The University Of Sheffield.

Understanding Peroxidase immobilisation on Bioinspired Silicas and application of the biocatalyst for dye removal

Eleni Routoula

A thesis submitted in partial fulfilment of the requirements for the degree of Doctor of Philosophy

Department of Chemical and Biological Engineering

Faculty of Engineering

University of Sheffield

2019

List of Publications and Conferences

Publications

Patel H., Routoula E., Patwardhan S., Removal of Water Pollutant Remazol Brilliant Blue R (RB19) Using Bioinspired Silica, (in preparation)

Routoula E., Patwardhan S., Using Peroxidase immobilised on Bioinspired Silicas to understand the difference between development and application of a biocatalyst, (in preparation)

Routoula E., Patwardhan S., Degradation of anthraquinone dyes from effluents: a review focusing on enzymatic dye degradation with industrial potential, *Env. Sci. Technol.* 54, 2, 647-664 (2020).

Manning J., Routoula E., Patwardhan S., Preparation of Functional Silica Using a Bioinspired Method, *J. Vis. Exp.* (138), e57730, doi:10.3791/57730 (2018).

Attended Conferences

Oral presentations

Catalysis and Reaction Engineering Symposium organised by IChemE, 31/05/2017, Sheffield, UK, "Peroxidase immobilisation on bioinspired silicas for dye degradation"

Engineering Research Symposium, 26/6/2018, Sheffield, UK, "Enzyme immobilisation on Bioinspired-Silicas for pollutant degradation" (winner of 1st prize "Research communicator of the year")

Oxizymes, 8-10/7/2018, Belfast, UK, "Peroxidase immobilisation on bioinspired silicas for dye degradation"

ISME workshop on "Role of enzymes in securing our sustainable future", 10-11/7/2018, Belfast, UK, "Peroxidase immobilisation on bioinspired silicas for dye degradation"

Poster presentations

ChemEngDayUK, 27-28/3/2017, Birmingham, UK, "Peroxidase immobilisation on bioinspired silicas for dye degradation" (winner of 1st poster prize in Catalysis and Sustainable Green Chemistry theme)

Engineering Research Symposium, 31/6/2017, Sheffield, UK, "Peroxidase immobilisation on Bioinspired Silica for dye degradation" (winner of first prize, "research poster of the year")

13th International Conference on Materials Chemistry (MC13), 10-13/7/2017, Liverpool, UK, "Peroxidase immobilisation on bioinspired silicas for dye degradation"

3rd EuCheMS Congress on Green and Sustainable Chemistry (EuGSC), 3-6/9/2017, York, UK, "Peroxidase immobilisation on bioinspired silicas for treating dye-polluted water"

WaRM (Waste and Resource Management) Conference, 20/6/2018, Milton Keynes, UK, "Green Silica-Enzyme composite for dye degradation" (winner of 1st poster prize)

9th International Congress on Biocatalysis, 26-30/8/2018, Hamburg, Germany, "Exploring immobilisation of Peroxidase in Bioinspired Silicas for dye degradation" (poster and 3-min talk position awarded but not accepted)

14th International Conference on Materials Chemistry (MC14), 8-11/7/2019, Birmingham, UK, "Anthraquinone dye removal from water using green nanomaterials with a twist" (poster position awarded but not accepted)

Abstract

Dyestuff industry is responsible for up to 20% of the industrial water pollution, due to dye loss in effluents. Compared to research on treatment of azo dyes (largest category), research of anthraquinone dyes (second largest category) is neglected. Environmental considerations about industrial chemical processes for water treatment have led to a shift towards green chemistry and biocatalysis. Although peroxidases are vastly applied in bioremediation, they cannot be industrially implemented due to low stability, lack of reusability and difficulty in scale-up. Immobilisation offers reusability and can improve the catalytic functions and operational stability of biocatalysts. Novel approaches, include bioinspired supports, synthesised fast and economically, avoiding the environmentally un-friendly methods used in "conventional" immobilisation.

This project focused on understanding the immobilisation of Horseradish Peroxidase (HRP) on bespoke Bioinspired Silicas (BIS), by examining factors affecting the synthesis and performance of the biocatalysts. We immobilised HRP on BIS via in-situ encapsulation and adsorption, and compared the outcomes to that of HRP adsorbed on commercial silicas. We also examined the effect of the controlled presence of amine functionalisation on BIS, of the point of HRP addition during synthesis of the biocatalyst and of increasing HRP concentration, to the immobilisation efficiency and performance of biocatalysts. BIS showed high potential as immobilisation supports, offering high loading (about 20% HRP on BIS-HRP composite) of active enzyme and their ability to protect HRP under exposure to non-optimal conditions. Biocatalysts were characterised for their morphology and porosity before assessing their performance a standard peroxidase assay based on 2,2′-azino-bis(3-ethylthiazoline-6-sulfonate acid oxidation (ABTS assay) and an application assay based on enzymatic degradation of a model anthraquinone dye, Reactive Blue 19 (RB19 assay). Further examination of the best performing BIS-HRP samples, revealed a competitive action of BIS to enzymatic activity, where the support acts as an excellent adsorbent, hindering the diffusion of substrate and product(s) through the pore network. Although free HRP outperforms immobilised HRP (especially via encapsulation), immobilisation results in a highly reusable biocatalyst, for up to 20 times with 60% performance retention towards dye removal, with enhanced storage stability, retaining almost 100% activity over 50 days of storage, compared to 3 days of storage reached with free HRP.

Through this work, we showed the importance of individual factors crucial for enzyme immobilisation, regarding both biocatalyst synthesis and expected performance, as well as the importance of the combination of enzyme, substrate and immobilisation support on biocatalyst performance. This work can be a great base for further optimisation of BIS as enzyme immobilisation support, and its exploration in other applications in the area of water treatment.

Acknowledgements

I would like to express my gratitude to my supervisor, Professor Siddharth Patwardhan, for his continuous support during our collaboration, his patience with my (super) long documents, his motivation, his advice and his critical judgement of my work. The choice to follow him from Glasgow was a correct one, which helped me grow and discover what I enjoy doing. Special thanks go to members of the Green Nanomaterials Research Group, in order of appearance, Joe, Mauro, Abi, Clive, Jake, Max, Manasi and Charles, for their support, stimulating discussions, advice and moments of joy.

I would like to deeply thank my second supervisor, Dr. Tuck Seng Wong for his advice on my research so far as well as his PhD candidate, Abdulrahman Alessa, for his time and support, and the kind donation of DyP4 for exploration of its potential. I would like to also deeply thank the following research groups in the Chemical and Biological Engineering department, for advice and help I received from their members: group of Dr. Peter Hall, group of Dr. James McGregor, group of Dr. Alan Dunbar. Last but not least, I would like to thank James Grinham, Duncan Scofield and Julie Swales, for their technical support, help and advice.

I would like to also thank Professor Gregory Beaucage, who introduced me to the potential of USAXS analysis and helped me with data interpretation. This research used resources of the Advanced Photon Source, a U.S. Department of Energy Office of Science User Facility operated for the DOE Office of Science by Argonne National Laboratory under Contract No. DE-AC02-06CH11357. The USAXS data was collected at the APS on the beamline 9-ID-C operated by Jan Ilavsky and his team at the X-ray Science Division.

I could not have completed this PhD without the continuous support and love from my family, who made sure to remind me that I can go through anything and find ways to manoeuvre around arising issues. Also, I would not be at the mental state I am today without the continuous support of my friends, in the UK, Greece, or elsewhere, who made sure to keep me laughing no matter what. Specifically, I would like to deeply thank Maria, Anna, Antonios, Sol, Gloria, Evi and Varvara, for handling my emotional load exceptionally well. An extra round of thanks is due to Jas, who was there for me almost from the beginning and held my hand in better and in worse. Those four years have been eye-opening, full of stress, joy, various experiences, travels, understanding and personal and professional growth and I could not have managed to go through it without this incredibly supportive network.

Table of Contents

Abbreviations

- ABTS: 2,2′-azino-bis(3-ethylthiazoline-6-sulfonate (typical peroxidase substrate)
- AOP: Advance Oxidation processes
- BET: Brunauer, Emmet and Teller equation on calculation of surface area via porosimetry
- BIS: Bioinspired silica (as produced from SVP group)
- BIS-PAH/BIS-PEHA: BIS produced with the specific additive
- BOD: Biological Oxygen Demand
- COD: Chemical Oxygen Demand
- Da: Dalton
- DMP: 2,6-dimethoxyphenol
- DyP: Dye-decolorising peroxidase
- FTIR: Fourier-Transformation Infrared Spectroscopy
- HRP: Horseradish Peroxidase
- PAH: polyallylamine hydrochloride
- PEHA: pentaethylenehexamine
- PEI: polyethyleneimines
- RB19 or RBBR: Remazol Brilliant Blue Reactive dye
- SEM: Scanning Electron Microscopy
- TOC: Total Organic Carbon
- TDS: total dissolved solids
- USAXS: ultra-small angle X-Ray scattering
- WRF: white rot fungi

List of figures

List of tables

List of equations

Chapter 1 : Introduction

In this chapter, the focus is to introduce the problem arising from presence of dyes in water effluents. Background information is given on the existing legislation with respect to dye content in water streams and a general overview of dye structure is discussed, focusing on anthraquinone dyes. The available methods used for decolorisation (mainly as part of water treatment facilities) are discussed and compared, and focus is merited in biological methods, specifically use of enzymes. An overview of biocatalytic actions and a thorough discussion of their advantages and disadvantages is given, resulting in the superiority of their performance, which is hindered by the cost and the instability of enzymes.

1.1. Problem faced from dyes in wastewaters

A very important factor of our life in every possible aspect is water, as it is not only vital for our physical existence but it is necessary for numerous activities in domestic and industrial fields, varying from cleaning and agriculture to cooking and product formation. Unsustainable exploitation and uncontrollable contamination are currently the "hot issues" regarding water management. The amount of freshwater available on Earth is 3% of the total water volume. Of that, the amount of water, in liquid form, available for human exploitation is 0.3%, making the percentage over the total water volume equal to 0.009% [1]. These limited water resources need to be adequately distributed and carefully used to fulfil the constantly rising demand due to population growth and consequent rising of the agricultural and industrial demands. Following that perspective, wastewater effluents need to be treated to a point of water being able to be recycled and reused [2].

1.1.1. Available legislation

Industrial use of water is the second largest freshwater consumer after agriculture [1], and amongst others, the textile and chemicals industry is recognised the most polluting, based both on the volume and the composition of its effluents [3]. Environmental protection awareness has increased, requiring minimisation of water usage and wastewater production, as well as limitation of the amounts of pollutants released to the environment. There are legislations that regulate and monitor the dyeing industry in Europe and the United States [4, 5], however these are not clearly defined and not comparable across countries with respect to the colour intensity of the discharged effluents [5]. These issues make the monitoring of coloured effluents released in the environment quite a challenge. The problem of the dye contaminated water is especially evident in Asia, which contributes to about 50% of textile exports and more than 50% of world's consumption of dyes [6]. However, many of the countries involved lack sufficient legislation about environmental protection relevant to textile industries [6], or there are no clearly set limits yet on the colour of the discarded effluents as they are for other pollutants [7]. A report produced by the World Bank with respect to the textile industry in Bangladesh [8] shows an overview of the textile industry in Bangladesh. 87% of the country's total exports in 2011 was based on garments, the majority of

environmental impacts with respect to water, energy and chemicals are attributed to the dyeing process, with percentages of 85%, 80% and 65% respectively. This report discusses available or potential sustainable solutions to mitigate those environmental implications, with reference to energy, water and chemicals overuse, with an added benefit of economic benefits. With respect to chemicals (dyes included), the proposed best practices are use of "eco" dyes and better dyeing recipes. However, there is no discussion about the current issues with dyes in terms of residual colour in water, although there are many photos illustrating the burning issue. Another case study from India [9], looked at the textile effluents of Tirupur city (also known as T-shirt city) in South India and performed a physical and chemical characterisation, comparing the results to the limits stated from the Bureau of Indian Standards. It was shown that the value of the effluents colour was over 200 times higher than the standard (as measured in Pt-Co units). Also, the previously reported practice of direct discharge of effluents in water streams despite the existing governmental rules [10], was also verified by Elango[9], indicating that the implementation of regulations is lacking and also pointing out that water streams are rendered unusable.

Although currently the relevant legislation might be vague and not properly applied [11-16], it is clear that not only the volume of discharged effluents needs to be minimized, but the quality of industrial effluents discharged in the environment needs to be fully monitored as well.

1.1.2. Quantification of the problem and potential implications

It is difficult to quantify the amount of dyes lost during production or during application on textiles, as the available figures on literature are based on estimations, or are representative of very specific types of dyes or applications. Dye production may vary between 10,000 [4] and 770,000 tons per year [17] and losses are estimated around 2% during production and around 10% during application, with wastewaters being discarded directly into the environment in developing countries [18]. Based on data from 2013, the annual production of textiles was around 30 million tons, increasing every year [17], especially production of cotton textiles [19]. Each ton of textile requires an average of 200 m^3 of water during its production [20, 21] (values depending on the type of textile), of which about 40 m^3 of water is attributed to the dyeing process. The dyestuff industry in total is responsible for about 20% of the industrial water pollution production [22]. It is also very difficult to estimate the concentration of dyes in effluents, mainly due to lack of information or consistency in measuring system, hence the range given in literature is quite vast, between 0.01g/L to 0.25g/L, or between 1000 to 12,500 ADMI units [23]. Dye (and other organic compounds) presence in water streams creates environmental issues such as difficulty of light penetration hence disturbance of aquatic photosynthesis and depletion of dissolved oxygen concentration due to the creation of films on the water surface [21, 24]. Also, there are aesthetic implications, given the fact that dyes in water can be detected from the eye at a concentration as low as 0.005 mg/L [25]. There is also a potential for health implications, although the toxicity of dyes is not fully identified yet, with some research being done on the toxicity of some common dyes, but no reports

monitoring the toxicity of chronic exposure or the intermediate products of dye degradation [19]. It is evident that water pollution from dyes is an existing and growing problem that demands attention.

1.2. Focus on anthraquinone dyes

The majority of dyes industrially used today are aromatic compounds with complex, reinforced structures. This indicates that their degradation will be more difficult compared to naturally occurring dyes and the structure suggests that there could be enhanced toxic effects related to them and the products of their decomposition [17]. Dye structure has been altered over the years, due to the need for dyes to be more stable (towards water, light, dry cleaning methods) and of higher colour intensity, without needing the use of additional chemicals as colour enhancers [7]. This indicates that conventional methods available for treating effluents from dye-industries could be ineffective [4, 26], so there is a particular need of innovation in the wastewater treatment sector. Of the industrially important dye categories, the most common "azo" dyes are making up of almost 60% of the synthetic dyes used industrially, followed by "anthraquinones" (15%), and indigoids in respect of the chromophore group present [27]. Chemically, what distinguishes azo dyes is the presence of one or more double bonds between nitrogen atoms (namely azo groups) in the dye molecule (Figure 1-1). Azo groups are able to absorb light in the visible spectrum and are broadly used due to the ease of their synthesis, their stability, the availability of colours and the low production cost [24], even if during their degradation from conventional methods they can generate toxic by-products [28].

While for azo dyes, relevant data is easily available, it is difficult to find current or accurate data for the annual production of anthraquinone dyes. Nevertheless, data found from previous years can be used to roughly estimate a production volume. For the US, within a period of about 15 years (1986-2002), the annual production of anthraquinone (a precursor for dyes and other chemicals) had a 5,000% increase (500 to 25,000 tons)[29], while a report from 1978 stated that for the 18 commercially most important anthraquinone dyes (among 145), the total production volume was slightly above 5,500 tons [30]. Given the increase in production volume of dyes (in general), it is safe to assume that the production of anthraquinone dyes increased as well. Based on the current volume of dyes production and the percentage that anthraquinone dyes hold, a rough estimation can be made, of about 100,000 tons of anthraquinone dyes produced per year.

The specific chemistry of the anthraquinone group is based on the anthracene and consists of three fused benzene rings (basic anthracene structure) with two carbonyl groups on the central ring, (Figure 1-1). This structure is naturally colourless, but substitution of the aromatic rings gives colour and controls its intensity [31]. Colour gets deeper with increased basicity of the substituents, for an aniline-based substituent (NHC_6H_5) is used, the maximum absorption length rises to from 327nm (case of H) to 508nm[31].

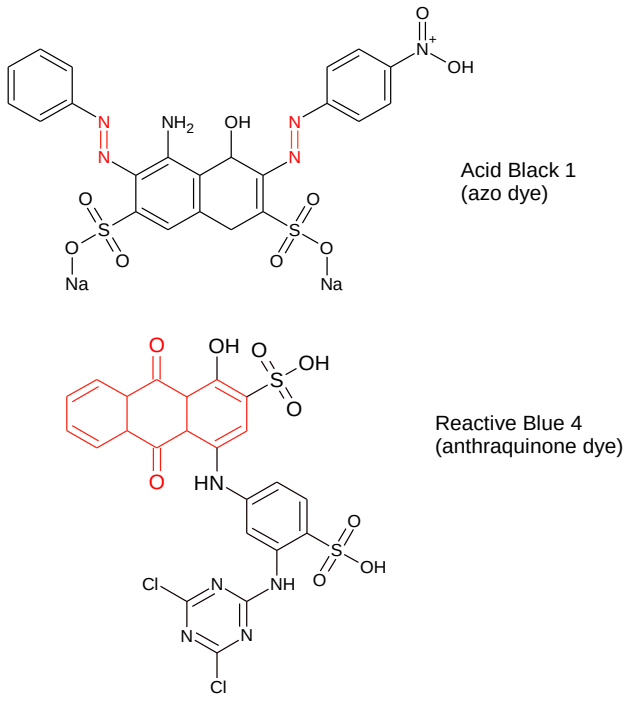

Figure 1-1 Representation of some important synthetic dyes, belonging to the two most important chromophore groups. The structure of the chromophore is shown in red.

Anthraquinone dyes are produced through many steps, including the production of intermediates such as haloanthraquinones, nitroanthraquinones and aminoanthraquinoes among others, as well as the addition of chemical groups to ease their solubility in water such as sulfonic groups [30]. Those groups however make the dye recalcitrant to degradation [32].

The difference from azo dyes is that in the anthraquinone structure, the carbonyl group acts as an electron acceptor, thus requiring an electron donor to react and break their structure [21]. This, combined with resonance effects among the anthracene structure leads to higher difficulty in anthraquinone dyes degradation compared to azo dyes [18, 33] and makes the choice of an appropriate degradation/decolorisation method challenging [34]. Due to their highly stable structure, anthraquinone dyes are known for their great fastness, stability and brightness[31].

It can be quite difficult to choose an appropriate method among the available conventional methods to treat anthraquinone dyes, due to their characteristics [35]. Also the lack of data on the intermediate products created during degradation makes it difficult to speculate any residual toxicity and its origin, as well as to find appropriate degradation pathways [34]. There are only a few reports about the toxicity of representative anthraquinone dyes and research has shown that not all anthraquinone dyes show toxicity, but some of them can be potentially toxic, few of them are mutagenic and some can be potentially carcinogenic [34, 36-39]. With respect to the degradation pathway of anthraquinone dyes, again few reports are produced which base their results on some experimental data and hypothesised routes due to absence of further evidence [40-44].

1.3. Available methods for decolorisation

1.3.1. Definition of decolorisation

Before elaborating on the available methods for colour removal from wastewaters, an explanation on relevant terminology should be given. There are three terms related to colour removal from dyed wastewaters, them being decolorisation, degradation and mineralisation [45]. Although all eventually describe the absence of colour, each term describes a different pathway towards that, resulting in the same "visible results" (no colour) but different "invisible results" (chemical structures). Decolorisation involves a slight chemical change of the chromophore/functional group of the dye molecule, leading to a colourless (or of less intense colour) solution, while degradation occurs when several parts of the dye molecule are "broken down", resulting in various, theoretically simpler intermediates [17]. On the other hand, mineralisation involves transformation of organic carbon to carbon dioxide, hence complete decomposition of the organic structures. It can be argued that mineralisation cannot occur without degradation or decolorisation of dye structure, however degradation or decolorisation do not necessarily lead to mineralised matter. Despite the vagueness of the specifications of the colour removal procedure, importance relies primarily on the percentage of colour removal. More rarely, analysis includes Chemical Oxygen Demand (COD) data [41] and, in the case of a specific need for mineralisation, the interest lies also on the percentage of Total Organic Carbon (TOC) transformed [46, 47].

1.3.2. Conventional methods of colour removal – Basic principles

Conventional wastewater treatments include mostly physical and chemical methods and to an extent biological in the terms of aerobic and anaerobic standard treatments used in municipal sewage treatment. The most known and extensively applied methods in the industry are adsorption, coagulation, membrane filtration, various oxidative or photocatalytic processes and biological processes [19, 48]. Before exploring relevant research done in enhancing aspects of each method, an overview of the basic operational principles will be discussed.

1.3.2.1. Adsorption

The mechanism of adsorption is based on physical and/or chemical interactions between the adsorbent and the substance to be removed from a usually aqueous solution.

Adsorption has been shown a preference over other methods of water treatment with respect to dye removal, as it offers lower initial cost, easy operation and flexibility compared to other methods. The important parameters for an efficient adsorbent are its capacity (amount of sorbed dye per mass of adsorbent), the equilibrium rate (how fast adsorption occurs) and the regeneration (how easy is to regenerate and reuse the adsorbent) [49]. The capacity of an adsorbent is judged by its porosity and available surface area. The bigger is not always the better, as there is a need for the optimum combination of pore size, porosity and surface area, alongside the chemistry of the adsorbent (functionalisation or available adsorption sites). The available surface area, porosity and chemistry can also affect the equilibrium rate, the time needed for capacity to be reached.

Also, these factors affect regeneration, based on the binding strength of the pollutant on the adsorbent and the porosity. It should be mentioned that biosorption is another type of adsorption, where pollutants are being adsorbed on dead (or inactive) biomass, through physical or chemical interactions, not related to metabolism. Bio-sorption is affected by the same factors as non-bio adsorbents (pH, T, ions among others), follows similar kinetic mechanisms and is subjected to the same techniques for characterisation [50]. Major differences between adsorption and biosorption are the delicate nature of some bio-sorbents (for example dead cells), the natural abundance of some biosorbents (for example agricultural biomass), and the valorisation of materials which are regarded as waste (for example dead cells that were used in other processes, agricultural biomass).

Amongst many adsorbents explored such as activated carbon, peat, silica-based adsorbents, zeolites or other naturally derived substances, activated carbon is widely studied for dye adsorption. It is also the dominant adsorbent in industry, based on its great adsorption ability, high surface area, stability and homogeneity [51]. Main issues with respect to use of activated carbon as a dye adsorbent, are the high cost of production and regeneration and the possibility of decreased efficiency due to material loss during regeneration [4, 52, 53]. When activated carbon from leaves was used for adsorption of Acid Green 25, adsorption was more effective in acidic solutions and that past the initial, external uptake, diffusional limitations due to pore structure delayed equilibrium, regardless of the over 900m^2/g surface area [54]. Another example using rice straw ash as adsorbent towards removal of Reactive Blue 19, showed that the physisorption was the dominant way of sorption, with electrostatic interactions being stronger again in highly acidic conditions (pH 1). In this case, despite the lower surface area (about 60m^2/g), adsorption capacity was high due to a mesoporous structure that prevented strong diffusional limitations [55]. Chu et al. studied the adsorption of an anthraquinone dye (X-BR) on activated carbon derived from aquatic biomass debris [56]. Decolorisation capacity (555mg dye/g adsorbent) of that type of activated carbon was found higher than commercial carbon products, potentially due to much higher surface area (around 1400m^2/g). Further, they revealed that acidic conditions favoured adsorption and the amount of adsorbent used was important as at higher adsorbent concentrations, aggregation of the adsorbent caused partial clogging of the adsorptive active sites. Another frequently discussed option in the area of adsorption, is the family of zeolites, materials abundant in nature, but with substantially lower adsorption capacity and again facing the issue of high regeneration costs [49, 57]. Besides activated carbon and zeolites, silicon based materials have been studied extensively for pollutants adsorption [58, 59]. Their interesting properties such as ability for a wide range of pore size and surface areas, durability, ease of functionalisation and relatively cheaper regeneration compared to activated carbon (lower temperature required), have made them excellent candidates for water treatment with many examples on dye adsorption [60-63]. However, issues such as manufacturing cost and diffusional limitations arising from high throughput in industrial scale applications combined with larger sized organic pollutants, have prevented them from being

widely implemented in water treatment. Despite those aforementioned difficulties, research is showing positive signs on their industrial implementation [64].

1.3.2.2. Coagulation - Electrocoagulation

Chemical coagulation or flocculation, although quite popular in the past, has been replaced by newer methods or is being used in combination with other methods, in order to reduce the effect of some major drawbacks such as sludge production and need for further treatment of the effluent [65]. The principle of coagulation and flocculation methods is the opposite charge between the soluble pollutant (e.g. dye) and coagulant, that makes the pollutant become insoluble[65]. Coagulants used are mostly based on aluminium and iron, sometimes assisted by polymeric coagulants. The factors of importance during coagulation are the type and dose of coagulant needed and the size and "sturdiness" of the coagulated pollutants (also known as floccs) which dominates their ease of removal [66]. Sludge production is a direct implication of coagulation, which poses one of the main concerns around the use of this method, as there is further treatment required, on a potentially more toxic waste stream than the original one. Recently, the process of coagulation was coupled with electrochemistry and electrochemical coagulation gained interest with respect to textile effluent decolorisation. Towards that direction, electrochemical coagulation producing in-situ coagulants based on aluminium or iron, showed great dye removal (RB19 as a representative anthraquinone dye, but other dyes were studied as well) and associated time [67]. That paper also presented an economic evaluation of some decolorisation processes, which suggested that electrochemical and oxidative processes are advantageous to adsorption, however, results can be considered inconclusive, as in this analysis biological methods were not included and some values on capital and operating costs for were not defined. What was only acknowledged but not commented further is sludge production and the need to deal with it, but, it was shown qualitatively that use of different conditions can have an effect on the amount and type of produced sludge.

1.3.2.3. (Advanced) Oxidation Processes (AOP)

Oxidation Processes belong to chemical methods that can be used for water treatment. The most widely known oxidation processes include Fenton's process, ozonation and use of hydrogen peroxide, and more recently, photocatalysis. The operating principle is the generation of free hydroxyl radicals that are able to oxidise organic molecules in a non-selective way and lead to their mineralisation [68]. In the case of Fenton process, the presence of ferric ions can lead to promotion of pollutants coagulation [69], combining aspects of both oxidation and coagulation processes. Photocatalysis is a relatively modern technique, where hydroxyl radicals are produced by the interaction of Ultra Violet light with a semiconductor photo-catalyst [70]. In every case, there are several factors of importance to the oxidation process used, such as the amount of oxidant produced and conditions of production, current, pH of solution, type and intensity of light source, mode of addition of the oxidant/semiconductor, structure of reactor and stability of the process.

All these factors are crucial for the time needed for mineralisation (or adequate results) and the cost effectiveness of the process.

What is worth highlighting with respect to AOP is the very short reaction times required, usually minutes, leading usually to very good efficiencies in reduction not only of colour, but also of COD/BOD levels. Main disadvantages of these methods are the cost of oxidative agents (ozone, peroxide) and radiation sources that can pose difficulties on their consideration of scale-up and also the production of sludge in the case of Fenton's reaction [71, 72].

Radovic [73] examined the degradation of RB19 dye using various AOP and their combinations, and a very high initial dye concentration (2,500mg/L, for reference, examined values in literature are usually within the range of a few hundred mg/L). They found that each process is affected differently by the dye structure and that UV radiation of peroxide is not as effective as Fenton's reagent and its variations (removal of 42% of colour by UV treatment compared to over 80% by Fenton's reagent or a combination of Fenton with photocatalysis). Also, upon examining simulated effluents instead of isolated dyes, the efficiency of the treatments dropped about 10%, fact expected, yet indicating that efficiency is still high. Similarly, Lovato [46] examined degradation of RB19 using ozonation and UV radiation. They found that UV radiation alone was not very effective, but ozonation or ozonation assisted by UV radiation were highly efficient, both removing almost 100% of the colour within 5mins. However, it was noticed that compared to ozonation, the combination with UV radiation lead to much higher mineralisation percentage (40% and more than 90% respectively). Two different studies also showed that ozonation can be quite effective for degradation of RB19 (both 100% in a matter of minutes), promoting its biodegradability based on reduction of the toxicity of the fragments [41] and showing the importance of the electrolytes to the decolorisation and identification of fragments [74]. Using a slightly different anthraquinone dye, Reactive Blue 4, Gozmen [75] examined its decolorisation using 4 different AOP, wet air and peroxide oxidation, photocatalysis using various oxides and Fenton's reagent. They found that although all treatments showed high effectiveness (100% colour removal in less than 60min) and relatively high removal of TOC, wet peroxide worked faster. However, this treatment required 35% w/w peroxide solution and a temperature of at least 100^{o}C, factors that might be limiting for industrial application.

1.3.2.4. Biological treatment

Biological methods have been used for water treatment for many years, especially in sewage water treatment, in the form of activated sludge. They can offer distinct advantages compared to physicochemical methods, but also challenges regarding their efficiency [48]. The most common categorisation is based on aerobic and anaerobic operation of the microorganisms involved, however, based on the ability to use isolated enzymes, there should have been a proposed categorisation in order to include them. Based on the latest argument, one could say that the available biological methods can be divided on whether they are performed inside a cell (of

bacteria, fungi, yeasts or algae), or using isolated enzymes. Others have proposed that use of enzymes falls in between chemical and biological treatment, as we are "taking advantage" of chemical reactions performed by isolated biological compounds [76].

Some of the clear differences between biological and non-biological methods include the lower starting concentration of dyes examined and the longer time needed for decolorisation in biological methods, leading to the conclusion that biological methods might not be as effective as physical and chemical methods. From the studies examined on biological treatment of anthraquinone dyes, the highest starting concentration was 300 mg/L of various anthraquinone dyes of acid and basic structure, using an *e-coli* culture [77]. This study showed that the structure of dye had an influence on the combination of mechanisms of removal; options being degradation due to metabolism, precipitation due to biotic effects and adsorption onto the cells. Specifically for anthraquinone dyes, dye decolorisation occurred primarily due to microbial induced precipitation, followed by adsorption on cells and cell metabolism. On a similar note, biological treatment of various anthraquinone dyes using a *Bacillus cereus* culture showed that the structure of dye lead to massively different degrees and times needed for decolorisation, around 90% removal of Acid Blue 25 in 6 hours and of Disperse Red 11 in 24 hours [78]. Another study [79] showed that when *Proteus species* were acting in a consortium, the decolorisation of anthraquinones Reactive Blue 4 and 19 was dramatically improved compared to lone action.

There are a few reviews compiling research done on the degradation of dyes by microorganisms [17, 24, 26, 80-83], either focusing on a specific species (e.g. bacterial), or a specific type of dyes (e.g. azo). The outcome of this collective research is that microbial decolorisation is quite effective, yet not so efficient, since there are many factors to be taken into consideration, such as nutrients, culture/species of the microorganism, concentration of pollutants and contact time involved.

On the other hand, use of isolated enzymes for dye decolorisation is not industrially applied yet due to limitations related to stability and scale up, but relevant research is flourishing [28, 84, 85]. The enzymes responsible for dye decolorisation belong to the family of oxidoreductases (EC: 1), which catalyse oxidation and reduction reactions, finding application in various domains varying from diagnostics to wastewater treatment and production of chemicals or potentially biofuels[86-92]. They have been studied extensively for dye decolorisation and bioremediation, with much research focusing on the oxidative action of laccases and peroxidases as well as the reductive action of azoreductases (azo dye specific enzymes), with many review papers available targeting dye degradation in general [84, 85, 93-95] or focusing on azo dyes [24, 28, 96]. Those enzymes have the ability to act on the dyes (and organic substrates in general) and either create precipitants that can be removed easier or transform the chemical substance into a compound that might be easily dealt with [97]. In literature there are numerous examples of isolated enzymes of the Oxidoreductase family for dye decolorisation, some of them focusing on anthraquinone dyes.

When Horseradish Peroxidase was used for degradation of RB19 dye, results were highly promising both based on removal percentage and toxicological analysis of residual products [98]. However, when the same enzyme was used on a 10fold higher concentration of the same dye solution, then inactivation was observed as well as precipitation of dye [99]. Other examples show that when Horseradish Peroxidase was applied on a single anthraquinone dye (Lanaset Blue 2R) decolorisation efficiency was very good, but when the enzyme was applied in real effluents, then its performance decreased [100]. Application of Laccase has been also well examined in dye degradation. Specifically for anthraquinone dyes, what Verma et al. found when applying Laccase for the degradation of Reactive Blue 4, was that equilibrium was reached fast, but decolorisation was not very efficient, due to the formation of coloured degradation products. However, when biosorption followed, those fragments could be almost fully removed. What their research showed is that although biosorption works better for dye removal (due to adsorption, not degradation), equilibrium is much slower, making the combination of enzymatic action followed by biosorption ideal for best results [101].

1.3.2.5. Emerging Methods for colour removal

A relatively new category of water treatment processing for pollutants' removal, including dyes, is use of advanced nanomaterials (or nanoparticles) with a size range of up to 100nm. Their action falls somewhere within chemical and physical methods, comprising aspects of both. Some examples of explored nanomaterials are metal oxides (zinc and titanium among others), carbon nanotubes, and nanochitosan. [102]. The application of nanomaterials for dye degradation from effluents is not yet thoroughly researched, but their advantages (such as durability, much higher surface area than conventional materials, unique confined spaces and conditionally easy scale up and low cost) lead to potential interest for their industrial application [103]. Nanomaterials can be used as adsorbents of dyes with very promising results, especially when coupled with AOP usually based on photocatalysis. Using zinc oxide nanoparticles to remove Reactive Blue 19 dye showed very good results, indicating high capacity, up to 167mg dye per g adsorbent and short contact time (max 20 minutes) [104]. The same adsorbent was tested for removal of an azo dye (Reactive Red 198) with the same auxochromes, and results were more promising compared to the anthraquinone dye, despite the bulkier structure and the almost double molecular weight. Research coupling use of zinc and titanium oxides with photocatalysis by irradiation showed that nanoparticles can be quite effective in assisting degradation of a model anthraquinone dye, but their efficiency depends on the structure of the dye [33]. A similar experiment looked at the optimisation of the degradation of Acid Green 25 using immobilised TiO_2 nanoparticles coupled with UV light photocatalysis [105], and further examined the importance of the chemical structure of dyes in degradation [106]. A more recent example examines the degradation of Reactive Blue 4 (another model anthraquinone dye) based on the coupled use of copper nanoparticles and showed that initially the dye gets adsorbed onto the nanoparticles and then is oxidised based on the production of hydroxyl radicals from added mediators and the action of monovalent copper [107].

While research shows is that nanoparticles can be a good approach for further investment into water treatment, there are some specific drawbacks to their use. Their toxicity is not thoroughly researched yet, however, there are strong indications that nanomaterials can be toxic to both humans and the aquatic environment [102]. Another disadvantage to their use as adsorbents is the need for regeneration (same as with conventional adsorbents).

1.3.2.6. Main issues with conventional methods

There are many research papers reviewing the industrially available methods and proposing new ones. Every category and method has advantages and disadvantages related to the following criteria: efficiency under various conditions, practicability, requirements of pre- and post-treatment and environmental impact; all of the aforementioned ultimately relate to cost (see Table 1-1 for a general comparison between physical, chemical and biological methods). Based on available literature, a method which could be universally applied and satisfy all demands simultaneously does not exist [21] and majority of methods cannot be used as a holistic approach [19]. As many researchers have proposed, the best dye removal approach should be a combination of available and under-development methods, combining their strong points and mitigating their disadvantages [26, 48].

What Table 1-1 shows is that some of the currently available physical and chemical methods may offer high effectiveness – especially depending on the combination of dye and method used, and there is a good amount of information about them since some of them (e.g. adsorption) have been extensively studied. However, alongside dye removal, there is sludge generation which can be difficult to handle, as well as the materials used cannot be regenerated easily, if at all. In addition some of these methods are not very efficient due to the large cost, time and space requirements [6]. It also shows that while AOPs are a quite promising category of methods, they still need refinement, whereas biological methods, past the traditional digestion, offer a novel approach to tackling the problem of dye presence in water. However, although enzymes work effectively towards dye degradation, there are issues about their industrial implementation that need to be addressed.

Table 1-1: General comparison of available decolorizing methods (adapted from [24, 26, 48, 86, 95, 108, 109])

Physical methods (adsorption, filtration)	**Chemical methods (coagulation / flocculation, (AOP, photocatalysis)**	**Biological methods (using microorganisms or isolated enzymes, or via bio-sorption)**
Advantages Industrially mature methods Highly efficient (conditional on combination of adsorbent / pollutant) Good knowledge of the processes and the physical chemistry required	**Advantages** Some industrially mature methods (e.g. coagulation, flocculation) Highly efficient, but not highly selective AOPs are quite fast (minutes – hours) and can lead to complete mineralisation Easily combined with other methods	**Advantages** Some industrially mature methods (e.g. activated sludge, aerobic digestion) Environmentally friendly, of lower cost, with lower water input required Dye structure is broken down to less toxic by-products, colour is removed or subdued Immobilisation can increase reusability, operational stability
Disadvantages Dye is removed but not degraded, so further treatment is required Difficulty in regenerating absorbents and filters/membranes Depend on the structure of the dye and the adsorbent Adsorbents might be of high cost Require long residence time (hours – days)	**Disadvantages** Some methods are not industrially mature yet (AOPs) Can lead to sludge production that is toxic and requires further treatment Costly due to energy requirements Unsustainable (use of harsh chemicals, production of secondary pollution) Coagulation/flocculation do not degrade dye structure	**Disadvantages** Some methods are not industrially mature yet (isolated enzymes) Limited knowledge and control of exact action and/or degradation pathway Many factors to be taken under consideration (T, pH, agitation, inhibitors, activators, chemistry of degradation, nutrients) Use of cultures requires high residence time (days) due to diffusion phenomena or the period of culture development

1.4. The shift to biocatalysis

The awareness and the environmental considerations about chemical processes and substances currently used in industry have led to a shift towards green chemistry [110]. Green chemistry, often termed sustainable chemistry, focuses on the molecular design of chemicals based on innovative and sustainable methods [110]. The goal is to reduce environmental and health impacts, minimise energy input and waste production and propose alternative, efficient solutions to existing problems, creating that way technologies economically competitive to existing ones [111].

Based on the principles of catalysis, biocatalysis –use of microorganisms or their enzymes [112]– has received much attention due to its many advantages (Table 1-2) [112, 113]. Inter-disciplinary cooperation has resulted in great advances in biocatalysis, creating biocatalysts with high versatility, selectivity and efficiency compared to "wild-type" enzymes [112, 114]. Those biocatalysts can be applied in many industrial areas, where absolute control of the molecule to be produced is needed, such as specific enantiomers in pharmaceutical production, and often chemical catalysis fails to guarantee the outcome [115, 116].

As with every technology, biocatalysis has specific advantages and disadvantages over regular catalysis or other available options. Use of "nature's" catalysts, enzymes, requires milder environments, hence lower temperature, pressure and absence of harsh chemicals. These requirements fulfil the creation of a sustainable process, as the energy usage (for heating, or holding high pressure among others) is minimised. Furthermore, by-products produced from enzymatic reactions, are generally considered less harmful compared to by-products produced from other processes with the same end goal and the end product is purer, requiring less downstream processing [117] . A good example to illustrate that is the production of sludge when chemical flocculation is used for decolorisation, as opposed to chemically lighter fragments (or even mineralisation) of the dye in case of enzymatic degradation. This sludge can be toxic and requires further treatment prior safe disposal in the environment, need that however is usually not openly discussed. With respect to efficiency, enzymes, similar to catalysts, have high turnover numbers (product per second from a unit of enzyme), with one of the greatest examples being carbonic anhydrase with up to 10^6 molecules of product produced by 1 molecule of enzyme in 1 second [118]. Turnover number can get even higher through optimisation of the enzyme, the substrate, the reaction medium or even their combination [117].

Disadvantages of biocatalysis are mostly relevant to the sensitivity of the microorganisms and their enzymes, as their operational conditions are mostly circumneutral. There are examples where microorganisms or enzymes show extreme thermal stability or stability in extreme pH values, but this is not usually the case, nor these examples are developed in an industrially exploitable scale [119]. Another major drawback of easy incorporation of biocatalysis in industrial scale is the amount of biocatalyst needed. The process to produce a specific cell culture or isolate an enzyme in a ready-to-use format is tedious and occasionally quite expensive, making industrial

implementation of biocatalysis difficult [120]. However, advances in scale-up production of specific enzymes of industrial importance (mainly lipase, amylase, glucose oxidase among others), have shown that scale-up is possible [120].

Table 1-2: Advantages and disadvantages of biocatalysis (adapted from [115, 119]).

Advantages	**Disadvantages**
Highly efficient processes	Narrow spectrum of operational parameters
Enzymes can be compatible with other enzymes (consortium, or cascade reactions)	The majority of enzymes show highest activity in aqueous solutions
Environmentally friendly, less energy usage, less waste production	Enzymes can be easily inhibited
Operation under mild conditions (room T, circumneutral pH, no harsh chemicals)	Industrial processes based on biocatalysis are difficult to establish
Potentially cheaper refining and purification procedures compared to conventional catalysis	Designing and developing a biocatalyst can be potentially expensive

Based on the advantages and disadvantages of biocatalytic processes as shown in Table 1-2, the challenge is to create methods for bioremediation, that can bypass the disadvantages of conventional, existing treatments (shown in Table 1-1) and be efficient, cost-effective and environmentally benign [76, 121].

With respect to the available biological methods (aerobic, anaerobic or enzymatic processes), they all use enzymes. In the enzymatic processes the enzymes are isolated, whereas in the aerobic/anaerobic treatment they are part of the microorganisms (bacteria, fungi, yeasts, algae). Exploitation of the enzymatic action in an isolated form and not as part of a microorganism has been developed relatively recently, since enzyme purification became widely available. Using isolated enzymes instead of the whole cell/micro-organism has divided scientists, as both options show considerable advantages and disadvantages (Table 1-3). The final decision depends on the targeted application and the specific conditions, but based on the specific advantages and disadvantages, it seems that isolated enzymes are more flexible to work with and potentially more powerful than whole cells. The enzymes responsible for dye degradation might be secreted intracellularly or extracellularly and they belong mainly to the family of oxidoreductases, including peroxidases (both peroxide dependent and independent), reductases and laccases [26, 122]. Those enzymes have the ability to act on the dyes (and organic substrates in general) and either create precipitants that can be removed easier or transform the chemical substance into a compound that might be easily dealt with [97].

Table 1-3: Points of interest in using whole cells or isolated enzymes.

Use of cells	Ref.	Use of enzymes	Ref.
Complemented/enhanced enzymatic action, ability for syntrophic mixed cultures, ability to deal with numerous compounds at once	[123, 124]	Use under conditions non-optimal to the microorganism is available	[94, 122]
Production in-situ of necessary co-factors	[26]	Faster reactions, no need to wait for culture growth	[125]
Cell structure can cause diffusional limitations or substrate adsorption before reaching the enzyme	[98, 126, 127]	High specificity, easily regulated catalytic activity, easier handling/storage, concentration not depending on culture growth rate	[4, 76, 124]
Use of cultures/cells is not as evolved in industrial level as the use of isolated (free/immobilised) enzymes, enzymes are more industrial-scale-friendly due to recombinant production	[95, 123]	Compromise of isolation and purification cost by production in recombinant hosts	[128]
Usually cannot remove pollutants to really low levels	[124]	Ability to develop faster, easier to implement methods	[124]

1.5. Peroxidases

Peroxidases (EC: 1.11) are part of the broader enzymatic class of Oxidoreductases (EC: 1) and as the name suggests, they catalyse reactions of oxidation and reduction, finding application in various domains such as in biosensors, diagnostic kits, industrial wastewater treatment, chemical production and potentially second generation biofuel production [86-92]. Their specific characteristic is that they contain a heme prosthetic group (iron (III) protoporphyrin IX), attached to the protein via a histidine residue [129].

The catalytic mechanism and the crystallography of peroxidases have been studied extensively using primarily horseradish and cytochrome C peroxidases, as representative enzymes of this category [130, 131]. Peroxidases catalyse the reduction of peroxides (mostly hydrogen peroxide due to steric hindrances arising from highly substituted peroxides [132]) and at the same time the oxidation of various organic and inorganic substrates. This “dual action” mechanism has been named “ping-pong bi bi” mechanism due to the fact that the electrons liberated by the enzyme for the reduction of hydrogen peroxide are recovered through the oxidation of the main substrate, with the aid of the intermediate compounds of the enzyme formulated during the enzymatic action [133].

During the catalytic action, 1 enzyme, using 1 molecule of peroxide, can oxidise 2 molecules of substrate (mainly aromatic phenols or phenolic acids, indoles, amines and sulfonates [132]) due to a “double charged” enzymatic form that requires two consecutive steps to return to its resting state (Equation 1-4) [134, 135]. This dual action can be represented in the following equations:

$$E + H_2O_2 \rightarrow EI + H_2O \text{ (EI contains a bound O molecule)}$$

Equation 1-1

$$EI + AH_2 \rightarrow EII + AH^{\cdot}$$

Equation 1-2

$$EII + AH_2 \rightarrow E + AH^{\cdot} + H_2O$$

Equation 1-3

$$\text{or in short: } H_2O_2 + 2AH_2 = 2H_2O + 2\ AH^{\cdot}\ .$$

Equation 1-4

E is the resting state of the enzyme (without showing catalytic action), EI is the enzyme in the "ultra-charged" state (namely Compound I), after providing 2 electrons to reduce the peroxide (Equation 1-1), EII is the "half charged" state (namely Compound II) of the enzyme, after accepting an electron from the substrate (AH_2, herein the chosen dye) and $AH^{\cdot}$ is the oxidised state of the substrate (Equation 1-2) [129]. After accepting another electron from a second molecule of substrate, thus reducing it, EII is transferred to the resting enzymatic state (Equation 1-3).

The intermediate compounds (I and II), are produced during the action of every heme peroxidase, independently of their structural differences [136] and the type of substrate can vary, independently of the redox potential of the intermediate compounds, including simpler or more complex phenolic and non-phenolic molecules [137]. It should be mentioned that the radicals produced during the catalytic cycle may not be identified due to their very short lifespan, and they could act as primers for further reactions with no dependence on the enzyme [129]. Decolorisation reactions are measured by the reduction of colour, hence, the spontaneous formation of radicals that may have a contribution towards the original dye structure deformation or creation of other coloured structures, could pose a factor of uncertainty on the pure enzymatic activity.

Research on the thermal deactivation and pH dependence of peroxidases showed that the heme group dissociates and gets degraded upon excessive heating [138], or in extreme pH values (below 5 or above 9 depending on the optimum pH for each peroxidase) [132, 139]. Alterations of pH can affect the thermal sensitivity of peroxidases, indicating that under suitable pH conditions the thermal tolerance of peroxidases can be increased or hindered [138].

Recently, a new category of peroxidases has attracted interest in the areas of decolorisation, lignin degradation and decontamination in general; peroxidases from white-rot fungi (WRF) [94, 140]. The applications of decolorisation and lignin degradation seem to be connected due to the similarities of those substrates in respect of the presence of substituted phenol rings [141, 142] and due to the non-specific substrate binding on these enzymes [143, 144]. In order to test the activity of specific

peroxidases towards lignin and dye degradation, some model representative compounds are being used, like veratryl alcohol, guaiacol, syringaldehyde, and pyrogallol to represent lignin. Remazol Brilliant Blue R or Reactive Blue 19 (RBBR or RB19), Poly R-478 are used as representative dyes and 2,2'-azino-bis(3-ethylthiazoline-6-sulfonate (ABTS) is used as a typical substrate for peroxidases [128, 141, 145-147].

Enzymes secreted from WRF include various peroxidases, like manganese peroxidase, lignin peroxidase and versatile peroxidase, which are known to degrade lignin [141, 143]. Apart from the mentioned enzymes, there is another family of enzymes secreted from WRF, namely dye decolorising peroxidases (DyP), which was firstly reported almost 20 years ago, showing a great activity over the decolorisation of dyes [148] and attributing its name to the ability of those enzymes to decolorise bulky dyes [149]. So far, DyP has been categorised as peroxidase as it shows activity over typical peroxidase substrates, varying from high to lower redox potential depending on the strain [150], and requires hydrogen peroxide [151]. However, due to indications of hybridised action of DyP between hydrolases and oxygenases [152] and their structural differences to "typical peroxidases", DyP cannot be categorised under any of the known peroxidase categories but it forms a new category [153]. The wide range of substrates indicates a family of enzymes with multiple potential applications [154], including dye decolorisation [155-157], lignin degradation [158, 159], synthesis of chemicals [160] and bleaching (in food industry) [161].

Due to the relatively short period of research on DyP, there is some data on the structure and mechanism of representative enzymes of this family, but information on the physiological role of these enzymes, or the exact structural or homology differences that mark the subfamilies is not fully mapped yet [84, 149, 150, 162-164]. With respect to the catalytic mechanism of DyP, different origin of DyPs may indicate differences in their catalytic mechanism as in which amino-acid residue serves as the base-acid catalyst (various distal residues, depending on the strain) [136, 165-168], thus leading to different preferred substrates and accordingly physiological roles. The mapped mechanism of DyP so far seems quite similar to the typical peroxidase mechanism as described in section 1.5 of Chapter 1. Recent reviews on characterisation of DyP can be of help for better understanding of this new enzyme family [151, 153, 163, 169]. Compared to other peroxidases, DyPs show distinguished advantages, not only when it comes to decolorisation and degradation of dyes, but in regard of other applications as well (Table 1-4). Besides extreme activity on degradation of anthraquinone dyes, DyPs show promising activity on lignin degradation fact that could be used towards valorisation of lignin biomass and production of chemicals [170]. One major disadvantage (as for all mediator-dependent enzymes), is their need for hydrogen peroxide and their conditional stability to high concentrations of it [128].

As far as the peroxidase action is concerned, DyP show activity over substrates of mainly anthraquinone structure [152, 162] but also show lignin degradation potential as well [171]. Anthraquinone dyes examined for decolorisation using DyPs include Reactive Blue 19 (RB19 or

RBBR) [148, 154, 159, 160, 172, 173] and Reactive Blue 5 (RB5) [150, 152, 157, 174-180]. Work on isolating and characterising DyP strains in their original hosts has been done by various researchers [148, 151, 153, 159, 175, 181, 182], as well as work on heterologous expression in recombinant hosts (indicating potential for scale up) [127, 128, 160, 172, 174, 178].

Table 1-4: Points of interest and limitations of DyP peroxidases.

Advantages – points of interest	**Reference**
Unprecedented activity towards anthraquinone dyes	131, 152, 158, 160, 177, 183
Activity on azo dyes (at some cases higher than azoreductases)	148, 183
Activity on model lignin-type compounds	128, 181, 184, 185
Ability to extend the substrate range by using mediators	84
Higher temperature and pH stability in and higher robustness compared to other peroxidases	152, 162, 164
Easier larger scale production through recombinant hosts compared to other peroxidases from WRF	166, 186
Limitations	**Reference**
The need of hydrogen peroxide limits industrial applicability	84, 127, 187
Excess of hydrogen peroxide causes inhibition	128
Decreased stability in "un-natural" environments, activity preservation and reuse potential	155

Examples of application of DyP for anthraquinone dye decolorisation show great results, such as research conducted by Shakeri et al. using recombinant DyP for RB19 degradation. They examined the enzymatic action in batch and fed batch reactor with stepwise or continuous addition of peroxide and showed that the enzyme had about 80% residual activity after 80 minutes. They also showed that –as expected– high concentrations of dye or peroxide lead to either reduction of decolorisation rate or deactivation of the enzyme and that in optimal conditions DyP had a capacity of 20mg of dye per unit of enzyme [127]. In a different example, Shoda et al. managed to completely decolorise Reactive Blue 5 by using a dual-peroxidase system; initially DyP fragmentised the dye and afterwards an in-house developed Versatile Peroxidase decolorised the degradation by-products [188].

It should be noted that researchers have developed artificial enzymes – namely nanozymes – that mimic specific enzymatic actions. Their action is based on a chemically synthesised active site very similar to the one of the targeted natural enzyme, focusing on enzymes that contain metals or metal oxides [189]. So far, the research is focused on mimicking the action of some peroxidases [190-194] and carbonic anhydrase [195-197]. Several reviews mention the progress of research so far, focusing on the ease of nanozyme usage over natural enzymes due to lower cost, easier scale-up production, durability, storage and operational stability. However, they also mention that the versatility of applications is very limited due to lack of selectivity and substrate binding ability, as well as they have comparably lower activity to natural enzymes [189, 198, 199].

Although literature shows that enzyme use in dye degradation specifically can be quite effective under laboratory, optimised conditions, application to an industrial scale has many limitations. The production cost (culture, isolation, equipment) and operational cost (use/reuse, downstream processing) of the enzymes [48, 86, 200-202] is definitely a burden. Also, high concentration of substrates or some of the by-products of dye degradation can inhibit the enzymatic action or potential reusability [176, 203, 204]. Furthermore, as the operational conditions (pH, temperature, buffers, mediators) are important for enzymatic action, difficulties can occur when treating real effluents [44, 100, 205] where conditions are not monitored.

In order to overcome some of these limitations –along with other limitations arising from the need to use enzymes outside of their optimum environment– there are mainly three strategies, which can be followed either alone or combined. The "invasive" one is by altering the properties of the enzyme via genetic engineering and molecular biology. The "excluding" one is by screening for new enzymes that will perform better than the so far known ones in the given conditions. The "external improvement" one refers to improvements that can be made without changing the enzyme, but utilising chemical engineering instead, to alter the stability of the enzyme, the reaction conditions or the downstream processing [123, 206]. The last option includes immobilisation which will be examined in detail in the next part.

1.6. Conclusion

In an overview, undoubtedly there is a major concern from the presence of organic pollutants, such as dyes, in water streams. All the methods currently used and potentially applied towards dye degradation have their strong and weak points, with respect to cost, efficiency, and sustainability. Historically, physical methods were developed first, followed by use of chemicals and implementation of activated sludge. Recently, novel approaches such as AOP implementing photocatalysis, use of isolated enzymes and nanomaterials are gaining way, as they allow for faster, better, cheaper results. However, none of them can be used as a standalone method for complete water treatment with respect to colour removal (or anything for that matter), so the target is to identify how further research can combine two or more methods in order to accentuate their potential and address their pitfalls. Out of the examined methods, Advanced Oxidation Processes and use of isolated enzymes were the most promising ones for partial or complete dye degradation. One could argue that Peroxidases fall between both categories, as enzymes that break down dyes based on oxidation with the use of peroxide. There are specific drawbacks in the use of isolated enzymes, which however can be overcome with suitable practices such as immobilisation.

Chapter 2 : Anthraquinone dye removal from immobilised oxidoreductases – a literature review

Enzymes are water soluble, so their separation from an aqueous solution is prevented, indicating that they cannot be separated from an aqueous system in order to be reused in another batch. Also, by nature, enzymes are sensitive to non-optimal operational conditions, so their use in native form can be industrially challenging. In this chapter the first point of interest is the use of immobilisation as a viable solution to tackle the main disadvantages of using enzymes. A brief, but critical overview is given on existing methods and supports for enzyme immobilisation (regardless of enzyme or application), identifying trends and challenges. Focus on the use of silicas as traditionally preferred immobilisation supports is merited, and then shifted to bioinspired silicas (BIS) as a promising solution to issues faced with other silicates. Literature is examined for examples of immobilised oxidoreductases applied for anthraquinone dye decolorisation and main conclusions are summarised.

2.1. Introduction to immobilisation

Immobilisation of enzymes is a technique that has been in use for almost a century [207]. Its main goals are to prevent the disturbance of enzymes' secondary (active) structure, as well as facilitate their separation and reuse by rendering them "not soluble" [208, 209]. Immobilisation, literally meaning non-mobile, occurs by "securely attaching" the enzyme onto usually solid supports that offer molecular rigidity [210]. Secondary goals evolved to be avoidance of product contamination by the enzymes, operational control, increased selectivity, ability of hydrophilic enzymes to operate under hydrophobic conditions and variety of bioreactors [200, 207], with the list not being exhaustive. It should be noted that immobilisation does not necessarily aim to make the enzyme perform better than its optimal operational conditions, but to increase its performance when the conditions are not optimal [211]. In some cases, an increase in activity over a specific substrate has been noted upon use of immobilised enzymes [212]. Examples of improved enzymatic activity after immobilisation include cellulase immobilised on magnesium oxide nanoparticles, targeting agricultural waste hydrolysis [213], manganese peroxidase immobilised in gelatine hydrogel targeting the degradation of an azo dye [214], or lipase immobilised on bioinspired silica [215] among others. It should be mentioned that the enhanced activity is measured with respect to kinetic parameters and/or conversion of a specific substrate. This does not mean that the biocatalyst will show enhanced activity towards any suitable substrate, but it shows the importance of optimisation of the combination of enzyme, support and substrate (the latter referring to the targeted application). The major advantage of immobilisation, ability of enzyme reuse, has been demonstrated through various examples, such as a spectacular reuse of immobilised Phytase, over 50 consecutive batch uses (use (cycle #1), separate, reuse (cycle #2)…), losing only 5% of its activity[216]. Other examples include ability of immobilised b-glucuronidase on a silica encapsulated alginate capsule to be reused for 10 cycles with barely any loss of activity [217] or a

20 cycle reuse with less than 20% activity loss of immobilised carbonic anhydrase on mesoporous silicas [218]. Also, it has been demonstrated that enzyme immobilisation allows for cascade reactions, trying to imitate the functions of a cell, without the need of controlling or catering for other biological functions. Selected examples of that, are work done by Rocha-Martin et al. [219], using horseradish peroxidase to degrade phenolic compounds, co-immobilised with formate dehydrogenase for in-situ hydrogen peroxide generation and work done by Wang et al. [220], building a multi-enzyme system for methanol production from carbon dioxide, using formate dehydrogenase, formaldehyde dehydrogenase and yeast alcohol dehydrogenase. On the other hand, a major disadvantage of immobilisation, confirmed by many researchers, is the potential of mass transfer or diffusional limitations, regarding the substrate and/or the product of the enzymatic reaction [221-224]. These issues arise from the confined environment around immobilised enzymes, usually porous channels, which can make transfer of bulky substrates or products difficult. Also, diffusional limitations have been observed when large enzyme quantities are immobilised on the support, where some enzyme molecules where packed on top of others, showing high surface loading, but not as high expected activity [225]. A brief summary of the most important advantages and disadvantages of immobilisation can be seen in Figure 2-1.

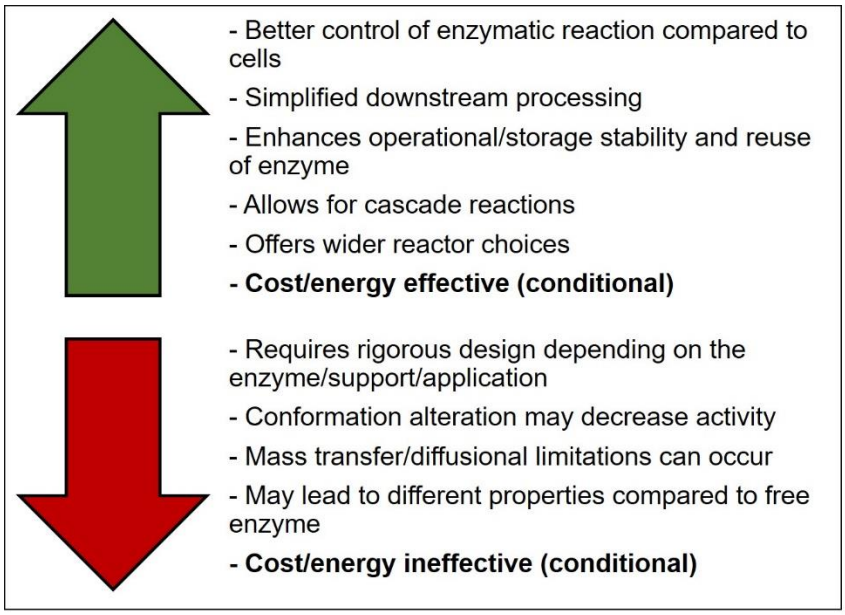

Figure 2-1: Advantages and disadvantages of immobilisation[207, 208, 226].

Enzyme immobilisation can be reversible or irreversible [208] and also can be chemical or physical, depending on the kind of interactions between the enzyme and the support [226]. There have been developed multiple ways of immobilisation over the years (Figure 2-2), majority of them incorporating a solid support as enzyme carrier, to facilitate removal of the biocatalyst from the reaction medium. In recent years, a novel way of immobilisation was introduced, namely cross linked enzyme aggregates (CLEAs) [227], in absence of a solid support. Each method has specific advantages and disadvantages (Figure 2-2) and finds applicability in different areas. For example,

adsorption is an overall easy method with no many steps required to create a biocatalyst, but it is based on weak physical interactions between the support and the enzyme, so it is prone to leaching (loss of enzyme). In order to use supports that have desired properties from the materials point of view but would not perform as great carriers for adsorbed enzyme, functionalisation is employed to increase their "stickiness" and promote enzyme's immobilisation. In the latter case, the immobilisation would be through chemical interactions (covalent bonding) between the chemical introduced (a very common example is glutaraldehyde) [228, 229]. Although immobilisation usually occurs under circumneutral conditions in order to preserve enzymatic activity, in the case of using strong chemicals or intense procedures the activity of the enzyme can be hampered [230].

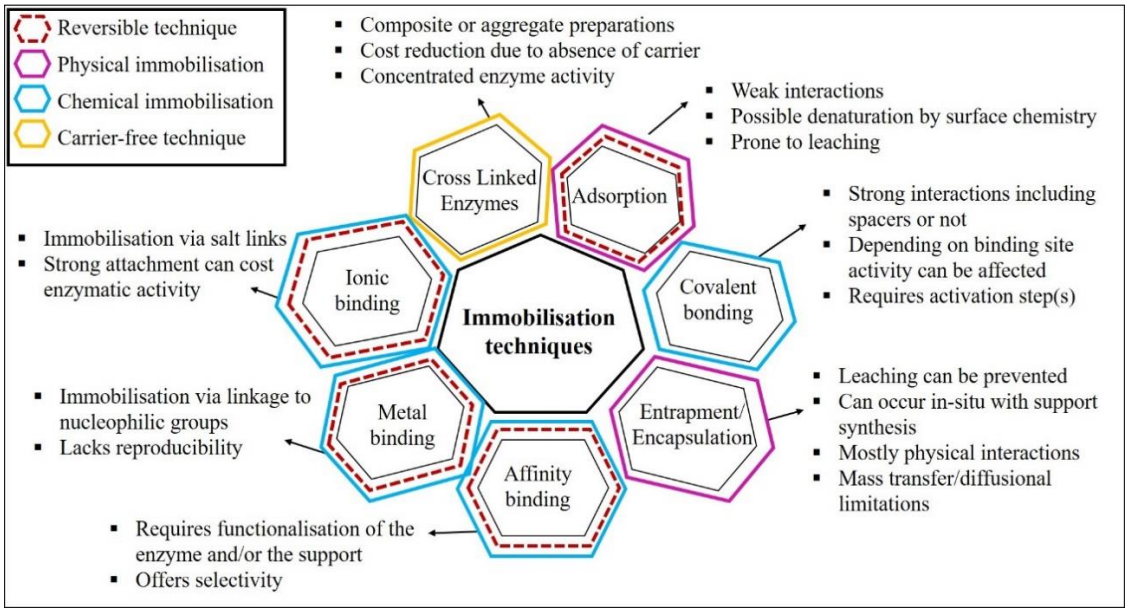

Figure 2-2: Brief description of immobilisation methods, (adapted from [208, 226, 227, 231, 232]).

Advances on the area of immobilisation have allowed for improvement of the activity, selectivity and reusability of the final product. Of course, there is no restriction in using only one method, as combination of methods may prove to be beneficial [227, 233]. Wang et al. [234] immobilised catalase by adsorption on silica and then encapsulated the biocatalyst in a layer of polyelectrolytes to minimise leaching. Another example of combination of methods for immobilisation is demonstrated for immobilised laccase by entrapment in an alginate capsule, which was then "reinforced" by encapsulation of the alginate beads in a silica layer [235]. A very interesting combination of immobilisation techniques was also shown by the immobilisation of yeast alcohol dehydrogenase inside bioinspired silica nanoparticles, which were then adsorbed on a poly-amine structure, creating a similar concept to CLEAs using immobilised enzymes as a start [236]. Out of the available methods for immobilisation, the most extensively used ones are adsorption, entrapment and covalent bonding [237], as well as their combinations. Despite the extensive knowledge on these methods and their establishment through many examples, there is area for advancement with respect to the supports used, the interactions between enzyme and support causing their bonding and the combination of methods in order to achieve the optimal outcome[231].

It has to be mentioned that the majority of the volume and mass of the final product is attributed to the support in contrast to the enzyme (usually with a ratio of 90:10) [227]. A way to avoid the non-catalytic mass present in immobilised enzymes, is by creating cross-linked enzyme crystals (CLECs) or aggregates with the aid of bi-functional agents (like glutaraldehyde, which however is toxic) [238].

Alongside different methods of immobilisation, there are many different support types as well, varying from soft gels to hard glassy materials, including both organics and inorganics, of natural or synthetic origin [239]. Also, there are many different structures of materials, such as crystals, amorphous structures, polymeric concoctions that can have a huge impact in the retained activity of the immobilised enzyme [240]. Depending on the targeted application, the choice of a hydrophobic or a hydrophilic support, or ability to create a hydrophobic or hydrophilic microenvironment can also be of a great importance [241, 242] fact known especially for lipase[243, 244].

There is not a single suitable combination of technique, support and enzyme, as efficient immobilisation highly depends on the targeted reaction/process, given conditions and possible interactions. A golden mean for the factors affecting its performance is based on optimisation and an understanding of the targeted system [232]. The selected combination should satisfy both the catalytic and non-catalytic requirements, such as productivity, stability and specificity for the former and control, separation, robustness and need for further processing for the latter [241]. When choosing an appropriate support, many factors should be taken into consideration with respect to the actual support and in general [210, 239], as immobilisation can affect the activity of the enzyme in many different ways [211]. A brief explanation of some important terms related to immobilisation can be seen in Table 0-3 of Appendix I. In general, the aim is to find a method and support compatible with the enzyme, which will lead to a stable and active biocatalyst that can be produced and applied on an industrial scale, all these at an acceptable cost [238, 242]. Many reviews have covered enzyme immobilisation from the aspect of the enzyme type and the targeted application, the aspect of method and support of immobilisation and in general covering the sense of immobilisation, as shown in Table 0-2 of Appendix I, with this list not being exhaustive. Some very specific examples have focused on the design process of a biocatalyst and the many aspects that need to be taken into consideration in order to build a system which is both effective and efficient [242, 245, 246]. In the next section, an economic evaluation of immobilisation is attempted and the design principles of biocatalysts are visited, in order to extract the most important points and identify potential culprits.

2.2. The need for improvement

2.2.1. Engineering approach and economic evaluation of immobilisation

2.2.1.1. Economic evaluation

It might seem that immobilising enzymes will increase the cost of the process, but this is not always the case. There are many factors that contribute to the total cost related to an enzymatic process such as production of the enzyme, immobilisation process, separation/regeneration, reuse of the biocatalyst and the necessary upstream and downstream processing [225, 247]. In this trail of costs, the cost of the enzyme may not necessarily be the highest.

The use of immobilised enzymes can be cost-effective if the cost of immobilisation (total cost of every step of the immobilisation process) is lower than the cost of separation of soluble enzymes from the product (including the cost of further product purification if needed) in addition to the cost of using fresh enzyme in every "catalytic round". In terms of production of a biocatalyst, a very crude estimation shows that if the biocatalyst can be produced in a scale of around 100 tons per year, then the per gram production cost is around 10$, price getting lower with increased production [248]. Furthermore, prolonged use of a biocatalyst towards production of a specific product can lower the production costs (negative exponential relation), as there is no extra biocatalyst cost involved and the output is –usually– high.

There is a great extent of literature on immobilisation of enzymes for numerous applications, but only a limited number of immobilised enzymes developed are actually used in an industrial scale[249]. A well-established example, used as "paradigm" for enzyme immobilisation, is immobilised glucose isomerase for the production of high-fructose corn syrup, with commercial products being available currently only from Novozyme® (Sweetzyme), with a turnover number of 18 ton of fructose per kg of biocatalyst [249, 250]. Another well-established example of an industrially implemented immobilised enzyme is lipase, immobilised on resins (Novozyme 435, Novozyme 40086), or silica gel (Lipozyme TL IM), all from Novozyme®, applied for enzymatic interesterification [251]. In both cases, the enzymes involved are well-studied and characterised, able to be produced on a large scale (kg or tons, compared to mg or g), and the immobilisation protocol is relatively simple, based on adsorption of enzyme on a solid support (silica gel or resin). These factors surely had an impact on the commercialisation of the immobilised enzymes, as the involved cost should have been lower compared to a newly isolated, novel enzyme, using a laborious immobilisation method on a novel support.

2.2.1.2. Engineering approach

The very limited number of industrially applied immobilised enzymes can be attributed to many issues arising mainly from the delicate nature of the enzymes, the cost for the immobilisation procedure and the efficiency of the final biocatalyst. A frequently occurring problem during enzyme immobilisation is the deactivation of the enzyme by the chemicals used to build the

support or attach the enzyme on it; strong chemical interactions cause disruption to the secondary conformation of the enzyme, leading to partial or total deactivation. This can be shown in results as reduced activity or reduced enzyme affinity to the substrate [155, 219, 222, 252]. Reduced activity can also be caused by other factors related to enzyme immobilisation, such as diffusional limitations and leaching. While diffusional limitations could be related to the application and the type of reactor used, both factors are greatly affected by the design of the immobilisation support and the process followed [248, 253]. Leaching describes the enzyme becoming un-attached to the immobilisation support, and occurs when the interactions between the enzyme and support are weak. Such was observed when carbonic anhydrase was immobilised on magnetic nanoparticles, where the biocatalyst lost 40% of its activity after the first round of use due to enzyme leaching from the support, when it was physically adsorbed compared to covalently bound [254]. It can also occur when an enzyme is encapsulated in a porous structure with pore openings larger than its size. Finally yet importantly, leaching can be observed in cases where enzyme is successfully encapsulated into a soft support, such as alginate beads, which, although great in theory and laboratory scale, do not possess the mechanical strength and durability needed to withstand industrial processes [255]. With respect to diffusional limitations, they can be categorised as internal or external. Internal diffusional limitations arise from the design of the biocatalyst for a specific application, as the enzyme needs to be accessible to the substrate and the product needs to be accessible to the bulk medium. If any of those two factors is not satisfied, then the design needs optimisation on the pore size and network of the support, compared to the size of the enzyme, substrate and product and/or their hydrophobic or hydrophilic interactions. Such issues were observed in immobilisation of lipase in silica aerogels, where the oily substrate could not diffuse through the narrow pores of the hydrophilic support [223]. In the case of immobilised phytase in mesoporous silica (KIT-6), it was again shown that access of substrate to the enzyme was limited due to diffusional limitations of the bulky substrate through the pore structure, leading to ostensibly lower activity [224]. In the case of external diffusional limitations, the problem of reduced activity is attributed to issues regarding the design of the support rather the accessibility of the enzyme. There are two factors affecting external diffusional limitations, them being mass transfer issues, or diffusion at the external area of biocatalyst. In the first case the issue can be resolved with efficient stirring [248].

Another usual issue to be bypassed regarding industrial implementation is the scale-up of the immobilisation process from laboratory scale to industrial scale. Research has shown that scaling up of a successful laboratory experiment is not a straightforward process, let alone when there are biological species involved. There are several factors that can affect scale-up from lab to large scale, such as mixing effects, reaction time, reaction volume, purity of reagents, easiness of synthesis and labour needed [256]. With respect to enzyme immobilisation, further issues that can delay or even prevent scale up are related to enzyme purification, characterisation with respect to

stability, kinetics and inhibition (looking at the specific application and substrate), the need for activators or ions for activity enhancement, the structure of the support and its formation [257]. Purification is related to higher specific activity and lower bulk of immobilised enzyme, however, the associated cost can be quite high, especially for a sensitive enzyme. The enzyme to be immobilised should be fully characterised and well researched in order to control potential harmful phenomena (interactions, pH and temperature conditions, inhibition). The support where the enzyme will be immobilised on should be of specifications that enhance the process (durability, cooperation with the choice of reactor, minimised diffusional limitations, low cost, ease of immobilisation). A protocol involving long waiting times and many different steps for support synthesis or immobilisation might render impractical for industrial implementation, regardless of ravishing results in laboratory scale. Also, an "easy" immobilisation protocol built around an enzyme in an underdeveloped state (still in the characterisation and purification process, without indications for mass production applicability), might be disregarded by the industry on the grounds of too much effort needed until complete implementation. There are many examples of successful immobilisation of promising enzymes that show improvement in their stability, storage, even in their activity in some cases. However, in many cases the process involves numerous steps (for materials' synthesis, immobilisation, or both, including activation, functionalisation, calcination, coatings, extensive adsorption time), waiting time, use of dangerous chemicals, production of potentially hard to deal with waste, making the biocatalyst potentially unwanted from industry. Some representative examples in literature where the biocatalyst production would not be easy to reach industrial scale are shown in Table 2-1.

Table 2-1: Major issues that can prevent a successfully immobilised enzyme from becoming industrially applicable.

Issue	**Why it is the problem**	**References**
Extended support synthesis time, including waiting times or many steps involved (>5h)	Time consuming, requirement of various steps/process changes	229, 254, 258-271
Calcination of material	High temperature for long time (~500ºC for 5h), unsustainable.	258, 260, 266, 269
Use chemical agents for functionalisation (e.g. glutaraldehyde, polyethylene glycol, epoxy agents)	Currently industrially applicable, but environmentally unsustainable and also not GRAS approved for use in specific industrial areas (e.g. food industry)	228, 229, 259, 262, 264, 266, 268, 271-277
Total synthesis-immobilisation procedure occurring in more than 24h	Time consuming	254, 258, 259, 261-264, 266, 269, 270, 272, 273, 278
Coating of synthesised material	Extra step required (time, cost, process change)	235, 254, 268, 269, 279
Extended time for enzyme adsorption or cross-linkage (>12h)	Time consuming, enzyme activity can be hampered	228, 262-264, 266, 270, 272, 273, 275, 278, 280-283

There are however examples of enzyme immobilisation where the immobilisation procedure used is not as lengthy or laborious. Encapsulation of invertase in germania nanoparticles was achieved by particle formation and simultaneous encapsulation/adsorption in under 60mins [284]. In a different example, lipase was immobilised in various economical supports exploring the cost effective aspect of immobilisation [285]. Industrially applicable immobilisation should be a matter of not only creating the "perfectly active enzyme", but keeping in mind the need for a simple method, reduced time, labour and cost constraints and respect for the environment.

2.2.2. Optimisation of immobilisation based on novel supports

Individual research examples, reviews and the number of industrially applied immobilised enzymes (a nice table of examples was created by Bornscheuer et al. [209]) indicate that immobilisation increases the industrial applicability of enzymes. That statement is conditional as it was discussed in section 2.2.1, and based on the available literature around the topic, enzyme immobilisation needs optimisation and tailoring. In the direction of optimisation and tailoring, there are some facts that undoubtedly favour some methods and supports over others.

Much research is devoted to nanomaterials and nanoparticles as supports for immobilisation due to the advantages they present compared to macro-scale materials. Those advantages include their higher surface area and smaller size that enhance enzyme loading and minimise diffusional limitations of the biocatalyst in the medium respectively. Also, nanomaterials offer enhanced robustness, hence enhanced number of possible applications [253, 286]. However, disadvantages of nanomaterials include the cost of fabrication and the difficulty in separation from the reaction medium, as well as the yet unidentified consequences their use can have on the environment [253]. Also, due to their nature, nanomaterials suffer in the scaling up of their production, as between lab scale and large scale the properties of the materials might change drastically, let alone the cost in developing the scale-up process [287]. Recent advances in the area have shown that there are ways to "bypass" those disadvantages by introducing for example magnetic properties for easier separation [286], or finding ways of preparation that do not require expensive raw materials, time and energy consuming processes that are unnecessarily wasteful [288-290] and use synthesis processes that are scalable [291].

In terms of the type of support used, there are some types of supports that have been examined and used extensively and through continuous optimisation have evolved to an even higher level. Among other extensively explored options like natural polymers (e.g. chitosan, cellulose), sepabeads (polystyrene/divinylbenzene), various oxides (e.g. alumina, zinc, titania), alginate beads, ceramics, precious metals, magnetic particles and various hybrid combinations of the aforementioned, silicon derived supports are a highly preferred option. Supports based on silicon can be in the form of silicates [237, 292], sol-gel materials [230], and more recently bioinspired silica [289].

2.2.3. Silicon-based supports

It is worth mentioning that silica (SiO_2-nH_2O) is one of the most important inorganic materials, due to its abundance, inert character and durability, with numerous applications in many disciplines, ranging from rubber filler to cosmetics [293]. Silicon derived materials have been used for enzyme immobilisation for many years due to their numerous advantages (Table 2-2). There are many different types of silica, resulting from different synthesis procedures (most commonly in solution) and having different characteristics. The most well-known silica formations used as carriers for enzymes, are sol-gel silicas [230, 294] and mesoporous silica nanoparticles like SBA-15, MCMs and FMS [237, 295, 296].

Table 2-2: Main advantages and disadvantages of silica as support for enzyme immobilisation [297-300].

Advantages	Disadvantages
+ Enhanced stability due to narrow pore size of ordered porous structure + Enzyme immobilisation via various methods + Possibility to obtain pore dimensions similar to those of biomolecules + Novel synthesis methods use mild conditions, are fast and inexpensive + Can be of tailored pore, channel size, surface properties, depending on the synthesis method + Usually there are no chemical interactions between the support and the enzyme unless functionalisation occurs + Ability of co-immobilisation of more than one enzymes + FDA approved, good biocompatibility and biodegradability, resistance to microbial attack	- Possibility of enzyme leaching from the support, hence decreased activity (applies primarily to enzymes adsorbed on silica through physical interactions) - Difficulty of entrapment of large molecules post-synthesis on traditional sol-gel silicas due to small pore openings - Depending on the synthesis method, may be energy and time consuming - Depending on synthesis method, reagents may be harmful/toxic to the environment and/or the enzyme - In case of sol-gel derived systems, low reproducibility of material properties due to non-uniform pore size

Although in principle sol-gel silicas and mesoporous silica nanoparticles are synthesised using the same method, with respect to enzyme immobilisation they are two different categories of supports. In the sol-gel case the enzyme can be entrapped inside the porous network during the last steps of the synthesis, whereas in the case of mesoporous silica nanoparticles, starting from a sol-gel procedure, templates are introduced (and then removed) in order to graft a specified pore structure and the enzyme is introduced to the support post-synthesis [296, 297]. Silica is synthesised by condensation of silicic acid, staring from polymerisation of monomers and formation of nuclei, growth of those particles and particle aggregation into formation of a network. Starting from an aqueous solution, the end product is a thickened gel. Silicic acid ($Si(OH)_4$) is produced by a silicate (also known as precursor) dissolved in water, and the condensation occurs by formation of siloxane bonds between a respective silicon and oxygen atom of 2 silicic acid monomers,

following a nucleophilic substitution reaction [301]. Moving past the formation of a dimer, polymerisation occurs based on the tendency of dimers to reduce the Si-OH groups to a minimum. Due to this tendency, further condensation is spontaneous, and leads to 3D structures that act as nuclei for further aggregation and eventually particle formation and growth. An illustration of silica synthesis is shown in Figure 2-3.

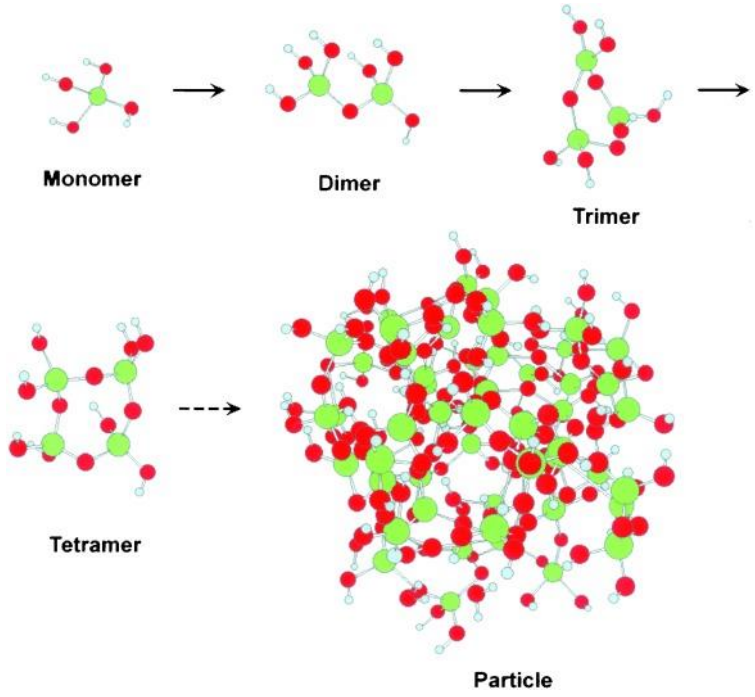

Figure 2-3: Silica synthesis based on condensation of silicic acid and further polymerisation, leading to formation of particles (image taken from [301]).

The conditions of the solution can affect both the rates of condensation and polymerisation, as well as the formation of particles, hence the final structure of the material (Figure 2-4). In acidic pH conditions, hydroxyl groups are protonated and do not repel the neutrally charged silica nuclei, so polymerisation is enhanced. Under basic pH conditions, particles are negatively charged, so polymerisation is not favoured. However, due to Ostwald ripening, which describes a constant state of dissolution and re-deposition, smaller particles are dissolved and re-deposited on larger particles, until the larger particles are too large for dissolution and there are no more smaller particles to be dissolved. At this stage, the solution with the ripe particles forms a "sol". The choice of precursor is also important for the properties of the final material, as well as the time allowed for development of the polymerisation ("gelation"). Widely explored silica precursors are alkoxysilanes (such Tetra-Meth-Oxy-Silane or Tetra-Et-Oxy-Silane) and metasilicates (such as sodium metasilicate, also known as water glass). [301]

In the case of alkoxysilanes, organic solvents are needed to facilitate dissolution of the precursors and lead to formation of silica. After the gel has formed, solvents can be removed and thus a pore structure is obtained. The ratio of solvent to water during synthesis can affect the formation rate of silica, as well as the structure of the gel. However, presence of organic solvents has been

characterised unwanted due to their toxicity, detrimental effect on biological compounds and un-sustainability, hence there were efforts to abolish their use and still improve the obtained materials [294, 300].

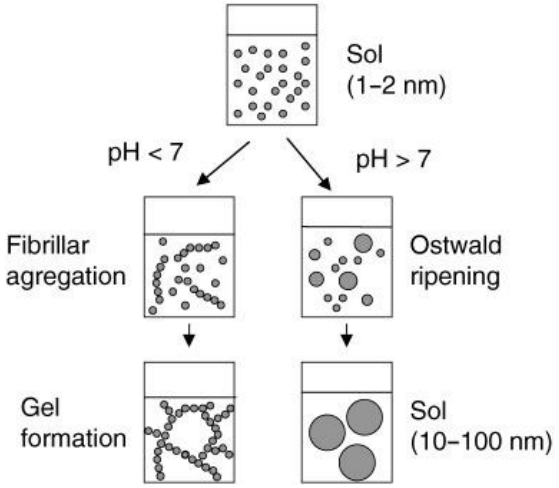

Figure 2-4: Importance of silica synthesis conditions for the end product (image taken from [301]).

The structure of sol-gel silica produced from condensation of silicic acid in presence of organic solvents, followed by evaporation of the solvent, is spontaneous, not easily reproducible and also can lead to fragile structures due to capillary condensation during solvent extraction. Furthermore, presence of organic solvents can affect the activity of biomolecules if they are mixed in the solution for in-situ encapsulation to silica synthesis [294]. Although some silica precursors do not require presence of solvents, standard sol-gel synthesis does not allow for controlled pore structure regarding the pore size or the communication channels. In order to address these issues, use of templates during silica synthesis was implemented, leading to the formation of a new class of materials with ordered, tuneable, mesoporous structure (referred to from now on as Mesoporous Silica Nanoparticles (MSN)) [302]. Depending on the template used, different pore structures and sizes can be achieved, in a self-assembly formation (Figure 2-5). Common template choices are lipids, block copolymers, biopolymers and various other surfactants with amino-residues. Depending on the choice (or combination) of templates, a pre-designed pore structure can be achieved [303]. In order for the pore structure to be usable and accessible, partial or complete template extraction is necessary, usually occurring via calcination or solvent extraction [304].

Upon template removal, MSN are readily usable, but due to the inert nature of silica, loading them with substances of interest (drugs, biomolecules) can only be effective by physical adsorption, which, as previously mentioned, is not based on strong interactions and usually suffers from leaching. In order to address this issue, functionalisation was introduced, where a "helping agent" is placed in the pore and acts as glue to any other substance introduced afterwards. Functionalisation can take place post-synthesis (after formation of MSN and removal of template), or during synthesis (template acts as carrier of the grafting agent, places it in the pore and upon template removal functionalisation is achieved) [302].

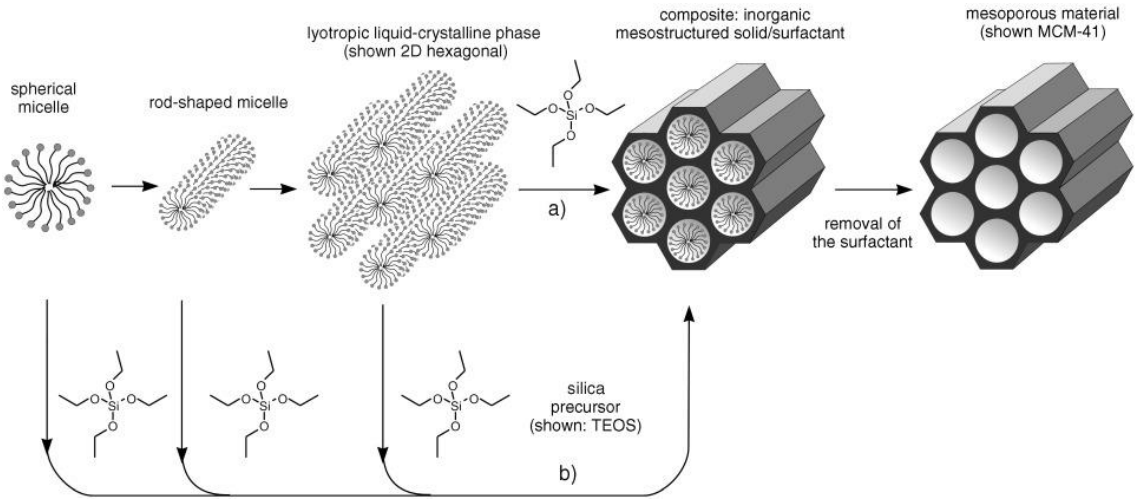

Figure 2-5: Directed self-assembly of mesoporous silica nanomaterials with the use –and subsequent removal– of templates (image taken from [302]).

After MSN are functionalised, they can be used for enzyme immobilisation, based on a combination of adsorption and covalent binding. At this point, the pore size and surface chemistry is of great importance for efficient immobilisation. If the pore size is smaller than the size of biomolecule to be immobilised, then the biomolecule will not enter inside the pore and it might get adsorbed on the material's external surface, facing the possibility of leaching. If the surface charge of the support repels the charge of the biomolecule at given circumstances, then regardless of a "correct" pore structure, immobilisation might be unsuccessful. This was demonstrated by Lynch et al. [305], who synthesised SBA-15 silica at accurately pre-determined pore sizes using chaperonins as templates, and used the supports for immobilisation of model compounds (lysozyme and myoglobin), examining the protective effect of immobilisation in various pH values. Although the free enzymes performed better under optimal pH conditions, immobilisation had a protective and enhancing effect on enzymatic activity when pH conditions allowed for attraction between the support and the enzyme given their isoelectric points. In a similar study examining immobilisation of a lysozyme on silica supports with different pore size it was shown that a larger pore structure could lead to tightly packed immobilised enzymes, showing high loading of protein on the support [306]. Examination of the secondary structure of lysozyme verified its perseverance, however, activity was not examined in order to rule out potential inhibition due to "overloading" that can cause steric hindrance and underuse of available catalyst.

There are multiple reviews on the use of silicas in enzyme immobilisation (Table 0-2 in Appendix I), referencing numerous examples of "traditional" immobilisation supports such as regular mesoporous silicates and "innovative" immobilisation supports like functionalised silicates or their fusions with other materials that give them advanced properties. The outcome of these examples is that the ideal immobilisation support has to be durable, in order to withstand industrial processing procedures, yet of tailorable porous structure, in order to make the perfect host for a given enzyme. Also, the immobilisation methods used the most are adsorption or covalent

bonding on a pre-functionalised support, encapsulation in a porous structure. Although functionalisation of silicon based supports is performed easily and adsorption of biomolecules is widely and successfully explored, there seems to be a preference towards the "protection" of a porous network, which is usually combined with internal adsorption/bonding of the biomolecule in order to strengthen the immobilisation.

Silicon based supports have been characterised as the most suitable for enzyme immobilisation targeted in industrial applications, due to the mechanical strength these materials hold and the ability to tailor their properties [207, 294]. However, there is a distinct disadvantage to the industrial use of the sophisticated silicon based materials, as well as many other emerging nanomaterials which are shown as promising enzyme immobilisation supports, that being the impracticability of their production at a –much– larger scale (kilograms or tons rather than milligrams or grams). The impracticability arises from the synthesis conditions, which often include high temperatures for prolonged time (hours), need for calcination in order to remove templates used to tailor pore structure, and low production yield, hence large waste volumes [290]. Also, regarding immobilisation of biomolecules, activity retention is of paramount importance and a protocol that does include the least amount of necessary steps and offers the most in terms of porosity tailoring is better received compared to laborious procedures. One step towards optimisation of enzyme immobilisation was made with the discovery of tailorable supports. The next step will have to be towards production of such promising supports at an industrial scale, without compromising cost, sustainability or performance. This step has already been made, with the development of bioinspired approaches towards synthesis of silica.

2.2.3.1. Bioinspired silica (BIS): Synthesis and properties

There is a need to overcome the major disadvantages of silicon-based supports when it comes to immobilisation, such as laborious synthesis protocols, need for post-synthetic functionalisation, inability for in-situ immobilisation, potential of leaching, low loading capacity and overall cost of the support synthesis and immobilisation procedure. Novel methods of silica synthesis have been developed, based on or inspired by nature, using less toxic reagents under milder and faster synthesis conditions and producing less or more easily managed waste. The inspiration comes from sponges and diatoms found in the ocean, which have the ability to synthesise silica as a protective shell around them (namely natural silica or biosilica). Biosilica is formed from monomeric silicon, which is dissolved in the ocean, and specific organic macromolecules, which are found on membranes of the aforementioned organisms [307]. Depending on the type of organism, the associated macromolecules are different, leading to different biosilica patterns and porosities (Figure 2-6). An in-depth analysis on biosilicification is given by Hildebrand [308]. Inspired by this natural way of silica synthesis, the synthesis procedure of BIS is based on the precipitation method, where a precursor (alkoxysilanes, silica complexes or silicates) creates silica clusters (nuclei) in aqueous environment when mixed appropriately with additives/surfactants and

catalysed by acid [291]. Those additives act as accelerators, assemblers, or "designers" of the surface properties and aggregation pattern of silica particles [309-311] and can be natural or synthetic, of organic or inorganic nature and of monomeric or polymeric structure [307, 310]. Some examples are R5 peptide, poly-peptides, polyethyleneimines, genetically engineered proteins and amines; the latter ones being among the most well studied additives for BIS synthesis [309, 312], with their cost depending on the difficulty of their procurement [313].

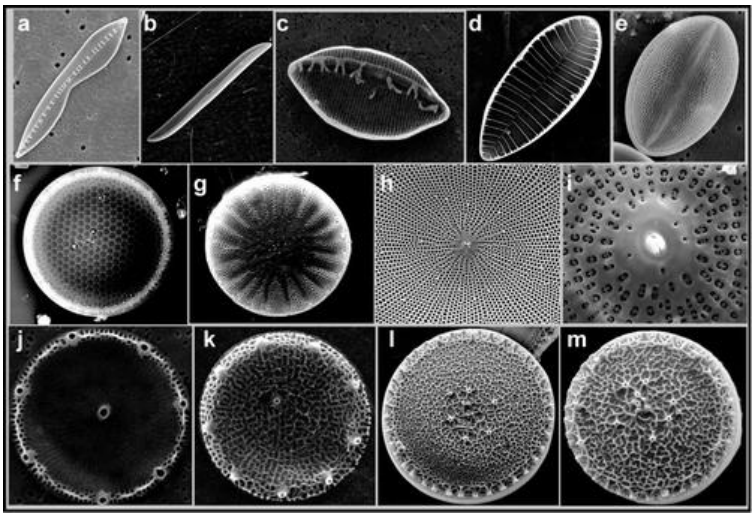

Figure 2-6: Different structures of silica formed by diatoms (image taken from [308]).

Competitive advantages of this type of silica as immobilisation support are primarily the ability to easily tailor its structure based on the choice of additives [310], ability for in-situ immobilisation[289], as well as the industrially feasible [291] and environmentally friendly synthesis procedure [298]. Addressing each of these claims separately, it has been shown that choice of additive used during BIS synthesis has a great effect on the porosity of the material, which affects potential applications. A vast range of pore sizes, aggregation patterns and particle sizes can be achieved with the choice of the correct additive [310, 314]. Pore structure can vary from almost nonporous when small, linear amines such as diethylenehexamine or pentaethylenehexamine are used, to mesoporous with the aid of a polyamine such as polyallylamine hydrochloride or polyethyleneimines [299, 315]. With respect to in-situ immobilisation, the ability to have an one-pot procedure for both synthesis and effective immobilisation is quite interesting and potentially feasible at an industrial level, compared to the laborious processes for MSN synthesis, functionalisation and use for immobilisation [289]. Furthermore, it has been shown that BIS synthesis is scalable, with the identified factors that can affect scalability being under control, hence allowing for its production at an industrial level without compromising the quality or properties of the material [291]. Also, BIS synthesis was proven to be environmentally friendlier and more sustainable than other methods of silica synthesis, as synthesis conditions are circumneutral, no heat, solvents or extreme acids/bases are required, synthesis is completed within 5 minutes and waste streams can be reused and recycled for subsequent synthesis rounds [64, 290]. Last but not least, it has been shown that immobilisation of enzymes by encapsulation in BIS offers higher loading

amount of enzyme [316, 317]. Achieving high enzyme loading is usually a hurdle with "regular" sol-gel silicas [304], while due to BIS's easily controlled nano structure and its ability of concurrent encapsulation of the enzyme alongside synthesis, as BIS is forming in an enzyme-containing solution, enzyme loading can be higher [317].

There are quite a few reports on immobilisation of enzymes in BIS, mainly through encapsulation, more rarely by adsorption. There have also been a few reports trying to mix methods of immobilisation and supports, by creating complex structures formed by distinguished layers of different materials that – at least theoretically – nullify each other's disadvantages (e.g. swelling of enzyme-containing alginate spheres) and offer specific advantages (rigidity and strength of biocatalyst, protection of compartmentalisation) [217, 235, 236, 279]. An important advantage is also the ability for cascade reactions by co-immobilisation of more than one enzymes with synergistic effects [220, 318] which can be advantageous for many enzymes, peroxidases included, due to their need for hydrogen peroxide. An overview is given in Table 2-3 based on the target of the research examples and the general findings, and a thorough review of each example is given in Table 0-4 of Appendix I.

Table 2-3: Overview of enzyme immobilisation in BIS.

Focus	**Enzyme**	**Ref**	**Immobilisation technique**	**General findings**
Immobilisation exploration or enhancement	Lipase, β-glucuronidase, laccase, manganese peroxidase, papain, yeast alcohol dehydrogenase, esterase, catalase, horseradish peroxidase	[212, 215, 217, 221, 235, 236, 288, 313, 319-322]	Encapsulation in situ, except 3 examples that used enzyme adsorption [322-324] and 1 example [325] that explored both techniques	Increased stability (T, pH, storage), high loading, reusability potential, minimal leaching (except in case of BIS formation over enzyme-containing alginate beads [217]), few examples [221, 313, 324, 325] identified diffusional limitations, 1 example showed shifted enzyme enantioselectivity [212], 1 example showed that performance of the immobilised biocatalyst surpassed the performance of commercialised product [325].
Biosensor	Glucose oxidase, horseradish peroxidase, combination of: Adenosine deaminase/nucleoside phosphorylase/xanthine oxidase	[311, 323, 324, 326]		
CO_2 sequestration	Carbonic anhydrase	[327-329]		
Production of esters	Lipase	[325]		

In the majority of the examined examples, the activity of the produced biocatalyst compared to the free enzyme is examined using a standard assay, not focusing on a specific – industrially relevant – application. Only in few cases an actual application was developed and tested, although the examined systems were treated as model systems using well-mapped enzymes. Examples include β-galactosidase immobilised on a biosensor to detect lactose [324], carbonic anhydrase encapsulated in BIS to mineralise carbon dioxide [327, 328], lipase encapsulate in BIS for ester production [325] or enzymes immobilised on BIS that can produce methanol through single or cascade reactions [220, 236]. So far, there has been no report on encapsulation of oxidoreductases (or any enzyme) in BIS, targeting bioremediation through exploration of an industrially relevant action. Despite the innovation of the support and the mix and match possibilities across various materials and methods, the majority of biocatalysts based on BIS present the disadvantage of diffusional limitations that hampers the ostensible activity of the enzyme. These are caused from the uncontrollably porous silica wall formed around the enzyme, or from silica particles aggregations that "block" existing pores [313]. Research has been focused on the accessibility of the enzyme, while securing its immobilisation, either by trying to enhance porosity during synthesis, or by "crafting" it afterwards [64, 294, 330].

Another disadvantage, as mentioned earlier, is the limitation of production scalability, and it should be mentioned that in some cases, BIS formation is based on not so environmentally friendly precursors and additives (such as alkoxysilanes, (e.g TMOS) and expensive peptides respectively). BIS scalability has been successfully addressed, showing the industrial potential of the synthesis method [64, 290]. Also, there have been efforts to obtain BIS using simpler and less expensive additives such as linear amines [309]. A limitation of using BIS as immobilisation support, (which applies to silica in general as well as metal oxides), is the limited pH range past pH 7, as BIS gets hydrolysed when introduced in pH environments above 9, limiting its applications to mildly basic or acidic pH [313]. Problems such as diffusional limitations and residual activity (un-related to inaccessibility of the enzyme) can be ameliorated and possibly resolved through careful design of the biocatalyst [212]. Biocatalyst's design may refer to the combination of types of reagents and their concentrations, buffers used, post-synthetic functionalisation, immobilisation conditions or targeted application and it definitely requires the optimisation of their coordination.

2.3. Use of immobilised peroxidases for anthraquinone dye decolorisation

There are some reviews available on water decontamination by immobilised enzymes, focusing either on specific pollutants or on specific enzymatic sub-categories of oxidoreductases [85, 93, 143, 331-333]. Generally, the operational stability of enzyme is enhanced by immobilisation but the activity of the enzyme is reduced. The decontamination efficiency is highly depending on the combination of enzyme and support used, as well as on the system investigated (dye structure and concentration, presence of other substances).

Khan et al. found that immobilised polyphenol oxidase on Celite resulted in higher percentage of decolorisation of the anthraquinone dye Reactive Blue 4 (amongst other dyes), but also in lower percentage of TOC compared to action of the free enzyme, indicating that immobilisation increased the enzymatic performance [334]. It has been also reported that immobilised DyP on mesocellular foam based on silica, could be reused effectively for 20 cycles of Reactive Blue 19 degradation, resulting in 10% residual activity after the last cycle. A cycle is referring to complete degradation (or no further dye removal) of a batch solution containing dye, immobilised enzyme and peroxide in appropriate medium. On the same paper it was reported that the operational pH was extremely important both for the enzymatic activity but for the efficiency of the immobilisation as well [156]. Similarly, Sun et al. immobilised HRP on a silica composite with ZnO nanowires using epoxy based cross linkers, and managed to achieve high loading (120mg HRP/g support) and very good activity of the biocatalyst (almost 100% degradation of Reactive Blue 19 and Acid Violet 109 within 1 hr). They also showed the importance of the immobilisation conditions for the immobilisation, mainly in terms of enzyme loading and prevention of leaching [335].

Immobilisation of laccase on silanised alumina pellets showed reduction of the inhibitory effects of components usually present in industrial dye-baths such as wetting, soaping or sequestering agents [336]. When decolorisation of two structurally similar anthraquinone dyes (Reactive Blue 19 and Acid Blue 25, both containing sulfonic, amine and N-phenyl auxiliaries at the same carbon spots) was examined using immobilized laccase in epoxy activated Sepabeads, researchers got greatly different results (almost 0% for Reactive Blue 19 and about 40% for Acid Blue 25) [281]. That indicates that structure of dye –even if of the same general type– has an important role in decolorisation. Presence of a mediator in the examined systems increased the decolorisation of Reactive Blue 19 from 0% to about 30%, whereas the effect on decolorisation of Acid Blue 25 was negligible. Following the same argument, researchers [270] studying the decolorisation of two anthraquinone dyes (Reactive Blue 19 and Acid green 25) using again laccase but immobilised on magnetic carbon nanoparticles, achieved highly positive results (more than 80% decolorisation efficiency, good reusability potential, stability) for both dyes. This shows that the immobilisation support also has a great effect on decolorisation efficiency, since using the same enzyme (laccase) acting on the same dye (Reactive Blue 19) yield different results when different supports were examined. Demonstrating the importance of the substrate used, studies from a research group on decolorisation of Acid Violet 109 using immobilised HRP, showed that when the enzyme was immobilised by the cross-linked aggregation method the decolorisation efficiency was more than 70% [337], whereas when immobilised on a sulfide electron the decolorisation efficiency was only about 40% [338]. A comprehensive table showing research examples of anthraquinone dye decolorisation using immobilised oxidoreductases was compiled, stating the combination of enzyme, immobilisation process and dye, as well as the decolorisation efficiency and the most

important findings (Table 0-5, in Appendix I, or refer to reference [339] for more extensive discussion).

An issue usually faced with immobilisation supports is adsorption of dye on the actual support instead of decolorisation due to enzymatic action, which might lead to false results if it is not accounted for correctly. Those results can either be higher decolorisation percentage, or lower decolorisation percentage. Examples in literature show that immobilised laccase on silica beads performed better than the free enzyme, because the dye got initially adsorbed onto the support and then was degraded more easily by the enzyme [274, 283]. In a different case, Zille et al. analysed thoroughly all the potential mechanisms leading to lower dye content in water when using an immobilised enzyme system, and found that there were three ways that dye got removed: mainly through adsorption on the immobilisation support, adsorption on the enzyme and degradation by the enzyme (laccase) [340]. As the reuse cycles progressed, it was shown that enzymatic degradation increased, probably due to decrease of available adsorption sites. Other examples that acknowledge the sorptive role of the support in the performance of the biocatalyst are shown for laccase immobilised on magnetic carbon nanocapsules [270] and HRP immobilised on a composite of zinc oxide and silica [335], or chitosan beads [271]. Another issue is the adsorption of degradation products onto the support [263, 283], which might lead to enzyme deactivation due to high concentration of inhibitors.

In terms of methods and matrices used for immobilisation of peroxidases for anthraquinone dye degradation, looking at Table 0-5 in Appendix I, one can see that adsorption on inorganic materials –usually silicates– is highly favoured over other combinations of methods and matrices. This trend is not only visible for this particular set of enzyme and application, as silicon-based materials are widely preferred for enzyme immobilisation in general. This is possibly due to the extensive research available on those materials [237, 292] and their wide industrial presence [310], thus allowing easier industrial implementation of the immobilized biocatalyst.

At this point, it is worth mentioning that none of those systems has been industrially implemented yet for applications around bioremediation. The most relevant example of oxidoreductases that have been industrially implemented is a liquid product of Novozyme® based on laccase, used for fibre modification and effluent treatment [341].

2.4. Conclusion

In this chapter, the term of enzyme immobilisation was revisited, focusing on the economic and industrial feasibility. Conventional methods and current trends were discussed and design parameters for an effective biocatalyst were defined. Those parameters are related to the design of the support with respect to surface characteristics and preservation of the enzymatic activity during and after immobilisation. Silica-based supports were discussed further, as their advantageous use for research and industrial purposes has rendered them the preferable type of

support for immobilisation. Special attention was given to bioinspired silica (BIS), as a novel and promising support for enzyme immobilisation. After an overview of examples of anthraquinone dye degradation using immobilised oxidoreductases, the crucial importance of the combination of the support, the enzyme and the targeted dye(s) was illustrated. It was shown that if one of these factors is changing, then results can be massively different, sometimes without identified reasoning, fact that can be related with the enzymatic activity or the breakdown pathway of the dye.

2.5. Aims and hypotheses of thesis

As it was mentioned in Chapter 1, the problem from dyes present in water effluents is big, potentially rising and the available decolorisation techniques are not sufficient on their own. Furthermore, there is an emerging need to focus on more sustainable solutions. Biocatalytic options have been explored to some extent, but the amount of ongoing research does not indicate any possibility of saturation in the near future. To this point, isolated peroxidases have not been implemented at an industrial level for water treatment due to difficulties arising from their use. Development of novel solutions is needed targeting easier manipulation of the design and the application of the biocatalyst.

The aim of this work is to provide understanding towards the formation of a sustainable biocatalyst based on peroxidase immobilised on BIS, for effective and efficient water decolorisation. The novelty of this work lays with the thorough exploration of peroxidase immobilisation on BIS, targeting a model anthraquinone dye degradation. Based on this aim and the available information about enzymes and BIS, the following general scientific questions were formed.

- Which factors affect the efficiency and effectiveness of peroxidase immobilisation on BIS and how can they be controlled?
- How does the activity of peroxidase immobilised in BIS compare to that of free enzyme, specifically for anthraquinone dye decolorisation?
- How does enzyme encapsulation in BIS compare with enzyme adsorption on BIS?

The hypotheses for this project are derived from the scientific exploration towards answering the aforementioned questions.

Hypothesis 1: The high tailorability of BIS leads to efficient immobilisation of peroxidase.

BIS offers the ability to control material properties primarily through the choice of additive, which can be quite useful for enzyme immobilisation. Herein, two additives were chosen for BIS synthesis, pentaethylenehexamine (PEHA) and polyallylamine hydrochloride (PAH), both already explored in BIS preparation. For immobilised enzymes through encapsulation –the main focus of this project– porosity has a great impact as it dictates mass transfer. Through the pore

structure the substrate accesses the enzyme and the product gets released to the bulk volume of the system. At the same time, the pore structure and potential adsorbing sites can prevent enzyme leaching from the matrix. That being said, a pore structure that is spacious enough for the substrate and the products to move in and out is needed, in combination with the ability to hold the entrapped enzyme in. By using these two additives, the creation of different pore structures and entrapment motifs can be explored [315]. Furthermore, partial or complete removal of the additive was attempted post synthesis by acid elution (quenching), as it has shown potential of crafting the surface of BIS, increasing the porosity and the surface area (PCT/GB2016/052705) [64].

This hypothesis is experimentally tested and discussed in Chapter 5.

Hypothesis 2: Immobilisation of peroxidase in BIS is affected by the immobilisation conditions.

Since BIS synthesis is pH dependant, it is expected that the point of addition of the enzyme in the system will affect immobilisation from the support formation part. That means that if the enzyme is added during nuclei formation (circumneutral pH) it will have a higher chance of being entrapped within the silica matrix. If the enzyme is added before BIS formation (alkaline pH) there might arise issues of aggregation of the enzyme which could lead to bigger particles and higher difficulty of effective immobilisation. On the other hand, pH has an influence on the enzymatic activity, meaning that if the pH of addition is out of the activity range for the enzyme chosen, there is the risk of partial temporary or permanent deactivation. Finally, based on the isoelectric point (pI) of the enzyme and the substances used (silicate, additives), speculations show that if the pH of addition lays in between the pI values then the charge of the enzyme will be opposite of the charge of the other substances, implying interactions between them that might have a stabilising effect and facilitate efficient immobilisation.

This hypothesis is experimentally tested and discussed in Chapter 6.

Hypothesis 3: Immobilised peroxidase performs better at un-natural conditions compared to free peroxidase.

As it was mentioned in section 2.1 of Chapter 2, one of the main reasons for the immobilisation of enzymes is their protection under un-natural conditions. This can be achieved by securing the active conformation of the enzyme through bond creation between the enzymatic structure and the immobilisation support. This can also be achieved by preserving mild conditions inside the confined environment of a porous support. Another major reason for immobilising enzymes is the ability to reuse them, since their soluble nature does not allow so. It is thus expected that peroxidase immobilised in BIS will be protected by the porous matrix and will be able to be reused.

This hypothesis is experimentally tested and discussed in Chapter 7 and Chapter 8.

Hypothesis 4: Since silicon-based materials are known for their use as adsorbents, BIS loaded with peroxidase will perform better compared to pure BIS.

As it was mentioned in section 1.3, adsorption is a well-studied and applied method when it comes to bioremediation and dye removal. Since silicon based materials have been explored as potential adsorbents for dyes, it is expected that BIS will adsorb dyes as well. Also, many adsorbents have been amino-functionalised in order to increase their sorptive ability, hence BIS synthesised using amines as additives is expected to show higher performance as a standalone sorbent compared to silica without amines present.

This hypothesis is experimentally tested and discussed partially in Chapter 6 and in Chapter 8.

To the best of the author's knowledge there is no other attempt to immobilise horseradish peroxidase on BIS with a clear application focus. Furthermore, a thorough investigation of the immobilisation conditions and their effect on the properties and the performance of the biocatalyst is made, which again, has not been explored before to this extent.

Chapter 3 : Materials and Methods

This chapter focuses on the materials and methods used in the experimental section of this thesis. Description of methods used is divided into two sections, with regards to the material synthesis and characterisation, and to enzyme characterisation (free or immobilised form), so that the two main aspects examined in this report are given separate attention.

3.1. Chemical reagents

Consumables used were plastic containers, plastic Eppendorf tubes, pipettes of 0.1, 1, 5 and 10ml with corresponding tips, crucibles, spatulas, glass test tubes, disposable cuvettes and quartz cuvettes. All chemicals (Table 3-1) were used as received and stored as advised from the supplier along with any produced dilutions. Prepared buffers were stored in the fridge. When a stock solution was created from lyophilised enzyme powder in appropriate buffer(s), it was stored in the fridge for no longer than 3 days and used appropriately. Aliquots of freshly prepared solutions were removed and stored in Eppendorf tubes in the freezer for future experiments. All diluted samples obtained from further dilution of stock solutions were stored in the fridge. When thawed, enzymatic solutions were not re-frozen, but were used as fresh and then discarded.

Table 3-1: Chemicals and materials used.

Purpose	**Chemical reagents**	**Source & Purity**
BIS synthesis	Sodium metasilicate pentahydrate	Fisher, Technical grade
	Pentaethylenehexamine (PEHA)	Sigma – Aldrich, Technical grade
	Poly allylamine hydrochloride (PAH)	Sigma – Aldrich, ≥95%
	Hydrochloric acid (HCl)	Fisher, Meets analytical specification of Ph. Eur. BP, USP, 1M
	Deionised water	Millipore, 120mΩ
	Horseradish Peroxidase (powder)	Sigma – Aldrich, N/A purity
Commercial silica	Syloid AL 1-FP	GRACE (PR sample)
Enzymatic assays for activity and protein concentration (includes reagents used for buffer production)	Sodium phosphate monobasic	Sigma – Aldrich , ≥99%
	Sodium phosphate dibasic	ACROS, ≥99%
	Citric acid monohydrate	Sigma – Aldrich , ≥98%
	Hydrogen peroxide solution (30% wt)	Sigma – Aldrich, 29.0-32.0%
	2,2′-Azino-bis(3-ethylbenzthiazoline-6-sulfonic acid (ABTS)	Sigma – Aldrich, 50mg ABTS per tablet
	Remazol Brilliant Blue (RBBR or RB19)	Sigma – Aldrich, N/A purity
	Potassium persulfate	Sigma – Aldrich, 99.99%
	Bovine Serum Albumin (BSA)	ACROS, ≥96%
	Bradford Reagent	Sigma – Aldrich

3.2. BIS synthesis and enzyme immobilisation

The methods presented herein were applied as described here throughout the experiments with no alteration. In every chapter, where necessary, methods specifically applied are presented in detail. BIS synthesis was examined as described elsewhere [330] using sodium metasilicate as a precursor and PEHA or PAH as additives. To ensure consistency in the method and the accuracy of preliminary measurements key experiments were conducted at least in triplicates. Briefly, aqueous solutions of silicate (concentration of Si in final solution: 30mM) and amine (for PEHA: 1:1 molar ratio of [N]:[Si], for PAH: 1mg/mL concentration in the final solution) were mixed. Addition of acid (HCl, 1M) initiated silica condensation, with final solution volume being 50mL. Depending on the experiment to be conducted, one or more of the following approaches were followed.

Approach 1: Synthesis of BIS

After acid initiated BIS condensation (final pH of 7.0 ± 0.1), BIS solution was left unstirred for 5min (Figure 3-1a). Solution was then centrifuged in thrice at 5,000rpm for 15min. In between centrifugation cycles, supernatants were collected and stored in the fridge for further analysis and precipitated BIS was re-washed with deionised water. After the final centrifugation round, BIS was freeze-dried. Silica yield was calculated after weighting the dry powder. BIS was stored in air-tight containers until further analysed.

Approach 2: Additive removal post-synthesis

After acid initiated BIS condensation (final pH of 7.0 ± 0.1), BIS solution was left unstirred for 5min. In order to proceed to additive removal (referred to as “acid elution” or “quenching”), more acid was then added until a target pH between 2.0 and 7.0 was reached [64] (Figure 3-1b). Then BIS solution was left unstirred for another 5 min and centrifuged and dried according to Approach 1.

Approach 3: Enzyme immobilisation by in-situ encapsulation

Pre-weighted amount of enzyme was added before or during silica’s precipitation and then one of the Approaches 1 or 2 was followed (Figure 3-1c). For every set of BIS samples containing bioactive substances, a control sample prepared using the same conditions but without the bioactive substance was made and used accordingly. Immobilisation efficiency (% of originally added protein loaded onto BIS) was determined by subtracting the quantity of protein present in the supernatant after centrifugation from the initially added quantity as described in section 3.4.1 of this Chapter. Protein content in BIS (% w/w) was determined as the weight of protein (as determined from the immobilisation efficiency) in the weight of the BIS-protein composite.

Approach 4: Enzyme immobilisation by post-synthetic adsorption

Bioactive substance was mixed with buffer at appropriate concentration and pre-weighted amount of BIS was added to the solution to obtain a set initial ratio of BIS to enzyme. The final solution was left in the fridge for up to 24h. During specified time points, samples were withdrawn, centrifuged and immobilisation efficiency was measured using the supernatant. Once amount of bioactive substance was stabilised (adsorption was completed), the initial sample was centrifuged, washed with specified buffer in triplicate and freeze-dried. Presence of bioactive substances was monitored during washings in order to define the final immobilisation efficiency based on a mass balance.

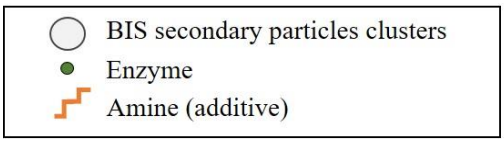

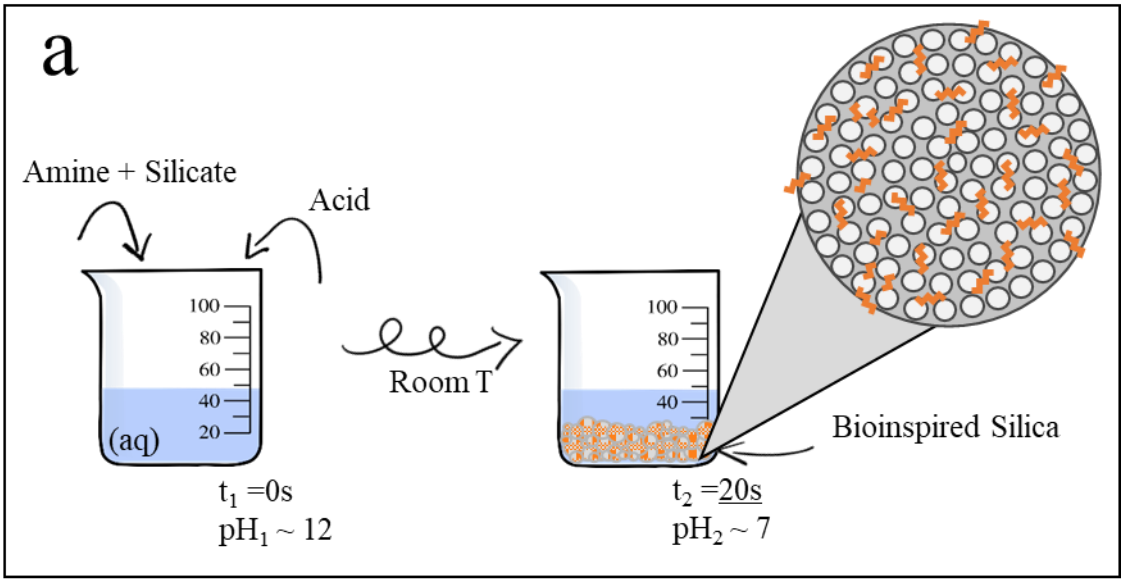

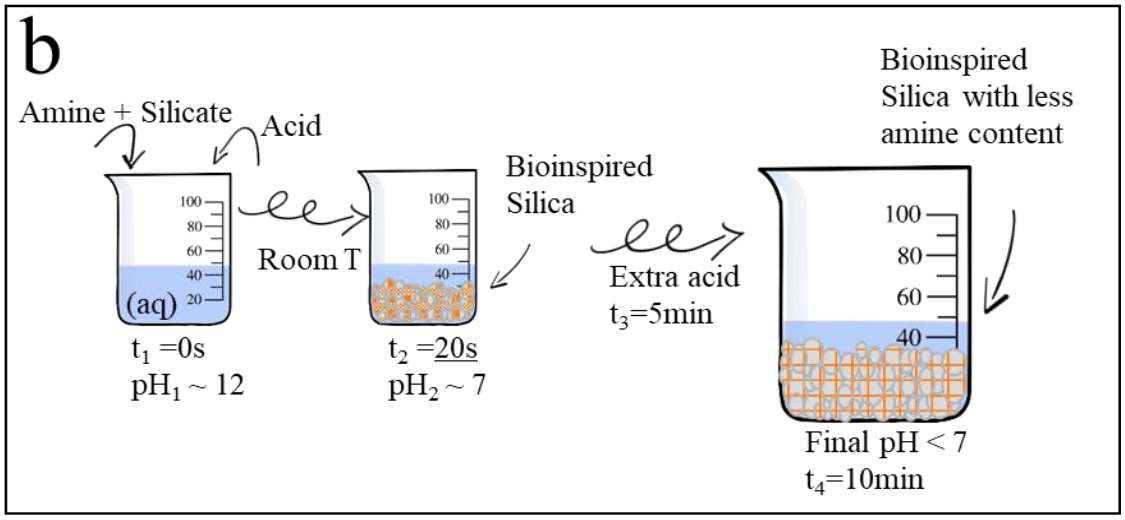

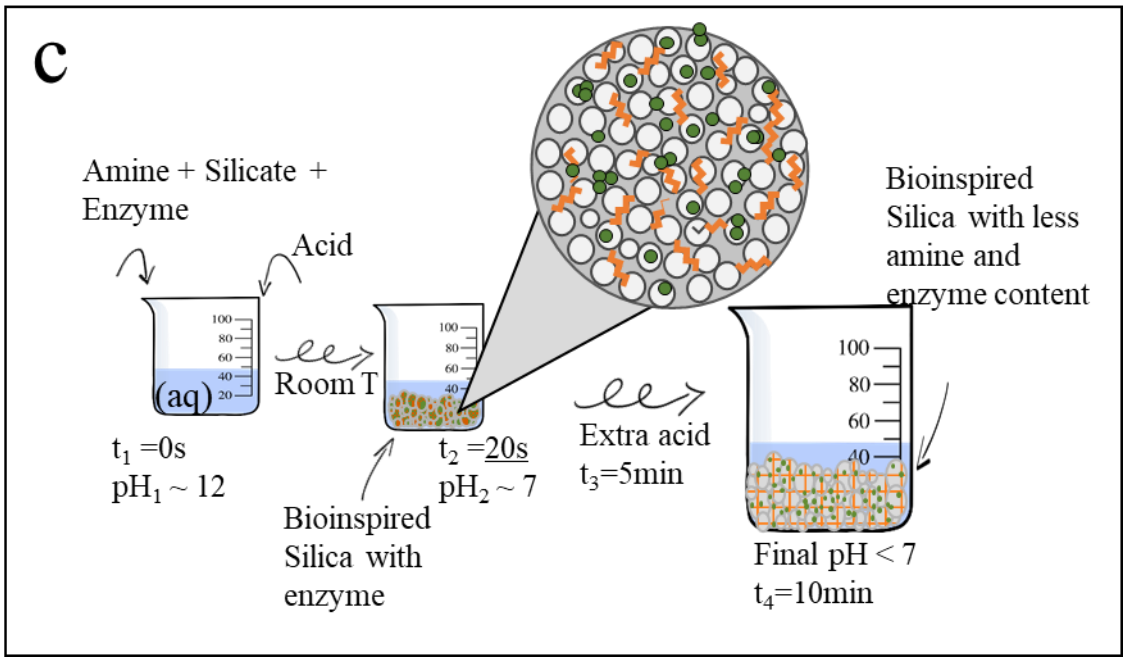

Figure 3-1: Schemes for better understanding of BIS synthesis and Approaches followed a) BIS standard synthesis (approach 1), b) post-synthesis modification by additive removal (approach 2), c) in-situ enzyme immobilisation (approach 3) and (optional) post-synthetic additive removal.

3.3. BIS characterisation

After reviewing methods used in literature that better describe systems of immobilised enzymes on solid supports, a list of measurements to be performed on the samples in terms of material characterisation (structural and surface properties) was compiled. In order to verify the chemical composition of BIS, Fourier Transformation Infra Red (FTIR) spectroscopy was used. In order to acquire information on the porosity and morphology (surface area, porosity, particle size) of BIS, N_2 adsorption and Scanning Electron Microscopy (SEM) and Ultra Small Angle X-Ray Scattering (USAXS) were used.

3.3.1. Fourier Transform Infra-Red (FTIR) spectroscopy

FTIR Spectroscopy is used to identify a chemical substance based on its unique spectrum of absorbance of infrared radiation. That spectrum is characteristic for molecules and molecular bonds and it can give information about the structure of the substance under examination, based on the vibrational energy of the existing bonds. Through FTIR spectroscopy both qualitative and quantitative analysis is possible, through various sampling techniques available (transmission, attenuated total reflection, specular reflection, diffuse reflectance). [342]

Through FTIR, all types of samples can be assayed (liquid, solid, gas), usually in the region of 4,000-400 cm^{-1} as most organic and inorganic substances absorb radiation at that region.

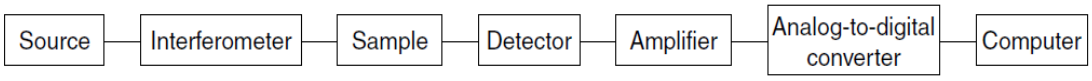

Figure 3-2: Instrumentation of a FTIR spectrophotometer (taken from [342]).

An optical signal is generated by a source via an interferometer, which encodes different frequencies to it. Data obtained by the interaction between the sample and the optical signal due to absorption of light, is passed through a detector, where it gets decoded using Fourier transformation in order to reveal information on which wavelengths the sample absorbed light at, based on the relationship of power density (or path length) and intensity (or wavenumber) (Figure 3-2) [342].

Formation of BIS (silica) was verified qualitatively through ATR-FTIR spectroscopy. Measurements were conducted on an IRAffinity-1S equipment (Schimadzu), using a resolution of 1cm^{-1}, taking 32 scans in each measurement and scanning the wavelengths between 400 and 4000 cm^{-1}. Prior to measurement, a background (empty, clean sample space) was scanned and the baseline was corrected. Powdered sample was then placed in the measurement space and the procured graph of the averaged intensity over wavelength was collected. Data was normalised based on the highest observed peak, in order to rule out any abnormalities and be able to have a fair comparison across samples. In order to reduce the noise, data was smoothed using the Adjacent-Averaging smoothing function of Origin software, with maximum 15 points of window, trying to ensure that the main peaks were not altered during the smoothing process.

3.3.2. Scanning Electron Microscopy (SEM)

SEM is used in order to examine samples in magnification much greater than 1,000x which is the maximum limit of optical microscopy, reaching up to 1,000,000x. The image procured through SEM is created from analysis of the secondary electrons, x-rays or photons (most usually secondary electrons or backscattered electrons are used to create the image) emitted from the sample's surface when it is exposed to an electron beam under vacuum (Figure 3-3). Secondary electrons are those that are emitted from the surface of the sample with an energy up to 50eV due to orbit disturbance by an incident electron, whereas backscattered electrons are produced due to scattering of their initial pathway because they approached too close to a nuclei. Secondary electrons can be produced also by backscattered ones once the latter are "travelling" to the surface. Out of those two types of secondary electrons, the "original" ones show more information on the topology under higher magnification, while the ones produced from backscattered electrons show the sample topology under lower magnification. Those emitted particles/signals can show information about the surface (max depth of 1μm) of the sample, without transmitting through it. Information shown is mainly about sample morphology and structure, but with specific measurements such Energy Dispersive X-ray Analysis, information on the chemical composition can be extracted. [343, 344]

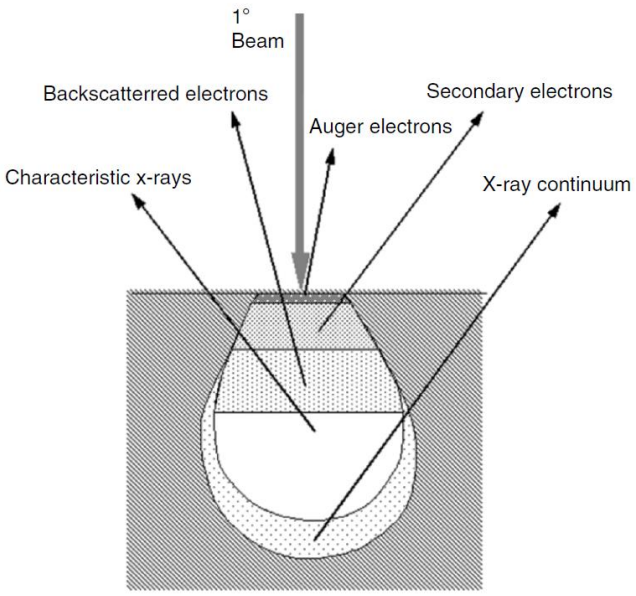

Figure 3-3: Different signals generated from an electron beam when it hits the sample (taken from [345]).

A usual problem faced in SEM image procurement is the low current in smaller probes which leads to unsatisfactory image acquisition depending on the energy threshold of the material examined and the limitation from emitted secondary electrons upon analysis, when the sample/area examined is smaller than 5nm and/or when the material examined is of a lower electron density. In order to deal with these issues, coating the sample with a metal film is suggested, in order to allow excess electrons to conduct and get earthed, since electrons emitted from metals give higher yield compared to carbon-based materials. [344, 345]

The main components of SEM machines are the electron gun which produces the electron beam which interacts with the sample (field emission gun, lanthanum hexaboride gun or tungsten electron gun), a lens which intensifies the focus of the electron beam, one or more detectors that captive the emitted electrons and signal generators and amplifiers (Figure 3-4). Once the electron beam is produced, demagnified and hits the sample, the detector detects emitted electrons and based on information acquired from them the image of the surface of the sample is synthesised.

The morphology and particle size of BIS samples were examined through SEM, using a FEI Sirion FEG SFM, with a 10 KV and 5 spot size, with the exception of a few samples where the images were collected with 8KV and 3 spot size due to poor quality images obtained with the original specifications. Fully dried BIS samples were lightly coated on sample holders with carbon tape. Samples were gold-coated for 3 minutes, allowing a deposition of about 15nm of gold. Images were collected for representative samples using 120,000 magnification.

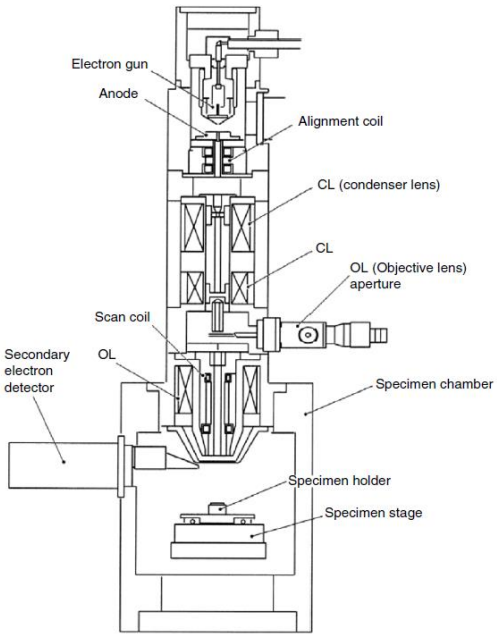

Figure 3-4: Instrumentation of SEM (taken from [345]).

3.3.3. Porosimetry via N_2 adsorption

Adsorption is the chemical or physical contact of components, the former named chemisorption and the later physisorption. In contrast to chemisorption, physisorption is a non-specific, spontaneous and reversible phenomenon. The contact occurs between the adsorbent (material under examination) and the adsorbate (material/probe used for the analysis, gas in gas adsorption, usually nitrogen). If the contact is monolayer, meaning one layer of adsorbate molecules is in touch with the surface of the adsorbent, then the adsorption is called interfacial. The corresponding reversed procedure of adsorptive removal from the adsorbent is called desorption.[346]

Adsorption is used to provide information on the surface area and the porosity of the material under examination, through the creation of the isotherm plots (of the adsorption and desorption procedures). Pre-determined amounts of gas are provided on a given solid, keeping the conditions of pressure and temperature stable. Gas is allowed to absorb (or desorb) on the solid until equilibrium is achieved at a certain pressure point, thus creating sets of values for pressure and quantity of gas adsorbed/desorbed that once plotted, form the isotherm curves. Theoretically, once plotted, adsorption and desorption curves should overlay, however due to the appearance of porosity this might not occur, especially in high pressure values (P/P_o higher than 0.8). Their "difference" is called hysteresis [346].

Information on pore sizes has distinguished three types of porosity based on pore size, namely being macro- (more than 50nm), meso- (between 2 and 50nm) and micro-porosity (up to 2nm). [346] Surface area is calculated by the monolayer adsorption that occurs until P/P_o equal to 0.3, before multilayer adsorption commences, by applying the theory developed by Brunauer, Emmet

and Teller –known as BET theory– [347]. The linear version of the BET theory is in Equation 3-1, where x is the relative pressure (P/P^o), y is $1/(n \times (1-P/P^o))$, n is the amount of gas adsorbed for a specific P/P^o value, n_m is the capacity of the monolayer and C is a parameter related to the energy of the monolayer adsorption that is required to be positive for correct application of the theory.

$$\frac{P/P^o}{n \times (1-\frac{P}{P^o})} = \frac{1}{n_m \times C} + \frac{C-1}{n_m \times C} \times (\frac{P}{P^o})$$

Equation 3-1

Surface area is calculated once the monolayer capacity is determined, given knowledge of the cross sectional area occupied by gas when monolayer adsorption is complete. When microporous materials are analysed, determination of the n_m factor might be difficult due to overlap with micropore filling. In this case, determination of surface area using the BET equation needs to be conducted using a relative pressure range where the quantity $n \times (1-P/P_o)$ is increasing with increasing relative pressure [348, 349].

Depending on the material's structure and porosity there are two types of surface area that can be identified. These are the external and the internal, corresponding either to general terms (external referring to area not occupied by pores and internal referring to area occupied by any type of pores) or to the pore size (internal referring to surface area occupied by micropore and external referring to the rest) [348].

Isotherm plots and hysteresis loop patterns can be slightly or greatly different depending on the type of adsorbent examined, but usually they fall under one of the identified categories as shown in Figure 3-5. Types II and IV (a, b) are typical for non-porous and mesoporous materials respectively. Type II is showing no hysteresis due to the absence of porosity that could create capillary condensation. Type IV (a) is showing hysteresis belonging to type H2, typical for siliceous materials. From the lower relative pressure range, information on the surface area and microporosity can be obtained as explained before, due to the formation of the monolayer and the graduate filling of the pores, starting with micropore. Information on micropore, especially the surface area and pore volume occupied by micropore, can be extracted by the t-plot, which is a plot that connects the thickness of the gas layer adsorbed on the material to the relative pressure [350]. Depending on the porosity of the material, t-plot can look quite different. A straight line passing by the origin is expected for nonporous materials since they can be considered as a flat surface due to equal adsorption behaviour. For microporous materials, a straight line is again expected, this time not passing by the origin, its intercept indicating an estimation for the micropore volume. For meso/macroporous materials, while the points of the t-plot corresponding to low relative pressures might form a straight line, points at higher relative pressures form a line that deviates from straight, representing increasing pore sizes. If the material is (expected to be) highly microporous, then analysis based on t-plot might be inaccurate due to overlapping of

micropore filling and monolayer formation at low pressures that leads to faulty determination of the gas layer thickness. [351]

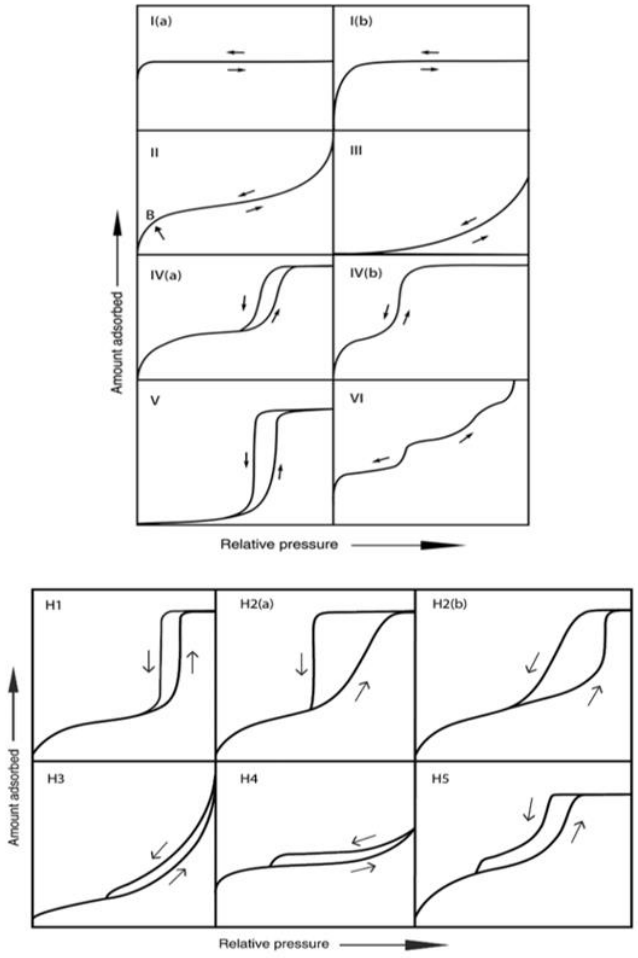

Figure 3-5: Classification of isotherms and hysteresis loops (taken from [348]).

By observing the isotherm at a higher relative pressure range, information on the mesopores and macropores can be extracted, especially when reviewing both the adsorption and desorption isotherms [348]. With respect to pore size and distribution analysis there are two widely used methods, Baret, Joyner and Halenda (BJH) and Density Functional Theory (DFT) respectively. Although the BJH method has been traditionally used over the years, it applies mainly to mesoporous structures and it does not represent microporous materials due to the assumptions made on the thickness layer and the perception of liquid meniscus of the gas adsorbed on the surface or in pores. In addition it does not take into account potential hysteresis between the adsorption and desorption isotherm although important information on pores is hiding there. On the other hand, the DFT method –consisting of various computational models nowadays– takes into account micropore filling and differences between the adsorption and desorption processes [352]. Amongst the various included models, Non Local Density Functional Theory (NLDFT) model using Tarazona's approach seems quite fitting for more accurate determination of pore sizes as it takes into account capillary condensation and evaporation as well as phase transition

phenomena that occur during gas adsorption, however this model fits better pure materials without surface functionalisation. Given that majority of examples in literature still use the BJH method, results were obtained using that over NLDFT.

Porosimetry of BIS was conducted through N_2 adsorption performed by a Micrometritics 3 Flex ASAP 2420 for samples of HRP encapsulated in BIS and by a Micromeritics TriStar for samples of HRP adsorbed on silicas, due to machine downtime reasons. Samples ranging from 50mg to 100mg were outgassed overnight at 105ºC under very low pressure (~20 mTorr) and immediately after were analysed. The equilibrium interval was 30s until 0.1 P/Po and 10s thereafter. The procured data points –after being fitted in the supplied software– formed an isotherm through which porosity characteristics were determined. Surface area was calculated using the Brunauer–Emmett–Teller (BET) equation and micropore surface area was determined from the t-plot between 0.8nm and 2nm aiming for correlation coefficients more than 0.8. Micropore and mesopore analysis (pore width, pore volume, pore size distribution) was performed using predominantly the Barrett-Joyner-Halenda (BJH) model [348].

3.3.4. (Ultra) Small Angle X-ray Scattering (USAXS/SAXS)

X-Ray Scattering analyses can offer information on the structure and morphology of samples in a non-destructive manner. The operation principal is based on observation of electrons scattered when the sample is being exposed to an X-Ray beam, as a function of the scattering angle, the wavelength, the energy or the polarisation. Given the much smaller wavelength of X-Ray beams compared to visible radiation, measurements using X-Rays are able to provide structural information of materials at much smaller dimensions than the obtained with light scattering [353].

USAXS analysis can provide valuable information on the size distribution of particles and the shape of them (mono/polydispersity), the pore size and the ordered, agglomerated or fractal nature of the material, especially in case on nanomaterials. It was developed as an extension to the SAXS measurement, in order to exploit all the range of scattering and allow for better estimation of particle size information in the range of a few nm. USAXS provides a higher detection range (enforced by the lower scattering vector values achieved, directly related to smaller angles used for scattering) [354]. Determination of such properties is feasible after analysis of scattering produced when electro-magnetic radiation interacts with the sample under examination. The typical (U)SAXS equipment, Bonse-Hart set-up, includes a radiation source, a "beam manipulator" consisting by a monochromator, mirrors and collimating crystals, a set of analyser crystals and a detector, as beautifully illustrated by Zhang et al. [354]. The initial data obtained during USAXS analysis the intensity distribution (I) and the scattering vector (q) values, the latter being related to the angle (θ) via this equation: $4\pi/\lambda \times \sin(\theta)$, with λ being the wavelength of the X-Ray beam and θ being the half of the scattering angle [353]. For reference, SAXS measurement can provide information for q values down to 0.1, whereas USAXS can provide information for q values as low almost 0.00001 [355]. After scattering data is obtained, it needs to be reduced to correct

for buffer/blank scattering subtraction, intensity calibration and desmearing. Of the most useful graphs obtained during USAXS data analysis is the plot of I v. q on normal or logarithmic scales, which shows 3 distinctive areas based on q values (Guinier, Fourier and Porod area respectively) (Figure 3-6). The Guinier law is directly related to the size of the particles (or their aggregates) as well as identification of polydispersity, through determination of the radius of gyration. This theory is applied in the lower q section of the obtained graph. The Porod law, as applied on the area of higher q values, trying to describe the asymptote of the scattering intensity, is directly related to surface characteristics of the particles (such as surface to volume ratio). Its application on the I/q plot can also provide information on the existence of fractals (irregular clusters of agglomerated particles). The area of the obtained line in-between the Guinier and Porod areas holds information on the shape of the particles examined, which can be defined by Fourier transformation equations. A descriptive analysis of the equations used during USAXS data analysis can be found in the following references [356, 357]. One needs to be careful during fitting obtained (U)SAXS data, as more than 1 possible interpretations might exist. The analysis can be quite informative about the morphology of a sample, but it is best when combined with other morphology characterisation measurements such as microscopy (Scanning or Transmission EM) or porosimetry in order to verify the findings.

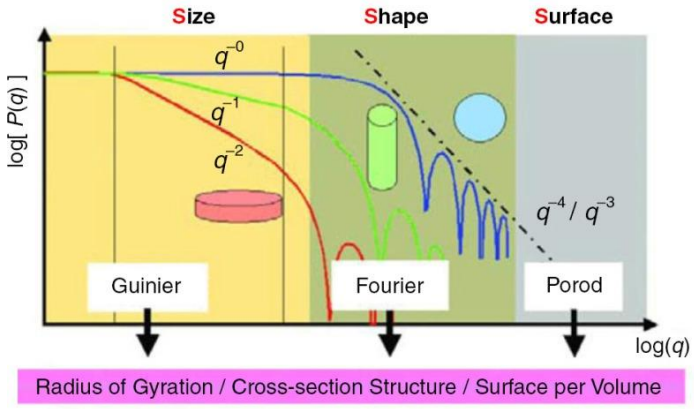

Figure 3-6: Regions of (U)SAXS obtained data (taken from [356]).

USAXS / SAXS / WAXS studies on representative samples were carried out at beamline 9 ID-C at the Advanced Photon Source, a U.S. Department of Energy (DOE) Office of Science User Facility by Argonne National Laboratory. This instrument is operated and maintained by Jan Ilavsky and his team [355, 358]. The Igor Pro 6.3 software was used for data analysis, using specific packages for specific procedures. Data reduction was performed using the "Nika"[359] and "Indra" analysis packages and analysis, fitting and evaluation was performed using the "Irena"[359, 360] package, in accordance with guidance from Professor Beaucage and the vital assistance of Alex McGlasson, Michael Chauby, and Kabir Rishi from the Chemical and Materials Engineering department at the University of Cincinnati in conducting the X-Ray scattering studies.

3.4. Assays for free or immobilised enzymes

In terms of biocatalyst performance, the measurements conducted initially were relevant to protein quantification, which will be used to assess the efficiency of immobilisation. Furthermore, two assays for the enzymatic activity were implemented in order to monitor quantitatively the activity of the biocatalyst in future experiments regarding the operational stability of the biocatalyst. The term "immobilisation efficiency" herein refers to how much enzyme (in terms of protein) is immobilised inside or on the support. The term "activity of the biocatalyst" refers to how active the enzyme is on specified substrates. Both terms are important for the design of systems for enzyme immobilisation, as they describe two different –but equally important– design criteria: the capacity of the support to host enzymes and the efficiency of those enzymes when immobilised, compared to the free form.

3.4.1. Immobilisation efficiency measurement

There are a few protein determination methods available that are used extensively, but they are not directly quantitative as they usually measure the protein content present in an unknown sample based on the quantification of a standard protein, usually bovine serum albumin [361]. A method that offers great sensitivity and is fairly simple to use, is protein quantification based on specific amino-acids present in the protein structure, by UV absorption [362], with a wavelength used around 280nm due to the absorbance of aromatic amino-acids Tyr and Trp [363]. In the case of heme-containing enzymes, such as HRP and DyP, there is also the possibility of quantification based on the heme content present, using its ability to absorb light in the wavelength range of 400-410nm (Soret band) [131, 161]. Last but not least, it has been shown that measuring the activity of enzyme can be used for quantification purposes in immobilisation of enzymes [155, 156, 364]. However, enzymatic activity can very easily be hampered by immobilisation conditions [365], so this method needs to be used cautiously as a seemingly low activity might not be indicative of the amount of enzyme present.

Herein three protein determination methods (UV absorption, Bradford assay and activity assay) were examined and compared to each other in order to define the optimal method for quantification of immobilisation efficiency. For UV absorption, supernatant or pre-prepared solution containing protein was inserted in a quartz cuvette and absorbance was measured at 280nm. For Bradford assay, appropriate amount of similar sample was mixed with Bradford reagent, left to develop for 10 min and absorbance was measured at 595nm, according to available standard protocols [330]. For the activity assay, the enzymatic assays used to quantify the activity of the enzyme (described in section 3.4.2) were also used to quantify the amount of enzyme. Protein determination was procured from absorbance readings based on calibration curves built accordingly for each method. The equipment used was a GENESIS 10 UV-Vis spectrophotometer from Fisher. During the standardisation of the methods, factors such as the optimum wavelength and the interference caused from water, buffers and various reagents present in the system were

studied. Appropriate solutions were used as blanks for each measurement to avoid falsified results. The development of these methods is discussed in detail in Chapter 4.

3.4.2. Enzymatic activity assay development

In order to monitor the enzymatic activity of peroxidase, two assays were employed. The first one is an assay used extensively with enzymes in the peroxidase family and is based on colour development (namely "ABTS assay"). The second one is an assay focusing on the efficiency of the enzyme in a potential application and is on colour disappearance of an industrially important, sturdy dye with a half-life of 46 years [366] (namely "RB19 assay"). Results in both cases were monitored in a GENESIS 10UV-Vis spectrophotometer by Fisher.

The ABTS assay measures the concentration of the intensely coloured product (dark green) produced upon oxidation of 2,2'-azino-bis(3-ethylbenzothiazoline-6-sulphonic acid) (light green) from peroxidase, in the presence of hydrogen peroxide. This reaction can be seen in Figure 3-7.

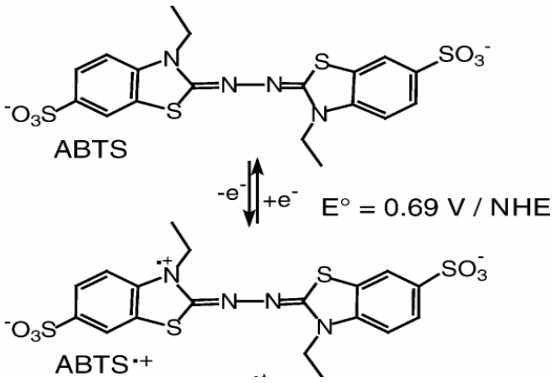

Figure 3-7: ABTS (light green) oxidation to $ABTS^{\cdot+}$ (dark green) from peroxidase (image taken from [367]).

In contrast, the RB19 (Reactive Blue 19 or Remazol Brilliant Blue Reactive, structure shown in Figure 3-8) assay measures the concentration decrease of a bright blue dye, which is usually used as a model pollutant, after peroxidase acts on it, in the presence of hydrogen peroxide.

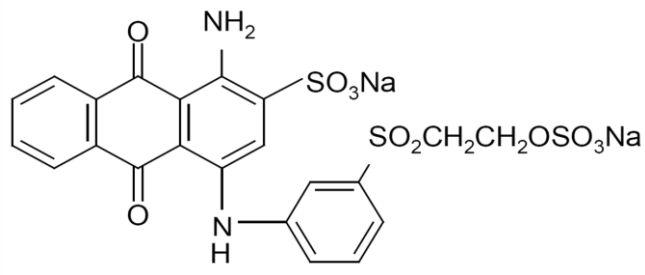

Figure 3-8: Structure of RB19 (taken from [20]).

Although the decolorisation products are not yet fully identified, based on the chemistry of reactive anthraquinone dyes [31, 368] and proposed degradation pathways for RB19 from other researchers [40-43, 46], the decolorisation reaction can be described as removing the auxochromes (position 1 and 2 substituents) and break down the anthraquinone structure. In both assays,

enzyme was mixed with H_2O_2 and measurable substrate (ABTS or RB19), in specified concentrations and buffered conditions. Since these assays were not provided by a standard lab kit, their optimisation and developing details are discussed in Chapter 4.

Although both assays have been used extensively in the literature, in every case there were some inconsistencies, indicating the need to optimise the conditions under which the assay was undertaken, based on the system to be applied to.

3.4.3. Determination of kinetic parameters of HRP

All kinetic models developed to understand enzymatic reactions are based on the initial reaction pathway describing a basic conversion of substrate to product using an enzyme that forms a complex to facilitate this conversion [369] (Equation 3-2). Enzyme (E) forms a complex (ES) with substrate (S), which is then converted to product (P) and enzyme is regenerated. Constant k_1 represents the complex formation (or substrate binding) constant, k_{-1} the complex dissociation constant and k_2 the product formation (or catalytic conversion) constant.

$$E + S \underset{k_{-1}}{\overset{k_1}{\longleftrightarrow}} ES \overset{k_2}{\rightarrow} E + P$$

Equation 3-2

In order to determine (theoretically and experimentally) the kinetic behaviour of an enzyme, the equation developed by Michaelis and Menten is widely implemented (Equation 3-3).

$$V_o = \frac{V_{max} \times [S]}{K_m + [S]}$$

Equation 3-3

This equation is derived from Equation 3-2 based on either the assumption of a steady state equilibrium, or the assumption of a fast equilibrium. In the first case, the concentration of the substrate is assumed to be much higher than the concentration of enzyme, (hence the complex formed between enzyme and substrate) and the rate of complex formation can be assumed as zero. Having this rate as zero, allows for further calculations on the derivation of an equation representing the rate of the reaction based on the complex. In the latter case, it is assumed that the rate of the formation and dissociation of the complex between substrate and enzyme is much faster than the rate of product formation, allowing an equilibrium between the free enzyme, the complex and the substrate. In the fast equilibrium case, the rates of formation and dissociation of the complex can be assumed equal. Both derivations can be seen in detail in Section 1 of Appendix II. Both derivations of the Michaelis Menten equation lead to the same final equation. V_{max} represents the maximum achievable rate (Equation 3-4) at the initial stage of the enzymatic reaction (measured in quantity of substrate consumed/time), $[E]_o$ being the initial amount of enzyme used. K_m is measured in concentration units and represents the concentration of the substrate needed for half the maximum achievable rate. K_m is also indicative of the enzyme's

affinity to the substrate, and depending on the assumption used for the derivation of the equation, it has the value of K_s (dissociation constant of the enzyme complex), or the value of K_s increased by the ratio of the turnover number (k_2) over the rate constant corresponding to complex formation (Equation 3-5).

$$V_{max} = k_2 \times [E]_0$$

Equation 3-4

$$K_m = K_S + \frac{k_2}{k_1} = \frac{k_{-1} + k_2}{k_1}$$

Equation 3-5

This equation is based on a saturation hypothesis, such that substrate consumption (and product appearance) is linear at first, reaching equilibrium at some point, and describes the enzymatic action mathematically, representing a very big number of the enzymes characterised so far [369]. This model however does not acknowledge possible inhibition of enzyme due to excess of substrate(s), excess of product/by-product formation, presence of inhibitors, or combination of any of the above, which can lead to lower reaction rates as substrate's concentration increases, hence deviation from the Michaelis-Menten model and far more complicated curves [370]. In order to include these possibilities, models based on the basic Michaelis-Menten have been developed, including besides V_{max} and K_m, other constants representatives of the inhibition type.

In the case of peroxide dependant peroxidases, where 2 substrates are used, although they can be characterised through the Michaelis-Menten, and this practice is usually followed in literature [20, 99, 108, 154, 172], there is another available model that incorporates their need for H_2O_2 as initial substrate (activator or co-substrate). This model is the Ping Pong Bi Bi model, as theoretically described in section 1.5 of Chapter 1 and is shown in Equation 3-6, as implemented by Sekuljka[133] examining activity of HRP on dyes. In this model, K_{mb} refers to the K_m of H_2O_2 and K_{ma} refers to the K_m of the dye (D) used as secondary substrate. Given the action of peroxidases on various substrates, D could also refer to ABTS or any other molecule prone to oxidation.

$$V_o = \frac{V_{max} \times [H_2O_2] \times [D]}{K_{mb} \times [H_2O_2] + K_{ma} \times [D] + [H_2O_2] \times [D]}$$

Equation 3-6

It could be argued that if the concentrations of substrates are in great excess to enzyme and substrate A is in great excess of substrate B, then the Ping Pong Bi Bi model could be re-written as the Michaelis-Menten model, where V_{max} and K_m would include substrate A concentration as a constant value [371].

In case of inhibition occurring due to one or both substrates, then the $K_{mx} \times [X]$ factor in Equation 3-6 is replaced by $K_{mx} \times [X] \times (1+ \frac{[X]}{K_{ix}})$, where X is the substrate that is potentially causing the inhibition (H_2O_2 and/or dye) and K_{ix} is the inhibition constant assigned to that substrate [133]. This model is theoretically more suited to describe the peroxidase action compared to the classic Michaelis-Menten model –even when substrate inhibition is accounted for– as it actively takes into account the presence of 2 substrates and the possibility of inhibition caused by either of them. As it was demonstrated by [133], the Ping Pong Bi Bi model with acknowledge of inhibition fitted experimental data of dye decolorisation using peroxidase in presence of peroxide much better than the simple Ping Pong Bi Bi model (Figure 3-9).

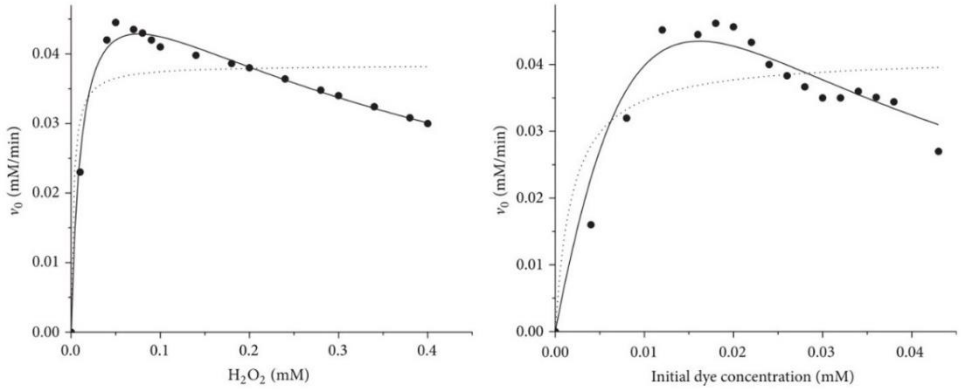

Figure 3-9: Fitting of experimental data (dots) with Ping Pong Bi Bi kinetic model without (dotted line) or with (solid line) acknowledgement of inhibition due to peroxide (left) or dye (right) concentration (taken from [133]).

So far, in literature examined, the classic Michaelis Menten model dominates, so for this project both models will be examined.

3.4.4. Activity examination of immobilised enzyme

In order to assess the activity of the system examined herein, the following methodology was used. Predetermined amount of immobilised enzyme was placed in a polyethylene cuvette. In a separate container, solution of substrate and solution of hydrogen peroxide were mixed to the ratio used in the assays. The volume of the free enzyme solution was replaced with the associated buffer. The mixture (total assay volume equal to the assay volume for the free enzyme) was added to the cuvette and cuvette was inserted in a UV-spectrophotometer where absorbance was recorded for 10mins in the appropriate wavelength, using an appropriate blank solution. After that, the cuvette was covered tightly with parafilm and left aside. The absorbance of the assay was measured in specific time intervals. In every case, BIS without enzyme was assayed as a control, using the same method to determine any activity caused by the immobilisation support.

3.4.5. Reusability examination of immobilised enzyme

In order to assess the reusability of the immobilised enzyme, the following methodology was used. After the first cycle, the contents of the cuvette (assay mixture and immobilised enzyme)

were carefully removed, placed in an Eppendorf vial and centrifuged at 20,000rpm for 5 min. Supernatant was removed and its absorbance was recorded. The immobilised enzyme was washed 3 times using the associated assay buffer. The washing procedure involved 1mL of buffer inserted in the Eppendorf vial, contents shaken vigorously, occasionally with the aid of a pipette to facilitate mixing, and then the Eppendorf vial was centrifuged at 20,000rpm for 5 min. Then supernatant was removed and washing was repeated. After the last washing, the immobilised enzyme was placed in a new cuvette and the activity assay was performed as described previously.

3.4.6. Leaching examination of immobilised enzyme

In order to assess enzyme leaching from the immobilisation support, the following procedure was used. Predetermined amounts of immobilised enzyme and support without presence of enzyme were mixed (separately) with the buffer used in the assay. A ratio of solids (mg) to buffer (mL) of 50:1 was used, in order to amplify any leaching potential. Mixtures were occasionally stirred and a sample was withdrawn in specific time intervals, placed in an Eppendorf vial and centrifuged at 20,000 rpm for 5 minutes. The supernatant was assayed both for protein content using the Bradford assay and for enzyme activity using one of the activity assays.

3.4.7. Storage stability examination of free and immobilised enzyme

In order to assess the storage stability of free enzyme, the following procedure was used. Lyophilised enzyme was mixed with buffer or other mediums in order to obtain a 1mg/mL concentration. Vials were sealed and placed in the fridge, at 4^{o}C. At specific time intervals, aliquots were withdrawn and checked for activity using one of the assays described in section 3.4.2. In order to assess the immobilised enzyme, the procedure was slightly different. Immobilised enzyme was stored after drying in airtight containers in the fridge, at 4^{o}C. At specific time intervals, predetermined amount of immobilised enzyme was withdrawn and its activity assayed.

3.5. Measurement of dye adsorption on silica

Measurement of dye adsorption on BIS was performed in two ways. The first was by applying the same assay used for determination of the enzymatic action on pure BIS, as discussed in Chapter 6 in order to obtain results necessary for pure enzymatic action determination. The second was by performing a complete adsorption profile, as shown in literature regarding dye removal by adsorption, discussed at the end of Chapter 8. Briefly, a stock solution RB19 dye was prepared by dissolving a specific amount of powdered dye into deionised water using a magnetic stirrer for 5 min. A stock solution of BIS was also prepared by dissolving 10 g/L of BIS into deionised water. Immediately prior to the adsorption tests, fresh sorbent solutions of desired concentration were prepared by diluting the stock solution. Samples were prepared by mixing dye and sorbent solutions in appropriate ratio. To ensure equal distribution of sorbent within each sample, the stock solution was mixed using a vortex at 1200 rpm for 30 s prior to ejection from the stock. The

dye-sorbent samples were then mixed using a vortex for 15 seconds to allow the dye and sorbent solutions to effectively mix.

The adsorption kinetics were studied as follows. Samples were introduced into a shaker water bath (25ºC and 180 rpm) and were extracted and analysed over regular time intervals until no further change in the dye concentration was observed. A maximum 7-day profile was considered in order to clearly understand and distinguish the adsorption mechanisms undertaken within the process. Extracted samples were centrifuged at 10,000 rpm for 5 min and residual dye was measured in the supernatant using a spectrophotometer as discussed in The adsorption capacity (q_t, mg/g) and removal efficiency (RE, %) of each sorbent was determined through the following equations:

$$q_t = \frac{(C_0 - C_e) \times (V)}{w}$$

Equation 3-7

$$\mathrm{RE} = \frac{\mathrm{C_0} - \mathrm{C_e}}{\mathrm{C_0}} \text{ x } 100$$

Equation 3-8

where C_0 and C_e are the initial and equilibrium concentration of RB19 in the solution (mg/L), V is the volume of solution (L) and w is the mass of the sorbent (g).

In order to obtain adsorption isotherms, a stock solution of RB19 was prepared and diluted to produce dye-sorbent samples at different initial dye concentrations (C_0, mg/L) ranging from 12.5 - 1500 mg/L. The adsorption tests were performed as described above. The samples allowed optimum contact time identified from the kinetic study for each sorbent.

The experiments and analysis of the sorption profile of BIS using RB19 were performed by Mr. Hinesh Patel, during his research project towards hid master of Engineering degree, under the guidance, supervision and help of the author.

3.6. Statistical analysis

Every BIS synthesis and enzyme immobilisation experiment was conducted at least in triplicate, where individual samples were prepared on the same or different days. Analysis of enzymatic activity conducted on these samples was performed in technical replicates (multiple samples from the original sample). In the case of assay development for enzyme quantification and activity measurement, every condition was examined in at least 3 individual replicates. In the case of FTIR and porosimetry, at least 3 individual BIS samples (with presence of enzyme or not) were analysed for each examined factor. In the case of SEM and USAXS, only selected samples were analysed in a single analysis as these techniques were used complimentary to FTIR and

porosimetry. Results were presented as average of the replicates with error bars representing one standard deviation.

Statistical analysis using t-test was conducted in order to identify significant differences between sample populations, when the average value of the replicates and the deviation rendered identification unclear. The hypothesis of unequal variance was used, with a 95% confidence level. Brief explanation of results is as follows. Assuming 2 different sample populations (Table 3-2), we aim to identify whether they differ significantly. Using the built-in function "t-test assuming unequal variations" of Excel™ and selecting the data sets, the t-test results are provided as shown in Table 3-3. From the procured results table, the values of importance are "t stat", "p" and "t critical". The relation between "t stat" and "t-critical" defines the difference between the 2 populations. If "t stat" > "t critical", then the null hypothesis (here: no significant differences between the populations) is rejected, as the calculated value (t stat) is larger than the set critical value (t critical) in order to accept the hypothesis. A second level of examination, is the probability that the extreme values of the data sets analysed will be observed, if the null hypothesis is true. Having a set level of confidence at 95%, indicates that if "p" > 0.05, then the null hypothesis is accepted and there are no significant differences between the 2 populations. For the examined example "t stat" > "t critical" and "p" < 0.05, hence the null hypothesis is rejected and the means of the populations are significantly different.

Table 3-2: Example used for explanation of t-test

Population 1	Population 2	Average	Standard deviation
74.5	70		
97	60.1		
75.7	55	Pop. 1: 79.38	Pop. 1: 9.905907
76.2	61.2	Pop. 2: 62.725	Pop. 2: 6.556809
73.5	58.6		
	71.45		

Table 3-3: Results procured from t-test using Excel built-in function.

	Variable 1	Variable 2
Mean	79.38	62.725
Variance	98.127	42.99175
Observations	5	6
Hypothesized Mean Difference	0	
df	7	
t Stat	3.217753	
P(T<=t) one-tail	0.00735	
t Critical one-tail	1.894579	
P(T<=t) two-tail	0.014699	
t Critical two-tail	2.364624	

Chapter 4 : Assay development

In this chapter the focus is the development of assays to be used for activity and protein concentration determination. This development was required because the relevant assays and information provided from literature were found insufficient and inapplicable in their existing state. Assays were developed with respect to activity measurement of the enzymatic action (either standard activity or based on the targeted application), as well as with respect to protein concentration determination. Although in the case of activity measurement the assay development was mainly straightforward, protein quantification was trickier. Factors of the system causing interference were identified and there was an effort to eliminate or control them. The outcome of this chapter is that although the system cannot be fully controlled, we were able to improve our knowledge of the limits and interferences in these assays. This knowledge was then further used in defining the protocols used herein.

4.1. Method development for activity assay based on ABTS

As mentioned in the section 3.4.2 of Chapter 3, the ABTS assay was used to monitor the peroxidase action, which is based on monitoring colour formation (production of oxidised ABTS).

Before proceeding to experimentation, the optimal wavelength of measurement should be identified. According to literature, the absorbance of oxidised ABTS is usually monitored in the area of 405-440nm [131, 150, 159, 173, 183, 372] or rarely at 735nm [373, 374]. After creating the oxidised form of ABTS, it was scanned (Figure 4-1) and 420nm was chosen as the optimum wavelength.

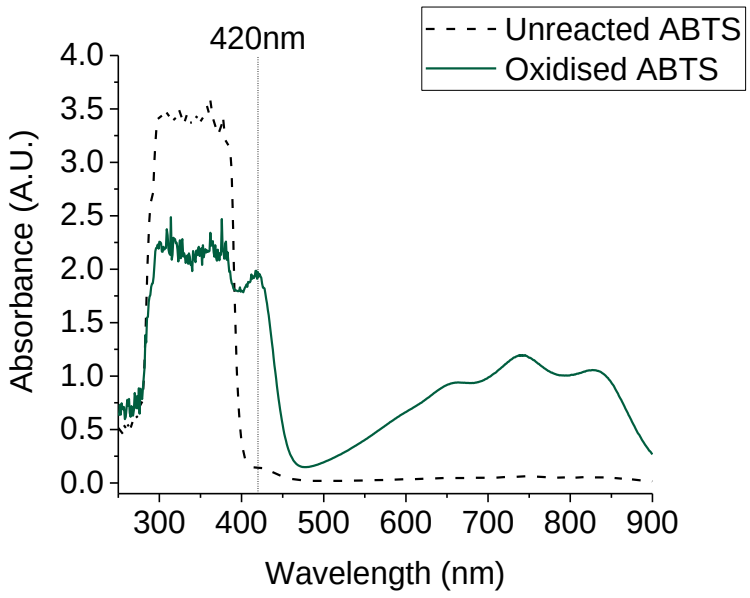

Figure 4-1: Scan of ABTS in unreacted and oxidised form in order to identify the optimum wavelength for absorbance monitoring of the oxidation.

4.1.1. ABTS calibration curve

In order to quantify the amount of oxidised ABTS produced from enzymatic oxidation and to analyse the activity of the enzyme, a calibration curve should be constructed to match the

absorbance with the quantity of the ion. According to literature [374, 375] a method to oxidise ABTS non enzymatically, is by using potassium persulfate. Herein, in order to achieve full oxidation of the ABTS which would allow to quantify the amount of oxidised ABTS produced, high excess of potassium persulfate was used. The reaction (chemical oxidation) was conducted in water (as suggested in literature) as well as in phosphate-citrate buffer of pH4 (as suggested in the proposed enzymatic assays) to monitor any differences. Necessary dilutions were made for creating calibration standards and absorbance was measured at 420nm using unreacted ABTS as a control (original absorbance: 0.142). Also, the absorbance of other reagents (unreacted potassium persulfate and sulphate ions) was monitored around the wavelength of interest to make sure that there was no added interference. The calibration curves are shown in Figure 4-2.

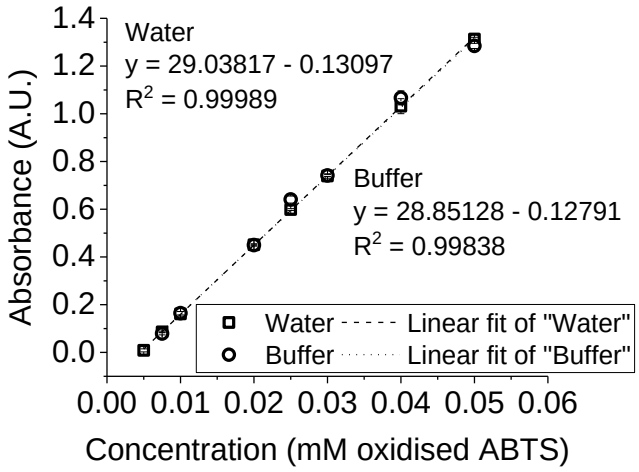

Figure 4-2: Calibration curve for oxidised ABTS produced from reaction with potassium persulfate in water and in phosphate-citrate buffer of pH4.

From the curves, it is clear that the use of water or buffer as a medium does not have a significant impact, however, for consistency reasons, the buffered system curve will be used for future reference. Scans of the ABTS ions produced with each method (chemical or enzymatic oxidation) showed matching structure, validating the choice made during method development (Figure 4-3).

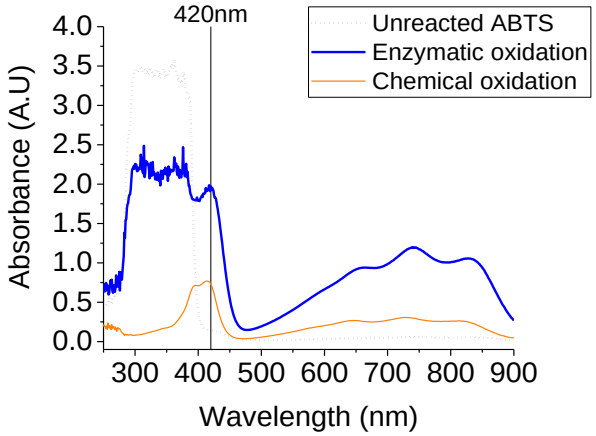

Figure 4-3: Scans of ABTS ion procured from enzymatic or chemical oxidation.

4.1.2. Developing the ABTS assay

The protocol followed for the ABTS assay was provided by the collaborating laboratory of Dr. Wong and upon implementation it was found that the original values were inappropriate for quantitative purposes and reaction monitoring, as discussed below.

In initial experiments, the importance of the concentration of H_2O_2 and the enzyme were examined, keeping the ABTS concentration constant (Figure 4-4). Using the assay protocol as received resulted in an immediate colour saturation (blue line in the graph). From the starting and final points in the graph, it can be concluded that decreasing by an order of magnitude the amount of enzyme and/or hydrogen peroxide, results in a very high colour intensity of the reaction product after seconds. These results indicate that both enzyme and peroxide concentrations are well in excess for appropriate measurements, even in the case of lower (0.1mg/mL) enzyme concentration.

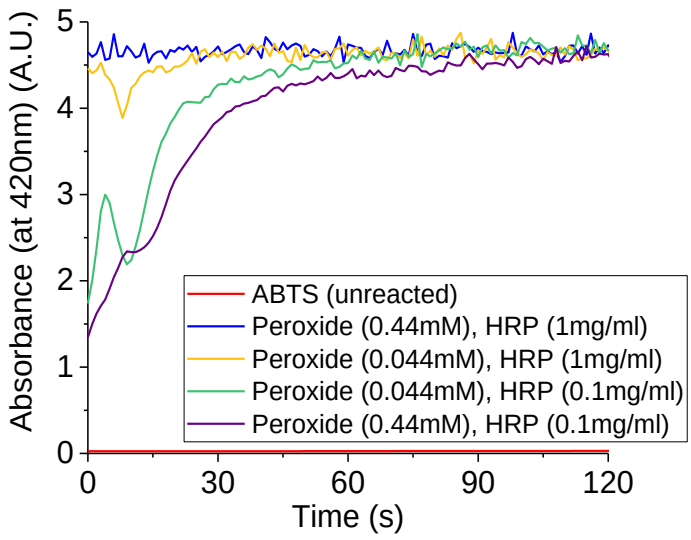

Figure 4-4: Kinetics of ABTS assay, having ABTS concentration of 1mM and altering the concentration of enzyme and hydrogen peroxide. Concentrations mentioned for HRP are initial concentrations of stock solutions.

Comparing qualitatively the kinetics with higher concentration of peroxide (0.44mM) and high concentration of enzyme (1mg/mL, blue line) or low (0.1mg/mL, purple line), one can see that lower enzyme concentration slows down the reaction rate, but the outcome is still a highly saturated coloured solution (quavery line of absorbance in the upper limit of detection). On the other hand, comparing the kinetics of the systems with high concentration of enzyme but high and low concentration of peroxide, one can see that the rate of colour formation is similar, indicating that even at low peroxide concentration the amount of peroxide present is more than enough for the amount of enzyme. A definite outcome of Figure 4-4 is that even the "lower" examined conditions, are incredibly high for quantitative analysis of the results (i.e. absorbance much higher than 1[376]). In order to identify conditions that would allow better kinetics monitoring,

experimentation with the concentration of enzyme was conducted, keeping the peroxide concentration constant, at 0.44mM.

In order to be able to conduct quantitative activity measurements, the concentration of the enzyme used should be lowered as required so that the absorbance generated from the oxidised ABTS to be lower than 1 for a substantial amount of time, so that we would be able to safely extract the reaction rate (Figure 4-5). Enzyme concentrations used are based on subsequent dilutions of an initial enzyme concentration of 1mg/ml just before the assay.

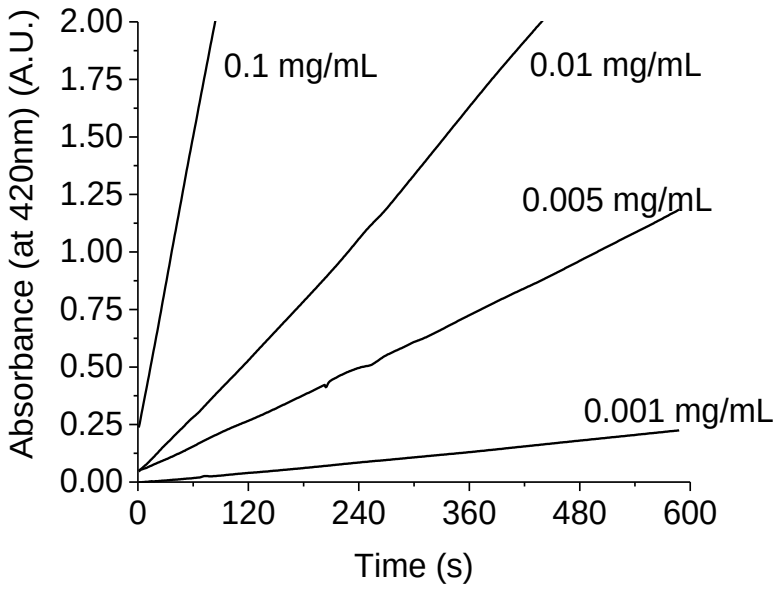

Figure 4-5: Examination of the effect of enzyme concentration on ABTS oxidation over the examined assay period. Assay concentrations: ABTS: 10mM, H_2O_2: 0.44mM. Initial enzyme concentrations used: 0.001-0.1 mgHRP/ml.

Based on the findings from Figure 4-5, the enzyme concentration used to conduct further experiments using HRP in free form, should be 0.005mg/ml (initial concentration of prepared enzymatic solution), as the other examined concentrations were too high (0.1, 0.01mg/ml).

After choosing a suitable concentration of free enzyme to fall within the appropriate absorbance range, replicates were conducted towards establishment of the stability of such a low enzyme concentration over time (Figure 4-6). It was found that the stability of HRP in such a low concentration was very low, even when stored in the appropriate buffer, as the activity of replicates originated from the same 0.005mg/mL solution decreased significantly, more than 80%, over a time lapse of about 1 hour. So for further experiments, dilutions of a stock solution of protein of 1mg/mL were prepared fresh directly before any enzymatic assay using ABTS.

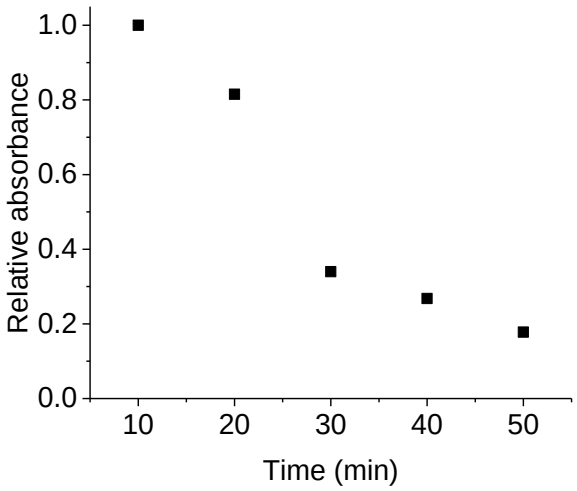

Figure 4-6: Replicates of ABTS activity assay using aliquots of a stock solution of enzyme of 0.005mg/ml. The absorbance was measured at 420nm at the end of the assay.

In order to examine the importance of the buffer to the assay, three different buffers were tested, of different ions present or pH, using the conditions as decided above (ABTS concentration of 10mM, peroxide concentration of 0.44mM, initial HRP concentration of 0.005mg/mL). Figure 4-7 shows a time comparison of 3 selected buffer conditions, phosphate citrate 0.1M of pH 4, phosphate (1st column) 0.1M of pH 4 (2nd column) and phosphate 0.1M of pH 7 (3rd column). The 1st photo represents the samples (and blanks) 1h after assay initiation, the 2nd photo shows the same samples after 24h and the 3rd after 7 days, with bottom row showing the blank and top row showing the oxidised sample. Results indicate - qualitatively - that the pH of the buffer is important for the stability of the produced radical, see comparison in across different buffers (in each photo) and over 7 days (comparison between 1st and last photo). We should mention that examination of the optimum pH regarding the enzymatic activity was performed and results are presented in section 8.1.1, as it was better suited at this point for continuity reasons.

The effect of ABTS "disappearance" can occur naturally, as the oxidised ABTS is condition dependant and generally more stable in lower pH [377]. Further consideration of research on the stability of ABTS radical was considered outside the scope of this project and was not pursued.

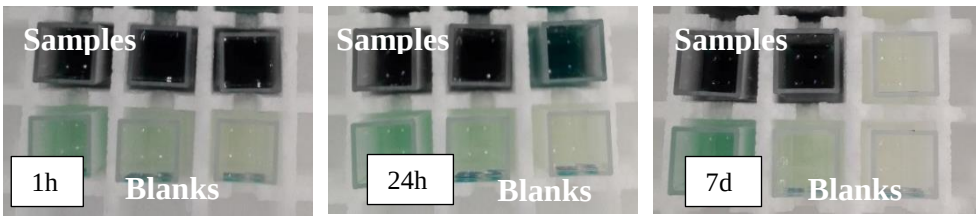

Figure 4-7: ABTS assay, buffer examination over time (1st column: citrate-phosphate buffer pH4, 2nd column: phosphate buffer pH4, 3rd column: phosphate buffer pH7)

Based on the findings from Figure 4-7, it was decided to follow the proposed buffer system (phosphate-citrate of pH4) for the activity measurement of HRP. In conclusion, the ABTS assay as developed so far, consists of an initial HRP concentration of 0.005mg/ml (quantity used: 50μl), assay concentration of peroxide 0.44mM (volume used: 15μl of a stock of 88mM) and assay concentration of ABTS of 10mM (volume used: 2.935ml of a stock of 10.2mM). For extraction of kinetics, the absorbance was monitored over 10mins, at 420nm. The full protocol followed can be seen in detail in Section 2 of Appendix III, or in short in Table 4-1.

Table 4-1: Concentrations and volumes of reagents used for ABTS assay.

Reagent	Conditions	Concentration in stock solution	Volume used (mL)	Final concentration in assay (mM)
ABTS	In phosphate-citrate buffer, pH 4	10.2mM	2.935	10
Peroxide	In deionised water	0.3% w/w	0.015	0.044
Peroxidase	In phosphate-citrate buffer, pH 4	0.005mg/mL	0.050	~ 0.19 x 10^{-5} (assuming M_w of 44KDa)

4.1.2.1. Extraction of reaction rate

It is unclear in literature how reaction rates are extracted from kinetic monitoring data. Based on the curves obtained for ABTS oxidation as shown in Figure 4-4 and in Figure 4-5, as well as on the description found in 1 source in literature [135], reaction rates were extracted by fitting data using exponential models. Upon experimentation with fitting, it was decided that the model to be used to fit obtained data would be the exponential model, as shown in Equation 4-1, and the rate would be extracted from the slope of the linear part of the curve, as obtained after differentiation (Equation 4-2).

$$y = Y_b + A\,(1 - e^{\frac{-(x-TD)}{\tau}})$$

Equation 4-1

$$\left.\frac{dy}{dx}\right|_{x=0} = A \times R_0 \times e^{R_0 \times x}$$

Equation 4-2

where Y_b is the baseline, A is the change in response, TD is the time offset and τ is the time constant. The meaning of the factors for the curve, as well as a sample calculation of the initial rate based on obtained data can be seen in Figure 4-8 a and b respectively.

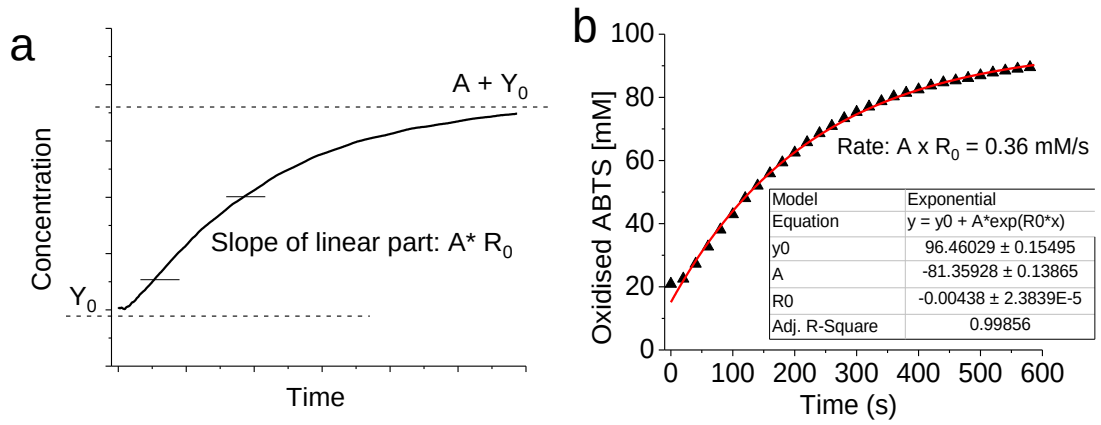

Figure 4-8: a) Explanation of the factors for exponential association fit of ABTS oxidation data, b) sample calculation of initial rate.

For all kinetic analysis using the ABTS assay, this equation was applied to identify the rate of the reaction, after fitting original data using the associated fitting function in Origin software.

4.2. Method development for activity assay based on RB19

As mentioned in section 3.4.2 of Chapter 3, the RB19 assay will be used to monitor the enzyme's performance in a potential application, based on monitoring of colour disappearance (RB19 decolorisation).

4.2.1. RB19 calibration curve

Before proceeding to any enzymatic reaction, a scan of dye in water was taken to identify the optimum wavelength for absorbance monitoring (dashed line in Figure 4-9). As proposed by other researchers [20, 42, 172] and also shown by the scan, 594nm was identified as the wavelength where RB19 shows maximum absorbance in the visible wavelength area. From the scans shown before and after enzymatic decolorisation of RB19 (Figure 4-9a), as well as the visual observation of the starting solution and the product after the assay (Figure 4-9b), one can see that enzymatic action does not result in complete decolorisation.

Although the peak between 500-700nm (blue hues) has considerably lowered, at the region of 400-500nm (where yellow and pink colour show absorbance) there was increase of absorbance, shown also visually from the pinkish-brownish shade of the final solution. This implies that although the blue colour is reduced, by-products are created, some of them coloured [42, 128, 172]. As mentioned in section 1.2, there have been efforts to identify the fragments created, but so far, a fully confirmed degradation pathway has not been announced, mainly due to the short life of some of the radicals or fragments created and the spontaneous reactions they cause [339].

Previously, during the degradation of a similar anthraquinone dye using a different peroxidase, the pinkish-brownish colour was attributed to the presence of 2,2-disulfonul azobenzene [128]. In that study, multiple anthraquinone dyes, were used for decolorisation experiments and it was found that the degradation pathway is dependent on the enzyme used as well as the dye applied

on as well. When monitoring dye degradation over several days selectively, no precipitation was observed. Other researchers showed that dye degradation using HRP may or may not result in precipitation, depending on the structure of the dye [99].

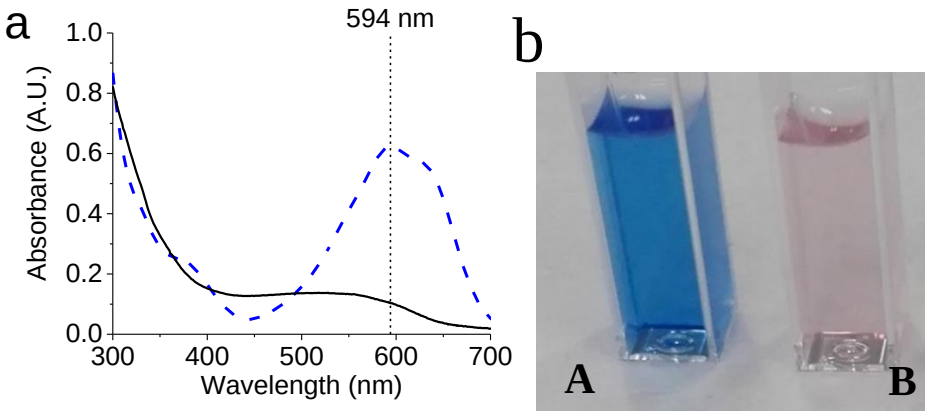

Figure 4-9: a) Scans of samples of RB19 before (dashed line) and after (solid line) action of HRP, b) visual decolorisation of RB19 (A: blank, unreacted dye sample before enzymatic action, B: after enzymatic action. Reaction conditions for 3mL assay: 0.125mM RB19 in 0.1M phosphate-citrate buffer pH 4, 0.044mM H_2O_2 and 50μg HRP).

At this point it should be mentioned that there are two methods of calculating the decolorisation degree. The one takes into consideration the absorbance of the examined dye at the wavelength of maximum absorbance and the other one measures the area under the absorbance spectrum curve between the edges of that curve (see Section 1 of Appendix III). Both methods are shown in literature, but they represent different outcomes. The first one examines the removal of the colour associated with the dye under examination [378] and the latter one examines the removal of total visible colour [20, 140]. Herein decolorisation was assayed primarily based on the absorbance at the optimum wavelength, unless stated otherwise, as this method is usually followed from literature and it would facilitate comparisons.

Knowing the optimum wavelength, a calibration curve was constructed using a stock solution of RB19 in water and serial dilutions and was used to match absorbance to quantity of RB19, when absorbance was measured at 594nm (Figure 4-10).

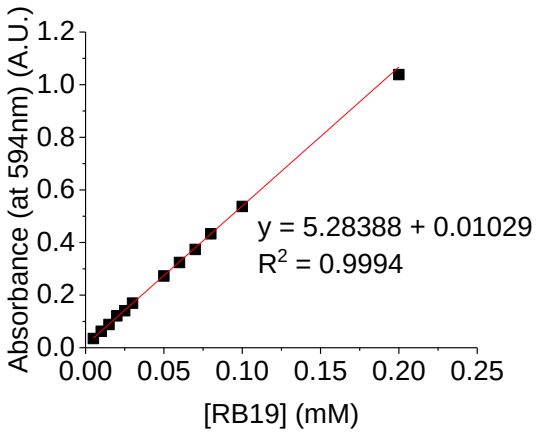

Figure 4-10: Calibration curve for RB19 (the standard deviation bars are present but very small).

4.2.2. Developing the RB19 assay

Having seen that the proposed conditions for enzymatic RB19 degradation were appropriate for quantitative measurement of colour degradation, exploration of the importance of reaction media was attempted, similarly to the ABTS assay. The thought behind exploration was that this project evolved around a potentially commercial application of immobilised peroxidase, decolorisation of industrial dyestuff effluents. Thus, enzymatic activity should –eventually– be explored under non-standard or recommended conditions but under realistic ones. In literature, pH of dye effluents is found to be usually around 7 since effluents are water with dyes and other organics/pollutants, not in a significant concentration to alter the pH drastically at most times[379, 380]. It should be mentioned that there are cases where HRP was used for decontamination of water with presence of phenols and optimum pH was found to be pH 7 [203, 381], but when decolorisation of dyes is attempted, the proposed mediums are usually of acidic pH [18, 20]. This could either be indicative of the enzyme used based on its origin or available iso-enzymes [382]), or the substrate used, as same enzymes obtained from different sources are not necessarily structurally the same, or one enzyme might show different optimum pH depending on the substrate [154].

The examined reaction media at this point were deionised water and 3 buffers of controlled pH (citrate-phosphate 0.1M / pH4, phosphate 0.1M / pH4, phosphate 0.1M / pH7), so that the importance of the reaction medium conditions could be explored. Figure 4-11 shows visual observation of enzymatic degradation in the different examined media (a) as well as the calculated decolorisation degree based on the assay's difference to the unreacted RB19 in the same media (b). Duplicates were performed within 10 min difference from each other, 1 round of assays per condition was examined before each condition was repeated. This means that by the time the 1st pH 7 assay was initiated, the 1st deionised water assay had been running for 40 min, and by the time the 2nd pH 7 assay was initiated, the 1st deionised water assay had been running for about 80 min. Visual results (Figure 4-11a) show that RB19 decolorisation in mediums of lower pH (4-6) occurs faster (based on observation of the left photo in Figure 4-11a, with assays performed in deionised water showing a slightly darker hue. In the case of phosphate buffer pH7 (last column

in photos shown in Figure 4-11a) there seems to be a delay in action, with results being equalised after a few hours (after 24h of observation both duplicates have the same colour as shown in the right photo in Figure 4-11a). The colour difference observed between the examined mediums is probably related to the pH and the composition of buffer. It has been shown that the buffer composition and the pH of the same buffer can highly affect the enzymatic action due to alteration of the conformational stability [383, 384]. Further analysis using HPLC or other analytic techniques could elaborate on the reasoning behind these changes, which are probably related to different by-products formed during degradation.

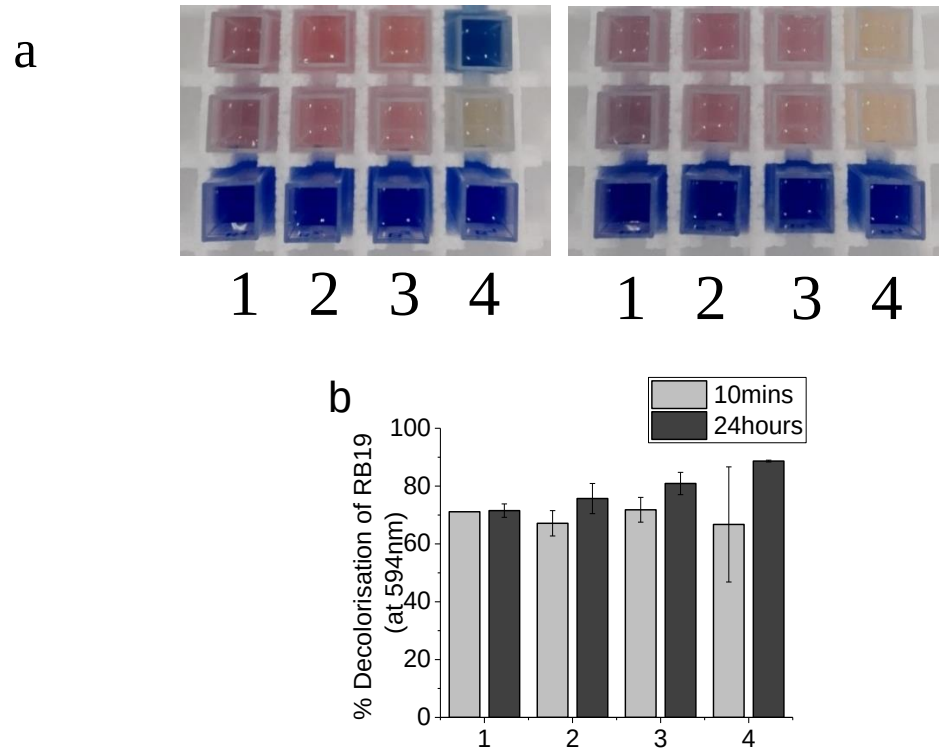

Figure 4-11: Decolorisation of RB19 from HRP in different mediums, a) visual observations of samples within 1h after the assay (left photo) and after 24h after assay initiation (right photo), b) % decolorisation based on absorbance difference from unreacted RB19, directly after assay (10mins) and after 24h. Media examined:1: deionised water (pH~6), 2: citrate-phosphate buffer 0.1M, pH 4, 3:phosphate buffer 0.1M, pH 4, 4:phosphate buffer 0.1M, pH 7. For all assays: 0.125mM RB19, 0.44mM H_2O_2, 50μg HRP. Bottom row: unreacted RB19 samples used as controls, middle and top rows: duplicates of assays.

As shown in Figure 4-11b, the degree of decolorisation was almost the same for the first 3 media examined (columns 1-3, deionised water, phosphate-citrate buffer pH 4 and phosphate buffer pH 4 respectively), progressing from around 70% after 10mins to almost 80% after 24h. In the case of phosphate buffer pH7 (column 4), the degree of decolorisation was lower just after the 10mins of initial monitoring, but after 24h it resulted to 88% of RB19 decolorisation, higher than the other media.

Based on the results shown above, the procedure of assaying RB19 decolorisation will be using phosphate-citrate buffer of pH4 as a reaction medium. This was decided as on the one hand the

proposed buffer provided by Dr. Wong's lab was phosphate-citrate of pH 4, and on the other hand, despite the similar obtained results, the pH of deionised water is not considered reliable and could potentially lead to uncontrolled results. With respect to the standard amount of dye to be used in the standard assay, it was decided to use a value close to values reported in literature for similar experiments, so a final assay concentration of 0.125mM was used. The concentration of free HRP was set at 50μg for a 3mL total assay volume, and the final concentration of H_2O_2 was set at 0.44mM. With respect to the amount of enzyme used it will be 50μl of solution with concentration 1mg/ml and the amount of H_2O_2 will be 15μl of solution with concentration 0.3%w/v. For extraction of kinetics, absorbance was monitored over 10mins, at 594nm. The full protocol followed can be seen in Section 2 of Appendix III, or briefly in Table 4-2.

Table 4-2: Concentrations and volumes of reagents used for RB19 assay.

Reagent	Conditions	Concentration in stock solution	Volume used (mL)	Final concentration in assay (mM)
RB19	In phosphate-citrate buffer, pH 4	0.127 mM	2.935	0.125
Peroxide	In deionised water	0.3% w/w	0.015	0.044
Peroxidase	In phosphate-citrate buffer, pH 4	1 mg/mL	0.050	~ 1.14×10^{-3} (assuming M_w of 44KDa)

4.2.2.1 Extraction of reaction rate

For the extraction of the reaction rate of the enzymatic breakdown of RB19, original absorbance data was transformed into dye concentration data using the calibration curve shown in Figure 4-11. Similarly to the issues faced with the calculation of the initial rate for the ABTS assay, literature is not very elaborated on how rates are calculated. In order to minimise errors, manual calculation of the rate from the linear part of the curve was omitted. Instead, fitting of the curve with available functions of the Origin software was attempted and the best fitting was found to be using exponential decay model (Equation 4-3).

$$y = A_1 \times e^{\frac{-x}{t_1}} + y_0$$

Equation 4-3

The maximum initial rate would be extracted from the slope of the linear part of the curve, as obtained after differentiation (Equation 4-4).

$$\left.\frac{dy}{dx}\right|_{x=0} = -\frac{A_1}{t_1} \times e^{\frac{-x}{t_1}}$$

Equation 4-4

where A_1 is the amplitude, $1/t_1$ is the time constant and y_0 is the plateau of the curve for infinite x. The meaning of the factors for the curve, as well as a sample calculation of the initial rate based on obtained data can be seen in Figure 4-12a and a sample rate calculation can be seen in Figure 4-12b. It was noticed that the spectrophotometer was not able to monitor the first few seconds of the reaction, so the obtained data could not be considered representative of the initial stage of the reaction. A "forged" initial point was added into the procured set of data, indicating the initial dye concentration of the reaction medium (Figure 4-12c).

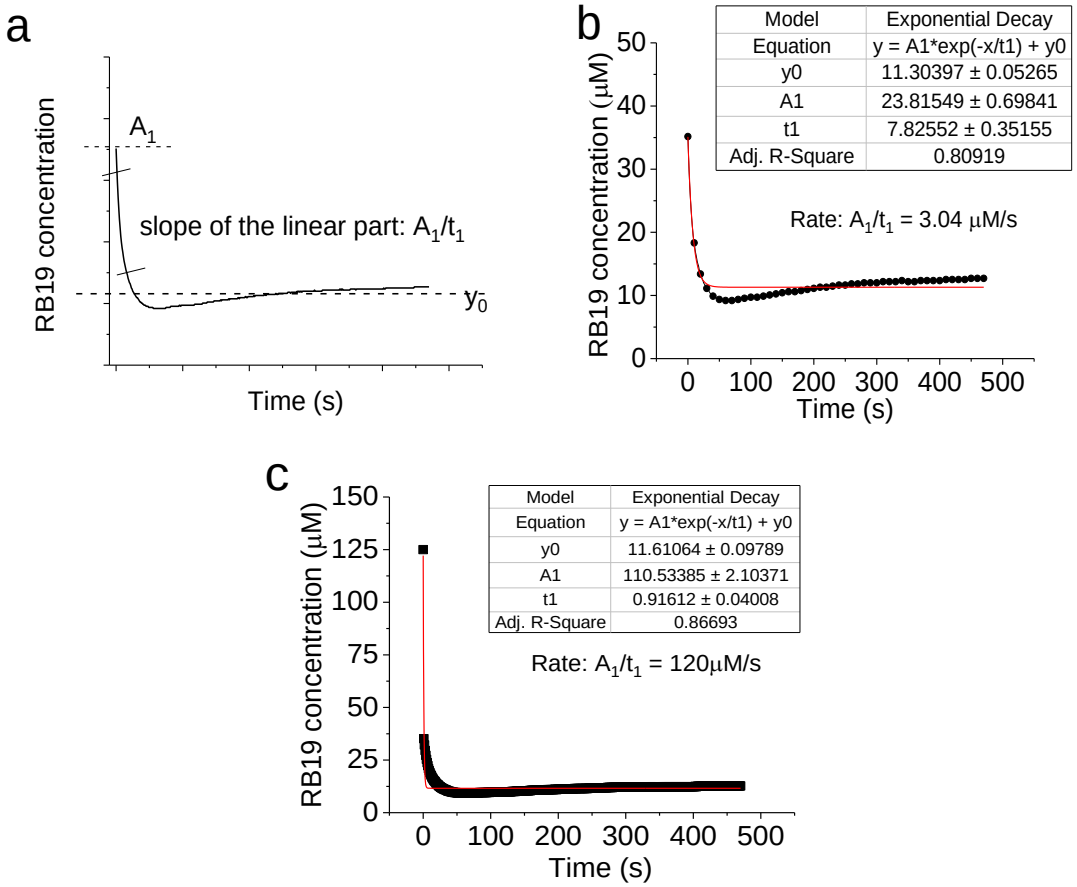

Figure 4-12: a) Explanation of the factors for exponential association fit of ABTS oxidation data, b) sample calculation of initial rate, c) sample calculation with forged initial point.

Rate was calculated for both cases to identify the difference that the first few seconds made. In the case of original, as produced, data, the calculated rate was 3 μM RB19/s. In the case of the data set with the forged initial point, the calculated rate was 120 μM RB19/s/. As one can see, there is a major difference between the two sets of data, even if the only difference is the starting point. Based on this observation, it was decided to insert a forged point as the initial point of the reaction, given the known initial RB19 concentration.

4.3. Measurement of immobilisation efficiency

4.3.1. Protein determination based on UV absorbance

During preliminary analysis, scans of deionised water and the decided assay buffer (phosphate-citrate 0.1M pH4), as well as scans of the individual reagents used for BIS synthesis (sodium

silicate and 2 additives, PEHA and PAH) and the resulted supernatants after the silicification were obtained (Figure 4-13 a and b respectively), all in absence of enzyme presence. Those scans were compared to the scan of HRP in deionised water (Figure 4-14). From Figure 4-13b one can see that only the scans related to PEHA have significant absorbance in the area of 280nm and 405nm (however without distinctive peaks) which are of importance for the protein quantitation.

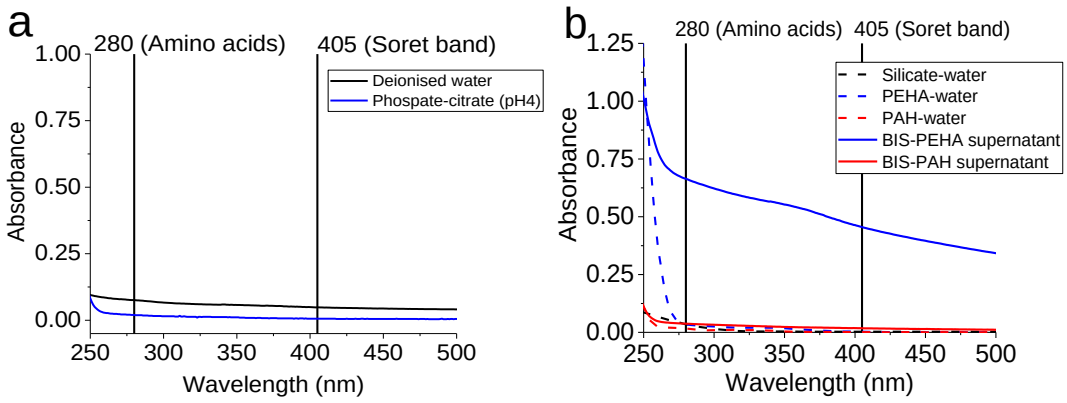

Figure 4-13: Scans of a) air, deionised water and phosphate-citrate 0.1M pH 4 buffer and b) individual BIS reagents (silicate, PEHA, PAH) and post-synthesis supernatants (BIS-PEHA, BIS-PAH). Concentrations of individual reagents are as required for BIS synthesis (30mM).

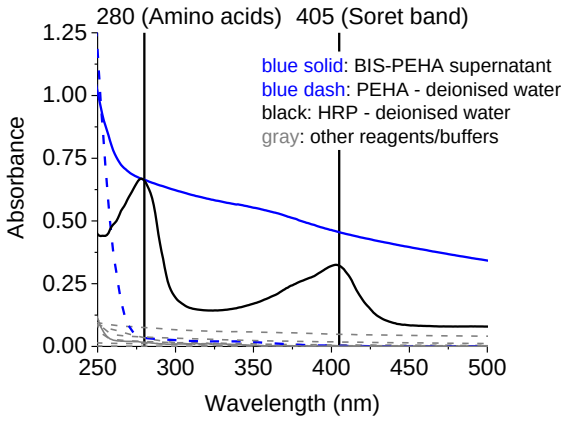

Figure 4-14: Comparison of scans for buffer, BIS reagents and supernatants to scan for HRP in deionised water (enzyme concentration 1mg/mL).

Given the fact that quantification of HRP would occur after BIS synthesis, based on enzyme present in supernatant, BIS supernatants procured with PEHA or PAH as additives were mixed with HRP in concentration of 1mg HRP/mL and their scan was obtained. This scan (HRP in supernatants) was compared to the scan of supernatants without enzyme, and also a few repeats were obtained in order to examine reproducibility (Figure 4-15). Repeats were based on procuring supernatant from freshly prepared BIS samples using either PAH or PEHA as additive and adding the same quantity of HRP. It can be noted that supernatants of BIS-PAH samples produce almost identical scans (peaks and intensity) under the same conditions, (either plain supernatant of mixed with HRP) and scans of BIS-PAH-HRP supernatants match the “expected” scan of HRP in water

(Figure 4-15a). However, in case of BIS-PEHA, the procured scans are not matching in terms of intensity across replicates, either for plain supernatants or when mixed with HRP, although the same peaks are observed (Figure 4-15b). This effect can be attributed to the presence of BIS colloids being present when BIS is synthesised with PEHA as additive, causing scattering of the absorbance measurements. It is known that due to longer chain length of PAH, it is more effective at flocculating nanoparticles from solution, leaving very few of them in suspension, compared to PEHA [299]. For reference, BIS-PEHA supernatants, if left undisturbed, showed "turbidity" within an hour of procurement while the same effect was observed for BIS-PAH supernatants after 24h.

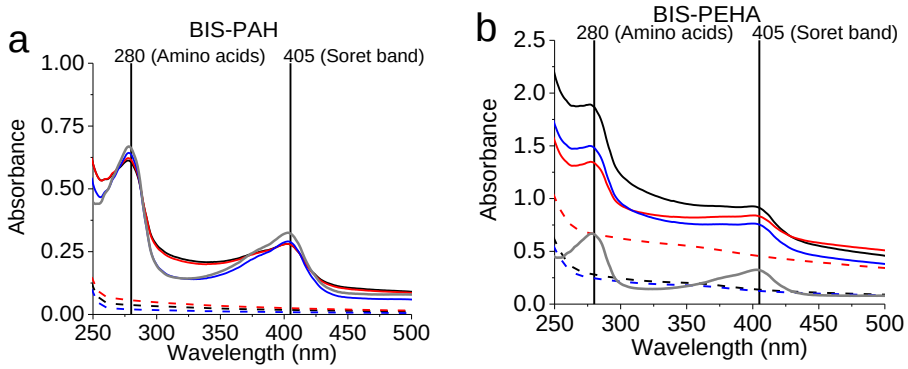

Figure 4-15: Replicates of scans of supernatants (dotted lines) and supernatants mixed with HRP (continuous lines) for a) BIS-PAH supernatant and b) BIS-PEHA supernatant. Grey line represents the scan of HRP in deionised water. For every HRP-containing scan, the enzyme concentration is 1mg/mL.

Looking closer to BIS-PEHA, in order to examine whether the presence of "leftover" nanoparticles in BIS-PEHA supernatants after the initial centrifugation can be controlled, further centrifugation of samples with developed turbidity was attempted. In Figure 4-16a we see scans of plain supernatant (red line) and supernatant mixed with HRP at a 1mg/mL concentration (blue line), as obtained after the initial centrifugation (dotted lines) and after further centrifugation (solid lines). For comparison, the scan of 1mg/mL HRP in deionised water is included (blackline).

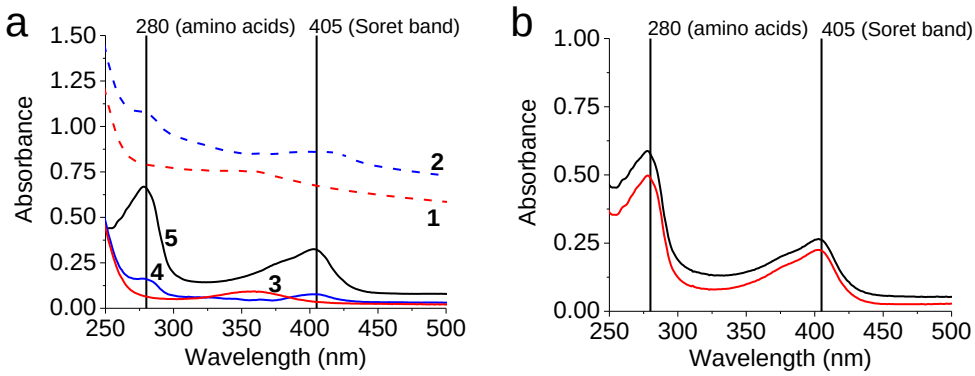

Figure 4-16: (a) Scans of BIS-PEHA supernatant, plain (red) or mixed with HRP (blue), before (dotted lines, 1/2) or after further centrifugation (solid lines 3/4), compared to scan of HRP in water (black/5), (b) Scans of phosphate-citrate buffer 0.1M, pH 4, mixed with HRP, before (black) and after centrifugation (red). All initial HRP concentrations were at 1mg/mL.

From Figure 4-16a it is clear that the absorbance of the further centrifuged samples is much lower, leading to the conclusion that BIS nanoparticles present in supernatant affect the detected amount of enzyme present. For comparison and completion reasons, solution of 1mg/mL HRP in phosphate-citrate 0.1M, pH4 buffer was prepared and its scan was obtained before and after centrifugation (Figure 4-16b). A 15% reduction in the absorbance was noted, indicative of partial sedimentation of HRP present. Further analysis is needed to characterise the effect of nanoparticles presence concomitantly with the enzyme. In any case, it is evident that an extra centrifuge cycle before measurement could possibly remove the interference caused by nanoparticles present, but would also result in significantly different results. In conclusion, measurement of protein based on UV absorbance was found impractical and in cases unreliable. Protein quantification based on the Bradford method was examined next.

4.3.2. Immobilisation efficiency based on Bradford assay

Protein quantification via Bradford method works based on the creation of a coloured complex between the Bradford reagent and specific amino acids present in the protein structure, mainly arginine [385, 386]. It is a well-known and trusted method used for protein determination in enzyme immobilisation studies. After initial control experiments it was found that the amines used in BIS synthesis were reacting with the Bradford reagent causing light to severe interference, which indicates that it should be factored in the assay's sensitivity and efficiency in protein determination. In order to examine the level of interference, solutions of all the reagents used for BIS synthesis were produced in separate pots and tested with the Bradford assay. As expected silicate did not cause any absorbance so it was ruled out for potential interference. To analyse further the extend of interference caused by the amines, both amines used (PEHA and PAH) were tested in 4 different concentrations for their binding on the Bradford reagent. Examined concentrations were: the actual concentration used for BIS synthesis (1) but also double (2), half (0.5), 1/10 (0.1) and 1/100 (0.01) of the concentration used for BIS synthesis. Given the different structure and [N] content of the additives used, the concentration of amine corresponding to these ratios was different between PEHA and PAH, (30mM, 60mM, 15mM, 3mM and 0.3mM respectively for PEHA and 0.06mM, 0.12mM, 0.03mM, 0.006mM and 0.0006mM for PAH). These amine concentrations were examined via Bradford assay using the "micro" and "macro" assay options, and results are shown in Figure 4-17a and b, with the x axis corresponding to the concentration ratio as explained before. Results showed that for PAH, regardless of the concentration present, the absorbance was stably high (about 0.2 for Macro and 0.8 for Micro assay, as shown from the red squares in Figure 4-17a and b respectively), indicating very strong interference, whereas for PEHA (blue circles in same graphs), interference was much lower, yet substantial for Micro assay.

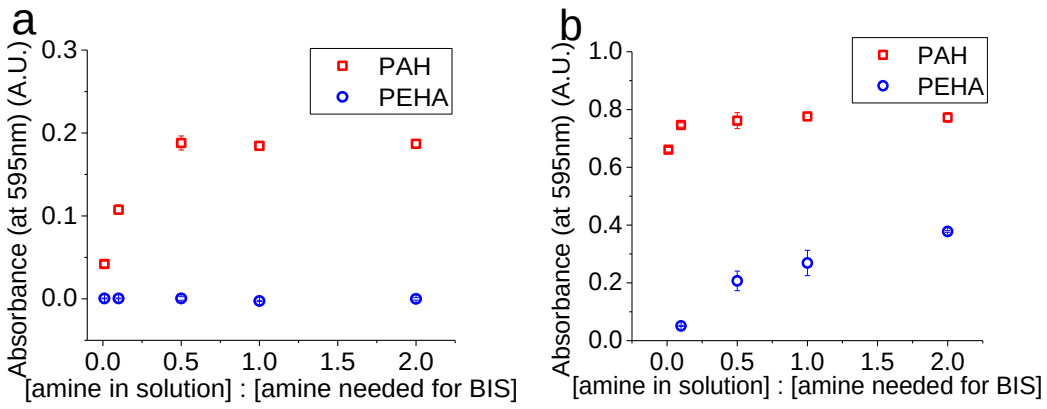

Figure 4-17: Bradford (a) "macro" assay and (b) "micro" assay of amines used in BIS synthesis (PAH, PEHA) in various ratios to the needed concentration for BIS formation. Results shown are the average of 2 or more replicates, with the error bar representing 1 standard deviation.

This can be explained from the high regional concentration of amine groups on the PAH molecule as opposed to PEHA. Since the interference of PEHA was not as high as of PAH, it could mean that the Bradford assay (at least the macro version of it) could be used to quantify protein immobilised on BIS made with PEHA and possibly with PAH, depending on the amount of residual amines from the additive being present. The amount of residual amine being present is relevant to the ability of it to be eluted post BIS synthesis. As it was explained in section 3.2. of Chapter 3, one of the main aspect of using BIS as immobilisation support, is the ability to elute the additive during synthesis, indicating a ratio of amine in solution post synthesis to amine initially needed for BIS ranging from very low (no additive elution) to almost 1 (complete additive elution).

It was also found that the amine content present in BIS supernatants after synthesis was not constant despite the standardised manner of BIS synthesis. This was observed by using the Bradford "macro" assay to examine supernatants from BIS samples synthesised on different days for amine content. These supernatants were from BIS samples synthesised either with PEHA (blue symbols) or PAH (red symbols) as additives, with the additive being left in BIS after synthesis at pH 7 (full symbols) or partially eluted using more acid until pH 5 (hollow symbols) and results are shown in Figure 4-18. There was not presence of any additional amine groups (protein/enzyme). What can definitely be seen in Figure 4-18, is that the response of the supernatants produced at pH 7 (full symbols) was lower that of those produced at pH 5 (hollow symbols), as predicted from the previous analysis done on the amount of amine present in solution. The very small deviations during BIS synthesis regarding weighting of reagents and experimental conditions (pH of reaction) and the higher observed differences in yield for sample replicates, which could not be assigned to experimental errors due to the protocol followed, leads us to assume unmapped presence of colloids during BIS formation, which has been mentioned before [387]. Presence of colloids could interact with the spectrophotometry measurement by causing scattering, but could also interfere with the assay, as the Coomassie Brilliant Blue dye

(used in the Bradford reagent) could possibly adsorb on the silica colloids being present, causing unmapped interference.

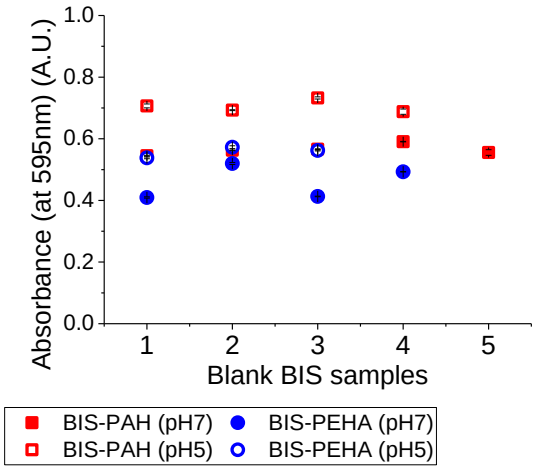

Figure 4-18: Examination of response to Bradford "macro" assay of BIS supernatants (control samples, no protein/enzyme added) produced on different days, using PAH or PEHA as additive, in zero or partial elution.

In order to reduce issues caused by amine presence other than aminoacids and to address the differences in amine held by BIS, an easily followed option is to create a calibration curve for each series of experiments per day, instead of using a standard curve produced on a different day. A few calibration curves were made for protein quantification via the Bradford method, using HRP instead of BSA, for higher accuracy, based on all the examined preparations of BIS. Curves produced for BIS with full additive content present (pH 7) are shown in Figure 4-19a and b, for BIS synthesised with PAH and PEHA as additive respectively. Curves produced for BIS with some additive eluted (pH 5) are shown in Figure 4-20a and b for BIS synthesised with PAH and PEHA as additive respectively. Curves for BIS with additive eluted to the highest extent (pH 2) are shown in Figure 4-21 for BIS synthesised with PAH or PEHA as additive respectively.

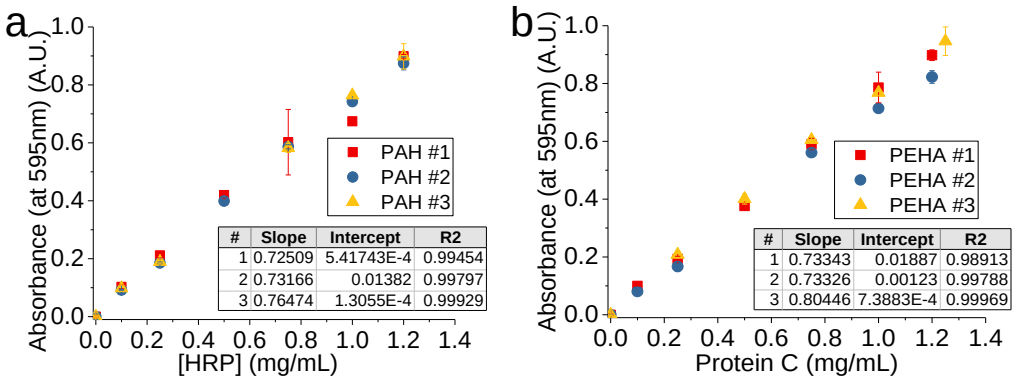

Figure 4-19: Independent calibration curves for Bradford assay using supernatant of freshly synthesised BIS with (a) PAH and (b) PEHA as additive, mixed with HRP. BIS samples were synthesised at pH7, no quenching was performed and supernatant was isolated after the 1st round of centrifugation.

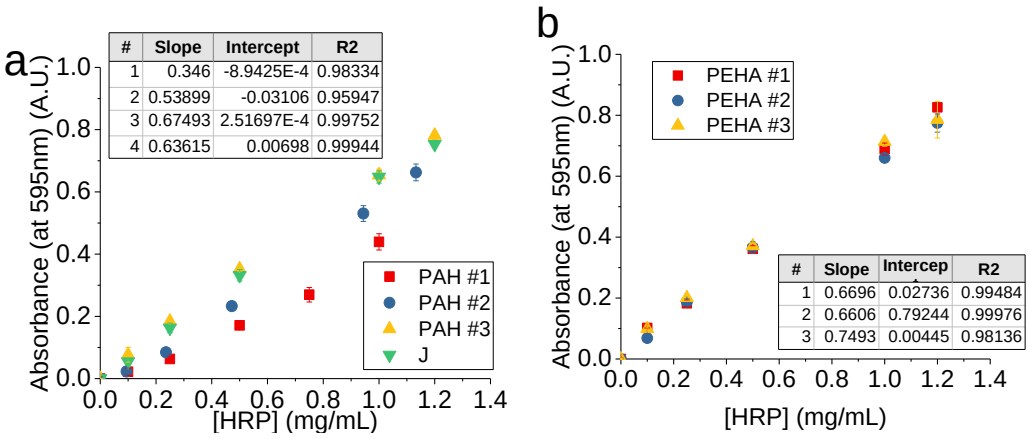

#	Slope	Intercept	R2
1	0.346	-8.9425E-4	0.98334
2	0.53899	-0.03106	0.95947
3	0.67493	2.51697E-4	0.99752
4	0.63615	0.00698	0.99944

#	Slope	Intercep	R2
1	0.6696	0.02736	0.99484
2	0.6606	0.79244	0.99976
3	0.7493	0.00445	0.98136

Figure 4-20: Independent calibration curves for Bradford assay using supernatant of freshly synthesised BIS with (a) PAH and (b) PEHA as additive, mixed with HRP. BIS samples were synthesised at pH7 and quenched at pH5. Supernatant was isolated after the 1st round of centrifugation.

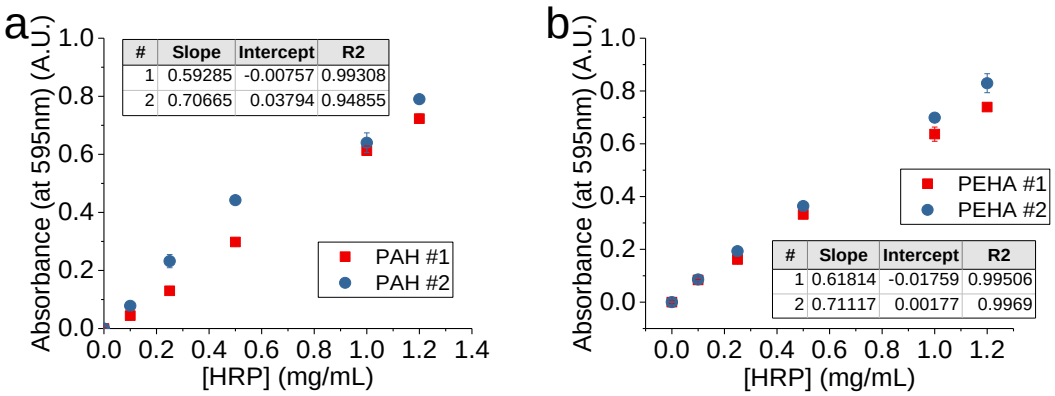

#	Slope	Intercept	R2
1	0.59285	-0.00757	0.99308
2	0.70665	0.03794	0.94855

#	Slope	Intercept	R2
1	0.61814	-0.01759	0.99506
2	0.71117	0.00177	0.9969

Figure 4-21: Independent calibration curves for Bradford assay using supernatant of freshly synthesised BIS with (a) PAH and (b) PEHA as additive, mixed with HRP. BIS samples were synthesised at pH7 and quenched at pH2. Supernatant was isolated after the 1st round of centrifugation.

Curves produced for the same type of BIS are slightly varying across different synthesis days, especially when PAH was used (Figure 4-19a). If we look a bit further than the curves, into the results they return for a given absorbance value, we can actually estimate the difference in the calculated values and see the magnitude of the calibration curves difference. Using a set absorbance value of 0.5 initially, we calculated the estimated HRP concentration using every calibration curve for each type of BIS and we compared the results. Table 4-3 shows the standard deviation (%) across the calculated values. We can see that for "standard" BIS samples, synthesised at pH 7 without further elution, the returned HRP concentration value (the "x" of the calibration curve) is within a 5% deviation for a 0.5 absorbance and closer to 10% for a 0.1 absorbance, which is considered on the lower scale. However, in the case of eluted additive either at pH 5 or at pH 2, regardless of the additive used, the deviation is rising above 10%, reaching very high values, up to almost 50%, which is very high. The uncertainty caused by the varying amine content and the presence of colloids as well as their interaction with the Bradford reagent even before adding any protein/enzyme in the mixture, was judged as too high to proceed using solely this method for protein quantification, especially when elution of the additive was performed.

Table 4-3: Calculated deviation (% over the average) for a hypothetical absorbance of 0.5 and 0.1, in order to test the variation of the calibration curves per BIS type examined.

Sample	Standard deviation for 0.5 absorbance value (%)	Standard deviation for 0.1 absorbance value (%)
BIS-PAH (pH 7)	2.69	7.67
BIS-PEHA (pH 7)	4.59	9.80
BIS-PAH (pH 5)	32.98	34.87
BIS-PEHA (pH 5)	44.28682	-152.353
BIS-PAH (pH 2)	18.94438	49.17122
BIS-PEHA (pH 2)	12.57569	22.44241

Interference using the Bradford assay is quite a common phenomenon, with many substances being categorised as competitors to protein with respect to binding on the dye and causing colour shifting, leading to overestimation or underestimation of protein [388]. There have been examples in literature, where Bradford assay (shown as Coomassie brilliant blue test) was used to indicate the charge of silica particles synthesised with PAH [389], or even attempt quantification of amines [390]. In a very similar research project, the quantity of lipase immobilised on functionalised magnetite nanoparticles was determined using different methods and their variations, and Bradford showed the highest variance, due to issues such as standard protein used for calibration instead of lipase, possible interference from nanoparticles present and from amine-containing reagents used for materials synthesis [391].

4.3.3. Immobilisation efficiency based on enzymatic activity

Another method that has been used in the literature for protein quantification is based on the activity of the enzyme left in the supernatant [156]. The limitation of this method is that the immobilisation procedure or reagents used can have an effect on the activity, causing false results. For example detection of lower activity in the supernatant can lead to the result of high immobilisation while it can be due to partially inactivated enzyme. On the other hand, residual activity of the enzyme in the supernatant after immobilisation could indicate the expected activity of the immobilised enzyme, by taking into account any deactivation during immobilisation. In order to examine whether any of the reagents used had an effect on the activity of the enzyme during the immobilisation, the stability of the enzyme was assayed under 7 different conditions, including initial reagents and supernatants after BIS synthesis, and was compared to the activity of enzyme stored in buffer. The conditions relevant to the initial reagents were based on the following hypothesis: the conditions of enzyme immobilisation can affect the degree of immobilisation. Based on this statement, HRP was mixed with BIS reagents individually (sodium metasilicate, PEHA, PAH), and it was also mixed with freshly collected supernatant obtained from silica synthesis using both PEHA and PAH in different final pH according (pH 7, 5 and 2). The concentration and pH of the reagents was the same one used for BIS synthesis, at the point of HRP addition. The pH of silicate, PEHA and PAH solutions was around 11-12, compared to

the regulated pH of the examined supernatants (pH 5 and pH 7) or the optimal conditions for enzymatic activity, of pH 4 in citrate-phosphate buffered medium). The activity (reaction rate) was examined over various time points (15mins, 1 hour and 24 hours after initial mixing), to monitor activity loss over prolonged exposure to adverse conditions, and was compared to the activity of HRP when in optimal storage conditions. Activity as measured using the standard RB19 assay. Based on the experimental procedure for immobilisation of enzyme in BIS, supernatant would be collected after 15 min of centrifugation. However due to multiple samples being synthesised at the same time and multiple supernatant samples to be examined, it could take up to 1 hr before enzyme activity of a supernatant could be assayed, so directly after centrifugation, supernatants were placed in the fridge.

In Figure 4-22a the actual rates are shown as calculated from the activity measurement, and in Figure 4-22b one can see the absorbance of standard RB19 assays, in absence of HRP, and in presence of the individual mediums used, in order to rule out any contribution from non-enzymatic degradation. In the case of HRP mixed with reagents used for BIS synthesis (silicate, PEHA and PAH), the activity of HRP is hampered quite substantially (almost 50% for PEHA and silicate and close to 100% for PAH). In the case of HRP mixed with silicate, the stability of HRP was hampered as well, as the activity reduction over time is evident (between initial measurement and measurement after 24 hr almost 100 of the activity was lost). The activity reduction is expected as the initial pH of the reagent solutions was quite alkaline and it is known that enzymatic activity in such high pH values is usually reduced. Specifically for silicate, the activity was initially high (almost 50% of expected) but quickly degraded, reaching almost zero (95% loss) after 24 hr. Evidence in literature shows that dissolved silica has an inhibitory effect on enzymatic activity, preventing cell growth [392]. This could potentially be attributed to the multivalent charge of dissolved silicate, leading to disfigurement of the enzyme's conformation, hence reduction of its activity. The reduced activity of HRP in presence of amines (PAH and PEHA) can be explained by the combination of ionic strength of the solutions and alkaline pH compared to optimal conditions and the effect they have on the electrostatic interactions amongst the enzyme's structure that can lead to its partial of complete unfolding and subsequent activity loss [393, 394]. Activity preservation when the concentration of amine or silicate were lower and the pH of the solution was closer to "normal" values (circumneutral to slightly acidic for HRP) corroborates the aforementioned arguments. It was not within the scope of this project to elaborate on the ionic strength examination of the solutions used, so further analysis on this area was not pursued. The findings from this analysis on stability allowed to use activity as a method of protein quantification reliably, only when addition of HRP was performed after BIS synthesis (pH around 7, reduced concentration of amine/silicate due to silica formation). Sample examination had to occur as soon as possible (maximum within 24 hours) after the immobilisation procedure. Having defined an activity measurement method as a means of protein quantification, calibration curves

were created for both RB19 and ABTS assays, as shown in Figure 4-23a and b respectively. Stock solutions of 1mg/mL HRP were used in both cases and appropriate dilutions were made, based on the sensitivity of the assay.

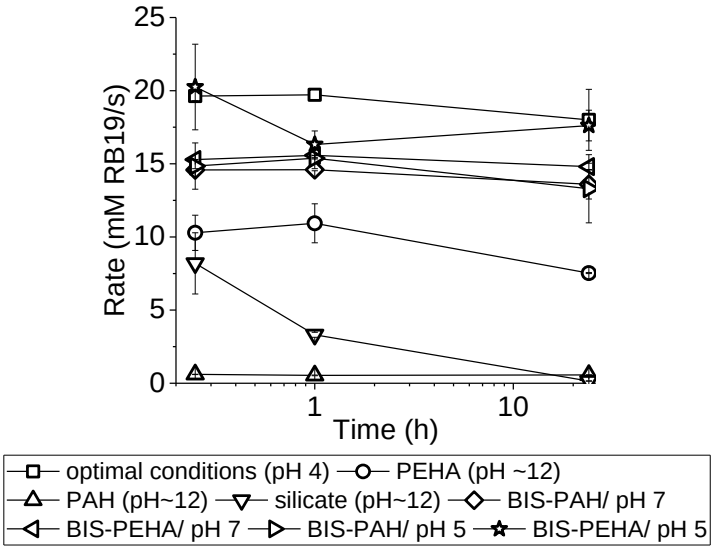

Figure 4-22: (a) Stability evaluation of HRP in initial reagents of BIS and in supernatants, activity measured using RB19 assay and (b) relevant rate for stability evaluation of HRP. Results shown are the average of triplicates, with the error bar representing 1 standard deviation.

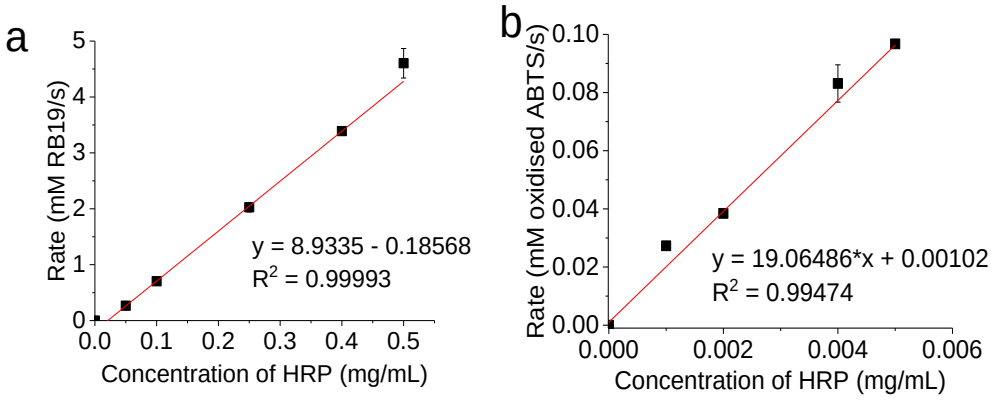

Figure 4-23: Calibration curve of HRP activity based on (a) RB19 and (b) ABTS for protein quantification.

It is worth mentioning that due to the sensitivity of the ABTS assay and the need for subsequent dilutions, the possibility of errors is much higher. It is also worth mentioning that for both assays, the idea of creating a calibration curve based on the product of the reaction was examined. In the case of RB19 assay this curve would connect amount of protein and degree of RB19 decolorisation, whereas in the case of ABTS assay the curve would connect amount of protein and amount of oxidised ABTS (using curve shown in Figure 4-2). However, creation of this curve for RB19 was not feasible, as while there was a difference in rate, the degree of decolorisation was almost identical at the end of the assay timeframe independently of the amount of enzyme present.

4.3.4. Verification of protein quantification method

In order to gain confidence that the use of activity as a method for protein quantification would produce reliable results, its verification was pursued. The idea behind this concept was that for a given solution of unknown HRP concentration, all three methods (Bradford assay, activity assay based on two substrates) should provide the same –at least in ballpark– end result in protein quantification. Verification was attempted in 2 layers. Initially a solution of HRP in water was subjected to protein quantification analysis (Figure 4-24a). Results showed that the most reliable method would be Bradford with only -2.39% deviation from the expected result, while the least trustworthy would be examination of ABTS activity with a deviation of +11%. This error could be partially attributed to subjected dilutions as was commented on earlier. At a secondary level, verification of the enzymatic activity as a quantification method was attempted for HRP solutions created with supernatants of BIS synthesis under various conditions, after 1 centrifugation cycle (Figure 4-24b). Results were interestingly different compared to the solution of HRP in water, as when activity was assayed using RB19 as substrate, the quantified protein was substantially different compared to protein quantification using the Bradford assay or activity based on ABTS. As shown from the calculated errors (insert table on Figure 4-24b), the error of quantification based on Bradford assay was almost double compared to the initial verification test (Figure 4-24a) and the error of quantification based on the RB19 assay was also substantially higher. One can see that for the solutions containing PAH, errors are slightly higher compared to solutions containing PEHA, indicative of the higher effect that PAH has both on the activity of the enzyme as well as on the Bradford assay as a factor that causes interference. With respect to the ABTS assay, the calculated error of protein estimation when HRP was mixed with BIS supernatants compared to optimal conditions, appears to be reduced. In terms of accuracy, the Bradford assay shows the lowest error in both verification tests, whereas activity assays are ranked 2nd and 3rd, with no trend being shown.

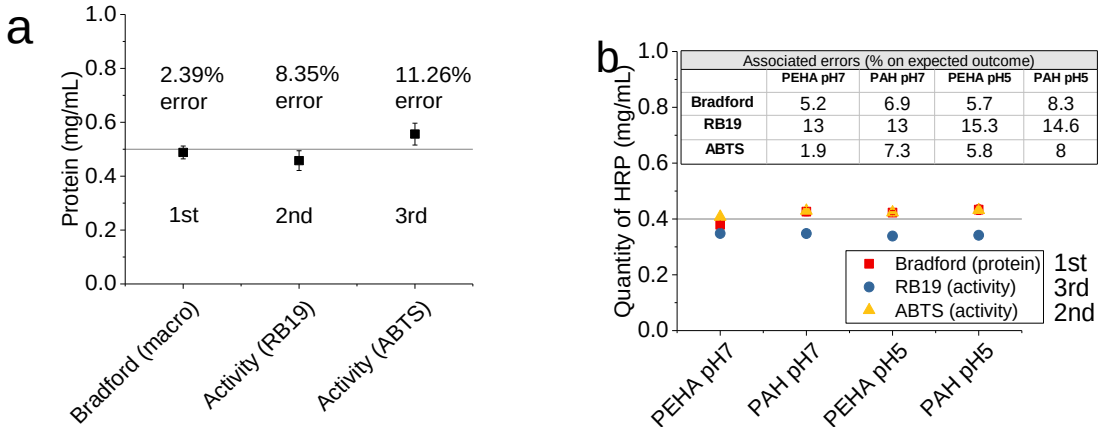

Figure 4-24: Quantification of HRP (a) under optimal conditions, using a standard solution of 0.5mg/mL HRP and (b) in various BIS supernatants prepared with PAH or PEHA, using a standard concentration of HRP equal to 0.4mg/mL, using 3 different methods (Bradford assay, or activity on RB19 and ABTS). Quantification methods have been ranked according to their accuracy from 1st (highest) to 3rd (lowest). Results shown are the average of 2 or more replicates, with the error bar representing 1 standard deviation.

4.4. Conclusions

In this chapter, the methods regarding the presence of enzyme in BIS in terms of activity or protein determination were developed based on existing protocols. With respect to enzymatic activity, two assays were chosen, one based on standard peroxidase activity (ABTS) and one based on a potential application of the biocatalyst (RB19). The initial conditions of the assays provided from literature or collaborating researchers were examined and were tweaked in order to achieve meaningful results. A more thorough examination on the effect of substrate concentration will take place in Chapter 6, as it is more suited there.

In terms of protein determination, methods usually used in the literature were employed. Contrary to other research examples where protocols are applied without a prior feasibility study, the suitability of these methods for this project was examined and a few ill-fitting points were identified. In this chapter, we examined many aspects of the provided protocols and tweaked the best performing ones to fit the purpose, which was to determine protein content as accurately as possible. If we were to apply these methods as they were provided, we would not be able to obtain accurate results. Protein determination based on UV absorbance was rejected altogether, and it was decided to use the Bradford assay in combination with activity assays as a means of protein determination. It should be mentioned that, the point of designing a biocatalyst is mainly preserving and/or enhancing the enzymatic action under continuous use or not optimal operational conditions. From an engineering point of view where mass balances are important, it is desirable to know the exact amount of enzyme immobilised. From a biochemical point of view, the quantity of enzyme immobilised is not important if it is not active. For this project, due to the difficulties faced during protein quantification, it was accepted that absolute quantification of the enzyme immobilised on bioinspired silica could not be feasible. For an as precise as possible estimation of the protein content, it was thought appropriate to use both Bradford assay and activity assays each time. A graphic summary of the methods examined and the respective findings is shown in Figure 4-25.

Future work could focus on trying to eliminate interference from substances found in the system. Such could be achieved by passing procured supernatant through an HPLC column of such affinity to attract anything but the enzyme. However, enzymes are known to be adsorbed on silica, material usually employed to build HPLC columns, so research and development of such a method would be required. Also, work could focus on fundamental understanding of bioinspired silica synthesis and how it can affect current methods.

UV-Vis Absorbance
Principle: protein backbone (amino acids) shows peaks at 220-280nm
Issue encountered here: turbidity/colloids/reagents cover those peaks
Possible solution: further centrifugation can help but some amount of protein settles as sediment with colloids

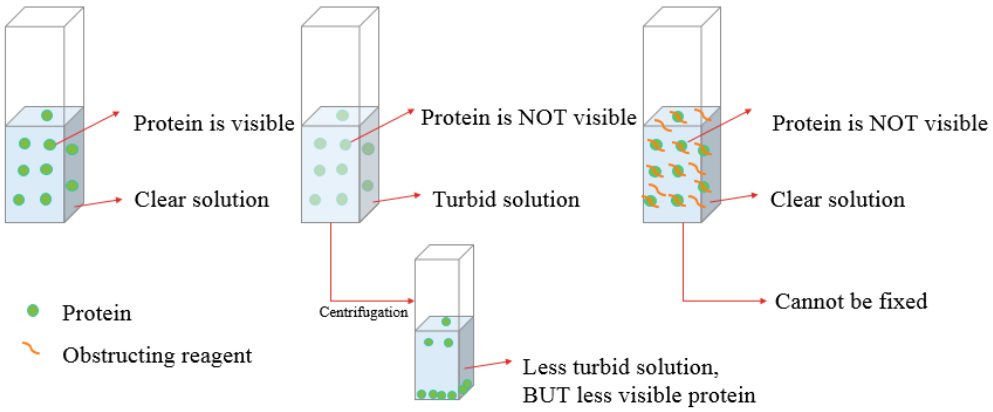

Bradford assay
Principle: amino acids react with Bradford reagent, leading to color formation, read at 595nm
Issue encountered here: turbidity/colloids/reagents react with Bradford reagent as well
Possible solution: awareness of contribution magnitude of non-protein substances, not easily applicable

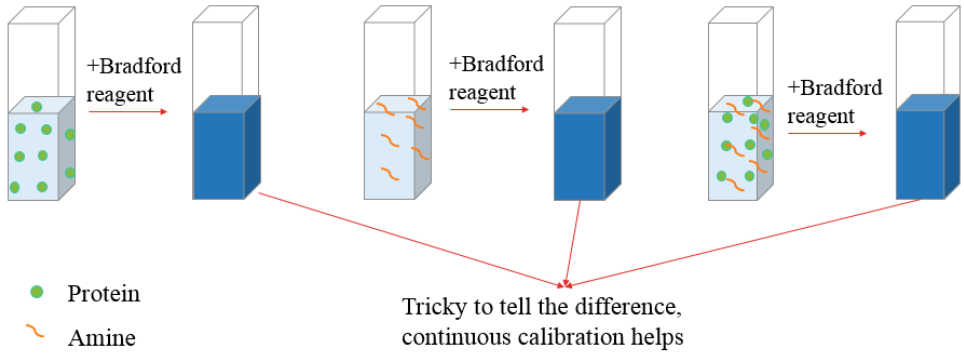

Activity assay
Principle: for very small protein concentration, linearity between activity and protein quantity occurs
Issue encountered here: enzymatic activity is affected by reagents present in the solution
Possible solution: awareness of possible deactivation and time "window" for activity preservation

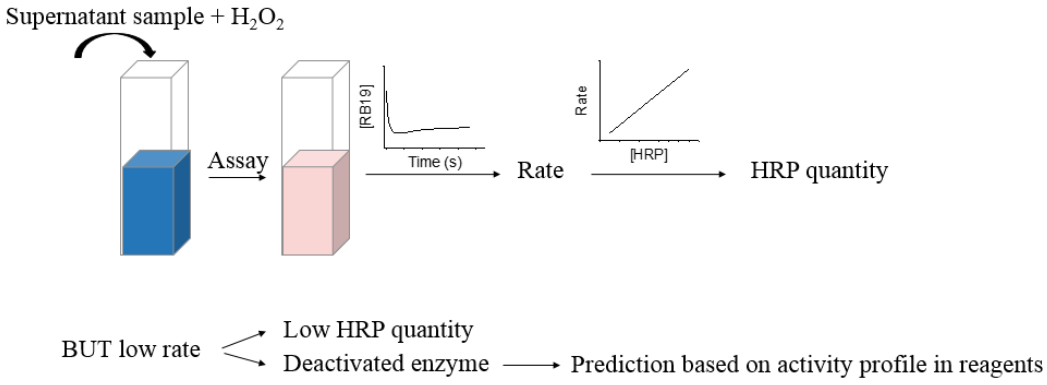

Figure 4-25: Summary of each of the 3 methods examined for protein quantification, UV-Vis absorbance, Bradford assay and Activity assay respectively.

Chapter 5 : Exploration of immobilisation of HRP in BIS

In this Chapter, the immobilisation of enzyme in BIS is explored. Focus is given on optimising the in-situ immobilisation procedure using commercial Horseradish Peroxidase (HRP), however for comparison reasons, immobilisation post-synthesis via adsorption was performed as well. The optimisation procedure is based on the factors identified for their potential influence on immobilisation, as pointed out in section 2.5 of Chapter 2. Immobilisation efficiency is measured in two different ways, as illustrated in Chapter 4, and results are critically analysed. Characterisation of the material is performed using mainly porosimetry, but also SEM and FTIR analyses. Conclusions are drawn, identifying the optimum method for efficient immobilisation in situ. Ex-situ immobilisation was also examined briefly, using BIS and a commercial silica to immobilise HRP via adsorption. A comparison between in situ and ex situ immobilisation allows useful conclusions to be drawn regarding specific advantages and disadvantages of BIS as immobilisation support overall.

5.1. Encapsulation of HRP in BIS

5.1.1. Effect of additive used on immobilisation and porosity

As it was pointed out in Chapter 2, functionalisation of silica supports enhances immobilisation, as the interactions between the enzyme and the chemical functionality are stronger compared to physical adsorption. In the case of Mesoporous Silica Nanoparticles, material is usually calcined post synthesis in order to remove the organic additive (also known as template) used, and then surface functionalisation can be introduced to enhance immobilisation [297]. In the case of BIS, the material is synthesised around the enzyme, encapsulating it inside the porous structure, in the presence of additives [317]. The additive used in BIS has a strong influence on the structure of the material, determining surface area, porosity, pore size and potentially the accessibility of pore structure [310]. During in-situ immobilisation in BIS, silica synthesis is initiated in the presence of the target enzyme and silica clusters are formed around the enzyme. Depending on the aggregation pattern and the availability of amino-residues –both relevant to the template used –the enzyme could be immobilised in-between particles during their aggregation, inside the pore structure of formed particles or by electrostatic interactions between “free” amino-residues of the additive used and some amino-acids of the protein (Scheme 5-1). Based on the aforementioned “localisation options”, it is quite difficult to identify where exactly is the enzyme inside BIS. In this project, 2 additives were used for BIS synthesis: a linear amine of low molecular weight (pentaethylenehexamine, PEHA) and a branched, polymeric amine of high molecular weight (polyallylamine hydrochloride, PAH), in order to identify the role of additive on immobilisation. It has been shown that the structure as well as the size of the nanoparticles of obtained BIS using PEHA and PAH are substantially different.

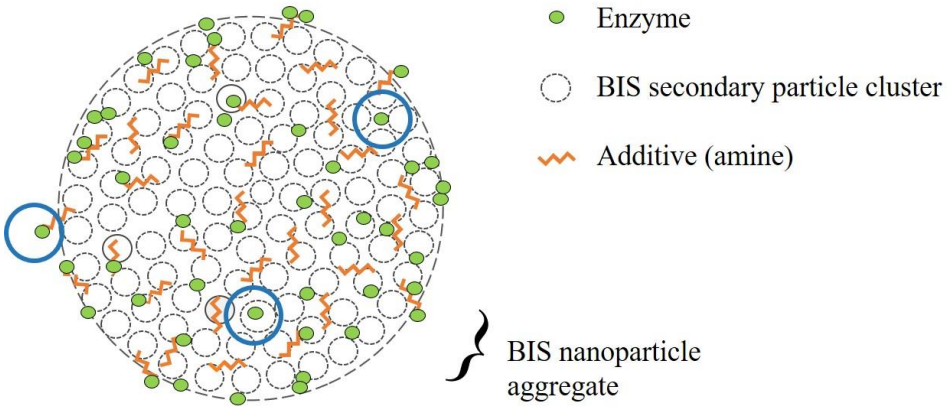

Scheme 5-1: Potential locations of enzyme in BIS nanoparticles.

BIS synthesised with PEHA (BIS-PEHA) has shown particles of larger size (few hundred nm), whereas BIS synthesised with PAH (BIS-PAH) leads to much smaller nanoparticles (less than 100nm). Furthermore, the porosity of BIS-PAH is much more enhanced compared to BIS-PEHA, which leads to almost nonporous silica [215, 299]. Both additives have been examined for BIS synthesis in combination with in-situ encapsulation of enzymes or drugs, leading to interesting findings, hence their choice seemed appropriate in order to examine two fundamentally different material structures, as host for the same bioactive molecule.

A standard amount of enzyme was added just after initiation of BIS formation, within 30s, at circumneutral pH, as it has been shown as the preferred way of in-situ immobilisation in BIS from previous work [215, 327]. If the enzyme would be added before pH neutralisation, to the silicate or additive solution, both with a very alkaline pH, the enzymatic activity could be severely hampered, as shown in Figure 4-22a. Immobilisation efficiency is expressed as a % of the initial amount of enzyme (Figure 5-1a) and results are also expressed as % of enzyme concentration in BIS obtained after drying (Figure 5-1b). % immobilisation efficiency was measured through the supernatant, using two assays: one based on protein content and the other based on enzymatic activity detected in supernatant, using the RB19 assay as explained in section 4.3 of Chapter 4.

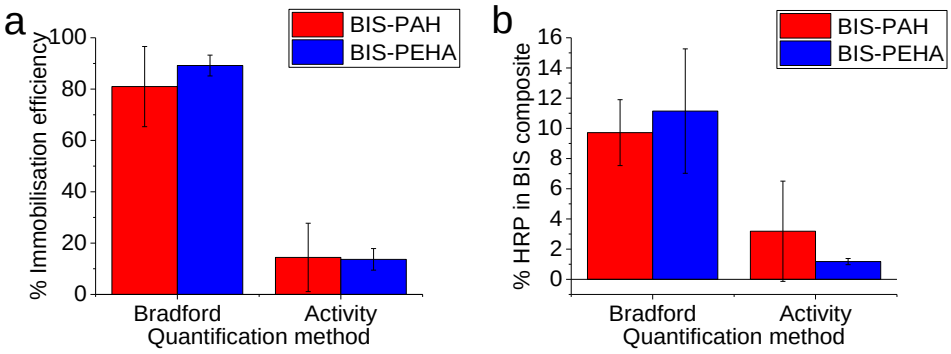

Figure 5-1: a) % Immobilisation efficiency and b) % HRP in BIS composite, for both templates used for BIS formation. Results shown are based on protein quantification based on Bradford assay, or enzymatic activity in the supernatant, using RB19 as a substrate. Results shown are the average of 3 or more replicates, with the error bar representing 1 standard deviation.

Comparing Figure 5-1a and b, three conclusions can be extracted. The first is that there is an obvious difference between the assays used for immobilisation efficiency, although it was shown in section 4.3 of Chapter 4 that protein measurement using any of the two assays should lead to very similar results. What was not accounted for in the exploration and validation of using both assays for measurement of protein content, was the actual reaction mixture and ongoing formation of BIS during immobilisation. During assay exploration as show in section 4.3 of Chapter 4, HRP was added in supernatant extracted from the centrifugation of freshly synthesised BIS, trying to simulate the synthesis conditions and predict any foreseeable inhibitory interactions. However, obtained results (Figure 5-1a) show that this simulation was not realistic. The second observation is that the average values in both plots indicate there is no significant difference on the immobilisation efficiency using any of the 2 additives, fact supported by a t-test conducted using the values collected. The third observation is the variation obtained by replicates illustrated by the error bars. Especially in the case of using PAH, irrespectively of the assay used to measure enzyme concentration, the error bars are quite high, showing high variation. This indicates that presence of PAH has an effect on both assays, inhibiting a clear and accurate illustration of immobilisation efficiency. Such an effect was predicted during the assay exploration (sections 4.3.2 and 4.3.3 of Chapter 4), however experimental data shows that it was underestimated.

The effect of PAH is probably relevant to the [N] density of the molecule and its effect on various aspects of the system. It has been shown that the ratio of [Si]:[N] as well as the size and structure of the additive are important for BIS properties [387] and for in-situ immobilisation of biomolecules, as it affects crucial properties of the material with respect to immobilisation, such as porosity [215, 299, 315]. Also, it was illustrated that both Bradford and activity assays were quite sensitive to the presence of PAH. These observations lead to the conclusion that the amount of residual [N] at the end of BIS synthesis and HRP immobilisation was not constant, regardless the constant synthesis conditions. In the case of BIS formation without presence of HRP, [N] is directly relevant to amount of PAH present, due to absence of other reagents with amine content (e.g. amino acids), whereas when HRP is present, [N] is derived from both additive and enzyme present in the supernatant.

One way of trying to understand the effect of the additive is by monitoring the yield of material produced, as – theoretically – the more additive engaged into BIS formation, should lead to more BIS, hence higher yield. The yield of BIS samples produced without HRP using either PEHA or PAH as additives, was compared to the yield of BIS samples produced with either PEHA or PAH, in presence of 12.5mg of HRP (Figure 5-2). Data was subjected to a t-test, which showed significant difference between BIS-PEHA samples in presence or not of HRP, indicating that yield of BIS-PEHA is higher in presence of HRP due to immobilised enzyme quantity (comparison of blue bars in Figure 5-2). However, there was no significant difference in the case of BIS-PAH yield in presence or not of HRP, indicating that the yield of BIS in presence of

enzyme was not affected by the added mas of immobilised enzyme. This indicates an undefined effect of PAH during BIS synthesis in presence of HRP. The action of HRP as an initiator of silica formation was examined and it was showed that BIS would not form in absence of an additive. This is in consistence with the literature, where carbonic anhydrase was unable to induce silica formation [328].

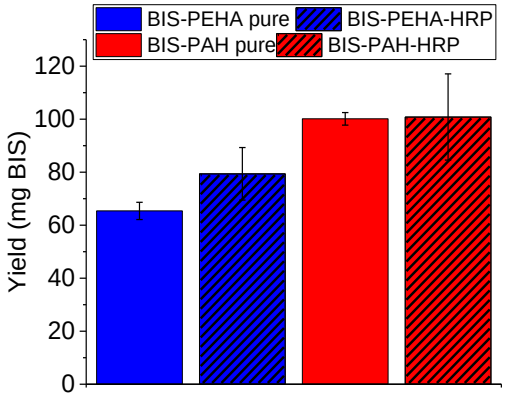

Figure 5-2: Yield of BIS in presence (textured) or not (plain) of enzyme, using PEHA (blue) or PAH (red) as additives. Results shown are the average of 3 or more replicates, with the error bar representing 1 standard deviation.

Speculations of the yet undefined relation between PAH and HRP during BIS formation, could be related to the formation of agglomerates between PAH (or PEHA) and HRP. The isoelectric point (pI) of HRP was estimated at pH 5.28, using the Expasy Prot Param online tool [395] based on enzyme sequence [396]. This indicates that at pH 7 HRP is negatively charged. On the other hand, amines have a high isoelectric point (pKa for PAH has been valued at 8.7 [315]), indicating that at pH 7 they are positively charged. Those opposite charges of PAH and HRP could indicate attraction of the molecules to form a composite. Work on ionisation of PAH [397] showed that in higher pH values (>pH 9), the molecule has the tendency to form spheroid to spherical conformations due to low ionisation, and that for pH values of 7 and above, the conformation of PAH is of bent spheroid. This conformation, combined with the tendency of charge interactions, could lead to PAH-HRP composites to form. Such structures might not be able to enter the already formed structure of BIS and due to lower rate of condensation at this point, "new" silica might not form around them. During centrifugation, these structures could sediment with BIS, leading to lower [N] being present in the supernatant, fact that is supported by the low response of Bradford assay on the original supernatant. However, when the 2nd supernatant (after washing BIS and re-centrifuging) was assayed for either protein or enzymatic activity, no response was obtained compared to BIS samples without presence of HRP. This indicates, that if the aforementioned speculation is correct, then the clusters were incorporated onto/into BIS. Another speculation on the effect of HRP to BIS formation, is that its presence reduced the amount of BIS made, hence the amount of material to act as a host for immobilisation. As it was discussed in

section 2.2.3.1 of Chapter 2, the role of the amine additive during the formation of BIS is of an accelerator, assembler and designer at the same time. Its reduced concentration or absence would make silica formation delayed compared to the 5 min timespan as it is examined here. Consequently, if amine's role is disturbed by the presence of HRP, that would lead to less BIS being made, possible with a lower degree of aggregation (and chance of immobilisation of HRP in-between the aggregates). This speculation could explain the statistically not different yield obtained with PAH used as additive, with or without the presence of HRP as shown in Figure 5-2. This speculation can also explain the higher variance of yield observed in the same Figure, when PEHA was used as additive, in presence of HRP. In the case of PEHA, BIS synthesis rate is much faster [299, 314], so BIS is almost completely formed by the time HRP is added, hence the effect of HRP on the yield disruption is not so strong. Similar effect of the rate of BIS formation (as affected by ionic strength) on immobilisation of lipase was observed by Cazaban et al. [325], who showed that a slower formation rate lead to higher protein entrapment into BIS.

BIS samples synthesised with PAH or PEHA, with or without presence of enzyme, were subjected to porosity analysis via N_2 adsorption (Figure 5-3, Figure 5-4) measurements, in order to monitor the effect of the additive and/or the enzyme presence. The surface areas shown in are leading to following observations. Firstly, BIS synthesised with either PAH or PEHA as additive shows similar values of total surface area, even in the presence of HRP (Figure 5-3a), as also shown for lipase encapsulated in BIS using the same method [215]. Secondly, surface area due to pores larger than 2nm is much more prominent for BIS synthesised with PAH compared to BIS synthesised with PEHA (Figure 5-3b). This can lead to the conclusion that PEHA forms almost micropore materials, whereas PAH can lead to formation of mesoporosity, which is consistent with literature reports for BIS synthesised with PEHA [64, 309].

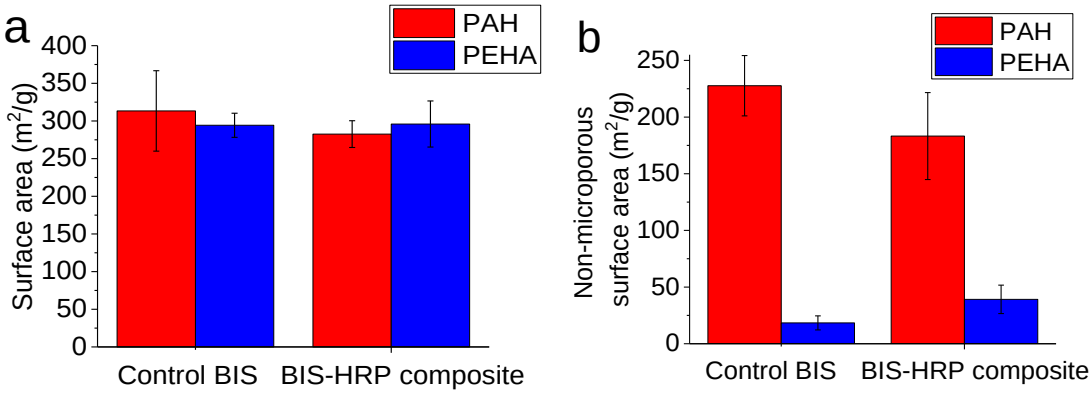

Figure 5-3: (a) Surface area measured using BET method and (b) non-microporous surface area calculated through t-plot, for BIS samples synthesised with PAH or PEHA, in presence or not of HRP. Results shown are the average of 3 or more replicates, with the error bar representing 1 standard deviation.

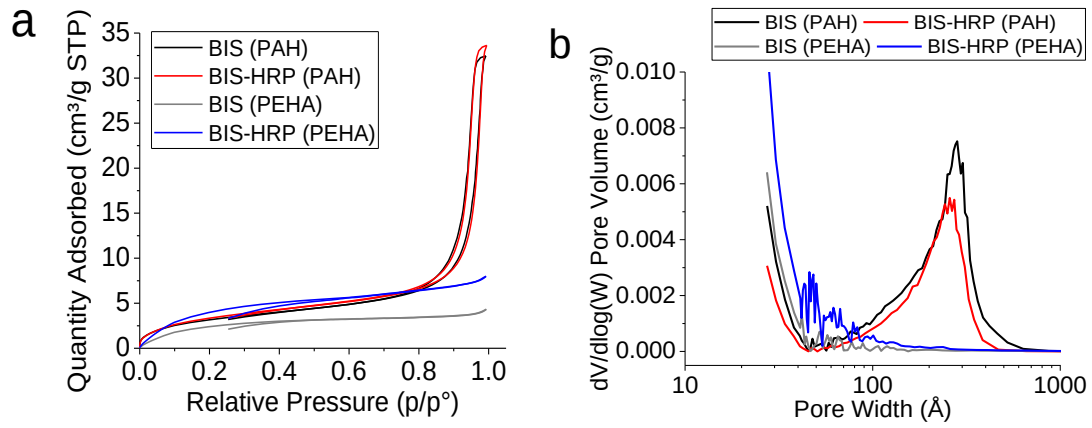

Figure 5-4: (a) isotherm plots and (b) pore size distribution for BIS samples made with PAH or PEHA as additives, in presence or not of enzyme.

The difference in porosity for BIS made with PAH or PEHA as additive is attributed to the nature of the additive, as it has been observed by work done previously within this group [299, 315]. When the surface area (total or non-microporous) of BIS-HRP composite is compared to the value of the unloaded BIS, results are not statistically different when PAH is used as additive, but they were statistically different when PEHA was used. This can be also seen from the procured isotherms (Figure 5-4a), where for BIS synthesised with PAH the isotherm has a type II (almost horizontal line to xx' axis) combined with type IV structure (increasing neck towards higher p/p_o), typical of materials which have some mesoporosity [348]. On the contrary, isotherms of BIS samples synthesised with PEHA, show a type II structure, typical for nonporous materials. A comparison of the pore size distribution (Figure 5-4b) also shows that in the case of BIS-PAH there is higher porosity than if PEHA is used as additive, evident from the peak around 25nm (250Å) for BIS-PAH (black and red line), compared to the almost "flat" lines corresponding to BIS synthesised with PEHA (blue and grey line). It should be mentioned that BIS samples synthesised with PEHA show increased porosity in the very low pore size area (less than 2nm) evident from the initial part of the graphs shown in Figure 5-4b. For both additives, differences in porosity caused in BIS in presence or absence of the enzyme are not significant (based on a series of repeats and not only one measurement as usually shown in literature). A summary of porosity information on BIS samples synthesised with both additives, in presence or absence of HRP, under various conditions examined in this Chapter, is shown in Table 5-4. It should be mentioned, that although speculations on the expected differences of BIS porosity before and after HRP encapsulation can be made, they cannot be conclusive at this point. In literature, for similar protocols followed for encapsulation, there is a tendency for the surface area to reduce upon enzyme encapsulation, as the enzyme is partially occupying the open pore volume [398, 399], whereas for the same protocol followed using a different enzyme, in-situ encapsulation did not lead to substantially different porosity [215].

SEM analysis of BIS produce using PEHA or PAH as additives was used to identify differences in the morphology of the particles (Figure 5-5). Results showed that particles produced with PAH

(Figure 5-5b) are fairly uniform in size and shape (about 30nm), and when PEHA was used as additive (Figure 5-5a) particles were significantly larger (about 200nm), with indications of smaller particles as well.

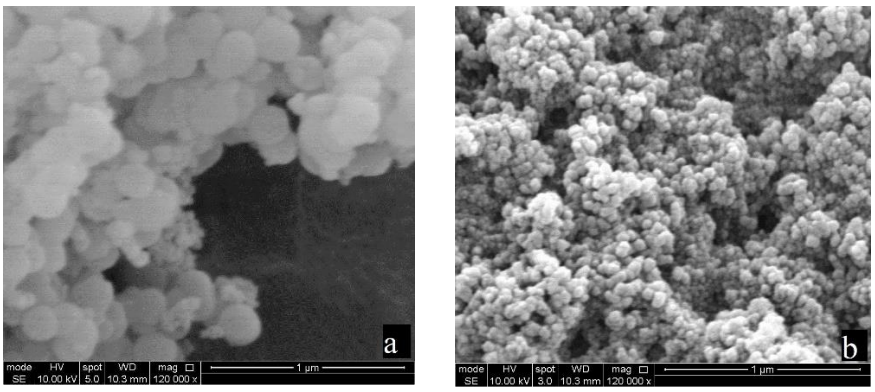

Figure 5-5: SEM images of BIS synthesised with PEHA (a) or PAH (b) as additives. Photos were captured using a 120K magnification.

Samples of BIS synthesised with PAH or PEHA as additives, in absence of HRP, were also analysed through USAXS, in order to gain more information on particle size and aggregation pattern. Scattering data were processed using appropriate analysis packages and characteristic plots were produced (Figure 5-6). From the unified fit of those plots we were able to gather information on the structure and particle size distribution of the examined samples. Results verify the difference in the observed particle size for BIS synthesised with PAH (top left graph) or PEHA (top right graph), as in the case of PAH there was only 1 particle size identified, around 10nm and in the case of PEHA 2 distinct particle sizes were shown, about 30nm and 300nm respectively. These particle sizes are comparable to the observed through SEM, as being in the same order of magnitude. When HRP was in-situ encapsulated in BIS synthesised with PAH or PEHA as additive, USAXS analysis reveals the same particle trend per additive, with slightly bigger size compared to "unloaded" BIS, around 14nm particles for BIS-PAH-HRP and 40nm and 400nm particles for BIS-PEHA-HRP. Fitting parameters identified during USAXS analysis are shown in Table 0-7 of Appendix III. We should say at this point, that given the structure of BIS and the sensitivity of USAXS, the different identified levels might not necessarily correspond to individual particle sizes, but be representative of primary and secondary particles. In order to identify which scenario serves better the truth, TEM analysis would be very useful. Literature on USAXS analysis for BIS samples synthesised with PAH agrees with the particle sizes observed herein [400]. It is also important to mention that besides the observed primary particles, both examined samples shown aggregated particle formations, described as fractals, as it has also been shown elsewhere [400]. As it was mentioned in the relevant experimental section, USAXS analysis was performed on selected samples, hence conclusive statements are not available at this point.

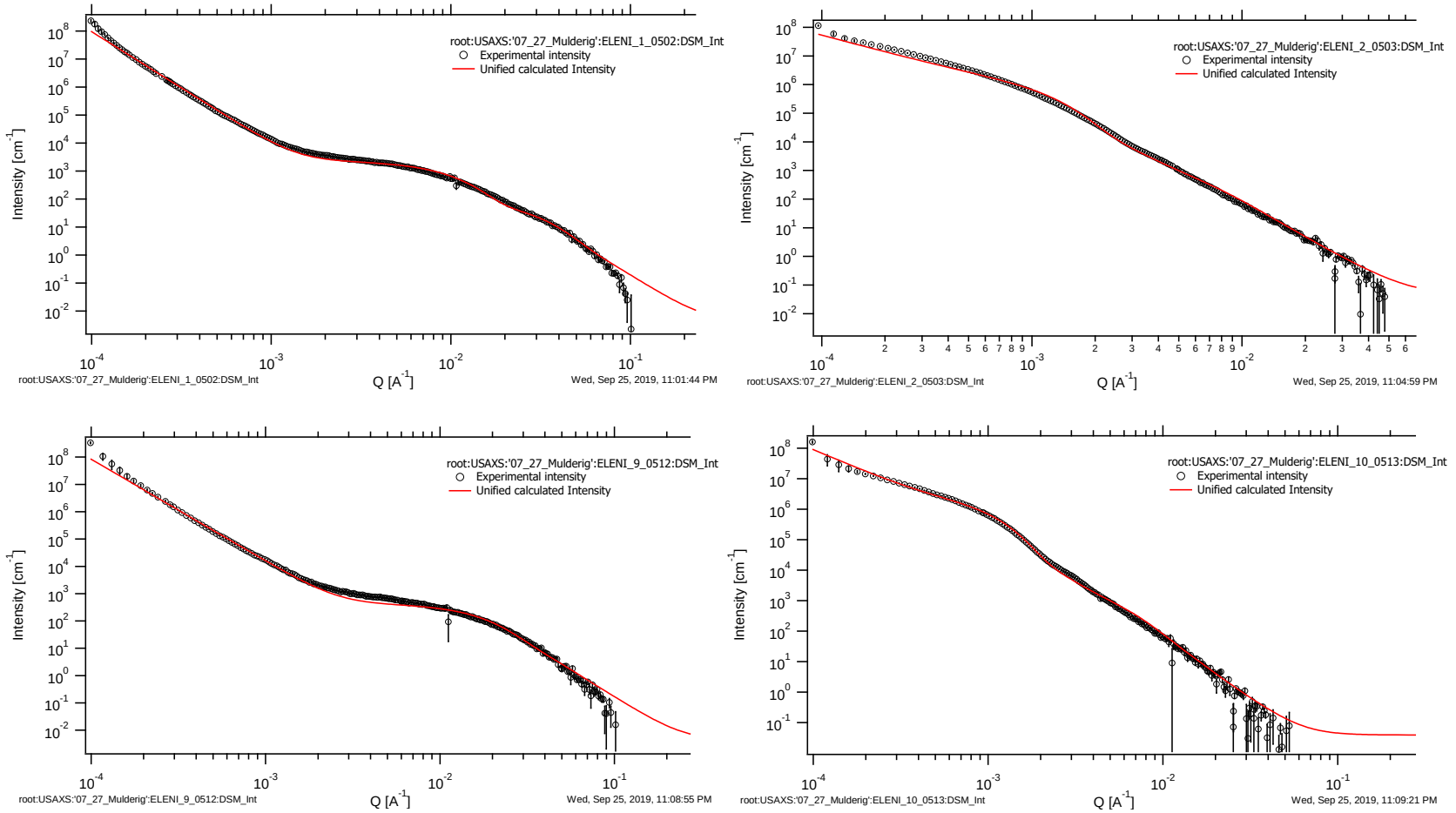

Figure 5-6: Logarithmic plot of intensity versus q for BIS (top) and BIS-HRP (bottom), synthesised with PAH (left) or PEHA (right) as additive, obtained from USAXS measurements.Red line represents the unified fit of the experimental data. Right x-axis represents the associated error for the fit.

When BIS was examined through FTIR (Figure 5-7), silica formation was verified by observation of the well documented FTIR spectra for silica, based on 3 characteristic peaks [401, 402]. Peak A (1035 cm^{-1}) and peak B (780 cm^{-1}) correspond to the Si-O-Si bond and peak C (955 cm^{-1}) corresponds to the ≡Si-OH bond.

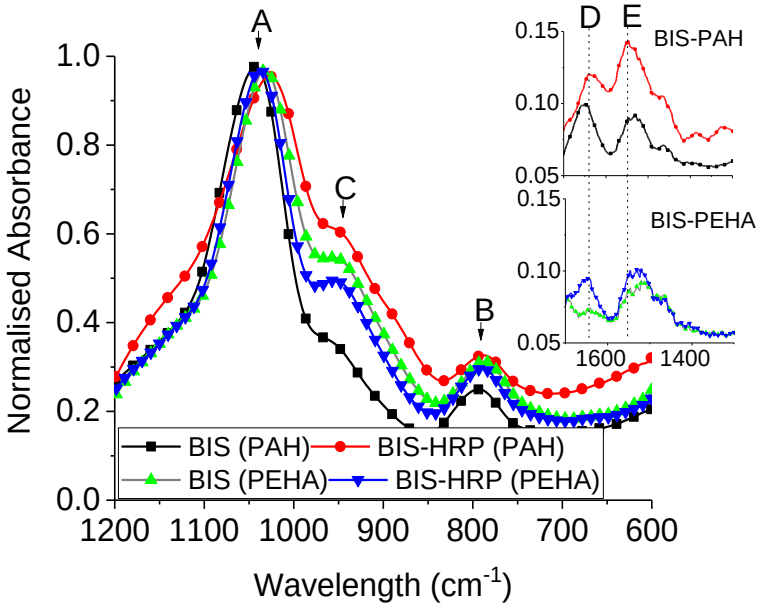

Figure 5-7: FTIR spectra of BIS synthesised with PAH or PEHA as additive, in presence or not of enzyme (HRP). Main graph focuses on BIS structure, insets refer to BIS with PAH as additive (top) and BIS with PEHA as additive (bottom).

In the insets, one can see the peaks related to contribution from the additives and/or presence of HRP, which overlap. Both additives contain primary amines and PEHA also contains secondary amines. Their characteristic peaks derive from N-H scissoring for primary or bending for secondary amines, at around 1615 cm^{-1} (peak D). Presence of HRP can be contribute to an FTIR spectrum by showing peaks from amide I and II being present. Those peaks are located at around 1650 cm^{-1} due to C=O stretching from amide I, at around 1620 cm^{-1} due to NH_2 bending from amide I (peak D), and at around 1550 cm^{-1} due to C-N stretching and N-H bending from amide II (peak E) [403]. Comparing the BIS spectra synthesised with PAH or PEHA (black and grey line in the inset graphs of Figure 5-7 respectively), one can see that the absorbance of BIS-HRP composites is higher, qualitatively corresponding to higher amount of amine present. This is expected, due to the structure and [N] local density of PAH compared to PEHA. Furthermore, comparing the spectra of BIS-HRP composite to pure BIS (sets of spectra in each inset), one can see that –again qualitatively– BIS-HRP composite shows higher absorbance, indicative of higher presence of amino-content. This can be attributed to the presence of enzyme, which contributes to the absorbance of amides due to the amino acid backbone of its structure.

5.1.2. Effects of point of HRP addition during BIS synthesis on immobilisation and porosity

As it has been discussed previously, conditions of immobilisation can affect drastically the amount of protein loaded on the support. In order to examine this approach for the systems examined herein and compare results, immobilisation of HRP was explored in different stages during the synthesis.

Although the approach examined so far for enzyme immobilisation in BIS from our group has been the introduction of enzyme during formation of silica [215, 327], developments in the area indicate that other avenues need to be explored as well. A thorough examination of the importance of the point of addition of a drug (calcein) during synthesis was conducted earlier from this group[299]. Addition points examined in that study are shown in Table 5-1, along with an explanation of steps followed for composite synthesis. It was found that the point of addition not only affected how much calcein got incorporated in the final material, but it also affected the yield of the composite. The yields ranged from 0 to almost 100%, with experiments O1, O2, O3 and O7 exhibiting the best silica yields (40% and above, compared to almost 0 observed for experiments O4, O5 and O6). A thorough analysis of protonation of each reagent for each experiment showed that the point of addition changed the initial ionisation for additive and calcein, which then changed their interactions with silicate, hence when interactions between calcein and additive were strong (e.g. O5), the interactions between silicate and additive were low, and BIS yield was also low. It is also noted, that in the examined work, the point of addition was examined for BIS samples synthesised with only one additive (PAH) and only for one of the examined addition points another additive (PEHA) was examined as a comparison point.

Table 5-1: Addition of drug in BIS during different stages of synthesis, in order to understand the effects in encapsulation (taken from [299]).

	Step 1	Step 2	Step 3	Step 4
O1	Drug + silicate solution	Dissolved PAH added to solution from step 1	pH adjusted to 7	N/A
O2	Drug + PAH solution	Dissolved silicate added to solution from step 1	pH adjusted to 7	N/A
O3	PAH + silicate solution	pH of solution from step 1 adjusted to 7	Dissolved drug added immediately to solution from step 2	N/A
O4	Drug + silicate solution	pH of solution from step 1 adjusted to 7	pH of PAH solution adjusted to pH 7	Solutions from steps 2 and 3 mixed
O5	Drug + PAH solution	pH of solution from step 1 adjusted to 7	Silicate solution acidified to pH 7	Solutions from steps 2 and 3 mixed
O6	pH of PAH solution adjusted to pH 7	Silicate solution acidified to pH 7	Solutions from step 1 and 2 mixed	N/A
O7	Identical to O5 but PAH replaced with PEHA.			

Given the design of experiments followed by Steven[299] and the associated results, it was decided to omit experiments O4, O5, O6 for the system examined here, due to the much lower obtained results, and the overall longer procedure required. We explored HRP immobilisation in BIS synthesised using 2 different additives and following the O1, O2, O3 approaches, adding one extra experiment (Table 5-2).

The yield of BIS-HRP composite using each additive for each different experiment is shown in in Figure 5-8. Examining the results for BIS produced using PEHA as additive, after conducting t-tests between the yield of control samples and BIS-HRP composite samples, it was shown that there was no statistical difference for experiments B and C, but average yield was statistically different for experiments A and D. When PAH was used as additive, yield of control samples and BIS-HRP composite showed no difference in the case of experiments C and D, but they were statistically different for experiments A and B.

Table 5-2: Procedure followed for exploration of HRP addition in different stages during BIS synthesis.

Experiment	Synthesis procedure followed
A	HRP added in silicate solution, then additive is added, combined solution is neutralised at pH 7 (equivalent to O1)
B	HRP added in additive solution, then additive is added, combined solution is neutralised at pH 7 (equivalent to O2)
C	Silicate and additive solution are mixed, then HRP is added, combined solution is neutralised at pH7
D	Silicate and additive solutions are mixed, neutralised at pH7, then HRP is added (equivalent to O3)

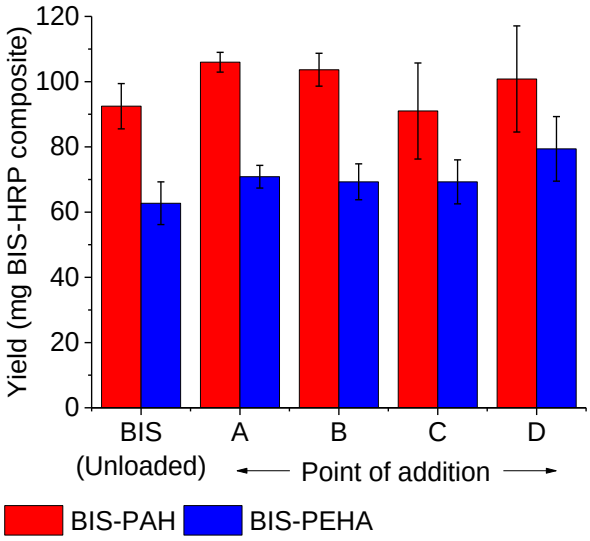

Figure 5-8: Effect of point of HRP addition during BIS synthesis, on yield of BIS-HRP composite synthesised with either PAH or PEHA as additive. Results shown are the average of 3 or more replicates, with the error bar representing 1 standard deviation.

Immobilisation efficiency and final HRP loading on BIS composite using the Bradford (protein) assay are shown in Figure 5-9a. An initial observation from Figure 5-9a is that the variance across data collected for BIS synthesised using PEHA as additive is much smaller, both between each experiment but also within each experiment compared to the variance observed for BIS synthesised with PAH. This indicates –as discussed earlier– that PAH has a stronger interference with immobilisation efficiency measurement, and potentially with BIS synthesis, in presence of HRP. Another observation is that the loading of HRP on BIS composite is not statistically different regardless of the additive used for BIS synthesis, or the point of addition of the enzyme.

The obtained values for both additives, with HRP being added at any examined point during synthesis, resulted at loading percentage of about 10% w/w. The constant value could indicate that the amount of enzyme added (12.5mg HRP per sample) is higher than the capacity of BIS synthesised with any additive to host biomolecules. Combined with the observations on the yield, the constant HRP load value could also indicate that there are unidentified effects between BIS reagents and HRP. Last but not least, the fact that there is no difference observed between the HRP load in BIS synthesised with PAH or PEHA, might mean that the initial hypothesis of a larger additive being related to higher immobilisation efficiency and enzyme load is false. The stage of enzyme addition was also attempted following the same procedure as shown in Table 5-2 using a different protein, Bovine Serum Albumin (BSA), instead of HRP, focusing only on PEHA as additive. In that case, results showed a clear difference in immobilisation efficiency of BSA, favouring addition points A, B and C [330]. This indicates that not only the presence of a biomolecule is of importance, but its composition as well. It should also been pointed out that analysis on the effect of individual amino acids on the formation and characteristics of BIS did show that there was an acceleration or reduction on the formation rate and a difference in the surface area of BIS obtained, depending on the isoelectric point of the amino acid [314]. Based on those indications and the nature of complex biomolecules, the prediction of an effect caused by enzyme presence with simultaneous presence of another additive can be validated, although the effect could not be quantified at this point.

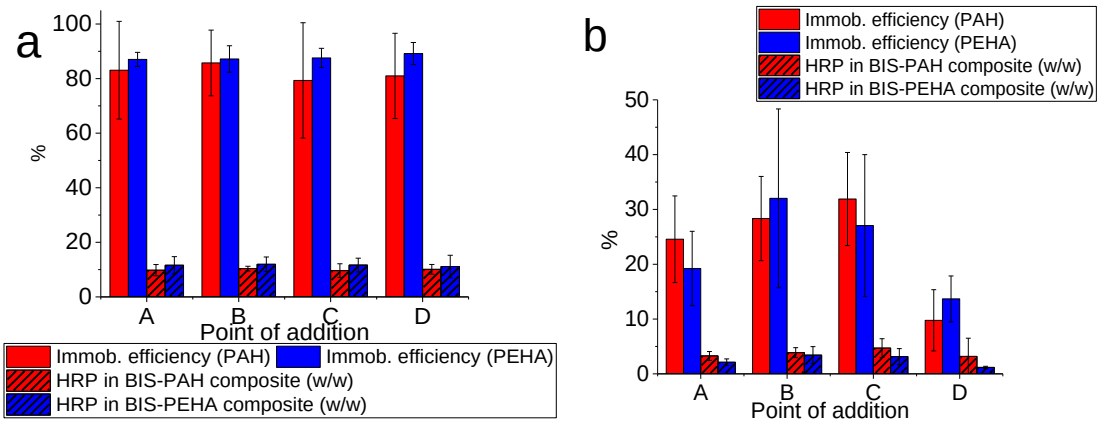

Figure 5-9: Effect of point of HRP addition during BIS synthesis, on immobilisation efficiency and HRP load on BIS composite synthesised with either PAH or PEHA as additive. Results procured through (a) Bradford assay, or (b) enzymatic activity assay using RB19 as substrate. Results shown are the average of 3 or more replicates, with the error bar representing 1 standard deviation.

Looking at the immobilisation efficiency and HRP loading on BIS based on measurements using the activity of the residual enzyme in the supernatant (Figure 5-9b), observations are slightly different. Although statistically the immobilisation efficiency for samples prepared with PEHA is not different regarding the stage of HRP addition, activity measurements show that there was less enzyme detected in the A, B and C cases, hence higher percentage of immobilisation. As it was discussed in section 4.3.3 of Chapter 4, protein quantification based on activity measurement is used herein based on examination of the stability of the enzyme in said conditions. However,

given the issues identified under in section 5.1.1 about the comparison of the 2 quantification methods, attention should be given to premature conclusions drawn. The pH of the initial solutions where HRP is added, was between 11 and 12. There is the potential that its activity was severely hampered and observed efficiency was based on false results. This speculation could be viable if protein measurement identified less quantities of HRP present in the supernatants, fact that did not occur given the Bradford assay response. In both cases of PEHA and PAH, the loading of HRP in BIS was determined at around 3% w/w using calculations based on enzymatic activity measurement, and was not statistically different between additives. As it was shown in work conducted by Davidson at al.[299] monitoring encapsulation of calcein in BIS prepared with both amines used herein, there was not a clear correlation between the amine and the loading efficiency of the drug, statement that is verified herein using HRP.

The relatively "low" loading (between 3% and 10% w/w) compared to previously reported values of about 20% w/w using very similar protocols[215] could be attributed to the interactions between charged HRP, silicate, additive or their mixture. The isoelectric points of sodium metasilicate, PAH and PEHA are estimated to be quite high (above pH13), based on calculations using SPARCS software [404]. In the A, B and C points of addition of HRP as shown in Table 5-2, addition of the enzyme occurred in a highly alkaline solution (around pH 11-12). Based on the pI of HRP (about pH 5), its charge will be highly negative at pH 11-12. On the other hand, PAH and PEHA's charge at pH12 is mostly neutral to slightly positive, indicating that no major interactions are occurring between the amines and HRP. At pH 7 however, both PEHA and PAH are mostly positively charged, hence they can interact with negatively charged HRP and cause disturbance of BIS formation by obscured interaction with also negatively charged silicate. These charge interactions could be the reason behind the unexpected yield values between BIS and BIS-HRP composite (Figure 5-8) and across the immobilisation efficiency as measured using the activity assay (Figure 5-9b).

Porosity analysis of BIS samples synthesised with PAH or PEHA exploring various points of HRP addition was performed, as this measurement can provide key information. A comparison of the surface area across BIS samples synthesised either with PAH or PEHA as additive, with HRP added at different points during synthesis shows variant results (Figure 5-10 and Table 5-4). When PAH was used as the additive, incorporation of HRP at high pH (experiments A, B and C) resulted in surface area values significantly lower than the surface area obtained for pure BIS samples. There was no statistical difference in the surface area for BIS-HRP composite when HRP was added at pH 7 (experiment D). Similar trends were observed for the pore size distribution profiles (Figure 5-11a). The profiles for samples A, B and C show much lower pore size compared to D and control sample (unloaded BIS). This indicates a change occurring in the structure of BIS upon incorporation of enzyme at specific points.

The absence of radical change between control sample and addition of HRP just after condensation of BIS (experiment D) could be attributed to the entrapment of HRP inside a small percentage of the pores of already formed BIS. In both cases, BIS formation was initiated in absence of "foreign" substances, other than silicate and amine, so the BIS formed is expected to be structurally similar. Absence of substantial mesoporosity in the case of A, B and C BIS-PAH-HRP samples could be attributed to the co-assembly of HRP and PAH molecules due to opposite charges and subsequent inhibition of PAH to direct mesopores. This could be a viable scenario given that at the point of mixing all the reagents together (for experiments A, B and C), silicate is positively charged, HRP is strongly negative and PAH has an almost neutral charge. Upon acidification, PAH acquires a positive charge, so the presence of negatively charged HRP potentially leads to PAH-HRP co-assembly, rather than solely BIS formation.

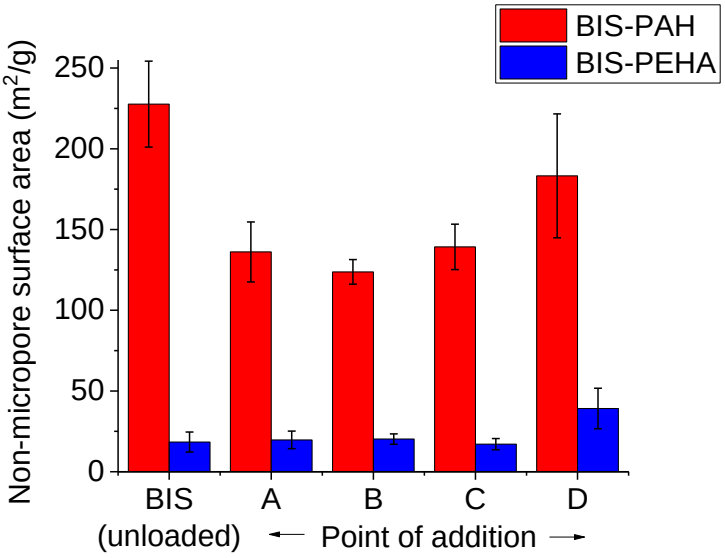

Figure 5-10: Non-micropore surface area of BIS samples prepared with PAH or PEHA as additives, examining the point of addition of HRP during synthesis. Results shown are the average of 3115) or more replicates, with the error bar representing 1 standard deviation.

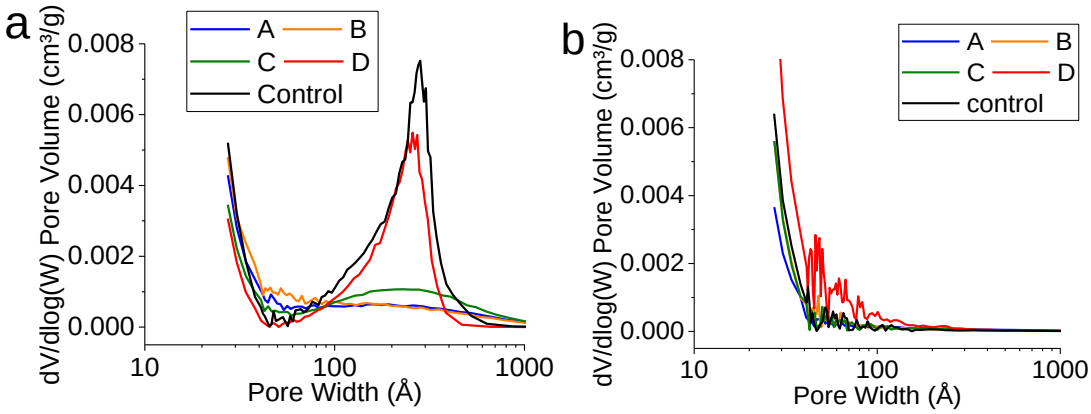

Figure 5-11: Pore size distribution for BIS samples prepared with (a) PAH or (b) PEHA as additive, examining addition of HRP at various points during synthesis. Results shown here are based on 1 sample per category.

In the case of PEHA, no significant differences were observed in the values of surface area of control BIS samples and BIS-HRP composite samples of A, B and C points of addition, however,

there are significant differences when the surface area of BIS-HRP composite at D point of addition is concerned. In this case the obtained surface area is significantly higher than that of control samples or samples of points A, B and C. This could possibly be attributed to the disturbance of BIS synthesis progress is "interrupted" by the addition of HRP, whereas in the cases of A, B and C, BIS formation is initiated in presence of HRP. Pore size distribution data when PEHA is used as additive cannot provide any further information on the effect of the point of HRP addition, as BIS is almost non porous Figure 5-11(b).

USAXS analysis of selected samples of BIS—PAH-HRP from every experiment, revealed that for experiments A and B there were 2 particle sizes identified, out of them 1 consistent with the identified for experiment D as it was discussed previously, at 14nm. The second particle size for experiment A was estimated at 72nm and for B at 51nm. In the case of experiment C, again 2 particle sizes were defined, of much bigger size though, at 43nm and 222nm respectively. A full disclosure of the fitting parameters and the associated USAXS plots can be found in Table 0-8 of Appendix III. The determination of 2 distinct sizes of particles for BIS-PAH-HRP, all of them bigger than the single particle size determined for BIS-PAH, indicates that presence of HRP probably has an effect in BIS formation. This effect could be the synthesis of larger particles due to encapsulation of HRP molecules in unaffected structure of BIS, or a fundamental change of the primary particle aggregation, leading to larger secondary particles. The much bigger size of particles observed when HRP is added to the mixture of silicate and additive solution prior neutralisation at pH 7, indicates either different magnitude of the aforementioned effect, or a new, unidentified effect in BIS formation. As it was discussed previously, since only one sample per case was used for USAXS measurement, conclusions cannot be final at this point.

Given the very similar HRP loading on BIS regardless of the point of addition, further experiments were conducted following point of addition D.

5.1.3. Effect of additive removal through acid elution on immobilisation and porosity

So far, the use of additives in order to render porosity or facilitate biomolecules encapsulation in solid supports has been well documented and discussed. However, the issue arising from the presence of "unwanted" organics in the final biocatalyst is also discussed, especially when the biocatalyst is applied in the food industry in order to reveal the pre-designed pore structure and purify the material. The most commonly used method of removing unwanted organics from a silica-based support is calcination, typically at 500^{o}C for 4-5hr [405]. Although this method is highly successful for removing templates, it cannot be applied post-immobilisation, because biomolecules will also burn off. Another method used for template removal is solvent extraction [405], which again cannot be applied without deactivating enzymes. Recent work from our group showed that both calcination and solvent extraction methods are highly unsustainable, due to the conditions and the chemicals required, and proposed acid elution as a means to remove the

additive(s) present in BIS, in a controllable way [64]. Acid elution removes the additives from BIS by modulating surface-charge interactions between the additive and the silica surface. It was shown that for small, linear amines (such as PEHA), the amount of acid used for elution (measured through the final pH of the solution) was related to the amount of additive removed, leading to 100% additive removal at pH2. Also, the amount of additive removed was correlated to increased surface area and pore volume. In the case of bigger amines (such as PAH), some removal was possible but full removal was not achieved by simple acidification.

Since this method of additive removal is gentler compared to the application of heat or refluxing in solvents, it was thought that it could be applied post-immobilisation without permanently deactivating the enzyme. In this way, in the same container where material synthesis and immobilisation occurred, acid elution could be applied in a 2nd step and lead to the final biocatalyst with increased porosity. In order to do this, 3 final solution pH values were examined, namely pH 7, pH 5 and pH 2. Note that these were pH values reached in a 2nd step after BIS synthesis was performed at pH 7 (refer to Figure 3-1b and Approach 2 as discussed in section 3.2 of Chapter 3). Figure 5-12 shows the product of BIS formation using PAH as additive at the 3 pH values examined. At pH 7 no additive is removed, at pH 5 there is partial removal and at pH 2 extended removal of the additive has occurred, at least for the smaller additive (PEHA). There is a noticeable difference between the samples, with respect to transparency. While at pH 7 BIS seems solid, opaque, at pH 5 there is translucency and at pH 2 BIS reassembles a gel (both consistency and appearance). It is worth mentioning that such an effect was not observed when PEHA was used as additive, in which case the only observable difference between samples of pH 7, 5 and 2 was the quantity of solid paste obtained.

Figure 5-12: BIS synthesised at pH 7 using PAH as additive, before removing the additive through acid elution. From left to right: BIS at pH7, BIS at pH 5 and BIS at pH 2.

Figure 5-13a and b show the immobilisation efficiency (how much enzyme made it in BIS) and the loading of enzyme (how much was the enzyme mass per mass of BIS composite), based on protein determination by Bradford or activity assay respectively. There is no protein determination data based on activity for pH2 shown in Figure 5-13b, as no activity was detected due to enzyme deactivation. Some direct conclusions are that BIS system using PAH is showing high deviation regardless of the method of measurement of the conditions of acidification. This can be related to effects of PAH on protein determination methods, combined with the higher presence of the additive in solution after its elution from BIS.

Based on the knowledge and understanding developed on the removal of additive through acid elution [64], there needs to be a comparison of the mass of procured silica in each case (both control samples without enzyme and samples with presence of enzyme), in order to be able to draw conclusions.

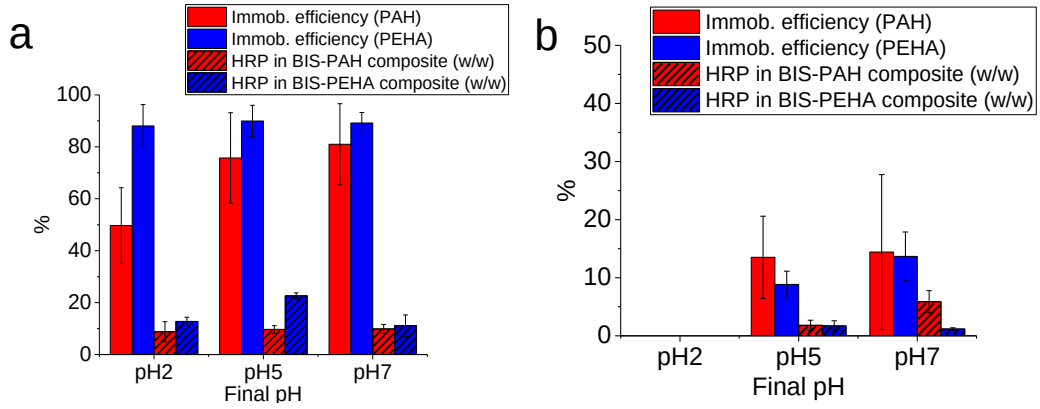

Figure 5-13: Effect of acid elution on immobilisation efficiency and loading of HRP in BIS composite synthesised with either PAH or PEHA as additive. Results procured through (a) Bradford assay or (b) enzymatic activity assay using RB19 as the substrate. Results shown are the average of 3 or more replicates, with the error bar representing 1 standard deviation.

As shown in Table 5-3, the mass of BIS (without presence of enzyme) procured is reduced with elution, which is expected due to removal of amine, as well as partial disintegration of silica clusters due to removal of amine. The effect is more noticeable for PAH, fact attributed to its ability to bridge many particles due to the larger molecular size compared to PEHA. Results were subjected to t-test analysis and it was shown that the yield difference between pH 7 and pH 5 is not significant, whereas for pH 2 there is significant loss of mass.

Table 5-3: Yield of BIS and BIS-HRP composite for samples produced either with PAH or PEHA as additive and underwent acid elution. Results shown are the average of 3 or more replicates, with the value in brackets representing 1 standard deviation.

	Yield (mg)			
	PAH		**PEHA**	
	BIS (no HRP)	**BIS composite (w/ HRP)**	**BIS (no HRP)**	**BIS composite (w/ HRP)**
pH 2	64.88 (8.89)	57.15 (7.74)	45.54 (3.10)	51.08 (3.54)
pH 5	101.98 (4.52)	94.40 (9.50)	58.35 (6.15)	53.40 (4.80)
pH 7	100.13 (2.37)	100.82 (16.26)	65.40 (3.26)	79.38 (9.91)

This is in alignment with previous findings [64], based on the estimation of amine loss in relevance to pH. They showed that between pH 7 and pH 5 there is almost 25% amine reduction (results based on PEHA) increasing to a 100% amine removal by acid elution at pH 2. They also showed preliminary results of the effect of acid elution on a polymeric amine, showing about 25% amine content reduction at pH 2, instead of 100% as shown with PEHA. In the same table (Table 5-3) the values of mass obtained for BIS samples in presence of HRP are also shown, side to side with the yield of BIS without enzyme present, for both additives used and for the 3 different values of

final pH of the solution. Subjecting the yield values in a t-test analysis, showed that when PAH is used as additive there is no significant difference to the yield of BIS of BIS-HRP composite for each stage of acid elution. However, in the case of PEHA there is statistical difference on the procured mass without acid elution taking place (pH 7), as well as in the case of acid elution at pH 2. The absence of statistical difference in the procured mass of silica with or without enzyme and the slightly lower procured values of BIS-HRP composite compared to pure BIS, indicate once again the existence of unidentified effects between HRP and PAH, in regards not only to immobilisation efficiency, but potentially to BIS formation. These effects might be attributed to charge interactions and their modulation from pH variance (from pH 12 to 7 for BIS synthesis and then to 5 or 2 depending on the elution degree), which can lead to disintegration of BIS and formation of colloids, affecting the yield, as well as the assays used. Due to lower mass of BIS obtained for elution at pH 2 and lower amount of enzyme being encapsulated, the ratio of BIS to HRP (% loading) appears the same for samples prepared with PAH across all 3 examined pH values. In the case of PEHA, it can be concluded that the % loading for samples undergoing acid elution at pH 5 is higher, due to the immobilisation efficiency being the same as for samples of pH 7, however the procured mass of the composite being lower than the equivalent of pH 7.

With respect to the effect of acid elution on porosity, BIS samples produced using either PAH or PEHA as additives, with or without presence of HRP, for every pH value examined, were subjected to porosimetry analysis using N_2. The available surface areas of BIS-PAH samples (Figure 5-14a), show no significant differences from acid elution or HRP presence. This can be attributed to the lesser extent of additive removal through acid elution, due to the polymeric nature of PAH, as it was also noted in previous work from our group [64]. When PEHA was used as additive (Figure 5-14b), the non-micropore surface area increased with acid elution, fact consistent with literature findings [64], trend also noticed for BIS-PEHA-HRP. What is notable, however, is that although for pH 7 and pH 5 there is significant difference between the measured non-micropore surface area of BIS and BIS-HRP composite, in the case of pH 2 there is no statistical difference. This indicates that at this case, either majority of HRP has been removed from BIS-HRP composite, or there are structural differences in BIS-HRP composite arising from presence of HRP, that upon removal of the additive lead to forming material with similar surface area. The later speculation is in alignment with the presence of HRP in BIS-HRP composite as observed by Bradford assay (Figure 5-13).

With respect to the pore size distribution of the materials produced when PEHA was used as additive (Figure 5-15b), there are considerable differences between BIS samples of pH 2 and BIS samples of pH 7 or 5, as expected based on previous findings [64]. Although there is not a distinct pore size distribution, Figure 5-15b reveals increased microporosity, with pore volumes ranging from about 0.1cm^3/g for BIS of pH 7 and 5 (black and red line), to 0.33 cm^3/g for BIS of pH 2 (blue line). Comparing BIS samples with BIS-HRP samples (black, red and blue lines with grey,

orange and light blue lines respectively), we can see that pore size distribution graph (values shown in Table 5-4) shows reduction of respective pore volume, except of the case of pH 7, where addition of HRP does not lead to considerable change.

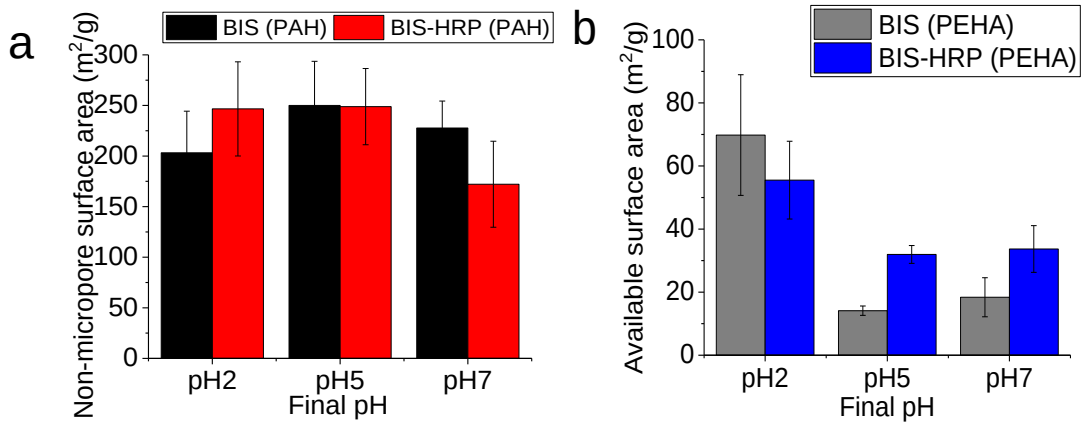

Figure 5-14: Available surface area of BIS samples synthesised with (a) PAH or (b) PEHA as additive, in presence or not of HRP, after post-synthetic acid elution treatment in 3 final pH values. Results shown are the average of 3 or more replicates, with the error bar representing 1 standard deviation.

Comparison of cumulative pore volume shows similar values for pH 7 and pH 5 BIS and BIS-HRP samples, and a considerable reduction of about 50% for pH 2 samples of BIS-HRP compared to BIS, with a value of 0.12 cm^3/g. This difference in behaviour between pH 2 and the rest of BIS samples upon incorporation of HRP, could be attributed to the pore volume of BIS being partially occupied from encapsulated HRP. While we would a pore volume reduction to occur once HRP is incorporated in BIS in the case of pH 7 and pH 5 samples, this is not observed, as probably HRP is incorporated in BIS in a way that does not block existing pores (pH 7) or crafted porosity upon atrial additive elution (pH 5).

When PAH was used as an additive, results on pore size distribution and pore volume for BIS and BIS-HRP samples of the 3 examined pH are shown in Figure 5-15a (values shown in Table 5-4). Compared to results shown for PEHA, BIS samples synthesised with PAH show a combination of micro- and meso-porosity, with distinct pore size distributions. Pore sizes are getting progressively reduced with additive elution (black, red and blue lines in Figure 5-15a , corresponding to BIS samples of pH 7, 5 and 2, with pore volumes of 1.186, 0.877 and 0.328 cm^3/g respectively). Based on Manning's findings, it would be expected to see an increase of porosity and pore size with the reduction of additive present, however, results indicate the opposite. This can be attributed to the pore network collapsing due to removal of PAH which is a bulky polymeric additive. Such an effect was observed before, when a different bulky additive (polyethyleneimine) was used as additive (unpublished data).

In the presence of HRP, pore size distribution data also show mesoporosity, but there is not apparent trend. At pH 7 pore size distribution for the BIS-HRP composite (grey line) is fairly similar to BIS (black line), with the cumulative pore volume of the composite being also similar

(about 1.00 cm^3/g). At pH 5 pore size distribution for the BIS-HRP composite (orange line) shows larger pore sizes compared to BIS (red line), but pore volumes are similar in both cases, about 0.76 cm^3/g. In the case of pH 2 pore size distribution for the BIS-HRP composite (light blue line), shows larger pore sizes compared to BIS (blue line), with cumulative pore volume of the composite being almost double than BIS (0.76 cm^3/g). For exact values and standard deviation please refer to Table 5-4.

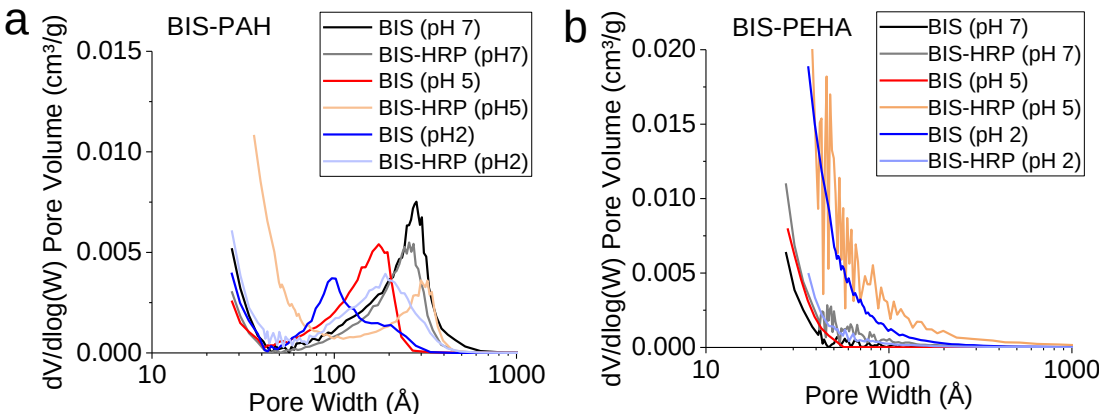

Figure 5-15: Pore size distribution for BIS samples prepared with (a) PAH or (b) PEHA as additive, examining removal of the additive through acid elution. Results shown here are based on 1 sample per category.

What can be concluded, is that there is minor difference in the porosity of BIS and BIS-HRP at pH 7 (slightly reduced pore volume), whereas porosity is starting to get enhanced upon additive elution, initially by increase in pore size (as shown for pH 5, pH 2) and upon further elution, increase in pore volume (shown only for pH 2). This could be attributed to potential localisation of HRP inside the porous structure of BIS synthesised with PAH, which upon elution of the additive can lead to the formation of bigger pores, while HRP still being encapsulated. Furthermore, removal of the additive can cause the network to collapse, as speculated for BIS samples, which, in the case of HRP being encapsulated, could lead to release of the enzyme and increase in the pore volume.

With respect to the particle morphology, Figure 5-16 shows SEM images of BIS samples synthesised with either PEHA or PAH as additives, followed by acid elution at the pH values examined. Although there were clear differences in porosity between BIS particles synthesised with PEHA or PAH, there were no visually observable differences upon acidification, indicating that acid elution does not alter the morphology of the particles. Given the absence of visual differences shown between BIS and BIS-HRP through SEM (Figure 5-5), there were no SEM images taken of BIS-HRP samples for pH 5 and 2.

USAXS measurement of BIS samples synthesised with either additive, acidified to pH of 7, 5 or 2, showed interesting results on particle size identification (Table 0-7 for BIS in absence and Table 0-8 in presence of HRP, found in Appendix III). In the case of BIS synthesised with PAH as additive, upon elution of the additive, BIS particles seem to develop polydispersity, as a second

slightly larger size of particles is detected only upon acidification. For BIS-PEHA, elution of the additive does not cause formation of a 3rd particle size, but although the 1st particle size is preserved at 30nm, the 2nd particle size is reduced upon additive elution, from 300nm to almost half, or less. This can be attributed to the collapse of BIS structure, which can lead to merging of smaller particles to form larger, distinct particles.

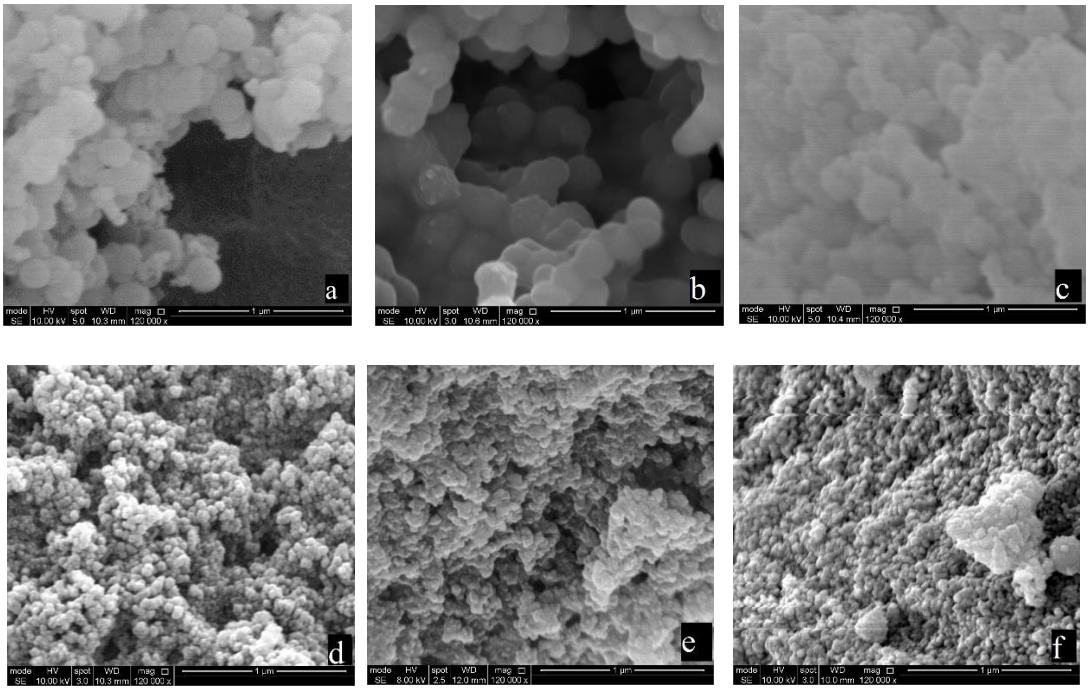

Figure 5-16: SEM images of BIS synthesised with PEHA (top) or PAH (bottom) as additive. a, b and c correspond to BIS synthesised with PEHA, with no acid elution (a), acid elution to pH 5 (b) or acid elution to pH 2 (c), d, e and f correspond to BIS synthesised with PAH, with no acid elution (d), acid elution to pH 5 (e), or acid elution to pH 2 (f). Magnification used is 120K. (Images b and e were captured by Mr. Max Yan under the author's supervision, images a and d were shown previously in Figure 5-5).

USAXS analysis of BIS-HRP particles, showed that upon additive elution there is a very similar effect observed, where when PAH is used as additive a 2nd particle size is being detected for elution at pH 5 and pH 2, slightly bigger than the 1st one, and both slightly bigger than BIS-PAH in absence of HRP. When PEHA is used as additive for BIS-HRP, additive elution leads to overall smaller particles compared to BIS-PEHA-HRP of pH 7, similarly to BIS-PEHA in absence of HRP, but also a 3rd size is being detected, in-between the 1st and the 2nd . These observations indicate the effect HRP has on BIS, but also that additive elution results in similar outcomes regardless the presence of enzyme, possibly attributed to structure crush upon additive removal. Again, given the measurement being conducted only for one sample for each additive and pH, further analysis is needed in order to be able to explain the findings with more confidence. Nevertheless, USAXS confirm microstructured effects of acidification, also noted for porosity.

The FTIR spectra produced from BIS samples made with PAH or PEHA as additive, following acidification at pH 7, 5 or 2 is shown in Figure 0-2 of Appendix III. For both additives, there are no clear differences on the extent of amine presence (as described by the absorbance of the respective C-N, N-H and C=O bonds in the region between 1400-1700cm^{-1}). FTIR spectra of BIS-

HRP composite for the 3 pH examined could not render usable results due to the combined effect of enhanced amine content due to enzyme and reduction of amine content due to acid elution.

To summarise the effect of post-synthetic acidification, we note that yield of BIS as well as its porosity is affected. As additive is being removed through elution, less BIS mass is obtained, with either improved porosity, in the case of PEHA, due to pore channel opening, or reduced porosity, in the case of PAH, due to pore channel collapse. When HRP is immobilised, yield and immobilisation efficiency results are not showing a clear trend. With respect to porosity of the BIS-HRP composite, there is an inversed trend between PEHA and PAH, similar to the one observed for BIS. Although the cumulative pore volume for BIS and BIS-HRP of pH 7 and 5 is similar, for pH 2 samples there is substantial difference between BIS and BIS-HRP samples; reduction in the case of PEHA, increase in the case of PAH. This can be related to the localisation of the HRP in the composite. While SEM did not show observable changes regarding acidification, USAXS analysis indicated structural changes, both across acidification and enzyme presence. Based on immobilisation efficiency and w/w HRP loading, as well as porosity results, post-synthetic additive elution at pH 5 was considered as the best option to continue investigating.

5.1.4. Effect of amount of HRP added on immobilisation and porosity

Having examined the effect of the type of the additive, the point of addition of HRP during BIS synthesis and the effect of acid elution, another factor to optimise a biocatalyst is the loading of enzyme. Loading could be measured either as mass of enzyme per mass of material [215] (as shown herein so far), but also it can be shown as activity of enzyme per mass of material (measured activity after immobilisation) [156]. Description of HRP loading based on mass was chosen herein in order to illustrate the point of BIS being able to host large amounts of enzyme. With respect to the activity of the enzyme loaded on BIS, it will be systematically discussed in Chapter 6. In order to identify the capacity of BIS as enzyme immobilisation support, 4 different initial concentrations of HRP were examined during BIS synthesis, following acid elution to pH 5, namely 0.1, 0.17, 0.25 and 0.4 mg/mL HRP in the initial solution (50mL). Results of the immobilisation efficiency and mass of enzyme per mass of composite are shown in Figure 5-17a and b respectively, using both Bradford and activity assay of the supernatant with RB19 as substrate. Comparing immobilisation efficiency when measured through the Bradford or the activity assay, we can see that again there is a large difference in the results obtained with each assay. Across the different HRP amounts added, immobilisation efficiency results show a variance, which however is not of major concern, except for the BIS-HRP samples obtained with PEHA and the largest amount of HRP. This is the only point where Bradford and activity assay return almost the same result, statistically no different, lower than usual for Bradford assay (51%) and higher than usual for activity assay (36%).

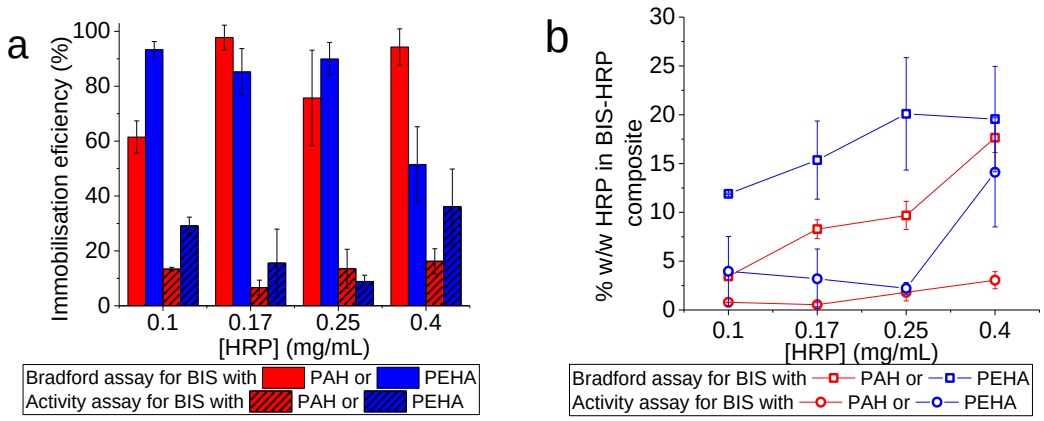

Figure 5-17: Effect of mass of HRP added a) on immobilisation efficiency and b) on w/w HRP loading on BIS-HRP composite synthesised with either PAH or PEHA as additive and examined with Bradford or activity assay using RB19 as substrate. Results shown are the average of 3 or more replicates, with the error bar representing 1 standard deviation.

Results procured via the Bradford assay on the w/w HRP loading (square symbols in Figure 5-17b) are fairly consistent with the idea of a maximum immobilisation capacity of enzyme being immobilised. For BIS synthesised with PEHA, a 20% w/w capacity was reached for HRP immobilisation in BIS. In the case of PAH, again there is a high variance, potentially due to interactions between PAH an HRP, and/or an effect of the amine on the assays used. For w/w HRP loading examined through the activity assay (circle symbols in Figure 5-17b), results for both BIS synthesised with PEHA or PAH are fairly similar, below 5%, until the 0.4mg/mL point, where loading for BIS-PEHA jumps to about 12%, whereas the value for BIS-PAH remains low. Higher amount of enzyme being added was not tested in this project, but it would be interesting to explore the option.

Looking at yield data from Figure 5-18, it is evident that the lowest examined quantity of HRP (0.1mg/mL initially added) has the maximum effect on BIS synthesis. Yield of BIS-HRP composite was significantly lower to control sample, regardless of the additive used. For HRP quantity higher than 0.1mg/mL, yield of composite showed no statistical differences regardless of the quantity of enzyme added. It is interesting to note that in the case of 0.4mg/mL HRP added, the incorporated amount into BIS composite was 15-20% measured with both protein determination assays (when PEHA was used as additive). Assuming a value of 50% immobilisation efficiency (roughly accurate by the values shown in Figure 5-17a for PEHA, when 0.4mg/mL HRP is added), about 10mg of HRP should be incorporated into BIS. Adding 10mg to the control BIS yield (58mg), returns a value of 68mg expected yield of BIS-HRP composite, while the yield recovered was about 50mg. The difference between the expected and the actual yield value is 22%, which is deemed not significant due to the variance observed between the replicates.

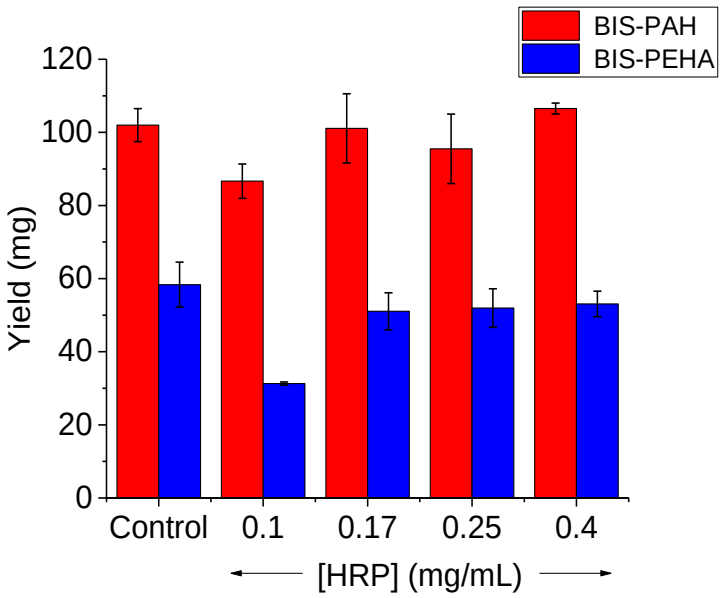

Figure 5-18: Effect of mass of HRP added on yield of BIS-HRP composite, synthesised either with PAH or PEHA as additive, compared to BIS with no enzyme presence. Results shown are the average of 3 or more replicates, with the error bar representing 1 standard deviation.

Same calculations in the case of 5mg added enzyme return a 47% difference of the obtained yield compared to expected when PEHA is used as an additive and a 15% difference when PAH is used as additive. These values can be used as evidence, supporting an effect between HRP and the additives, hindering BIS formation.

With respect to the effect of the mass of HRP incorporated into BIS on porosity of BIS-HRP composite, results on available surface area (Figure 5-19, blue columns) show a clear trend for BIS made with PEHA. Measured non-micropore surface area of BIS-HRP composite is higher compared to BIS without presence of HRP, and the surface area reduced with increased amount of HRP added. For the maximum amount of HRP incorporated (when 0.4mg/mL HRP was introduced), the surface area shows no statistical difference to the one observed for BIS without HRP. On the contrary, for the lowest amount of HRP present (when 0.1mg/mL was introduced), the observed surface area is more than quadruple the value of the control sample. This indicates that the more enzyme present, the lower the effect on porosity when PEHA is used as additive during BIS synthesis. As expected, there is no observed pore size peak for BIS samples synthesised with PEHA as additive, regardless of the amount of HRP present (Figure 5-20b). However, comparing the pore volume of BIS-HRP samples to the one of BIS, we can see that there is an increase, with the strongest effect shown for the BIS-HRP samples obtained by adding 0.1mg/mL HRP. Whereas the pore volume of the BIS sample in absence of HRP is 0.08cm^3/g, the pore volume for the BIS-HRP samples is 0.275, 0.14, 0.14 and 0.109 cm^3/g for increasing quantity of HRP added. A simple explanation to that could be attributed to electrostatic interactions between PEHA and HRP, which at lower enzyme concentrations could disturb the role of PEHA in BIS formation, or to the lower amount of enzyme entering BIS, which would

mean that acidification could lead to larger pore structures. The higher surface area obtained in presence of 0.1mg/mL HRP and the increased pore volume, could indicate a structural change of the obtained solids.

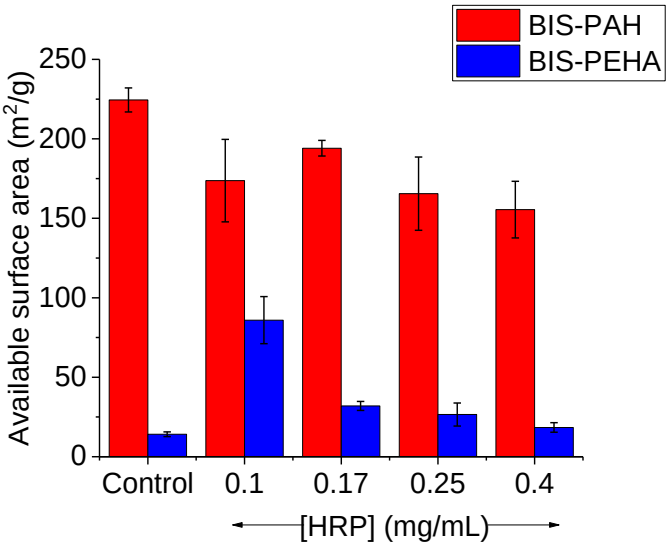

Figure 5-19: Effect of mass of HRP added on the available surface area yield of BIS synthesised either with PAH or PEHA as additive. Results shown are the average of 2 or more replicates, with the error bar representing 1 standard deviation.

When PAH is used as additive, the observed effect on the available surface area is almost inversed (Figure 5-19, red columns). All BIS samples in presence of HRP showed lower surface area compared to control samples and there was no statistically significant difference across different amounts of HRP introduced (and retained). This effect can be attributed to the presence of enzyme inside and in-between BIS particles, which occupies the available pore space and surface area. This explanation can be corroborated by data on pore size distribution (Figure 5-20a), which shows that for BIS-HRP composite the pore size is larger than the pore size of BIS in the absence of enzyme, regardless of the amount of enzyme added.

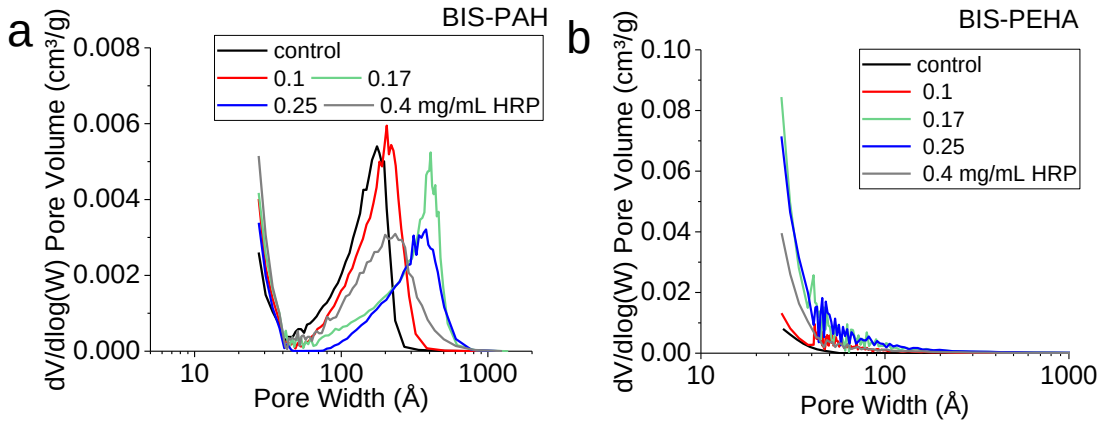

Figure 5-20: Pore size distribution for BIS samples prepared with (a) PAH or (b) PEHA as additive, examining amount of HRP added for encapsulation. Results shown here are based on 1 sample per category.

Also, it is worth commenting on the cumulative pore volume being almost stable across all BIS-PAH and BIS-PAH-HRP samples, with values between 0.75 and 0.85 cm^3/g supporting even

more the speculation of the effect of enzyme on porosity, as given the lower surface areas shown for BIS-HRP, we would expect a difference to be observed for pore volume. Tabulated results on porosity characteristics can be found in Table 5-4.

As discussed earlier, FTIR spectra could not be used to draw relevant conclusions due to the complicated effect of HRP presence during BIS formation. SEM images were collected for BIS-HRP composites with the highest amount of enzyme and were compared to images of BIS without the presence of HRP in order to identify any differences (Figure 5-21). No differences were observed with respect to enzyme presence, the only observable difference was attributed to the different amine used as additive during BIS synthesis, as illustrated also in Figure 5-5. Such an effect is not unexpected, as BIS secondary particles synthesised with PEHA or PAH as additive have a size of about 300nm and 60nm respectively, resulting in a volume of a few thousand nm^3, and the size of HRP is about 6 nm x 4 nm x 1 nm, resulting in a volume of about $30nm^3$. Based on these volumes, its encapsulation within secondary particles would not have made such a visible difference in the material. Also, HRP could be residing within the pore structure of the material, as suggested by porosity results, but SEM confirms no effects on the morphologies.

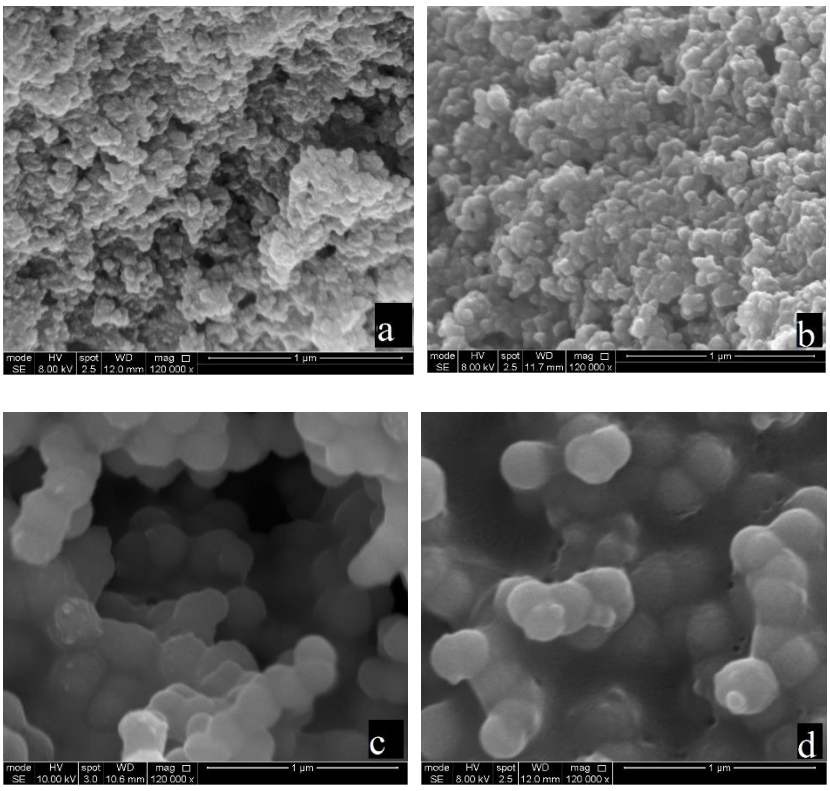

Figure 5-21: SEM images of BIS synthesised with PAH (top) or PEHA (bottom) as additive. a and c correspond to BIS without presence of HRP, b and d correspond to BIS-HRP composite with the 0.4mg/mL HRP introduced. Magnification used is 120K. Images b, c and d were captured by Mr. Max Yan under the author's supervision.

Comparison of USAXS measurements for BIS-HRP of 0.25mg/mL and 0.4mg/mL introduced concentration of HRP showed that in the second case, particle sizes detected were almost identical to BIS in absence of enzyme (for each additive respectively). When 0.25mg/mL were added for

encapsulation, there were some slight differences as discussed earlier (fitting parameters, including particle sizes can be seen in Table 0-8 of Appendix III).

A very thorough analysis on localisation of encapsulated protein in BIS was done by Cardoso [406], who however used protein –lysozyme– as the additive to initiate silica formation. Their findings indicate that protein is localised in closely packed particle aggregates, leading to lower surface area compared to silica in the absence of protein, fact that is also supported from data found herein. In similar research from our group, localisation of lipase encapsulated in BIS could not be confidently concluded either based on SEM and N_2 adsorption data [215].

Summarising the findings in this section, we can see that we were able to achieve a 20% w/w HRP in BIS-HRP composite, value quite high compared to general literature as it will be discussed later. We also once again showed that there is an unidentified effect of the presence of HRP in BIS formation, especially for lower quantity of HRP added. Although morphologically we were not able to observe any differences, porosity data suggest structural differences of BIS upon addition of HRP.

Table 5-4: Comparison of porosity of silicas used for HRP encapsulation, before and after enzyme incorporation for all the experiments conducted (additive elution, point of addition, quantity of HRP). Results represent the average value of 2 or more replicates, with the value in parenthesis being 1 standard deviation.

	Type of silica	Total surface area (m^2/g)	Non micropore surface area (m^2/g)	Pore volume (cm^3/g)	Average pore size (nm)
Silica	BIS (PAH) pH2	285 (93)	158 (19)	0.328 (0.079)	9.8 (2)
	BIS (PAH) pH5	294 (19)	224 (7)	0.877 (0.383)	10 (3)
	BIS (PAH) pH7	313 (53)	223 (20)	1.186 (0.124)	21 (2)
	BIS (PEHA) pH2	603 (12)	72 (17)	0.344 (0.194)	3 (3)
	BIS (PEHA) pH5	174 (20)	14 (1)	0.079 (0.026)	3 (0.4)
	BIS (PEHA) pH7	294 (16)	18 (6)	0.121 (0.031)	6 (1)
Silica-HRP	BIS (PAH) pH2-HRP [pH7, 0.25]	374 (25)	246 (46)	0.793 (0.065)	15.7 (4)
	BIS (PAH) pH5-HRP [pH7, 0.25]	267 (29)	165 (23)	0.835 (0.106)	18.8 (9)
	BIS (PAH) pH7-HRP [pH7, 0.25]	294 (31)	159 (54)	1.018 (0.154)	16.8 (7)
	BIS (PEHA) pH2-HRP [pH7, 0.25]	306 (138)	55 (12)	0.259 (0.195)	6.2 (1.8)
	BIS (PEHA) pH5-HRP [pH7, 0.25]	357 (55)	26 (7)	0.134 (0.016)	5.3 (0.5)
	BIS (PEHA) pH 7-HRP [pH7, 0.25]	295 (30)	33 (7)	0.171 (0.058)	5.4 (0.3)
	BIS (PAH) pH7-HRP [amine, 0.25]	220 (23)	136 (18)	0.513 (0.029)	18 (3)
	BIS (PAH) pH7-HRP [silicate, 0.25]	203 (31)	123 (7)	0.521 (0.056)	17 (3.7)
	BIS (PAH) pH7-HRP [mixture, 0.25]	214 (27)	139 (14)	0.541 (0.096)	17 (3)
	BIS (PEHA) pH 7-HRP [amine, 0.25]	218 (46)	20 (5)	0.105 (0.007)	7.3 (1)
	BIS (PEHA) pH 7-HRP [silicate, 0.25]	256 (45)	20 (3)	0.107 (0.005)	7 (1)
	BIS (PEHA) pH 7-HRP [mixture, 0.25]	231 (42)	17 (3)	0.095 (0.017)	7 (2)
	BIS (PAH) pH5-HRP [pH7, 0.1]	260 (30)	173 (26)	0.748 (0.097)	17 (2)
	BIS (PAH) pH5-HRP [pH7, 0.17]	286 (24)	194 (5)	0.868 (0.383)	18 (8)
	BIS (PAH) pH5-HRP [pH7, 0.4]	344 (0)	155 (17)	0.831 (0.049)	18 (2)
	BIS (PEHA) pH5-HRP [pH7, 0.1]	449 (42)	86 (15)	0.275 (0.103)	5.7 (0.4)
	BIS (PEHA) pH5-HRP [pH7, 0.17]	385 (14)	32 (3)	0.140 (0.002)	6 (0.6)
	BIS (PEHA) pH5-HRP [pH7, 0.4]	239 (36)	18 (3)	0.109 (0.045)	4 (2)

5.2. Adsorption of HRP on BIS

Adsorption of HRP on BIS and on commercial silica was examined in order to compare in-situ immobilisation with traditional adsorption. Adsorption has been well established as an immobilisation method as discussed in section 2.1, especially when a functionalised support is used to enhance retention of an enzyme. Given the built-in functionality of BIS derived from the presence of amines used as building blocks, BIS is expected to perform better than pure silica without functionalisation as a support for enzyme adsorption. The point of this comparison is not to examine in detail the potential of BIS as an immobilisation support for enzyme adsorption, but to directly compare with encapsulation. Similar work in terms of comparison was done by our group [315] examining encapsulation of ibuprofen in BIS during formation and compared it with adsorption of ibuprofen on MCM-41. It was shown that despite the higher immobilisation efficiency achieved with MCM-41, drug content was much lower than in examined BIS samples. Similarly, immobilisation of lipase was examined by in-situ encapsulation in BIS and by adsorption post material synthesis, showing higher immobilisation efficiency for encapsulation, but higher activity retention for adsorption [325]. Herein, immobilisation of HRP on BIS in situ is compared to both adsorption of HRP on BIS post synthesis as well as adsorption of HRP on a commercial silica.

5.2.1. Effect of type of silica in ex situ HRP immobilisation

BIS was synthesised using PEHA or PAH as additive and furthermore post-synthetic acid elution was performed to obtain BIS with full amount of additive present (pH 7), partial additive removal (pH 5) or more extended additive removal (pH 2). The commercial silica, Syloid, type AL – 1FP, was used as a comparison with purified BIS (pH 2). AL – 1FP is a product of GRACE® [407], applied in drug delivery [408]. It was chosen over other silicas, such as MCM-41, because it is already commercially available in a large scale, while other mesoporous silicas (e.g. MCM-41) are not. A comparison of porosity of Syloid and BIS before HRP adsorption (Table 5-5) showed that Syloid has considerable higher surface area compared to BIS (almost double of BIS-PAH). Syloid appeared to be microporous, as the non micropore surface area was estimated at about a sixth of the total surface area, 100 m^2/g. Syloid was deemed similar to BIS synthesised with PEHA as additive, due to the similar value of available surface area pore volume.

Comparing BIS synthesised herein with mesoporous materials found in literature, BIS shows similar pore size to many ordered silicas with pore range of up to 20nm [405], however, BIS is not ordered, and the measured pore size is not representative of the bulk material. Although surface area and pore volume values for BIS synthesised with PAH as additive are high and imply high expectations, it does not mean that the full potential of the material is exploitable, as pores might be too narrow, tortuous, or not connected to a pore network. We will engage in further analysis on this argument in Chapter 6.

Table 5-5: Comparison of porosity of silicas used for HRP adsorption, before and after enzyme adsorption. Results represent the average value of 2 or more replicates, with the value in parenthesis being 1 standard deviation.

	Type of silica	Total surface area (m^2/g)	Non micropore surface area (m^2/g)	Pore volume (cm^3/g)	Average pore size (nm)
Silica	Syloid Al-1FP	664 (5)	103 (17)	0.210 (0.005)	2.5 (0.1)
	BIS (PAH) pH2	285 (93)	203 (41)	0.381 (0.149)	15.4 (3.2)
	BIS (PAH) pH5	294 (19)	224 (8)	0.747 (0.098)	15.4 (2.8)
	BIS (PAH) pH7	313 (53)	227 (27)	1.141 (0.060)	21.1 (2.2)
	BIS (PEHA) pH2	604 (12)	69 (19)	0.337 (0.182)	5.1 (1.8)
	BIS (PEHA) pH5	174 (20)	14 (1)	0.079 (0.026)	3.4 (1.4)
	BIS (PEHA) pH 7	294 (16)	18 (6)	0.109 (0.016)	6.1 (0.7)
Silica-HRP	Syloid Al-1FP-HRP	632 (18)	38.3 (2.8)	0.119 (0.010)	2.50 (0.01)
	BIS (PAH) pH2-HRP	49.0 (0.4)	47.1 (3.2)	0.106 (0.004)	6.6 (0.7)
	BIS (PAH) pH5-HRP	115.0 (0.4)	110 (6)	0.16 (0.01)	5.7 (0.3)
	BIS (PAH) pH7-HRP	122.4 (0.3)	118.0 (0.8)	0.200 (0.007)	6.90 (0.01)
	BIS (PEHA) pH2-HRP	90.8 (16.8)	15.9 (2.5)	0.020 (0.003)	4.1 (1.6)
	BIS (PEHA) pH5-HRP	16.1 (6.6)	7.71 (0.06)	0.013 (0.003)	4.0 (0.5)
	BIS (PEHA) pH 7-HRP	18.8 (0.4)	16.7 (0.6)	0.021 (0.002)	5.12 (0.86)

Maintaining standard conditions during immobilisation with respect to time and temperature of adsorption, as well as a ratio of support to available concentration of HRP calculated to ensure equal availability to encapsulation experiments, the adsorption of HRP on different silicas was examined. For the adsorption of HRP on Syloid, the conditions used were the same as for BIS-PEHA pH 2 samples. This was deemed equivalent based on the similarity of the material. The rationale behind calculating the equivalent HRP quantities to be used for adsorption, was to have the same starting basis of silica and enzyme, as in the case of in-situ encapsulation. This was decided due to the non-linear or straightforward trends shown in the case of in-situ encapsulation, due to the unidentified contribution of HRP during BIS synthesis. Therefore, trying to keep a common point and facilitate comparison, the initial enzyme mass to adsorbent mass was chosen, based on obtained mass for BIS in absence of HRP. From the obtained results on HRP adsorption, it was noted that for most examined silica samples, majority of HRP was adsorbed within 1-4h (Figure 5-22). This behaviour is quite typical for adsorption of substances onto supports and has been observed also for adsorption of enzymes on solid supports [18, 324, 335]

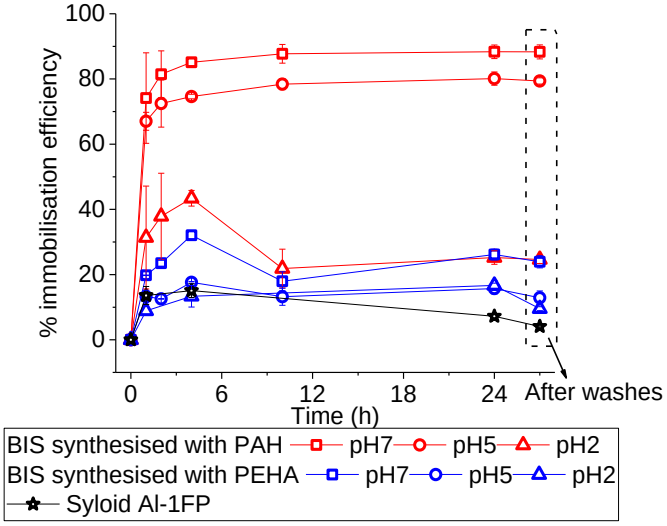

Figure 5-22: Immobilisation efficiency over time and after washing for HRP adsorbed on different type of silicas. Efficiency was measured using Bradford assay. Results shown are the average of 2 or more replicates, with the error bar representing 1 standard deviation.

It was noticed that for silicas with absence or lower presence of functionalisation, or with pore sizes larger than the HRP size (largest dimension is about 6nm), there was a small percentage of HRP desorption over time, until a new equilibrium was reached. This can be attributed to the weak initial adsorption, which over time equilibrated to the actual capacity. Similar effects have been observed in literature. For cellulase adsorption on cellulose, it was shown that after a rapid adsorption, desorption followed, leading to equilibrium about 50% lower than initially adsorbed[409]. In order to test the robustness of immobilisation by adsorption, after the 24hr of adsorption, samples were isolated and washed twice, with water and supernatants were assessed for protein content using Bradford assay. From the results it was clear that HRP adsorption on BIS-PAH was robust, regardless of pH, as hardly any loss of adsorbed enzyme was observed. However, for all other samples (BIS-PEHA and Syloid), HRP loss was increased upon washing. As the HRP adsorption is governed by the pore sizes, surface area and the surface chemistry, these results are not surprising. For BIS-PAH samples, amine functionalisation to available surface area and in the mesopore range allows for higher loading into the pores rather than just extended surface. In the case of Syloid and BIS-PEHA pH 5 and pH 2 (partial and complete removal of additive respectively), immobilisation of HRP is only achieved through weak physisorption on the surface area of the material, predominantly externally. For BIS-PEHA pH 7 samples, adsorption is enhanced compared to BIS-PEHA pH 5 and pH 2, fact attributed to the presence of amine functionalisation on the surface area, but results are not as high as for BIS-PAH. The w/w loading of HRP on BIS achieved through adsorption is shown in Figure 5-23. As we can see, BIS-PAH pH 7 and pH 5 show the highest loading, around 10%, followed by BIS-PEHA pH 7 at 5%. Loading for BIS-PAH pH 2, BIS-PEHA pH 5 and BIS-PEHA pH 2 is similar, around 3% and Syloid shows the weakest performance, with just about 1% HRP per mass of composite.

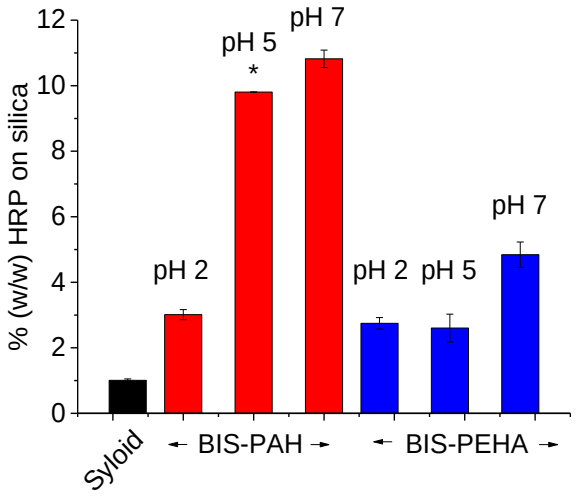

Figure 5-23: w/w of enzyme per support mass for HRP adsorbed on different silicas after 24h. Results shown are the average of 2 or more replicates, with the error bar representing 1 standard deviation. For BIS-PAH, pH 5, standard deviation is 0.00613, hence the error bar is not visible.

The results showed in both Figure 5-22 and Figure 5-23 are in good agreement with porosity of the composite materials as shown in Table 5-5. In every case of HRP adsorption on silica there was reduction in the surface area and the pore volume of the composite after adsorption, indicative of HRP occupation of pores. BIS synthesised with PAH with no additive removal (pH7) showed the best immobilisation efficiency and HRP retention on BIS, which is expected given the higher pore volume and pore size compared to other BIS. BIS-PAH pH 5 showed similar, only slightly lower, HRP loading. This is expected, as both BIS-PAH pH 7 and pH 5 samples had a high pore volume and similar surface area and pore sizes. Further, for polymeric additives like PAH, the removal of the additive through elution at pH 5 is small. For BIS-PEHA samples, only small parts of the additive are available on the external surface area and due to the pore sizes only small part of the porous structure is accessible by HRP during immobilisation. PAH, being a polymeric amine, theoretically allows for higher concentration of available attachment points for HRP as it was indirectly indicated by FTIR measurements of the amine-derived peaks due to C-N, N-H and C=O bonds (Figure 5-7). Scheme 5-2 shows graphically the differences between the 3 main supports used for enzyme adsorption, BIS-PAH, BIS-PEHA and Syloid, based on the aforementioned discussion. There are various examples in literature that examine the adsorption of enzymes on functionalised supports, leading to a conclusion that, up to a point, higher density of functional groups leads to generally higher immobilisation efficiency [229, 410, 411]. Results in Figure 5-23 also show that BIS with all 100% of the additive present shows higher protein loading efficiency compared to BIS treated post synthesis via acid elution (pH 7 vs pH 5 and pH 2).

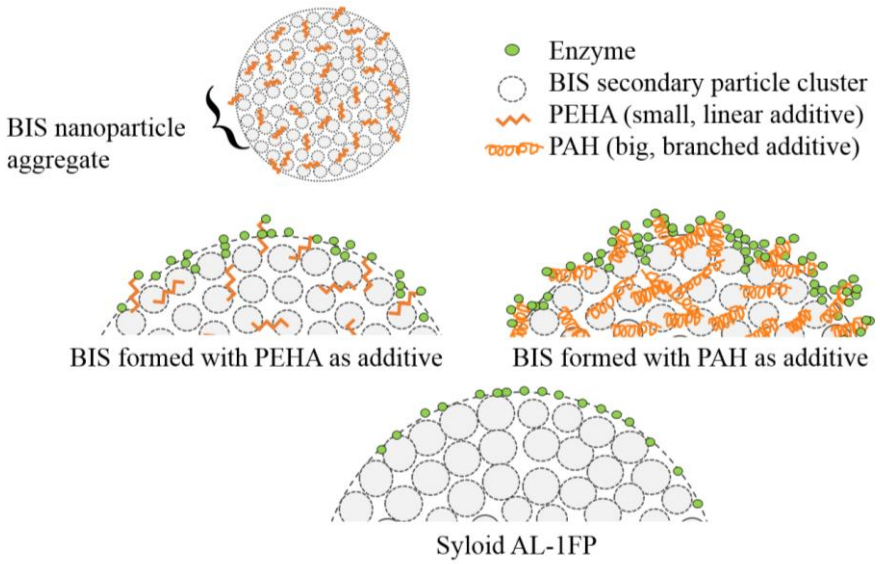

Scheme 5-2: Illustration of HRP adsorption on BIS and Syloid.

Another very important factor when adsorption of enzymes on solid supports is examined, is the surface area and the pore size of the material. As also verified here, materials with very small pore size are not very successful immobilisation supports for enzymes of molecular size larger than the pore opening, as adsorption occurs predominately in the external surface area [412, 413]. Through an extensive analysis of adsorption of various enzymes on various MSNs under varying conditions, it was shown that besides the porosity of the materials, charges are also massively affecting immobilisation, as they affect electrostatic interactions between the support and the enzyme [412]. As discussed earlier, silica is negatively charged in any pH above 2-3 (isolelectric point of silica). Furthermore, given the isolelectric point of HRP around pH 5, in any solution of pH higher than that, HRP is negatively charged. Given the pH 7 of the solution during adsorption, HRP is slightly negatively charged, fact that indicates possibility of weak interactions between the positively charged areas of the enzyme and the predominantly negatively charged support. Last but not least, amines are positively charged in any solution of pH lower than 13. Since adsorption of HRP in BIS and Syloid occurs in deionised water (measured pH of about 6), the charge of HRP is partially negative, charge of silica is mostly negative and the charge of the additive present is mostly positive. This can also explain the lower immobilisation efficiency in absence –or lower presence– of positively charged additive, as was demonstrated in detail be Deere [412]. Herein this is illustrated by the relatively low adsorption of HRP on Syloid (about 10%) and on BIS synthesised either with PEHA or PAH with the additive being eluted at pH 2 (efficiency of 12% and 21% respectively). There are similar examples in literature, examining efficiency of enzyme adsorption on solid supports with alternating pH of the system's solution, showing that the higher the difference in charge between the support and the enzyme, the higher the adsorption efficiency. This was clearly demonstrated by Shakeri [156] who examined adsorption of DyP4 (isoelectric point of 4.2) in functionalised mesocellular foams in a pH range of 3 to 6. They showed that solution's pH was crucial for adsorption, as it affected the charge, hence the

interactions between the support and the protein. In another relevant study[296], Hudson et al. showed comprehensively the importance of surface charge interactions between the silica supports and the enzyme for immobilisation, concluding that it is difficult to differentiate between hydrophobic and electrostatic interactions and that not all supports are equally prominent for adsorption of a specific enzyme. This is in alignment with work shown herein, as two different supports are examined, showing different adsorption efficiency for the same enzyme.

5.2.2. Effect of amount of HRP in ex situ immobilisation

In order to compare the capacity of BIS for HRP immobilisation via adsorption with that measured for encapsulation, BIS synthesised with PAH or PEHA as additive, with acid elution to partially remove the additive (pH5) were used as the adsorbents. Results (Figure 5-24) indicate a clear superiority of encapsulation as an immobilisation method, with respect to how much enzyme was able to be immobilised.

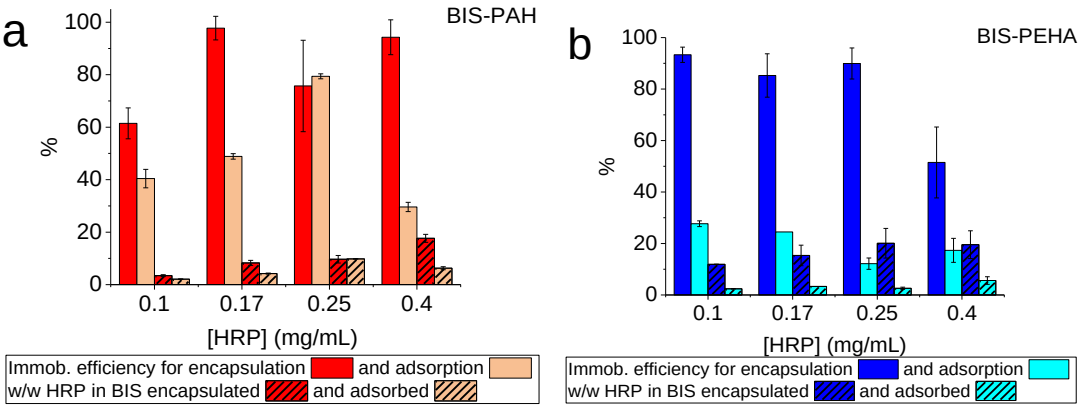

Figure 5-24: Comparison of immobilisation efficiency and HRP in BIS composite (w/w) between encapsulation and adsorption of HRP on BIS synthesised with a) PAH or b) PEHA as additive, with the additive eluted at pH5. Results shown are the average of triplicates, with the error bar representing 1 standard deviation.

Especially when PEHA was used as the additive, immobilisation via encapsulation lead to almost five times higher efficiency compared to adsorption for the lower amounts of enzyme. When immobilisation of the highest quantity of HRP was examined, encapsulation was just over 2 times more effective than adsorption. In the case of PAH, results again favour encapsulation over adsorption, but not as prominently as PEHA. These results could be potentially explained by the concentration of enzyme during the adsorption experiments. Although the ratio of BIS to HRP was kept the same as in encapsulation, the system volume was different. In encapsulation experiments, system's volume was 50mL, whereas in adsorption experiments system's volume was 25mL. Given the circumneutral conditions of the experiment, higher enzyme concentration could indicate intensification of lateral repulsion between negatively charged HRP molecules, which might have resulted in their stabilisation in solution and repulsion from the positively charged amines present. This, combined with the negatively charged silica bed, could lead to reduced adsorption efficiency. Furthermore, another issue that could be occurring is the adsorption of HRP molecules at the entrance of pores, preventing diffusion and adsorption of

enzyme inside the pore structure. It has been shown in literature that high concentrations of enzyme might lead to immobilisation efficiency lower than the assumed capacity of the adsorbent, due to competitive interactions or collisions between the enzyme molecules and the sites for adsorption [264, 414].

For reference, adsorption of increasing quantity of HRP was also examined for Syloid AL-1FP and results were compared to adsorption of HRP on BIS (Figure 5-25).

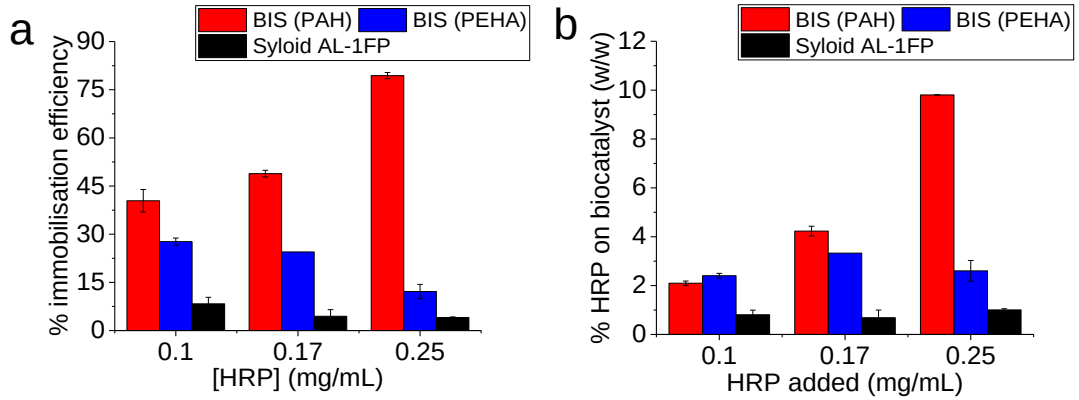

Figure 5-25: Comparison of effect of added mass of HRP on a) immobilisation efficiency and b) quantity of HRP on the biocatalyst. Results shown are the average of triplicates, with the error bar representing 1 standard deviation.

There is an evident superiority of BIS compared to commercial silica as a support for enzyme adsorption, regardless of the quantity of enzyme added. Even at a low initial concentration (5mg HRP added at 50mg support, leading to 0.1mg/mL initial HR concentration), Syloid shows very low ability to adsorb HRP, leading to a mere 1% of enzyme on the biocatalyst (Figure 5-25b). Given the constant amount of enzyme adsorbed on Syloid regardless of the increased initial mass of HRP, it is safe to assume that about 1% is the maximum achieved loading of HRP on Syloid, compared to the almost 10% achieved when BIS was used as immobilisation support for adsorption. The difference between BIS and Syloid AL-1FP is attributed to amine functionalisation being present in BIS given the use of amino-containing additives for its synthesis (PAH and PEHA).

5.3. Leaching

Given the encapsulation of enzyme occurs during the formation of BIS nanoparticles, hence entrapped within the porous structure, it is expected that leaching will not be high. Leaching studies on in-situ enzyme encapsulation in BIS showed minimal to no release of enzyme over time, fact attributed to the small pore channels of BIS, which prevented leak of entrapped enzymes [215, 221, 236, 327]. Herein, leaching of HRP from the BIS structure was observed over 48h, for selected BIS-HRP samples synthesised with PAH or PEHA as additive, using suitable BIS controls to rule out BIS contribution to the assays. Supernatants were assayed both using the Bradford assay and an activity assay. Results (Figure 5-26a) show an interesting pattern, where there is a high value of protein detected by the Bradford assay during the 1st hour of the study, which however reduces

over the duration of the study. When assayed for enzymatic activity (round, overlapping symbols in Figure 5-26a for all measured samples) using the very sensitive ABTS assay, supernatants showed no activity. The absence of activity could be attributed to either absence of enzyme in the solution, or enzyme being present but deactivated, hence showing no activity. Given the low stability of low concentration of HRP in solution, as shown in Figure 4-6 of Chapter 4, the latter explanation could be plausible. However, if such occurred, Bradford assay should show indications of protein presence in the consecutive time points as well, not only the 1st one. There are two possible explanations for the discrepancy observed between Bradford and activity assay. The first would be that there is HRP leaching from the composite during the 1st hour, which however gets adsorbed on BIS, hence the reduction in the subsequent measurements. The absence of enzymatic activity determination at the 1hr point would mean that the enzyme is deactivated. The second explanation would be that the initial measurement based on Bradford assay has wrongly identified HRP being present, and the enzymatic activity corroborates this statement. The obtained signal could be due to either nanoparticles in the supernatant sample which caused scattering, or due to released amines which caused a colour-forming reaction with the Bradford reagent. Given the previous analysis on issues faced with the Bradford assay (see section 4.3.2 in Chapter 2), the 2nd explanation is deemed as more plausible.

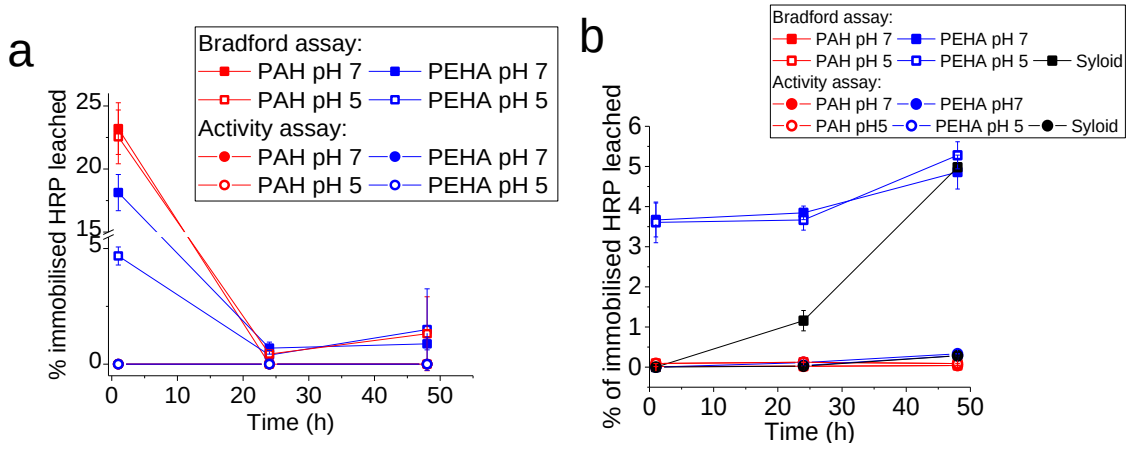

Figure 5-26: Leaching examination of HRP a) from BIS-HRP composites obtained via in-situ encapsulation and b) from BIS-HRP and Syloid-HRP composites obtained via adsorption. 2 assays were used, Bradford assay and activity assay using ABTS as substrate. Results shown are the average of 2 or more replicates, with the error bar representing 1 standard deviation.

When immobilised HRP on BIS or Syloid via adsorption was examined, (Figure 5-26b) HRP adsorbed on BIS-PAH samples showed no leaching, regardless of the presence of additive, indicating a strong adsorption. For BIS-PEHA of pH 7 and pH 5 some leaching was noticed within the 1st hour of examination, which progressively increased until the end of the examination period, reaching a 5% of adsorbed enzyme loss. Syloid also showed leaching, resulting in a similar value at the end of the examination. It is worth mentioning that the aforementioned results were obtained using the Bradford assay for protein detection, while the activity assay using ABTS as substrate did not return any results for any of the examined samples (flat, horizontal lines in (Figure 5-26b).

The difference shown between the assays could be attributed to amines or nanoparticles being present in the system, causing interference to the Bradford assay, in addition to leached enzyme gradually getting deactivated over time.

In any case, the highest leached amount of HRP by the end of the leaching study for encapsulated HRP was no more than 2.5% of the HRP quantity originally present in the composite and no more than 5% of the HRP quantity originally present in the composite in the case of adsorbed HRP on BIS or Syloid. This low percentage shows that BIS is a reliable support for leach-proof immobilisation of enzymes.

5.4. Comparison of findings for BIS-HRP with literature (w/w loading, porosity, leaching)

5.4.1. Loading of HRP on BIS

With respect to the obtained mass of enzyme per mass of BIS composite, the maximum value obtained herein –just below 20% w/w for 20mg HRP added during BIS synthesis with subsequent additive removal through acid elution at pH5– as shown in Figure 5-25b is comparable with other reports of enzyme immobilisation in BIS. Luckarift reported a 20% (w/w) loading of butyrylcholinesterase [415], while a just over 20% (w/w) for lipase in BIS was reported by Forsyth [215] and a range between 10-30% (w/w) was reported by Steven [299] for calcein encapsulated in BIS. The value reported here is higher than the maximum value reported for enzyme immobilisation in sol-gel materials (about 5% w/w with some great examples reaching 10% w/w) [416]. In some outstanding cases, immobilisation was able to achieve just over 50% w/w loading of carbonic anhydrase on functionalised mesoporous silica supports [417] and of lysozyme on mesoporous silica supports [418]. Such a high loading was possible due to advantageous interactions between the enzyme and the support and a combination of large pore structures. Research examples specifically looking at immobilisation of HRP that report a final loading of enzyme mass per support mass were difficult to find as majority of examples focus on activity. A vague report by [416], shows a range between 1-5% (w/w), without details being disclosed, and [419] reported a value of 3.4mg HRP adsorbed on fumed silica, corresponding to a 0.34% w/w, followed by a later report [18] of a value of almost 3mg HRP adsorbed per g kaolin, corresponding to 0.3% w/w. Another report resulted at an almost 5% w/w of HRP immobilised on Eupergit®C support via covalent bonding [420]. The maximum values found in literature were almost 13%, reported for immobilised HRP on zinc oxide using epoxy cross linkers [335], 10%, reported for immobilised HRP on graphene oxide by adsorption [381] and 8% w/w reported for co-precipitated HRP with $CaCO_3$, before cross-linking the loaded particles with glutaraldehyde and remove the inorganic template [421].

5.4.2. Porosity

Compared to mesoporous silica materials, BIS does not exhibit the ordered pore structure. In this case, the synthesis method dictates random aggregation of primary particles to form nanoparticles

and as a result the final materials, might show large surface area and promising pore volumes (such as 603m^2/g and 0.344cm^3/g respectively for BIS-PEHA pH 2). However, in reality, due to large tortuosity and non-ordered structure of the pore channels, BIS materials might not offer a viable system for immobilisation of large molecules. Difficulties arise from the high micropore volumes, which might indicate large porosity, however porosity might not be usable if the molecules to be diffused (e.g. substrate, product) are larger than not only the pore opening, but the pore channel width as well, which for uneven and tortuous channels can be significantly different and unpredictable. Using the BIS-PEHA pH 2 example, the non micropore surface area is 72m^2/g, indicating that the rest is due to micropores existence (pore size < 2nm). An illustration of the aforementioned arguments is given in Figure 5-27 and Figure 5-28a and b, showing the pore hierarchy, potential pore shapes and the assumed porosity of BIS respectively.

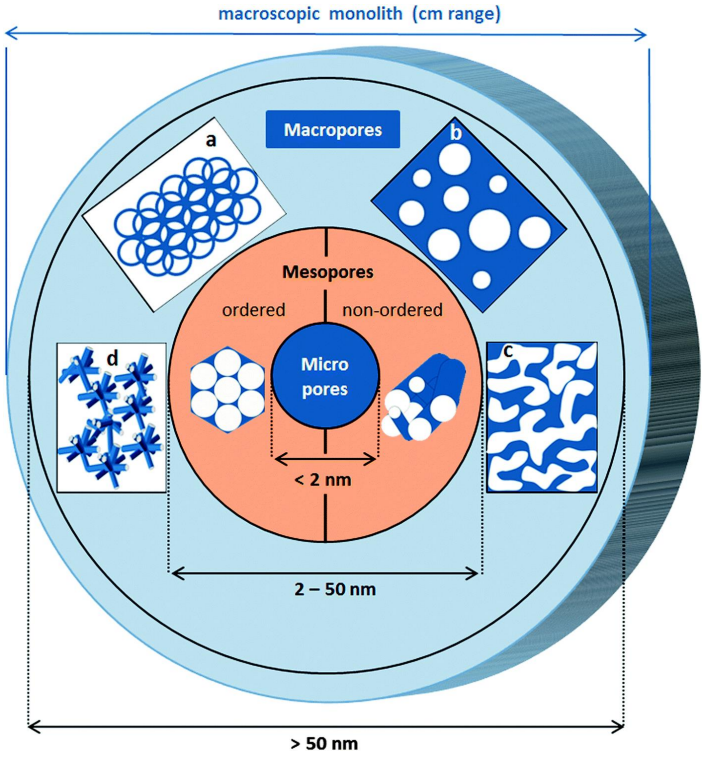

Figure 5-27: Pore size hierarchy and pore shapes in porous materials. 3 size ranges of pores, macropores (light blue circle, >50nm), mesopores (orange circle, 2-50nm) and micropores (dark blue circle, <2nm. Different pore arrangements are shown, such as (a) inverse opal-like structures, (b) isolated pores, (c) co-continuous porosity, and (d) a cellular build-up (in the scheme, the blue part represents the solid network, the white part is the pore space). Furthermore, well-organized pores with monomodal character as shown for a 2D hex structure (left hand side in orange circle) or disordered pore arrangements (right hand side in orange circle) are possible. Image taken from [422].

Due to the disordered nature of BIS pore network, it is assumed that pores can have all possible shapes shown in Figure 5-28a. Based on the difference between the pore size estimation from the adsorption and desorption isotherm produced from porosimetry measurements; the later showing reduced values, pore shapes are expected to be closer to (ii) and (iv) type, potentially with large pore opening, leading to micropore networks. These arguments on BIS pore channel tortuosity and disordered shape of pores can explain why loading was not higher, given the available pore volume. With respect to the effect of enzyme immobilisation on porosity of the composite, we

can say that although there was not an overall commendable difference on porosity when HRP was encapsulated, for specific samples there was substantial difference. In such cases, porosity difference was attributed to fundamental changes to BIS aggregation pattern and structure, as indicated by USAXS analysis.

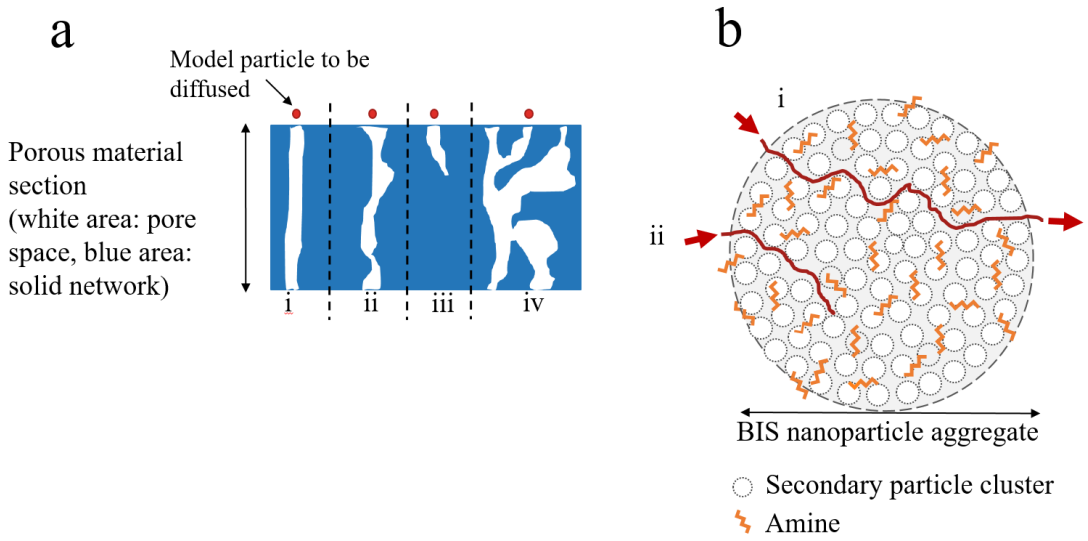

Figure 5-28:Illustration of a) pore channel structures and b) BIS nanoparticle aggregate based on secondary particle clusters connected with amines. a) i: ordered, uniform sized pore, ii: tortuous pore, iii: dead-end pore, iv: connected pore network. Diffusion of a model particle (red) is possible only in cases (i) and (iv), b) points (i) and (ii) represent the ability for diffusion or not respectively, due to tortuosity and micropore structures.

On the other hand, there was substantial porosity reduction upon adsorption of HRP on BIS or Syloid, given the expected volume occupation by HRP. Such behaviour has been observed in literature, with many examples of immobilised enzymes via adsorption, such as lipase and BSA adsorbed on mesoporous silicas, showing a 20-30% and 50-60% pore volume reduction respectively [423]. Another example showed a considerable reduction of surface area and pore volume (up to almost 50% and 25% respectively) upon adsorption of carbonic anhydrase and HRP on colloidal mesoporous silica nanoparticles [424]. When adsorption of lysozyme on mesoporous silicas was examined, it was shown that due to the large pores and small enzyme size, as well as favourable charge interactions, surface area was significantly reduced (more than 80% for bimodal UVM silicas), indicating high enzyme loading (up to 35% w/w was measured)[425]. On a lower scale, upon adsorption of HRP on mesoporous silica (SBA-15), surface area and pore volume of the composite were reduced after the immobilisation, but not substantially compared to the initial values, indicating residence of the enzyme in micro-channels of the material as opposed to the "bulk pore volume" [426].

5.4.3. Leaching

During enzyme immobilisation, the ability of the support to securely hold the enzyme is of great importance, affecting mainly the reusability of the biocatalyst and purity of the reaction bulk, but ultimately being linked to the cost of the process. There are many systems that can be used successfully in immobilisation, but due to adverse operational conditions the enzyme leaches

from the support. One such system is use of alginate beads, due to large pores and the lack of mechanical strength, which leads to easy rupture and enzyme loss, especially if immobilisation conditions are not optimised [97, 108, 235, 427]. It has been shown however that incorporation of a silica layer around alginate-based immobilised enzyme systems can minimise leaching, due to higher mechanical strength and better control of porosity [217, 235, 428].

In the case of mesoporous silicates, leaching can occur when the attachment of enzyme on the porous support is due to weak (or pH dependant) electrostatic interactions [266, 296]. In one example, a "layering" methodology was used, in order to protect adsorbed catalase on mesoporous silicates. It was shown that although during the layering of the loaded silicate with a polyelectrolyte, enzyme got partially desorbed, the residual enzyme quantity got entrapped into the pores and its stability was enhanced [234]. An extensive analysis by Lynch [305] on leaching of physically adsorbed enzymes on SBA-15 of controlled various pore sizes, showed that leaching depends both on the pore size, as well as on the electrostatic interactions between the support and the enzyme. It was shown that up to 35% of myoglobin can leach at pH 7.6, but with increased pore size of the support, leaching can be reduced to 15%. This was attributed to the neutral charge of myoglobin at this pH, which reduced electrostatic interaction with the support. When immobilisation of HRP was attempted on composites of zinc oxide and silica using either physical adsorption or a cross linking approach, an analysis on leaching of enzyme over 50 h showed that HRP adsorbed on the composite leached 100% more compared to the cross linked enzyme, leading to a loss of 40% of initially bound enzyme [335].

With respect to in-situ entrapment of enzymes in BIS, it was shown from our group for lipase and carbonic anhydrase immobilisation, that leaching was either not observed at all, in the case of lipase, [215], or was less than 10%, in the case of carbonic anhydrase over the course of 1 week [327]. This indicates successful and secure encapsulation inside the pore network, supporting the findings of this project, where leaching was not observed in the case of HRP encapsulated in BIS and it was less than 5% of the immobilised enzyme in the case of HRP adsorbed on BIS. Other research examples of enzymes in-situ encapsulated in bioinspired and biomimetic silicas, looking at carbonic anhydrase [328], β-glucuronidase [221, 364], butyrylcholinesterase [415] and horseradish peroxidase [429], also support our findings, as leaching of immobilised enzyme was not observed.

5.5. Conclusions

In this chapter, the immobilisation of Horseradish Peroxidase (HRP) was explored via in-situ encapsulation in Bioinspired Silicas (BIS) and post-synthetic adsorption on BIS. Through a systematic approach, factors affecting immobilisation were identified and their effects analysed. These factors included the type of additive used for BIS synthesis and the controlled removal of it post-synthesis, the point during synthesis at which HRP was added for in-situ immobilisation and the amount of HRP added for immobilisation. When HRP was adsorbed on BIS, the examined

factors were the type of BIS used (based on additive used for its synthesis and the post-synthetic removal of it) and the amount of HRP added for immobilisation via adsorption.

The conditions of immobilisation are important for the efficiency of the procedure in regards both to how much enzyme is retained and how much is the percentage of enzyme on the final mass of the biocatalyst. The findings from examining the point of addition of HRP during BIS synthesis indicate a yet undefined effect of the presence of protein during materials synthesis and in-situ immobilisation, influencing synthesis and porosity of procured materials, as well as the efficiency of immobilisation. Although further extensive work is needed to fully explain this effect, speculations point to the direction of electrostatic interactions between HRP and additives, which strongly affect BIS synthesis. The exploration of in-situ immobilisation and additive removal through acid elution was also examined in order to develop a 1-pot procedure allowing tailored synthesis and immobilisation. It was shown that additive elution had an effect on the porosity of the obtained materials, and also on the amount of retained HRP, as the enzyme got partially eluted as well. Increasing the quantity of HRP introduced for in-situ immobilisation led to a plateau and even slight decrease of the amount of enzyme retained. Upon examination for leaching, none of the examined samples showed considerable leaching of HRP.

A comparison between encapsulation and adsorption of enzyme in the same types of BIS, showed that the type of additive which is used to initiate BIS synthesis has an important role in adsorption, as it acts in a similar way to post-synthetic chemical functionalisation, enhancing immobilisation efficiency through strong electrostatic interactions. It was shown that higher functionalisation present (i.e. no additive eluted) led to higher percentage of HRP adsorbed on BIS. Increasing the amount of HRP introduced for adsorption led to increased amount of HRP retained, up to a point where higher quantity made no difference. When compared with a commercial silica, BIS shows much higher potential as immobilisation support based on the amount of enzyme that can be encapsulated or adsorbed. Immobilisation of HRP in BIS resulted in a maximum of 20% mass of HRP per mass of biocatalyst composite, value higher than other examples found in literature. Analysis of leaching of immobilised HRP from the obtained biocatalysts resulted in no leaching in the case of in-situ encapsulation and minimal leaching (less than 5%) in the case of adsorption. This corroborates the argument that BIS is a promising support for immobilisation, which however still needs optimisation in order to enhance results even more.

Chapter 6 : Performance screening of free and immobilised Horseradish Peroxidase (HRP)

After having explored different immobilisation strategies of HRP with respect to immobilisation efficiency, porosity and morphology, in this chapter, we explore the performance of the immobilised HRP samples. The parameters examined for their effect on immobilisation efficiency in Chapter 5 (immobilisation by encapsulation or adsorption, additive used during BIS synthesis, point of HRP addition during encapsulation, the possibility for additive elution, amount of HRP added for immobilisation) are examined again, in terms of their effect on the biocatalyst's activity. This Chapter results with the identification of the samples to be taken forward for further characterisation of the immobilised HRP. The aim is to identify the optimum immobilisation strategy for best performance, while simultaneously describing what "best performance" is. Performance is assayed using 2 different assays as described in Chapter 4. The first assay is directly relevant to peroxidase activity and the second one is based on a realistic application, in order to explore the industrial potential of the biocatalyst.

6.1. HRP encapsulated in BIS in-situ

6.1.1. Effect of additive used

As discussed in section 5.1.1 but also throughout Chapter 5, the additive is quite important during BIS synthesis, as it leads to materials with different structure, porosity and functionalisation. Use of PEHA (small, linear amine) led to mostly microporous materials, whereas use of PAH forms BIS with distinct pore sizes and increased pore volume and available surface areas. Given the structural differences of the biocatalysts produced via encapsulation of HRP in BIS synthesised with PAH or PEHA as additives, different performance is expected. Performance was assayed using both the ABTS and RB19 standard assays, on the same quantity of BIS-HRP composite. This indicates that the amount of HRP present might not be the same, but corrective measures were put in place in an effort to normalise the results and be able to compare the results. Samples examined in this instance are BIS-HRP composites synthesised by addition of an initial concentration of HRP equal to 0.25mg/mL, during synthesis of BIS using PAH or PEHA as additive, at a circumneutral pH (pH 7.0 ± 0.1). Obtained results using the ABTS or the RB19 assay are shown in Figure 6-1, examining the performance over a course of 48h with 4 time points of observation. The extension of the assay to 48h was deemed necessary, as upon initial experimentation with the original 10min of assaying the absorbance (as developed for the free enzyme), results were not conclusive on the potential of the biocatalysts.

What is immediately noticeable from both graphs of Figure 6-1 is that BIS-HRP synthesised with PAH performs generally better (higher production of oxidised ABTS and higher decolorisation of RB19). Looking at the performance of the samples based on the ABTS assay, a common trend

is identified, where while oxidation of ABTS seems to increase, after a point a noticeable drop is occurring.

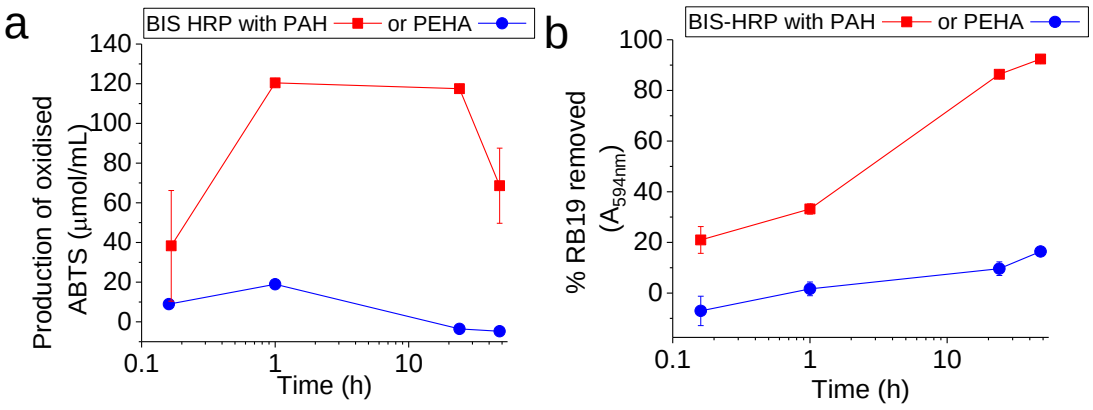

Figure 6-1: Performance of BIS-HRP synthesised with either PAH or PEHA as additive, with the same initial amount of HRP added for in situ encapsulation, examined under standard assay procedure using a) ABTS or b) RB19 as substrate. Results shown are the average of 3 or more replicates, with the error bar representing 1 standard deviation.

In order to explain these observations, a few points need to be discussed. These points are: a) concentration of HRP in BIS-HRP, b) structural differences between samples, c) mechanism behind assay, and d) contribution of the support. Starting with the concentration of HRP in the BIS-HRP composites, although the amount of HRP added during immobilisation was the same, the amount retained was different. Looking at Figure 5-1a of Chapter 5, we can see that the amount of HRP present in BIS-HRP composite is about 10% (w/w) in both cases. This indicates that observed differences are not due to less HRP being present, but they might be due to less enzyme being available.

This leads us to examination of the second point, the structural differences between the composites. Characterisation of the samples done through porosimetry showed that PAH leads to BIS with much higher porosity (pore volumes can be over 1 cm^3/g and available surface areas are much higher, compared to 0.1 cm^3/g and low surface areas measured for BIS-PEHA samples, please refer to Table 5-4 and Figures 5-3 and 5-4 in Chapter 5). This knowledge, combined with the performance of the samples in both assays, indicates that structure of BIS-HRP synthesised with PAH offers better accessibility of the enzyme (pores of average size of 20nm were measured, compared to 6nm average size of BIS-PEHA pores), allowing substrate to reach the inside of the structure and product to flow to the bulk. In the case of BIS-HRP synthesised with PEHA, the enzyme is there, but is not accessible to substrates, probably due to the combination of micro porosity, tortuosity and the localisation of HRP in the composite.

Moving on to having a closer look at the mechanism of action of the assays in presence of BIS-HRP composite, there are some interesting observations to be made. In the case of ABTS assay, unreacted ABTS needs to diffuse through the pore system and find the HRP which should be excited by the presence of peroxide. Then, initial oxidation should occur, leading to the generation

of ABTS radicals, which need to diffuse out of the porous network to be measured. In the case of RB19, similarly, dye molecules need to diffuse through the pores, and find the excited HRP in ordered to get decolorised. In this case however, since we are measuring the colour reduction, adsorbed but unreacted dye molecules will result in an overestimation of enzymatic dye degradation.

BIS-HRP contain PAH or PEHA and hence are amino-functionalised silicas. The properties of amino-functionalised silicas as adsorbents are quite well known and studied, with many examples examining dye removal [59, 63]. This indicates that there is a high chance that the BIS support alone can have a contribution, or interference to the measurement of colour during each assay. In the case of ABTS assay, unreacted or oxidised ABTS might get adsorbed on the BIS bed. This leads to lower observable colour, hence ostensibly lower performance of immobilised HRP. In the case of RB19 assay, dye or dye degradation products might get adsorbed on the BIS bed. This leads to lower observable colour, hence ostensibly higher performance of immobilised HRP. An illustrative depiction of the potential interference and contribution from the BIS support for both assays is shown in Figure 6-2. In the case of ABTS assay, substrate gets adsorbed on BIS and eventually moves inside the pore structure, where is get oxidised by the enzyme. Based on the observed results, this process probably lasts for about 1h. Then oxidised ABTS gets diffused in the bulk (increase in measured colour), before get adsorbed on the BIS structure again. In the case of RB19, dye initially gets adsorbed on BIS, and eventually it diffuses through the porous structure towards the enzyme. Upon degradation, by-products might either diffuse back in the bulk or get adsorbed on the BIS bed as well. These results are supported by the visual observations of the samples, 48h after assay initiation (Figure 6-3). The qualitative contribution of the support is clear, especially in the case of BIS synthesised with PAH, where the bed (BIS, with no HRP present) is visibly coloured with adsorbed unreacted ABTS or RB19 dye.

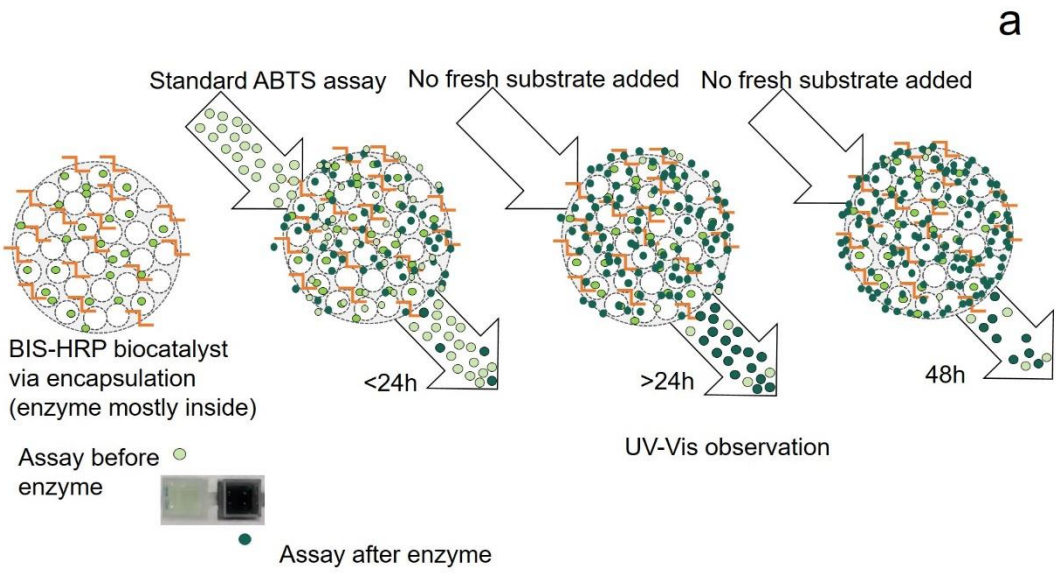

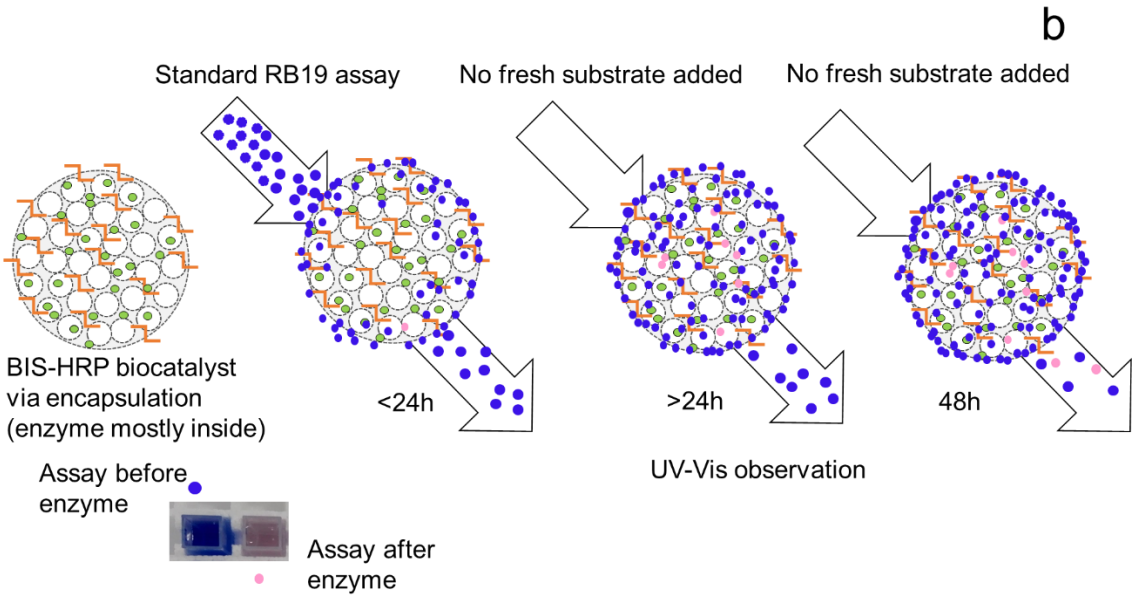

Figure 6-2: Illustration of BIS-HRP obtained via encapsulation performance during a) ABTS assay and b) RB19 assay. Arrow coming in represents the addition of substrate, arrow coming out represents the observable outcome via UV-Vis. From left to right, illustrations show the progress of the assay over time (0, up to 48h). For an explanation on BIS-HRP structure, please refer to Scheme 5-1and Scheme 5-2 of Chapter 5.

Furthermore, the enzymatic contribution is more distinguishable for BIS-HRP samples synthesised with PAH, as the characteristic dark green colour is evident in the bulk solution (middle cuvette, left top side), and also for the decolorised sample, bulk solution has less of a blue tint (comparison between left and middle photos on right top side). In the case of PEHA being used as an additive towards BIS synthesis and in-situ HRP immobilisation, visual results are barely noticeable, with the Blank ABTS solution being slightly more coloured than both BIS and BIS-HRP sample (bottom left set of photos). In the case of RB19 decolorisation there is barely any difference between the BIS and BIS-HRP samples, both being slightly less intensely coloured than the Blank sample (bottom right set of photos).

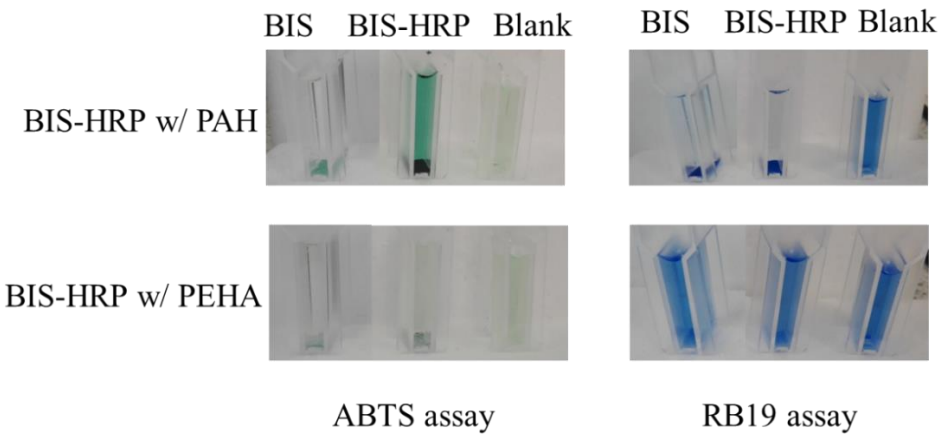

Figure 6-3: Snapshots of BIS-HRP assay, illustrating the difference between PAH and PEHA additives used for BIS synthesis. Photos were taken 48h after assay initiation.

It is quite difficult to quantify the contribution of the BIS support to the observed results and answer questions such as “how much does adsorption of unreacted ABTS affect the rate of the reaction?”, or “how much ABTS is oxidised during the examined time?”, due to technical difficulties. Such difficulties arise from the simultaneous need for quantification of unreacted ABTS adsorption on BIS and its localisation in BIS structure, as well as quantification of the oxidation of ABTS accounting for the amount of oxidised ABTS adsorbed on BIS during or after production. However, we can quantify the contribution of BIS to RB19 decolorisation, by examining the same quantity of BIS for dye adsorption over the examined time and subtracting the quantity adsorbed from the result obtained using BIS-HRP. Obtained results for the quantification of the contribution of BIS using the RB19 assay, are shown in Figure 6-4.

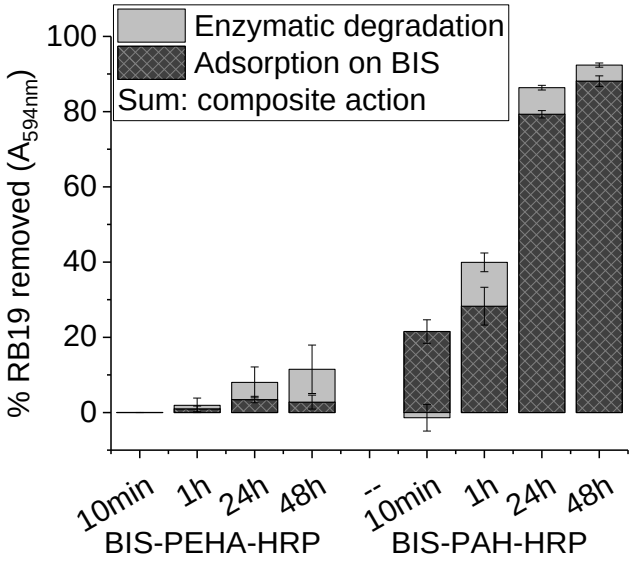

Figure 6-4: Examination of RB19 removal by BIS-HRP and BIS samples in order to distinguish the contribution of adsorption and enzymatic degradation. Samples were examined using the standard RB19 assay. RB19 removal was recorded at 4 specific time points for samples of immobilised HRP on BIS and corresponding BIS supports in absence of HRP. Results shown are the average of 2 or more replicates, with the error bar representing 1 standard deviation.

Looking at the ratio of adsorption to enzymatic degradation for both BIS-HRP preparations, we can see that in the case of PAH, adsorption dominates, with the enzymatic contribution being visible later in the assay. In the case of PEHA the enzymatic dye degradation seems to be dominating over adsorption. This can be attributed to the combination of adsorption sites being present and the porosity of each sample. Higher density of amines in bigger pores (BIS-PAH) facilitates faster adsorption, whereas smaller pore structures and less amine presence (BIS-PEHA) makes it easier for RB19 to reach the enzyme.

6.1.2. Effect of point of addition

Having analysed the observed phenomena and the effect that BIS synthesised with different additives have in each assay in the previous section, here we focus at the point of addition of the enzyme during BIS-HRP synthesis. As explained in detail in section 5.1.2, addition of HRP during 4 different stages during BIS synthesis was attempted, resulting in 4 types of BIS-HRP for each

additive examined. These stages were mixing HRP with the additive (A), with silicate (B), or with their mixture (C) before acidification (pH ~12), or adding it just after acidification, at pH 7 (D). The initial amount of HRP added was kept the same across all samples. Samples were examined using both assays and in the case of RB19 assay, the contribution of the BIS support was estimated as shown in the previous sub-section. Results obtained through the ABTS assay are shown in Figure 6-5. Given the very similar immobilisation efficiency obtained across samples synthesised with PAH and across samples synthesised with PEHA, regardless of the point of addition of HRP (please refer to Figure 5-9 in Chapter 5), results are presented as received, with no normalised correction.

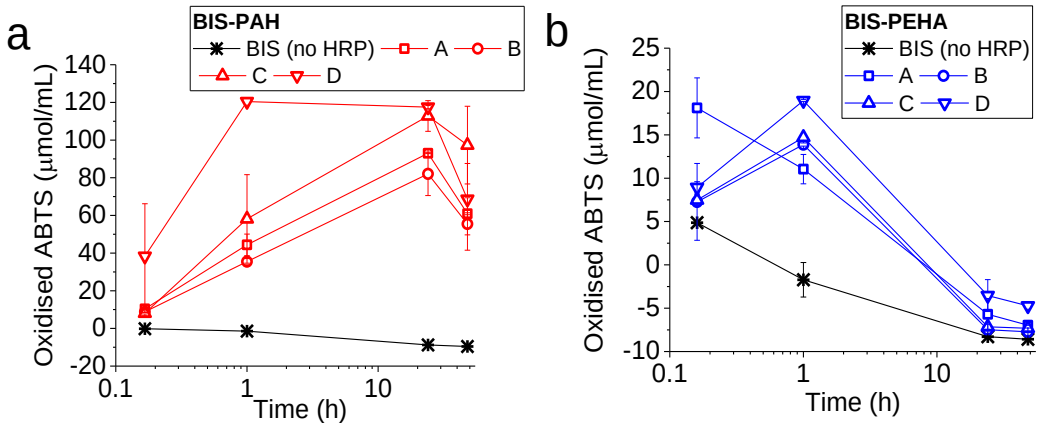

Figure 6-5: Oxidation of ABTS by BIS-HRP produced using a) PAH or b) PEHA as additive, with the enzyme added in different stages during BIS synthesis. A: addition of HRP to the additive before mixing with silicate and acidification to pH 7, B: addition of HRP to the silicate before mixing with additive and acidification to pH 7, C: addition of HRP to the mix of additive and silicate before acidification to pH 7 and D: addition of HRP just after acidification, at pH 7. Results shown are the average of 2 or more replicates, with the error bar representing 1 standard deviation.

From the oxidised ABTS measured across all different preparations of BIS-HRP, adding the enzyme just after acidification of the amine-silicate solution, offers the highest measured ABTS oxidation in both cases of PAH and PEHA as additives. Given the complexity of the system though, with BIS having such a strong adsorption effect for the substrate and the product, it is difficult to confidently identify the best result. The negative results obtained when BIS without HRP was examined under the ABTS assay (star symbol lines in Figure 6-5), indicate removal of unreacted ABTS from solution and the slightly coloured BIS bed implies adsorption of unreacted ABTS on it ("BIS" sample on photos related to the ABTS assay shown in Figure 6-3). It is worth mentioning again the much higher measured oxidation in the case of BIS-PAH-HRP compared to BIS-PEHA-HRP, as well as the almost uniform trend regarding the assay development over time. Absorbance for BIS-PAH-HRP samples increases up to the 24h mark before reduction, as opposed to the 1h mark shown for BIS-PEHA-HRP. For points of addition A, B and C, the performance of the biocatalyst does not show any significant difference for BIS-PAH-HRP.

Comparing the performance of the different BIS-HRP preparations via the RB19 assay (Figure 6-6) one can see that there is no considerable difference for BIS-HRP samples produced with

PAH as additive. In the case of PEHA, the results on decolorisation are generally much lower compared to PAH, despite the concentration of the immobilised HRP being relatively similar (difference of 5% at the most). However, in the case of PEHA, the action of the enzyme compared to the action of the support is clearer, as there is a distinct difference between the performance of the control sample (star symbol) and the HRP-containing samples, clear mostly from the 24h mark. Mixing HRP with the silicate solution or with the mixture of additive and silicate solution, before acidification, results in a better performance, substantially different to BIS-HRP produced by mixing the enzyme with PEHA before BIS production, or adding in during silicification. This difference in performance could be related to either accessibility of the enzyme to substrate, or to its residual activity. Having run initial checks regarding the preservation of enzymatic activity during synthesis (refer to Figure 4-22 in section 4.3.3), we can confidently assume that HRP is not deactivated in any of the cases examined, so the difference in activity is probably related to structural differences across the composites.

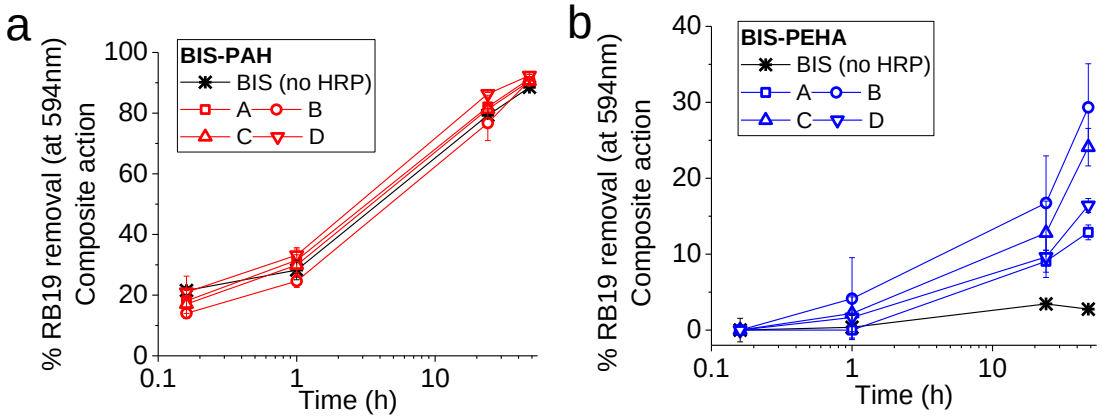

Figure 6-6: Removal of RB19 by BIS-HRP produced using a) PAH or b) PEHA as additive, with the enzyme added in different stages during BIS synthesis. A: addition of HRP to the additive before mixing with silicate and acidification to pH 7, B: addition of HRP to the silicate before mixing with additive and acidification to pH 7, C: addition of HRP to the mix of additive and silicate before acidification to pH 7 and D: addition of HRP just after acidification, at pH7. Results shown are the average of 3 or more replicates, with the error bar representing 1 standard deviation.

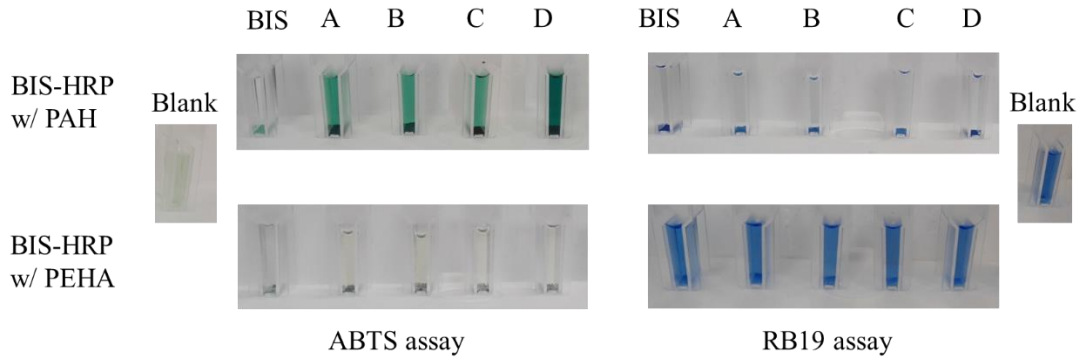

Figure 6-7: Snapshots of BIS-HRP assay 48hr after initiation, illustrating the difference between PAH and PEHA additives used for BIS synthesis, as well as the importance of the point of HRP addition during BIS synthesis (A: addition of HRP to the additive before mixing with silicate and acidification to pH 7, B: addition of HRP to the silicate before mixing with additive and acidification to pH 7, C: addition of HRP to the mix of additive and silicate before acidification to pH 7 and D: addition of HRP just after acidification, at pH 7).

Figure 6-7 shows photos taken of the examined samples 48h after assay initiation. Again, the superiority of PAH as an additive for BIS synthesis and effective HRP immobilisation is visibly shown (darker green for ABTS assay, less blue for RB19 assay). Whereas similar work was produced in terms of loading efficiency of drug upon its addition during different stages of BIS synthesis [299], obtained composites were not tested for drug release, so a comparison benchmark is not available for the observations made here.

From the aforementioned results, for the 4 different points of addition examined, it was decided to choose point D (addition of HRP during silicification, at pH 7) for further consideration, for both amines examined.

6.1.3. Effect of post-synthetic acid elution

As it was mentioned in section 5.1.3, elution of the additive was examined post synthesis in order to tune the properties of the obtained biocatalysts. Elution was performed by adding more acid to the obtained BIS-HRP composite, to lower the pH from 7 to 5 or 2. BIS-HRP was produced by addition of the same initial amount of HRP during silicification of samples produced with PAH or PEHA. Due to the varying loading of HRP across the different preparations, obtained results were normalised to the extrapolated performance per mg of HRP present in the assay, focusing on the enzymatic action of the biocatalyst. A comparison of the performance of BIS-HRP composites with increasing elution of additive through the ABTS assay is shown in Figure 6-8.

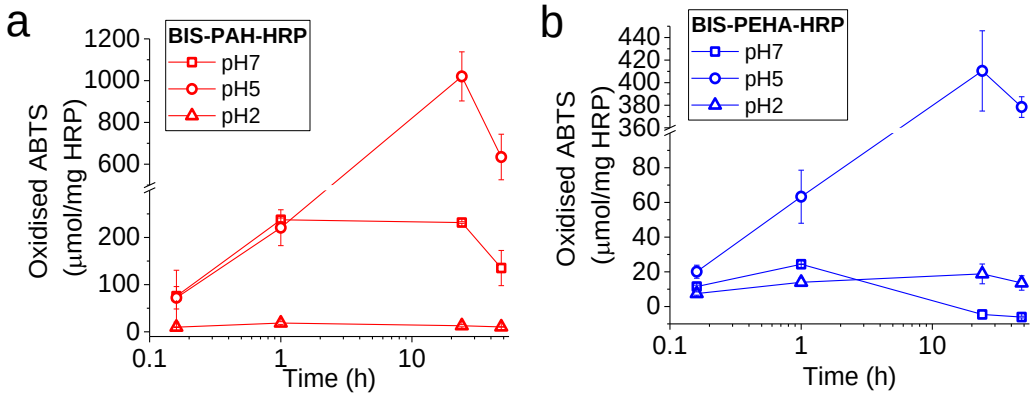

Figure 6-8: Normalised oxidation of ABTS for BIS-HRP samples produced with a) PAH or b) PEHA, with the additive either completely present (pH7), or eluted with more acid until pH 5 (partial elution) or pH 2 (close to complete elution). Results shown are the average of 3 or more replicates, with the error bar representing 1 standard deviation.

Regardless of the additive used for BIS synthesis, its removal shows a clear difference for the BIS-HRP samples examined. In both cases, eluting the additive partially (pH 5) produced the best results in terms of observed product over time. This sample, in both cases, shows a significantly higher product compared to samples as-made (pH 7) or with highest amount of additive removed (pH 2). This effect can be attributed to the accessibility of HRP for unreacted ABTS due to the removal of additives. It is worth mentioning that there was no substantial difference observed in the surface areas between BIS-HRP samples with 100% or partial additive presence per additive

case (around 200m^2/g for BIS-PAH-HRP and 30m^2/g for BIS-PEHA-HRP as shown in Figure 5-14 of section 5.1.3). This implies that improved performance can be due to the increased accessibility of enzyme and the reduction of available sites for adsorption of unreacted ABTS. This suggests that more molecules of ABTS can reach the enzyme, in a shorter period of time, with not much retention of the oxidised product from lack of adsorption. For pH 2 samples, regardless the additive, the performance of the immobilised HRP is very low. This is noteworthy, as elution at pH 2 represents the highest amount of additive removed, thus providing higher porosity and better access to HRP. However, pH 2 is too acidic for HRP and leads to activity loss, explaining the much lower performance of the biocatalyst despite the improved accessibility.

Examining the BIS-HRP samples using the RB19 assay, we can again see distinguishable differences depending on the additive elution point for both additives (Figure 6-9a for BIS-PAH and b for BIS-PEHA), where samples with the additive eluted at pH 5 show the best performance in terms of % of dye removal based on the action of the BIS-HRP composite.

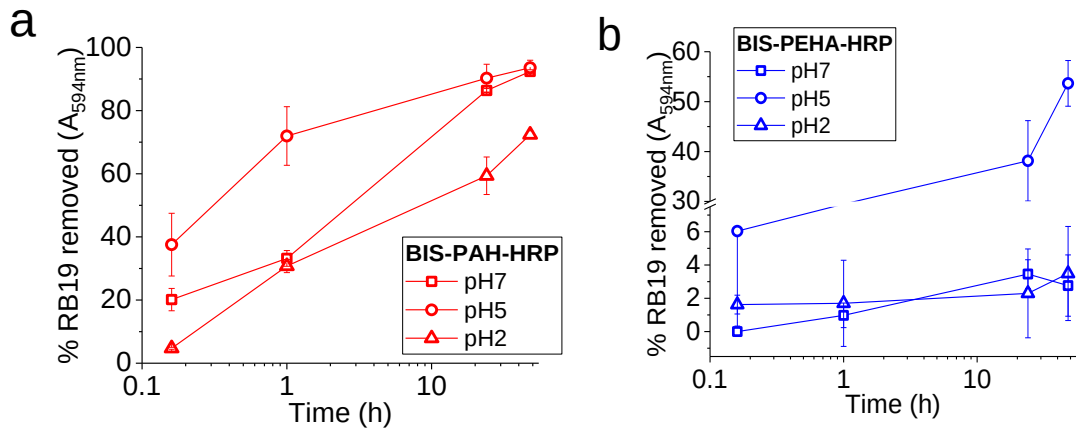

Figure 6-9: Removal of RB19 based on the composite action of BIS-HRP produced with a) PAH or b) PEHA, with the additive either completely present (pH7), or eluted with more acid until pH 5 (partial elution) or pH 2 (close to complete elution). Results shown are the average of 3 or more replicates, with the error bar representing 1 standard deviation.

Isolating the enzymatic performance by subtracting the amount of dye adsorbed on corresponding samples of BIS with the additive eluted and normalising the response to the extrapolated value of quantity of dye removed by 1 mg HRP, results show an interesting trend (Figure 6-10). In the case of BIS-HRP produced with PAH (Figure 6-10a), all samples start with negative enzymatic contribution, indicating dominant adsorption of dye on BIS. By the 1h mark, enzymatic contribution is substantially higher than dye adsorption, leading to almost 30nmol of RB19 removed per mg of immobilised HRP. Progressively, the enzymatic contribution reduces to a value of almost 10nM per mg HRP. In the case where PAH is eluted to pH 2 (triangles), dye adsorption is dominant throughout the assay. On the contrary, the contribution attributed to enzymatic degradation in the case of BIS-HRP produced with PEHA progressively increases (Figure 6-10b). This effect is highly noticeable in the cases of full or partial presence of additive

on the BIS-HRP composite (pH 7 and pH 5 samples), whereas in the case of additive eluted to pH2, the enzymatic response is almost zero, similar to the case of ABTS assay.

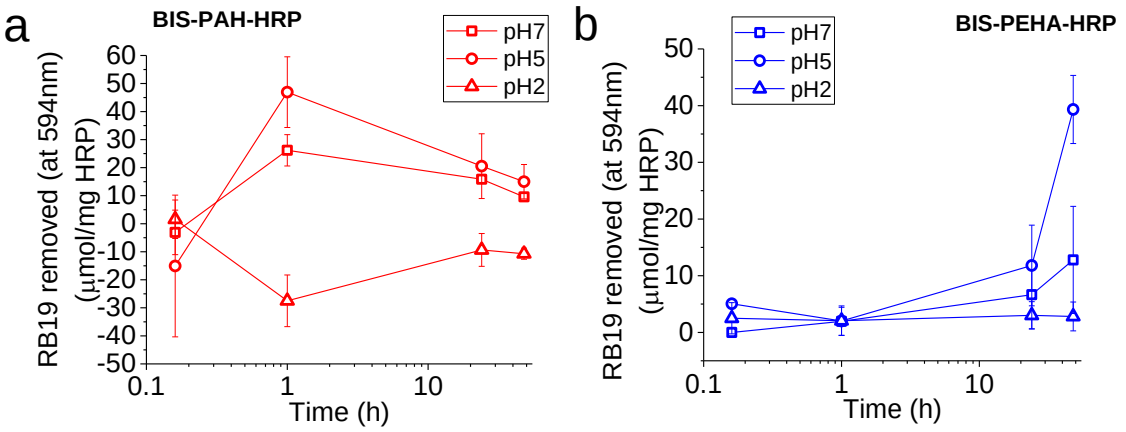

Figure 6-10: Quantity of RB19 removed over time due to enzymatic contribution of BIS-HRP produced with a) PAH or b) PEHA, with the additive either completely present (pH7), or eluted with more acid until pH 5 (partial elution) or pH 2 (close to complete elution). Results shown are the average of 3 or more replicates, with the error bar representing 1 standard deviation.

Based on the observations made with both the ABTS and RB19 assays, we can see that partial elution of the additive offers the best results for both PAH and PEHA. This is due to a "sweet spot" between porosity, accessibility of HRP, the presence of amines in the composite and enzyme stability.

6.1.4. Effect of amount of HRP encapsulated

Having seen the effects of increasing quantity in immobilisation efficiency on immobilisation efficiency and porosity of BIS-HRP composites (refer to Figure 5-17 of section 5.1.4), it is interesting to see whether the amount of encapsulated HRP had an influence on activity. Results for BIS-HRP synthesised with PAH or PEHA, with increasing initial concentration of HRP added for immobilisation are shown in Figure 6-11 using the ABTS assay. Since the loading efficiency is different for each sample, results are presented by normalising per mg HRP present. This helps compare how much ABTS would 1mg of immobilised HRP can oxidise. If there were no structural/porosity differences, we would expect to see the same results after normalisation to 1mg of HRP. Hence, any observed differences would be attributed to factors such as porosity of BIS, accessibility to HRP and adsorption of ABTS (unreacted or oxidised) on BIS. In the case where BIS is synthesised with PEHA (Figure 6-11b), the increase of initial amount of HRP added for immobilisation leads to an increase in the oxidation of ABTS. In the case where BIS is synthesised with PAH (Figure 6-11a), results are showing a different response. For BIS-PAH-HRP samples, during the earlier stages of the assay (up to 1h), samples with 0.17mg/mL and 0.4mg/mL initially added HRP show the quickest highest response, which gets reduced as assay progresses. In the case of BIS-HRP samples created with 0.1mg/mL or 0.25mg/mL of initially added HRP, response is delayed, but results to high amount of oxidised ABTS around the 24h mark. Trying to correlate the observed response with the obtained information on porosity for

BIS-PAH samples synthesised with PAH (refer to Figure 5-19 and Figure 5-20 of section 5.1.4), there seems to be no obvious correlation. That leads to assume an undefined effect by the presence of HRP during BIS synthesis, depending on the quantity added.

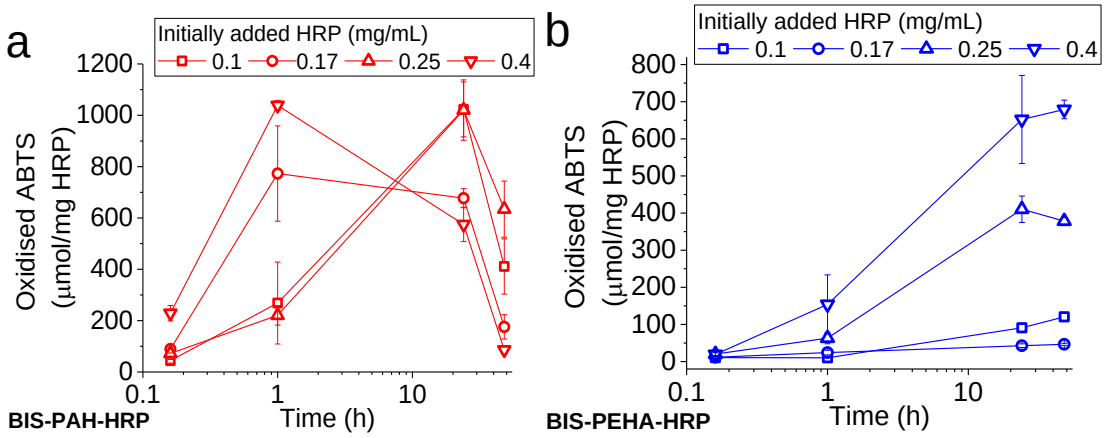

Figure 6-11: Normalised oxidation of ABTS by BIS-HRP samples produced with a) PAH or b) PEHA, with the additive partially eluted, examining the effect of increasing the initially added mass of HRP. Results shown are the average of 3 or more replicates, with the error bar representing 1 standard deviation.

The effect of initially added quantity of HRP to produce BIS-HRP via encapsulation was examined through the RB19 assay as well. Results on the BIS-HRP composite action are shown in Figure 6-12 (as observed, no normalisation taking place). Regardless of the initially added quantity or the type of amine used, RB19 removal shows a sharp initial increase within 1h of assay initiation, slowing down after the 24h mark, except from the 0.17 and 0.25mg/mL samples for BIS-PEHA, where there is a sharp decolorisation increase between 24h and 48h.

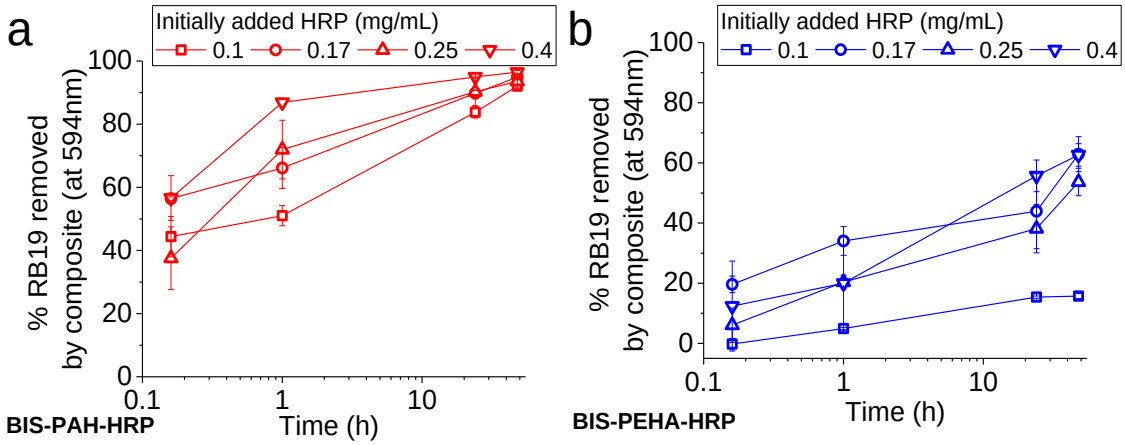

Figure 6-12: As observed percentage removal or RB19 by BIS-HRP samples produced with a) PAH or b) PEHA, with the additive partially eluted, examining the effect of increasing the initially added mass of HRP. Results shown are the average of 3 or more replicates, with the error bar representing 1 standard deviation.

The composite action of BIS-HRP synthesised with PAH (Figure 6-12a) results in very high colour removal percentage (80-90% within 48h) for every quantity of HRP examined except from the 0.1mg/mL. When PEHA was used as additive (Figure 6-12a), there is a substantial difference to the colour removal achieved for different initial HRP quantities, with the higher initially added

quantities of HRP leading to higher percentage of removal at the 48h mark. This performance is not surprising, given the increased quantity of theoretically available HRP.

In order to isolate the enzymatic action from the composite action, the contribution of dye adsorption on BIS samples was subtracted and obtained results were extrapolated to the expectation of dye degradation by 1mg HRP being present in the assay (Figure 6-13). Looking at BIS-PAH-HRP samples (Figure 6-13a), we see that for the higher initial concentrations of HRP (upward and downward triangle respectively), the enzymatic contribution is increasing until the 1h mark, reaching a value of almost 30nmol RB19 per mg of HRP in both cases and stabilises later, to a value around 10nmol RB19 per mg of HRP. Interestingly, the HRP contribution when 0.17mg/mL of HRP are initially added (circles) shows a high value at the beginning of the assay, which is almost halved by the end of the assay. For the case of 0.1mg/mL HRP initially added (squares), the presence of enzyme in BIS-HRP does not enhance colour removal, as BIS in absence of HRP performs better than BIS-HRP, hence the negative results.

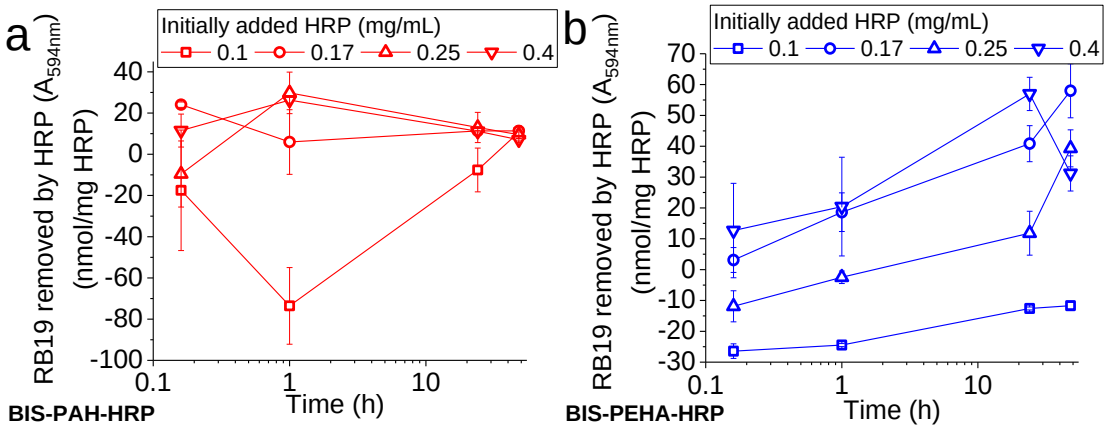

Figure 6-13: Normalised enzymatic degradation of RB19 by BIS-HRP samples produced with a) PAH or b) PEHA, with the additive partially eluted, examining the effect of increasing the initially added mass of HRP. Results shown are the average of 3 or more replicates, with the error bar representing 1 standard deviation.

When PEHA is used as additive (Figure 6-13b), results are more on the "expected" side, where the contribution of the higher initial quantities of HRP (upward and downward triangle) is significantly higher than in the lower added mass cases (square and circle). Interestingly, this trend is inversed as the assay progresses, showing a delayed activity from lower quantities of HRP present. Comparing Graphs a and b, we can see that BIS-PEHA-HRP does not overshadow enzymatic contribution as much as observed in the case of BIS-PAH-HRP, as past the initial 10min, results are increasing and are overall positive. Based on the so far observations, it looks like dye is fast adsorbed on BIS synthesised with PAH before dye molecules are able to access the enzyme. Higher quantity of HRP present generally enhances obtained response, with a clear difference between 0.1mg/mL and higher concentrations, whereas for the 3 higher quantities examined there is not a clearly observed trend.

Having seen the response of BIS-HRP with varying quantity of HRP using both ABTS and RB19 assay, it is clear that although for the ABTS assay there is a clear trend, with increased response when quantity of HRP is higher, in the case of RB19 there is no clear trend.

6.2. HRP adsorbed on BIS or Syloid AL-1FP ex-situ

6.2.1. Effect of additive used

As it was shown in the case of in-situ encapsulation of HRP, the choice of additive has a great contribution to the performance of BIS-HRP, mainly due to differences on the porosity of BIS-HRP composites and presence of different type of amines. In the case of BIS-HRP obtained by adsorption of HRP on pre-synthesised BIS, the enzyme is theoretically more easily accessible, hence the performance is expected to be enhanced compared to the encapsulated version. Examining the effect of amine first, BIS-HRP was synthesised via adsorption of the same initial quantity of HRP on BIS synthesised with PAH or PEHA, without elution of the additive (Figure 6-14). BIS-HRP with HRP being adsorbed (from now on referred to as BIS-ads-HRP) shows the same performance trend regardless of the additive used (Figure 6-14a). However, when PAH is used (red circles), the performance of the composite is almost half of the one obtained for BIS-HRP where PEHA was used as support (blue squares). This can be partially attributed to the accessibility of enzyme in each case. HRP accessibility can be affected by the structure of BIS (porous and functionalised in the case of PAH, almost non-porous with no much surface functionalisation in the case of PEHA), or the "over-loading" of HRP on BIS, implying high potential but underperforming due to clutter. We should also not forget the adsorptive ability of BIS (especially BIS-PAH), which probably did contribute to the lower observation of ABTS oxidation due to adsorption of unreacted ABTS preventing its oxidation from HRP, or oxidised ABTS, preventing its diffusion in bulk volume.

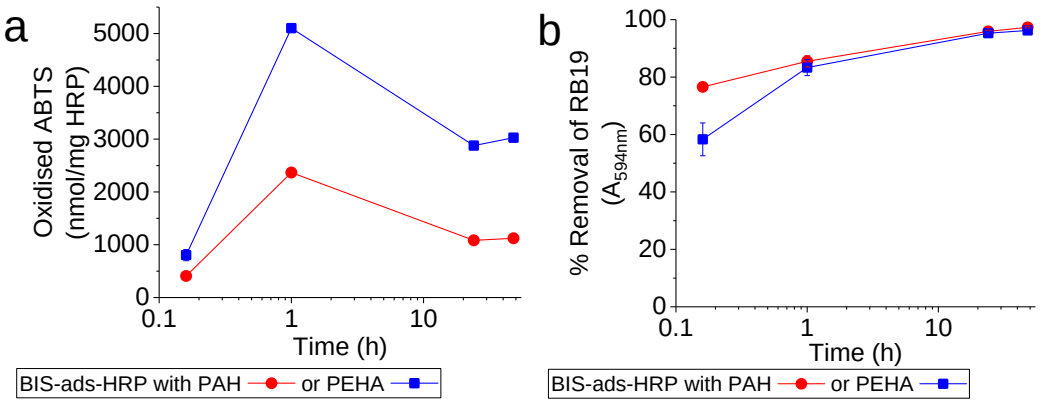

Figure 6-14: Performance of BIS-HRP synthesised with either PAH or PEHA as additive, with the same initial amount of HRP added for adsorption on pre-synthesised BIS, examined under standard assay procedure using a) ABTS or b) RB19 as substrate. Results shown are the average of 2 or more replicates, with the error bar representing 1 standard deviation.

Moving to the examination of the effect of amine on the performance of BIS-ads-HRP using the RB19 assay (Figure 6-14b), we can see that the removal percentage is quite high for both

preparations and past the 1h point, with the obtained colour removal being identical. The results obtained with the RB19 assay are not complete at this point, as the contribution of the BIS as adsorbent needs to be subtracted as discussed in the case of encapsulated HRP. Once the enzymatic contribution is isolated and shown as a percentage of the total performance, it is clear that the enzymatic contribution of HRP synthesised with PEHA is much higher than the enzymatic contribution shown in the case of PAH being used as additive, with higher initial and progressive contribution (Figure 6-15). Based on the comparison of Figure 6-4 and Figure 6-15, we can see that when HRP is adsorbed on BIS as opposed to encapsulated, the enzymatic contribution is much more apparent and fast. In the case of encapsulated HRP, the enzymatic contribution towards decolorisation was not more than about 10% of the composite action, regardless the time point of the additive used, whereas for adsorbed HRP the enzymatic contribution is quite high even from the 10min time point, with more than 50% contribution.

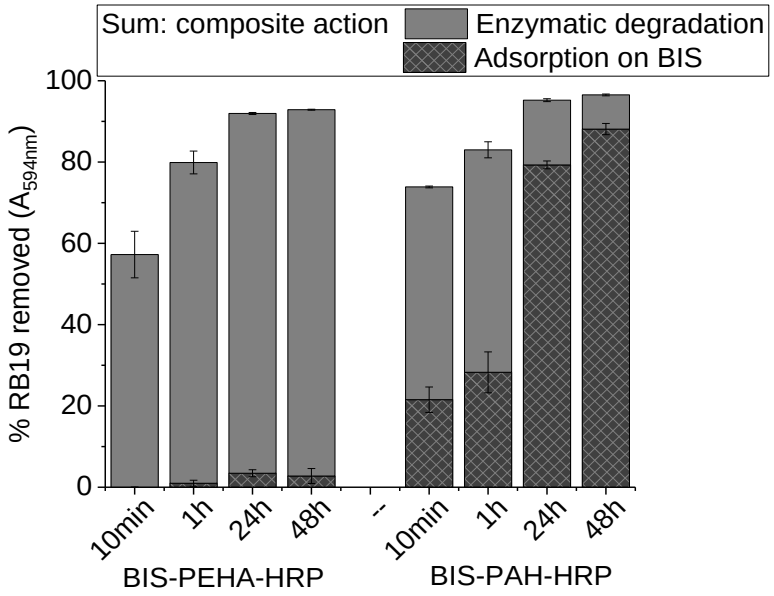

Figure 6-15: Examination of RB19 removal by BIS-HRP and BIS samples in order to distinguish the contribution of adsorption and enzymatic degradation. Samples were examined using the standard RB19 assay. RB19 removal was recorded at 4 specific time points for samples of immobilised HRP on BIS and corresponding BIS supports in absence of HRP. Results shown are the average of 2 or more replicates, with the error bar representing 1 standard deviation.

When results are normalised to the presence of 1mg HRP in the assay and enzymatic performance is isolated (Figure 6-16), the much higher performance of HRP adsorbed on BIS synthesised with PEHA is clear. This effect might be explained based on 2 possible scenarios, which can occur independently, or have a cooperative effect. Adsorbing HRP on BIS synthesised with PEHA led to an almost 5% w/w concentration of HRP on BIS-HRP composite, whereas when PAH was used that concentration was just over 10% w/w. This indicates a higher concentration of HRP being immobilised, which could have led to aggregation of enzyme molecules and blocking of their action [229, 277, 430]. Furthermore, we need to think where is adsorption of HRP taking place in each BIS case. Based on porosity analysis of BIS synthesised with PEHA or PAH, we showed that in the case of PEHA we have an almost non porous material with low available surface area

($18m^2/g$), whereas in the case of PAH, BIS is significantly more porous, with much higher available surface area ($180m^2/g$). This indicates that HRP will get adsorbed predominately on the external surface area of BIS synthesised with PEHA, whereas in the case of PAH there will be partial adsorption on the internal pore structure. Introduced substrate in each assay will easily "find" the excited HRP in the case of BIS synthesised with PEHA, but in the case of PAH it will get adsorbed initially on BIS, before reaching the enzyme which is adsorbed in the pores of the material.

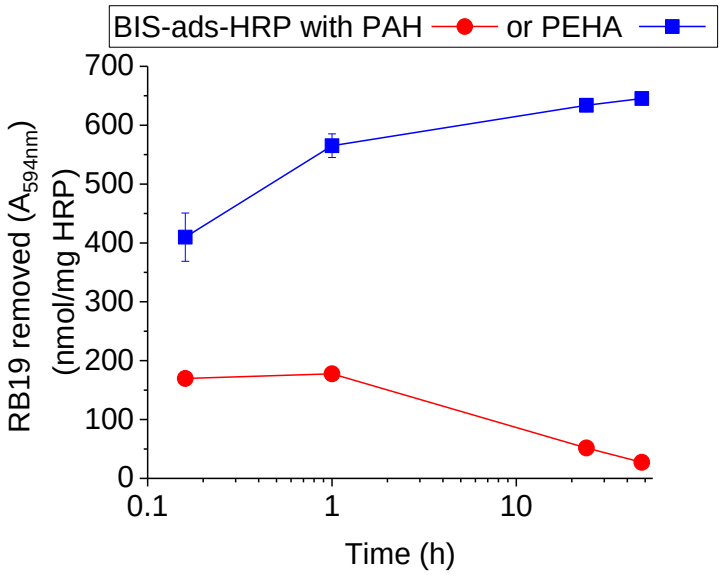

Figure 6-16: Enzymatic contribution of HRP adsorbed on BIS synthesised with PAH or PEHA as additive, extrapolated to 1 mg of HRP being present in the assay. Results shown are the average of 2 or more replicates, with the error bar representing 1 standard deviation.

Similar to the depiction shown for encapsulated HRP in Figure 6-2, an.illustrative depiction of the potential interference and contribution from the BIS support for both assays, for the case of adsorbed HRP is shown in Figure 6-17. In the case of ABTS assay (Figure 6-17a), substrate gets easily in touch with the HRP adsorbed on the surface of BIS and oxidation occurs quickly, leading to high absorbance readings up until the 1h point. Due to the high adsorbing ability of BIS (especially with PAH used as the additive) oxidised ABTS can then adsorb on BIS, and since oxidation reaction has finished, we do see a reduction in the absorbance of the assay, as product is being adsorbed but no fresh product is generated. Over the examined period of 48h, more and more product is being adsorbed, up to the 24h point, where it seems that adsorption is reaching a limit, since the concentration of oxidised ABTS present in the assay is stable (Figure 6-14a). In the case of RB19 degradation (Figure 6-17b), dye gets quickly oxidised by HRP being easily accessible on the surface of BIS, before adsorption of residual dye and/or dye fragments on BIS takes place.

The comparison of the 2 additives was clear for encapsulation of HRP, with PAH favouring faster communication between the bulk solution and the enzyme due to the larger pore network. In the case of adsorbed HRP, presence of an amine loaded pore network seems to be obstructing the

enzymatic performance. Based on this observation, it is interesting to examine the performance of BIS-HRP obtained via adsorption on BIS synthesised with either PAH or PEHA, with elution of the additive prior the immobilisation

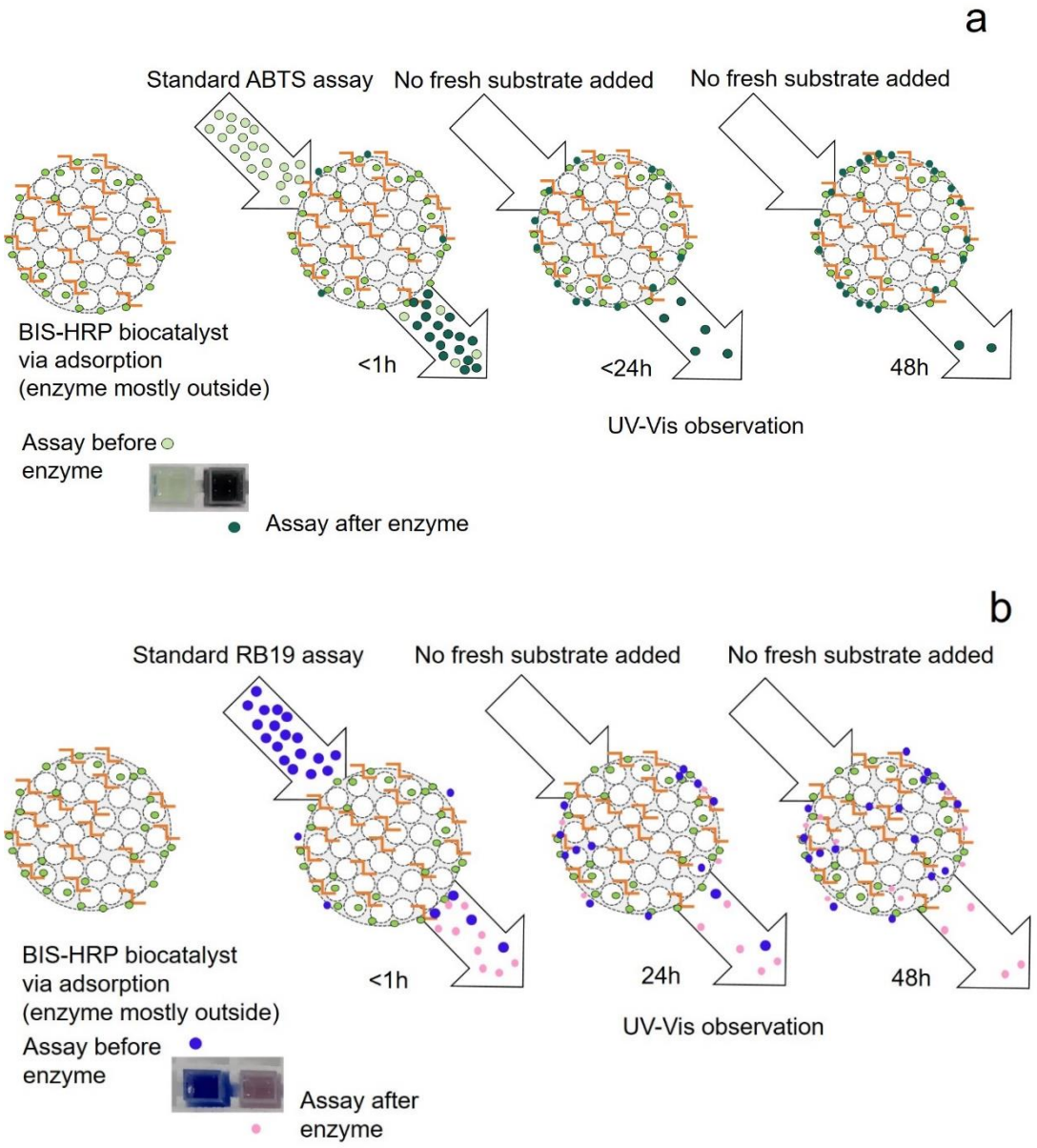

Figure 6-17: Illustration of the performance of BIS-HRP obtained via adsorption during a) ABTS assay and b) RB19 assay. Arrow coming in represents the addition of substrate, arrow coming out represents the observable outcome via UV-Vis. From left to right, illustrations show the progress of the assay over time (0, up to 48h). For an explanation on BIS-HRP structure, please refer to Scheme 5-1and Scheme 5-2 of Chapter 5.

6.2.2. Effect of acid elution

Similarly to examining the effect of additive elution for the performance of encapsulated HRP, the effect of using BIS with various stages of additive elution as immobilisation support for HRP on the performance of the enzyme was examined. The same 3 pH levels were examined, where additive was either fully present in BIS ("pH 7", BIS as synthesised), partially eluted ("pH 5", BIS synthesis at pH 7, then extra acid was added until pH 5), or further eluted ("pH 2", BIS synthesis at pH 7, then extra acid was added until pH 2). The initial amount of HRP added was

the same, but immobilisation efficiencies were quite different per pH and per additive used (shown in Figure 5-23 of section 5.2.1). Hence, results are normalised to 1 mg of HRP being present in the assay was employed again. Results for the ABTS assay are shown in Figure 6-18a and b for BIS-PAH and BIS-PEHA respectively.

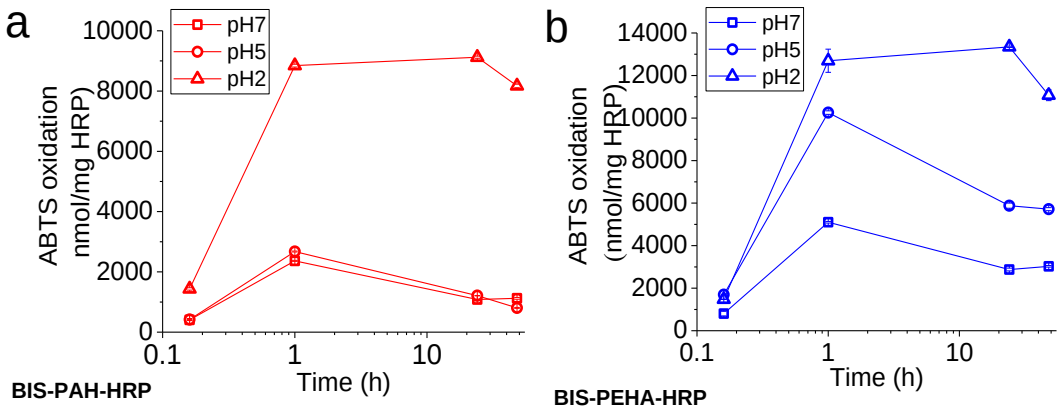

Figure 6-18: Normalised oxidation of ABTS for BIS-HRP samples produced by adsorption of HRP on BIS synthesised with a) PAH or b) PEHA, with the additive either completely present (pH7), or eluted with more acid until pH 5 (partial elution) or pH 2 (close to complete elution). Results shown are the average of 3 or more replicates, with the error bar representing 1 standard deviation.

Regardless of the additive used for BIS synthesis, the highest degree of elution (pH 2) leads to the highest performance of immobilised HRP (about 9 mmol or 13 mmol of ABTS oxidised per mg of HRP for the case of PAH or PEHA being used for BIS synthesis respectively). Obtained results for pH 7 and pH 5 samples were almost identical, whereas pH 2 showed a substantial difference (Figure 6-18a). We speculate that this difference is due to the lower amount of PAH present in the case of pH 2, leading to less available sites for adsorption of ABTS, hence less adsorption of oxidised product and subsequently less interference towards product measurement. In the case of PEHA used as the additive (Figure 6-18b) there is a noticeable difference across all 3 examined sample sets. This difference could be attributed, again, to the lower presence of available sites for oxidised ABTS adsorption, as well as to the lower amount of HRP present (in the case of pH 2), which can promote better activity as shown earlier. The difference in performance of HRP depending on the degree of elution is more noticeable in the case of PEHA, probably due to the more controlled elution of additive upon addition of more acid, compared to PAH [64].

Examining the same samples using the RB19 assay, we initially present colour removal as observed, before the enzymatic contribution normalisation, for BIS synthesised with PAH or PEHA (Figure 6-19a and b respectively). For both examined additives, results obtained based on the composite action favour HRP adsorbed on BIS after partial additive elution (pH 5), as even from the 10min mark the colour removal is almost as high as the final time point of the assay (more than 80% colour removal in both cases). Furthermore, for both additives, the performance of BIS-HRP for BIS with majority of additive eluted (pH 2, triangle shape lines in both graphs of

Figure 6-19) starts considerably lower compared to the pH 7 and pH 5 cases, but by the end of the assay colour removal is close to the maximum obtained with the other samples.

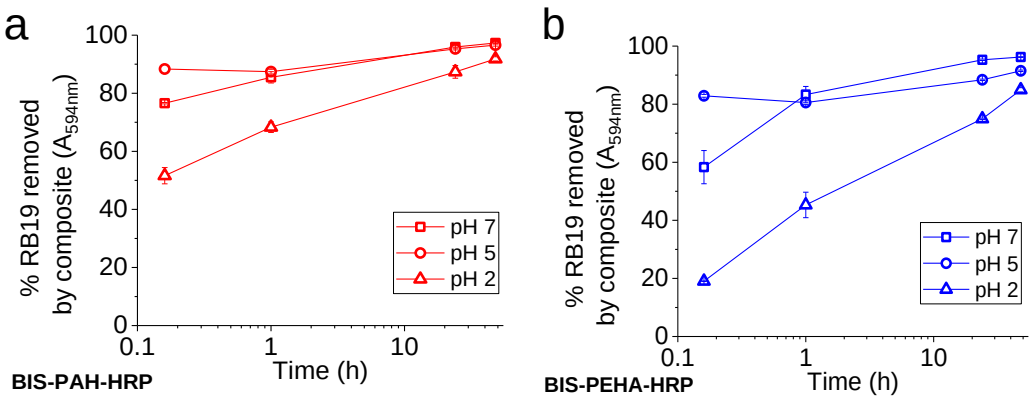

Figure 6-19: Removal of RB19 based on the composite action of BIS-HRP produced by adsorption of HRP on BIS synthesised with a) PAH or b) PEHA, with the additive either completely present (pH7), or eluted with more acid until pH 5 (partial elution) or pH 2 (close to complete elution). Results shown are the average of 3 or more replicates, with the error bar representing 1 standard deviation.

When the contribution from the support is subtracted and the enzymatic contribution is normalised to the extrapolated quantity of RB19 removed by 1 mg HRP being present in each case (Figure 6-20), results follow the trend shown for ABTS only in the case of PAH used as additive (Figure 6-20a). The performance of HRP adsorbed on "pH 2" BIS is substantially higher compared to other types of BIS. In the case of PEHA being used as additive, when BIS-HRP is examined using the RB19 assay, results obtained for the enzymatic contribution are almost opposite to the ones shown using the ABTS assay (Figure 6-20b). The pH 5 set is showing a stably high enzymatic contribution and pH 2 set is showing an increasingly high performance, which eventually, by the end of the assay is approaching the one measured for pH 5 set.

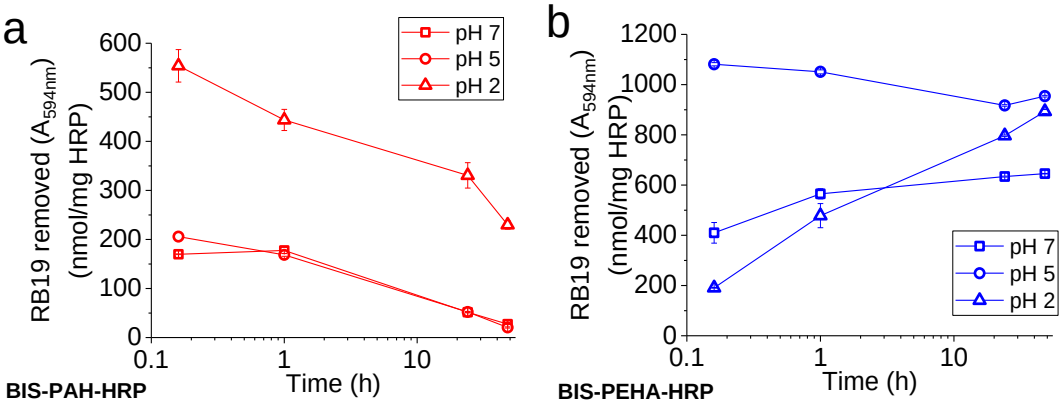

Figure 6-20: Normalised quantity of RB19 removed over time due to enzymatic contribution of BIS-HRP produced by adsorption of HRP on BIS synthesised with a) PAH or b) PEHA, with the additive either completely present (pH7), or eluted with more acid until pH 5 (partial elution) or pH 2 (close to complete elution). Results shown are the average of 3 or more replicates, with the error bar representing 1 standard deviation.

It is worth commenting on the maximum contribution observed with BIS-HRP when PAH was used as additive compared to the use of PEHA. For the former the maximum observed contribution form immobilised HRP is almost 600nmol RB19 per mg HRP, at the beginning of

the assay, before contribution from BIS overpowers HRP. For the latter, this number is almost double, measured at almost 1100nmol RB19 per mg HRP, showing a stable performance overtime. This difference can possibly be attributed the accessibility of HRP, with BIS synthesised with PAH offering a porous network lined with amines (quantity depending on elution), hence potentially obstructing the dye from reaching HRP adsorbed in the pores. The adsorbing ability of BIS is also the reason for the inversed trend on the enzymatic contribution observed for BIS-PAH and BIS-PEHA. For BIS-PAH the enzymatic performance is decreasing with time, as RB19 gets adsorbed on BIS, not allowing contact with HRP. On the other hand, for BIS-PEHA the adsorption is not as prominent, allowing enzymatic activity to occur (and develop) without obstacles.

Although the performance of BIS-ads-HRP samples showed very high performance for BIS synthesised with either PAH or PEHA, with the additive eluted at pH 2, BIS materials selected for further study were BIS with additive eluted at pH 5, in order to keep a common point for comparison with the encapsulated HRP.

6.2.3. Effect of amount of HRP adsorbed

Similarly to section 6.1.4, the performance of progressively increased amount of initially added HRP for immobilisation via adsorption on BIS or Syloid Al-1FP was examined using both assays. Obtained results using the ABTS assay are shown in Figure 6-21. Before looking in detail at each type of silica used as immobilisation support, we will compare the maximum estimated value of oxidised ABTS per mg of HRP immobilised on each different support. Comparing the maximum observed point of each Graph of Figure 6-21, we can see that the best performance is by far shown from HRP immobilised on Syloid AL-1FP, with a 45μmol ABTS oxidised per mg HRP, compared to about 12 μmol and 6 μmol ABTS for HRP immobilised on BIS synthesised with PEHA or PAH respectively.

Examining the effect of increasing quantity of HRP, there is not a consistent trend shown for any of the 3 supports examined. When BIS-PAH was used (Figure 6-21a), the biocatalyst with the lowest amount of HRP present (0.1mg/mL initial HRP concentration showed the lowest performance (square symbols). Disregarding the face value of the rest sets but looking at the obtained immobilisation efficiency (0.25 > 0.4 > 0.17mg/mL as shown in Figure 5-25 of section 5.2.2), there is a trend, where lowest amount of HRP present shows higher potential of ABTS oxidation. Given that results shown in Figure 6-21 are based on the same amount of HRP being present in the composites, the difference in performance could be explained by the ratio of HRP to available amine for adsorption of ABTS. Theoretically, higher amount of HRP retained from BIS indicates higher amount of amine residues engaged with it, hence lower amount of amine residues available for dye adsorption. In the case of 0.1mg/mL the amount of HRP present is almost half compared to 0.17mg/mL or 0.4mg/mL and is almost the 1/5 of HRP present on the 0.25mg/mL samples (Figure 5-24a in section 5.2.2).

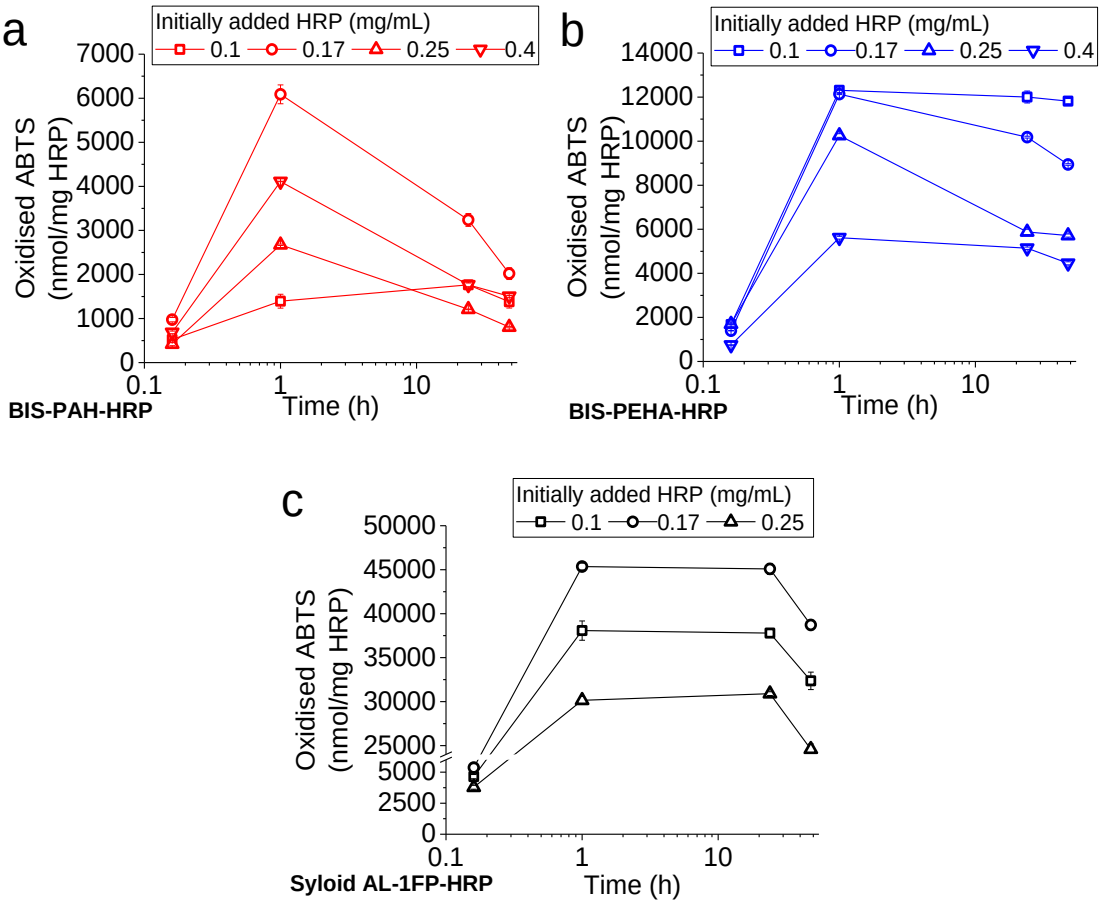

Figure 6-21: Normalised oxidation of ABTS by immobilised HRP samples on a) BIS synthesised with PAH or b) BIS synthesised with PEHA, with the additive partially eluted, or on c) Syloid AL-1FP, examining the effect of increasing the initially added mass of HRP. Results shown are the average of 3 or more replicates, with the error bar representing 1 standard deviation.

Looking at Figure 6-21b, where BIS-PEHA was used as support, results show that the sets of 0.1mg/mL, 0.17mg/mL and 0.25mg/mL of initial HRP concentration, have a similar performance, at least until the 1h point. These samples have similar content of HRP (2.3%, 3.2% and 2.5% w/w HRP/BIS-HRP as shown in Figure 5-25b of section 5.2.2). On the other hand, the sample of BIS-PEHA with the higher amount of HRP adsorbed (0.4mg/mL initial concentration, leading to 5.5% w/w HRP/BIS-HRP) shows the lowest performance. This shows the potential of activity hinder due to larger amount of HRP present. Last but not least, when HRP was immobilised on Syloid AL-1FP, oxidation of ABTS was correlated to immobilisation efficiency of HRP on the composite, with lower amounts of HRP oxidising more ABTS.

Results on colour removal from immobilised HRP obtained through the RB19 assay for each of the 3 supports used (Figure 6-22), show a distinctively lower performance for the lowest HRP concentration present for both BIS-HRP preparations, with the other 3 quantities examined showing a similar performance (comparison between Figure 6-22a and b). In the case of HRP adsorbed on Syloid AL-1FP, the observed colour removal is showing the exact opposite trend shown for ABTS previously, where lower quantity of HRP results in lower percentage of colour removal (Figure 6-22c).

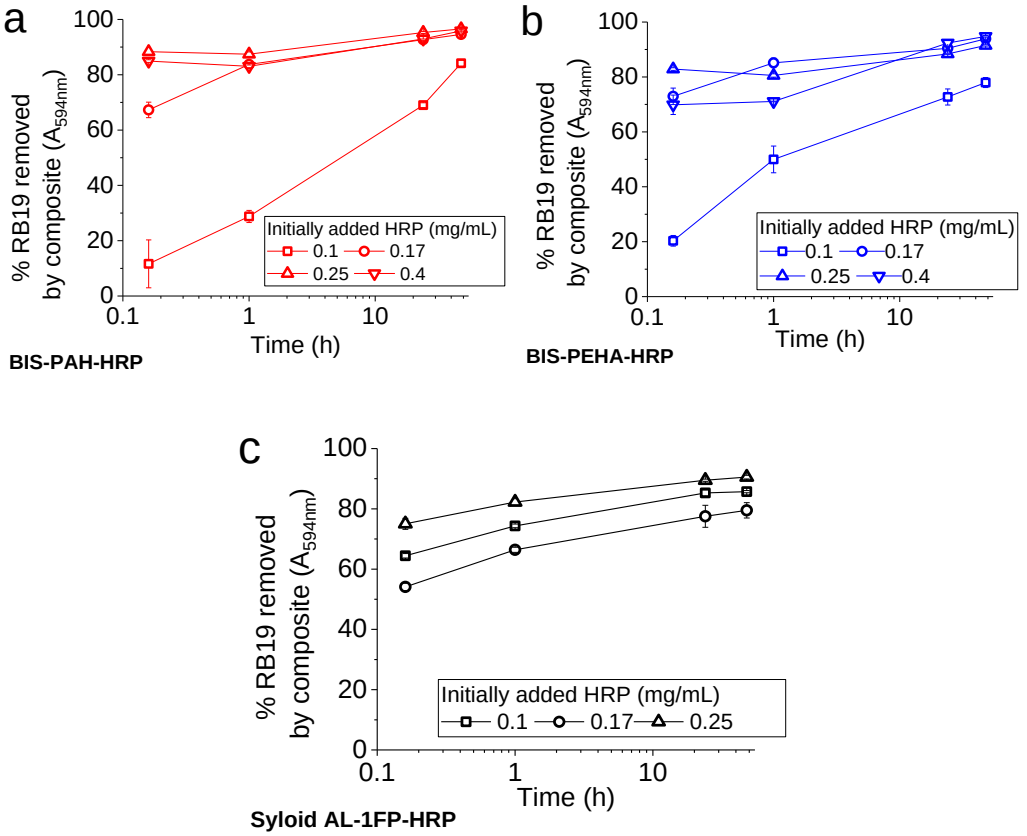

Figure 6-22: Effect of HRP mass on as observed percentage removal or RB19 by immobilised HRP samples via adsorption on a) BIS synthesised with PAH or b) BIS synthesised with PEHA, with the additive partially eluted, or on c) Syloid AL-1FP. Results shown are the average of 3 or more replicates, with the error bar representing 1 standard deviation.

Results of enzymatic contribution to RB19 degradation, after subtracting the contribution of the silica support and normalising the enzymatic contribution per mg HRP present in the assay for each case, are shown in Figure 6-23. We can see that – as observed for the ABTS assay – the amount of RB19 enzymatically degraded by HRP is lower by an order of magnitude between HRP immobilised on BIS-PAH (Figure 6-23a) or on Syloid AL-1FP (Figure 6-23c), with the performance of HRP adsorbed on BIS-PEHA (Figure 6-23b) being in between. It should be pointed out that for HRP adsorbed on BIS synthesised with PAH, the enzymatic contribution of HRP at the lowest quantity added (0.1mg/mL) was negative (not shown on Figure 6-24a), indicating that BIS in absence of HRP performed better. For the other quantities, obtained results are consistent with the ABTS assay, where less quantity of HRP present leads to higher removal of RB19. When HRP is adsorbed on BIS synthesised with PEHA, increasing the concentration of HRP present in the assay leads to mixed results, until the highest concentration (obtained for 0.4mg/mL HRP added for immobilisation), where the performance of immobilised HRP is the lowest. Last but not least, HRP adsorbed on Syloid AL-1FP shows a performance similar to the observed for the ABTS assay, where higher amount of HRP present in the assay leads to smaller quantity of RB19 being degraded, although the effect is not as noticeable as in the case of ABTS.

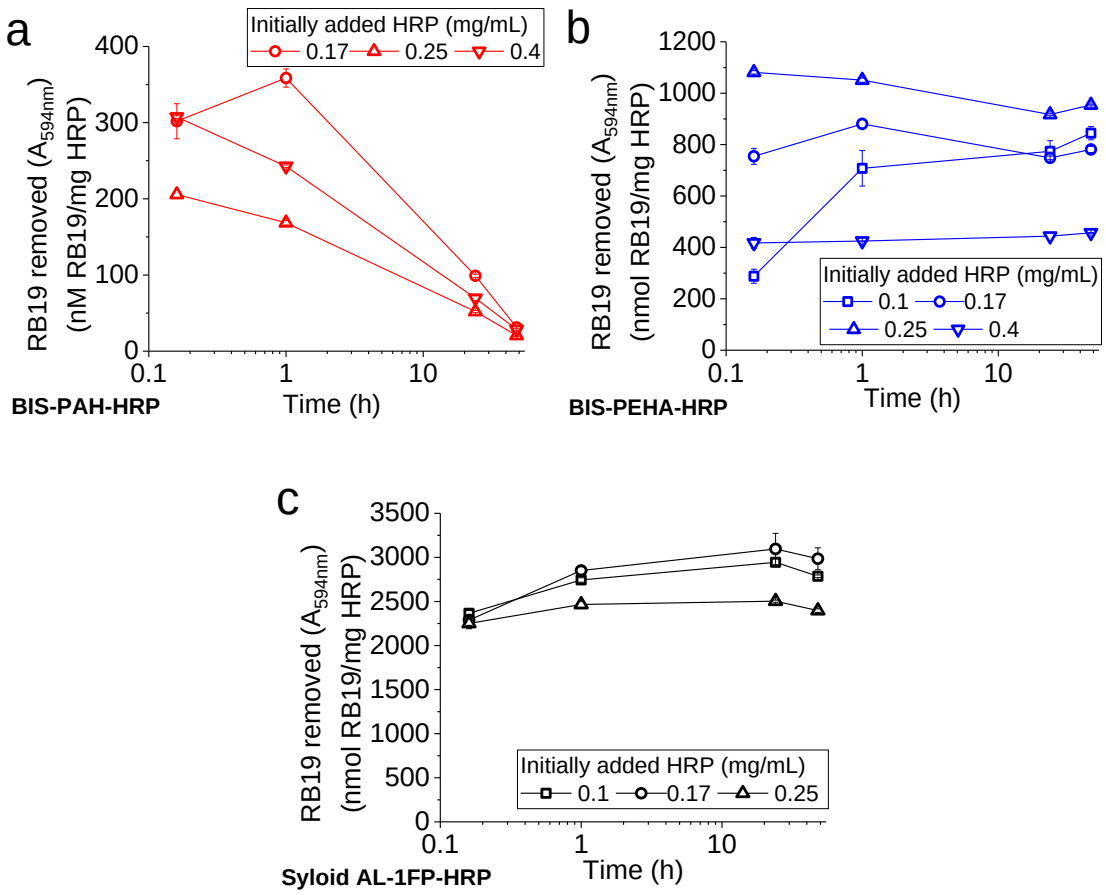

Figure 6-23: Normalised enzymatic degradation of RB19 by immobilised HRP samples produced via adsorption on a) BIS synthesised with PAH or b) BIS synthesised with PEHA, with the additive partially eluted, or on c) Syloid AL-1FP, examining the effect of increasing the initially added mass of HRP. Results shown are the average of 3 or more replicates, with the error bar representing 1 standard deviation.

In conclusion, lower amount of HRP being immobilised led overall to better results, except from the case of BIS synthesised with PAH, where for the lowest amount of HRP present, performance was the lowest observed, indicating the possibility of a "threshold" to be reached by enzymatic action to overcome the contribution from the support.

6.3. Conclusion and comparison with literature

In this Chapter, we examined the performance of the synthesised biocatalysts, after their characterisation as shown in Chapter 5. So far, presented results were categorised based on the form of immobilisation of HRP (encapsulation or adsorption) and secondly based on an optimisation of the porosity of the BIS support (based on type of amine and amount of amine present) or of the amount of HRP immobilised. The ultimate goal through the exploration of those factors is to understand their importance for the performance of the BIS-HRP composite, using 2 different assays. A commercial silica (Syloid AL-1FP) was used as a control, in order to examine how the in-house produced BIS compares as an immobilisation support with an already commercialised material.

Based on the results as shown for immobilised HRP via encapsulation or adsorption, the adsorbed enzyme shows a much faster and higher response, when examined under the same conditions as

the encapsulated, regardless of the assay used. This is mainly attributed to the localisation of HRP in each immobilisation system. In the encapsulation case the enzyme is buried deep inside the pore structure (mostly micropore in the case of PEHA, some mesopores in the case of PAH), with no clear "channels of communication" with the bulk solution of the assay. In the adsorption case, HRP is located mainly on the external surface area, or in easily accessible pore channels, allowing for easier interaction with the substrates.

Narrowing down the comparison of the systems examined in this section, 2 graphs were created, based on the normalised enzymatic ABTS oxidation or RB19 removal. The value selected to represent each system in each graph was the maximum detected during the assay, across the same cohort, i.e. amount of HRP initially added, point of addition, elution state of the additive, representing both additives examined. A tabulated matrix showing the best identified options is shown in Table 6-1. Results for ABTS for all the best performing samples (including HRP adsorbed on Syloid AL-1FP) are shown in Figure 6-24a and equivalent results for RB19 are shown in Figure 6-24b. Through those collective graphs, one can see the clustered performance of HRP encapsulated of adsorbed on BIS, as well as the overall higher performance of HRP adsorbed on Syloid AL-1FP. When HRP is assayed using the – much more sensitive – ABTS assay, there is a difference of an order of a magnitude between the best immobilised HRP version and the free enzyme (Figure 6-24a), whereas, for RB19, the performance of free and immobilised enzyme is more comparable (Figure 6-24b).

At this point we have to mention the very high interaction that BIS had with both assays used. BIS proved to be a very good adsorbent for both substrate and product of each assay used, leading to spectacular results when it came to colour removal. Isolating the enzymatic contribution and identifying the "real" measurement in each case was difficult. It should also be pointed out that only a few literature examples on enzyme immobilisation for dye decolorisation acknowledge the potential contribution of the immobilisation support to dye removal, such as [108, 271, 274, 283, 431, 432], and there is only 1 report of thorough examination of decolorisation due to dye adsorption on the support of immobilised laccase [340]. In this example, the contribution of the alumina support and the presence of not catalytically active protein (bovine serum albumin) was examined to dye removal, similarly to how we tried to isolate the contribution from the support used in this work. It was found that adsorption of dye was overall more prominent compared to enzymatic degradation, with results similar to the obtained for HRP encapsulated in BIS. Many reports do not state the use of appropriate controls needed for monitoring of adsorption contribution to colour removal [97, 261, 263, 381, 433-435], despite the fact either that the supports under question (silicas, alginate beads) are known for their adsorbing abilities. In other cases, there is a brief mention dye adsorption potential on the support without further analysis [155, 156, 335, 436].

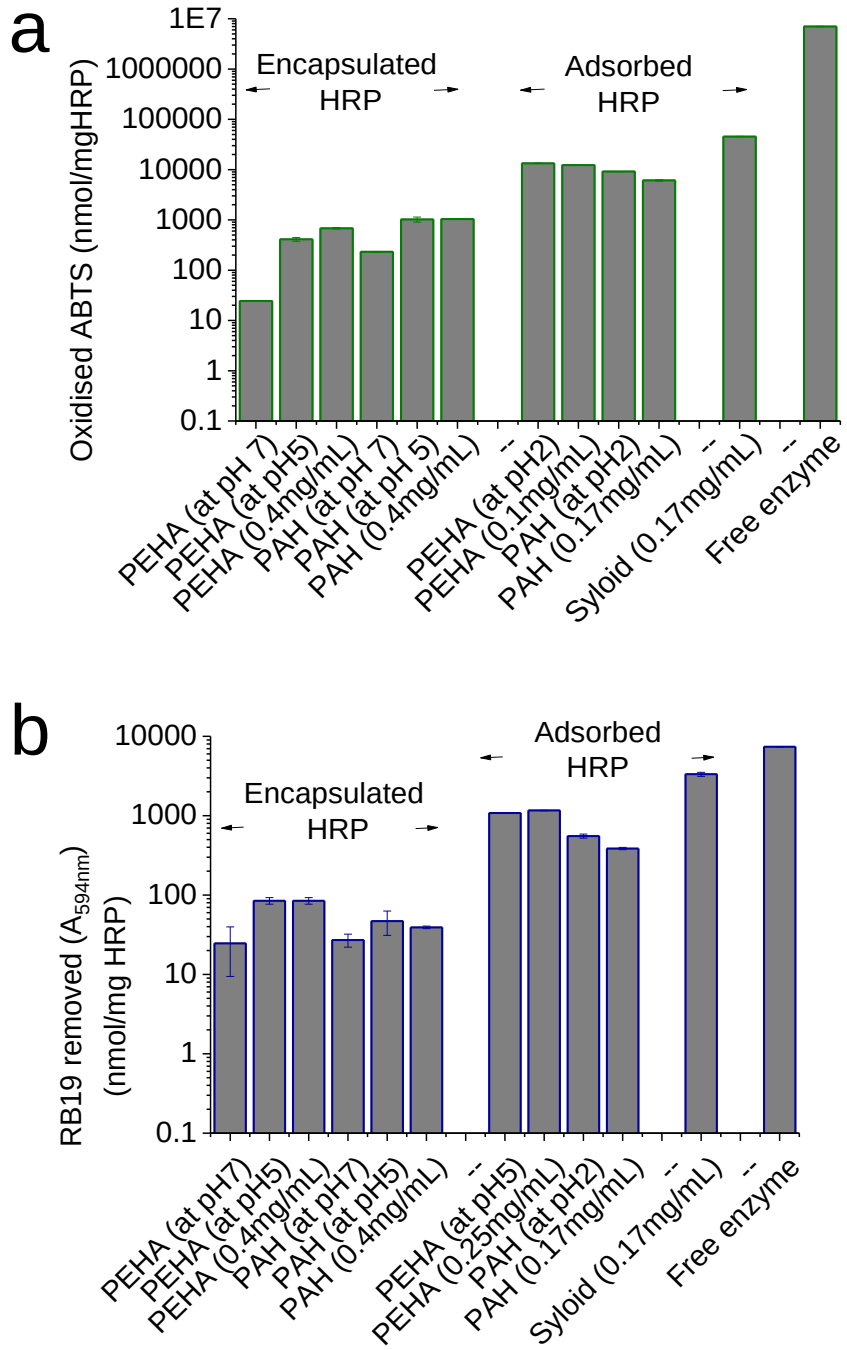

Figure 6-24: Best performing samples of immobilised HRP as shown in Table 6-1, compared with free HRP, examined through the a) ABTS and b) RB19 assay. Results shown are based on the normalised per mg HRP approach, of the maximum observed value of each sample during the assay. Results shown are the average of 3 or more replicates, with the error bar representing 1 standard deviation.

Table 6-1: Matrix of best results achieved from each assay, for each amine used for BIS synthesis, for each immobilisation method of HRP.

Encapsulation of HRP in BIS using PEHA	**Best (time point, h)**	**Adsorption of HRP on BIS using PEHA**	**Best (time point, h)**
ABTS assay			
Point of addition	at pH 7 (1)	Elution of additive	at pH 2 (24)
Elution of additive	at pH 5 (1)	Mass of HRP initially added	0.1 or 0.17mg/mL (1)
Mass of HRP initially added	0.4mg/mL (48)		
RB19 assay			
Point of addition	Any (48)	Elution of additive	at pH5 (0.16)
Elution of additive	at pH 5 (48)	Mass of HRP initially added	0.25mg/mL (0.16)
Mass of HRP initially added	0.4mg/mL (24)		

Encapsulation of HRP in BIS using PAH	**Best (time point)**	**Adsorption of HRP on BIS using PAH**	**Best (time point)**
ABTS assay			
Point of addition	at pH 7 (24)	Elution of additive	at pH 2 (24)
Elution of additive	at pH 5 (1)	Mass of HRP initially added	0.17mg/mL (1)
Mass of HRP initially added	0.4mg/mL (1)		
RB19 assay			
Point of addition	at pH 7 (1)	Elution of additive	at pH 2 (0.16)
Elution of additive	at pH 5 (1)	Mass of HRP initially added	0.17mg/mL (1)
Mass of HRP initially added	0.4mg/mL (1)		

In conclusion, answering the question on whether using BIS as immobilisation support is an effective option, the answer is a conditional yes. BIS achieves high loadings of enzyme, and the enzyme shows activity upon examination. We were able to identify optimised conditions of immobilisation which led to higher results in terms of ABTS oxidation or RB19 degradation. However, results obtained with BIS-HRP biocatalysts (regardless of immobilisation type, amine or mass of enzyme), where not as high as achieved results with HRP immobilised on Syloid AL-1FP. Based on the experimental observations and speculations about the BIS-HRP systems, this is attributed to a) contribution from the BIS support on the assays and b) amount of HRP present in the assay.

A comparison with literature regarding the factors examined in this Chapter, shows that although there are many reports examining the effect of different factors on the immobilisation efficiency (as we showed in Chapter 4); few reports examine the effect of these factors on the performance of the biocatalyst. As it was showed in this Chapter, more often than not, samples with lower amount of immobilised HRP showed much higher response to both oxidation of ABTS and degradation of RB19, so it should be advised that samples are biocatalysts are tested for enzymatic activity regardless of the amount of enzyme loaded. A great report which does that was produced by Janovic et al, who looked at immobilisation of HRP on various supports and immobilisation systems and examined their performance. It was shown that systems with high performance were not necessarily rich in immobilised HRP and vice versa, as well as encapsulated HRP performed lower compared to adsorbed or covalently bound HRP, due to higher enzyme availability [271], verifying the observations made herein. There are a few reports which examine the optimisation of the synthesis of immobilised enzyme systems, such as the one reported by Mansor [267], regarding laccase entrapped in mesoporous silicas synthesised via the sol-gel method, examining the ratio of silica precursor to water, the quantity of amine present and the quantity of enzyme present during the synthesis of biocatalysts. Their analysis resulted in a set of design parameters where amine concentration was on the lower side of the examined spectrum and enzyme concentration on the higher side of the examine spectrum [267], aligning with the observations herein, where elution of additive from BIS leads to biocatalysts with higher enzymatic activity. Another example compared the performance of immobilised HRP in alginate or acrylamide beads, resulting in higher performance of the latter, increased compared to free HRP [435]. Furthermore, the decolorisation potential of laccase immobilised on imidazole-modified silica, ionic resin and modified montmorillonite was examined, showing that the lower amount immobilised on the silica support offered the highest results on dye removal [432]. Sekulijca examined the effect of glutaraldehyde and bovine serum albumin concentration used for aggregation of HRP to form CLEAs and showed that higher amount of both leads to higher recovery of aggregates, but with lower enzymatic activity [337]. Temocin showed that higher amount of HRP present in biocatalysts synthesised by HRP immobilised on modified acrylamide fibers resulted in higher activity up to

a point, when activity was stable regardless of the increasing quantity of HRP [264]. Similarly, increasing the concentration of a DyP immobilised in alginate beads resulted in increase of the retained activity, up to a maximum, followed by a drop [436]. Many of the literature examples on immobilised enzyme systems examined on dye decolorisation show a quite high decolorisation degree, comparable or even higher to the observed for the free enzyme [108, 274, 337, 434] . However, having seen the contribution of the BIS support in this case and being aware of the lack of information on the contribution of immobilisation supports in literature examples, a comparison with literature should be taken with a pinch of salt.

A takeaway message from this Chapter is that researchers ought to be more careful during data collection using immobilised enzymes. Attention is needed in order to identify all factors that might have an effect on the observed results and try to quantify the contribution. In this way, we can increase understanding of the system and create a solid base for further development and potential future work. Also, a correlation between enzyme loading and activity of the biocatalyst reveals that higher amount of enzyme present does not always imply high activity. Diffusional limitations can affect the enzyme-activity balance (as it was the case for encapsulated HRP), but also presence of excessive amount of enzyme can cause reduced activity response (as it was the case for HRP adsorbed on BIS or Syloid AL-1FP). Last but not least, what we saw in this chapter, was that activity response of immobilised enzyme might by substantially delayed, fact mainly attributed to diffusional limitations and adsorbing abilities of the immobilisation supports used. If the assay time was kept constant at 10min as it was for free HRP, we would not have been able to observe and assess the enzymatic activity of immobilised HRP, neither witness the adsorbing ability of BIS, or build understanding around the response time needed for different systems.

For HRP encapsulated in BIS, regardless of the additive used, the best results were identified when the additive was eluted at pH 5 and the initial concentration of HRP to be incorporated was 0.4mg/mL. Given the identified contribution of BIS to the response of the assays, in order to have a fair comparison with the BIS-HRP samples produced by in-situ encapsulation, the selected BIS-HRP samples produced by adsorption to be used for comparison reasons were again of BIS pH 5. This decision was made based on the levels of complexity which would be involved if too many factors changed at the same time.

Chapter 7 : Kinetics of enzymatic action of free and immobilised Horseradish Peroxidase

In Chapter 6 we identified the best performing samples of immobilised HRP either through encapsulation in BIS or adsorption on BIS using standard assays. In this chapter we further explore the performance of those immobilised HRP samples, comparing it to that of free HRP, regarding the kinetics of enzymatic action. Characterising the kinetic behaviour of enzymes in free or immobilised from is a quite common way of examining and comparing their performance, using the initial rate of controlled enzymatic reaction. The most common kinetic model which described enzymatic activity was developed by Michaelis and Menten [437]. Most of enzymes can be characterised using this model, under controlled conditions. When conditions are different than the "appropriate", then behaviour does not fit with the simple Michaelis-Menten model and further corrections need to be applied as mentioned and described in section 3.4.3 of chapter 3. Given the use of both H_2O_2 and "coloured" substrate (ABTS or RB19) used for HRP, kinetic characteristics were determined for both cases, using both ABTS and RB19 assays.

It should be mentioned that HRP is a fairly well characterised enzyme, which however, as for every enzyme, can have a different performance depending on the origin of the enzyme, the isoenzyme type, the concentrations of reagents used and the substrates used [133, 134, 382, 438]. The added level of complexity due to immobilisation can potentially lead to even higher ambiguity of obtained results. Furthermore, there is not explicit information in the literature on how the initial rates for enzymatic conversions are obtained, a fact which can lead to substantially different results as we will explain later.

In order to define the kinetic characteristics of HRP – in free or immobilised form – under standard assay conditions, all parameters were kept constant except from the concentration of one substrate at a time. Results are shown initially for the free enzyme, followed by a section for the immobilised preparations.

7.1. Studies on free HRP

7.1.1. Effect of RB19 and ABTS concentration

Keeping the concentration of HRP and H_2O_2 constant, (at 0.017 mg/mL and 0.044mM final concentration in the assay respectively), the concentration of RB19 was varied from 0.05 to 0.5mM, kinetics were monitored (Figure 7-1), adding the "forged" initial point, as it was explained in section 4.2.2.1 and illustrated in Figure 4-12 of Chapter 4. From Figure 7-1 it is evident that for higher dye concentrations, HRP does not reach complete colour removal (at least to the extent observed for lower concentrations), as it can also be observed from the actual samples visually (Figure 7-2).

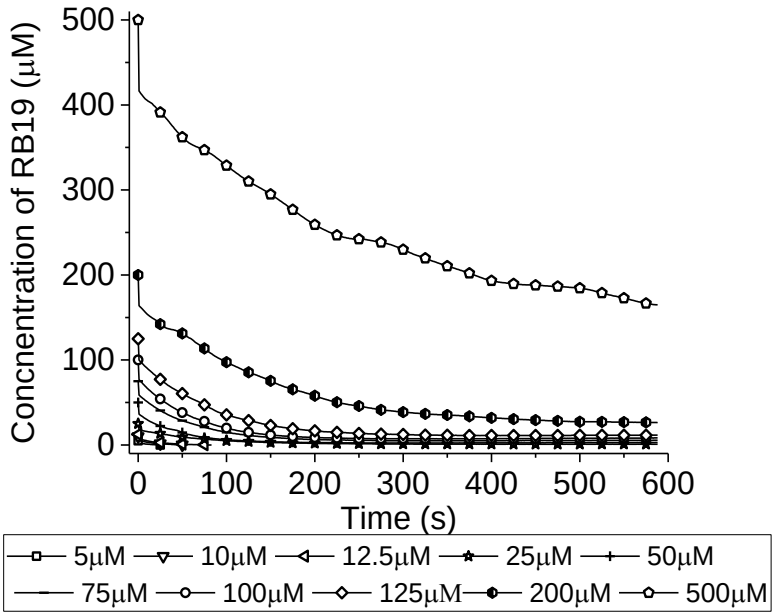

Figure 7-1: Kinetics monitoring of enzymatic RB19 degradation. One sample per RB19 concentration examined is shown and the point skipping function is used for clarity.

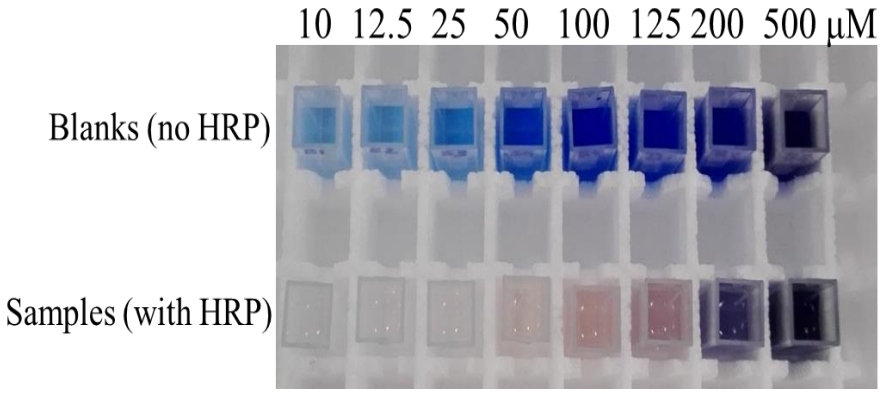

Figure 7-2: Snapshot of enzymatic degradation of RB19 upon increasing concentration of dye. Photos were taken about 1h after assay initiation.

The initial rate of the decolorisation reaction was determined by fitting the kinetics using the exponential decay model as it was demonstrated in section 4.2.2.1 and plotted for increasing substrate concentration in Figure 7-3. Table 7-1 shows the kinetic parameters as obtained through fitting. With respect to the kinetic parameters, given that measured rates were kept at a more or less constant value past the concentration of 75μM and until 500 μM, inhibition (reduction of measured rate) was not occurring for the measured dye concentration range. Fittings were performed with the classic Michaelis Menten model and the Ping Pong Bi Bi model [133], as discussed in section 3.4.3 of Chapter 3. The measured maximum initial rate (V_{max}) was almost 3.5μM RB19/s and the Michaelis Menten constant (K_m) was calculated at 25.16μM. Another study of the same system, decolorisation of RB19 using HRP, resulted in kinetic parameters an order of magnitude higher than calculated here (V_{max} was 1.8 μM/min and K_m was 455 μM, but there is no information on how rates were calculated. Furthermore there are concerns about the quality of the result, as the calculated K_m is an order of magnitude higher than the concentration

range examined in their study [20]. A similar study (same enzyme, different dyes) resulted in kinetic parameters within the same order of magnitude as observed herein (K_m equal to 46 and 58 μM for Reactive Blue 221 and Reactive Blue 198 respectively) [433].

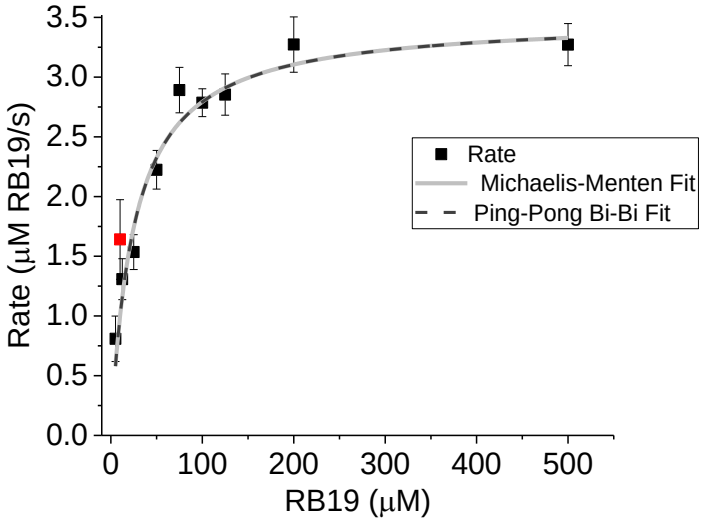

Figure 7-3: Initial rate of RB19 degradation by free HRP with increasing substrate concentration and determination of kinetic parameters. Results shown are the average of 3 or more replicates, with the error bar representing 1 standard deviation. Red symbol signifies point out of order which prevented fitting, hence it was excluded during fitting.

Table 7-1: Determination of kinetic parameters for models shown in Figure 7-2. Values shown are in the format of "returned value (error)". Values shown have been rounded to max 4 significant digits.

	Model	
	Michaelis-Menten	**Ping Pong Bi Bi (inhibition)**
Equation	$y = {V_{max} \times x}/{(K_m + x)}$	$y = {0.44 \times V_{max} \times x}/{A}$ $A = \left((K_{mb} \times 0.044) + K_{ma} \times x \times \left(1 + \left({x}/{K_{ib}}\right)\right)\right) + (0.044 \times x)$
V_{max} (μM/s)	3.50 (0.16)	3.50 (0.17)
K_m (μM)	25.16 (4.07)	--
K_{ma} (μM)	--	2.94E-15 (0.00)
K_{mb} (μM)	--	25.17 (4.83)
K_{ib} (μM)	--	130.09 (0.00)
R^2	0.9591	0.9428

Work from Sekulijca (same enzyme, different dye, examining inhibition) resulted either in V_{max} 2 orders of magnitude higher than calculated here and K_m 1 order of magnitude higher [133], or in similar K_m and 2 orders of magnitude higher V_{max} [18]. The aforementioned examples and some research examples examining the activity of HRP on non-dye substrates can be seen tabulated in Table 0-9 and Table 0-10 of Appendix III. These results show high variance, mainly attributed to either the examined system (type and concentration of reagents), or to the generation of data (calculation of rates, fitting models). Hence, it is not uncommon to not find a good match between the data produced here and the literature.

Although the focus of this section is the determination of kinetic parameters, further analysis past this point was conducted. In order to be consistent with the assay procedure, the concentration of the examined samples was monitored over 48h (Figure 7-4). Results show that beyond the first 10min, dye content was not significantly reduced over the 48h time period, indicating the fast action of free HRP and the absence of subsequent spontaneous oxidation. It should be mentioned that points for t=0s and t=10s are connected by a straight line for illustrative reasons.

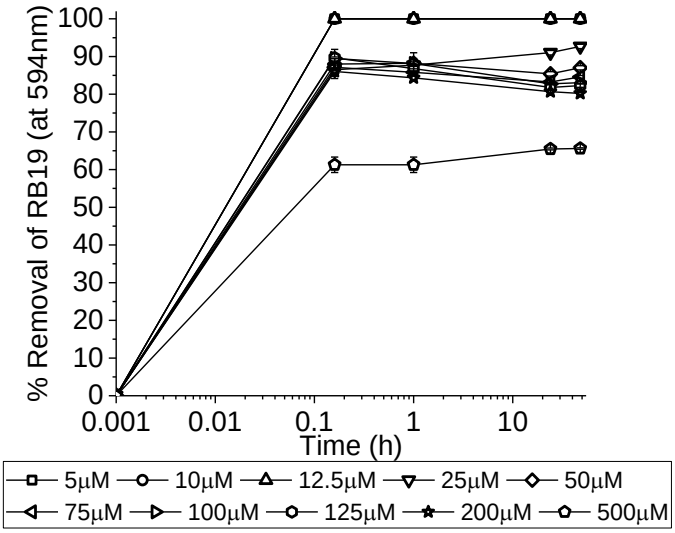

Figure 7-4: Removal of RB19 by free HRP over the assay period, examining different initial concentrations of RB19. Results shown are the average of 3 replicates, with the error bar representing 1 standard deviation.

Similarly for ABTS, kinetic parameters were determined by monitoring of kinetics (Figure 7-5) and calculation of the initial reaction rate. Substrate concentration was varied from to 0.01mM to 10mM, keeping the concentration of other reagents stable (0.044mM for H_2O_2 and 0.084μg/mL HRP). From Figure 7-5 it is clear that with increasing initial concentration of ABTS the oxidation rate and production of ABTS radical increases, up to a point where rate (and production) starts decreasing (after 0.5mM ABTS). The rate of the oxidation reaction was determined (Figure 7-6) by fitting of the kinetic monitoring data with the exponential model, as demonstrated in section 4.1.2.1. of Chapter 4. Figure 7-6 shows a typical inhibition based on substrate concentration, indicating deactivation of HRP as initial concentration of ABTS increases. The classic Michaelis-Menten model is not appropriate to fit the data, but models taking inhibition into consideration

reach a good fit level (Figure 7-6, Table 7-2). Inhibition can be attributed to dead-end complexes formed between the enzyme and the oxidation products, as described by Sekulijca when examined excess concentrations of dye using HRP [133].

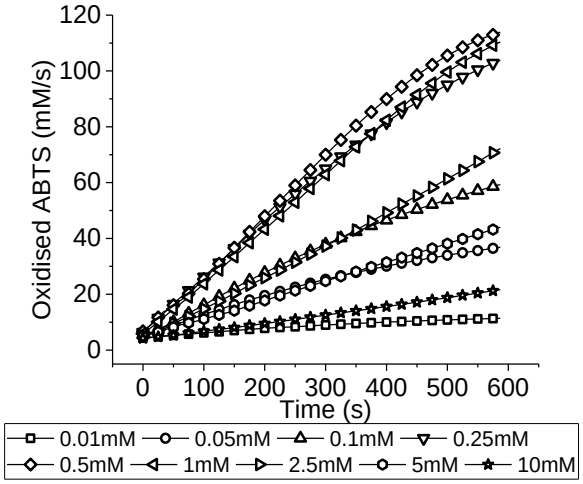

Figure 7-5: Kinetics monitoring of enzymatic ABTS oxidation. One sample per ABTS concentration examined is shown and the point skipping function is used for clarity..

Interestingly, if the higher ABTS concentrations are omitted from the plot and data gets re-fitted with the same models, inhibition is not present (Figure 7-7) and classic Michaelis-Menten model fits very well (Table 7-3). Again, given the discrepancy shown for kinetic parameters obtained with B19, a comparison with literature on the kinetic parameters obtained with ABTS would not provide any useful information.

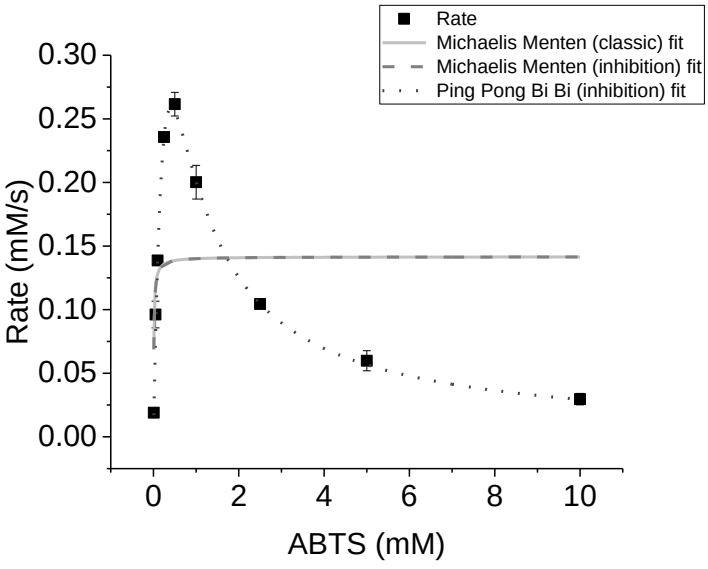

Figure 7-6: Fitting of calculated ABTS oxidation rates for ABTS concentration varying from 0 to 10mM. Results shown are the average of 3 replicates, with the error bars representing 1 standard deviation.

Table 7-2: Determination of kinetic parameters for models shown in Figure 7-6. Values shown are in the format of "returned value (error)". Values shown have been rounded to max 4 significant digits.

	Model		
	Michaelis-Menten	**Michaelis-Menten (inhibition)**	**Ping Pong Bi Bi (inhibition)**
Equation	$y = {V_{max} \times x}/{(K_m + x)}$	$y = \frac{V_{max} \times x}{(K_m + x \times (1 + {x}/{K_i}))}$	$y = {0.044 \times V_{max} \times x}/{A}$ $A = \left((K_{mb} \times 0.044) + K_{ma} \times x \times \left(1 + \left({x}/{K_{ib}}\right)\right)\right) + (0.044 \times x))$
V_{max} (mM/s)	0.14 (0.03)	0.89 (0.06)	0.14 (0.03)
K_m (mM)	0.01 (0.02)	0.51 (0.04)	--
K_{ma} (mM)	--	--	1.28E-20 (0)
K_{mb} (mM)	--	--	0.01 (0.03)
K_{ib} (mM)	--	0.34 (0.03)	0.37 (0)
R^2	0.0278	0.9988	-0.3611

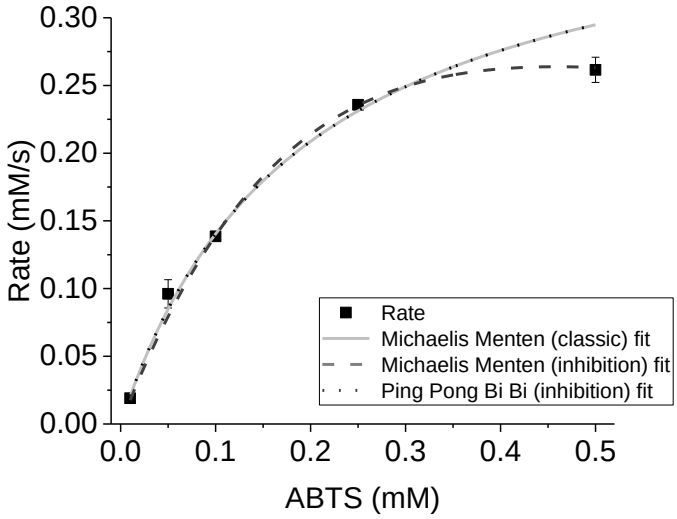

Figure 7-7: Re-fitting of calculated ABTS oxidation rates for ABTS concentration varying from 0 to 0.5mM, while keeping every other factor constant. Results shown are the average of 3 replicates, with the error bars representing 1 standard deviation.

Table 7-3: Determination of kinetic parameters for models shown in Figure 7-7. Values shown are in the format of "returned value (error)". Values shown have been rounded to max 4 significant digits.

	Model		
	Michaelis Menten	**Michaelis Menten (inhibition)**	**Ping Pong Bi Bi (inhibition)**
Equation	$y = {V_{max} \times x}/{(K_m + x)}$	$y = \frac{V_{max} \times x}{(K_m + x \times (1 + {x}/{K_i}))}$	$y = {0.044 \times V_{max} \times x}/{A}$ $A = \left((K_{mb} \times 0.044) + K_{ma} \times x \times \left(1 + \left({x}/{K_{ib}}\right)\right)\right) + (0.044 \times x)$
V_{max} (mM /s)	0.41 (0.03)	0.73 (0.19)	0.41 (0.06)
K_m (mM)	0.19 (0.03)	0.41 (0.13)	--
K_{ma} (mM)	--	--	0 (0)
K_{mb} (mM)	--	--	0.19 (0.05)
K_{ib} (mM)	--	0.52 (0.30)	0.31 (0)
R^2	0.9915	0.9981	0.9745

Similarly to RB19, 48h monitoring of ABTS oxidation for the initial ABTS concentrations examined is shown in Figure 7-8, where it is clear that for the lower concentrations of ABTS (up to 1mM), oxidation is completed by the 1st hour, whereas for the higher concentrations, the slower rate of enzymatic activity dictates a longer time until reaction is completed. Having seen the effect that RB19 and ABTS initial concentration has on enzymatic activity, we can conclude that for both substrates, if the concentration is kept at values up to 0.5mM, there is no inhibition present, whereas for higher concentrations enzymatic activity can get severely hampered.

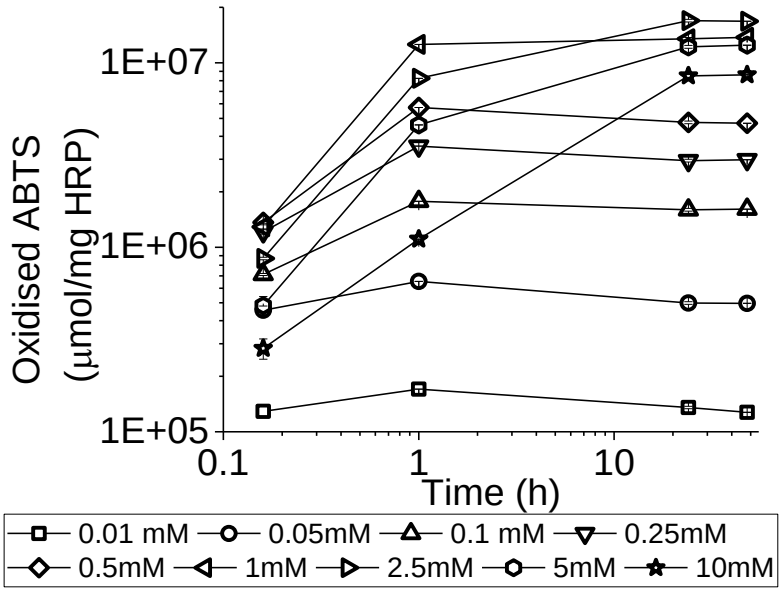

Figure 7-8: Oxidation of ABTS by free HRP over the assay period, examining different initial concentrations of ABTS. Results shown are the average of 3 replicates, with the error bar representing 1 standard deviation.

Furthermore, it should be pointed out that given the different structure and oxidation mechanism of the 2 substrates, resulting in different kinetic parameters in each case is not surprising. Examples in literature have shown a very different performance of the same enzyme towards different substrates [154, 177, 185].

7.1.2. Effect of H_2O_2 concentration

During the previous examination, concentration of hydrogen peroxide was being kept constant, but since it is also a substrate, its effect on enzymatic activity should be examined as well. The low stability of peroxide-dependant peroxidases to hydrogen peroxide is a well-known issue with those enzymes, as it is considered a limiting factor for their industrial implementation [439]. Much research is done in order to understand and increase the stability of peroxidases to peroxides, with main research avenues being through molecular biology or immobilisation [87, 187, 440]. The initial rate of the enzymatic oxidation of ABTS or RB19 was monitored while concentrations of ABTS or RB19 were kept constant and H_2O_2 concentration varied from 0.015mM to 44mM (final assay concentration).

Results obtained for RB19 oxidation based on kinetic monitoring of the first 10min of the reaction are shown in Figure 7-9. It is clear that for the extreme concentrations of peroxide (0.0147mM and 44.1mM) the enzymatic activity is substantially different compared to the rest, given the considerably higher RB19 concentration left by the end of the monitoring. This is also evident by the snapshots of the examined samples just after the assay (Figure 7-10).

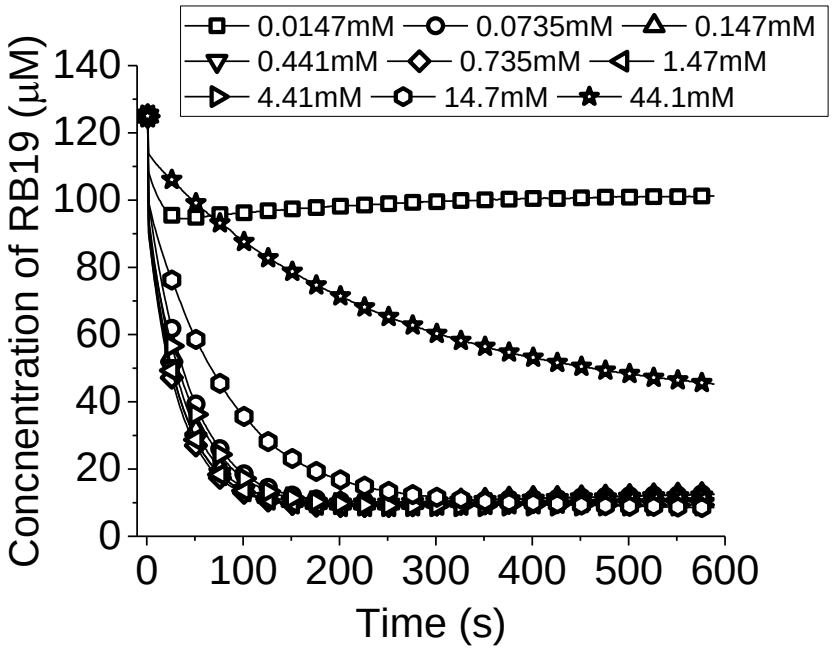

Figure 7-9: Kinetics monitoring of enzymatic RB19 degradation. One sample per H_2O_2 concentration examined is shown and the point skipping function is used for clarity..

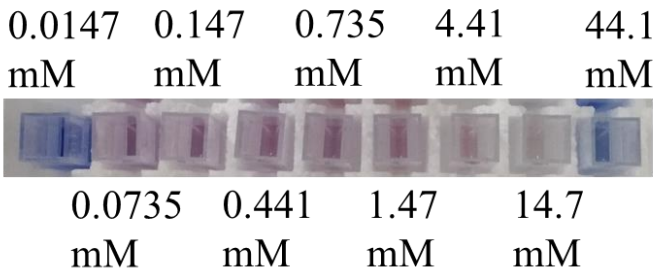

Figure 7-10: Snapshots of enzymatic degradation of RB19 with increasing concentration of H_2O_2, keeping every other factor constant.

Determination of the initial rates of the enzymatic reactions showed that highest rate was observed for peroxide concentration of 0.44mM, with high rates being also observed within the range between 0.0735 to 0.735mM H_2O_2 (inset of Figure 7-11). The only model reaching a fit was the Michaelis Menten including inhibition (Table 7-4), leading to a V_{max} of 4.6mM RB19/s, a K_m of 0.04mM and an inhibition constant (K_i) of 6.8mM.

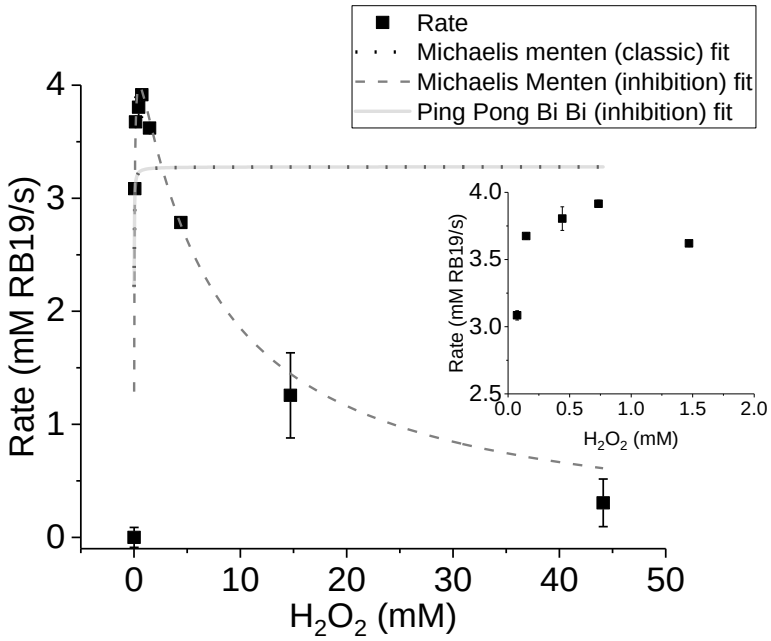

Figure 7-11: a) Fitting of calculated RB19 degradation rates and b) determination of kinetic parameters, for H_2O_2 concentration varying from 0.0147 to 44.01mM, while keeping every other factor constant. Results shown are the average of 3 replicates, with the error bar representing 1 standard deviation.

As discussed previously, comparison of these results to literature cannot offer any constructive information, other than the similarity of the inhibition trend [133]. Attempting to identify the non-inhibitory concentration range of peroxide for the enzymatic activity, obtained rates were re-fitted, for peroxide concentration ranging from 0.0147mM to 0.147mM (Figure 7-12), indicating a better fit with the Michaelis Menten model than before, although still fitting better with the inhibition model, as shown in Table 7-5. It should be pointed out that although the Ping Pong Bi Bi model seems to reach a fit, the R^2 value is poor, indicating falsified converging.

Table 7-4: Determination of kinetic parameters for models shown in Figure 7-11. Values shown are in the format of "returned value (error)". Values shown have been rounded to max 4 significant digits.

	Model		
	Michaelis Menten	**Michaelis Menten (inhibition)**	**Ping Pong Bi Bi (inhibition)**
Equation	$y = {V_{max} \times x}/{(K_m + x)}$	$y = \frac{V_{max} \times x}{(K_m + x \times (1 + {x}/{K_i}))}$	$y = {0.125 \times V_{max} \times x}/{A}$ $A = \left((K_{mb} \times 0.125) + K_{ma} \times x \times \left(1 + \left({x}/{K_{ib}}\right)\right)\right) + (0.125 \times x))$
V_{max} (mM/s)	3.27 (0.24)	4.58 (0.24)	7.57856 (4.03802)
K_m (mM)	0.007 (0.014)	0.037 (0.009)	--
K_{ma} (mM)	--	--	1 (0)
K_{mb} (mM)	--	--	1 (0)
K_i (mM)	--	6.79 (1.18)	1 (0)
R^2	-0.0346	0.9160	-28.15

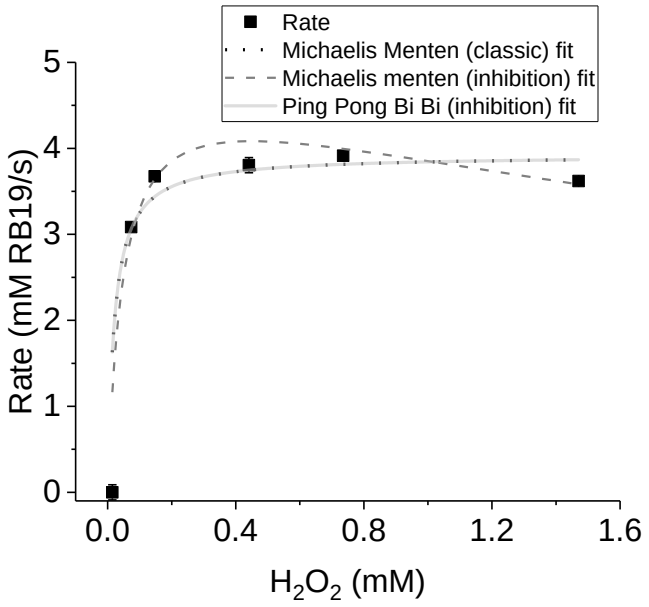

Figure 7-12: Re-fitting of calculated RB19 degradation rates for H_2O_2 concentration varying from 0.0147 to 1.47mM, while keeping every other factor constant. Results shown are the average of 3 replicates, with the error bar representing 1 standard deviation.

Table 7-5: Determination of kinetic parameters for models shown in Figure 7-12. Values shown are in the format of "returned value (error)". Values shown have been rounded to max 4 significant digits.

	Model		
	Michaelis Menten	**Michaelis Menten (inhibition)**	**Ping Pong Bi Bi (inhibition)**
Equation	$y = {V_{max} \times x}/{(K_m + x)}$	$y = \frac{V_{max} \times x}{(K_m + x \times (1 + {x}/{K_i}))}$	$y = {0.125 \times V_{max} \times x}/{A}$ $A = \left((K_{mb} \times 0.125) + K_{ma} \times x \times \left(1 + \left({x}/{K_{ib}}\right)\right)\right) + (0.125 \times x)$
V_{max} (mM/s)	3.92 (0.22)	4.95 (0.70)	3.92 (0.31)
K_m (mM)	0.020 (0.011)	0.047 (0.023)	--
K_{ma} (mM)	--	--	2.44E-19 (0)
K_{mb} (mM)	--	--	0.02 (0.01)
K_i (mM)	--	4.18 (2.60)	0.15 (0)
R^2	0.6399	0.9160	0.2799

Repeating the same procedure but using ABTS as substrate this time, kinetics monitoring for peroxide concentrations ranging from 0.0147mM to 44.1mM while keeping all other factors constant, is shown in Figure 7-13 and determination of kinetic parameters are shown in Table 7-6. It is evident that the examined concentration of peroxide does not pose such an inhibitory effect to HRP when it comes to ABTS oxidation, as opposed to RB19 degradation, as for higher concentration of peroxide oxidation rate of ABTS is not decreasing as drastically as in the case of RB19. Given the different structure and oxidation mechanism of the 2 substrates, such an observation is again not surprising. The fitting of the models should be commented at this point, as for all 3 models fit is quite acceptable (high R^2 obtained), but only in the case of Michaelis Menten with accounted inhibition model the fitting line passes by all the experimental points, indicating a better representation of the data.

So far, we saw the performance of HRP in free form, on a range of concentrations of each substrate, keeping all other factors constant. The obtained profiles and the kinetic characterisation give us information on the effect each substrate has on the enzyme, and the inhibitory potential. Trying to fit the experimental data with the available models shows that although in many cases a fit to the classic Michaelis Menten model is obtainable, data fits better to more complicated models, accounting for inhibition by excessive substrate concentration. Furthermore, comparing the fit obtained with the classic Michaelis Menten model and the Ping Pong Bi Bi model with accounted inhibition, we can see that they are identical in every case. The K_{ma} factor (Michaelis Menten constant representative of the substrate with the varying concentration) is practically 0, nullifying the relevant portion of the model, leading to a classic Michaelis Menten expression.

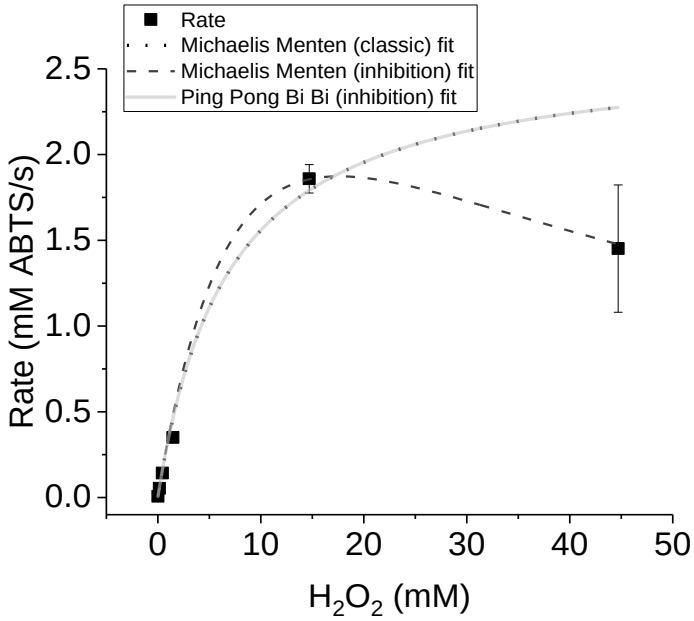

Figure 7-13: Fitting of calculated ABTS oxidation rates for H_2O_2 concentration varying from 0.0147 to 44.01mM, while keeping every other factor constant. Results shown are the average of 3 replicates, with the error bar representing 1 standard deviation.

Table 7-6: Determination of kinetic parameters for models shown in Figure 7-13. Values shown are in the format of "returned value (error)". Values shown have been rounded to max 4 significant digits.

	Model		
	Michaelis Menten	**Michaelis Menten (inhibition)**	**Ping Pong Bi Bi (inhibition)**
Equation	$y = {V_{max} \times x}/{(K_m + x)}$	$y = \frac{V_{max} \times x}{(K_m + x \times (1 + {x}/{K_i}))}$	$y = {10 \times V_{max} \times x}/{A}$ $A = \left((K_{mb} \times 10) + K_{ma} \times x \times \left(1 + \left({x}/{K_{ib}}\right)\right)\right) + (10 \times x)$
V_{max} (mM/s)	2.62 (0.26)	4.40 (1.68)	2.62 (0.37)
K_m (mM)	6.83 (1.20)	11.86 (4.83)	--
K_{ma} (mM)	--	--	0 (0)
K_{mb} (mM)	--	--	6.83 (1.71)
K_i (mM)	--	26.08 (25.56)	73.02 (0)
R^2	0.9842	0.9933	0.9685

In literature there has been extensive work trying to characterise peroxidases based on determination and quantification of the intermediate compounds formed, determination of kinetic parameters under various operational conditions and even in the presence of known inhibitors [134, 135, 275, 371]. In this project the scope of kinetic characterisation of the enzyme is being done only to compare between the free and immobilised form of HRP, without looking into further detail, as it is considered beyond the scope.

7.2. Studies on immobilised HRP

Given the ultimate goal of enzyme immobilisation which is the preservation of enzymatic activity under "normal" conditions and enhancement of it under "unnatural" conditions, it is interesting to compare the kinetic characteristics of the free enzyme with the immobilised preparation. In many cases there are diffusional limitations, preventing us from observing the real activity and allowing us only to see the apparent activity. Such effects are more pronounced in immobilised enzyme preparations where the enzyme is entrapped or encapsulated in a matrix, or immobilised in a pore structure, given the higher possibility for diffusional limitations [215, 441]. Given the physical meaning of maximum initial rate (V_{max}) and Michaelis Menten constant (K_m), we are able to distinguish the nature of the difference between the kinetics in free or immobilised form of an enzyme. V_{max} is directly associated with the activity of the enzyme, whereas K_m is associated with the affinity of the enzyme to substrate [369]. When K_m is higher for the immobilised preparation, it indicates a lower affinity to the substrate, leading to lower enzymatic rate. Lower affinity is usually related to changed conformation of the enzyme rather than delayed action of it. Usually, obtained parameters are compromised for the immobilised preparation of the enzyme, ranging from "worse, but comparable" values of marginally lower V_{max} and slightly higher K_m [215, 218, 323], to "significantly compromised values" of much higher K_m or much lower V_{max}, by at least 50% compared to free enzyme [18, 222, 254, 365, 421, 441, 442]. In some cases, immobilisation has led to enhancement of the kinetic characteristics of the enzyme, showing higher V_{max} and/or lower K_m compared to free enzyme, indicating higher activity and affinity of the enzyme to the substrate [214, 222, 322, 443]. This is usually attributed to a more stable active conformation, allowing for better enzymatic activity. Given the sensitivity of enzymatic reactions using different substrates and the added complexity of immobilisation, there are reports where kinetic characteristics of immobilised enzyme had a different relation to those of free enzyme for different examined substrates [444]. In addition, there are reports showing higher K_m (worse affinity for the substrate) but higher V_{max} (faster reaction) [108, 261], or the opposite [321]. These results indicate that designing a biocatalyst with good retained activity, high(er) reaction rates and high(er) affinity for the substrate under examination, let alone every potential substrate, is very challenging.

Given the very strong prominent adsorption of RB19 on BIS, examination of immobilised HRP kinetics using RB19 as a substrate was omitted from the scope, and kinetic characterisation was performed using ABTS as measurable substrate. The BIS-HRP samples chosen for kinetic characterisation were in-situ encapsulated HRP during BIS synthesis using PAH as additive, with the additive partially eluted at pH 5 and HRP adsorbed on BIS synthesised with PAH as additive, with the additive eluted at pH 5. In both cases the HRP concentration initially introduced for immobilisation was 0.4mg/mL. Such a choice was justified by two criteria, the highest response of ABTS oxidation obtained from encapsulated HRP (as shown in the conclusive Table 6-1 of section 6.3) and also the need to have as few factors changing in our system as possible due to the

adsorbing abilities of BIS. Based on the second criterion and since all of the BIS-HRP-ads showed a decent-to-great response towards ABTS oxidation (as shown in Figure 6-18 and Figure 6-21), the chosen sample as a representative from this cohort was HRP adsorbed on BIS-PAH with partial elution of additive at pH 5. Experiments and subsequent data analysis was performed using the same methodology as in the case of free HRP.

7.2.1. Effect of ABTS concentration

Monitoring of HRP activity of BIS-HRP samples using varying concentrations of ABTS, shows a clear difference between encapsulated and adsorbed HRP on BIS with respect to the time needed to reach a maximum (Figure 7-14a and b for encapsulated and adsorbed HRP respectively), hinting the comparison of the procured rates and the trend of the curve.

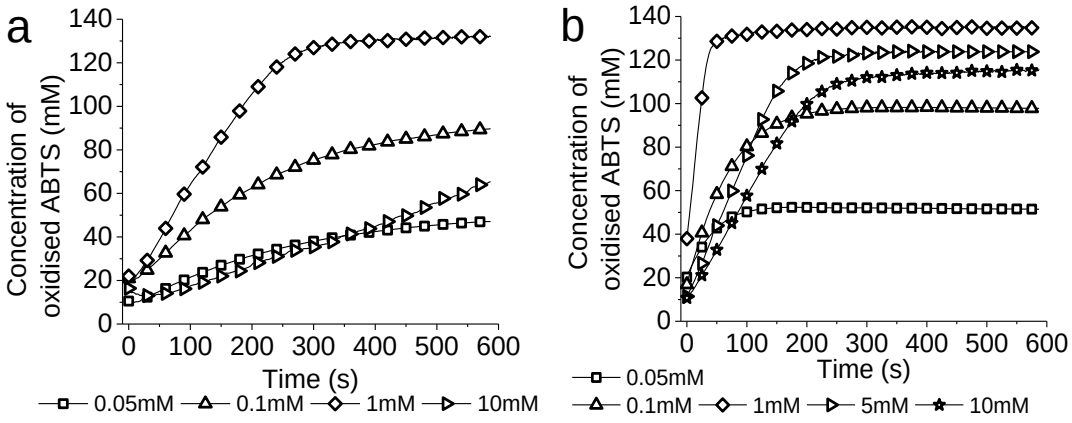

Figure 7-14: Kinetics monitoring of enzymatic ABTS oxidation by a) encapsulated HRP in BIS and b) adsorbed HRP on BIS.. One sample per ABTS concentration examined is shown.

Given the different concentrations of HRP being present in each case, procured rates cannot be compared directly, but initial observations can be drawn. It should be mentioned that the HRP quantity present in each case was 0.88mg for encapsulated HRP assays and 0.17mg for adsorbed HRP assays. Looking at Figure 7-15 we can see that the rates calculated for adsorbed HRP are significantly higher compared to the ones for encapsulated HRP, despite the lower concentration of HRP. This could be attributed either to excessive amount of enzyme in the encapsulated preparation, leading to less product due to active site blockage, or – more realistically – to severe diffusional limitations in the case of encapsulated HRP which prevent fast contact of ABTS to HRP or diffusion of oxidised ABTS. Trying to fit the obtained rates with the models used in section 0 (Table 7-7) we can see that although fit seems successful for the Michaelis Menten model with accounted inhibition, the actual parameter estimation leads to untrustworthy results, with extremely high estimated values and even higher associated error. For example, V_{max} for encapsulated HRP was estimated at 2,364 mM/s using the Michaelis Menten inhibition model, with error of 2.2E06 for the aforementioned V_{max} value and a R^2 of 0.97. In the case of adsorbed HRP returned results seem more realistic, but the error value does not allow us to accept them.

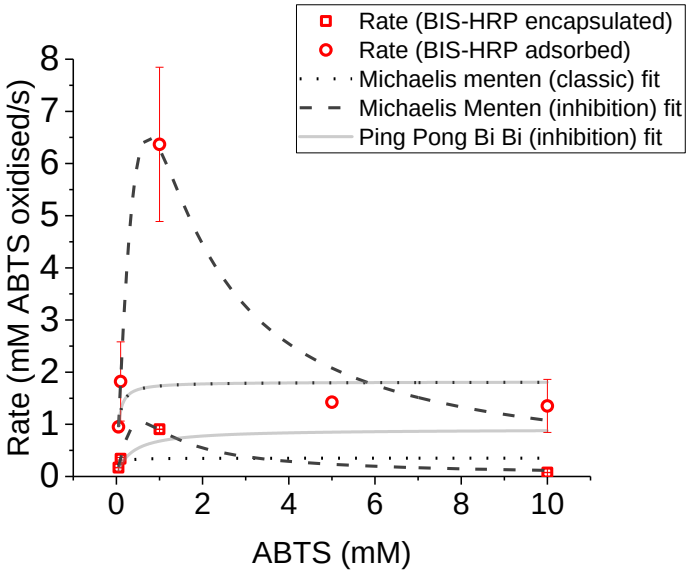

Figure 7-15: Fitting of calculated ABTS oxidation rates for ABTS concentration varying from 0.05 to 10mM, using immobilised HRP, while keeping every other factor constant. Results shown are the average of duplicates, with the error bar representing 1 standard deviation.

In an effort to see which system shows higher inhibition from increasing ABTS concentration, obtained rates (including the obtained ones for free HRP) were normalised to the maximum observed value in each case. Results (Figure 7-16) show that immobilisation of HRP expands the tolerance of the enzyme to ABTS, as the maximum rate is observed for higher concentration in the case of encapsulated and adsorbed HRP (at 1mM, compared to 0.5mM for the free enzyme). The relatively higher rates observed for lower ABTS concentrations from free HRP compared to immobilised are expected, as enzymatic activity is not being inhibited at this point for free HRP, whereas diffusional limitations and adsorption of produced ABTS radical is a occurring.

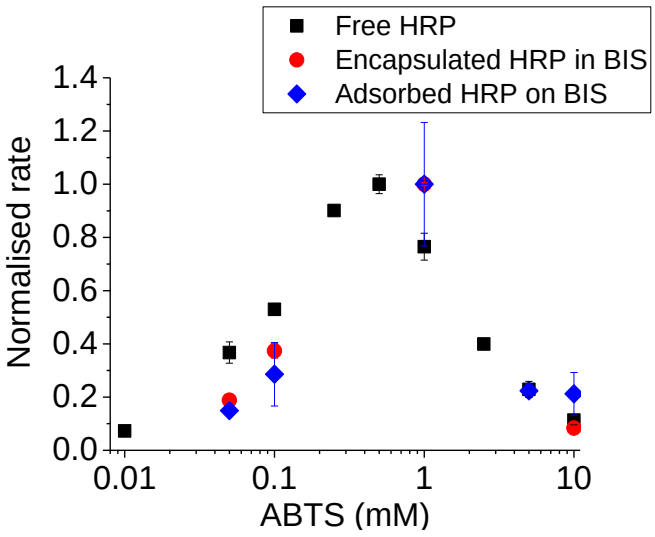

Figure 7-16: Normalised rates for the 3 systems examined, with respect to performance upon increasing ABTS concentration, keeping every other factor constant.

Table 7-7: Determination of kinetic parameters for models shown in Figure 7-15. Values shown are in the format of average (error), as calculated from OriginPro® software.

	Model		
	Michaelis Menten	**Michaelis Menten (inhibition)**	**Ping Pong Bi Bi**
	Encapsulated BIS-HRP		
Equation	$y = {V_{max} \times x}/{(K_m + x)}$	$y = \frac{V_{max} \times x}{(K_m + x \times (1 + {x}/{K_i}))}$	$y = {0.044 \times V_{max} \times x}/{A}$ $A = \left((K_{mb} \times 0.044) + K_{ma} \times x \times \left(1 + \left({x}/{K_{ib}}\right)\right)\right) + (0.044 \times x))$
V_{max} (mM/s)	0.35 (0.29)	2364 (2.20E6)	0.90 (0)
K_m (mM)	0.032 (0.167)	650.7 (606437)	--
K_{ma} (mM)	--	--	0 (0)
K_{mb} (mM)	--	--	0.34 (0)
K_i (mM)	--	5.00E-4 (0.46)	1.02 (0)
R^2	-0.4253	0.9776	0
	Adsorbed BIS-HRP		
V_{max} (mM/s)	1.81 (0.85)	58.48 (125.80)	1.81 (1.48)
K_m (mM)	0.044 (0.047)	3.01 (6.6)	--
K_{ma} (mM)	--	--	0 (0)
K_{mb} (mM)	--	--	0.044 (0.082)
K_i (mM)	--	0.18 (0.44)	1.39 (0)
R^2	0.0188	0.9050	-1.944

Looking at snapshots of the examined samples, we can visually observe the difference of the effect of ABTS concentration (Figure 7-17). What is worth pointing out is that for the lower concentrations used (0.05mM, 0.1mM), BIS particles transformed from white to green (upon adsorption of ABTS substrate and/or oxidised ABTS) to purple (close-up shown in Figure 7-18 upper photo). The reasoning behind this colour transformation cannot be explained further at this point, other than there is an effect of BIS-HRP and oxidised ABTS.

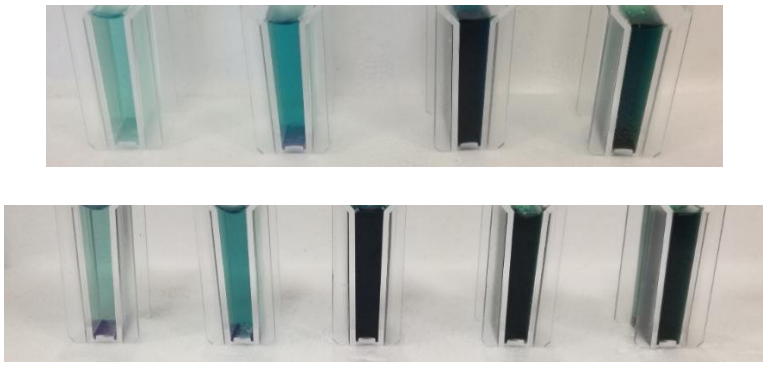

Figure 7-17: Snapshots of enzymatic oxidation of ABTS using HRP-BIS immobilised by encapsulation (top) or adsorption (bottom), examining increase of ABTS.

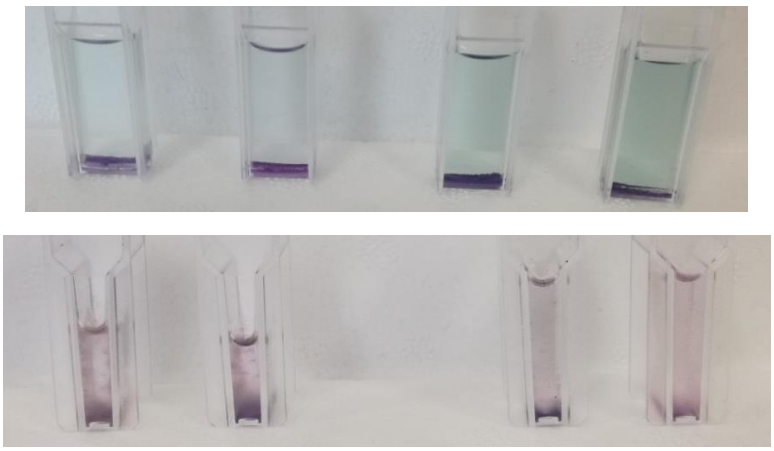

Figure 7-18: Snapshot of 0.05mM and 0.1mM ABTS assays for BIS-HRP samples produced by adsorption (2 cuvettes on the left) or encapsulation (2 cuvettes on the right), soon after assay initiation (Up) and 30 days after assay initiation (Down).

The purple colour was only observed in the presence of BIS loaded with HRP, as control samples of BIS in presence of the ABTS assay mixture did not show this behaviour, neither did the samples of free HRP when assayed under the same conditions. When the same samples were reviewed 30 days after assay initiation, solution and BIS-HRP bed was pink (Figure 7-18 lower photo), phenomenon that had not been observed before for the ABTS assay before (standard ABTS concentration: 10mM). In literature there is only 1 relevant study which mentions a pink coloured product as a result of the savaging action of antioxidants on formed ABTS radical [445]. Although to the best of our knowledge there is no presence of antioxidant compounds in the assay, there might be a side reaction occurring between the ABTS radical and amines contained in BIS, evident due to the considerably lower concentration of ABTS radical compared to higher initial concentrations of ABTS. The examined samples of immobilised HRP were monitored over 48h and obtained concentrations were normalised to the expected per mg of HRP present in the assay (Figure 7-19). Results show that in both immobilised HRP preparations, maximum oxidation of ABTS was reached by 1h after assay initiation. In the case of encapsulation of HRP in BIS the adsorption of oxidised ABTS on the silica bed was much more prominent compared to adsorbed HRP (max reduction of 84% compared to 63% respectively), probably attributed to the unoccupied external pore structure of BIS.

It is worth comparing the maximum oxidation of ABTS per mg of immobilised HRP with the equivalent quantity calculated for the free HRP (see Figure 7-8). The difference between the production of ABTS radical for the free and immobilised HRP is of about 4 orders of magnitude (compared for the same initial concentration of ABTS, 1mM), indicating severe diffusional limitations for the immobilised preparations.

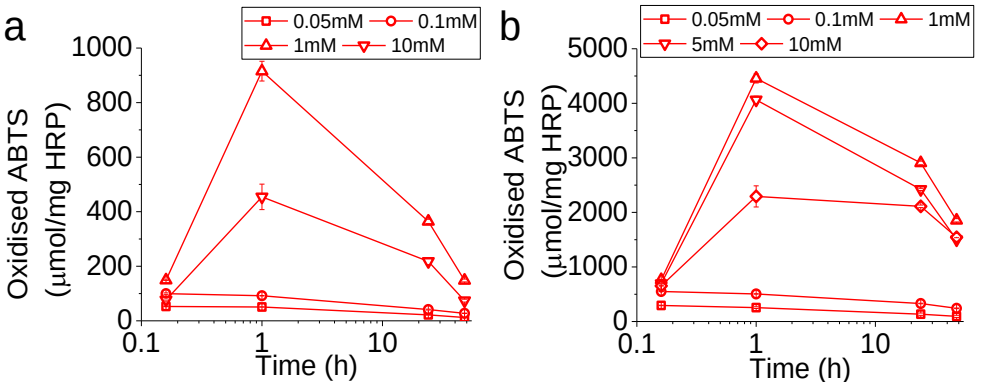

Figure 7-19: Oxidation of ABTS by immobilised HRP via a) encapsulation in BIS or b) adsorption on BIS, over the assay period, examining different initial concentrations of ABTS. Results shown are the average of 3 replicates, with the error bar representing 1 standard deviation.

7.2.2. Effect of H_2O_2 concentration

The effect of initial peroxide concentration was examined on the activity of BIS-HRP samples in the same way as for the free enzyme. Monitoring of kinetics for both encapsulated and adsorbed HRP shows again a considerable difference, regarding the time needed for maximum oxidation, indicating that adsorbed HRP performs better than encapsulated HRP (Figure 7-20). Furthermore, in both immobilised HRP preparations, there is a difference between concentrations below and above the range of 0.44-1.47mM. As stated in the previous section, given the difference in HRP loading, a direct comparison or rates or performance is not advisable.

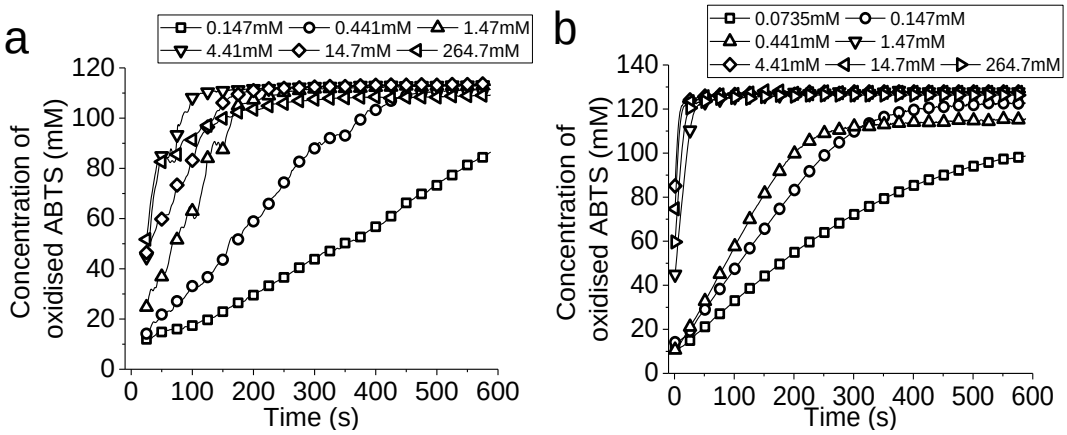

Figure 7-20: Kinetics monitoring of enzymatic ABTS oxidation by a) encapsulated HRP in BIS and b) adsorbed HRP on BIS, with varying initial concentration of H_2O_2. One sample per ABTS concentration examined is shown..

Looking at the rate profile (Figure 7-21), we can see that the performance of adsorbed HRP on BIS seems more prominent than the encapsulated preparation, probably due to the accessibility of enzyme, allowing for faster and higher results. Upon fitting of the obtained rate values with the models used so far (Table 7-8) we can see that the Michaelis Menten model accounting for inhibition seems the best fitting one for both preparations based on the R^2 value, however the same issue as previously is shown. Estimated values for the kinetic parameters and the associated errors are unreasonably high (especially for encapsulated HRP). Looking at the fit and parameters returned for the classic Michaelis Menten model, in both cases returned values are within acceptable range and the R^2 value is also acceptable. In the case of the Ping Pong Bi Bi model

with accounted inhibition, whereas for the adsorbed HRP the response is exactly the same as the Michaelis Menten model, for the encapsulated HRP fit is not acceptable.

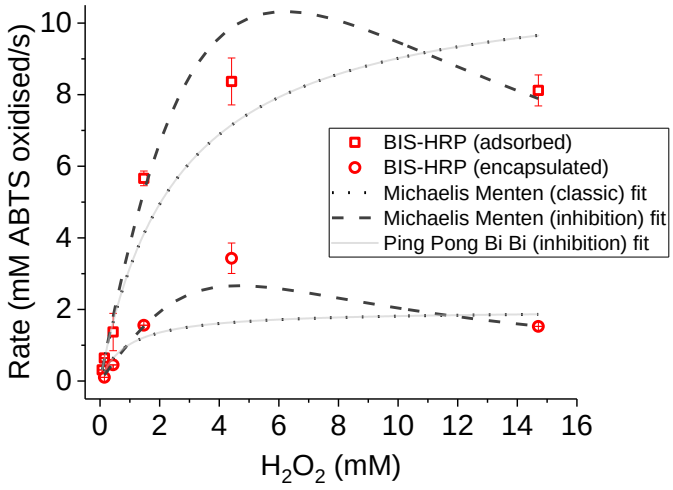

Figure 7-21: Fitting of calculated ABTS oxidation rates and b) determination of kinetic parameters, for H_2O_2 concentration varying from 0.075 to 14.705mM, while keeping every other factor constant.Results shown are the average of duplicates, with the error bars representing 1 standard deviation.

Table 7-8: Determination of kinetic parameters for models shown in Figure 7-21 Values shown are in the format of average (error), as calculated from OriginPro® software.

	Model		
	Michaelis Menten	**Michaelis Menten (inhibition)**	**Ping Pong Bi Bi**
	Adsorbed BIS-HRP		
Equation	$y = {V_{max} \times x}/{(K_m + x)}$	$y = \frac{V_{max} \times x}{(K_m + x \times (1 + {x}/{K_i}))}$	$y = {10 \times V_{max} \times x}/{A}$ $A = \left((K_{mb} \times 10) + K_{ma} \times x \times \left(1 + \left({x}/{K_{ib}}\right)\right)\right) + (10 \times x)$
V_{max} (mM/s)	11.36 (2.39)	46.59 (30.06)	11.35 (3.39)
K_m (mM)	2.59 (0.56)	10.90 (7.09)	--
K_{ma} (mM)	--	--	6.68E-24 (0)
K_{mb} (mM)	--	--	2.59 (0.81)
K_i (mM)	--	3.53 (3.01)	3.46 (0)
R^2	0.9393	0.9872	0.8787
	Encapsulated BIS-HRP		
V_{max} (mM/s)	1.98 (0.53)	17955 (2.86E7)	1.98 (0.92)
K_m (mM)	0.93 (0.60)	15726 (2.506E7)	--
K_{ma} (mM)	--	--	0 (0)
K_{mb} (mM)	--	--	0.93 (1.05)
K_i (mM)	--	0.0013 (2.2044)	5.39 (0)
R^2	0.7179	0.9884	0.1538

In order to compare the obtained results between the two immobilised systems and the free HRP, normalisation of the rates was employed again, to the maximum observed value for each case (Figure 7-22). Comparing the observed trends, we can say that free HRP shows a slow increase up to 1.4mM peroxide until the rate spikes at 14mM peroxide, but in the case of adsorbed HRP on BIS rate shows a steeper increase and reaches maximum value at 4.4mM peroxide, slightly faster than the free enzyme. Encapsulated HRP in BIS shows a similar increase in rate with increasing concentration of peroxide present, but it quickly drops after reaching the maximum at 4.4mM peroxide. Based on this "relevant" representation of data, we could argue that immobilisation of HRP allows the enzyme to reach maximum rate using a lower concentration of peroxide. This could be advantageous if the obtained rates for immobilised enzyme were comparable to the ones obtained for immobilised enzyme, which is not the case here.

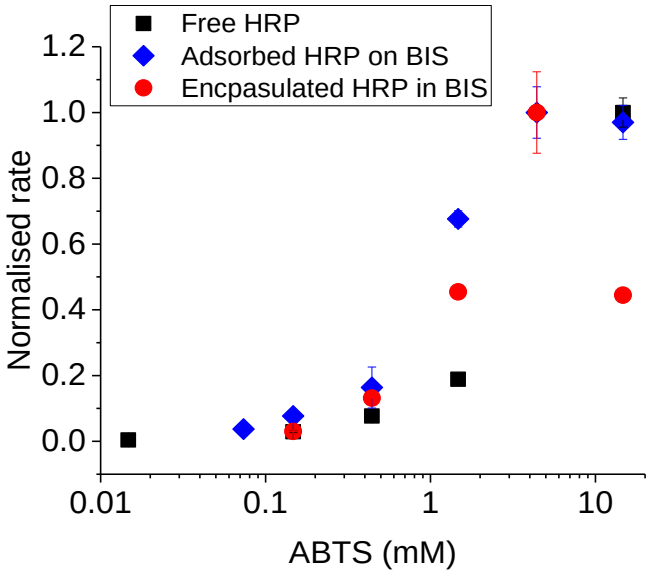

Figure 7-22: Normalised rates for the 3 systems examined, with respect to performance upon increasing H_2O_2 concentration, keeping every other factor constant.

Observing the over time performance of the 2 systems of immobilised HRP (encapsulation shown in Figure 7-23a and adsorption shown in Figure 7-23b), we can clearly see the performance difference between the adsorbed and encapsulated HRP in terms of oxidation of ABTS. Again, this is most likely attributed to the strong diffusional limitations for the encapsulated system, arising from both the porosity and the action of BIS as adsorbent. Unfortunately a direct point-to-point comparison with the free enzyme is not possible as this data was not collected. However, observing the trend shown for immobilised HRP (much higher production of oxidised ABTS for peroxide concentration between 1.47mM and 14.7mM) and having in mind the 4-order of magnitude of difference between free and immobilised HRP performance for 0.441mM peroxide (as commented for Figure 7-19), we can safely assume that there is no meaning in comparing the performance of the free to immobilised HRP.

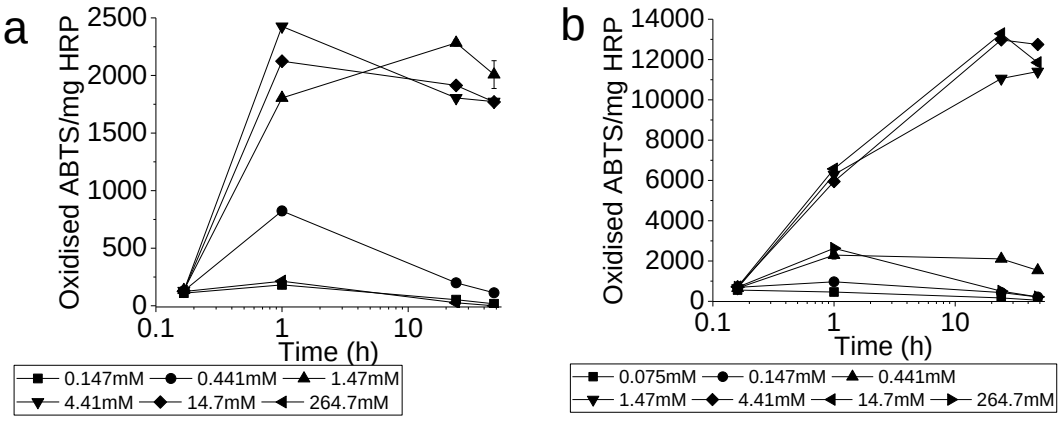

Figure 7-23: Oxidation of ABTS by immobilised HRP via a) encapsulation in BIS or b) adsorption on BIS, over the assay period, examining different initial concentrations of H_2O_2. Results shown are the average of 3 replicates, with the error bar representing 1 standard deviation.

7.3. Conclusions

In this Chapter se saw the kinetic characterisation of HRP using the 2 substrates of the enzymatic assays used in this project (RB19 and ABTS), but also hydrogen peroxide, which is the main peroxidase substrate. Kinetic characterisation was performed in both free and immobilised HRP, the latter including both encapsulated and adsorbed preparations. Determination of kinetic parameters was cumbersome for the case of immobilised HRP, due to the major diffusional limitations the BIS system poses. Free HRP obeys the classic Michaelis-Menten kinetics under specific considerations and upon high concentrations of any of the 3 substrates (peroxide, ABTS, RB19) the enzymatic activity is inhibited. Although a direct comparison of the obtained kinetic parameters is not applicable for the examined systems due to the different concentration of HRP used, monitoring of the enzymatic performance in each case over the time, oxidation of ABTS shows the inferiority of the immobilised systems. On a positive side, there is a clear superiority of immobilisation by adsorption between the 2 immobilisation techniques examined, due to the lower diffusional limitations. A comparison of normalised reaction rates between free HRP and adsorbed HRP on BIS, shows that immobilisation might be offering some protection to HRP in high concentrations of ABTS and is facilitating higher – relevant –rates for lower concentrations of peroxide. However, much optimisation is needed before these results can actually have an applicable meaning.

Chapter 8 : Examination of stability and reusability of Horseradish Peroxidase in free and immobilised form

In Chapter 7 we examined the performance of immobilised HRP with respect to its kinetic characteristics and compared it to the performance of free HRP. Although knowledge on the kinetic parameters of an enzymatic system can reveal much information, they are not the only way of performance evaluation. Other important attributes of an immobilised enzyme are its stability under various conditions and its ability to be reused, given industrial requirements. In this chapter, we are looking at the operational stability, as affected by pH, the thermal stability and the storage stability of selected BIS-HRP samples, comparing it to the respective values obtained for the free enzyme. Due to issues related to adsorption of RB19 on BIS-HRP samples, the RB19 assay was omitted in some cases. Also, due to reasons related to BIS-HRP performance and need for measurable results, only BIS-PAH-HRP samples were examined for operational and thermal stability. Furthermore, we are exploring the reusability potential of immobilised HRP, trying to separate the enzymatic contribution from the contribution of the support, using both ABTS and RB19 assay, for selected samples of BIS-HRP prepared with PAH or PEHA and comparing them to the performance of Syloid FP-1AL-HRP. Last but not least, motivated by the unexpected performance of BIS as adsorbent, we are looking a bit further into its potential, exploring adsorption kinetics and isotherm evaluation of BIS-PEHA samples.

8.1. Effect of pH on the operational stability of free or immobilised HRP

One of the main effects of immobilisation is the protection of enzyme under non-optimal operational conditions. Such conditions might include pH values outside of the optimal for the specific enzyme. There are many immobilisation reports which show an improvement on the observed enzymatic activity in pH conditions where free enzyme is not showing the highest activity (measured through the reaction rate, amount of product or other metrics) [213, 229, 264, 442, 444, 446-448]. Some reports manage to preserve the activity profile of the enzyme intact after immobilisation [279, 443, 449, 450], or with slightly improved enzymatic activity following the trend of the free enzyme [97, 228, 235, 266, 284].

There is a need to distinguish between operational and storage pH stability, as the first measures the adaptability of the enzyme in different operational conditions than the optimal ones. The second describes whether the enzyme can preserve its activity after it has been exposed in non-optimal storage or treatment pH conditions. Herein, we chose to focus on the operational stability of HRP under various pH values, as we believe it is more relevant for potential industrial implementation.

The comparison between reaction rate (or activity) and decolorisation percentage over time, as well as the monitoring of decolorisation over an extended period of time, has not been studied in much detail in literature. What is usually shown regarding dye decolorisation (or generally water treatment) monitoring, is the exploration of the rate of the reaction – or the activity – using a standard assay and the percentage of decolorisation (or pollutant removal) as an application of the enzyme [42, 97, 99, 204, 261, 274, 281, 335]. Some reports show only the percentage of decolorisation or pollutant removal, without any mention to rates or activity [18, 20, 133, 203, 433, 451]. Very few examples are actually comparing the reaction rate with the decolorisation percentage, such as [271, 435], providing a different perspective into very complex systems such as enzymatic reactions. These observations can be useful when deciding on the specifications for a system

8.1.1. Studies on free HRP

Operational stability was examined by changing the pH of the assay medium and keeping every other parameters of the assay unchanged (ratio of reagents, ions present, and enzyme storage conditions). The pH was varied from 3 to 7, as usually this is the examined pH range for Horseradish Peroxidase [20, 99, 337]. Results shown in Figure 8-1 represent the performance of HRP under different operational pH using ABTS as a substrate. Figure 8-1a depicts the difference of the ABTS oxidation rate under different pH conditions and Figure 8-1b depicts the production of oxidised ABTS (ABTS ion or radical) over a course of 48h.

What can be instantly observed is the substantial difference of the reaction rates for the different operational pH values examined, where at pH 5 the enzyme clearly performs much better than at any other pH. Usually, enzymatic activity shows a sharp peak at the optimal pH and the activity can be substantially lower for pH values not much different to the optimal one. This is due to the charge alteration of amino acids, which can lead to them getting displaced from the active configuration of the enzyme, hence, leading to lower, or even zero, activity [369] and the optimal pH can change drastically depending on the substrate [154].

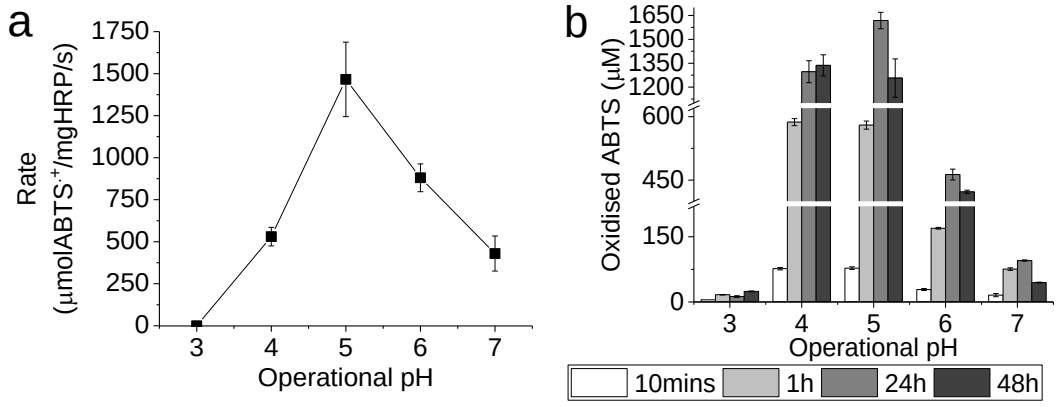

Figure 8-1: Effect of pH on a) initial rate for ABTS oxidation by free HRP and b) 48h monitoring of product formation, using the standard ABTSassay, in buffered medioum of pH ranging from 3 to 7. Each point is based on triplicates, with the error bar representing one standard deviation.

Comparing the rate profile with the product concentration over time, it seems that HRP performs better at pH 5, even up to 48h, where the concentration of the produced ion gets substantially reduced. These observations contrast slightly with the optimal pH values shown in literature for horseradish peroxidase using ABTS as the substrate. The most often reported value is pH 6 [452, 453], with some reports indicating pH 7 [134], or pH 5 [454, 455] and one report showing an optimal pH value for HRP at pH 2 [435]. However, we should not forget that HRP is an enzyme with many different isoenzyme forms, showing a big range of isoelectric points [382], hence potential for many different optimal pH values. Research conducted on the stability of the produced ABTS ion via chemical oxidation showed that stability (hence observed absorbance) gets reduced in the alkaline pH, with the best results shown in the area of pH 4-5 [456]. The lower stability of the ion could explain the lower measured product at 48h compared to earlier time points.

Having seen the obtained results with ABTS, the RB19 assay was applied as well (as described in section 4.2), in order to explore the effect of pH during a potential application. Both initial rate of reaction and absorbance in specific time points after assay initiation were monitored in order to obtain an accurate picture. Herein, based on the rate of decolorisation (Figure 8-2a), the optimum pH is pH 4, with a difference of two orders of magnitude between the other pH values examined. It has been pointed out that the optimum pH may differ even for the same enzyme, depending on the origin of the enzyme and the system it is applied to [20]. When HRP is applied on dye decolorisation, the optimum pH is shown to be either around pH 4-5 or pH 6-7. Monitoring the reactions over the course of 48h allowed for some very interesting observations with respect to the progress of decolorisation over time (Figure 8-2b), as well as the final product (Figure 8-3).

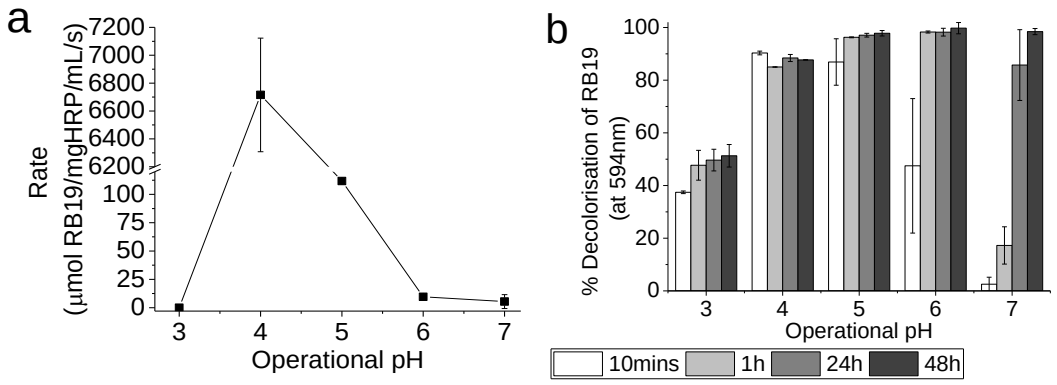

Figure 8-2: Effect of pH on a) initial rate for RB19 decolorisation by free HRP and b) 48h monitoring of decolorisation, using the standard RB19 assay, in buffered mediom of pH ranging from 3 to 7. Each point is based on triplicates, with the error bar representing one standard deviation.

As it can be seen in both figures, for pH values 6 and 7 there is a dramatic difference over time, leading to almost colourless solutions. Furthermore, it is notable that although there was a great difference in the initial rate of the reaction for pH 3 and 4, the end product appeared very similar (red-pink hues shown in Figure 8-3).

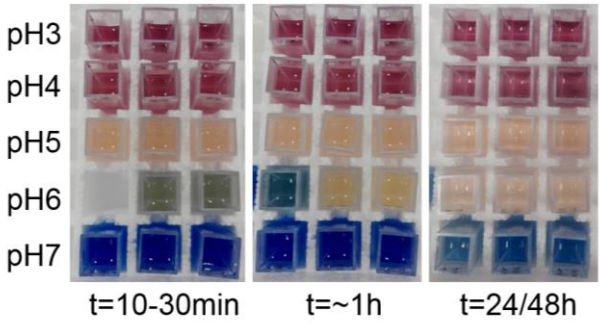

Figure 8-3: Visual observations of RB19 decolorisation from HRP using standard RB19 assay in buffered medium of pH ranging from 3 to 7. Rows represent triplicates.

Based on measured decolorisation efficiency after 24 to 48h, as well as the visual observation of the samples, one could argue that the best pH would be 6. It is then a matter of preference on what "best" signifies, depending on the need for speed and stable results (pH 4), or the need for maximum decolorisation over a more extended period of time (pH 5-6). Having mentioned earlier about the measurement of decolorisation based on the area under the curve instead of the absorbance difference at a specific wavelength (section 4.2), it would be interesting to see the comparison of the two methods in this case, where such a visual difference between results is observed. A scan was obtained for 1 reaction from each triplicate, in the area of visible wavelength (350-700nm) and the area under the curve between these wavelengths was calculated using the Peak Analyzer function of Origin software. Results are shown in Figure 8-4a and b. These results verify the observations made earlier about the lighter colour obtained over an extended period of time compared to not as visibly decolorised solutions obtained faster, and show the importance of the pH for dye decolorisation by free HRP. The lower rate (and lower dye removal percentage for the first few minutes/hours) is expected, given the sensitivity of enzymes to operational conditions as described earlier for the ABTS assay.

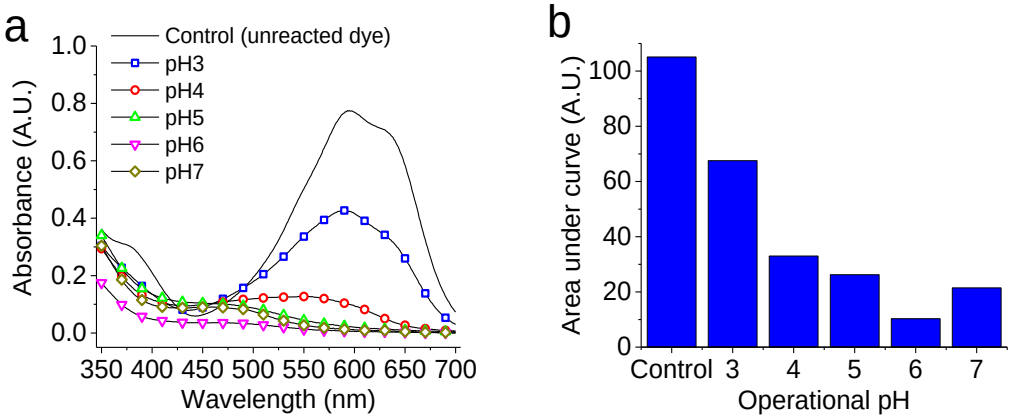

Figure 8-4: a) absorbance spectra and b) calculated area under curve for decolorisation of RB19 using free HRP in buffered medium of H ranging from 3 to 7. Region of interest was between 350nm and 700nm (visible region). Baseline used was of 0 absorbance. Results represent 1 sample from each different condition. Control (unreacted dye) sample is of pH 4, as a representative, as there was no observable difference across control unreacted dye samples of different pH.

With respect to the high degree of decolorisation for samples with a low reaction rate (e.g. at pH 6 or pH 7), we should mention that degradation of RB19 is an oxidation reaction, where upon initial formation of radicals due to the enzymatic excitation by peroxide, can be spontaneous and uncontrollable. Studies on Reactive Black 4 (RB4), another anthraquinone dye with structure similar to RB19, showed that there are 3 predominant, deprotonated species of RB4 in a range of pH from 4 to 14 [457]. This indicates 3 different "starting structures" for enzymatic degradation depending on the pH, which can potentially lead to different fragments. This speculation can explain the different colours observed during degradation and at the end of the assay as shown in Figure 8-3.

Work on RB19 degradation using photocatalysis with hydrogen peroxide, showed that degradation of the dye in solution of higher pH was faster [458]. During photocatalysis, hydrogen peroxide generates hydroxyl radicals, which "attack" ionisable groups of the organic molecule and lead to the structure disruption. Given the similarity of this procedure to the enzymatic decolorisation, where hydroxyl radicals are produced by hydrogen peroxide via the activity mechanism of peroxidase as alternatively presented by Rodriguez-Lopez [135], a mixed effect between the reduced production of hydroxyl radicals and the different starting structures can be assumed.

Examining the operational stability of HRP we saw that results follow 2 trends, depending on the perspective one want to focus on. If the interest lays with fast reaction (high initial rate), then the optimal pH for HRP was pH 4, showing maximum initial rate, but not as colourless products as in other cases. If the interest lays with most effective decolorisation (% of dye removal either by measurement at the optimal wavelength or by area under curve, regardless of time needed), then the optimal pH for free HRP was pH 6. From a point of industrial interest, both angles are important. An efficient biocatalyst should be working fast, producing optimal results (in our case colour reduction). In the next section we will examine the operational stability of immobilised HRP, looking at how immobilisation affects the aforementioned results.

8.1.2. Studies on immobilised HRP

As it has been mentioned earlier, one of the aspects that makes enzyme immobilisation very valuable, is the ability to protect the enzyme under conditions different than the determined as optimal. In the previous section the optimal operational pH conditions for free HRP were identified and observations for the performance of the enzyme were made using the 2 different assays. In this section, selected samples of immobilised HRP were assayed under the same conditions, in order to compare the performance of HRP in immobilised form, using samples procured with both encapsulation and adsorption of HRP on BIS. The selected samples of immobilised HRP were the same as shown in Chapter 7, based on best performance and need for consistency. Encapsulated HRP sample chosen was HRP in BIS synthesised with PAH and subsequent elution of amine at pH 5, with an initial HRP concentration of 0.4mg/mL. Adsorbed

HRP sample chosen was HRP adsorbed on BIS synthesised also with PAH, with the amine eluted at pH5 and a HRP quantity introduced for immobilisation of 0.4mg/ml. The assay of the bio-composites was performed as described in section 3.4.4. As it was noted in Chapter 6, both assays interacted one way or another with the substrates, especially in the case of RB19, so control samples of pure BIS were used in order to extract the portion of the enzymatic performance. In Figure 8-5 the comparison of the initial rates of ABTS oxidation using HRP in free form and in 2 different immobilised forms is shown, depicting the actual (Figure 8-5a) as well as the normalised rates (Figure 8-5), using the maximum observed value of each sample for the latest. Comparing the actual values for the initial rate of ABTS oxidation, it is clear that neither of the immobilised preparations of HRP can perform to the same extent as the free enzyme. There is a difference of 4 orders of magnitude between the free and adsorbed HRP and a difference of 7 orders of magnitude between encapsulated and free HRP, indicating that in both cases there are serious issues regarding the enzymatic activity. It is worth mentioning that there is some activity measured at pH 3 for HRP adsorbed on BIS, whereas no activity was detected for either free or encapsulated enzyme. It should also be pointed out based on what he have witnessed so far, that the accessibility of enzyme to ABTS and oxidised ABTS to bulk volume is considerably different. Despite the low performance of immobilised HRP compared to expectations, if rates are normalised to the maximum observed value per case, results are very interesting (Figure 8-5). There is a common point between the 2 preparations of immobilised HRP, which is the considerably higher activity shown at pH 4, compared to the free enzyme. For operational pH of 5, 6 and 7, free HRP and HRP adsorbed on BIS show basically the same descending trend, whereas HRP encapsulated in BIS shows a semi-stable profile for pH 4, 5 and 6 and an increase activity for pH 7.

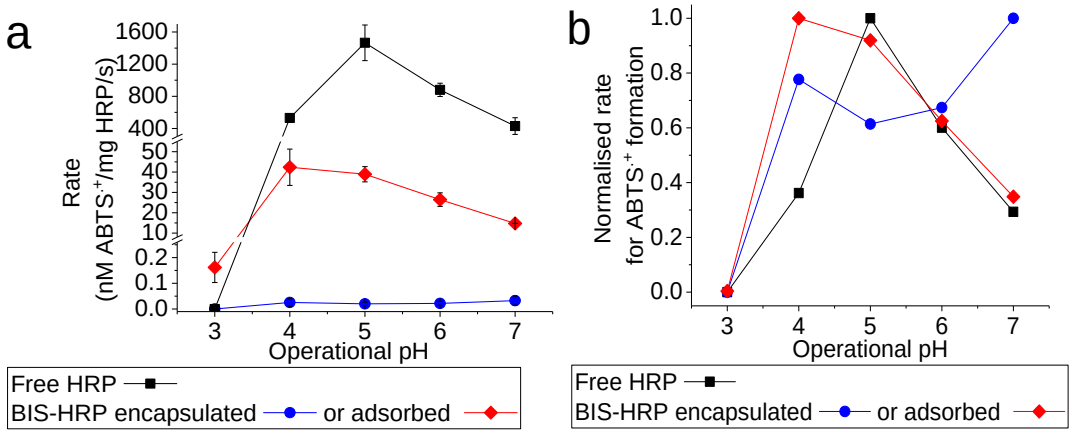

Figure 8-5: Initial rates of ABTS oxidation using the standard ABTS assay, for free HRP, HRP immobilised in BIS via encapsulation and HRP immobilised in BIS via adsorption. a) values of initial rates as calculated using collected data, b) normalised rates to the maximum value observed for each BIS preparation. Each point is based on triplicates, with the error bar representing one standard deviation.

Interestingly, all 3 HRP preparations show the same relative effect for pH 6. As it was pointed out earlier, the dislocation of the optimal point or the perseverance of the same profile and even the lower observed activity are fairly often observed in enzyme immobilisation. Addressing the

move of the optimal performance point between the free HRP and HRP adsorbed on BIS, this can be possible given the attachment of HRP on BIS, which could provide protection of the active conformation of the enzyme for this operational pH.

The absence of the same protective effect for pH 6 and 7, could be due to stronger interactions and charge alterations of HRP aminoacids at these pH values, compared to the offered protection from BIS. On the other hand, when HRP is encapsulated in BIS, the overall oxidation rate was much lower, but it did not show the sharp decrease either side of the optimal pH point such as in the case of free and adsorbed HRP. Results show that the maximum rate for encapsulated HRP was observed at pH 7. Activity between pH 4 and pH 6 is lower by only 20% from the optimal. This indicates a stronger protective effect of BIS to HRP, which could be attributed to the encapsulation procedure and the reduction of full exposure of the enzyme to operational conditions. When HRP is adsorbed on BIS, the enzyme is mostly located on the external surface area. When HRP is in-situ encapsulated, the bulk of the enzyme is located inside the pore structure of BIS, with some quantity potentially adsorbed on the external surface area. It has been argued before that encapsulating enzymes into immobilisation supports can preserve the active microenvironment around the enzyme, hence help the composite show a higher activity compared to the free enzyme [459] under non-optimal conditions. It has also been shown that introduction of drastic pH changes could lead to desorption of enzymes from a solid support [155, 156, 413], when immobilisation was based on weak charge interactions, so this could be a possibility to take into consideration here. Trying to investigate the effect of some of the aforementioned possibilities, an exploration of the oxidation of ABTS per time point could offer some enlightenment.

In Figure 8-6, the production of oxidised ABTS is shown over time for the 3 systems examined, in each of the pH conditions (graphs a to e corresponding to pH 3 to 7). Presented results are shown as an expectation of ABTS oxidation per mg of HRP, based on the measured results for the given HRP amount in each case. What is immediately noticeable is the magnitude of difference between the performance of the free enzyme compared to the immobilised form, as it was also established through the initial rate comparison (Figure 8-5a). Another observation is the much lower observed product by the 48h point for the BIS-HRP samples compared to the maximum observed measurement, especially when HRP was adsorbed on BIS (shown be the decrease of the red lines over time in graphs a-e of Figure 8-6). The maximum observed reduction in observed product in the case of free HRP was shown at pH 7 (Figure 8-6e), where the maximum observed value was at 24 h and by 48 h the oxidised ABTS concentration was reduced by 53%, which is most probably relevant to the stability of the oxidised ABTS as explained in section 8.1.1. For pH 3 and 4 (Figure 8-6a, b) there was no observable difference throughout the time points examined and for pH 5 and 6 (Figure 8-6c, d) there was a difference between the maximum value (observed again 24 h after assay initiation for both cases) of 22% and 8% respectively. These observations indicate that once ABTS is oxidised by free HRP, its concentration stays

mainly unchanged throughout the assay. With respect to the immobilised HRP preparations, results are different. In case of pH 3 (Figure 8-6a), both preparations lead to a zero value (lower compared to control sample of unreacted ABTS) of observed oxidised ABTS 48h after assay initiation. The stable oxidised ABTS concentration in the case of free HRP at pH 3, leads to the conclusion that in the case of BIS-HRP, at pH 3, all the produced ABTS ion is getting adsorbed on BIS. For pH 4 (Figure 8-6b), where again the performance of free HRP was stable over time, maximum oxidised ABTS concentration for BIS-HRP (both preparations) is shown at 1h. After this point, encapsulated HRP assays show a reduction of about 63% for observed ABTS ion and adsorbed HRP assays show a reduction of about 76% respectively, 48h after assay initiation, again, indicating adsorption of the coloured product on BIS. For pH 5 (Figure 8-6c) the respective reduction is 22% and 61% for encapsulated and adsorbed HRP, whereas for pH 6 (Figure 8-6d) the values move to 14% and 43% respectively. Last but not least, at pH 7 (Figure 8-6e), the observed product 48h after the assay initiation is 12% and 30% reduced for encapsulated and adsorbed HRP respectively, compared to the maximum observed value in each case. It is worth mentioning that in the case of immobilised HRP preparations the maximum observed concentration for oxidised ABTS is measured at 24h and 1h for encapsulated and adsorbed HRP respectively, consistently through the different operational pH values explored.

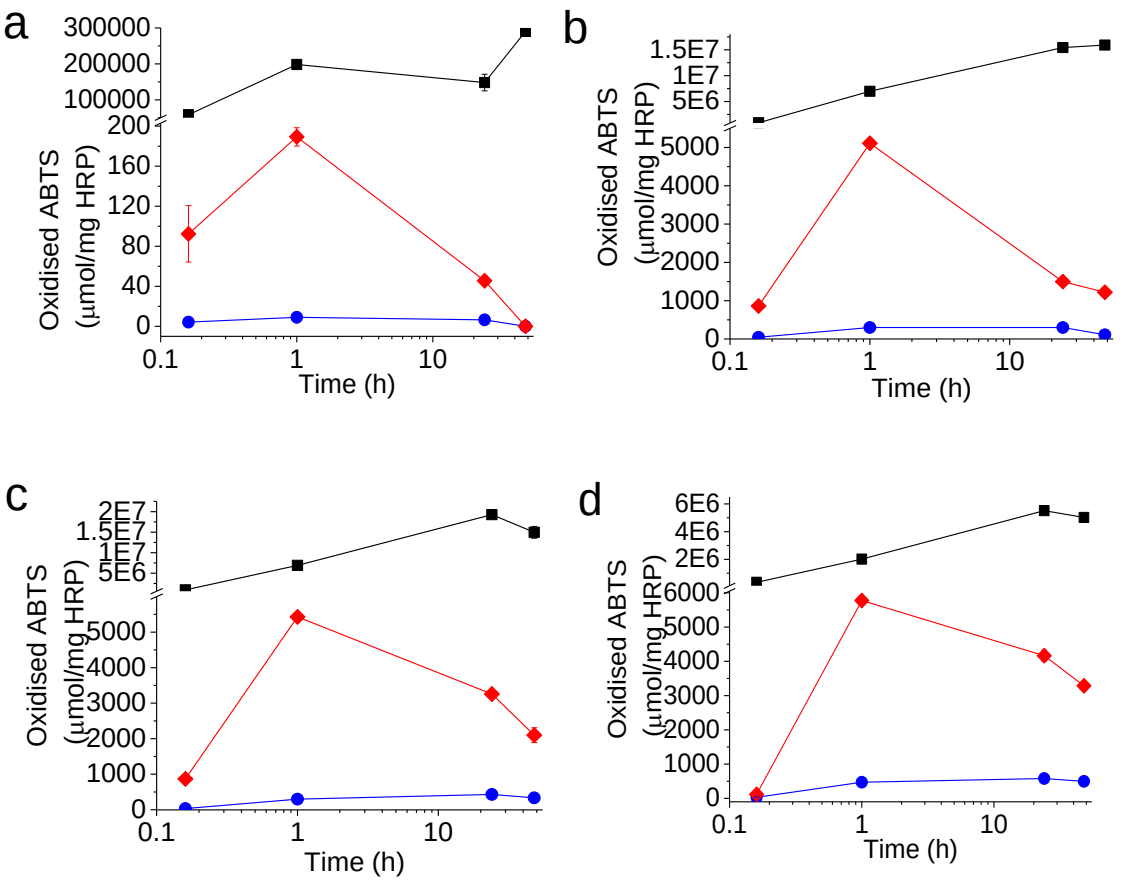

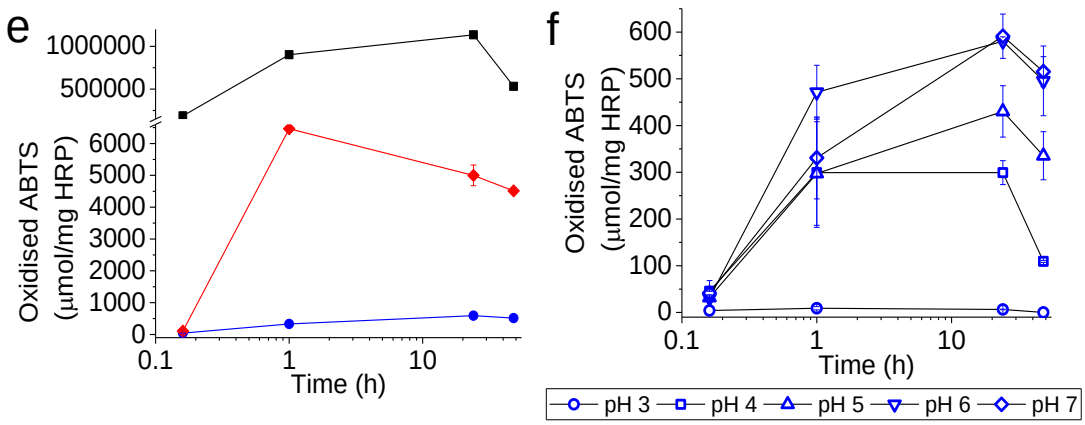

Figure 8-6: Effect of pH on oxidation of ABTS over time for free HRP (black squares), BIS-HRP via encapsulation (blue circles) and BIS-HRP via adsorption (red diamonds) in operational pH conditions varying from pH 3 (a) to pH 7 (e), f: Collection of same results for BIS-HRP via encapsulation for a more focused view. Each point is based on triplicates, with the error bar representing one standard deviation.

The great difference of product concentration between 10min and 1-24h for immobilised HRP (circles, diamonds), opposed to the almost stable product concentration already from the 10min point for free HRP (squares), as well as the time delay between the encapsulated and the adsorbed HRP are indicative of the difficulty of substrate and product movement through the BIS network. Comparing the observed product reduction over time for the immobilised HRP systems, assuming that is it due to adsorption of oxidised ABTS on the BIS support, it seems like the adsorption abilities of BIS to ABTS ion are much better at lower pH, which is reasonable. BIS is almost neutrally charged (pI is at pH 2), probably slightly positive from the presence of PAH and ABTS is negatively charged. Similar analysis conducted with HRP immobilised in silica and used for ABTS oxidation confirmed this observation [460].

When HRP immobilised on BIS was examined under different operational pH conditions using the RB19 assay, obtained results were different compared to the ABTS assay, showing the importance of the substrate when designing a biocatalyst. Due to the high adsorptive capacity of BIS, monitoring of rates for RB19 degradation was not possible, so this point of comparison to the free enzyme was omitted. Data collected represent the decolorisation degree over time for the 2 different BIS-HRP preparations under the examined pH conditions, with respect to the specific wavelength for RB19, as well as the area under the curve obtained at the end of the assay. Control BIS samples were also assayed for RB19 dye removal and their performance was subtracted from the one of the composite, trying to identify the extent of the enzymatic decolorisation from its combination with dye adsorption on the BIS support. Looking initially at the performance of the BIS-HRP composite, Figure 8-7a shows the performance of the 2 different BIS-HRP preparations in comparison to free HRP and BIS without presence of enzyme. What is instantly noticeable is the almost inversed effect between free enzyme and BIS, where BIS is performing much better at lower pH and enzyme shows better performance at higher pH values (with respect to colour removal). The improved performance of BIS at more acidic pH can be explained by the

electrostatic interactions between silica and dye, where the first is negatively charged but very close to neutral charge (pI of silica is at pH 2), and the second is negatively charged as being an anionic dye. Furthermore, the presence of positively charged amines (pI of PAH is around pH11), offers chemisorption points as it will be explained later in more detail. However, at higher pH (pH 6 or 7), the negative charge of silica possible overcomes the positive charge of amines present, making the adsorption ability of BIS less powerful.

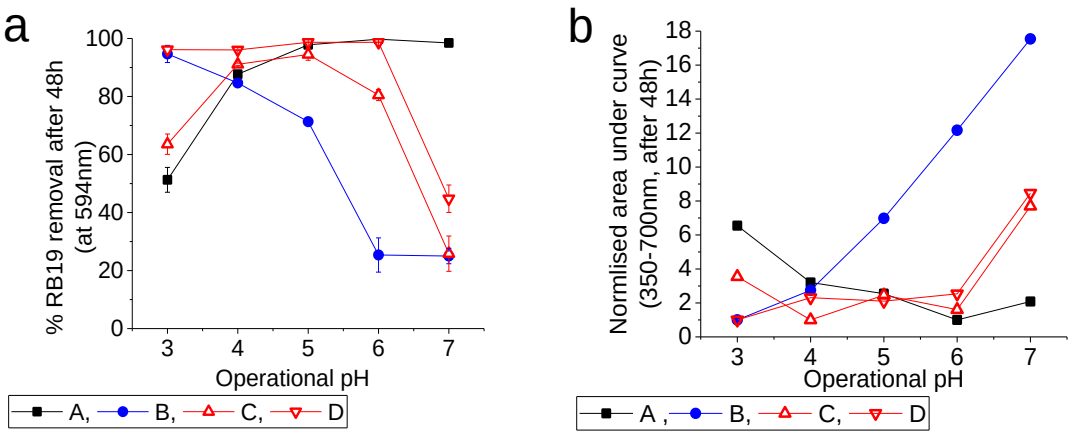

Figure 8-7: Effect of pH on decolorisation of RB19 using the standard RB19 assay ,by free HRP (A), BIS (B), BIS-HRP obtained via encapsulation (C) and BIS-HRP obtained via adsorption (D) measured 48h after assay initiation (a) as concentration difference at the optimal wavelength and (b) as area under the curve obtained through a scan at the area of visible wavelength, normalised to the minimum area obtained per case. Each point of graph (a) is based on triplicates, with the error bar representing one standard deviation, points for graph (b) were obtained by single scans.

Comparing the performance of the BIS-HRP preparations (points of lines C and D on the same figure), we can see that in pH values approaching neutrality their performance is comparable, while in acidic conditions BIS-HRP via adsorption performs considerably better than BIS-HRP via encapsulation. Interestingly the expectation was the opposite, since for adsorbed HRP the majority of enzyme is located on the surface and is occupying the positively charged sites of PAH, whereas in the case of encapsulated HRP, the bulk of the enzyme is located inside the pore structure of BIS. The high ability of adsorbed HRP to decolorise RB19 at pH 3, might be an indication of improved enzymatic activity caused by immobilisation, specifically towards RB19 decolorisation, since a similar effect was not observed for ABTS. As it can be seen by comparing the performance of free HRP to the performance of both BIS-HRP samples for pH 4, 5 and 6, all 3 systems are having a high performance. Specifically for pH 4, the BIS-HRP via adsorption sample shows a 9% and BIS-HRP via encapsulation shows about a 3% increase in RB19 removal compared to free enzyme. Having explored the performance of each system on dye decolorisation based on reduction of absorbance at the dedicated wavelength, it would be interesting to compare that with the area under the curve, as calculated by area integration from a scan of the assays. As it was shown visually for the free enzyme, different operational conditions can lead to different degradation patterns, which can affect the residual colour, not only necessarily to the original dye, but due to formation of coloured by-products. What each line in Figure 8-7b shows, is the ratio

between the lowest calculated area (representing optimal performance of decolorisation) under the obtained curve for each sample, to the area(s) obtained in other pH conditions. This ration can be a measure to express how many times that specific sample at that specific pH was better than the same sample in other pH values. It is interesting that both BIS and BIS-HRP via adsorption showed the lowest area when assayed for RB19 decolorisation at pH 3, whereas the lowest area for free HRP was obtained at pH 6 and for BIS-HRP via encapsulation at pH4. The other interesting observation is the relatively small ratio or areas observed for the enzymatic preparations. No sample was more than 8 times "worse" than the best performing one, whereas for BIS without presence of enzyme, the ratio of the "worst" sample was an almost 18 at pH 7 and a 12 at pH 6, indicating 18 and 12 times larger areas under the curve respectively. For comparison purposes, the lowest area under curve for the free enzyme was 10.31, for BIS it was 3.45, for BIS-HRP via encapsulation it was 9.77 and for BIS-HRP via adsorption is was 6.60 (all in arbitrary units). This indicates that presence of BIS had a positive effect in the area reduction, probably due to the combination of enzymatic degradation and adsorption.

In an effort to see the contribution of the enzymatic degradation on the BIS-HRP composite action, results obtained for the composite were reduced by the performance of BIS. Figure 8-8a and b show the % contribution of immobilised HRP to decolorisation of RB19 for encapsulated or adsorbed HRP respectively. Immediately we can notice the much higher enzymatic contribution in the case of adsorbed HRP, as for every pH and time point, it is superior to the observed for encapsulated HRP. Knowing that the concentration of HRP in encapsulated form is much higher than that of adsorbed form, we can assume that the difference is due to diffusional limitations, mainly arising from the localisation of the enzyme as discussed previously. As it had been analysed previously, HRP being buried deep inside the pore structures in the case of encapsulation, does not allow easy contact of RB19 with the enzyme, as the pores might be tortuous or too small, or, the presence of amine facilitates adsorption of dye on BIS.

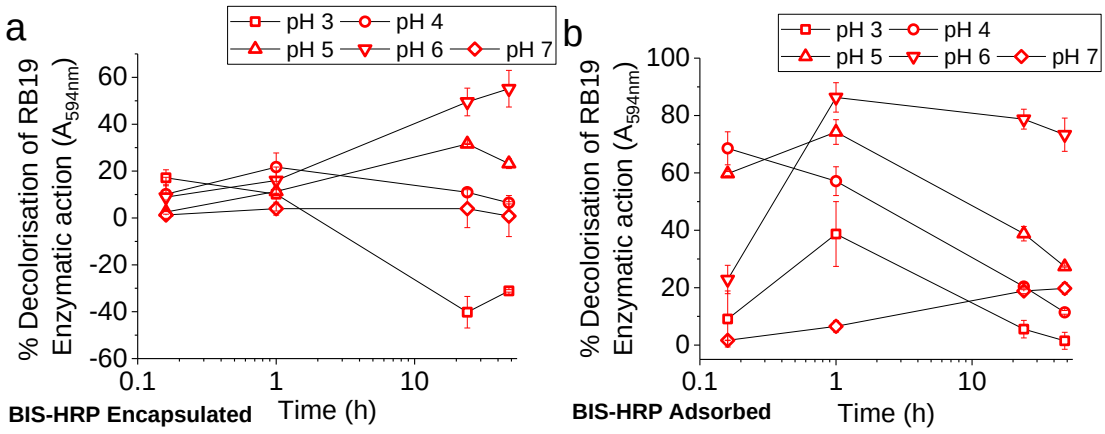

Figure 8-8: Enzymatic contribution to decolorisation of RB19 by BIS-HRPproduced via a) in-situ encapsulation and b) adsorption, in relation to pH. Each point is based on triplicates, with the error bar representing one standard deviation.

All these speculations could explain the time delay before noticing an optimum of enzymatic decolorisation for encapsulated HRP, as well as the overall low values (Figure 8-8a). In the case of pH 3, the negative enzymatic contribution indicates that BIS in absence of HRP is removing RB19 better than BIS-HRP, indicating that presence of enzyme hinders the adsorbing ability of BIS. In the case of adsorbed HRP (Figure 8-8b), we can see that enzymatic contribution is reaching a maximum within the 1st hour of assay, dropping afterwards. This shows that due to easier accessibility, HRP overpowers BIS on RB19 decolorisation, before adsorption kicks in. This is mostly evident in the lower pH values (3-5), as adsorption of RB19 on BIS is stronger due to charge interactions (line B in Figure 8-7a).

In order to compare the output of free HRP and immobilised HRP, an extrapolation on the productivity (μM RB19 destroyed) per mg HRP was made, using the highest observed decolorisation output during the assay. Results are shown in Figure 8-9 for free HRP and the 2 immobilised HRP preparations. As a reminder, the assay contains about 125μM RB19 and the enzyme quantities present during assay are 0.0168mg free HRP, about 0.9mg immobilised HRP via encapsulation and about 0.18mg immobilised HRP via adsorption. The trend for the expected productivity of HRP in free and immobilised form for RB19 degradation as shown in Figure 8-9 is similar to the trend observed for the expected oxidation of ABTS. Free HRP shows a difference of about 3 orders of magnitude compared to encapsulated HRP and about 2 orders of magnitude compared to adsorbed HRP. These results are reasonable, on the basis of competitive action between dye adsorption on BIS and enzymatic degradation of dye, as well as due to diffusional limitations.

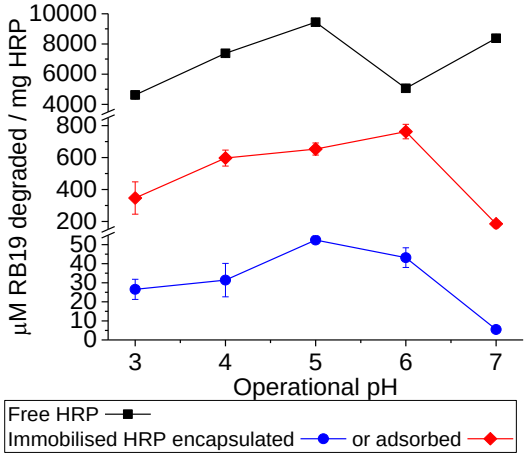

Figure 8-9: Expected productivity –based on extrapolation– per mg of HRP in free or immobilised form, depending on operational pH conditions. Each point is based on triplicates, with the error bar representing one standard deviation.

In conclusion, regarding the operational stability of HRP in free and immobilised form, looking past the incomparable productivity of the free form to the immobilised preparations, we can see that immobilisation can offer protection of the enzyme in pH conditions other than the optimal. In addition, for the examined application of dye decolorisation, the choice of pH can offer very

good results based on the combined action of the BIS-HRP composite. In both cases, there are substantial issues arising from the interaction of BIS with the substrates and their products upon exposure to enzymatic activity.

8.2. Thermal stability of free or immobilised HRP

As mentioned in previous sections, immobilisation of enzymes is primarily used for easy separation, ability of reuse and protection of the enzymatic activity under non-optimal conditions. Such conditions might be different operational pH (as examined in section Chapter 8), or different temperature, as needed from the targeted industrial application. Specifically regarding temperature, much research is devoted into the molecular design of enzymes which offer high thermotolerance [461, 462]. Immobilising enzymes on solid supports as opposed to immobilisations in gels or via aggregation is thought of offering higher thermostability, and silicas are known for their high thermotolerance [237, 297].

For this project, free HRP and immobilised HRP were incubated in temperatures ranging from 20°C to 70 °C for 10mins and their activity was then examined using the standard ABTS assay. The immobilised preparations of HRP selected to be examined for their stability were chosen having in mind the contribution of the support, as well as the need to see some measurable concentration of product. Based on the best performing samples of BIS-HRP as identified in Chapter 6, the chosen sample was HRP encapsulated in BIS synthesised with PAH, with the additive partially eluted at pH 5 and initial concentration of HRP introduced being 0.4mg/mL. In order to keep the effect of the support as similar as possible and avoid confusion, the selected sample from the adsorbed HRP cohort was HRP adsorbed at BIS-PAH, with the additive partially eluted at pH 5 and initial amount of HRP added being again 20mg. Response was initially measured by the initial rate of the enzymatic oxidation of ABTS (Figure 8-10), and data is presented as received (Figure 8-10a) and after normalisation to the best observed value per system (Figure 8-10b).

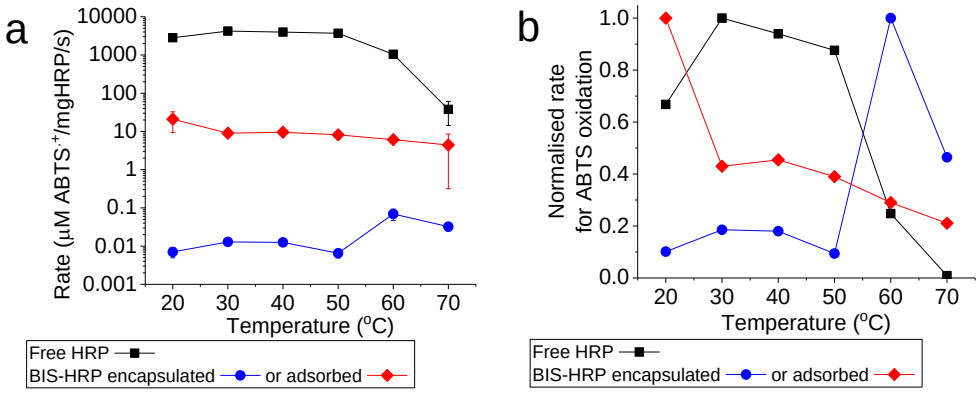

Figure 8-10: a) rate of ABTS oxidation from free HRP (black), HRP encapsulated in BIS (blue), or adsorbed on BIS (red), when exposed to various temperatures in order to explore enzymatic stability. Rate was calculated per mg of HRP present in the assay by extrapolation of the measured rate in each case. Each point is based on triplicates, with the error bar representing one standard deviation. b) normalised rate values to the maximum observed for each system.

Looking at the actual rates, there is a clear difference between the 3 systems, with the free enzyme having by far the best performance, by 2 orders of magnitude higher than adsorbed HRP on BIS and 5 orders of magnitude higher compared to encapsulated HRP in BIS. What is also noticeable is that free HRP shows the sharpest drop at high temperatures, compared to the immobilised systems, having a 99% drop in activity at 70^{o}C from the observed max at 30^{o}C, compared to the drop of just over 50% for encapsulated HRP and about 80% for adsorbed HRP. This indicates some protection of HRP by its immobilisation, although the actual rate values are not at all comparable. Last but not least, looking at the relative rates as observed for each system (Graph b), we need to point out the maximum performance for each sample, this being at 30^{o}C for free HRP, at 60^{o} for encapsulated HRP and at 20^{o}C for adsorbed HRP. The temperature profile observed for free HRP looks reasonable and comparable with similar studies on free HRP found in literature [97, 133, 263, 264, 276], whereas for the immobilise systems the maximum observed points are substantially different to the neighbouring ones. At this point, it is not clear why this might be happening. As it has been shown previously, the contribution of the BIS support could lead to inaccuracy of rate measurement, due to a) diffusional limitations, b) adsorption of substrate and/or product on the BIS support hence, lower measured activity compared to "real" one.

Observation of ABTS oxidation during the designated time points of the assay was conducted for each examined system and temperature (presented as the extrapolated expectation of 1mg HRP being present in the assay) is shown in Figure 8-11a, b and c, for free, encapsulated and adsorbed HRP respectively. Looking at the oxidised ABTS production as observed for the free HRP (Figure 8-11a), we can clearly see a correlation between the generally much lower observed product for 70^{o}C and the initially lower observed product for 60^{o}C, with the observed rates in Figure 8-10a. For the rest of examined temperatures, ABTS oxidation over time is almost identical, correlating with the very similar rates observed. Comparing Figure 8-10b to Figure 8-11b and c with respect to the performance of the immobilised HRP systems, we can say that the difference between the production of oxidised ABTS over time is not as big as in the case of free HRP compared to the observed difference of the measured rates. This could be related to the generally lower observed values and the unknown performance of BIS as adsorbent upon heating. The delayed increase of maximum oxidised ABTS concentration in the case of encapsulated HRP (max shown at 24h), compared to the adsorbed HRP (max shown at 1h) can be attributed to the localisation of the enzyme and the diffusional limitations posed in each case, as discussed before.

Briefly, does immobilisation of HRP offer protection against exposure to temperature other than the optimal? Conditionally, yes. Both immobilised systems showed a higher relative performance compared to free HRP, encapsulated HRP was better in terms of temperature optimum and adsorbed HRP showed preservation of the activity around the temperature range.

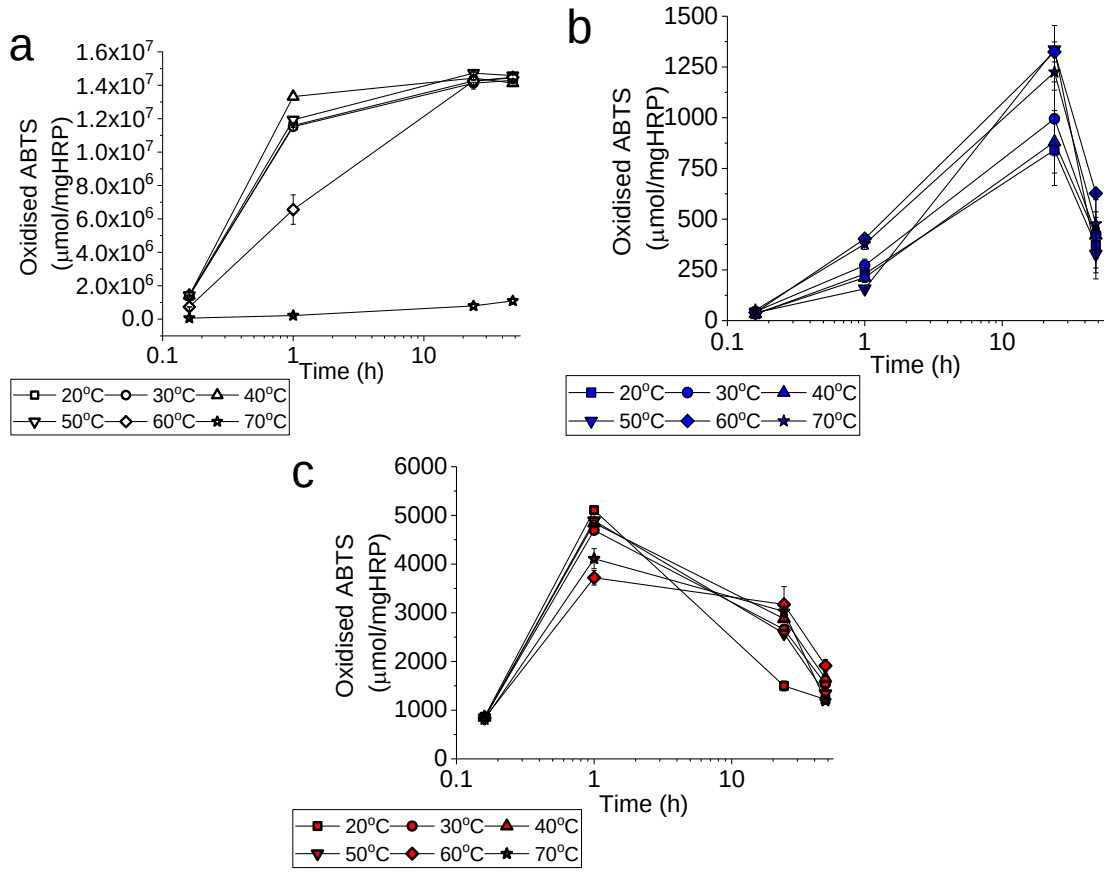

Figure 8-11: Measured production of oxidised ABTS per time point during the assay, for a) free HRP, b) HRP encapsulated in BIS and c) HRP adsorbed on BIS, when exposed to different temperatures, in order to examine the stability of the enzyme. Each point is based on triplicates, with the error bar representing one standard deviation.

A protective effect upon immobilisation of HRP was also observed by Celebi, using polysulfone supports, managing to enhance HRP activity at higher temperatures compared to the free enzyme, although for lower temperatures (below 50°C) free HRP showed a better performance [263]. A similar protective effect was also observed when HRP was immobilised in alginate beads, where relative stability at temperatures above 40°C was greatly enhanced, up to 80°C where enzymatic activity was not observed for either free or immobilised enzyme [97]. Again immobilised in alginate beads with assistance of crosslinking this time, showed higher and more stable performance at higher temperatures compared to free HRP, identifying the same optimum temperatures for free and immobilised HRP as shown herein [463]. Another great example of protection of HRP upon exposure to high temperatures was shown by Fernandes, who used polyaniline as immobilisation support, achieving a stably high performance at lower temperatures and much higher percentage of preserved activity at higher temperatures compared to free HRP [276]. When HRP was immobilised on magnetic nanoparticles and subsequently on a fibrous support, showed higher activity in higher temperatures compared to the free enzyme, owning the effect to the protection achieved with immobilisation [464]. Similarly, HRP immobilised on a polymeric matrix grafted by radiation showed substantial prevention of activity loss at higher temperatures compared to free HRP [453]. Literature shows that immobilisation has extended the thermal stability of other

peroxidases as well, with examples of immobilised laccase [228, 235, 261, 266] or other peroxidases [214, 447, 465, 466].

The higher activity retention in higher temperatures for immobilised enzymes is generally attributed to the prevention of the inevitable unfolding and alteration of the secondary conformation. When enzymes are securely attached on a support by covalent binding, or securely encapsulated inside the pore structure of a thermostable material, then unfolding can be delayed. However, it should be pointed out that the majority of examined cases (including this project) showed slightly or significantly lower activity of the immobilised enzyme for lower temperatures.

8.3. Storage stability of free or immobilised HRP

Stability of a biocatalyst is a very important attribute when it comes to industrial implementation, as it helps reduce the associated costs, by producing the biocatalyst in bulk and being able to store it for prolonged periods of time, with high activity retention, hence reproducibility of results. Immobilisation has been shown to improve the storage stability of enzymes [207], with examples in literature ranging from days to months of high activity recovery [203, 215], compared to the much lower activity recovery during storage of enzymes in free form [218, 320].

In order to examine the storage stability of immobilised HRP, selected samples were stored directly after preparation and their activity was examined via both assays at specific time points, for a course of 50 days. The selected samples of immobilised HRP were the best performing samples, obtained with either PAH or PEHA used as an additive for BIS synthesis, and using both encapsulation or adsorption as method of immobilisation. Storage stability examined via the ABTS assay is shown in Figure 8-12, regarding formed product, as detected at the end of the assay (48h), and normalised to the first time point of examination.

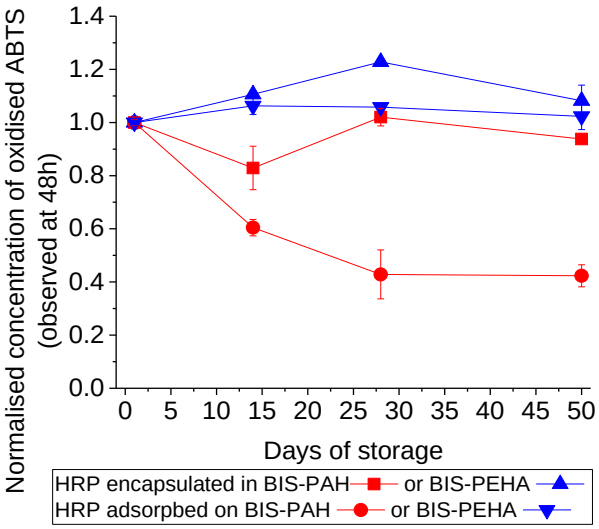

Figure 8-12: Storage stability of HRP immobilised in BIS based on the oxidation of ABTS, examined through the standard ABTS assay, as recorded after 48h of assay. Each point is based on triplicates, with the error bar representing one standard deviation.

From an initial observation, it looks like the method of immobilisation did not have an effect on the storage stability when PEHA was used as an additive for BIS synthesis. During the 50 days of examination, the obtained product at the end of the assay was similar to the initial measurement, indicating high stability under storage. In the case where PAH was used as an additive for BIS synthesis, results are different. Whereas when HRP is encapsulated, storage stability shows an almost linear trend, in the case of HRP adsorption on BIS, the observed concentration is decreasing with increased storage time, resulting to about 40% of the initially observed value. This behaviour indicates that the enzymatic performance degrades faster when immobilised by adsorption on BIS synthesised with PAH, over any other immobilisation method and support examined. However, given the peculiarities of the BIS-HRP system as described before, further analysis is necessary before finalising conclusions. Although Figure 8-12 shows the observed concentration of the oxidised ABTS ion at the end of the assay, it is important to see the pathway of the ABTS oxidation, given the fact that BIS was shown to be a prominent adsorbent of this particular product. Based on the performance of BIS-HRP samples from the screening section (Figure 6-1a and Figure 6-14a of Chapter 6) and in an effort to avoid unnecessary or repeated information, we only show the maximum value of expected product per mg HRP present in the biocatalysts, also stating the time point of the assay (Table 8-1). We can see that for BIS-PAH-HRP samples, maximum values are observed consistently within 1h during the assay, during the course of storage time. We can also see that for both BIS-PAH-HRP preparations the observed values are more or less stable during storage examination. This contradicts previous observations for BIS-PAH-HRP via adsorption, where observations at the 48h mark showed reduced product observation over time (Figure 8-12). An explanation to that could be that over time, the adsorbing capacity of BIS-PAH-HRP with adsorbed enzyme increases, which however cannot be looked further into at this point.

Table 8-1: Time point for maximum value of observed oxidised ABTS by BIS-HRP and associated value, for BIS-HRP samples synthesised with PAH or PEHA and HRP being encapsulated or adsorbed. Stated value is the extrapolated expectation of ABTS oxidation, based on original value collected and amount of HRP present in each sample, in μg oxidised BATS/mg HRP units. Presentation format: average (standard deviation). Each point is based on triplicates, with the error bar representing one standard deviation.

	BIS-PAH-HRP (encapsulated)	**BIS-PEHA-HRP (encapsulated)**	**BIS-PAH-HRP (adsorbed)**	**BIS-PEHA-HRP (adsorbed)**
Day 1 (h)	1	1	1	1
Max value	826.38 (39.51)	900.96 (4.52)	1853.81 (9.91)	5617.50 (64.56)
Day 14 (h)	1	1	1	24
Max value	771.68 (7.79)	806.10 (6.02)	2029.83 (90.41)	5501.29 (270.01)
Day 28 (h)	1	48	1	1
Max value	733.89 (7.79)	744.28 (7.03)	2267.16 (76.79)	6532.72 (55.76)
Day 50 (h)	1	24	1	1
Max value	745.70 (74.58)	730.07 (37.18)	2261.03 (241.51)	5181.68 (64.57)

Looking at BIS-PEHA-HRP, we can see that there is not a very clear trend, neither for the point of max value observation, or the value itself. For BIS-PEHA-HRP via encapsulation the maximum observed value is slowly decreasing over time, and similarly do values for BIS-PEHA-HRP via adsorption, except for the 28th day one, which is considerably higher than the others. Interestingly, the trend shown in Table 8-1 (max product) does not match with results shown in Figure 8-12 (product at the end of the assay), fact potentially associated with the adsorbing abilities of BIS rather than an alteration of enzymatic activity. Having seen the effect storage has on the biocatalyst through it performance using the ABTS assay, it is interesting to see if the effect is the same using the RB19 assay, where the observations are based on colour disappearance over time. Examining samples of the same biocatalysts, under the same time points with respect to assay development and storage stability, results are shown in Figure 8-13a. These results represent the decolorisation of RB19 based on the combined action of adsorption and dye degradation, given the complexity of the biocatalyst composite as described earlier. Similarly to the approach taken for the ABTS assay, obtained results were normalised to the value obtained on the first day of examination. Based on the performance of the composite, the only sample with stable performance over the storage period of 50 days is HRP in-situ encapsulated in BIS synthesised with PAH as additive, as its performance was literally unchanged.

For every other sample, there was a reduction on the degree of RB19 decolorisation over time, especially after day 28, indicating that the performance of the biocatalyst deteriorated over storage. Knowing the very strong ability of BIS to adsorb RB19, and since the focus of this project on the enzymatic performance, it deemed necessary to separate the enzymatic degradation from the adsorption of dye and judge the preservation of the former. This was done, as explained before, by assaying BIS samples without HRP, using the standard RB19 assay. Once the adsorption contribution was removed, obtained results were normalised per sample, to the initial observation of maximum detected enzymatic decolorisation (Figure 8-13b).

Looking at the enzymatic performance of the biocatalyst over the examined period of storage, it is clear that it would be wrong to assume that the biocatalysts are as stable as shown in Figure 8-13a and claim that BIS offer unaffected protection of HRP. There is definitely a protective effect since there is enzymatic activity detected at such a prolonged storage period, however, for every examined sample, the enzymatic degradation of RB19 decreased over time. Comparing the performance of the composite and the isolated enzymatic activity of BIS-PAH-HRP samples (red lines in Figure 8-13a and b respectively) one can see that especially in the case of adsorbed HRP on BIS (red circles), the drop of enzymatic activity over time is not negligible, whereas based on the composite action, RB19 removal seems stable.

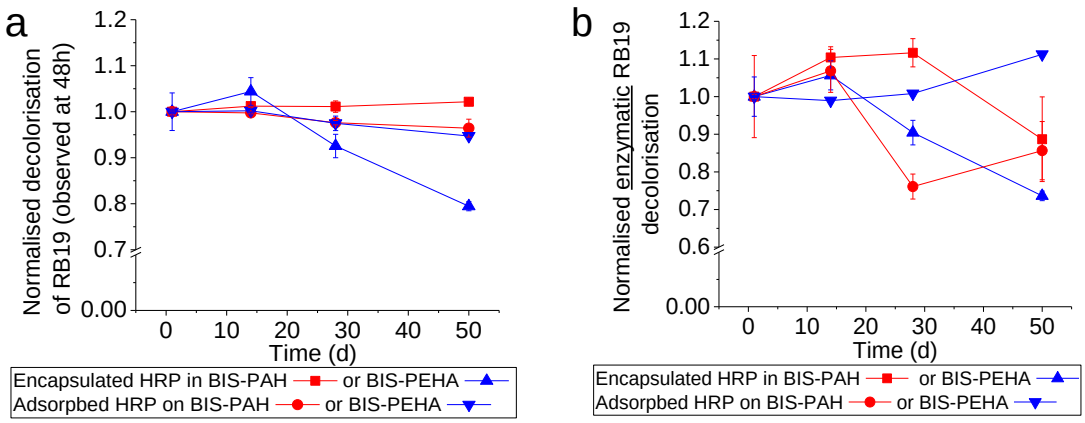

Figure 8-13:Normalised storage stability of HRP immobilised in BIS based on the decolorisation of RB19, using the standard RB19 assay, as recorded after 48h of assay, a) based on the action of BIS-HRP composite and b) based on enzymatic activity. Each point is based on triplicates, with the error bar representing one standard deviation.

Looking at these results from a broader perspective and focusing on the commercial potential of BIS-HRP biocatalyst, for every examined case, the decrease observed in either composite or enzymatic action was not larger than 20% from the originally observed value, with the exception of HRP encapsulated in BIS synthesised with PEHA as additive. This indicates an overall positive and quite promising effect of immobilisation on the storage stability of HRP. Furthermore, regarding the enzymatic decolorisation, it was noted that the time point of the maximum value observed during the 48h assay was kept constant over the 4 points of storage examination (Table 8-2), showing that the enzyme did not showed a considerably delayed action, despite the decrease in enzymatic activity.

Table 8-2: Time point in assay where the maximum value of enzymatic contribution to decolorisation of RB19 was observed for BIS-HRP composites and associated value. Values represent the average of triplicates, and values shown in parentheses represent 1 standard deviation.

	Day 1		Day 14		Day 28		Day 50	
Sample	**Time point (h)**	**Max value (% RB19 removed)**	**Time point (h)**	**Max value (% RB19 removed)**	**Time point (h)**	**Max value (% RB19 removed)**	**Time point (h)**	**Max value (% RB19 removed)**
BIS-PAH-HRP Encapsulated	1	37.59 (4.10)	1	41.50 (1.07)	1	41.97 (1.41)	1	33.33 (4.23)
BIS-PEHA-HRP Encapsulated	48	64.75 (3.39)	48	68.41 (2.49)	48	58.56 (2.11)	48	47.68 (0.82)
BIS-PAH-HRP Adsorbed	0.16	51.62 (0.27)	0.16	55.15 (2.94)	0.16	39.28 (1.72)	0.16	44.21 (3.99)
BIS-PEHA-HRP Adsorbed	1	77.36 (0.09)	48	76.54 (0.27)	1	77.99 (0.46)	1	86.05 (0.47)

The only difference was shown for HRP adsorbed on BIS synthesised with PEHA, where the maximum observed value for enzymatic degradation was at 48h, however, statistically this value was not different to the one observed at 1 h of assay. Overall, immobilisation of HRP on BIS extends the shelf life of the enzyme, allowing for use after 50 days of storage with good activity retention. Results are slightly different using the two different assays, but this is expected, given the different response of HRP to each substrate, as well as the contribution of BIS's presence to the observed results.

Comparing the performance of BIS-HRP samples on RB19 decolorisation after extended storage, to examples found in literature, findings from this work show a better performance than other systems of HRP immobilisation. HRP immobilised on aluminum-pillared clay lost 65% of activity over a 65 day storage period [203]. In a different study, it was found that HRP immobilised on polysulfones supports showed 29% activity towards dye decolorisation after 15 days of storage, which dropped to 12% after 48 days [263]. For reference, monitoring the activity of free HRP, stored in buffer, under the same temperature conditions, showed that the enzyme was highly active for the first day of storage, with the activity substantially decreasing after day 2 and the enzyme being almost inactive by day 3 (Figure 8-14). Comparing results obtained on storage stability for the free and immobilised enzyme, we can see that immobilisation definitely offers protection of the enzymatic activity over time, maintaining the activity levels almost intact over the 50 day period of examination. Depending on the immobilisation method and the additive used to synthesise BIS there are some differences on the ability of the support to protect HRP (e.g. in the case of HRP adsorbed on BIS synthesised with PAH, when biocatalyst was examined using the standard ABTS assay). Literature on storage stability of immobilised peroxidases shows similar results, where immobilised preparations preserved high enzymatic activity for longer compared to free enzyme, for periods of usually more than 30 days [108, 229, 263, 264, 381, 447, 467].

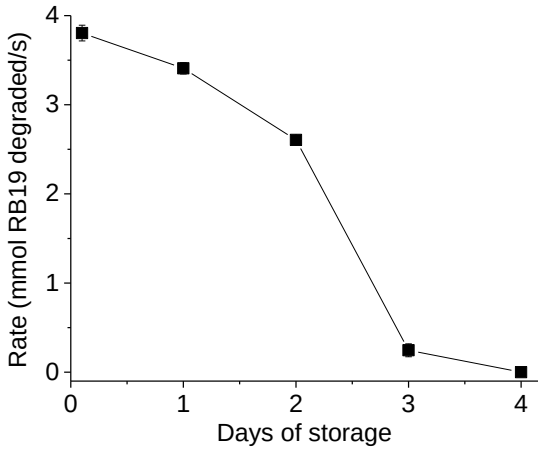

Figure 8-14: Storage stability of free HRP using the standard RB19 assay. Storage conditions: in phosphate-citrate buffer 0.1M, pH 4, at 4°C. Each point is based on triplicates, with the error bar representing one standard deviation.

It should be commented that in many of the examined examples, free HRP had a relatively high activity for many more days compared to the only 4 shown here [229, 264, 381]. This difference could related to the initial concentration of HRP used, or the fact that HRP used in this project was obtained as a lyophilised powder. It is unknown whether there were other contaminants present during lyophilisation (salts, buffers, possibly contaminants), which could potentially interfere with the buffer used here, but this could probably explain the results shown.

8.4. Reusability of immobilised HRP

As discussed in sections 2.1 and 2.2 of Chapter 2, the ability to reuse a (bio)catalyst is of paramount importance, given the operating principles and the associated costs. A major drawback of free enzymes is the absence of reusability, due to their soluble nature. Although a theoretical solution would be to add more substrate in a contained space, for practical reasons (finite volume of container, potential poisoning from product accumulation, severe dilution of enzyme's initial concentration) this is not applicable. A "good" immobilised enzyme system should allow for prolonged reuse, with a relatively stable performance, ideally close to the initial cycle. In order to examine the potential of BIS as an immobilisation support which could offer reuse of HRP, selected samples of BIS-HRP obtained by encapsulation or adsorption, using PAH and PEHA as additives, were assayed via the standard ABTS and RB19 assays as developed in sections 4.1 and 4.2 respectively. The samples examined to illustrate the potential of BIS as an enzyme immobilisation support which allows for reusability of the enzyme, where the best performing BIS-HRP composites derived from in-situ HRP encapsulation, as identified in Table 6-1 of Chapter 6. These were composites derived from encapsulation of an initial concentration of HRP introduced being 0.4mg/mL, added just after acid neutralisation, around pH 7, on BIS supports synthesised with PAH or PEHA, followed by acid elution to pH 5. For completion, their performance was compared to the reusability of BIS-HRP composites derived by adsorption of the same initial amount of HRP on premade BIS using PAH or PEHA and acid elution at pH 5. Furthermore, a Syloid Al-1FP – HRP composite was assessed for reusability, in order to compare the potential of reusing a BIS-based biocatalyst with a commercial silica-based biocatalyst.

8.4.1. Examination through the ABTS assay

Results of the production of ABTS ion through enzymatic oxidation after consecutive cycles are shown in Figure 8-15. Values shown were measured at the end of the 48h assay and normalised to the maximum observed value for each system, to rule out the effect of parameters such as different concentration of enzyme present in each system. A few observations can be extracted from this graph. Initially, it can be noted that the behaviour of all examined samples is decreasing with repetition, regardless of the type of silica used or the immobilisation method. Furthermore, samples of BIS-HRP synthesised with PAH show an increasing trend, followed by a plateau and then a rapid decrease in performance, whereas BIS-HRP samples synthesised with PEHA show a more "expected" performance, higher at the beginning, decreasing after a few cycles. The last

observation is about the maximum product observed, which for the majority of samples except from 1 (BIS-HRP synthesised with PEHA, with in-situ encapsulation), is shown in consecutive cycles instead of the initial one.

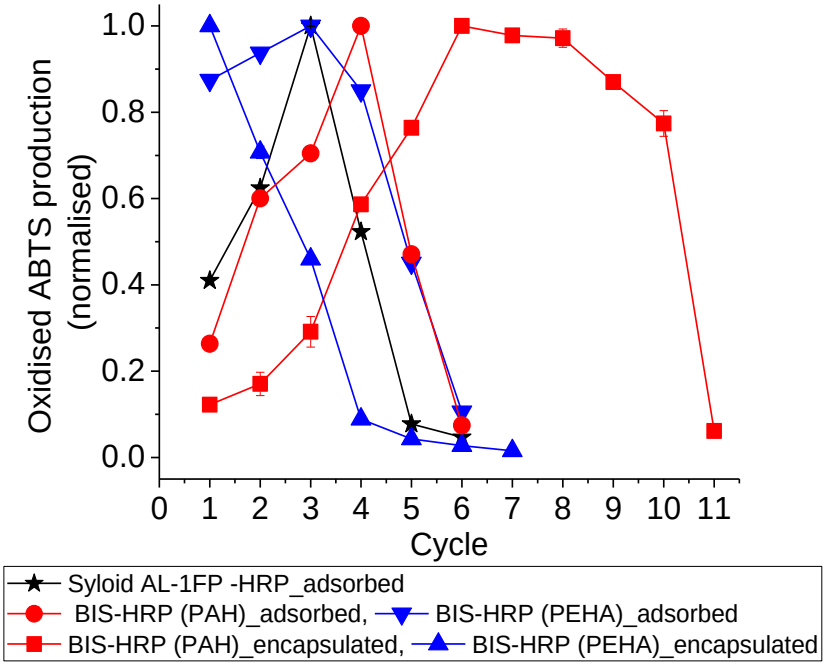

Figure 8-15: Effect of repeated use on performance of immobilised HRP using the standard ABTS assay. ABTS oxidation was recorded after 48h and values were normalised based on the maximum value recorded across all cycles per sample. Each point is based on triplicates, with the error bar representing one standard deviation.

The increasing trend of ABTS oxidation for the first few cycles for BIS-PAH-HRP samples could be explained by the very good performance of BIS as an adsorbent. Based on our developed knowledge on the performance of BIS-PAH-HRP during the ABTS assay and on the observed behaviour of BIS-PAH-HRP samples upon reuse, we can reach another conclusion, besides the excellent adsorbing capacity of BIS. The other conclusion is an estimation on the capacity of BIS to adsorb ABTS radical. This conclusion is derived from the fact that –assuming the ABTS has to diffuse in and out of the pores– after a point (cycle 4 for adsorbed and cycle 6 for encapsulated HRP on BIS synthesised with PAH as shown in Figure 8-15), we are able to see a maximum in the observed production of oxidised ABTS. This could be indicative of the adsorbing capacity of BIS being reached, allowing "easier" diffusion through the pore structure, as amino residues from PAH would not be available. The aforementioned argument can be further supported from the surface characteristics of the biocatalyst. Based on porosimetry data on porosity and surface area, as discussed in various sections of Chapter 5, BIS-HRP samples synthesised with PAH as additive offer large surface areas and a mesoporous profile, allowing – theoretically – for easier flow of reagents. However, given the knowledge on the structure of BIS, there is a high probability of the pore channels being "lined" with amine residues, where reagents can get adsorbed. As we saw for every ABTS assay of BIS-PAH-HRP so far, this is most definitely happening with both unoxidised and oxidised ABTS. A speculation would be that initially formed ABTS radical gets

adsorbed on the BIS structure by favourable electrostatic interactions, and once at least a monolayer is formed, "newly" oxidised ABTS is easier to diffuse outside the pore structure. When HRP is adsorbed on BIS, then the enzyme is more easily accessible by the substrate, hence observation of ABTS oxidation occurs faster and more intensely. However, reduction of the absorbance intensity occurs faster as well, due to adsorption of the ion on the biocatalyst. An attempt to depict this speculation was shown in Figure 6-2a and Figure 6-17a of Chapter 6 for encapsulated and adsorbed HRP on BIS respectively.

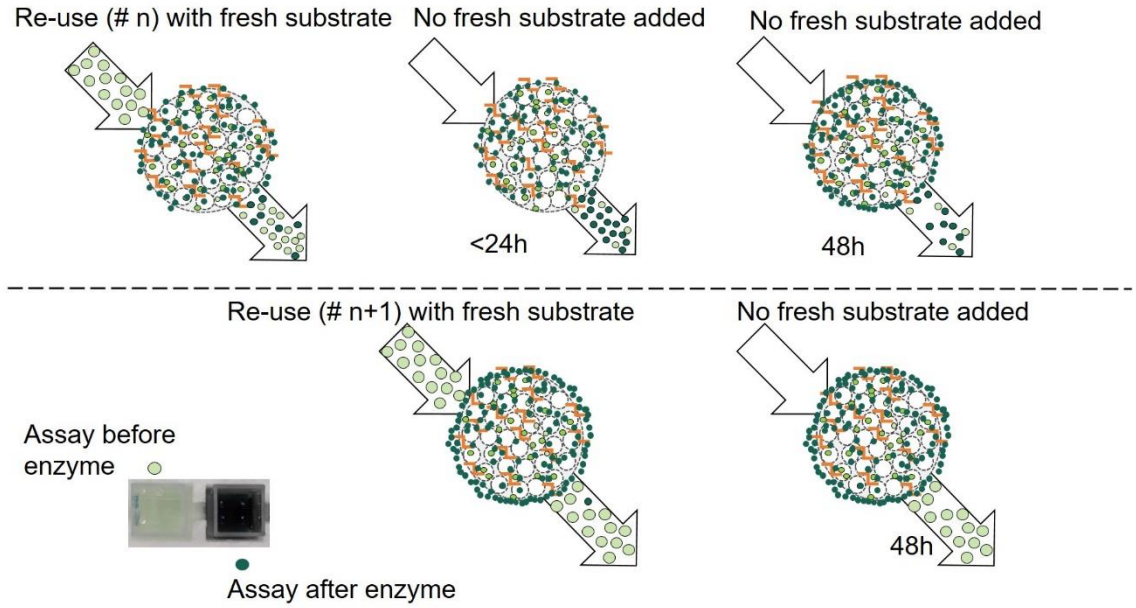

Figure 8-16: Depiction of BIS-HRP biocatalyst using ABTS assay, during consecutive cycles of reuse. Arrow coming in represents the addition of substrate, arrow coming out represents the observable outcome via UV-Vis. From left to right, illustrations show the progress of the assay over time (0, up to 48h).

Having established that reacted ABTS gets adsorbed on the BIS-HRP biocatalyst during or after production, the question of what happens during reuse arises. Based on the observations made from the collected data, a speculation on the difference between the encapsulated and adsorbed HRP system can be made. Given the few cycles of reusability, before noticeable reduction on ABTS production, we believe that during the initial first few cycles accessibility of HRP is more or less stable, until the peak absorbance is observed. After this point, reduction of the observed concentration of oxidised ABTS is documented. This could mean either higher adsorption of produced radical on BIS, or lower generation of produced radical by HRP. Given the finite capacity of BIS as adsorbent and the few reuse cycles already occurred, the acceleration of adsorption of ion on BIS is not a plausible scenario. This leaves the reduction of ABTS oxidation as the only reason for the reduced observed concentration. Decrease in the generation of ABTS ion can occur either due to inactivation of the enzyme, or difficulty of the substrate to reach it. The first scenario would imply poisoning of HRP due to high accumulation of product and the second scenario would imply a clogged pore network, possibly due to adsorbed ABTS. Such scenarios for the explanation of reduced apparent enzymatic activity over prolonged reuse of

immobilised enzyme systems have been proposed in literature [108, 468]. In both immobilised HRP systems, there is the possibility of a decrease in the observed value for ABTS ion concentration due to loss of biocatalyst during the separation and washing procedure, which however is not considered based on the leaching analysis shown in section 5.4.3. An illustration of the prolonged reuse and subsequent termination of observed enzymatic activity is shown in Figure 8-16.

Comparing the method of immobilisation, still referring to BIS-PAH-HRP, it is obvious that the delay until the cycle with the maximum ABTS ion observation is higher in the case of encapsulated HRP (squares in Figure 8-15) compared to adsorbed HRP (circles in Figure 8-15). Furthermore, the plateau observed for encapsulated HRP (about 5 cycles) does not occur in the case of adsorbed HRP (rapid decrease after max value is observed). These observations could be attributed to the localisation of HRP in the BIS-HRP composite in each case. When HRP is immobilised in-situ, during BIS synthesis, it is expected that the majority of the enzyme will be entrapped within particle aggregates, deep inside the pore structure. In the case of HRP being adsorbed on BIS, the enzyme will enter the pore structure when allowed from the pore size and potentially the tortuosity, but predominantly, it will be localised in the external surface area, adsorbed strongly on the embedded amine and through weak interactions on the silica. This realisation, can lead to the assumption that protection of the enzyme is enhanced in the encapsulated system, hence showing a prolonged plateau of "max" observed ABTS ion. Having said that, even when the maximum concentration of ABTS ion is observed for the encapsulated HRP system, certainty on this amount corresponding to the maximum produced from the enzyme present cannot be acquired. Uncertainty is merited to the absence of accurate knowledge on the quantity of enzyme present as well as its accessibility to the substrate. Furthermore, although the assumed explanation on why there is such a trend during reuse of BIS-HRP in presence of PAH seems reasonable, further analysis is needed to convert the assumption into a confident statement.

In the case of reuse BIS-PEHA-HRP systems, results are different to PAH, as shown in Figure 8-15 (blue data sets). Here, the performance of the biocatalyst starts high and then either drops quickly (for encapsulated HRP, triangles), or retains high values before a rapid decrease (for adsorbed HRP, inverted triangles). This behaviour could be attributed to the structure of the material, which – as shown from the porosimetry analysis – is much less porous, and with considerably lower surface area. Furthermore, although both PEHA and PAH have amino-residues where oxidised ABTS can adsorb on, in the case of PEHA, the concentration of nitrogen is less, allowing for fewer adsorption points. The effect of less prominent adsorption of the oxidised ABTS on BIS synthesised with PEHA compared to PAH, was also shown from the time points measured during the assay, as shown earlier, since the absorbance of the solution would not reduce over time, as it was observed in the case of BIS-PAH. Comparing the method of immobilisation, based on obtained results, adsorbed HRP (inverted triangles in Figure 8-15) seems to perform better when reused, as it allowed for 3 cycles before observing a reduction of

the performance. On the other hand, in the case of encapsulated HRP, performance was drastically reduced after the initial cycle (triangles in Figure 8-15). The rapid performance reduction for encapsulated HRP can be attributed, again, to the localisation of enzyme in the composite combined with the reduced accessibility of it, especially if the narrow pore channels were blocked with adsorbed ABTS (oxidised or not). In the case of adsorbed HRP, the relative performance of the biocatalyst was similar to the relative performance of HRP adsorbed on BIS synthesised with PAH, although in the case of PAH, an additional 2 cycles of high performance were obtained before decrease occurred.

Last but not least, the performance of HRP adsorbed on Syloid AL-1FP is interesting, as the expectation was to see a trend similar to the observed for HRP adsorbed on BIS-PEHA, given the very narrow pores and the absence of functionalisation. On the contrary, HRP adsorbed on Syloid shows a behaviour similar to the one observed for HRP adsorbed on BIS-PAH, where consecutive to the initial cycles show a higher performance –purely based on product measurement, before there is a decrease and a subsequent termination of enzymatic activity. There is no clear understanding on why such a behaviour might have occurred, but initial assumptions could be based on loosely adsorbed oxidised ABTS molecules on the silica particles, which desorbed upon consecutive cycles, showing an ostensible increase in enzymatic performance.

Putting numbers on the normalised approach used so far, the maximum obtained concentration of oxidised ABTS per mg of HRP present on each examined composite, based on the maximum observed absorbance value is shown in Table 8-3. One can see that the best performing samples in terms of observed ABTS oxidation are by far BIS-PEHA-HRP where HRP is adsorbed post-synthesis and Syloid AL-1FP-HRP. In both these cases, adsorption of oxidised ABTS on the support is not as favoured as in the other cases, either due to lack of strong attachment points (e.g. amines), or due to lack of porosity.

Table 8-3: Maximum oxidised ABTS production per examined composite. Value was obtained by extrapolation to 1 mg HRP being present in assay. Each value is based on triplicates, with the value in parenthesis representing one standard deviation.

Sample examined	Maximum oxidised ABTS concentration / mg HRP (μM)	Cycle where maximum production is observed
BIS-PAH-HRP encapsulated	701.64 (5.01)	5
BIS-PEHA-HRP encapsulated	641.26 (25.12)	1
BIS-PAH-HRP adsorbed	5,805.02 (235.81)	4
BIS-PAH-HRP adsorbed	10,228.80 (45.72)	3
Syloid AL-1FP – HRP	18,634.53 (425.09)	3
Free HRP (for reference)	15,915,744 (789,455)	-

It is worth mentioning that these 2 samples had the lowest HRP loading amongst the examined samples (as estimated via the Bradford assay). Specifically, Syloid Al-1FP – HRP had half the

HRP loading of BIS-HRP synthesised with PEHA. The fact that the maximum oxidised ABTS concentration calculated for each sample is representative of the loading ratio, shows that the samples perform in a similar way. Comparing the HRP loading of BIS-HRP composite derived by adsorption of HRP on BIS synthesised with PAH and with PEHA, in the case of PAH, the loading is almost 50% higher than in the case of PEHA. However, maximum production results show an inversed effect, as the performance of BIS-HRP synthesised with PAH is almost half of the equivalent synthesised with PEHA. This can be attributed to a few factors, mentioned below. Firstly, there are structural differences between BIS-PAH and BIS-PEHA, leading to biocatalysts with potentially different localisation of HRP. When PAH is used, larger pores are created, allowing HRP to be immobilised "internally" as well, compared to the almost only "external" adsorption in the case of BIS made with PEHA, where material's morphology is mostly nonporous. Secondly, the effect of amine presence during the ABTS assay showed a strong interaction between PAH and ABTS (oxidised or not). Formed product would not get diffused in the bulk solution allowing for us to measure it, but it would get adsorbed upon its creation, maybe slowly released over time and then re-adsorbed on the BIS particles, making accurate quantification very difficult. Thirdly, substrate and product accumulation can be detrimental to enzymatic activity, fact that might have contributed to reduced performance of HRP compared to expected, as the immobilisation support acted as a "sponge" for both substrate and product, which could have led to deactivation of HRP. Last but not least, accumulation of adsorbed substrate and/or product could have caused blocking of active sites of HRP, leading to lower activity.

The behaviour observed during reuse of BIS-HRP composites for ABTS oxidation is not expected based on the usual expectations and available observations for immobilised enzyme reuse. Most systems in literature show either a stable performance for the number of cycles examined [156, 469, 470], or an initially high and subsequently decreasing performance, attributed to various factors as noted in literature. Such factors are enzyme leaching from the support [217], biocatalyst loss during reuse [221], enzyme deactivation upon prolonged reuse [264, 471], blocked access to substrate [203], or even easier deactivation under specific assay conditions [156]. However, there are many examples where an explanation on the activity or performance reduction over prolonged use is not given [18, 97, 155, 195, 218, 262, 277, 321, 430, 431, 435, 442, 472], showing that there is a need for more in depth understanding of the dynamics during reuse of immobilised enzymes. Being able to explain the mechanisms that enhance or hinder reuse is fundamental for designing better biocatalysts.

8.4.2. Examination through the RB19 assay

Throughout the recycling of the BIS-HRP composite samples for the monitoring of colour removal, the blank samples were recycled as well, to gain understanding for the capacity of the support as adsorbent. In order to identify the contribution of the enzymatic degradation on the observed reduction of colour over time, the contribution of the support was removed as shown previously. As a reminder, the samples examined for reusability where the identified as best

performing BIS-HRP composites via in-situ encapsulation for each additive, with corresponding samples from the adsorbed HRP cohort. Furthermore, a Syloid Al-1FP – HRP composite was assessed for reusability, in order to compare the potential of reusing a BIS-based biocatalyst with a commercial silica-based one. Similarly to previous cases, results per sample are presented after normalising the performance to the best observed one, in to avoid complications arising from the unequal concentration of immobilised (and available) HRP in each case (Figure 8-17). Putting some figures on the normalised results presented, the RB19 removal (after 48h) for the first cycle was 96%, 62%, 95%, 94% and 40% for the examined samples, with the order of appearance on Figure 8-17. There is a statistically significant reduction of performance after the initial cycle across all examined samples, with residual performance reaching between 60-80% for BIS-HRP samples and being almost 0 for Syloid AL-1FP-HRP. For subsequent cycles, the performance of most BIS-HRP samples retained, with the exception of HRP adsorbed on BIS-PEHA, where performance drastically reduces over repeated use. A simple explanation for the reduction in performance would be leaching of enzyme, which however is probably not the case here, as it was shown in section 5.4.3 of Chapter 5. There is a similarity on the reusability performance trend observed for Syloid AL-1FP-HRP and BIS-PEHA-HRP via adsorption, where in both cases, past the initial use, the performance rapidly traces off, with performances significantly lower than the initial one. Furthermore, there are structural similarities of the 2 materials, BIS-PEHA is almost nonporous, with some porosity obtained after acid elution, but not at substantial level, and Syloid AL-1FP is categorised as "mesoporous" with a pore size of 2nm, hence, on the verge of microporous area. Given those 2 observations, we can explain the rapid performance reduction as reduction of the adsorbent's capacity (especially since a portion of adsorption sites was occupied with HRP), combined with blocked active sites, or inactivation of the adsorbed enzyme.

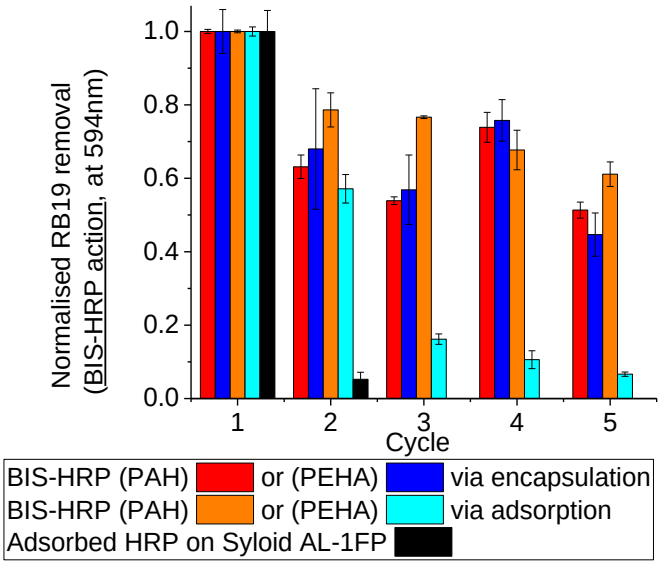

Figure 8-17: Effect of repeated use on performance of immobilised HRP using the standard RB19 assay. RB19 removal was recorded after 48h and values were normalised based on the maximum value recorded across all cycles per sample. Results represent the performance of the composite action. Each point is based on triplicates, with the error bar representing one standard deviation.

Another point for consideration is potential loss of biocatalyst particles during the recycling process, as the composite had to be separated from the assay volume and washed with buffer at least 2 times. This is a valid concern especially in the case of Syloid Al-1FP, since the commercial product sample was received as very finely milled powder, compared to the untreated particle aggregates of BIS. It should be emphasised that the performance observed in Figure 8-17 is the combination of the adsorbing action of silicas and the catalytic degradation by immobilised HRP. Since the point of this project is the preservation of the enzymatic activity, it was crucial to extract the portion of the performance which corresponded to each portion of the composite. That was done by subtracting the performance of BIS types used for immobilisation and Syloid AL-1FP, when assayed for adsorption of RB19 over the same number of cycles as the immobilised HRP samples. In an effort to present those results in an understandable manner, and illustrate the aforementioned points, a "per time point approach was chosen", focusing on the first and the last cycle of each of the 5 immobilised HRP preparations examined (Figure 8-18).

In this figure, graphs have been colour coded. Grey bars represent the contribution of enzymatic degradation of RB19 during the assay and textured bars represent the portion of RB19 being adsorbed on the support. Graphs a and b describe encapsulated HRP in BIS-PAH and BIS-PEHA respectively, graphs c and d describe adsorbed HRP on BIS-PAH and BIS-PEHA respectively and graph e represents the commercial silica, Syloid AL-1FP as support for HRP adsorption. Given the uneven amounts of HRP being present, absolute % RB19 removal should not be compared across graphs, but only within the same graph. A comparison of the performance on that factor is being done later. What we are focusing on is the ratio between the contribution of the support and the contribution of the enzyme on the total performance, as time during the assay progresses, as well as between the first and last cycle. Specifically looking at the performance of BIS-PAH-HRP composites (Figure 8-18a and c), we can see that for the first cycle the contribution of the enzyme is higher at the beginning of the assay (10min to 1h). However, for the last cycle, the enzyme shows a higher contribution towards the end of the assay, with the overall contribution not being comparable to the contribution from dye adsorption. This shows that in these immobilised HRP preparations, the initially fast action of the enzyme is substituted by a slower enzymatic contribution, as dye adsorption on BIS takes over. It also shows that although in the first cycle the maximum colour removal was more or less reached within 1h for encapsulated HRP and within the first 10min for adsorbed HRP, with a more than 50% contribution of the enzyme, by the end of the reuse study, the maximum result is reached by 48h, depending almost solely on dye adsorption. Focusing on Figure 8-18b and d, for BIS-PEHA-HRP samples by encapsulation and adsorption respectively, we can see that for both initial and last cycle, the composite performance is highly dependent on enzymatic degradation, as the dye adsorbed on the support accounts for a small part of the performance and appears later in the assay. Looking at Figure 8-18e, representing the performance of Syloid AL-1FP-HRP, we can

see that adsorption of RB19 on the support steadily increases during the assay, but the highest contribution of the enzyme is not shown until the 24h time point during the first cycle, implying a delay on the enzymatic activity. The second – and last – cycle run for this preparation implies that dye removal based on the action of the support is better than the action of the composite, as subtracting the "support only" contribution from the performance of composite led to negative results.

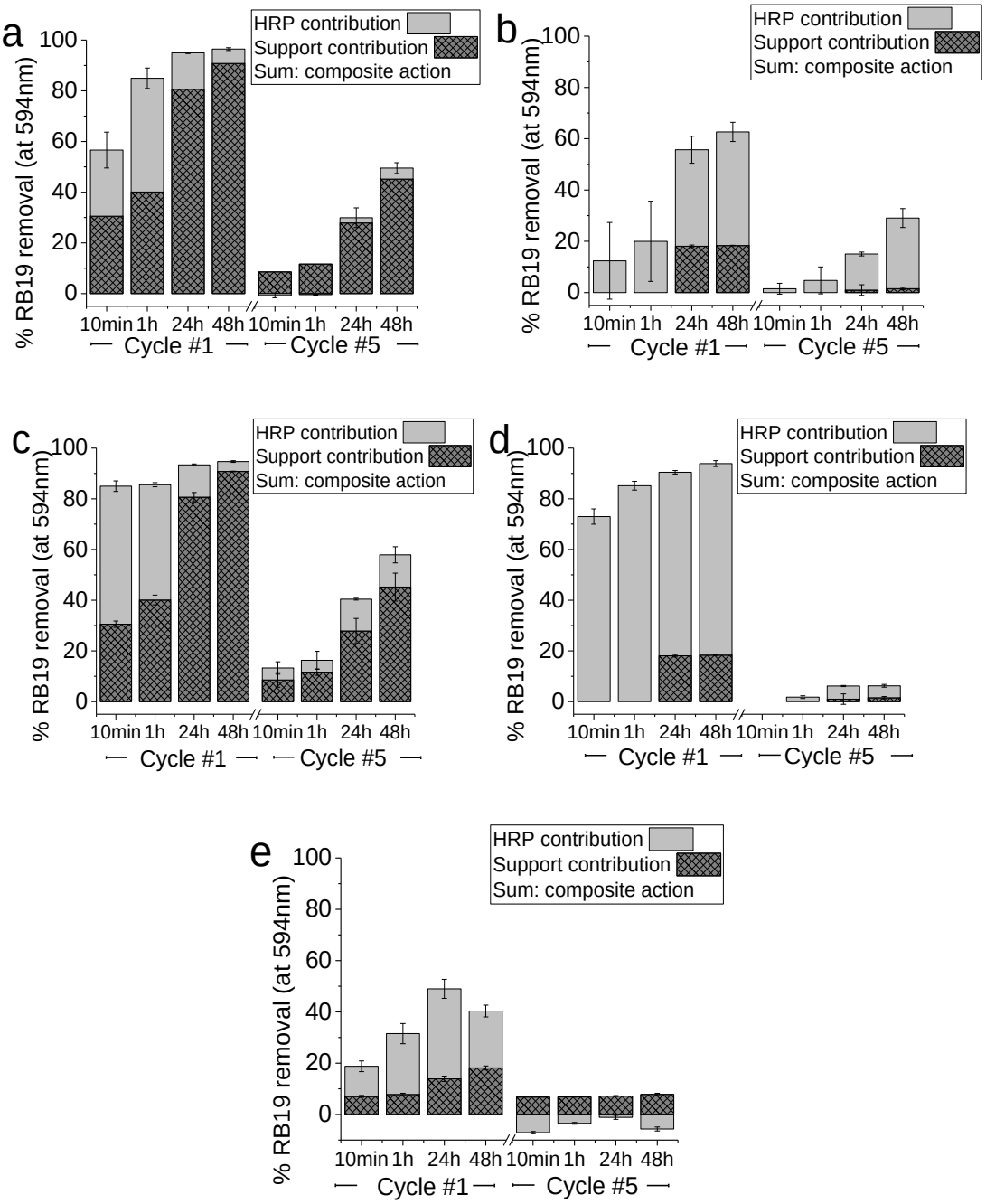

Figure 8-18: Performance of immobilised HRP being reused using the standard RB19 assay. RB19 removal was recorded at 4 specific time points for samples of immobilised HRP and corresponding supports, in order to distinguish the contribution of adsorption and enzymatic degradation. Results shown here are for the initial and 5th cycle of reuse, for a) BIS-PAH-HRP via encapsulation, b) BIS-PEHA-HRP via encapsulation, c) BIS-PAH-HRP via adsorption, d) BIS-PEHA-HRP via adsorption and e) Syloid AL-1FP-HRP. Each point is based on triplicates, with the error bar representing one standard deviation.

Comparing the contributions of the 3 different supports used for immobilisation of HRP (Figure 8-18a and c for BIS-PAH, b and d for BIS-PEHA and e for Syloid AL-1FP), we can see that presence of PAH makes BIS a very prominent adsorbent. Even after 5 cycles of reuse, its performance is reduced by almost 50%, compared to the more than 90% reduction in the performance of BIS synthesised with PEHA. The performance of Syloid AL-1FP as adsorbent is reduced by almost 50% within 2 cycles and the composite loses all enzymatic activity, whereas in every other case, a percentage up to almost 30% is preserved.

Trying to explain these findings, we need to consider not only the type of support used and the method of immobilisation, but also the procedure of dye degradation. RB19 is oxidised by HRP previously activated with peroxide. That means that both peroxide and dye molecules need to get in the vicinity of the enzyme, which might be located primarily on the external surface of the support (if adsorbed), or deep inside the pore structure (if encapsulated). Given the presence of moieties located on the support, that facilitate adsorption of the dye based on weaker or stronger electrostatic interactions, and depending where the enzyme is, adsorption might dominate compared to enzymatic degradation. This is mostly observed in the case of BIS synthesised with PAH, as the presence of protonated amine residues interacts strongly with the anionic sulfonate groups of RB19. Until the available moieties for adsorption are covered and dye molecules can diffuse further inside the pore structure to find the excited enzyme, adsorption will dominate over enzymatic activity. However, if the enzyme is "easily available", on the external surface of the composite, such as is the case when adsorbed, then enzymatic degradation is much more prominent and faster than adsorption, as shown in Graphs c, d and e of Figure 8-18. Again, dye adsorption is occurring, but given the direct availability of excited enzyme, enzymatic degradation is dominating, until either peroxide concentration is substantially reduced, or the active conformation of the enzyme is distorted. The pore structure of BIS has been discussed before, on the context of not having enough information about the shape of the pores and the tortuosity effects caused by the not ordered formation of the material. A not ordered pore structure can cause delayed expression of enzymatic activity, fact illustrated for BIS-HRP composites where HRP is encapsulated, especially in the case of PEHA.

As recycling occurs, there are fewer adsorption sites during each subsequent cycle, as the capacity of BIS as sorbent is being approached. The strong adsorption of RB19 on BIS support can have various effects which affect the composite's performance. Due to the increased concentration of dye on, in and around the support, HRP present might get poisoned, as excessive concentration of substrate has been seen to have this effect. Furthermore, adsorption of RB19 on the external surface area and diffusion of RB19 through larger pores and subsequent adsorption of it in there, can cause delayed of event blocked access to HRP residing in the pores, hence much lower enzymatic contribution to observed colour removal.

In conclusion, based on the so far presented results, there is a distinct advantage of BIS-HRP compared to Syloid AL-1FP-HRP, that being the prolonged reuse of the composite with some enzymatic activity being detected. Furthermore, there is a an advantage of faster initial action of HRP adsorbed on BIS compared to the encapsulated composite, which however does not carry the trend over multiple uses.

Trying to examine these results from a more quantitative point of view and compare across samples, we are employing the method used previously. We normalise the observed enzymatic contributions from the mass of HRP present in the assay, to 1 mg HRP; how much dye would be decolorised if 1mg HRP was present in the assay within the specific composite. In this approach, we do not take into consideration the contribution of the support, as a different type of analysis is needed for that. The observed enzymatic contribution used is the maximum one observed per cycle, irrespective of the time point. Results are shown per cycle for every preparation of immobilised HRP in Table 8-4. At a first glance, one can observe that the maximum value of enzymatically degraded dye is shown for BIS-PEHA-HRP via adsorption, at 1865 μM, followed by BIS-PAH-HRP via adsorption. For reference, the maximum quantity of RB19 decolorised by 1mg of free HRP using the standard RB19 assay was calculated around 7000 μM.

Table 8-4: Arbitrary estimation of maximum enzymatic decolorisation using immobilised HRP, based on max enzymatic decolorisation observed per sample per cycle and extrapolated to 1mg of HRP present. Values are based on triplicates, with the value in parenthesis representing one standard deviation.

	Maximum enzymatic decolorisation (μM RB19/mg HRP present on composite)					
Sample	**Cycle #1**	**Cycle #2**	**Cycle #3**	**Cycle #4**	**Cycle #5**	**Sum**
BIS-PAH-HRP (encapsulated)	62.00 (5.56) at 1h	5.26 (11.2) at 24h	7.73 (1.39) at 48h	38.90 (5.44) at 48h	6.01 (2.92) at 48h	119.92
BIS-PEHA-HRP (encapsulated)	55.27 (4.67) at 48h	47.48 (12.82) at 48h	44.45 (7.40) at 48h	55.77 (4.42) at 48h	34.34 (4.59) at 48h	237.31
BIS-PAH-HRP (adsorbed)	433.48 (16.55) at 10min	176.71 (56.08) at 24h	208.54 (2.76) at 48h	187.82 (110.51) at 24h	99.81 (2.91) at 48h	1106.37
BIS-PEHA-HRP (adsorbed)	1037.07 (21.10) at 1h	598.04 (44.51) at 48h	109.58 (16.18) at 48h	57.28 (14.70) at 48h	63.14 (2.65) at 24h	1865.11
Syloid AL-1FP - HRP	917.39 (96.55) at 24h	-	-	-	-	917.39

Results for Syloid AL-1FP-HRP are close to the aforementioned for adsorbed HRP on BIS, although collected over only 1 cycle. When it comes to encapsulated HRP in BIS, the enzymatic contribution is considerably less. Looking at the per cycle results, as reuse progresses, enzymatic

dye degradation reduces for the adsorbed HRP faster than for encapsulated HRP. Furthermore, looking at the time point for the as observed maximum enzymatic degradation contribution, it gets delayed in every case, but the encapsulated HRP in BIS synthesised with PEHA, where the maximum result is constantly observed at the 48h point. These observations are reasonable given the localisation of HRP in each immobilised preparation, and the action of the support as a dye adsorbent based on presence of porosity and functionalisation induced from amine presence.

The different processes occurring during the initial cycle of the RB19 assay as discussed above, are shown illustratively in Figure 6-2b and Figure 6-17b of Chapter 6. Looking at prolonged use of BIS-HRP samples for dye degradation, the performance is similar to the observed for ABTS oxidation, where after a point the capacity of BIS as adsorbent of RB19 is reached and adsorbed dye is blocking access to immobilised enzyme, or enzyme has been deactivated. These effects are illustrated in Figure 8-19. So far, reuse potential of immobilised HRP was examined over 5 cycles. However, after the last cycle, some of the samples were still showing high decolorisation ability. Hence, it was decided to keep recycling them in order to identify a) when obtained decolorisation would completely degrade and b) get an estimation of the adsorbing capacity of different BIS. The samples selected for this purpose were BIS-HRP samples with encapsulated HRP in BIS synthesised with PAH or PEHA. They were reused for a total of 20 cycles, results of enzymatic and adsorption contribution shown in Figure 8-20.

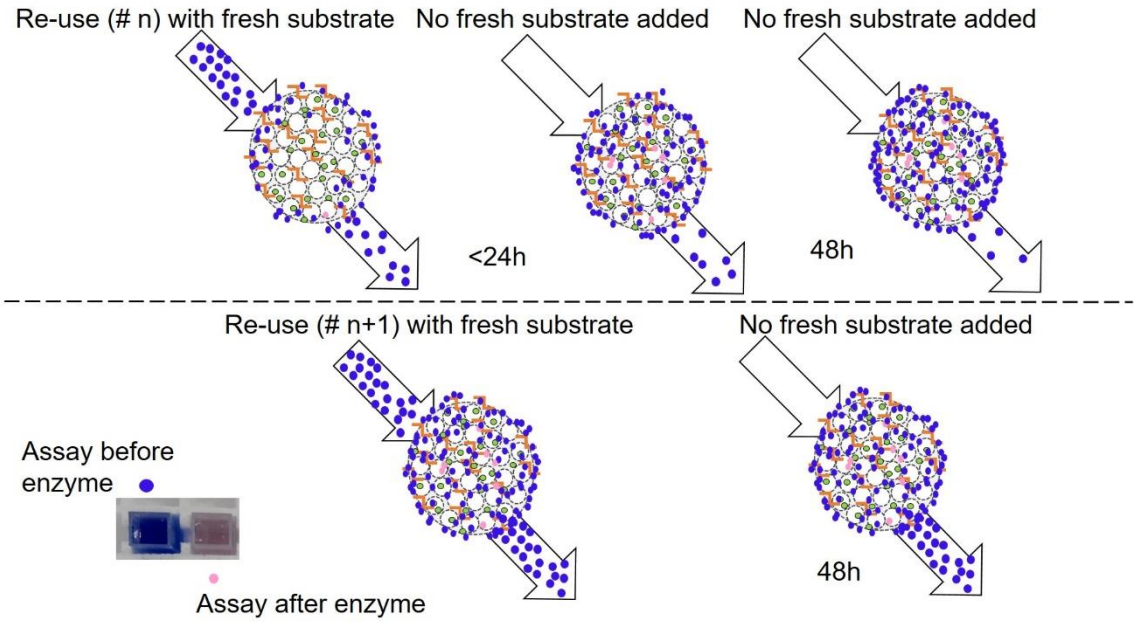

Figure 8-19: Depiction of BIS-HRP biocatalyst using RB19 assay, during consecutive cycles of reuse. Arrow coming in represents the addition of substrate, arrow coming out represents the observable outcome via UV-Vis. From left to right, illustrations show the progress of the assay over time (0, up to 48h).

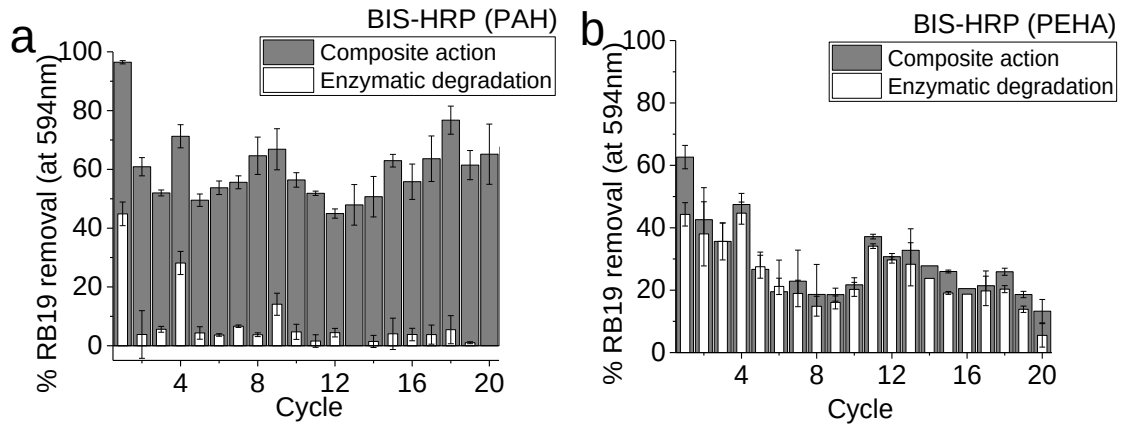

Figure 8-20: Repeated use of immobilised HRP by encapsulation in BIS synthesised with a) PAH or b) as additive, over 20 cycles. Light grey bars represent the enzymatic contribution to colour removal, coloured bars show the colour removal based on the action of the composite. Values are based on triplicates, with the error bar representing one standard deviation.

It is clear that the observed decolorisation potential in the case of BIS-PAH-HRP is attributed mainly to adsorption of dye on the composite (red bars being much bigger than grey bars), whereas in the case of BIS-PEHA-HRP colour removal is due to enzymatic action (grey bars being almost equal to blue bars). It is worth mentioning the relatively stable performance over the course of 20 cycles in the case of BIS-PAH-HRP, where colour removal past the initial cycle is hovering around 60%. In the case of BIS-PEHA-HRP the performance is reduced by about 66% by the end of the 20 cycles. In both cases, by cycle 20 the contribution of immobilised HRP to the overall colour removal was severely degraded, reaching 0 and 5% for BIS-HRP synthesised with PAH or PEHA as additive respectively. Calculating the dye removed by this point based on the action of the composite, we result at 0.19 and 0.088mg RB19 removed per mg BIS-HRP composite synthesised with PAH and PEHA respectively. This analysis is not conclusive, just indicative of the potential of BIS-HRP, as especially in the case of BIS-HRP synthesised with PAH, the adsorbing performance still showed considerable potential even after 20 continuous cycles of reuse, without regeneration taking place.

Comparing the performance of the different preparations of BIS-HRP examined for dye decolorisation with examples of immobilised HRP found in literature (Table 8-5), some of the systems examined herein perform much better than in other cases, where the biocatalyst could not last for more than a few cycles (e.g. immobilisation in alginate beads). However, there are some examples in literature which show great potential based on the number of cycles of reuse and the retained activity percentage (e.g. [271, 335, 453, 473], where for more than 7 cycles, the retained activity on dye decolorisation was higher than 50%).

Table 8-5: Examples of immobilised HRP and its reusability potential on dye decolorisation.

System	Cycles of reuse	% or performance retained by last cycle compared to initial	Reference
BIS-HRP (encapsulated, using PAH)	20	67	This study
BIS-HRP (encapsulated, using PEHA)	20	21	This study
BIS-HRP (adsorbed, using PAH)	5	61	This study
BIS-HRP (adsorbed, using PEHA)	5	7	This study
HRP adsorbed on polysulfones supports	7	17	[263]
HRP encapsulated in alginate beads	3	14	[433]
HRP encapsulated in alginate beads	5	36	[435]
HRP adsorbed on acrylamide gel	5	37	[435]
HRP adsorbed on kaolin	6	40	[18]
HRP adsorbed on ZnO/silica nanowires	12	80	[335]
HRP bound on chitosan	5	0	[474]
HRP encapsulated in alginate beads	10	11-13 (multiple dyes examined)	[97]
HRP immobilised by cross-linking with glutaraldehyde on chitosan or aluminum oxide/gelatin composites	7	50-80 (multiple immobilisation preparations examined)	[271]
HRP immobilised as CLEA with magnetic nanoparticles, with or without glucose oxidase	8	60 (for both preparations)	[473]
HRP immobilised in porous structure in presence or absence of $CaCO_3$	7	55-63 (multiple immobilisation preparations examined)	[421]
HRP immobilised as CLEA and used in batch or packed bed reactor	7	26-66 (multiple uses of immobilised HRP)	[337]
HRP immobilised on functionalised polypropylene films	10	90	[453]
HRP encapsulated in alginate beads	7	44-55 (multiple dyes examined)	[463]

8.5. Exploring the adsorbing potential of BIS

Having seen the significant contribution of the immobilisation supports as adsorbents during examining the performance of immobilised HRP preparations, it was deemed interesting to examine the adsorbing capacity of various silicas in absence of enzyme. This research project was carried out by Mr. Hinesh Patel, in fulfilment of the degree of Master of Engineering, under the author's supervision and guidance. The adsorption profile of 4 different silicas was examined.

The chosen silicas were BIS synthesised with PEHA, with the amine either fully present (pH 7), partially removed (pH 5), or fully removed (pH 2) and Syloid Al-1FP. The choice of silicas was as such, due to the more controlled amine content compared with BIS synthesised with PAH as additive [64].

8.5.1. Adsorption kinetics and mechanisms

Initially, the adsorption of RB19 was examined by the 4 selected types of silica, over a period of 7 days. Results show that silicas with absence of amine content (BIS with fully removed amine and Syloid Al-1FP) were not as effective sorbents as BIS in full or partial presence of the initial amine content. This is attributed to the absence of functionalisation of these materials and the negatively charged silica surface and anionic dye. The uptake of RB19 onto BIS in presence of amine is denoted by 2 phases: (a) a slow initial rate of removal for approximately 4 hours where 20-30% of dye was adsorbed, and (b) a faster rate of adsorption after 1-day. It is likely that the first phase represents the time taken for large dye molecules (diameter of RB19 is calculated to 2nm) to diffuse through the smaller pores, while the second phase may represent greater and faster interactions between the functionalised sorbent surface and the sorbate. The enhancement of dye uptake onto BIS with full or partial amine content (BIS pH 7 and BIS pH 5) is most likely to be through electrostatic interactions between the anionic sulfonate groups of the dye arising following dissociation in water and the protonated amino groups on the sorbent. After 7 days, the maximum dye removal (%) was 85% (BIS pH 5) and 94% (BIS pH 7).

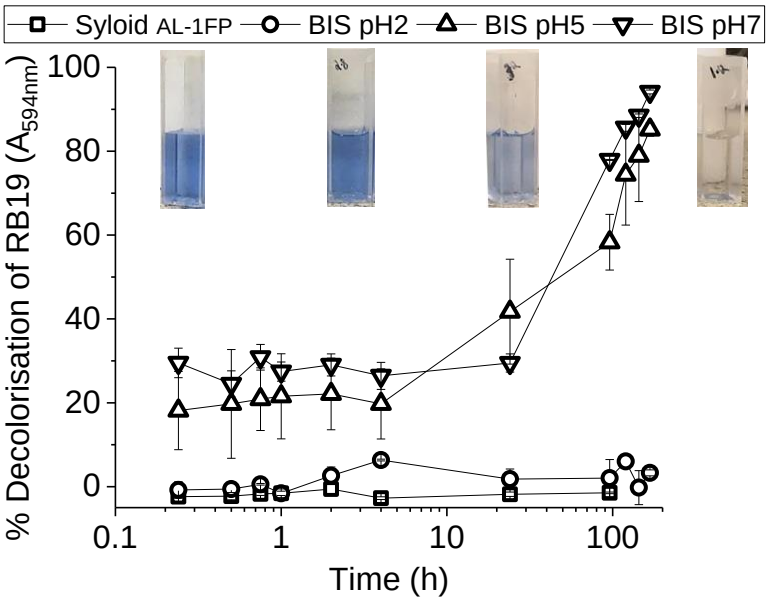

Figure 8-21: Effect of sorbent on RB19 decolorisation over time (7 day study).The insets show the photos of samples at the beginning (t≈0) and end of adsorption for various samples. Values are based on triplicates, with the error bar representing one standard deviation.

Given the complexity of the adsorption, which as we saw for BIS-HRP samples includes effects from porosity, surface chemistry, chemisorption and diffusion, using established models to describe the adsorption kinetics can provide valuable mechanistic information. With this view,

the adsorption data obtained for the best performing BIS pH 7 and BIS pH 5 were fitted using non-linear regression analysis against a pseudo-first order model [475] (Equation 8-1), a second-order model [476] (Equation 8-2), and an intraparticle diffusion model (Equation 8-3). These models are commonly used to describe an adsorption process between dye molecules and sorbents [477, 478], with the first one described mainly physisorption, the second one includes chemisorption and the third one accounts for diffusional limitations during adsorption.

$$q_t = q_e - q_{e,calc} \times e^{-k_1 t}$$

Equation 8-1

where k_1 (days^{-1}) is the pseudo-first-order rate constant, q_e and q_t (mg/g) are the adsorption capacities at equilibrium and time t, and $q_{e,calc}$ (mg/g) is the modelled equilibrium capacity respectively.

$$\frac{t}{q_t} = \frac{1}{k_2 q_{e,calc}^2} + \frac{1}{q_{e,calc}} t$$

Equation 8-2

where k_2 (g/mg/day) is the second order rate constant and the $k_2 \times q^2_{e,calc}$ (mg/g/day) is the initial rate of adsorption.

$$q_t = k_i t^{0.5} + C_i$$

Equation 8-3

where k_i is the intraparticle diffusion rate (mg/g/day$^{0.5}$) and C_i is the boundary layer constant.

Results (Table 8-6) show that the pseudo-first order model does not fit the data as good as the second order model, due to the high value of χ^2, despite the also high R^2 value. The intra-particle diffusion model is showing the best fit. The unsuitability of the pseudo-first model is expected because this model is most suitable for systems with physisorption on flat or smooth surfaces, while in this case, BIS are porous materials with potential for chemisorption derived from amine functionalisation. The good fit of the data with the second order model provides evidence for chemisorption as the main adsorption mechanism. The chemisorption is via electrostatic interactions between the anionic sulfonate groups from the dye molecules and protonated amines from the additive molecules present on the silica surface. The not high R^2 (0.8255) in the case of BIS pH 5 indicates that the model does not provide a great fit for all the data points, fact attributed to the not consistent functionalisation presence on the material. As demonstrated by Manning [64] and also discussed in Chapter 5, partial elution of the additive at pH 5 leaves a porous external surface, with additive being present mainly on the inside area of the material. This leads to physisorption on the external surface of BIS pH 5 sample, followed by chemisorption on the internal pores, while for BIS pH 7, chemisorption is dominating as all available surfaces are amine

functionalised. These observations clearly suggest that, in addition to chemisorption, the diffusion of the dye molecules into the pores of silica particles is a rate determining step [479-482].

Table 8-6: Kinetic parameters for sorption of RB19 onto BIS pH 7 and BIS pH 5.

	Sorbent	**BIS pH 5**	**BIS pH 7**
Model	**Parameter**		
Pseudo-first order	**k_1 (day^{-1})**	0.359	0.393
	$q_{e(calc)}$ ($mg\ g^{-1}$)	5.191	5.524
	R^2	0.948	0.966
	χ^2	0.276	0.424
Second order	**k_2 ($g\ mg^{-1}$)**	0.25	1.69
	$q_{e(calc)}$ ($mg\ g^{-1}$)	5.67	6.16
	$k_2 \times q^2_{e,calc}$ ($mg\ g^{-1}\ day^{-1}$)	7.99	64.3
	R^2	0.826	0.991
	χ^2	0.016	0.001
Webber-Morris (intraparticle diffusion)	**k_i ($mg\ g^{-1}\ d^{-0.5}$)**	1.96	1.96
	C_i ($mg\ g^{-1}$)	1.16	1.91
	R^2	0.996	0.991

It is interesting to note that the diffusion rate constant for both samples is identical, which suggests that the pores in both samples have similar physical and chemical properties (e.g. sizes, structure and surface chemistry). This corroborates earlier findings [330] and the fact that both samples had the same origin, with BIS pH 5 undergoing an additional acid wash at pH 5 in order to remove only the external amines and retain the internal amines.

8.5.2. Adsorption isotherms

The best performing samples as identified in the previous section (namely BIS pH 5 and BIS pH 7) were used for exploration of the sorbents capacity upon exposure to increasing dye concentrations (adsorption isotherm). Dye concentrations examined were up to 1500mg/mL, with the study period being 7 days. Results (Figure 8-22) show that BIS pH 5 and BIS pH 7 exhibited high dye removal capacities at lower initial dye concentration (92 and 97% for BIS pH 5 and BIS pH 7 respectively). These decreased with increasing initial dye concentration, reaching to 44 and 75% respectively for BIS pH 5 and BIS pH 7, for initial dye concentration of 1500mg/L. A drop in capacity is expected with the increasing sorbate concentration due to a reduction in available adsorption sites, however, it is worth noting that the dye removal by BIS pH 7 dropped only to 75%, at a relatively high initial dye concentration compared to literature [483] thereby showing excellent potential.

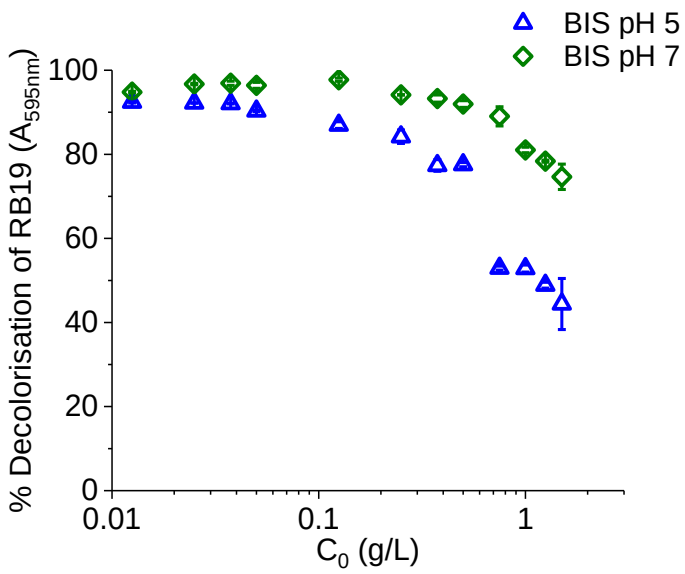

Figure 8-22: Effect of initial RB19 concentration on the dye removal by silica samples. Values are based on triplicates, with the error bar representing one standard deviation.

Data obtained from adsorption isotherms was fitted using the Langmuir and Freundlich models (Equation 8-4, Equation 8-5) to explain the mechanisms undertaken within the sorption of RB19 onto these sorbents.

$$q_e = \frac{q_m b C_e}{1 + b C_e}$$

Equation 8-4

$$q_e = K_F C_e^{\frac{1}{n}}$$

Equation 8-5

where q_e and q_m are the equilibrium capacity (mg/g) and the maximum adsorption capacity (mg/g) of the sorbent respectively, C_e is the equilibrium dye concentration (mg/L), b is a Langmuir equilibrium constant, and K_F and 1/n are the Freundlich constants.

The Langmuir isotherm model is used to describe monolayer surface coverage at specific homogenous sites within an adsorbent and that adsorption can no longer take place at a site once occupied by a dye molecule [484]. The Freundlich isotherm model unlike the Langmuir model assumes multilayer adsorption on a heterogeneous surface and that adsorption can still occur at an occupied site [485]. The 1/n factor is used to indicate the affinity and hence favourability of the sorbent (examined silicas) towards the sorbate (dye): $0 < 1/n < 1$ indicates strong interactions between RB19 and their respective sorbent and hence favourability [480]. Fitting the experimental adsorption isotherms for RB19 uptake onto BIS pH 5 and BIS pH 7 samples showed that while the data in both cases was well represented by the Freundlich model, only BIS pH 7 followed the Langmuir model (Table 8-7). In the case of PS7, the observed higher adsorption affinity (see KF

values in Table 8-7), a good fit with Langmuir model and a higher maximum capacity (q_m) when compared to BIS pH 5 sample strongly support the presence of chemisorption through electrostatic interactions identified from the 2nd order kinetics model.

Table 8-7: Determined parameters of RB19 adsorption on BIS, using the Langmuir and Freundlich adsorption models.

Sorbent	Langmuir			Freundlich		
	q_m (mg/g)	B (L/mg)	R^2	1/n	KF($mg^{1-1/n}$ $L^{1/n}$ /g)	R^2
BIS pH 5	103*	0.009*	0.895*	0.65	1.74	0.966
BIS pH 7	334	0.0052	0.995	0.67	4.56	0.997

* Due to a poor fit of PS5 with Langmuir model, these values are show for completeness and they should not be used to draw quantitative inferences.

The adsorption capacity of PS7 reported in this study (334 mg/g) is significantly higher than the highest capacity reported previously for any sorbent (221 mg/g) [55], and it is an order of magnitude higher than most competing sorbent materials. Additionally, excellent removal efficiencies were observed for BIS pH 7 for dye concentrations as high as 1500 mg/L, which surpass those reported in the literature [486-488]. These results highlight that bioinspired silica can be extensively used to remove high concentrations of RB19 that are likely to pose greater environmental and health concerns. It is important to mention at this point that these results were based on BIS produced with PEHA as an additive. Having seen the much faster and better adsorbing performance of BIS when synthesised with PAH as additive, it is safe to assume that we can expect much better results upon further investigation.

8.6. Conclusions

In this Chapter we explored the ability of BIS as immobilisation support for HRP to protect the enzyme, enhance its stability and facilitate reusability, based on the performance of the BIS-HRP composite using 2 substrates. Comparing the performance of HRP and BIS-HRP samples for stability in operational pH and exposure to temperature, it was found that comparison of actual performance does not show any advantage of immobilisation. However, relative performance (for each sample under the examined set of conditions), shows that immobilisation can offer protection of HRP in non-optimal conditions, and maintain the activity of the enzyme for prolonged periods of storage. With respect to immobilisation, we showed that BIS-HRP is highly reusable, fact attributed not only to the protection of the enzyme and facilitation of its removal, but also to the adsorbing abilities of BIS. We found that BIS-HRP could be reused for 20 times with 20% or more than 60% performance retention, depending on the additive used for BIS synthesis (PEHA and PAH respectively), overpowering Syloid Al-1FP-HRP which could be reused only up to 5 times. Upon extended reuse, we were able to identify the different tentacles of this system leading to observations during the assays, them being enzymatic performance which is obscured by diffusional limitations and adsorption of substrate and/or product on BIS, blocking of the pores and eventually deactivation of the catalyst.

In the last section we explored the potential of BIS as an adsorbent, given the identified adsorbing abilities during the BIS-HRP composite action. Analysis was done using BIS synthesised with PEHA, with the additive present in full (pH 7), partially (pH 5), or absent (pH 2), comparing the findings to Syloid AL-1FP as a commercial benchmark. Results showed that BIS-PEHA pH 7 performs best as a dye adsorbent, due to the presence of functionalisation which allows for chemisorption on top of physisorption into the existing porosity. We were able to describe the adsorption kinetics and mechanism and estimate the capacity of the sorbent, which was found on the higher end of the spectrum of values shown in literature. Although the aim of this work was to design and optimise efficient biocatalysts, we nevertheless managed to identify materials with great adsorbing potential, which can be enhanced by the added value of enzymatic action.

Chapter 9 : General remarks and Future work

9.1. Motivation

This work was motivated by the need to preserve the already limited freshwater reservoirs, as industrial processes are polluting them to an extent of not only rendering them unsuited for recycle and reuse, but also dangerous for aquatic and human life and aesthetically unpleasant. The focus of this work was treatment of polluted water effluents from the textile industry in order to remove dyes. Specifically, the dyes we focused on were of anthraquinone structure, as they are more resistant to degradation and less thoroughly researched compared to azo dyes. Upon exploration of the currently available and emerging water treatment methods, biocatalysis – use of enzymes – is showing very good potential towards complete breakdown of organic pollutants. However, enzymes are sensitive to operational conditions and cannot be easily reused, if at all, making them not an ideal solution to tackle the given problem. In order to assist their reusability and potentially preserve their activity under non-optimal conditions, immobilisation is an interesting approach, where the enzyme is being attached on or encapsulated in a solid support. Although enzyme immobilisation is a quite well-studied area, the results are highly dependent on the enzyme, the targeted enzymatic action and substrate and the immobilisation support used, indicating that the guidelines established so far might not offer a straightforward understanding. Furthermore, in an effort to optimise the support and the immobilisation method to offer higher enzymatic activity, factors relevant to industrial implementation of biocatalysts, such as cost and manufacturing time involved, are commonly overlooked. In this project, we systematically investigated how the performance of horseradish peroxidase (HRP) is affected upon immobilisation using bioinspired silica (BIS) as support, via the oxidation of 2 different substrates, in an effort to understand how to create effective biocatalysts for water treatment, using more environmentally friendly materials and methods.

9.2. Main findings and how they improved our understanding

On the methods used for protein determination

There are quite a few methods used for enzyme quantification, based on protein determination, through quantification of aminoacids via colorimetric assays or their UV absorbance, or more rarely, based on their activity. The quantification of HRP with respect to the immobilisation system was examined in this project using UV absorbance, Bradford assay and activity measurement using RB19 or ABTS as substrates. Based on thorough experimentation, it was found that the widely used methods for protein quantification based on UV absorbance (at the range of 200-280nm, as well as the peroxidase-specific absorbance in the Soret range ~400nm) were not appropriate, due to interference caused by other reagents in the system. Protein quantification using the Bradford assay was also problematic, as the amine additives used for BIS formation were causing interference by reacting with the Bradford reagent. Given the strong pH

dependence of BIS synthesis, any subtle changes (beyond those accurately detectable) caused occasionally considerable differences and led to our inability to be able to fully control this source of interference. Last but not least, we tried to standardise enzymatic activity observations, in order to be able to use activity measurement as an accurate method for enzyme quantification. We did so by exposing the enzyme in conditions that would possibly occur during in-situ encapsulation. These conditions were identified by the point of HRP addition during BIS synthesis, specifically exposure to amine solution (PAH or PEHA), silicate solution and freshly produced supernatants of BIS synthesis. Results showed that this method could actually be trustworthy, if activity measurements were taken within a specific time limit, given the effect some of the reagents had on HRP. Under fully controlled conditions, we were able to validate results between HRP quantification using Bradford assay and quantification using enzymatic activity assays. Although there have been research examples questioning the suitability of Bradford assay for certain systems of immobilisation and proposing ways to bypass difficulties, to the best of our knowledge, a thorough comparison and validation of enzyme quantification using both the protein nature and the activity of the enzyme has not been shown.

It should be mentioned that the detected interferences with HRP quantification were further investigated using detailed design of controlled experiments, based on individual or mixed reagents occurring during the immobilisation protocol. The identification of these interferences, show that a) not every method is applicable to every system, regardless of how well studied the method or the system is, and b) there is a need for appropriate control samples, in order to make sure that the methods chosen are working towards the selected goal. If interference was not identified, then obtained results would have led to ostensibly correct but in principle false conclusions. Unfortunately, if a method is known to be working for a system, its suitability for similar systems or even upon altering a parameter on the original system is not often questioned. This culture of not questioning pre-established decisions and protocols might be detrimental for the quality of data collected and the conclusions or further experiments correction or avoidance of potential errors. The importance of the analysis done on protein quantification is based on the need to know how much enzyme is immobilised and connect this quantity with the observed activity of the biocatalyst and the expected activity of the biocatalyst.

At this point we need to mention the difference in observed performance of HRP using ABTS or RB19 as substrate. The sensitivity of the enzyme to ABTS was much higher compared to RB19, leading to more noticeable results upon minor change of conditions. This could be due to the different structure of the substrate and the different radicals – and their subsequent reaction products – created. It would be wrong to assume that the performance of an enzyme will be equal or even comparable when examining its activity on different substrates. Adding the contribution of BIS as an adsorbent to the equation when assaying immobilised HRP, it would be wrong to imply that the performance of BIS-HRP using ABTS will be the same with the performance of

BIS-HRP using RB19. This identifies another gap in the literature, where, again, in the absence of correct control samples or in-depth characterisation of the examined system, results shown are not representative of the real performance of the system examined. In many literature cases, it was noticed that controls were missing or were insufficient to rule out any potential contribution to the observed "enzymatic" activity of an immobilised biocatalyst. It is of paramount importance to identify factors that might affect the performance of the examined system and try to understand the extent of their contribution, in order to be able to tune the system towards a specific route.

On the immobilisation of peroxidase

The focus of this work was mainly the exploration of in-situ encapsulation of HRP in BIS, as a biocatalyst using a fast method and a sustainable and tailorable support, in contrast to the laborious and environmentally unfriendly protocols reported in the literature. As a brief reminder, BIS is formed within seconds, by the acidification of sodium silicate, in the presence of a bioinspired additive (amine). Upon BIS formation, additive presence can be reduced or completely eliminated with further acidification of the material. We initially examined the effect of specific factors on the amount of HRP immobilised in BIS. Those factors were relevant to the synthesis and structure of BIS (additive used, partial or complete additive removal) and of in-situ incorporation of HRP (point of addition during BIS synthesis, amount of HRP added). In order to have a point of reference, adsorption of HRP on BIS was also examined, using the same factors where applicable (type of additive used, partial or complete additive removal, amount of HRP added), as well as on a commercial silica (Syloid AL-1FP).

It was found that in-situ encapsulation of HRP in BIS offers almost double retention of HRP in the support (~20% w/w) compared to adsorption of HRP on BIS (max 10% w/w) or commercial silica (max 5% w/w), when similar immobilisation conditions are examined. This effect is mainly attributed to BIS synthesis and/or nanoparticle formation around the enzyme during in-situ encapsulation, leading to HRP localisation mostly inside BIS, as opposed to the adsorption of HRP on available adsorption sites and localisation mainly on the outside. Analysis of the structure of silica revealed an almost non-porous structure, with low available surface areas when a small additive (PEHA) was used and slightly increased porosity and available surface areas when a larger polymeric additive (PAH) was used. Differences in structure and functionalisation between BIS synthesised using different additives, or upon elution of additives were relevant to the amount of HRP retained, especially during adsorption of the enzyme. During in-situ encapsulation of HRP in BIS, obtained results based on immobilisation efficiency, percentage of HRP in BIS and porosity analysis indicated a yet undefined effect of the presence of protein during BIS synthesis, attributed to tangled interactions between charged molecules. These findings indicate that **Hypothesis 1** and **Hypothesis 2** (section 2.5 of Chapter 2) **are confirmed**.

On the performance of peroxidase

BIS offers a promising option as immobilisation support, based on the amount of enzyme retained and the immobilisation method, compared to other supports and methods examined in literature. That being said, a high enzyme load on a solid support is not scientifically or industrially appreciated if the enzyme does not show the expected activity.

The performance of HRP was assessed using 2 different substrates. The first was a typical peroxidase substrate, 2,2′-azino-bis(3-ethylthiazoline-6-sulfonate acid (ABTS), measuring colour appearance. The second one was a model anthraquinone dye, Reactive Blue 19 (RB19), measuring colour disappearance. HRP activity was examined in free and immobilised form, and results were compared, in order to examine the efficiency of immobilisation. Findings from the comparison of the enzymatic action of HRP in free and immobilised form indicate that the observed activity of immobilised HRP is substantially lower compared to the one of free HRP. Based on a systematic experimentation on the effect of immobilisation procedure followed (process and reagents) on the activity of HRP, we can argue that the much lower activity is ostensible and attributed to 2 factors. The first arises from the structure of the biocatalyst, which posed severe diffusional limitations. The second one arises from the functionalisation present in the biocatalyst, which hindered our ability to actively measure the product. These assumptions are corroborated from the much higher activity observed for adsorbed HRP compared to encapsulated HRP (almost 10 fold difference) due to the easier accessibility of enzyme from the substrate and of product to bulk volume. Furthermore, the quite higher activity shown from HRP adsorbed on supports with absence of porosity or functionalisation (Syloid AL-1FP and BIS synthesised with PEHA, with the additive fully eluted) also point to the aforementioned direction.

Trends within each enzymatic system (free, encapsulated, adsorbed) obtained by converting the observed results to relative values based on the maximum observed per sample, showed a different pattern. Immobilisation (both methods) was able to offer protection of HRP under lower pH and higher temperature conditions, and led to higher relative activities upon exposure to high concentrations of substrates. Furthermore, various immobilised HRP preparations using BIS as support showed a practically stably high performance over an examination period of 50 days and were able to be reused for more than 20 cycles. In specific cases, such as examination of operational stability at various pH values using the RB19 assay, the performance of BIS-HRP surpassed that of free HRP, indicating the selective superiority of immobilisation, attributed to the presence of BIS support. These findings indicate that **Hypothesis 3 and Hypothesis 4** (section 2.5 of Chapter 2) **are conditionally confirmed or rejected**, depending on the specific conditions under examination.

As mentioned at the end of Chapter 6, we were able to synthesise an active biocatalyst using BIS to immobilise HRP. However, upon initial experimentation, the contribution of the support as a

potentially powerful adsorbent was noticed in both assays, so exploration of the adsorbing abilities of BIS became a partial part of the scope of this project. Examining in depth the adsorbing performance of BIS synthesised with PEHA, with the additive present in full, partially, or removed and comparing it to a commercial silica (Syloid AL-1FP), we were able to describe and quantify the adsorbing potential of BIS. Results on RB19 removal showed that both physisorption (due to porosity) and chemisorption (due to amine presence) were responsible for dye adsorption, and that diffusional limitations were also present. Overall the capacity of the best performing adsorbent (BIS-PEHA with amine fully present) was calculated higher than other values in literature, showing the superiority of BIS also as adsorbent, besides immobilisation support.

Connecting the activity results with the HRP retention results upon immobilisation and building on the knowledge acquired so far for this system, we can say that high functionalisation offers higher enzyme retention, but also leads to enhanced performance of BIS as an adsorbent of substrates (and/or products), hence hindering the enzymatic action. Answering whether BIS-HRP is an effective biocatalyst with performance comparable to the free enzyme, the answer is yes, but it highly depends on the substrate. Similarly, answering whether BIS-HRP can be effectively used for dye decolorisation compared to free HRP, the answer is yes, but the performance is highly affected by the support as well. In order to reduce the effect of the "but" in the previous answers, further work is needed, in order to expand our understanding on the complexities identified in the BIS-HRP systems examined here.

9.3. Avenues for further exploration

During this research project we discussed some limitations arising by the systems examined, the available methods and their combination. We also examined a systematic approach towards the exploration of BIS as support for enzyme immobilisation, and we were able to identify the potential of BIS as an adsorbent. Although there are many factors examined in this thesis, there are also many ideas generated for future exploration, in order to better understand the systems described herein and take a step further with the exploration of BIS's wider applicability. Furthermore, this project allowed us to improve our understanding culprits that can prevent a researcher form conducting rigorous research.

Improvement in understanding of BIS formation in presence of charged molecules and characterisation of materials

Based on the protein determination difficulties and the unspecified contribution of HRP to BIS formation, as highlighted by differences in porosity and yield, it would be interesting to investigate further the effect of an additional charged molecule being present during BIS synthesis. Similar work has been done by our group before using relatively simpler surfactants and molecules, but an approach of exploring the effect of an added factor in a – theoretically – well characterised system has not been pursued. A potential starting point would be exploration

of the co-presence of more than one additives during BIS formation, followed by substitution of 1 additive for a small protein and subsequently a larger protein. Based on the porosity difference shown for the presence of low quantity of HRP during BIS formation, further elaboration on the quantity and/or molar ratio of reagents would be interesting. This would improve deeper understanding of fundamental changes during BIS formation, and allow optimisation of the material itself but also immobilisation of protein present.

The characterisation methods used herein are well established in materials science, but they were not enough to fully characterise this type of nanomaterials. The main issue is the unconventional structure of BIS, not fully fitting the assumptions of built-in models for characterisation (e.g. BJH or NL-DFT porosity models), with particles and pores quite small to be observed in SEM. A combination of gas adsorption, microscopy (including TEM) and small angle scattering techniques (USAXS, SAXS, SANS), performed in a substantial amount of samples, would help tremendously to improve our knowledge on the structure of the materials obtained and trace it back to the origin for difference. Individually each method can offer valuable information, but only through combination and corroboration we will be able to have an accurate picture, as in many cases there might be more than 1 plausible scenarios (e.g. while fitting USAXS data or deciding whether a formation is an aggregate in SEM/TEM). Additional to these characterisation measurements, elemental analysis and silicon speciation analysis could offer more information on the chemistry of the materials, helping us to compose a more complete picture. For all of the aforementioned techniques, especially for the ones incorporating chemical reactions, it is of paramount importance to use appropriate control samples, in order to identify any potential interference and be reassured that collected data represent the factor under examination each time.

By having a complete picture of materials structure, we will be in a much better position to explain the origin and extent of diffusional limitations and the internal pore network structure, leading us to identify or design potential applications more suited to these materials.

Further optimisation of enzyme immobilisation using BIS as support

Based on the comparison between adsorbed and encapsulated HRP using BIS as support, we can say that the adsorbed enzyme seems to offer a higher enzymatic performance, excluding the action of BIS as adsorbent. In the case of encapsulated HRP, adsorption of substrate and/or product on BIS seems to be the driving force, leading to subsequent enzymatic activity. In order to improve those systems with respect to enzymatic activity, a few ideas could be investigated. It was shown that the best performing systems of BIS-HRP when HRP was adsorbed, were those where BIS carried the least amount of additive present, as absence of amine functionalisation indicated less obstruction of the substrate to reach the enzyme. On the other hand, amine functionalisation assisted with the adsorption of HRP on BIS due to strong charge interactions. A way to maintain strong attachment of the enzyme, but reduce any other functionalisation, would be to introduce

specific "new" functionalisation post-additive removal, added at an appropriate ratio in order not to leave residual unoccupied functionality post immobilisation (overlooking the additional labour/cost/time required). Another approach would be to use a different functionalisation for the purpose of immobilisation, which would allow the enzyme to be attached further from the BIS surface (space-arm approach). Both methods would mean introduction of at least an additional step to the immobilisation protocol and furthermore added cost, depending on the type of chemicals used. Both approaches have been explored in literature, but not using BIS and peroxidase for the purpose of water treatment.

In order to improve the performance of encapsulated HRP in BIS, post synthetic approaches would probably not work, so changes should occur at an earlier stage. Herein we examined 2 fundamentally different additives, a small linear amine (PEHA) and a large polymeric and tangled amine (PAH). The creation of porosity in the case of BIS-PAH was beneficial for the interaction of encapsulated HRP with the bulk volume, but the embedded presence of PAH caused enzymatic activity to be delayed. Partial removal of the additive was beneficial, but it was not enough, and additive removal by eluting the composite with acid at a low pH was detrimental for HRP. A mid-ground approach could be further explored, examining the effect of additive elution at pH lower than 5, but not as low as 2. Based on previous work from our group, a "sweet spot" was found for BIS synthesised with PEHA upon acid elution in terms of structural differences [64], but such work is not done for PAH.

Further exploration of BIS as an adsorbent

Although the focus of this project was the exploration of immobilisation of HRP for application in dye removal, through experimentation and development of the biocatalysts, the contribution of BIS as adsorbent was realised and pursued further, examining the potential of BIS synthesised with PEHA as additive, as it was shown in section 8.5 of Chapter 8. However, it was shown that BIS synthesised with PAH showed much higher potential as an adsorbent, both towards RB19 but also towards reacted and unreacted ABTS. It would be interesting to explore the adsorbing potential of BIS synthesised with a variety of additives, and identify the contribution from the structure and from the embedded functionalisation. Furthermore, it would be interesting to see the adsorbing potential of BIS towards other pollutants. Some work has already been done in this area [489], but more exploration would be beneficial in order to identify the extend of the potential of BIS.

Ideas for future exploration based on knowledge from BIS-HRP performance

An interesting idea would be the exploration of immobilising a more selective peroxidase towards dyes, such a Dye decolorising Peroxidase (DyP). As briefly described in section 1.5, DyPs show high selectivity towards anthraquinone dyes. Using an in-house developed DyP, generously gifted from Dr. Wong and his PhD student, we were able to partially characterise the enzyme and

compare the findings to the relevant for HRP. It was shown that DyP exceeded by far the storage stability of HRP (Figure 9-1a), however it was also more sensitive towards excessive concentration of peroxide (Figure 9-1b). The difficulty to model DyP's performance in order to determine its kinetic parameters (Figure 9-2, Table 9-1) might be due to the early stage of enzyme's development and purification, or its performance based on a different reaction mechanism. Further experimentation using DyP4 was not conducted at this time, due to the limited quantity of DyP available. It would be interesting to see though how DyP would perform upon adsorption on BIS.

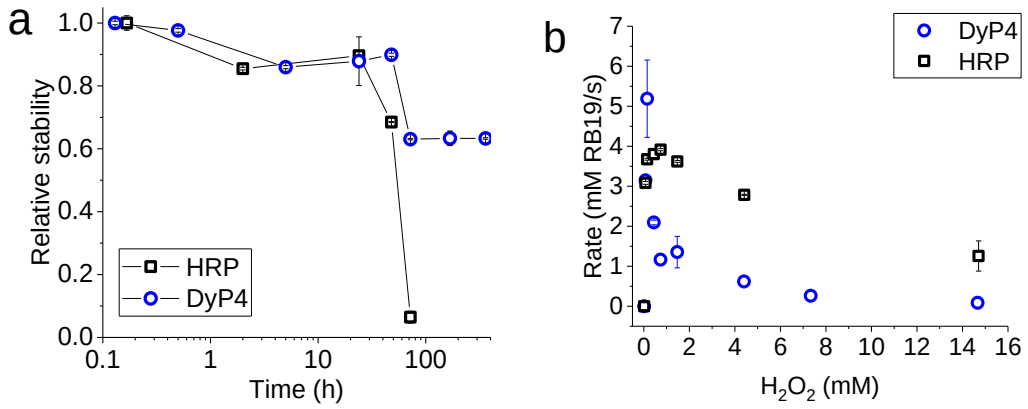

Figure 9-1: Early-stage comparison between HRP and DyP4 a) Comparison of storage stability of HRP and DyP4, examined using the RB19 standard assay. Enzyme solutions were stored in the fridge and aliquots were subtracted at specific time points, b) comparison of stability of HRP and DyP4 for H_2O_2 concentration varying from 0.0147 to 14.7mM, while keeping every other factor constant. Values are based on at least replicates, with the error bars representing 1 standard deviation.

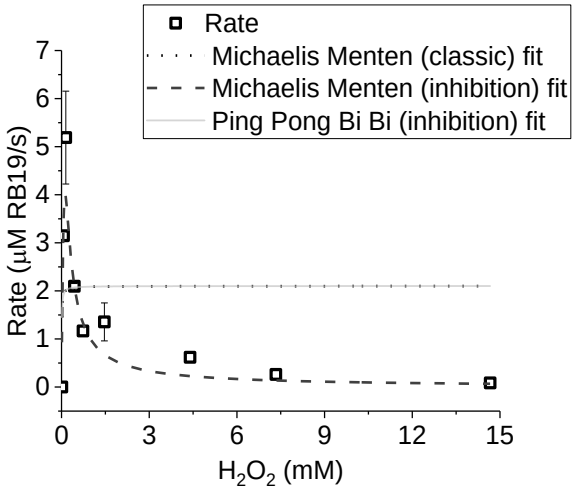

Figure 9-2: Fitting of calculated RB19 degradation rates using DyP4 for H_2O_2 concentration varying from 0.0147 to 14.7mM, while keeping every other factor constant. Results shown are the average of at least duplicates, with the error bar representing 1 standard deviation.

Assuming a further optimised system with controlled diffusional limitations, using BIS as immobilisation support, another idea would be co-immobilisation of glucose oxidase or another peroxide producing enzyme, in order to reduce the need for external addition of hydrogen peroxide. This idea is not new and such an approach could be industrially preferred, compared to the need of peroxide addition as a requirement for enzymatic activity. Controlling the activity of

glucose oxidase for optimal peroxide production for the encapsulated peroxidase, deactivation of peroxidase due to excess peroxide can be prevented. However, this approach comes with other problems, such as the need of ensuring activity of the oxidase and controlling cascade reactions.

Table 9-1: Determination of kinetic parameters for models shown in Figure 9-2. Values shown are in the format of average (error), as calculated from OriginPro® software.

	Model		
	Michaelis-Menten	**Michaelis-Menten (inhibition)**	**Ping Pong Bi Bi**
Equation	$y = {V_{max} \times x}/{(K_m + x)}$	$y = \frac{V_{max} \times x}{(K_m + x \times (1 + {x}/{K_i}))}$	$y = {10 \times V_{max} \times x}/{A}$ $A = \left((K_{mb} \times 10) + K_{ma} \times x \times \left(1 + \left({x}/{K_{ib}}\right)\right)\right) + (10 \times x))$
V_{max} (mM/s)	2.10 (0.18)	758.35 (97122)	2.10 (0.21)
K_m (mM)	0.006 (0.029)	11.75 (1530)	--
K_{ma} (mM)	--	--	6.85E-23 (0)
K_{mb} (mM)	--	--	0.006 (0.034)
K_i (mM)	--	0.0013 (0.1716)	0.80 (0)
R^2	-0.1071	0.7378	-0.5499

Advice on how to work with complex systems

Some systems are more difficult to work than others, although at a doctorate level of research there is not such a term as a "straightforward system". What arose from this work that is of immense importance, was the establishment of control samples and measurements before any key data collection. It is not very common to examine every factor of a system individually for their contribution to a specific phenomenon, as many times factors work synergistically. However, if the additives used for BIS formation were not analysed for their effect on the UV assay or their reaction with Bradford reagent, or if BIS without presence of HRP was not analysed using the assays used for the enzymatic activity, the extracted results would have been wrong, as those important sources of interference and added contribution would have been missed. In addition, when working with systems that show randomness regarding structure and patterns, repeating measurements in triplicate might not lead to a consistent value. Assuming that the error is not caused by the researcher or experimental apparatus, more replicates are advisable, in order to reach a conclusion, which might be that a consistent value cannot be achieved. A final piece of advice is that when a system consists of too many factors with potentially unidentified effects, a "given" solution or method by someone else should not be taken as granted, but it should be adequately tested for its suitability to the examined system.

References

1. DuPlessis, A., Freshwater Challenges of South Africa and its Upper Vaal River: Current State and Outlook. *Freshwater Challenges of South Africa and Its Upper Vaal River: Current State and Outlook* **2017**, 1.
2. UNW-DPAC, U.-W. D. P. o. A. a. C. In *Challenges and opportunities for water in the transition to a green economy*, UN-Water Conference 'Water in the Green Economy in Practice: Towards Rio+20', Zaragoza, Spain, 2011; Communication, U.-W. D. P. o. A. a., Ed. UNDESA (United Nations Department of Economic and Scoial Affairs), Water for Life, UN-WATER: Zaragoza, Spain, 2011.
3. Reid, R., Go green - A sound business decision .1. *J. Soc. Dye. Colour* **1996,** *112*, (4), 103.
4. Forgacs, E.; Cserhati, T.; Oros, G., Removal of synthetic dyes from wastewaters: a review. *Environment International* **2004,** *30*, (7), 953.
5. Hessel, C.; Allegre, C.; Maisseu, M.; Charbit, F.; Moulin, P., Guidelines and legislation for dye house effluents. *Journal of Environmental Management* **2007,** *83*, (2), 171.
6. Ghaly, A.; Ananthashankar, R.; Alhattab, M.; Ramakrishnan, V. V., Production, Characterization and Treatment of Textile Effluents: A Critical Review. *J Chem Eng Process Technol* **2014,** *5*, (1), 182.
7. Laing, I. G., The impact of regulations on the dyeing industry. *Rev. Prog. Coloration* **1991,** *21*, 56.
8. World Bank *The Bangladesh Responsible Sourcing Initiative, A new model for green growth?*; The World Bank, International Finance Corporation (IFC), Natural Resources Defense Council (NRDC): 2014.
9. Elango, G.; Rathika, G.; Elango, S., Physico-Chemical Parameters of Textile Dyeing Effluent and Its Impacts with Casestudy. *Int. J. Res. Chem. Environ* **2017,** *7*, (1), 17.
10. Rajaram, T.; Das, A., Water pollution by industrial effluents in India: Discharge scenarios and case for participatory ecosystem specific local regulation. *Futures* **2008,** *40*, (1), 56.
11. European Communities *Directive 98/83/EC on water intended for human consumption*; http://eur-lex.europa.eu/legal-content/EN/TXT/?uri=CELEX:31998L0083, 1998.
12. European Communities *Directive 75/440/EEC on surface water*; https://www.eea.europa.eu/policy-documents/council-directive-75-440-eec, 1975.
13. EPA *Waste from the Production Of Dyes and Pigments Listed as Hazardous*; United States Environmental Protection Agency: https://www.epa.gov/hw/documents-related-hazardous-waste-listing-dyes-and-pigments, 2005.
14. GmBh, H. L. *Objective colour assessment and quality control in the chemical pharmaceutical and cosmetic industry*; Hach Lange GmBh: 2016.
15. Hazardous Waste Consultant *Hazardous Waste Listing for Dye and Pigment Production Wastes Finalized* 2005.
16. EPA Water Quality Standards: Regulations and Resources (https://www.epa.gov/wqs-tech). (02/02/17),
17. Ali, H., Biodegradation of Synthetic Dyes-A Review. *Water Air and Soil Pollution* **2010,** *213*, (1-4), 251.
18. Sekuljica, N. Z.; Prlainovic, N. Z.; Jovanovic, J. R.; Stefanovic, A. B.; Djokic, V. R.; Mijin, D. Z.; Knezevic-Jugovic, Z. D., Immobilization of horseradish peroxidase onto kaolin. *Bioprocess and Biosystems Engineering* **2016,** *39*, (3), 461.
19. Vandevivere, P. C.; Bianchi, R.; Verstraete, W., Treatment and reuse of wastewater from the textile wet-processing industry: Review of emerging technologies. *Journal of Chemical Technology and Biotechnology* **1998,** *72*, (4), 289.
20. Celebi, M.; Altikatoglu, M.; Akdeste, Z. M.; Yildirim, H., Determination of decolorization properties of Reactive Blue 19 dye using Horseradish Peroxidase enzyme. *Turkish Journal of Biochemistry-Turk Biyokimya Dergisi* **2013,** *38*, (2), 200.
21. Pereira, L.; Alves, M., Dyes—Environmental Impact and Remediation. In *Environmental Protection Strategies for Sustainable Development*, Malik Abdul ; Elisabeth, G., Eds. Springer Netherlands: **2012;** pp 111.

22. Kant, R., Textile dyeing industry an environmental hazard. *Natural Science* **2012,** *4*, (1), 22.
23. O'Neill, C.; Hawkes, F. R.; Hawkes, D. L.; Lourenco, N. D.; Pinheiro, H. M.; Delee, W., Colour in textile effluents - sources, measurement, discharge consents and simulation: a review. *Journal of Chemical Technology and Biotechnology* **1999,** *74*, (11), 1009.
24. Saratale, R. G.; Saratale, G. D.; Chang, J. S.; Govindwar, S. P., Bacterial decolorization and degradation of azo dyes: A review. *Journal of the Taiwan Institute of Chemical Engineers* **2011,** *42*, (1), 138.
25. Willmott, N.; Guthrie, J.; Nelson, G., The biotechnology approach to colour removal from textile effluent. *J. Soc. Dye. Colour* **1998,** *114*, (2), 38.
26. Kaushik, P.; Malik, A., Fungal dye decolourization: Recent advances and future potential. *Environment International* **2009,** *35*, (1), 127.
27. Easton, J. R., The dye maker's view. In *Colour in Dyehouse Effluent*, P., C., Ed. Society of Dyers and Colourists, The Alden Press: Oxford, **1995;** pp 9.
28. Singh, R. L.; Singh, P. K.; Singh, R. P., Enzymatic decolorization and degradation of azo dyes - A review. *International Biodeterioration & Biodegradation* **2015,** *104*, 21.
29. IARC IARC Monographs - Anthraquinone. (01/02/17 http://monographs.iarc.fr/ENG/Monographs/vol101/mono101-001.pdf),
30. Gwinn, J. E.; Bomberger, D. C. *Wastes from manufacture of dyes and pigments: Volume 4. Anthraquinone dyes and pigments*; Industrial Environmental Research Laboratory; Office of Research and Development: Cincinnati, Ohio, 45268, 1984.
31. Gregory, P., Important Chemical Chromophores of Dye Classes. In *Industrial Dyes: Chemistry, Properties, Applications* Hunger, K., Ed. Wiley-VCH: Federal Republic of Germany, **2003;** pp 35.
32. Aubert, S.; Schwitzguebel, J. P., Screening of plant species for the phytotreatment of wastewater containing sulphonated anthraquinones. *Water Research* **2004,** *38*, (16), 3569.
33. Lizama, C.; Freer, J.; Baeza, J.; Mansilla, H. D., Optimized photodegradation of Reactive Blue 19 on TiO2 and ZnO suspensions. *Catalysis Today* **2002,** *76*, (2-4), 235.
34. dos Santos, A. B.; Bisschops, I. A. E.; Cervantes, F. J.; van Lier, J. B., The transformation and toxicity of anthraquinone dyes during thermophilic (55 degrees C) and mesophilic (30 degrees C) anaerobic treatments. *Journal of Biotechnology* **2005,** *115*, (4), 345.
35. Julkapli, N.; Bagheri, S.; Abd Hamid, S. B., Recent Advances in Heterogeneous Photocatalytic Decolorization of Synthetic Dyes. *Scientific World Journal* **2014**, 25.
36. Novotny, C.; Dias, N.; Kapanen, A.; Malachova, K.; Vandrovcova, M.; Itavaara, M.; Lima, N., Comparative use of bacterial, algal and protozoan tests to study toxicity of azo- and anthraquinone dyes. *Chemosphere* **2006,** *63*, (9), 1436.
37. Malachova, K.; Pavlickova, Z.; Novotny, C.; Svobodova, K.; Lednicka, D.; Musilkova, E., Reduction in the mutagenicity of synthetic dyes by successive treatment with activated sludge and the ligninolytic fungus, Irpex lacteus. *Environmental and Molecular Mutagenesis* **2006,** *47*, (7), 533.
38. Harrington-Brock, K.; Parker, L.; Doerr, C.; Cimino, M. C.; Moore, M. M., Analysis of the genotoxicity of anthraquinone dyes in the mouse lymphoma assay *Mutagenesis* **1991,** *6*, (1), 35.
39. Leme, D. M.; de Oliveira, G. A. R.; Meireles, G.; Brito, L. B.; Rodrigues, L. D.; de Oliveira, D. P., Eco- and Genotoxicological Assessments of Two Reactive Textile Dyes. *Journal of Toxicology and Environmental Health-Part a-Current Issues* **2015,** *78*, (5), 287.
40. He, Z. Q.; Lin, L. L.; Song, S.; Xia, M.; Xu, L. J.; Ying, H. P.; Chen, J. M., Mineralization of CI Reactive Blue 19 by ozonation combined with sonolysis: Performance optimization and degradation mechanism. *Separation and Purification Technology* **2008,** *62*, (2), 376.
41. Fanchiang, J. M.; Tseng, D. H., Degradation of anthraquinone dye CI Reactive Blue 19 in aqueous solution by ozonation. *Chemosphere* **2009,** *77*, (2), 214.
42. Osma, J. F.; Toca-Herrera, J. L.; Rodriguez-Couto, S., Transformation pathway of Remazol Brilliant Blue R by immobilised laccase. *Bioresource Technology* **2010,** *101*, (22), 8509.

43. Siddique, M.; Farooq, R.; Khan, Z. M.; Khan, Z.; Shaukat, S. F., Enhanced decomposition of reactive blue 19 dye in ultrasound assisted electrochemical reactor. *Ultrasonics Sonochemistry* **2011,** *18*, (1), 190.
44. Andleeb, S.; Atiq, N.; Robson, G. D.; Ahmed, S., An investigation of anthraquinone dye biodegradation by immobilized Aspergillus flavus in fluidized bed bioreactor. *Environmental Science and Pollution Research* **2012,** *19*, (5), 1728.
45. Hao, O. J.; Kim, H.; Chiang, P.-C., Decolorization of Wastewater. *Critical Reviews in Environmental Science and Technology* **2000,** *30*, (4), 449.
46. Lovato, M. E.; Fiasconaro, M. L.; Martin, C. A., Degradation and toxicity depletion of RB19 anthraquinone dye in water by ozone-based technologies. *Water Science and Technology* **2017,** *75*, (4), 813.
47. Peralta-Zamora, P.; Kunz, A.; de Moraes, S. G.; Pelegrini, R.; Moleiro, P. D.; Reyes, J.; Duran, N., Degradation of reactive dyes - I. A comparative study of ozonation, enzymatic and photochemical processes. *Chemosphere* **1999,** *38*, (4), 835.
48. Robinson, T.; McMullan, G.; Marchant, R.; Nigam, P., Remediation of dyes in textile effluent: a critical review on current treatment technologies with a proposed alternative. *Bioresource Technology* **2001,** *77*, (3), 247.
49. Bhatnagar, A.; Minocha, A. K., Conventional and non-conventional adsorbents for removal of pollutants from water - A review. *Indian J. Chem. Technol.* **2006,** *13*, (3), 203.
50. Asgher, M., Biosorption of Reactive Dyes: A Review. *Water Air and Soil Pollution* **2012,** *223*, (5), 2417.
51. Aljeboree, A. M.; Alshirifi, A. N.; Alkaim, A. F., Kinetics and equilibrium study for the adsorption of textile dyes on coconut shell activated carbon. *Arab. J. Chem.* **2017,** *10*, S3381.
52. Qu, J. H., Research progress of novel adsorption processes in water purification: A review. *J. Environ. Sci.* **2008,** *20*, (1), 1.
53. Salleh, M. A. M.; Mahmoud, D. K.; Karim, W.; Idris, A., Cationic and anionic dye adsorption by agricultural solid wastes: A comprehensive review. *Desalination* **2011,** *280*, (1-3), 1.
54. Parimalam, R.; Raj, V.; Sivakumar, P., Removal of Acid Green 25 from Aqueous Solution by Adsorption. *E-J. Chem.* **2012,** *9*, (4), 1683.
55. El-Bindary, A. A.; Abd El-Kawi, M. A.; Hafez, A. M.; Rashed, I. G. A.; Aboelnaga, E. E., Removal of reactive blue 19 from aqueous solution using rice straw fly ash. *J. Mater. Environ. Sci* **2016,** *7*, (3), 1023.
56. Chu, S. Y.; Xiao, J. B.; Tian, G. M.; Wong, M. H., Preparation and characterization of activated carbon from aquatic macrophyte debris and its ability to adsorb anthraquinone dyes. *Journal of Industrial and Engineering Chemistry* **2014,** *20*, (5), 3461.
57. Wang, S. B.; Li, H.; Xu, L. Y., Application of zeolite MCM-22 for basic dye removal from wastewater. *J. Colloid Interface Sci.* **2006,** *295*, (1), 71.
58. Gibson, L. T., Mesosilica materials and organic pollutant adsorption: part B removal from aqueous solution. *Chemical Society Reviews* **2014,** *43*, (15), 5173.
59. Diagboya, P. N. E.; Dikio, E. D., Silica-based mesoporous materials; emerging designer adsorbents for aqueous pollutants removal and water treatment. *Microporous and Mesoporous Materials* **2018,** *266*, 252.
60. Babu, B. K.; Purayil, J. V.; Padinhattatyil, H.; Shukla, S.; Warrier, K. G., Silica-Based NTPC-Fly Ash for Dye-Removal Application and Effect of Its Modification. *International Journal of Applied Ceramic Technology* **2013,** *10*, (1), 186.
61. Banaei, A.; Ebrahimi, S.; Vojoudi, H.; Karimi, S.; Badiei, A.; Pourbasheer, E., Adsorption equilibrium and thermodynamics of anionic reactive dyes from aqueous solutions by using a new modified silica gel with 2,2 '-(pentane-1,5-diylbis(oxy))dibenzaldehyde. *Chemical Engineering Research & Design* **2017,** *123*, 50.
62. Krysztafkiewicz, A.; Binkowski, S.; Jesionowski, T., Adsorption of dyes on a silica surface. *Applied Surface Science* **2002,** *199*, (1–4), 31.
63. Mahmoodi, N. M.; Khorramfar, S.; Najafi, F., Amine-functionalized silica nanoparticle: Preparation, characterization and anionic dye removal ability. *Desalination* **2011,** *279*, (1), 61.
64. Manning, J. R. H.; Yip, T. W. S.; Centi, A.; Jorge, M.; Patwardhan, S. V., An Eco-Friendly, Tunable and Scalable Method for Producing Porous Functional Nanomaterials Designed Using Molecular Interactions. *ChemSusChem* **2017,** *10*, (8), 1683.

65. Khandegar, V.; Saroha, A. K., Electrocoagulation for the treatment of textile industry effluent - A review. *Journal of Environmental Management* **2013,** *128*, 949.
66. Barbot, E.; Moustier, S.; Bottero, J. Y.; Moulin, P., Coagulation and ultrafiltration: Understanding of the key parameters of the hybrid process. *Journal of Membrane Science* **2008,** *325*, (2), 520.
67. Yang, C. L.; McGarrahan, J., Electrochemical coagulation for textile effluent decolorization. *Journal of Hazardous Materials* **2005,** *127*, (1-3), 40.
68. Nidheesh, P. V.; Gandhimathi, R.; Ramesh, S. T., Degradation of dyes from aqueous solution by Fenton processes: a review. *Environmental Science and Pollution Research* **2013,** *20*, (4), 2099.
69. Guo, W. Q.; Yang, Z. Z.; Zhou, X. J.; Wu, Q. L., Degradation and mineralization of dyes with advanced oxidation processes (AOPs): A brief review. *Proceedings of the 2015 International Forum on Energy, Environment Science and Materials* **2015,** *40*, 341.
70. Thiruvenkatachari, R.; Vigneswaran, S.; Moon, I. S., A review on UV/TiO2 photocatalytic oxidation process. *Korean Journal of Chemical Engineering* **2008,** *25*, (1), 64.
71. Castro, E.; Avellaneda, A.; Marco, P., Combination of Advanced Oxidation Processes and Biological Treatment for the Removal of Benzidine-Derived Dyes. *Environ. Prog. Sustain. Energy* **2014,** *33*, (3), 873.
72. Cesaro A., N. V., Belgiorno V., Wastewater Treatment by Combination of Advanced Oxidation Processes and Conventional Biological Systems. *Journal of Bioremediation & Biodegradation* **2013,** *4*, (208).
73. Radovic, M. D.; Mitrovic, J. Z.; Kostic, M. M.; Bojic, D. V.; Petrovic, M. M.; Najdanovic, S. M.; Bojic, A. L., Comparison of ultraviolet radiation/hydrogen peroxide, Fenton and photo-Fenton processes for the decolorization of reactive dyes. *Hem. Ind.* **2015,** *69*, (6), 657.
74. Tehrani-Bagha, A. R.; Mahmoodi, N. M.; Menger, F. M., Degradation of a persistent organic dye from colored textile wastewater by ozonation. *Desalination* **2010,** *260*, (1-3), 34.
75. Gözmen, B.; Kayan, B.; Gizir, A. M.; Hesenov, A., Oxidative degradations of reactive blue 4 dye by different advanced oxidation methods. *Journal of Hazardous Materials* **2009,** *168*, (1), 129.
76. Husain, Q.; Ulber, R., Immobilized Peroxidase as a Valuable Tool in the Remediation of Aromatic Pollutants and Xenobiotic Compounds: A Review. *Critical Reviews in Environmental Science and Technology* **2011,** *41*, (8), 770.
77. Cerboneschi, M.; Corsi, M.; Bianchini, R.; Bonanni, M.; Tegli, S., Decolorization of acid and basic dyes: understanding the metabolic degradation and cell-induced adsorption/precipitation by Escherichia coli. *Applied Microbiology and Biotechnology* **2015,** *99*, (19), 8235.
78. Deng, D. Y.; Guo, J.; Zeng, G. Q.; Sun, G. P., Decolorization of anthraquinone, triphenylmethane and azo dyes by a new isolated Bacillus cereus strain DC11. *International Biodeterioration & Biodegradation* **2008,** *62*, (3), 263.
79. Parmar, N.; Shukla, S. R., Microbial Decolorization of Reactive Dye Solutions. *Clean-Soil Air Water* **2015,** *43*, (10), 1426.
80. Srinivasan, A.; Viraraghavan, T., Decolorization of dye wastewaters by biosorbents: A review. *Journal of Environmental Management* **2010,** *91*, (10), 1915.
81. Chengalroyen, M. D.; Dabbs, E. R., The microbial degradation of azo dyes: minireview. *World Journal of Microbiology & Biotechnology* **2013,** *29*, (3), 389.
82. Mahmood, S.; Khalid, A.; Arshad, M.; Mahmood, T.; Crowley, D. E., Detoxification of azo dyes by bacterial oxidoreductase enzymes. *Critical Reviews in Biotechnology* **2016,** *36*, (4), 639.
83. Wesenberg, D.; Kyriakides, I.; Agathos, S. N., White-rot fungi and their enzymes for the treatment of industrial dye effluents. *Biotechnology Advances* **2003,** *22*, (1-2), 161.
84. Ogola, H. J. O.; Ashida, H.; Ishikawa, T.; Sawa, Y., Explorations and Applications of Enzyme-linked Bioremediation of Synthetic Dyes. In *Advances in Bioremediation of Wastewater and Polluted Soil*, Shiomi, N., Ed. Intech Europe: Rijeka, **2015;** pp 111.
85. Husain, Q., Potential applications of the oxidoreductive enzymes in the decolorization and detoxification of textile and other synthetic dyes from polluted water: A review. *Critical Reviews in Biotechnology* **2006,** *26*, (4), 201.

86. Regalado, C.; Garcia-Almendarez, B. E.; Duarte-Vazquez, M. A., Biotechnological applications of peroxidases. *Phytochemistry Reviews* **2004,** *3*, (1-2), 243.
87. Hamid, M.; Khalil ur, R., Potential applications of peroxidases. *Food Chemistry* **2009,** *115*, (4), 1177.
88. Bansal, N.; Kanwar, S. S., Peroxidase(s) in Environment Protection. *Scientific World Journal* **2013**, 9.
89. Lopes, G. R.; Pinto, D.; Silva, A. M. S., Horseradish peroxidase (HRP) as a tool in green chemistry. *Rsc Advances* **2014,** *4*, (70), 37244.
90. Burnette, F. S., Peroxidase and its relationship to food flavor and quality - Review. *Journal of Food Science* **1977,** *42*, (1), 1.
91. Azevedo, A. M.; Martins, V. C.; Prazeres, D. M. F.; Vojinovic, V.; Cabral, J. M. S.; Fonseca, L. P., Horseradish peroxidase: a valuable tool in biotechnology. *Biotechnology Annual Review, Vol 9* **2003,** *9*, 199.
92. Araujo, R.; Casal, M.; Cavaco-Paulo, A., Application of enzymes for textile fibres processing. *Biocatalysis and Biotransformation* **2008,** *26*, (5), 332.
93. Husain, Q., Peroxidase mediated decolorization and remediation of wastewater containing industrial dyes: a review. *Reviews in Environmental Science and Bio-Technology* **2010,** *9*, (2), 117.
94. Gianfreda, L.; Rao, M. A., Potential of extra cellular enzymes in remediation of polluted soils: a review. *Enzyme and Microbial Technology* **2004,** *35*, (4), 339.
95. Rao, M. A.; Scelza, R.; Scotti, R.; Gianfreda, L., Role of Enzymes in the Remediation of Polluted Environments. *J. Soil Sci. Plant Nutr.* **2010,** *10*, (3), 333.
96. Sen, S. K.; Raut, S.; Bandyopadhyay, P., Fungal decolouration and degradation of azo dyes: A review. *Fungal Biol. Rev.* **2016,** *30*, (3), 112.
97. Gholami-Borujeni, F.; Mahvi, A. H.; Naseri, S.; Faramarzi, M. A.; Nabizadeh, R.; Alimohammadi, M., Application of immobilized horseradish peroxidase for removal and detoxification of azo dye from aqueous solution. *Research Journal of Chemistry and Environment* **2011,** *15*, (2), 217.
98. da Silva, M. R.; de Sa, L. R. V.; Russo, C.; Scio, E.; Ferreira-Leitao, V. S., The Use of HRP in Decolorization of Reactive Dyes and Toxicological Evaluation of Their Products. *Enzyme research* **2011,** *2010*, 703824.
99. Bhunia, A.; Durani, S.; Wangikar, P. P., Horseradish peroxidase catalyzed degradation of industrially important dyes. *Biotechnology and Bioengineering* **2001,** *72*, (5), 562.
100. de Souza, S.; Forgiarini, E.; de Souza, A. A. U., Toxicity of textile dyes and their degradation by the enzyme horseradish peroxidase (HRP). *Journal of Hazardous Materials* **2007,** *147*, (3), 1073.
101. Verma, A. K.; Raghukumar, C.; Parvatkar, R. R.; Naik, C. G., A Rapid Two-Step Bioremediation of the Anthraquinone Dye, Reactive Blue 4 by a Marine-Derived Fungus. *Water Air and Soil Pollution* **2012,** *223*, (6), 3499.
102. Tan, K. B.; Vakili, M.; Hord, B. A.; Poh, P. E.; Abdullah, A. Z.; Salamatinia, B., Adsorption of dyes by nanomaterials: Recent developments and adsorption mechanisms. *Separation and Purification Technology* **2015,** *150*, 229.
103. Amin, M. T.; Alazba, A. A.; Manzoor, U., A Review of Removal of Pollutants from Water/Wastewater Using Different Types of Nanomaterials. *Adv. Mater. Sci. Eng.* **2014**, 24.
104. Moussavi, G.; Mahmoudi, M., Removal of azo and anthraquinone reactive dyes from industrial wastewaters using MgO nanoparticles. *Journal of Hazardous Materials* **2009,** *168*, (2-3), 806.
105. Khataee, A. R.; Zarei, M.; Fathinia, M.; Jafari, M. K., Photocatalytic degradation of an anthraquinone dye on immobilized TiO2 nanoparticles in a rectangular reactor: Destruction pathway and response surface approach. *Desalination* **2011,** *268*, (1-3), 126.
106. Khataee, A. R.; Kasiri, M. B., Photocatalytic degradation of organic dyes in the presence of nanostructured titanium dioxide: Influence of the chemical structure of dyes. *Journal of Molecular Catalysis A: Chemical* **2010,** *328*, (1–2), 8.
107. Marcelo, C. R.; Puiatti, G. A.; Nascimento, M. A.; Oliveira, A. F.; Lopes, R. P., Degradation of the Reactive Blue 4 Dye in Aqueous Solution Using Zero-Valent Copper Nanoparticles. *Journal of Nanomaterials* **2018**, 9.

108. Bilal, M.; Asgher, M., Dye decolorization and detoxification potential of Ca-alginate beads immobilized manganese peroxidase. *Bmc Biotechnology* **2015,** *15*, 14.
109. Gupta, V. K.; Khamparia, S.; Tyagi, I.; Jaspal, D.; Malviya, A., Decolorization of mixture of dyes: A critical review. *Global Journal of Environmental Science and Management-Gjesm* **2015,** *1*, (1), 71.
110. Iles, A., Shifting To Green Chemistry: The Need for Innovations in Sustainability Marketing. *Business Strategy and the Environment* **2006,** *17*, (8), 524.
111. Anastas, P. T.; Kirchhoff, M. M.; Williamson, T. C., Catalysis as a foundational pillar of green chemistry. *Applied Catalysis a-General* **2001,** *221*, (1-2), 3.
112. Azerad, R., Chemical biotechnology - Better enzymes for green chemistry - Editorial overview. *Current Opinion in Biotechnology* **2001,** *12*, (6), 533.
113. Alcalde, M.; Ferrer, M.; Plou, F. J.; Ballesteros, A., Environmental biocatalysis: from remediation with enzymes to novel green processes. *Trends in Biotechnology* **2006,** *24*, (6), 281.
114. Illanes, A.; Cauerhff, A.; Wilson, L.; Castro, G. R., Recent trends in biocatalysis engineering. *Bioresource Technology* **2012,** *115*, 48.
115. Kulkarni, K.; A.D.Kulkarni; Hussein, H. S., Application of Biocatalyst in Chemical Engineering. *International Journal of Advanced Engineering Technology* **2011,** *II*, (IV).
116. Sheldon, R. A.; van Pelt, S., Enzyme immobilisation in biocatalysis: why, what and how. *Chemical Society Reviews* **2013,** *42*, (15), 6223.
117. Sheldon, R. A.; Pereira, P. C., Biocatalysis engineering: the big picture. *Chemical Society Reviews* **2017,** *46*, (10), 2678.
118. Di Fiore, A.; Alterio, V.; Monti, S. M.; De Simone, G.; D'Ambrosio, K., Thermostable Carbonic Anhydrases in Biotechnological Applications. *International Journal of Molecular Sciences* **2015,** *16*, (7), 15456.
119. Adrio, J. L.; Demain, A. L., Microbial enzymes: tools for biotechnological processes. *Biomolecules* **2014,** *4*, (1), 117.
120. Narancic, T.; Davis, R.; Nikodinovic-Runic, J.; O'Connor, K. E., Recent developments in biocatalysis beyond the laboratory. *Biotechnology Letters* **2015,** *37*, (5), 943.
121. Whiteley, C. G.; Lee, D. J., Enzyme technology and biological remediation. *Enzyme and Microbial Technology* **2006,** *38*, (3-4), 291.
122. Fu, Y. Z.; Viraraghavan, T., Fungal decolorization of dye wastewaters: a review. *Bioresource Technology* **2001,** *79*, (3), 251.
123. Sanchez, S.; Demain, A. L., Enzymes and Bioconversions of Industrial, Pharmaceutical, and Biotechnological Significance. *Organic Process Research & Development* **2011,** *15*, (1), 224.
124. Nicell, J. A., Environmental applications of enzymes. *Interdisciplinary Environmental Review* **2001,** *3*, 14.
125. Soares, G. M. B.; de Amorim, M. T. P.; Costa-Ferreira, M., Use of laccase together with redox mediators to decolourize Remazol Brilliant Blue R. *Journal of Biotechnology* **2001,** *89*, (2-3), 123.
126. Daassi, D.; Mechichi, T.; Nasri, M.; Rodriguez-Couto, S., Decolorization of the metal textile dye Lanaset Grey G by immobilized white-rot fungi. *Journal of Environmental Management* **2013,** *129*, 324.
127. Shakeri, M.; Shoda, M., Change in turnover capacity of crude recombinant dye-decolorizing peroxidase (rDyP) in batch and fed-batch decolorization of Remazol Brilliant Blue R. *Applied Microbiology and Biotechnology* **2007,** *76*, (4), 919.
128. Ogola, H. J. O.; Kamiike, T.; Hashimoto, N.; Ashida, H.; Ishikawa, T.; Shibata, H.; Sawa, Y., Molecular Characterization of a Novel Peroxidase from the Cyanobacterium Anabaena sp Strain PCC 7120. *Applied and Environmental Microbiology* **2009,** *75*, (23), 7509.
129. Veitch, N. C., Horseradish peroxidase: a modern view of a classic enzyme. *Phytochemistry* **2004,** *65*, (3), 249.
130. Poulos, T. L., Thirty years of heme peroxidase structural biology. *Archives of Biochemistry and Biophysics* **2010,** *500*, (1), 3.
131. Sezer, M.; Genebra, T.; Mendes, S.; Martins, L. O.; Todorovic, S., A DyP-type peroxidase at a bio-compatible interface: structural and mechanistic insights. *Soft Matter* **2012,** *8*, (40), 10314.

132. Chance, B., The properties of the enzyme-substrate compounds of Horse-radish and Lacto-Peroxidase. *Science* **1949,** *109*, (2826), 204.
133. Sekuljica, N. Z.; Prlainovic, N. Z.; Stefanovic, A. B.; Zuza, M. G.; Cickaric, D. Z.; Mijin, D. Z.; Knezevic-Jugovic, Z. D., Decolorization of anthraquinonic dyes from textile effluent using horseradish peroxidase: optimization and kinetic study. *TheScientificWorldJournal* **2015,** *2015*, 371625.
134. Rodriguez-Lopez, J. N.; Gilabert, M. A.; Tudela, J.; Thorneley, R. N. F.; Garcia-Canovas, F., Reactivity of horseradish peroxidase compound II toward substrates: Kinetic evidence for a two-step mechanism. *Biochemistry* **2000,** *39*, (43), 13201.
135. Rodriguez-Lopez, J. N.; Lowe, D. J.; Hernandez-Ruiz, J.; Hiner, A. N. P.; Garcia-Canovas, F.; Thorneley, R. N. F., Mechanism of reaction of hydrogen peroxide with horseradish peroxidase: Identification of intermediates in the catalytic cycle. *Journal of the American Chemical Society* **2001,** *123*, (48), 11838.
136. Zubieta, C.; Joseph, R.; Krishna, S. S.; McMullan, D.; Kapoor, M.; Axelrod, H. L.; Miller, M. D.; Abdubek, P.; Acosta, C.; Astakhova, T.; Carlton, D.; Chiu, H. J.; Clayton, T.; Deller, M. C.; Duan, L.; Elias, Y.; Elsliger, M. A.; Feuerhelm, J.; Grzechnik, S. K.; Hale, J.; Han, G. W.; Jaroszewski, L.; Jin, K. K.; Klock, H. E.; Knuth, M. W.; Kozbial, P.; Kumar, A.; Marciano, D.; Morse, A. T.; Murphy, K. D.; Nigoghossian, E.; Okach, L.; Oommachen, S.; Reyes, R.; Rife, C. L.; Schimmel, P.; Trout, C. V.; van den Bedem, H.; Weekes, D.; White, A.; Xu, Q. P.; Hodgson, K. O.; Wooley, J.; Deacon, A. M.; Godzik, A.; Lesley, S. A.; Wilson, I. A., Identification and structural characterization of heme binding in a novel dye-decolorizing peroxidase, TyrA. *Proteins-Structure Function and Bioinformatics* **2007,** *69*, (2), 234.
137. Liers, C.; Aranda, E.; Strittmatter, E.; Piontek, K.; Plattner, D. A.; Zorn, H.; Ullrich, R.; Hofrichter, M., Phenol oxidation by DyP-type peroxidases in comparison to fungal and plant peroxidases. *Journal of Molecular Catalysis B-Enzymatic* **2014,** *103*, 41.
138. Lemos, M. A.; Oliveira, J. C.; Saraiva, J. A., Influence of pH on the thermal inactivation kinetics of horseradish peroxidase in aqueous solution. *Lebensmittel-Wissenschaft Und-Technologie-Food Science and Technology* **2000,** *33*, (5), 362.
139. Machado, M. F.; Saraiva, J., Inactivation and reactivation kinetics of horseradish peroxidase in phosphate buffer and buffer-dimethylformamide solutions. *Journal of Molecular Catalysis B-Enzymatic* **2002,** *19*, 451.
140. Palmieri, G.; Cennamo, G.; Sannia, G., Remazol Brilliant Blue R decolourisation by the fungus Pleurotus ostreatus and its oxidative enzymatic system. *Enzyme and Microbial Technology* **2005,** *36*, (1), 17.
141. Shah, V.; Nerud, F., Lignin degrading system of white-rot fungi and its exploitation for dye decolorization. *Canadian Journal of Microbiology* **2002,** *48*, (10), 857.
142. Chander, M.; Arora, D. S., Evaluation of some white-rot fungi for their potential to decolourise industrial dyes. *Dyes and Pigments* **2007,** *72*, (2), 192.
143. Couto, S. R., Dye removal by immobilised fungi. *Biotechnology Advances* **2009,** *27*, (3), 227.
144. Chengalroyen, M. D.; Dabbs, E. R., The microbial degradation of azo dyes: minireview. *World Journal of Microbiology & Biotechnology* **2013,** *29*, (3), 389.
145. Ahmad, M.; Taylor, C. R.; Pink, D.; Burton, K.; Eastwood, D.; Bending, G. D.; Bugg, T. D. H., Development of novel assays for lignin degradation: comparative analysis of bacterial and fungal lignin degraders. *Molecular Biosystems* **2010,** *6*, (5), 815.
146. Min, K.; Gong, G.; Woo, H. M.; Kim, Y.; Um, Y., A dye-decolorizing peroxidase from Bacillus subtilis exhibiting substrate-dependent optimum temperature for dyes and beta-ether lignin dimer. *Scientific Reports* **2015,** *5*, 8.
147. Vyas, B. R. M.; Molitoris, H. P., Involvement of an extracellular H2O2-dependent ligninolytic activity of the white-rot fungus pleurotus-ostreatus in the decolorization of Remazol-Brilliant-Blue-R. *Applied and Environmental Microbiology* **1995,** *61*, (11), 3919.
148. Kim, S. J.; Ishikawa, K.; Hirai, M.; Shoda, M., Characteristics of a newly isolated fungus, Geotrichum-Candidum Dec-1, which decolorizes various dyes. *Journal of Fermentation and Bioengineering* **1995,** *79*, (6), 601.
149. Zamocky, M.; Hofbauer, S.; Schaffner, I.; Gasselhuber, B.; Nicolussi, A.; Soudi, M.; Pirker, K. F.; Furamuller, P. G.; Obinger, C., Independent evolution of four heme peroxidase superfamilies. *Archives of Biochemistry and Biophysics* **2015,** *574*, 108.

150. Liers, C.; Pecyna, M. J.; Kellner, H.; Worrich, A.; Zorn, H.; Steffen, K. T.; Hofrichter, M.; Ullrich, R., Substrate oxidation by dye-decolorizing peroxidases (DyPs) from wood-and litter-degrading agaricomycetes compared to other fungal and plant heme-peroxidases. *Applied Microbiology and Biotechnology* **2013,** *97*, (13), 5839.
151. Sugano, Y.; Muramatsu, R.; Ichiyanagi, A.; Sato, T.; Shoda, M., DyP, a unique dye-decolorizing peroxidase, represents a novel heme peroxidase family. *Journal of Biological Chemistry* **2007,** *282*, (50), 36652.
152. Sugano, Y.; Matsushima, Y.; Tsuchiya, K.; Aoki, H.; Hirai, M.; Shoda, M., Degradation pathway of an anthraquinone dye catalyzed by a unique peroxidase DyP from Thanatephorus cucumeris Dec 1. *Biodegradation* **2009,** *20*, (3), 433.
153. Sugano, Y., DyP-type peroxidases comprise a novel heme peroxidase family. *Cellular and Molecular Life Sciences* **2009,** *66*, (8), 1387.
154. Fernandez-Fueyo, E.; Linde, D.; Almendral, D.; Lopez-Lucendo, M. F.; Ruiz-Duenas, F. J.; Martinez, A. T., Description of the first fungal dye-decolorizing peroxidase oxidizing manganese(II). *Applied Microbiology and Biotechnology* **2015,** *99*, (21), 8927.
155. Shakeri, M.; Shoda, M., Decolorization of an anthraquinone dye by the recombinant dye-decolorizing peroxidase (rDyP) immobilized on mesoporous materials. *Journal of Molecular Catalysis B-Enzymatic* **2008,** *54*, (1-2), 42.
156. Shakeri, M.; Shoda, M., Efficient decolorization of an anthraquinone dye by recombinant dye-decolorizing peroxidase (rDyP) immobilized in silica-based mesocellular foam. *Journal of Molecular Catalysis B-Enzymatic* **2010,** *62*, (3-4), 277.
157. Shimokawa, T.; Hirai, M.; Shoda, M.; Sugano, Y., Efficient Dye Decolorization and Production of Dye Decolorizing Enzymes by the Basidiomycete Thanatephorus cucumeris Dec 1 in a Liquid and Solid Hybrid Culture. *Journal of Bioscience and Bioengineering* **2008,** *106*, (5), 481.
158. Yu, W. N.; Liu, W. N.; Huang, H. Q.; Zheng, F.; Wang, X. Y.; Wu, Y. Y.; Li, K. J.; Xie, X. M.; Jin, Y., Application of a Novel Alkali-Tolerant Thermostable DyP-Type Peroxidase from Saccharomonospora viridis DSM 43017 in Biobleaching of Eucalyptus Kraft Pulp. *Plos One* **2014,** *9*, (10).
159. Salvachua, D.; Prieto, A.; Martinez, A. T.; Martinez, M. J., Characterization of a Novel Dye-Decolorizing Peroxidase (DyP)-Type Enzyme from Irpex lacteus and Its Application in Enzymatic Hydrolysis of Wheat Straw. *Applied and Environmental Microbiology* **2013,** *79*, (14), 4316.
160. van Bloois, E.; Pazmino, D. E. T.; Winter, R. T.; Fraaije, M. W., A robust and extracellular heme-containing peroxidase from Thermobifida fusca as prototype of a bacterial peroxidase superfamily. *Applied Microbiology and Biotechnology* **2010,** *86*, (5), 1419.
161. Scheibner, M.; Hulsdau, B.; Zelena, K.; Nimtz, M.; de Boer, L.; Berger, R. G.; Zorn, H., Novel peroxidases of Marasmius scorodonius degrade beta-carotene. *Applied Microbiology and Biotechnology* **2008,** *77*, (6), 1241.
162. Hofrichter, M.; Ullrich, R.; Pecyna, M. J.; Liers, C.; Lundell, T., New and classic families of secreted fungal heme peroxidases. *Applied Microbiology and Biotechnology* **2010,** *87*, (3), 871.
163. Colpa, D. I.; Fraaije, M. W.; van Bloois, E., DyP-type peroxidases: a promising and versatile class of enzymes. *Journal of Industrial Microbiology & Biotechnology* **2014,** *41*, (1), 1.
164. Singh, R.; Eltis, L. D., The multihued palette of dye-decolorizing peroxidases. *Archives of Biochemistry and Biophysics* **2015,** *574*, 56.
165. Singh, R.; Grigg, J. C.; Armstrong, Z.; Murphy, M. E. P.; Eltis, L. D., Distal Heme Pocket Residues of B-type Dye-decolorizing Peroxidase *Journal of Biological Chemistry* **2012,** *287*, (13), 10623.
166. Sugano, Y.; Ishii, Y.; Shoda, M., Role of H164 in a unique dye-decolorizing heme peroxidase DyP. *Biochemical and Biophysical Research Communications* **2004,** *322*, (1), 126.
167. Yoshida, T.; Tsuge, H.; Konno, H.; Hisabori, T.; Sugano, Y., The catalytic mechanism of dye-decolorizing peroxidase DyP may require the swinging movement of an aspartic acid residue. *Febs Journal* **2011,** *278*, (13), 2387.
168. Yoshida, T.; Tsuge, H.; Hisabori, T.; Sugano, Y., Crystal structures of dye-decolorizing peroxidase with ascorbic acid and 2,6-dimethoxyphenol. *Febs Letters* **2012,** *586*, (24), 4351.

169. Yoshida, T.; Sugano, Y., A structural and functional perspective of DyP-type peroxidase family. *Archives of Biochemistry and Biophysics* **2015,** *574*, 49.
170. Bugg, T. D. H.; Rahmanpour, R., Enzymatic conversion of lignin into renewable chemicals. *Current Opinion in Chemical Biology* **2015,** *29*, 10.
171. Colpa, D. I.; Fraaije, M. W.; van Bloois, E., DyP-type peroxidases: a promising and versatile class of enzymes. *Journal of Industrial Microbiology & Biotechnology* **2014,** *41*, (1), 1.
172. Uchida, T.; Sasaki, M.; Tanaka, Y.; Ishimorit, K., A Dye-Decolorizing Peroxidase from Vibrio cholerae. *Biochemistry* **2015,** *54*, (43), 6610.
173. Linde, D.; Coscolin, C.; Liers, C.; Hofrichter, M.; Martinez, A. T.; Ruiz-Duenas, F. J., Heterologous expression and physicochemical characterization of a fungal dye-decolorizing peroxidase from Auricularia auricula-judae. *Protein Expression and Purification* **2014,** *103*, 28.
174. Sugano, Y.; Nakano, R.; Sasaki, K.; Shoda, M., Efficient heterologous expression in Aspergillus oryzae of a unique dye-decolorizing peroxidase, DyP, of Geotrichum candidum Dec 1. *Applied and Environmental Microbiology* **2000,** *66*, (4), 1754.
175. Kim, S. J.; Shoda, M., Decolorization of molasses and a dye by a newly isolated strain of the fungus Geotrichum candidum Dec 1. *Biotechnology and Bioengineering* **1999,** *62*, (1), 114.
176. Kim, S. J.; Shoda, M., Purification and characterization of a novel peroxidase from Geotrichum candidum Dec 1 involved in decolorization of dyes. *Applied and Environmental Microbiology* **1999,** *65*, (3), 1029.
177. Chen, C.; Shrestha, R.; Jia, K.; Gao, P. F.; Geisbrecht, B. V.; Bossmann, S. H.; Shi, J. S.; Li, P., Characterization of Dye-decolorizing Peroxidase (DyP) from Thermomonospora curvata Reveals Unique Catalytic Properties of A-type DyPs. *Journal of Biological Chemistry* **2015,** *290*, (38), 23447.
178. Shakeri, M.; Sugano, Y.; Shoda, M., Stable repeated-batch production of recombinant dye-decolorizing peroxidase (rDyP) from Aspergillus oryzae. *Journal of Bioscience and Bioengineering* **2008,** *105*, (6), 683.
179. Brown, M. E.; Barros, T.; Chang, M. C. Y., Identification and Characterization of a Multifunctional Dye Peroxidase from a Lignin-Reactive Bacterium. *Acs Chemical Biology* **2012,** *7*, (12), 2074.
180. Li, J.; Liu, C.; Li, B. Z.; Yuan, H. L.; Yang, J. S.; Zheng, B. W., Identification and Molecular Characterization of a Novel DyP-Type Peroxidase from Pseudomonas aeruginosa PKE117. *Applied Biochemistry and Biotechnology* **2012,** *166*, (3), 774.
181. Ahmad, M.; Roberts, J. N.; Hardiman, E. M.; Singh, R.; Eltis, L. D.; Bugg, T. D. H., Identification of DypB from Rhodococcus jostii RHA1 as a Lignin Peroxidase. *Biochemistry* **2011,** *50*, (23), 5096.
182. Roberts, J. N.; Singh, R.; Grigg, J. C.; Murphy, M. E. P.; Bugg, T. D. H.; Eltis, L. D., Characterization of Dye-Decolorizing Peroxidases from Rhodococcus jostii RHA1. *Biochemistry* **2011,** *50*, (23), 5108.
183. Santos, A.; Mendes, S.; Brissos, V.; Martins, L. O., New dye-decolorizing peroxidases from Bacillus subtilis and Pseudomonas putida MET94: towards biotechnological applications. *Applied Microbiology and Biotechnology* **2014,** *98*, (5), 2053.
184. Rahmanpour, R.; Bugg, T. D. H., Characterisation of Dyp-type peroxidases from Pseudomonas fluorescens Pf-5: Oxidation of Mn(II) and polymeric lignin by Dyp1B. *Archives of Biochemistry and Biophysics* **2015,** *574*, 93.
185. Liers, C.; Bobeth, C.; Pecyna, M.; Ullrich, R.; Hofrichter, M., DyP-like peroxidases of the jelly fungus Auricularia auricula-judae oxidize nonphenolic lignin model compounds and high-redox potential dyes. *Applied Microbiology and Biotechnology* **2010,** *85*, (6), 1869.
186. Sato, T.; Hara, S.; Matsui, T.; Sazaki, G.; Saijo, S.; Ganbe, T.; Tanaka, N.; Sugano, Y.; Shoda, M., A unique dye-decolorizing peroxidase, DyP, from Thanatephorus cucumeris Dec 1: heterologous expression, crystallization and preliminary X-ray analysis. *Acta Crystallographica Section D-Biological Crystallography* **2004,** *60*, 149.
187. Guzik, U.; Hupert-Kocurek, K.; Wojcieszynska, D., Immobilization as a Strategy for Improving Enzyme Properties-Application to Oxidoreductases. *Molecules* **2014,** *19*, (7), 8995.

188. Sugano, Y.; Matsushima, Y.; Shoda, M., Complete decolorization of the anthraquinone dye Reactive blue 5 by the concerted action of two peroxidases from Thanatephorus cucumeris Dec 1. *Applied Microbiology and Biotechnology* **2006,** *73*, (4), 862.
189. Shin, H. Y.; Park, T. J.; Kim, M. I., Recent Research Trends and Future Prospects in Nanozymes. *Journal of Nanomaterials* **2015**, 11.
190. Han, L.; Li, C. C.; Zhang, T.; Lang, Q. L.; Liu, A. H., Au@Ag Heterogeneous Nanorods as Nanozyme Interfaces with Peroxidase-Like Activity and Their Application for One-Pot Analysis of Glucose at Nearly Neutral pH. *Acs Applied Materials & Interfaces* **2015,** *7*, (26), 14463.
191. Shi, W. B.; Wang, Q. L.; Long, Y. J.; Cheng, Z. L.; Chen, S. H.; Zheng, H. Z.; Huang, Y. M., Carbon nanodots as peroxidase mimetics and their applications to glucose detection. *Chemical Communications* **2011,** *47*, (23), 6695.
192. Wang, H.; Huang, Y. M., Prussian-blue-modified iron oxide magnetic nanoparticles as effective peroxidase-like catalysts to degrade methylene blue with H2O2. *Journal of Hazardous Materials* **2011,** *191*, (1-3), 163.
193. Nirala, N. R.; Abraham, S.; Kumar, V.; Bansal, A.; Srivastava, A.; Saxena, P. S., Colorimetric detection of cholesterol based on highly efficient peroxidase mimetic activity of graphene quantum dots. *Sensors and Actuators B-Chemical* **2015,** *218*, 42.
194. Gao, L. Z.; Zhuang, J.; Nie, L.; Zhang, J. B.; Zhang, Y.; Gu, N.; Wang, T. H.; Feng, J.; Yang, D. L.; Perrett, S.; Yan, X., Intrinsic peroxidase-like activity of ferromagnetic nanoparticles. *Nature Nanotechnology* **2007,** *2*, (9), 577.
195. Cheng, L. Y.; Long, Y. T.; Kraatz, H. B.; Tian, H., Evaluation of an immobilized artificial carbonic anhydrase model for CO2 sequestration. *Chemical Science* **2011,** *2*, (8), 1515.
196. Sahoo, P. C.; Jang, Y. N.; Lee, S. W., Immobilization of carbonic anhydrase and an artificial Zn(II) complex on a magnetic support for biomimetic carbon dioxide sequestration. *Journal of Molecular Catalysis B-Enzymatic* **2012,** *82*, 37.
197. Sahoo, P. C.; Jang, Y. N.; Suh, Y. J.; Lee, S. W., Bioinspired design of mesoporous silica complex based on active site of carbonic anhydrase. *Journal of Molecular Catalysis a-Chemical* **2014,** *390*, 105.
198. Wei, H.; Wang, E. K., Nanomaterials with enzyme-like characteristics (nanozymes): next-generation artificial enzymes. *Chemical Society Reviews* **2013,** *42*, (14), 6060.
199. Lin, Y. H.; Ren, J. S.; Qu, X. G., Catalytically Active Nanomaterials: A Promising Candidate for Artificial Enzymes. *Accounts of Chemical Research* **2014,** *47*, (4), 1097.
200. Cantone, S.; Ferrario, V.; Corici, L.; Ebert, C.; Fattor, D.; Spizzo, P.; Gardossi, L., Efficient immobilisation of industrial biocatalysts: criteria and constraints for the selection of organic polymeric carriers and immobilisation methods. *Chemical Society Reviews* **2013,** *42*, (15), 6262.
201. Osma, J. F.; Toca-Herrera, J. L.; Rodríguez-Couto, S., Cost analysis in laccase production. *Journal of Environmental Management* **2011,** *92*, (11), 2907.
202. Elnashar, M. M. M., Review Article: Immobilized Molecules Using Biomaterials and Nanobiotechnology. *Journal of Biomaterials and Nanobiotechnology* **2010,** *1*, (1), 61.
203. Cheng, J.; Yu, S. M.; Zuo, P., Horseradish peroxidase immobilized on aluminum-pillaredinterlayered clay for the catalytic oxidadon of phenolic wastewater. *Water Research* **2006,** *40*, (2), 283.
204. Arabaci, G.; Usluoglu, A., The Enzymatic Decolorization of Textile Dyes by the Immobilized Polyphenol Oxidase from Quince Leaves. *Scientific World Journal* **2014**, 5.
205. Matto, M.; Satar, R.; Husain, Q., Application of Calcium Alginate-Starch Entrapped Bitter Gourd (Momordica charantia) Peroxidase for the Removal of Colored Compounds from a Textile Effluent in Batch as well as in Continuous Reactor. *Applied Biochemistry and Biotechnology* **2009,** *158*, (3), 512.
206. Reetz, M. T., Biocatalysis in organic chemistry and biotechnology: past, present, and future. *J Am Chem Soc* **2013,** *135*, (34), 12480.
207. Homaei, A. A.; Sariri, R.; Vianello, F.; Stevanato, R., Enzyme immobilization: an update. *Journal of chemical biology* **2013,** *6*, (4), 185.
208. Brena, B. M.; Batista-Viera, F., Immobilization of Enzymes, A Literature Survey. In *Methods in Biotechnology: Immobilization of Enzymes and Cells, Second Edition*, Humana Press Inc: Totowa NJ, **2006;** pp 15.

209. Bornscheuer, U. T.; Buchholz, K., Highlights in biocatalysis - Historical landmarks and current trends. *Engineering in Life Sciences* **2005,** *5*, (4), 309.
210. Iyer, P. V.; Ananthanarayan, L., Enzyme stability and stabilization - Aqueous and non-aqueous environment. *Process Biochemistry* **2008,** *43*, (10), 1019.
211. Rodrigues, R. C.; Ortiz, C.; Berenguer-Murcia, A.; Torres, R.; Fernandez-Lafuente, R., Modifying enzyme activity and selectivity by immobilization. *Chemical Society Reviews* **2013,** *42*, (15), 6290.
212. Emond, S.; Guieysse, D.; Lechevallier, S.; Dexpert-Ghys, J.; Monsan, P.; Remaud-Simeon, M., Alteration of enzyme activity and enantioselectivity by biomimetic encapsulation in silica particles. *Chemical Communications* **2012,** *48*, (9), 1314.
213. Cherian, E.; Dharmendirakumar, M.; Baskar, G., Immobilization of cellulase onto MnO2 nanoparticles for bioethanol production by enhanced hydrolysis of agricultural waste. *Chinese Journal of Catalysis* **2015,** *36*, (8), 1223.
214. Bilal, M.; Asgher, M.; Hu, H. B.; Zhang, X. H., Kinetic characterization, thermo-stability and Reactive Red 195A dye detoxifying properties of manganese peroxidase-coupled gelatin hydrogel. *Water Science and Technology* **2016,** *74*, (8), 1809.
215. Forsyth, C.; Patwardhan, S. V., Controlling performance of lipase immobilised on bioinspired silica. *Journal of Materials Chemistry B* **2013,** *1*, (8), 1164.
216. Greiner, R.; Konietzny, U.; Blackburn, D. M.; Jorquera, M. A., Production of partially phosphorylated myo-inositol phosphates using phytases immobilised on magnetic nanoparticles. *Bioresource Technology* **2013,** *142*, 375.
217. Zhang, Y.; Wu, H.; Li, J.; Li, L.; Jiang, Y.; Jiang, Z., Protamine-templated biomimetic hybrid capsules: Efficient and stable carrier for enzyme encapsulation. *Chemistry of Materials* **2008,** *20*, (3), 1041.
218. Fei, X. Y.; Chen, S. Y.; Huang, C. J.; Liu, D.; Zhang, Y. C., Immobilization of bovine carbonic anhydrase on glycidoxypropyl-functionalized nanostructured mesoporous silicas for carbonation reaction. *Journal of Molecular Catalysis B-Enzymatic* **2015,** *116*, 134.
219. Rocha-Martin, J.; Velasco-Lozano, S.; Guisan, J. M.; Lopez-Gallego, F., Oxidation of phenolic compounds catalyzed by immobilized multi-enzyme systems with integrated hydrogen peroxide production. *Green Chemistry* **2014,** *16*, (1), 303.
220. Wang, X. L.; Li, Z.; Shi, J. F.; Wu, H.; Jiang, Z. Y.; Zhang, W. Y.; Song, X. K.; Ai, Q. H., Bioinspired Approach to Multienzyme Cascade System Construction for Efficient Carbon Dioxide Reduction. *Acs Catalysis* **2014,** *4*, (3), 962.
221. Li, L.; Jiang, Z. Y.; Wu, H.; Feng, Y. N.; Li, J., Protamine-induced biosilica as efficient enzyme immobilization carrier with high loading and improved stability. *Materials Science & Engineering C-Materials for Biological Applications* **2009,** *29*, (6), 2029.
222. Rojas-Melgarejo, F.; Rodriguez-Lopez, J. N.; Garcia-Canovas, F.; Garcia-Ruiz, P. A., Stability of horseradish peroxidase immobilized on different cinnamic carbohydrate esters. *Journal of Chemical Technology and Biotechnology* **2004,** *79*, (10), 1148.
223. Orcaire, O.; Buisson, P.; Pierre, A. C., Application of silica aerogel encapsulated lipases in the synthesis of biodiesel by transesterification reactions. *Journal of Molecular Catalysis B-Enzymatic* **2006,** *42*, (3-4), 106.
224. Trouillefou, C. M.; Le Cadre, E.; Cacciaguerra, T.; Cunin, F.; Plassard, C.; Belamie, E., Protected activity of a phytase immobilized in mesoporous silica with benefits to plant phosphorus nutrition. *Journal of Sol-Gel Science and Technology* **2015,** *74*, (1), 55.
225. Swaisgood, H., The use of immobilized enzymes to improve functionality. In *Proteins in Food Processing*, Yada, R., Ed. Woodhead Publishing Limited and CRC Press LLC: **2004;** pp 608.
226. Nisha, S.; Arun, K. S.; Gobi, N., A Review on Methods, Application and Properties of Immobilized Enzyme. *Che Sci Rev Lett* **2012,** *1*, (3), 148.
227. Sheldon, R. A., Cross-linked enzyme aggregates (CLEA (R) s): stable and recyclable biocatalysts. *Biochemical Society Transactions* **2007,** *35*, 1583.
228. D'Annibale, A.; Stazi, S. R.; Vinciguerra, V.; Di Mattia, E.; Sermanni, G. G., Characterization of immobilized laccase from Lentinula edodes and its use in olive-mill wastewater treatment. *Process Biochemistry* **1999,** *34*, (6-7), 697.

229. Liu, W.; Wang, W. C.; Li, H. S.; Zhou, X., Immobilization of horseradish peroxidase on silane-modified ceramics and their properties: potential for oily wastewater treatment. *Water Science and Technology* **2011,** *63*, (8), 1621.
230. Gill, I.; Ballesteros, A., Bioencapsulation within synthetic polymers (Part 1): sol-gel encapsulated biologicals. *Trends in Biotechnology* **2000,** *18*, (7), 282.
231. Spahn, C.; Minteer, S. D., Enzyme Immobilization in Biotechnology. *Recent Patents on Engineering* **2008,** *2*, 195.
232. Khan, A. A.; M.A., A., Recent Advances and Applications of Immobilised Enzyme Technologies: A Review. *Research Journal of Biological Sciences* **2010,** *5*, (8), 565.
233. Velasco-Lozano, S.; López-Gallego, F.; Mateos-Díaz, J. C.; Favela-Torres, E., Cross-linked enzyme aggregates (CLEA) in enzyme improvement – a review. *Biocatalysis* **2015,** *1*, 166.
234. Wang, Y.; Caruso, F., Enzyme encapsulation in nanoporous silica spheres. *Chemical Communications* **2004**, (13), 1528.
235. Wang, J. Y.; Yu, H. R.; Xie, R.; Ju, X. J.; Yu, Y. L.; Chu, L. Y.; Zhang, Z. B., Alginate/Protamine/Silica Hybrid Capsules with Ultrathin Membranes for Laccase Immobilization. *Aiche Journal* **2013,** *59*, (2), 380.
236. Shi, J. F.; Jiang, Z. Y., An efficient and recyclable enzyme catalytic system constructed through the synergy between biomimetic mineralization and polyamine-salt aggregate assembly. *Journal of Materials Chemistry B* **2014,** *2*, (28), 4435.
237. Magner, E., Immobilisation of enzymes on mesoporous silicate materials. *Chemical Society Reviews* **2013,** *42*, (15), 6213.
238. Contesini, F. J.; Figueira, J. D.; Kawaguti, H. Y.; Fernandes, P. C. B.; Carvalho, P. D.; Nascimento, M. D.; Sato, H. H., Potential Applications of Carbohydrases Immobilization in the Food Industry. *International Journal of Molecular Sciences* **2013,** *14*, (1), 1335.
239. Datta, S.; Christena, L. R.; Rajaram, Y. R. S., Enzyme immobilization: an overview on techniques and support materials. *3 Biotech* **2013,** *3*, (1), 1.
240. Tischer, W.; Kasche, V., Immobilized enzymes: crystals or carriers? *Trends in Biotechnology* **1999,** *17*, (8), 326.
241. Cao, L., Immobilised enzymes: science or art? *Current Opinion in Chemical Biology* **2005,** *9*, 217.
242. Hanefeld, U.; Gardossi, L.; Magner, E., Understanding enzyme immobilisation. *Chemical Society Reviews* **2009,** *38*, (2), 453.
243. Adlercreutz, P., Immobilisation and application of lipases in organic media. *Chemical Society Reviews* **2013,** *42*, (15), 6406.
244. Christensen, M. W.; Andersen, L.; Husum, T. L.; Kirk, O., Industrial lipase immobilization. *European Journal of Lipid Science and Technology* **2003,** *105*, (6), 318.
245. Mateo, C.; Palomo, J. M.; Fernandez-Lorente, G.; Guisan, J. M.; Fernandez-Lafuente, R., Improvement of enzyme activity, stability and selectivity via immobilization techniques. *Enzyme and Microbial Technology* **2007,** *40*, (6), 1451.
246. Garcia-Galan, C.; Berenguer-Murcia, A.; Fernandez-Lafuente, R.; Rodrigues, R. C., Potential of Different Enzyme Immobilization Strategies to Improve Enzyme Performance. *Advanced Synthesis & Catalysis* **2011,** *353*, (16), 2885.
247. Smith, A. C., The potential for destructuring of food processing waste by combination processing. In *Handbook of waste management and co-product recovery in food processing* Keith, W., Ed. CRC Press, Woodhead Publishing Limited: **2007;** Vol. Volume 1, pp 165.
248. Tischer, W.; Wedekind, F., Immobilized Enzymes: Methods and Applications. In *Biocatalysis - From Discovery to Application*, W.-D. Fessner, A. A., D. C. Demirjian, R. Furstoss,; H. Griengl, K.-E. J., E Morls-Varas,; R. 0hrlein, M. T. R., J.-L. Reymond, M. Schmidt,; S. Servi, E. C. S., W. Tischer, F. Wedekind, Eds. Springer Berlin Heidelberg: **1999;** Vol. 200, pp 95.
249. DiCosimo, R.; McAuliffe, J.; Poulose, A. J.; Bohlmann, G., Industrial use of immobilized enzymes. *Chemical Society Reviews* **2013,** *42*, (15), 6437.
250. Novozymes Effective fructose syrup production with isomerization. (21/1/2019),
251. Novozymes No trans fats or chemicals with Lypozyme^{R} TL IM. (21/1/2019),

252. Sahutoglu, A. S.; Akgul, C., Immobilisation of Aspergillus oryzae α-amylase and Aspergillus niger glucoamylase enzymes as cross-linked enzyme aggregates. *Chemical Papers* **2015,** *69*, (3).
253. Ahmad, R.; Sardar, M., Enzyme Immobilization: An Overview on Nanoparticles as Immobilization Matrix. *Biochem Anal Biochem* **2015,** *4*, (2), 178.
254. Jing, G. H.; Pan, F. J.; Lv, B. H.; Zhou, Z. M., Immobilization of carbonic anhydrase on epoxy-functionalized magnetic polymer microspheres for CO2 capture. *Process Biochemistry* **2015,** *50*, (12), 2234.
255. Cha, C.; Kim, S. R.; Jin, Y. S.; Kong, H., Tuning structural durability of yeast-encapsulating alginate gel beads with interpenetrating networks for sustained bioethanol production. *Biotechnology and Bioengineering* **2012,** *109*, (1), 63.
256. Gerdenbach, D.; Cooper, B. L., Scale up issues from bench to pilot. In *AlChE Annual Meeting*, Nashville, TN, 2009.
257. Weetall, H. H.; Pitcher, W. H., Scaling up an immobilised enzyme-system. *Science* **1986,** *232*, (4756), 1396.
258. Bellino, M. G.; Regazzoni, A. E.; Soler-Illia, G., Amylase-Functionalized Mesoporous Silica Thin Films as Robust Biocatalyst Platforms. *Acs Applied Materials & Interfaces* **2010,** *2*, (2), 360.
259. Tomin, A.; Weiser, D.; Hellner, G.; Bata, Z.; Corici, L.; Peter, F.; Koczka, B.; Poppe, L., Fine-tuning the second generation sol-gel lipase immobilization with ternary alkoxysilane precursor systems. *Process Biochemistry* **2011,** *46*, (1), 52.
260. Galarneau, A.; Mureseanu, M.; Atger, S.; Renard, G.; Fajula, F., Immobilization of lipase on silicas. Relevance of textural and interfacial properties on activity and selectivity. *New Journal of Chemistry* **2006,** *30*, (4), 562.
261. Singh, N.; Basu, S.; Vankelecom, I. F. J.; Balakrishnan, M., Covalently Immobilized Laccase for Decolourization of Glucose-Glycine Maillard Products as Colourant of Distillery Wastewater. *Applied Biochemistry and Biotechnology* **2015,** *177*, (1), 76.
262. Rojas-Melgarejo, F.; Marin-Iniesta, F.; Rodriguez-Lopez, J. N.; Garcia-Canovas, F.; Garcia-Ruiz, P. A., Cinnamic carbohydrate esters show great versatility as supports for the immobilization of different enzymes. *Enzyme and Microbial Technology* **2006,** *38*, (6), 748.
263. Celebi, M.; Kaya, M. A.; Altikatoglu, M.; Yildirim, H., Enzymatic Decolorization of Anthraquinone and Diazo Dyes Using Horseradish Peroxidase Enzyme Immobilized onto Various Polysulfone Supports. *Applied Biochemistry and Biotechnology* **2013,** *171*, (3), 716.
264. Temocin, Z.; Yigitoglu, M., Studies on the activity and stability of immobilized horseradish peroxidase on poly(ethylene terephthalate) grafted acrylamide fiber. *Bioprocess and Biosystems Engineering* **2009,** *32*, (4), 467.
265. Wang, B.; Zhang, J.-J.; Pan, Z.-Y.; Tao, X.-Q.; Wang, H.-S., A novel hydrogen peroxide sensor based on the direct electron transfer of horseradish peroxidase immobilized on silica–hydroxyapatite hybrid film. *Biosensors and Bioelectronics* **2009,** *24*, (5), 1141.
266. Zhu, Y.; Kaskel, S.; Shi, J.; Wage, T.; van Pee, K. H., Immobilization of Trametes versicolor laccase on magnetically separable mesoporous silica spheres. *Chemistry of Materials* **2007,** *19*, (26), 6408.
267. Mansor, A. F.; Mohidem, N. A.; Zawawi, W.; Othman, N. S.; Endud, S.; Mat, H., The optimization of synthesis conditions for laccase entrapment in mesoporous silica microparticles by response surface methodology. *Microporous and Mesoporous Materials* **2016,** *220*, 308.
268. Sharma, A.; Bhattacharya, A.; Shrivastava, A., Biomimetic CO2 sequestration using purified carbonic anhydrase from indigenous bacterial strains immobilized on biopolymeric materials. *Enzyme and Microbial Technology* **2011,** *48*, (4-5), 416.
269. Woo, K. M.; Lee, I.; Hong, S. G.; An, S.; Lee, J.; Oh, E.; Kim, J., Crosslinked chitosan coating on magnetic mesoporous silica with pre-adsorbed carbonic anhydrase for carbon dioxide conversion. *Chemical Engineering Journal* **2015,** *276*, 232.
270. Valle-Vigon, P.; Fuertes, A. B., Magnetically separable carbon capsules loaded with laccase and their application to dye degradation. *Rsc Advances* **2011,** *1*, (9), 1756.
271. Janovic, B. S.; Vicovac, M. L. M.; Vujcic, Z. M.; Vujcic, M. T., Tailor-made biocatalysts based on scarcely studied acidic horseradish peroxidase for biodegradation of reactive dyes. *Environmental Science and Pollution Research* **2017,** *24*, (4), 3923.

272. Blank, K.; Morfill, J.; Gaub, H. E., Site-specific immobilization of genetically engineered variants of Candida antarctica lipase B. *ChemBioChem* **2006,** *7*, (9), 1349.
273. David, A. E.; Wang, N. S.; Yang, V. C.; Yang, A. J., Chemically surface modified gel (CSMG): An excellent enzyme-immobilization matrix for industrial processes. *Journal of Biotechnology* **2006,** *125*, (3), 395.
274. Champagne, P. P.; Ramsay, J. A., Dye decolorization and detoxification by laccase immobilized on porous glass beads. *Bioresource Technology* **2010,** *101*, (7), 2230.
275. Vojinovic, V.; Carvalho, R. H.; Lemos, F.; Cabral, J. M. S.; Fonseca, L. P.; Ferreira, B. S., Kinetics of soluble and immobilized horseradish peroxidase-mediated oxidation of phenolic compounds. *Biochemical Engineering Journal* **2007,** *35*, (2), 126.
276. Fernandes, K. F.; Lima, C. S.; Lopes, F. M.; Collins, C. H., Properties of horseradish peroxidase immobilised onto polyaniline. *Process Biochemistry* **2004,** *39*, (8), 957.
277. Jiang, D. S.; Long, S. Y.; Huang, J.; Xiao, H. Y.; Zhou, J. Y., Immobilization of Pycnoporus sanguineus laccase on magnetic chitosan microspheres. *Biochemical Engineering Journal* **2005,** *25*, (1), 15.
278. Voss, R.; Brook, M. A.; Thompson, J.; Chen, Y.; Pelton, R. H.; Brennan, J. D., Non-destructive horseradish peroxidase immobilization in porous silica nanoparticles. *Journal of Materials Chemistry* **2007,** *17*, (46), 4854.
279. Mei, L.; Xie, R.; Yang, C.; Ju, X. J.; Wang, J. Y.; Zhang, Z. B.; Chu, L. Y., Bio-inspired mini-eggs with pH-responsive membrane for enzyme immobilization. *Journal of Membrane Science* **2013,** *429*, 313.
280. Hilterhaus, L.; Minow, B.; Muller, J.; Berheide, M.; Quitmann, H.; Katzer, M.; Thum, O.; Antranikian, G.; Zeng, A. P.; Liese, A., Practical application of different enzymes immobilized on sepabeads. *Bioprocess and Biosystems Engineering* **2008,** *31*, (3), 163.
281. Kunamneni, A.; Ghazi, I.; Camarero, S.; Ballesteros, A.; Plou, F. J.; Alcalde, M., Decolorization of synthetic dyes by laccase immobilized on epoxy-activated carriers. *Process Biochemistry* **2008,** *43*, (2), 169.
282. Khan, A. A.; Akhtar, S.; Husain, Q., Direct immobilization of polyphenol oxidases on Celite 545 from ammonium sulphate fractionated proteins of potato (Solanum tuberosum). *Journal of Molecular Catalysis B-Enzymatic* **2006,** *40*, (1-2), 58.
283. Champagne, P.-P.; Ramsay, J. A., Reactive blue 19 decolouration by laccase immobilized on silica beads. *Applied Microbiology and Biotechnology* **2007,** *77*, (4), 819.
284. Regan, M. R.; Banerjee, I. A., Immobilization of invertase in germania matrix and a study of its enzymatic activity. *Journal of Sol-Gel Science and Technology* **2007,** *43*, (1), 27.
285. Tufvesson, P.; Tornvall, U.; Carvalho, J.; Karlsson, A. J.; Hatti-Kaul, R., Towards a cost-effective immobilized lipase for specialty chemicals. *Journal of Molecular Catalysis B-Enzymatic* **2011,** *68*, (2), 200.
286. Ansari, S. A.; Husain, Q., Potential applications of enzymes immobilized on/in nano materials: A review. *Biotechnology Advances* **2012,** *30*, (3), 512.
287. A matter of scale. *Nature Nanotechnology* **2016,** *11*, (9), 733.
288. Naik, R. R.; Tomczak, M. M.; Luckarift, H. R.; Spain, J. C.; Stone, M. O., Entrapment of enzymes and nanoparticles using biomimetically synthesized silica. *Chemical Communications* **2004**, (15), 1684.
289. Forsyth , C.; Patwardhan, S. V., Bioinsired silica for enzyme immobilisation: a comparison with traditional methods. In *Bio-Inspired Silicon-Based Materials, Advances in Silicon Science 5*, Springer Science: **2014**.
290. Patwardhan, S. V.; Manning, J. R. H.; Chiacchia, M., Bioinspired synthesis as a potential green method for the preparation of nanomaterials: Opportunities and challenges. *Curr. Opin. Green Sustain. Chem.* **2018,** *12*, 110.
291. Drummond, C.; McCann, R.; Patwardhan, S. V., A feasibility study of the biologically inspired green manufacturing of precipitated silica. *Chemical Engineering Journal* **2014,** *244*, 483.
292. Hartmann, M.; Kostrov, X., Immobilization of enzymes on porous silicas - benefits and challenges. *Chemical Society Reviews* **2013,** *42*, (15), 6277.
293. Ciullo, P. A., *Industrial Minerals and their Uses, A handbook and formulary*. Noyes Publication: United States of America, **1996**.

294. Pierre, A. C., The sol-gel encapsulation of enzymes. *Biocatalysis and Biotransformation* **2004,** *22*, (3), 145.
295. Hartmann, M.; Jung, D., Biocatalysis with enzymes immobilized on mesoporous hosts: the status quo and future trends. *Journal of Materials Chemistry* **2010,** *20*, (5), 844.
296. Hudson, S.; Magner, E.; Cooney, J.; Hodnett, B. K., Methodology for the immobilization of enzymes onto mesoporous materials. *Journal of Physical Chemistry B* **2005,** *109*, (41), 19496.
297. Hudson, S.; Cooney, J.; Magner, E., Proteins in mesoporous silicates. *Angewandte Chemie* **2008,** *47*, (45), 8582.
298. Livage, J.; Coradin, T.; Roux, C., Encapsulation of biomolecules in silica gels. *Journal of Physics: Condensed Matter* 2001.
299. Steven, C. R.; Busby, G. A.; Mather, C.; Tariq, B.; Briuglia, M. L.; Lamprou, D. A.; Urquhart, A. J.; Grant, M. H.; Patwardhan, S. V., Bioinspired silica as drug delivery systems and their biocompatibility. *Journal of Materials Chemistry B* **2014,** *2*, (31), 5028.
300. Patwardhan, S. V., Biomimetic and bioinspired silica: recent developments and applications. *Chem Commun (Camb)* **2011,** *47*, (27), 7567.
301. Coradin, T.; Lopez, P. J., Biogenic silica patterning: Simple chemistry or subtle biology? *ChemBioChem* **2003,** *4*, (4), 251.
302. Hoffmann, F.; Cornelius, M.; Morell, J.; Froba, M., Silica-based mesoporous organic-inorganic hybrid materials. *Angew. Chem.-Int. Edit.* **2006,** *45*, (20), 3216.
303. Malgras, V.; Ji, Q. M.; Kamachi, Y.; Mori, T.; Shieh, F. K.; Wu, K. C. W.; Ariga, K.; Yamauchi, Y., Templated Synthesis for Nanoarchitectured Porous Materials. *Bull. Chem. Soc. Jpn.* **2015,** *88*, (9), 1171.
304. Tang, F. Q.; Li, L. L.; Chen, D., Mesoporous Silica Nanoparticles: Synthesis, Biocompatibility and Drug Delivery. *Advanced Materials* **2012,** *24*, (12), 1504.
305. Lynch, M. M.; Liu, J. C.; Nigra, M.; Coppens, M. O., Chaperonin-Inspired pH Protection by Mesoporous Silica SBA-15 on Myoglobin and Lysozyme. *Langmuir* **2016,** *32*, (37), 9604.
306. Vinu, A.; Murugesan, V.; Hartmann, M., Adsorption of lysozyme over mesoporous molecular sieves MCM-41 and SBA-15: Influence of pH and aluminum incorporation. *Journal of Physical Chemistry B* **2004,** *108*, (22), 7323.
307. Belton, D. J.; Patwardhan, S. V.; Annenkov, V. V.; Danilovtseva, E. N.; Perry, C. C., From biosilicification to tailored materials: optimizing hydrophobic domains and resistance to protonation of polyamines. *Proc Natl Acad Sci U S A* **2008,** *105*, (16), 5963.
308. Hildebrand, M., Diatoms, Biomineralization Processes, and Genomics. *Chemical Reviews* **2008,** *108*, (11), 4855.
309. Belton, D. J.; Patwardhan, S. V.; Perry, C. C., Spermine, spermidine and their analogues generate tailored silicas. *Journal of Materials Chemistry* **2005,** *15*, (43), 4629.
310. Patwardhan, S. V.; Clarson, S. J.; Perry, C. C., On the role(s) of additives in bioinspired silicification. *Chemical Communications* **2005**, (9), 1113.
311. Tian, F. M.; Wu, W. J.; Broderick, M.; Vamvakaki, V.; Chaniotakis, N.; Dale, N., Novel microbiosensors prepared utilizing biomimetic silicification method. *Biosensors & Bioelectronics* **2010,** *25*, (11), 2408.
312. Roth, K. M.; Zhou, Y.; Yang, W. J.; Morse, D. E., Bifunctional small molecules are biomimetic catalysts for silica synthesis at neutral pH. *Journal of the American Chemical Society* **2005,** *127*, (1), 325.
313. Kuan, I. C.; Wu, J. C.; Lee, S. L.; Tsai, C. W.; Chuang, C. A.; Yu, C. Y., Stabilization of D-amino acid oxidase from Rhodosporidium toruloides by encapsulation in polyallylamine-mediated biomimetic silica. *Biochemical Engineering Journal* **2010,** *49*, (3), 408.
314. Belton, D.; Paine, G.; Patwardhan, S. V.; Perry, C. C., Towards an understanding of (bio)silicification: the role of amino acids and lysine oligomers in silicification. *Journal of Materials Chemistry* **2004,** *14*, (14), 2231.
315. Davidson, S.; Lamprou, D. A.; Urquhart, A. J.; Grant, M. H.; Patwardhan, S. V., Bioinspired Silica Offers a Novel, Green, and Biocompatible Alternative to Traditional Drug Delivery Systems. *ACS Biomaterials Science & Engineering* **2016,** *2*, (9), 1493.

316. Li, L.; Jiang, Z. Y.; Wu, H.; Feng, Y. N.; Li, J., Protamine-induced biosilica as efficient enzyme immobilization carrier with high loading and improved stability. *Materials Science & Engineering C-Materials for Biological Applications* **2009,** *29*, (6), 2029.
317. Betancor, L.; Luckarift, H. R., Bioinspired enzyme encapsulation for biocatalysis. *Trends in Biotechnology* **2008,** *26*, (10), 566.
318. Shi, J. F.; Zhang, L.; Jiang, Z. Y., Facile Construction of Multicompartment Multienzyme System through Layer-by-Layer Self-Assembly and Biomimetic Mineralization. *Acs Applied Materials & Interfaces* **2011,** *3*, (3), 881.
319. Luan, P. P.; Jiang, Y. J.; Zhang, S. P.; Gao, J.; Su, Z. G.; Ma, G. H.; Zhang, Y. F., Chitosan-mediated formation of biomimetic silica nanoparticles: An effective method for manganese peroxidase immobilization and stabilization. *Journal of Bioscience and Bioengineering* **2014,** *118*, (5), 575.
320. Chen, G. C.; Kuan, I. C.; Hong, J. R.; Tsai, B. H.; Lee, S. L.; Yu, C. Y., Activity enhancement and stabilization of lipase from Pseudomonas cepacia in polyallylamine-mediated biomimetic silica. *Biotechnology Letters* **2011,** *33*, (3), 525.
321. Lai, J. K.; Chuang, T. H.; Jan, J. S.; Wang, S. S. S., Efficient and stable enzyme immobilization in a block copolypeptide vesicle-templated biomimetic silica support. *Colloids and Surfaces B-Biointerfaces* **2010,** *80*, (1), 51.
322. Rao, A.; Bankar, A.; Shinde, A.; Kumar, A. R.; Gosavi, S.; Zinjarde, S., Phyto-inspired Silica Nanowires: Characterization and Application in Lipase Immobilization. *Acs Applied Materials & Interfaces* **2012,** *4*, (2), 871.
323. Haase, N. R.; Shian, S.; Sandhage, K. H.; Kroger, N., Biocatalytic Nanoscale Coatings Through Biomimetic Layer-by-Layer Mineralization. *Advanced Functional Materials* **2011,** *21*, (22), 4243.
324. Betancor, L.; Luckarift, H. R.; Seo, J. H.; Brand, O.; Spain, J. C., Three-dimensional immobilization of beta-galactosidase on a silicon surface. *Biotechnology and Bioengineering* **2008,** *99*, (2), 261.
325. Cazaban, D.; Illanes, A.; Wilson, L.; Betancor, L., Bio-inspired silica lipase nanobiocatalysts for the synthesis of fatty acid methyl esters. *Process Biochemistry* **2018,** *74*, 86.
326. Zamora, P.; Narvaez, A.; Dominguez, E., Enzyme-modified nanoparticles using biomimetically synthesized silica. *Bioelectrochemistry* **2009,** *76*, (1-2), 100.
327. Forsyth, C.; Yip, T. W. S.; Patwardhan, S. V., CO2 sequestration by enzyme immobilized onto bioinspired silica. *Chemical Communications* **2013,** *49*, (31), 3191.
328. Jo, B. H.; Seo, J. H.; Yang, Y. J.; Baek, K.; Choi, Y. S.; Pack, S. P.; Oh, S. H.; Cha, H. J., Bioinspired Silica Nanocomposite with Autoencapsulated Carbonic Anhydrase as a Robust Biocatalyst for CO2 Sequestration. *Acs Catalysis* **2014,** *4*, (12), 4332.
329. Min, K. H.; Son, R. G.; Ki, M. R.; Choi, Y. S.; Pack, S. P., High expression and biosilica encapsulation of alkaline-active carbonic anhydrase for CO2 sequestration system development. *Chemosphere* **2016,** *143*, 128.
330. Manning, J. R.; Routoula, E.; Patwardhan, S. V., Preparation of Functional Silica Using a Bioinspired Method. *JoVE* **2018**, (138), e57730.
331. Duran, N.; Rosa, M. A.; D'Annibale, A.; Gianfreda, L., Applications of laccases and tyrosinases (phenoloxidases) immobilized on different supports: a review. *Enzyme and Microbial Technology* **2002,** *31*, (7), 907.
332. Fernandez-Fernandez, M.; Sanroman, M. A.; Moldes, D., Recent developments and applications of immobilized laccase. *Biotechnology Advances* **2013,** *31*, (8), 1808.
333. Bilal, M.; Asgher, M.; Parra-Saldivar, R.; Hu, H. B.; Wang, W.; Zhang, X. H.; Iqbal, H. M. N., Immobilized ligninolytic enzymes: An innovative and environmental responsive technology to tackle dye-based industrial pollutants - A review. *Sci. Total Environ.* **2017,** *576*, 646.
334. Khan, A. A.; Husain, Q., Decolorization and removal of textile and non-textile dyes from polluted wastewater and dyeing effluent by using potato (Solanum tuberosum) soluble and immobilized polyphenol oxidase. *Bioresource Technology* **2007,** *98*, (5), 1012.
335. Sun, H. Y.; Jin, X. Y.; Jiang, F.; Zhang, R. F., Immobilization of horseradish peroxidase on ZnO nanowires/macroporous SiO2 composites for the complete decolorization of anthraquinone dyes. *Biotechnology and Applied Biochemistry* **2018,** *65*, (2), 220.

336. Abadulla, E.; Tzanov, T.; Costa, S.; Robra, K. H.; Cavaco-Paulo, A.; Gubitz, G. M., Decolorization and detoxification of textile dyes with a laccase from Trametes hirsuta. *Applied and Environmental Microbiology* **2000,** *66*, (8), 3357.
337. Sekuljica, N. Z.; Prlainovic, N. Z.; Jakovetic, S. M.; Grbavcic, S. Z.; Ognjanovic, N. D.; Knezevic-Jugovic, Z. D.; Mijin, D. Z., Removal of Anthraquinone Dye by Cross-Linked Enzyme Aggregates From Fresh Horseradish Extract. *Clean-Soil Air Water* **2016,** *44*, (7), 891.
338. Sekuljica, N. Z.; Gvozdenovic, M. M.; Knezevic-Jugovic, Z. D.; Jugovic, B. Z.; Grgur, B. N., Biofuel cell based on horseradish peroxidase immobilized on copper sulfide as anode for decolorization of anthraquinone AV109 dye. *J. Energy Chem.* **2016,** *25*, (3), 403.
339. E. Routoula, S. V. P., Degradation of Anthraquinone Dyes from Effluents: A Review Focusing on Enzymatic Dye Degradation with Industrial Potential. *Environ. Sci. Technol.* **2020,** *54*, (2), 647.
340. Zille, A.; Tzanov, T.; Gubitz, G. M.; Cavaco-Paulo, A., Immobilized laccase for decolourization of Reactive Black 5 dyeing effluent. *Biotechnology Letters* **2003,** *25*, (17), 1473.
341. Novozymes Forest Products - Standard product range. (18/1/19),
342. Stuart, B., Experimental methods. In *Infrared Spectroscopy: Fundamentals and Applications*, Stuart, B., Ed. John Wiley & Sons, Ltd: Wiltshire, UK, **2004;** pp 15.
343. Vernon-Parry, K. D., Scanning electron microscopy: an introduction. *III-Vs Review* **2000,** *13*, (4), 40.
344. Joy, D. C., The thory and practice of high-resolution scanning electron-microscopy. *Ultramicroscopy* **1991,** *37*, (1-4), 216.
345. Zhou , W.; Apkarian, R.; Wang, Z. L.; Joy, D., Fundamentals of Scanning Electron Microscopy (SEM). In *Scanning Microscopy for NanotechnologyTechniques and Applications*, **Zhou** , W.; W**ang ,** Z. L., Eds. Springer: New York, **2007;** pp 1.
346. Sing, K. S. W.; Everett, D. H.; Haul, R. A. W.; Moscou, L.; Pierotti, R. A.; Rouquerol, J.; Siemieniewska, T., Reporting physisorption data for gas solid systems with special reference to the determination of surface area and porosity (recommentations 1984). *Pure Appl. Chem.* **1985,** *57*, (4), 603.
347. Sing, K. S. W.; Williams, R. T., Physisorption hysteresis loops and the characterization of nanoporous materials. *Adsorption Science & Technology* **2004,** *22*, (10), 773.
348. Thommes, M.; Kaneko, K.; Neimark, A. V.; Olivier, J. P.; Rodriguez-Reinoso, F.; Rouquerol, J.; Sing, K. S. W., Physisorption of gases, with special reference to the evaluation of surface area and pore size distribution (IUPAC Technical Report). *Pure Appl. Chem.* **2015,** *87*, (9-10), 1051.
349. Rouquerol, J.; Llewellyn, P.; Rouquerol, F., Is the bet equation applicable to microporous adsorbents? In *Studies in Surface Science and Catalysis*, Llewellyn, P. L.; Rodriquez-Reinoso, F.; Rouqerol, J.; Seaton, N., Eds. Elsevier: **2007;** Vol. 160, pp 49.
350. Mikhail, R. S.; Brunauer, S.; Bodor, E. E., Investigations of a complete pore structure analysis. I. Analysis of micropores. *J. Colloid Interface Sci.* **1968,** *26*, (1), 45.
351. Galarneau, A.; Villemot, F.; Rodriguez, J.; Fajula, F.; Coasne, B., Validity of the t-plot Method to Assess Microporosity in Hierarchical Micro/Mesoporous Materials. *Langmuir* **2014,** *30*, (44), 13266.
352. Tarazona, P.; Marconi, U. M. B.; Evans, R., Phase-equilibria of fluid interfaces and confined fluids - NonLocal versus Local Density functionals *Mol. Phys.* **1987,** *60*, (3), 573.
353. Young, R. J.; Lovell, P. A., Characterization. In *Introduction to polymers*, Young, R. J. L., P.A.;, Ed. Nelson Thornes Ltd: **1991**.
354. Zhang, F.; Ilavsky, J., Ultra-Small-Angle X-ray Scattering of Polymers. *Polym. Rev.* **2010,** *50*, (1), 59.
355. Ilavsky, J.; Zhang, F.; Allen, A. J.; Levine, L. E.; Jemian, P. R.; Long, G. G., Ultra-Small-Angle X-ray Scattering Instrument at the Advanced Photon Source: History, Recent Development, and Current Status. *Metall. Mater. Trans. A-Phys. Metall. Mater. Sci.* **2013,** *44A*, (1), 68.
356. Boldon, L.; Laliberte, F.; Liu, L., Review of the fundamental theories behind small angle X-ray scattering, molecular dynamics simulations, and relevant integrated application. *Nano Rev. Exp.* **2015,** *6*, (1), 21.

357. Beaucage, G.; Kammler, H. K.; Pratsinis, S. E., Particle size distributions from small-angle scattering using global scattering functions. *J. Appl. Crystallogr.* **2004,** *37*, 523.
358. Ilavsky, J.; Zhang, F.; Andrews, R. N.; Kuzmenko, I.; Jemian, P. R.; Levine, L. E.; Allen, A. J., Development of combined microstructure and structure characterization facility for in situ and operando studies at the Advanced Photon Source. *J. Appl. Crystallogr.* **2018,** *51*, 867.
359. Ilavsky, J., Nika: software for two-dimensional data reduction. *J. Appl. Crystallogr.* **2012,** *45*, 324.
360. Ilavsky, J.; Jemian, P. R., Irena: tool suite for modeling and analysis of small-angle scattering. *J. Appl. Crystallogr.* **2009,** *42*, 347.
361. Roach, P.; Shirtcliffe, N. J.; Farrar, D.; Perry, C. C., Quantification of surface-bound proteins by fluorometric assay: Comparison with quartz crystal microbalance and amido black assay. *Journal of Physical Chemistry B* **2006,** *110*, (41), 20572.
362. Aitken, A.; Learmonth, M. P., Protein Determination by UV Absorption. In *The Protein Protocols Handbook, 2nd Edition*, J. M. Walker Ed. Humana Press Inc.: Totowa, NJ, **2003;** pp 3.
363. Dartigalongue, T.; Niezborala, C.; Hache, F., Subpicosecond UV spectroscopy of carbonmonoxy-myoglobin: absorption and circular dichroism studies. *Physical Chemistry Chemical Physics* **2007,** *9*, (13), 1611.
364. Song, X. K.; Jiang, Z. Y.; Li, L.; Wu, H., Immobilization of beta-glucuronidase in lysozyme-induced biosilica particles to improve its stability. *Front. Chem. Sci. Eng.* **2014,** *8*, (3), 353.
365. Arica, M. Y.; Yavuz, H.; Patir, S.; Denizli, A., Immobilization of glucoamylase onto spacer-arm attached magnetic poly(methylmethacrylate) microspheres: characterization and application to a continuous flow reactor. *Journal of Molecular Catalysis B-Enzymatic* **2000,** *11*, (2-3), 127.
366. Chequer Drumond, F. M.; Rodrigues de Oliveira, G. A.; Ferraz, E. R. A.; Cardoso, J. C.; Zanoni, M. V. B.; de Oliveira, D. P., Textile Dyes: Dyeing Process and Environmental Impact. In *Eco-Friendly Textile Dyeing and Finishing*, Gunay, M., Ed. InTech: **2013;** pp 151.
367. Branchi, B.; Galli, C.; Gentili, P., Kinetics of oxidation of benzyl alcohols by the dication and radical cation of ABTS. Comparison with laccase-ABTS oxidations: an apparent paradox. *Org. Biomol. Chem.* **2005,** *3*, (14), 2604.
368. dos Santos, A. B.; Cervantes, F. J.; van Lier, J. B., Review paper on current technologies for decolourisation of textile wastewaters: Perspectives for anaerobic biotechnology. *Bioresource Technology* **2007,** *98*, (12), 2369.
369. Shuler, M. L.; Kargi, F., Chapter 3: Enzymes. In *Bioprocess Engineering, Basic Concepts, 2nd edition*, Shuler, M. L.; Kargi, F., Eds. Prentice Hall PTR: **2002;** pp 57.
370. Bardsley, W. G.; Leff, P.; Kavanagh, J.; Waight, R. D., Deviations from Michaelis-Menten kinetics - The possibility of complicated curves for simple kinetic schemes and the computer fitting of experimental-data for acetycholin-esterase, acid-phosphatase, adenosine-deaminase, arylsulfatase, benzylamine oxidase, chymotrypsin, fumarase, galactose dehydrogenase, beta-galactosidase, lactate-dehydrogenase, peroxidase and xanthine-oxidase-d. *Biochemical Journal* **1980,** *187*, (3), 739.
371. Galende, P. P.; Cuadrado, N. H.; Kostetsky, E. Y.; Roig, M. G.; Villar, E.; Shnyrov, V. L.; Kennedy, J. F., Kinetics of Spanish broom peroxidase obeys a Ping-Pong Bi-Bi mechanism with competitive inhibition by substrates. *International Journal of Biological Macromolecules* **2015,** *81*, 1005.
372. Singh, P.; Gupta, P.; Singh, R.; Sharma, R., Activity and stability of immobilized alpha-amylase produced by Bacillus acidocaldarius. *International Journal of Pharmacy and LifeSciences* 2012.
373. Woo, S. H.; Cho, J. S.; Lee, B. S.; Kim, E. K., Decolorization of melanin by lignin peroxidase from Phanerochaete chrysosporium. *Biotechnology and Bioprocess Engineering* **2004,** *9*, (4), 256.
374. Re, R.; Pellegrini, N.; Proteggente, A.; Pannala, A.; Yang, M.; Rice-Evans, C., Antioxidant activity applying an improved ABTS radical cation decolorization assay. *Free Radic. Biol. Med.* **1999,** *26*, (9-10), 1231.

375. Gulcin, I.; Huyut, Z.; Elmastas, M.; Aboul-Enein, H. Y., Radical scavenging and antioxidant activity of tannic acid. *Arab. J. Chem.* **2010,** *3*, (1), 43.
376. Owen, T., Sample handling and measurement In *Fundamentals of Modern UV-Visible Spectroscopy : A Primer*

Owen, T., Ed. Hewlett Packard: Germany, **1996;** pp 64.
377. Asghar, M. N.; Khan, I. U.; Zia, I.; Ahmad, M.; Qureshi, F. A., Modified 2,2 '-azinobis(3-ethylbenzo thiazoline)-6-sulphonic acid radical cation decolorization assay for antioxidant activity of human plasma and extracts of traditional medicinal plants. *Acta Chim. Slov.* **2008,** *55*, (2), 408.
378. Rodriguez-Couto, S.; Osma, J. F.; Toca-Herrera, J. L., Removal of synthetic dyes by an eco-friendly strategy. *Engineering in Life Sciences* **2009,** *9*, (2), 116.
379. Jolly, Y. N.; Islam, A., Characterization of dye industry effluent and assessment of its suitability for irrigation purpose. *Journal of Bangladesh Academy of Sciences* **2009,** *33*, (1), 99.
380. Islam, A.; Guha, A. K., Removal of pH, TDS and Color from Textile Effluent by Using Coagulants and Aquatic/Non Aquatic Plants as Adsorbents. *Resources and Environment* **2013,** *3*, (5), 101.
381. Zhang, F.; Zheng, B.; Zhang, J. L.; Huang, X. L.; Liu, H.; Guo, S. W.; Zhang, J. Y., Horseradish Peroxidase Immobilized on Graphene Oxide: Physical Properties and Applications in Phenolic Compound Removal. *Journal of Physical Chemistry C* **2010,** *114*, (18), 8469.
382. Krainer, F. W.; Glieder, A., An updated view on horseradish peroxidases: recombinant production and biotechnological applications. *Applied Microbiology and Biotechnology* **2015,** *99*, (4), 1611.
383. Ballou, A., Gerald; Murray, L., The effects of different buffers on the activity of beta-amylase. *J. Biol. Chem.* **1941,** *139*, 233.
384. Ugwu, S. O.; Apte, S. P., The Effect of Buffers on Protein Conformational Stability. *Pharmaceutical Technology* **2004,** *28*, 86.
385. Bradford, M. M., A Rapid and Sensitive Method for the Quantitation of Microgram Quantities of Protein Utilizing the Principle of Protein-Dye Binding. *Anal. Biochem.* **1976,** *72*, 248.
386. Lu, T.-S.; Yiao, S.-Y.; Lim, K.; Jensen, R. V.; Hsiao, L.-L., Interpretation of biological and mechanical variations between the Lowry versus Bradford method for protein quantification. *N Am J Med Sci* **2010,** *2*, (7), 325.
387. Manning, J. R. H. Sustainable Chemistry & Process Intensification of Bioinspired Silica Materials. The University of Sheffield, Sheffield, **2019**.
388. Compton, S. J.; Jones, C. G., Mechanism of dye response and interference in the Bradford protein assay. *Analytical Biochemistry* **1985,** *151*, (2), 369.
389. Nguyen, Q. X.; Belgard, T. G.; Taylor, J. J.; Murthy, V. S.; Halas, N. J.; Wong, M. S., Water-Phase Synthesis of Cationic Silica/Polyamine Nanoparticles. *Chemistry of Materials* **2012,** *24*, (8), 1426.
390. Noel, S.; Liberelle, B.; Robitaille, L.; De Crescenzo, G., Quantification of Primary Amine Groups Available for Subsequent Biofunctionalization of Polymer Surfaces. *Bioconjugate Chem.* **2011,** *22*, (8), 1690.
391. Nicolas, P.; Lassalle, V. L.; Ferreira, M. L., Quantification of immobilized Candida antarctica lipase B (CALB) using ICP-AES combined with Bradford method. *Enzyme and Microbial Technology* **2017,** *97*, 97.
392. Ge, Y.; Chen, Y.; Li, C.; Wei, M.; Lv, J.; Meng, K., Inhibitory effects of sodium silicate on the fungal growth and secretion of cell wall-degrading enzymes by Trichothecium roseum. *Journal of Phytopathology* **2017,** *165*, (9), 620.
393. Wu, X. Y.; Narsimhan, G., Effect of surface concentration on secondary and tertiary conformational changes of lysozyme adsorbed on silica nanoparticles. *Biochimica Et Biophysica Acta-Proteins and Proteomics* **2008,** *1784*, (11), 1694.
394. Jensen, H. B.; Kleppe, K., Effect of ionic strength, pH, amines and divalent cations on lytic activity of T4 Lysozyme. *European Journal of Biochemistry* **1972,** *28*, (1), 116.
395. Gasteiger, E.; Christine, H.; Alexandre, G.; Séverine, D.; Wilkins, M. R.; Appel, R. D.; Bairoch, a. A., Protein Identification and Analysis Tools on the ExPASy Server. In *The*

Proteomics Protocols Handbook, Walker, J. M., Ed. Humana Press Inc: Totowa, NJ, **2005;** pp 571.
396. Welinder, K. G., Amino-acid sequence studies of horseradish-peroxidase. Amino and carboxyl termini, cyanogen-bromide and tryptic fragments, the complete sequence, and some structural characteristics of horseradish peroxidase-c. *European Journal of Biochemistry* **1979,** *96*, (3), 483.
397. Jachimska, B.; Jasinski, T.; Warszynski, P.; Adamczyk, Z., Conformations of poly(allylamine hydrochloride) in electrolyte solutions: Experimental measurements and theoretical modeling. *Colloid Surf. A-Physicochem. Eng. Asp.* **2010,** *355*, (1-3), 7.
398. Wei, Y.; Xu, J. G.; Feng, Q. W.; Dong, H.; Lin, M. D., Encapsulation of enzymes in mesoporous host materials via the nonsurfactant-templated sol-gel process. *Materials Letters* **2000,** *44*, (1), 6.
399. Tsai, H. C.; Doong, R. A., Preparation and characterization of urease-encapsulated biosensors in poly(vinyl alcohol)-modified silica sol-gel materials. *Biosens Bioelectron* **2007,** *23*, (1), 66.
400. Patwardhan, S. V.; Taori, V. P.; Hassan, M.; Agashe, N. R.; Franklin, J. E.; Beaucage, G.; Mark, J. E.; Clarson, S. J., An investigation of the properties of poly(dimethylsiloxane)-bioinspired silica hybrids. *Eur. Polym. J.* **2006,** *42*, (1), 167.
401. Grill, A., Porous pSiCOH Ultralow-kDielectrics for Chip Interconnects Prepared by PECVD. *Annual Review of Materials Research* **2009,** *39*, (1), 49.
402. Munusamy, P.; Sanghavi, S.; Varga, T.; Suntharampillai, T., Silica supported ceria nanoparticles: a hybrid nanostructure to increase stability and surface reactivity of nano-crystalline ceria. *Rsc Advances* **2014,** *4*, (17), 8421.
403. Barth, A., Infrared spectroscopy of proteins. *Biochimica et biophysica acta* **2007,** *1767*, (9), 1073.
404. Hilal, S. H.; Karickhoff, S. W.; Carreira, L. A., A rigorous test for SPARC's chemical reactivity models: Estimation of more than 4300 ionization pK(a)s. *Quant. Struct.-Act. Relat.* **1995,** *14*, (4), 348.
405. Lee, C.-H.; Lin, T.-S.; Mou, C.-Y., Mesoporous materials for encapsulating enzymes. *Nano Today* 2009.
406. Cardoso, M. B.; Luckarift, H. R.; Urban, V. S.; O'Neill, H.; Johnson, G. R., Protein Localization in Silica Nanospheres Derived via Biomimetic Mineralization. *Advanced Functional Materials* **2010,** *20*, (18), 3031.
407. Grace&Co.-Conn.;, W. R. *Syloid FP Silica*; Online, 2014.
408. Waters, L. J.; Hanrahan, J. P.; Tobin, J. M.; Finch, C. V.; Parkes, G. M. B.; Ahmad, S. A.; Mohammad, F.; Saleem, M., Enhancing the dissolution of phenylbutazone using Syloid based mesoporous silicas for oral equine applications. *J. Pharm. Anal.* **2018,** *8*, (3), 181.
409. Zheng, Y.; Zhang, S.; Miao, S.; Su, Z.; Wang, P., Temperature sensitivity of cellulase adsorption on lignin and its impact on enzymatic hydrolysis of lignocellulosic biomass. *Journal of Biotechnology* **2013,** *166*, (3), 135.
410. Zhang, X.; Guan, R. F.; Wu, D. Q.; Chan, K. Y., Enzyme immobilization on amino-functionalized mesostructured cellular foam surfaces, characterization and catalytic properties. *Journal of Molecular Catalysis B-Enzymatic* **2005,** *33*, (1-2), 43.
411. Szymańska, K.; Bryjak, J.; Mrowiec-Białoń, J.; Jarzębski, A. B., Application and properties of siliceous mesostructured cellular foams as enzymes carriers to obtain efficient biocatalysts. *Microporous and Mesoporous Materials* **2007,** *99*, (1-2), 167.
412. Deere, J.; Magner, E.; Wall, J. G.; Hodnett, B. K., Mechanistic and structural features of protein adsorption onto mesoporous silicates. *Journal of Physical Chemistry B* **2002,** *106*, (29), 7340.
413. Diaz, J. F.; Balkus, K. J., Enzyme immobilization in MCM-41 molecular sieve. *Journal of Molecular Catalysis B-Enzymatic* **1996,** *2*, (2-3), 115.
414. Andrade, J. D.; Hlady, V., Protein Adsorption and Materials Biocompatability - A tutorial review and suggested hypotheses. *Adv. Polym. Sci.* **1986,** *79*, 1.
415. Luckarift, H. R.; Spain, J. C.; Naik, R. R.; Stone, M. O., Enzyme immobilization in a biomimetic silica support. *Nature biotechnology* **2004,** *22*, (2), 211.

416. Gill, I.; Ballesteros, A., Encapsulation of biologicals within silicate, siloxane, and hybrid sol-gel polymers: An efficient and generic approach. *Journal of the American Chemical Society* **1998,** *120*, (34), 8587.
417. Yu, Y. H.; Chen, B. W.; Qi, W.; Li, X. L.; Shin, Y.; Lei, C. H.; Liu, J., Enzymatic conversion of CO2 to bicarbonate in functionalized mesoporous silica. *Microporous and Mesoporous Materials* **2012,** *153*, 166.
418. Fan, J.; Lei, J.; Wang, L. M.; Yu, C. Z.; Tu, B.; Zhao, D. Y., Rapid and high-capacity immobilization of enzymes based on mesoporous silicas with controlled morphologies. *Chemical Communications* **2003**, (17), 2140.
419. Sekuljica, N. Z.; Prlainovic, N. Z.; Lucic, N. Z.; Aleksandra, M. J.; Grbavcic, S. Z.; Dusan, Ţ. M.; Zorica, D.; Knejevic-Jugovic, Immobilization of peroxidase from fresh horseradish extract for anthraquinone dye decolorization. *Zastita Materijala* **2015,** *56*, (3), 335.
420. Pramparo, L.; Stuber, F.; Font, J.; Fortuny, A.; Fabregat, A.; Bengoa, C., Immobilisation of horseradish peroxidase on Eupergit (R) C for the enzymatic elimination of phenol. *Journal of Hazardous Materials* **2010,** *177*, (1-3), 990.
421. Jiang, Y. J.; Cui, C. C.; Zhou, L. Y.; He, Y.; Gao, J., Preparation and Characterization of Porous Horseradish Peroxidase Microspheres for the Removal of Phenolic Compound and Dye. *Industrial & Engineering Chemistry Research* **2014,** *53*, (18), 7591.
422. Feinle, A.; Elsaesser, M. S.; Husing, N., Sol-gel synthesis of monolithic materials with hierarchical porosity. *Chemical Society Reviews* **2016,** *45*, (12), 3377.
423. Zadeh, P. S. N.; Akerman, B., Immobilization of Enzymes in Mesoporous Silica Particles: Protein Concentration and Rotational Mobility in the Pores. *Journal of Physical Chemistry B* **2017,** *121*, (12), 2575.
424. Gossl, D.; Singer, H.; Chiu, H. Y.; Schmidt, A.; Lichtnecker, M.; Engelke, H.; Bein, T., Highly active enzymes immobilized in large pore colloidal mesoporous silica nanoparticles. *New Journal of Chemistry* **2019,** *43*, (4), 1671.
425. Tortajada, M.; Ramon, N.; Beltran, D.; Amoros, P., Hierarchical bimodal porous silicas and organosilicas for enzyme immobilization. *Journal of Materials Chemistry* **2005,** *15*, (35-36), 3859.
426. Chen, C.-C.; Do, J.-S.; Gu, Y., Immobilization of HRP in Mesoporous Silica and Its Application for the Construction of Polyaniline Modified Hydrogen Peroxide Biosensor. *Sensors* **2009,** *9*, (6), 4635.
427. Nguyen, L. T.; Lau, Y. S.; Yang, K. L., Entrapment of cross-linked cellulase colloids in alginate beads for hydrolysis of cellulose. *Colloids and Surfaces B-Biointerfaces* **2016,** *145*, 862.
428. Zhang, W. Z.; Xu, F., Hierarchical Composites Promoting Immobilization and Stabilization of Phytase via Transesterification/Silification of Modulated Alginate Hydrogels. *ACS Sustainable Chemistry & Engineering* **2015,** *3*, (11), 2694.
429. Cao, X. D.; Yu, J. C.; Zhang, Z. Q.; Liu, S. Q., Bioactivity of horseradish peroxidase entrapped in silica nanospheres. *Biosensors & Bioelectronics* **2012,** *35*, (1), 101.
430. Rodriguez, J.; Soria, F.; Geronazzo, H.; Destefanis, H., alpha-Amylase Aspergillus oryzae Immobilized on Modified Expanded Perlite. *International Journal of Chemical Reactor Engineering* **2014,** *12*, (1), 10.
431. Kandelbauer, A.; Maute, O.; Kessler, R. W.; Erlacher, A.; Gubitz, G. M., Study of dye decolorization in an immobilized laccase enzyme-reactor using online spectroscopy. *Biotechnology and Bioengineering* **2004,** *87*, (4), 552.
432. Peralta-Zamora, P.; Pereira, C. M.; Tiburtius, E. R. L.; Moraes, S. G.; Rosa, M. A.; Minussi, R. C.; Duran, N., Decolorization of reactive dyes by immobilized laccase. *Applied Catalysis B-Environmental* **2003,** *42*, (2), 131.
433. Farias, S.; Mayer, D. A.; de Oliveira, D.; de Souza, S.; de Souza, A. A. U., Free and Ca-Alginate Beads Immobilized Horseradish Peroxidase for the Removal of Reactive Dyes: an Experimental and Modeling Study. *Applied Biochemistry and Biotechnology* **2017,** *182*, (4), 1290.
434. Vasquez, C.; Anderson, D.; Oyarzun, M.; Carvajal, A.; Palma, C., Method for the stabilization and immobilization of enzymatic extracts and its application to the decolorization of textile dyes. *Biotechnology Letters* **2014,** *36*, (10), 1999.

435. Mohan, S. V.; Prasad, K. K.; Rao, N. C.; Sarma, P. N., Acid azo dye degradation by free and immobilized horseradish peroxidase (HRP) catalyzed process. *Chemosphere* **2005,** *58*, (8), 1097.
436. Wasak, A.; Drozd, R.; Struk, L.; Grygorcewicz, B., Entrapment of DyP-type peroxidase from Pseudomonas fluorescens Pf-5 into Ca-alginate magnetic beads. *Biotechnology and Applied Biochemistry* **2018,** *65*, (2), 238.
437. Johnson, K. A.; Goody, R. S., The Original Michaelis Constant: Translation of the 1913 Michaelis-Menten Paper. *Biochemistry* **2011,** *50*, (39), 8264.
438. Krainer, F. W.; Pletzenauer, R.; Rossetti, L.; Herwig, C.; Glieder, A.; Spadiut, O., Purification and basic biochemical characterization of 19 recombinant plant peroxidase isoenzymes produced in Pichia pastoris. *Protein Expression and Purification* **2014,** *95*, 104.
439. Valderrama, B.; Ayala, M.; Vazquez-Duhalt, R., Suicide inactivation of peroxidases and the challenge of engineering more robust enzymes. *Chem. Biol.* **2002,** *9*, (5), 555.
440. Ogola, H. J. O.; Hashimoto, N.; Miyabe, S.; Ashida, H.; Ishikawa, T.; Shibata, H.; Sawa, Y., Enhancement of hydrogen peroxide stability of a novel Anabaena sp DyP-type peroxidase by site-directed mutagenesis of methionine residues. *Applied Microbiology and Biotechnology* **2010,** *87*, (5), 1727.
441. Jaladi, H.; Katiyar, A.; Thiel, S. W.; Guliants, V. V.; Pinto, N. G., Effect of pore diffusional resistance on biocatalytic activity of Burkholderia cepacia lipase immobilized on SBA-15 hosts. *Chemical Engineering Science* **2009,** *64*, (7), 1474.
442. Patel, A. C.; Li, S. X.; Yuan, J. M.; Wei, Y., In situ encapsulation of horseradish peroxidase in electrospun porous silica fibers for potential biosensor applications. *Nano Letters* **2006,** *6*, (5), 1042.
443. Amaya-Delgado, L.; Hidalgo-Lara, M. E.; Montes-Horcasitas, M. C., Hydrolysis of sucrose by invertase immobilized on nylon-6 microbeads. *Food Chemistry* **2006,** *99*, (2), 299.
444. Lettera, V.; Pezzella, C.; Cicatiello, P.; Piscitelli, A.; Giacobelli, V. G.; Galano, E.; Amoresano, A.; Sannia, G., Efficient immobilization of a fungal laccase and its exploitation in fruit juice clarification. *Food Chemistry* **2016,** *196*, 1272.
445. Arnao, M. B.; SanchezBravo, J.; Acosta, M., Indole-3-carbinol as a scavenger of free radicals. *Biochem. Mol. Biol. Int.* **1996,** *39*, (6), 1125.
446. Hosseinkhani, S.; Nemat-Gorgani, M., Partial unfolding of carbonic anhydrase provides a method for its immobilization on hydrophobic adsorbents and protects it against irreversible thermoinactivation. *Enzyme and Microbial Technology* **2003,** *33*, (2-3), 179.
447. Cui, R.; Bai, C. H.; Jiang, Y. C.; Hu, M. C.; Li, S. N.; Zhai, Q. G., Well-defined bioarchitecture for immobilization of chloroperoxidase on magnetic nanoparticles and its application in dye decolorization. *Chemical Engineering Journal* **2015,** *259*, 640.
448. Chakrabarti, S.; Bhattacharya, S.; Bhattacharya, S. K., Immobilization of D-ribulose-1,5-bisphosphate carboxylase/oxygenase - A step toward carbon dioxide fixation bioprocess. *Biotechnology and Bioengineering* **2003,** *81*, (6), 705.
449. Pawar, S. H.; Bohara, R. A.; Thorat, N. D., Immobilization of cellulase on functionalized cobalt ferrite nanoparticles. *The Korean Journal of Chemical Engineering* **2016,** *33*, (1), 216.
450. Greiner, R.; Sajidan, Production of D-myo-inositol(1,2,4,5,6)pentakisphosphate using alginate-entrapped recombinant Pantoea agglomerans glucose-1-phosphatase. *Brazilian Archives of Biology and Technology* **2008,** *51*, (2), 235.
451. Mahmoodi, N. M.; Arabloo, M.; Abdi, J., Laccase immobilized manganese ferrite nanoparticle: Synthesis and LSSVM intelligent modeling of decolorization. *Water Research* **2014,** *67*, 216.
452. Al-Bagmi, M. S.; Khan, M. S.; Ismael, M. A.; Al-Senaidy, A. M.; Ben Bacha, A.; Husain, F. M.; Alamery, S. F., An efficient methodology for the purification of date palm peroxidase: Stability comparison with horseradish peroxidase (HRP). *Saudi J. Biol. Sci.* **2019,** *26*, (2), 301.
453. Kumar, V.; Misra, N.; Goel, N. K.; Thakar, R.; Gupta, J.; Varshney, L., A horseradish peroxidase immobilized radiation grafted polymer matrix: a biocatalytic system for dye waste water treatment. *Rsc Advances* **2016,** *6*, (4), 2974.
454. Humer, D.; Spadiut, O., Improving the Performance of Horseradish Peroxidase by Site-Directed Mutagenesis. *International Journal of Molecular Sciences* **2019,** *20*, (4), 14.

455. Goodwin, D. C.; Yamazaki, I.; Aust, S. D.; Grover, T. A., Determination of rate constants for rapid Peroxidase reactions. *Analytical Biochemistry* **1995,** *231*, (2), 333.
456. Ozgen, M.; Reese, R. N.; Tulio, A. Z.; Scheerens, J. C.; Miller, A. R., Modified 2,2-azino-bis-3-ethylbenzothiazoline-6-sulfonic acid (ABTS) method to measure antioxidant capacity of selected small fruits and comparison to ferric reducing antioxidant power (FRAP) and 2,2 '-diphenyl-1-picrylhydrazyl (DPPH) methods. *Journal of Agricultural and Food Chemistry* **2006,** *54*, (4), 1151.
457. Epolito, W. J.; Lee, Y. H.; Bottomley, L. A.; Pavlostathis, S. G., Characterization of the textile anthraquinone dye Reactive Blue 4. *Dyes and Pigments* **2005,** *67*, (1), 35.
458. Radovic, M. D.; Mitrovic, J. Z.; Bojic, D. V.; Antonijevic, M. D.; Kostic, M. M.; Baosic, R. M.; Bojic, A. L., Effects of system parameters and inorganic salts on the photodecolourisation of textile dye Reactive Blue 19 by UV/H2O2 process. *Water SA* **2014,** *40*, (3), 571.
459. Mohamad, N. R.; Marzuki, N. H.; Buang, N. A.; Huyop, F.; Wahab, R. A., An overview of technologies for immobilization of enzymes and surface analysis techniques for immobilized enzymes. *Biotechnology, biotechnological equipment* **2015,** *29*, (2), 205.
460. Kadnikova, E. N.; Kostic, N. M., Oxidation of ABTS by hydrogen peroxide catalyzed by horseradish peroxidase encapsulated into sol-gel glass. Effects of glass matrix on reactivity. *Journal of Molecular Catalysis B-Enzymatic* **2002,** *18*, (1-3), 39.
461. Haki, G., Developments in industrially important thermostable enzymes: a review. *Bioresource Technology* **2003,** *89*, (1), 17.
462. Vieille, C.; Zeikus, G. J., Hyperthermophilic enzymes: sources, uses, and molecular mechanisms for thermostability. *Microbiology and molecular biology reviews : MMBR* **2001,** *65*, (1), 1.
463. Bilal, M.; Iqbal, H. M. N.; Shah, S. Z. H.; Hu, H. B.; Wang, W.; Zhang, X. H., Horseradish peroxidase-assisted approach to decolorize and detoxify dye pollutants in a packed bed bioreactor. *Journal of Environmental Management* **2016,** *183*, 836.
464. Xu, R.; Yuan, J. M.; Si, Y. F.; Li, F. T.; Zhang, B. R., Estrone removal by horseradish peroxidase immobilized on a nanofibrous support with Fe3O4 nanoparticles. *Rsc Advances* **2016,** *6*, (5), 3927.
465. Akhtar, S.; Husain, Q., Potential applications of immobilized bitter gourd (Momordica charantia) peroxidase in the removal of phenols from polluted water. *Chemosphere* **2006,** *65*, (7), 1228.
466. Guerrero, E.; Aburto, P.; Terres, E.; Villegas, O.; Gonzalez, E.; Zayas, T.; Hernandez, F.; Torres, E., Improvement of catalytic efficiency of chloroperoxidase by its covalent immobilization on SBA-15 for azo dye oxidation. *Journal of Porous Materials* **2013,** *20*, (2), 387.
467. Iqbal, H. M. N.; Asgher, M., Decolorization applicability of sol-gel matrix immobilized manganese peroxidase produced from an indigenous white rot fungal strain Ganoderma lucidum. *Bmc Biotechnology* **2013,** *13*, 7.
468. Chagas, P. M. B.; Torres, J. A.; Silva, M. C.; Correa, A. D., Immobilized soybean hull peroxidase for the oxidation of phenolic compounds in coffee processing wastewater. *International Journal of Biological Macromolecules* **2015,** *81*, 568.
469. Ozdemir, E., Biomimetic CO2 Sequestration: 1. Immobilization of Carbonic Anhydrase within Polyurethane Foam. *Energy & Fuels* **2009,** *23*, 5725.
470. Bakker, M.; van de Velde, F.; van Ranwijk, F.; Sheldon, R. A., Highly efficient immobilization of glycosylated enzymes into polyurethane foams. *Biotechnology and Bioengineering* **2000,** *70*, (3), 342.
471. Tzialla, A. A.; Pavlidis, I. V.; Felicissimo, M. P.; Rudolf, P.; Gournis, D.; Stamatis, H., Lipase immobilization on smectite nanoclays: Characterization and application to the epoxidation of alpha-pinene. *Bioresource Technology* **2010,** *101*, (6), 1587.
472. Wanjari, S.; Prabhu, C.; Labhsetwar, N.; Rayalu, S., Biomimetic carbon dioxide sequestration using immobilized bio-composite materials. *Journal of Molecular Catalysis B-Enzymatic* **2013,** *93*, 15.
473. Zhou, L. Y.; Tang, W.; Jiang, Y. J.; Ma, L.; He, Y.; Gao, J., Magnetic combined cross-linked enzyme aggregates of horseradish peroxidase and glucose oxidase: an efficient biocatalyst for dye decolourization. *Rsc Advances* **2016,** *6*, (93), 90061.

474. Cordoba, A.; Magario, I.; Ferreira, M. L., Modified chitosan as an economical support for hematin: application in the decolorization of anthraquinone and azo dyes. *Journal of Chemical Technology and Biotechnology* **2015,** *90*, (9), 1665.
475. Lagergren, S., About the Theory of so Called Adsorption of Soluble Substances. *Kungliga Svenska Vetenskapsakademiens Handlingar* **1898,** *24*, 1.
476. Ho, Y. S.; McKay, G., Sorption of dye from aqueous solution by peat. *Chemical Engineering Journal* **1998,** *70*, (2), 115.
477. Robati, D., Pseudo-second-order kinetic equations for modeling adsorption systems for removal of lead ions using multi-walled carbon nanotube. *Journal of Nanostructure in Chemistry* **2013,** *3*, (1), 55.
478. Deniz, F.; Karaman, S., Removal of an azo-metal complex textile dye from colored aqueous solutions using an agro-residue. *Microchem J.* **2011,** *99*, (2), 296.
479. Weber, W. J.; Morris, J. C., Kinetics of Adsorption on Carbon from Solution. *Journal of the Sanitary Engineering Division* **1963,** *89*, (2), 31.
480. Elwakeel, K. Z.; El-Bindary, A. A.; Ismail, A.; Morshidy, A. M., Sorptive removal of Remazol Brilliant Blue R from aqueous solution by diethylenetriamine functionalized magnetic macro-reticular hybrid material. *Rsc Advances* **2016,** *6*, (27), 22395.
481. Vadivelan, V.; Kumar, K. V., Equilibrium, kinetics, mechanism, and process design for the sorption of methylene blue onto rice husk. *J. Colloid Interface Sci.* **2005,** *286*, (1), 90.
482. Fierro, V.; Torne-Fernandez, V.; Montane, D.; Celzard, A., Adsorption of phenol onto activated carbons having different textural and surface properties. *Microporous and Mesoporous Materials* **2008,** *111*, (1-3), 276.
483. Routoula E.; Patwardhan, S. V., Degradation of anthraquinone dyes from effluents: a review focusing on enzymatic dye degradation. *under review* **2019**.
484. Santhi;, M.; Kumar;, P. E., Removal of Basic Dye Rhodamine-B by Activated Carbon-MnO2-Nanocomposite and Activated Carbon-A Comparative Study. *International Journal of Science and Research (IJSR)* **2013,** *4*, (5), 1968.
485. Freundlich, H. M. F., Over the Adsorption in Solution. *The Journal of Physical Chemistry* **1906,** *57*, 385.
486. Khoshhesab, Z. M.; Ahmadi, M., Removal of reactive blue 19 from aqueous solutions using NiO nanoparticles: equilibrium and kinetic studies. *Desalin. Water Treat.* **2016,** *57*, (42), 20037.
487. Nair, V.; Panigrahy, A.; Vinu, R., Development of Novel Chitosan-Lignin Composites for Adsorption of Dyes and Metal Ions from Wastewater. *Chemical Engineering Journal* **2014,** *254*, 491
488. Alrozi, R.; Anuar, N.; Senusi, F.; Kamaruddin, M., Enhancement of Remazol Brilliant Blue R Adsorption Capacity by Using Modified Clinoptilolite. *Iranica Journal of Energy and Environment* **2016,** *7*, (2), 129
489. Alotaibi, K. M.; Shiels, L.; Lacaze, L.; Peshkur, T. A.; Anderson, P.; Machala, L.; Critchley, K.; Patwardhan, S. V.; Gibson, L. T., Iron supported on bioinspired green silica for water remediation. *Chemical Science* **2017,** *8*, (1), 567.
490. Singh, S., A comparative study on immobilisation of alpha amylase on different matrices. *International Journal of Plant, Animal and Environmental Studies* 2014.
491. Kotwal, S. M.; Shankar, V., Immobilized invertase. *Biotechnology Advances* **2009,** *27*, (4), 311.
492. Verma, M. L.; Puri, M.; Barrow, C. J., Recent trends in nanomaterials immobilised enzymes for biofuel production. *Critical Reviews in Biotechnology* **2016,** *36*, (1), 108.
493. Zhang, B. H.; Weng, Y. Q.; Xu, H.; Mao, Z. P., Enzyme immobilization for biodiesel production. *Applied Microbiology and Biotechnology* **2012,** *93*, (1), 61.
494. Walsh, M. K., Immobilised enzyme technology for food applications. In *Novel Enzyme Technology for Food Applications*, R., R., Ed. Elsevier: **2007;** pp 60.
495. Gassara-Chatti, F.; Brar, S. K.; Ajila, C. M.; Verma, M.; Tyagi, R. D.; Valero, J. R., Encapsulation of ligninolytic enzymes and its application in clarification of juice. *Food Chemistry* **2013,** *137*, (1-4), 18.
496. Kim, J.; Grate, J. W.; Wang, P., Nanostructures for enzyme stabilization. *Chemical Engineering Science* **2006,** *61*, (3), 1017.

497. Yiu, H. H. P.; Wright, P. A., Enzymes supported on ordered mesoporous solids: a special case of an inorganic-organic hybrid. *Journal of Materials Chemistry* **2005,** *15*, (35-36), 3690.
498. Barbosa, O.; Torres, R.; Ortiz, C.; Berenguer-Murcia, A.; Rodrigues, R. C.; Fernandez-Lafuente, R., Heterofunctional Supports in Enzyme Immobilization: From Traditional Immobilization Protocols to Opportunities in Tuning Enzyme Properties. *Biomacromolecules* **2013,** *14*, (8), 2433.
499. Zucca, P.; Sanjust, E., Inorganic Materials as Supports for Covalent Enzyme Immobilization: Methods and Mechanisms. *Molecules* **2014,** *19*, (9), 14139.
500. Sheldon, R. A., Enzyme immobilization: The quest for optimum performance. *Advanced Synthesis & Catalysis* **2007,** *349*, (8-9), 1289.
501. Hanefeld, U.; Cao, L. Q.; Magner, E., Enzyme immobilisation: fundamentals and application. *Chemical Society Reviews* **2013,** *42*, (15), 6211.
502. Asgher, M.; Shahid, M.; Kamal, S.; Iqbal, H. M. N., Recent trends and valorization of immobilization strategies and ligninolytic enzymes by industrial biotechnology. *Journal of Molecular Catalysis B-Enzymatic* **2014,** *101*, 56.
503. Podrepsek, G. H.; Primozic, M.; Knez, Z.; Habulin, M., Immobilization of Cellulase for Industrial Production. *Ibic2012: International Conference on Industrial Biotechnology* **2012,** *27*, 235.
504. Singh, R. K.; Tiwari, K. M.; Singh, R.; Lee, J.-K., From protein engineeirng to immobilisation: promising strategies for the update of industrial enzymes. *International Journal of Molecular Sciences* 2013.
505. Shaffiqu, T. S.; Roy, J. J.; Nair, R. A.; Abraham, T. E., Degradation of textile dyes mediated by plant peroxidases. *Applied Biochemistry and Biotechnology* **2002,** *102*, 315.
506. Ikemoto, H.; Chi, Q. J.; Ulstrup, J., Stability and Catalytic Kinetics of Horseradish Peroxidase Confined in Nanoporous SBA-15. *Journal of Physical Chemistry C* **2010,** *114*, (39), 16174.

Appendices

Appendix I

Supporting information for Chapter 2

Table 0-1: Examples of literature on isolated strains of DyP from various microorganisms and the substrates on which they were assayed.

Microorganism	**Substrate used for characterisation**	**Reference**
Thanatephorus cucumeris Dec 1	ABTS, RB5	151, 152, 157
Geotrichum candidum Dec 1	RBlue5,	148, 175, 176
Rhodococcus jostii RHA1	H_2O_2, ABTS, wheat lignin	181, 182
A. auricula-judae	ABTS, DMP, RB5 (black/blue), RB19	150, 185
Bacillus subtilis	veratryl glycerol-b-guaiacyl ether, ABTS, RB19, RBlue5	146
Basidiomycete I. lacteus	ABTS, DMP, RB19, RBlack5, Veratryl alcohol	159
Recombinant production of DyP (as comparison to wild type or sole focus of paper)	ABTS, various dyes, lignin derivatives	127, 128, 131, 146, 150, 158, 160, 165, 172-174, 177, 178, 180, 181, 183

Table 0-2: Reviews covering enzyme immobilisation from different points of view

Interest	**Description**	**Reference**
Enzyme	Immobilisation of lipases for their application in organic media (hydrophilic enzyme in hydrophobic application)	243
	Immobilisation of alpha-amylase using various supports	490
	Immobilisation of invertase	491
Enzyme + application	Immobilisation of fungi to be used in dye removal	143
	Immobilisation of laccases and phenoloxidases using various supports	331
	Immobilisation of enzymes for biofuel production	492, 493
	Immobilisation of enzymes to be used in food industry	238, 494, 495
Support used for immobilisation	Nanoparticles and nanomaterials as immobilisation matrix	253, 286, 496
	Silicates as immobilisation matrix	237, 292, 295-298, 405, 497
	Sepabeads as immobilisation matrix	280
	Heterofunctional immobilisation matrices	498
	Bioinspired silica as immobilisation matrix	289
	Inorganic materials combined with covalent bonding	499
Method of immobilisation	Absence of immobilisation carrier (cross-linked enzyme aggregates)	227, 233
	Sol-gel encapsulation (mostly referred to silicon supports, but other options are referenced as well)	230, 294
General	Information on importance of immobilisation, examples of immobilised enzymes and procedures followed, categorisation depending on the type of application or the method of immobilisation	116, 207, 211, 239, 241, 242, 245, 246, 500, 501
Industrial aspect	Information on existing applications of immobilised enzymes in industrial processes	200, 244, 249, 502-504

Table 0-3: Terminology related to enzyme immobilisation (adapted from [116, 200, 248]).

Parameter	**Definition/equation**
Immobilisation yield (x100, %): how much enzyme is bound to the carrier based on the residual activity of the supernatant	Immobilised activity/starting activity
Immobilisation efficiency (x100, %): how much enzyme is bound to the carrier, based on the activity observed activity of the immobilisate. Can be done based on the protein measurement but it may be misleading.	Observed activity/immobilised activity
Immobilised activity	Starting activity – Activity in supernatant
Activity recovery (x100, %): comparison between the observed activity of the immobilisate and the starting activity of the enzyme	Immobilisation yield*immobilisation efficiency = Observed activity/starting activity
Leaching (x100, %): how much activity is lost during each consecutive cycle	(Immobilised activity – immobilised activity after 1 cycle)/immobilised activity
Total activity (preferred for comparable results)	Units (mol/min)
Specific activity	Unit/mL or Unit/mg
Efficiency coefficient (or effectiveness factor): shows the mass transfer control by comparing the conversion rate between soluble and immobilised enzyme	Substrate conversion rate for immobilised enzyme/substrate conversion rate for free enzyme

Table 0-4: Examples of enzymes immobilised on BIS

Focus	**Enzyme**	**Additive/method used**	**Findings**	**Ref.**
Enhancement of immobilisation efficiency	β-glucuronidase	protamine/ encapsulation of enzyme-containing alginate beads	Mechanics/chemistry of immobilisation, enhanced activity and reuse potential, there was leaching during reuse due to stirring	[217]
Enhancement of immobilisation efficiency	β-glucuronidase	protamine encapsulation	High loading achieved (5% w/w), enhanced stability in T/pH/storage, decent reuse potential, diffusional limitations, no leaching occurred	[316]
Enhancement of stability	β-glucuronidase	Lysozyme/encapsulation	Immobilisation efficiency based on activity, mixing enzyme with the additive first facilitates effective immobilisation due to electrostatic attraction, increased pH and storage stability, decreased V_{max} (reduced activity) and increased K_m (reduced substrate affinity), 12 cycle reusability	[364]
CO_2 sequestration	Carbonic anhydrase	DETA/encapsulation	high immobilisation efficiency, decent residual activity, comparable Km but lower Vmax, decent reusability, minor leaching, increased thermal stability, high CO_2 removal	[327]
CO_2 sequestration	Carbonic anhydrase	fused R5 peptide/encapsulation	Full material characterisation, enhanced thermal/storage stability/reusability, outer surface catalytically more important	[328]
Immobilisation efficiency	Catalase and horseradish peroxidase	R5/encapsulation	Confirmation of entrapment over immobilisation by adsorption, activity comparable to free enzyme, increased thermal stability, use of magnetic nanoparticles	[288]

Immobilisation efficiency	Esterase and lipase	R5, PEI, fused R5 peptide/encapsulation	Higher immobilisation efficiency of fusions compared to enzyme plus additive, basic material characterisation, low retained activity, biosilicification shifts enantioselectivity	[212]
Biosensor	Glucose oxidase	protamine/adsorption	Basic material characterisation, retained enzymatic activity, enhanced thermal/biochemical stability	[323]
Biosensor	Horseradish peroxidase	poly-L-lycine, PEI, PAMAM/encapsulation	PEI is better compared to PANAM, qualitative analysis, material characterisation based on SEM	[326]
Enhancement of immobilisation efficiency	Laccase	protamine/protective layer	Enhanced storage/pH/T stability, prolonged reusability, extended SEM analysis as part of material characterisation	[235]
Enhancement of immobilisation efficiency	Lipase	DETA,TETA,TEPA,PEHA/ encapsulation	High immobilisation efficiency, no leaching, good reuse potential, comparable residual activity to free enzyme and Novozyme 435	[215]
Enhancement of immobilisation efficiency	Lipase	polyallylamine/encapsulation	High immobilisation efficiency but low retained activity, enhanced thermal/storage stability, experimentation with different silica precursors	[320]
Enhancement of immobilisation efficiency	Lipase	pomegranate leaf extract/adsorption	Basic material characterisation, enhanced pH/T optimum, enhanced T stability, favourable reaction microenvironment, good reusability	[322]

Enhancement of immobilisation efficiency	Manganese Peroxidase	chitosan/encapsulation	Enzyme pre-incubation with the additive enhances immobilisation efficiency, comparable kinetics, enhanced stability in solvents	[319]
Enhancement of immobilisation efficiency	Papain	R5/encapsulation	Full material characterisation, enhanced stability under various conditions (including pH T), decent reuse potential, enhanced affinity but decreased activity	[321]
Enhancement of immobilisation efficiency	Yeast alcohol dehydrogenase	PEI, PAH/encapsulation	Full material characterisation, enhanced activity and performance of the biocatalyst, decent to good reuse potential, enhanced storage stability	[236]
Biosensor	β-galctosidase	R5/encapsulation, adsorption	Immobilisation by adsorption showed higher efficiency than encapsulation, good storage stability, mass transfer limitations	[324]
Enhancement of immobilisation efficiency	d-amino-acid oxidase	PAH/encapsulation	Basic material characterisation, higher immobilisation efficiency results in decreased recovered activity, enhanced pH/T stability, mass transfer limitations, almost decent reusability, enhanced stability to H_2O_2	[313]
Biosensor	Adenosine deaminase/nucleoside phosphorylase/xanthine oxidase	poly-L-lysine/encapsulation	good storage stability, no material characterisation, mild preparation conditions	[311]

Immobilisation efficiency/ CO_2 sequestration	Carbonic anhydrase	spermine/encapsulation	Results mostly based on esterase activity rather than actual application, enhanced T and almost preserved pH stability, great reusability (shown up to 10 cycles)	329
Immobilisation efficiency/ FAME production	Lipase	PEI/adsorption and encapsulation	Exploration of immobilisation conditions, adsorbed lipase shows better performance on synthesis of FAME but encapsulated lipase shows better standard catalytic potential, both perform better than commercial product, poor reusability (up to 20% activity after 5 cycles), mention of diffusional limitations	325

Table 0-5: Decolorisation of anthraquinone dyes by immobilised oxidoreductases.

Enzyme	**Method/Support**	**Dye name/ concentration (mg/L)**	**Throughput (mg/L/h)****	**Summary of findings**	**Ref.**
Horseradish peroxidase	Covalent binding/ methacrylated polysulfones	Reactive Blue 19/ 40	34	85% decolorisation within 1h, decent reuse potential (7 times, 20% activity left by 7th), increased storage stability. Increased T stability	263
Horseradish peroxidase	Covalent binding/ chitosan + glutaraldehyde	Reactive Blue 19/ 100	17	Multiple immobilisation approached examined, chitosan was the best support, 68% decolorisation of RB19 within 4h, high activity retention, further analysis conducted with azo dyes, but overall the biocatalyst had improved performance to free enzyme, up to 7 cycles of reuse with good activity retention (70%), no difference to decolorisation degree between high and low dye concentration.	271
Laccase	Covalent binding/ functionalised controlled porosity silica beads	Reactive Blue 19/ 22.5, Dispersed Blue 3 /21.3	1.68, 0.93	Between 70-80% within 30mins for free enzyme and within 10hours and 17hours for immobilised enzyme respectively. Dye gets adsorbed onto support and then enzymatically decolorised by enzyme, dyes do not affect enzymatic activity, increased toxicity after degradation	274
Dye-decolorising peroxidase	Adsorption/ immobilized FSM-16 and AlSBA-15	Reactive Blue 19 /150	**1800**	100% removal within 5mins, immobilisation support affects enzymatic activity hence decolorisation, pH affects decolorisation and enzyme leaching from support	155

Dye-decolorising peroxidase	Adsorption/ MCF	Reactive Blue 19 /150	**3600**	High adsorption yield but low residual activity, pH affects decolorisation and enzyme leaching from support, very good reuse potential (20 cycles) in pH4	156
Polyphenol oxidase	Adsorption/ Celite 545	Reactive Blue 4 /50-100	43.5-87	Immobilised enzyme shows better results than free, pH affects decolorisation, immobilized enzyme treatment leads to reduced TOC post-treatment compared to free enzyme	334
Laccase	Adsorption-covalent bonding/ Silanised alumina	Reactive Blue 19 /150	N/A	Decent activity recovery of immobilised enzyme (68%), higher thermal stability and stability to inhibitors, higher detoxification of anthraquinone dyes	336
Horseradish peroxidase	Encapsulation/ Ca-alginate beads	Acid Blue 25 /10.4	8.32	High encapsulation efficiency and low leakage, slight improvement of pH stability and considerable improvement on thermal stability, max removal (80%) was reached within an hour, decent reusability (~10% reduction after 4 cycles, 86% after 10), reduced toxicity after decolorisation	97
Laccase	Covalent adsorption/ Epoxy activated polymers	Acid Blue 25, Reactive Blue 19, Acid green 27 /20 (all)	~0.5	Decent immobilisation efficiency (17-32%) and activity recovery, improved pH, thermal, storage stability, slightly improved solvent stability, use of mediator (HBT) aids decolorisation of some dyes, max decolorisation degree for AQ dyes was ~60% (24h), no comparison with free enzyme	281
Laccase	Adsorption/ alumina pellets	Reactive Blue 19 /100	1.07	Good immobilisation efficiency and activity recovery (~70% both), ~45% decolorisation over 42h, slightly reversed results after 70h, identification of degradation pathway, reduced toxicity	42
Horseradish Peroxidase	Cross linked Enzyme Aggregates	Acid Violet 109 /30	36-46	High decolorisation degree (70-90%), decolorisation experiments in batch/packed bed reactors (packed bed performs better), enhanced pH stability and higher dye and peroxide concentration tolerance, reduced toxicity after enzymatic treatment of dye solution	337
Horseradish Peroxidase	Adsorption/activated kaolin	Acid Violet 109 /40	52.2	Adsorption conditions examined, good decolorisation (87% after 40mins), improved pH stability during decolorisation, better tolerance of high dye concentration, considerably lower substrate affinity but not very lower initial rate, high (7) reuse cycles (35% activity left)	18
Horseradish Peroxidase	Adsorption/ sulfide electrode	Acid Violet 109/ 30	14.4	Study examined the potential of energy generation while decolorising a dye, max efficiency achieved was about 40% within 50min	338

Laccase	Adsorption/ Silica beads	Reactive Blue 19 /25	3.04	Dye initially adsorbed to matrix but decolorisation was due to enzymatic action (97,5%), better reaction rate than free enzyme, increased storage stability	283
Hematin (not enzyme, but of structure resembling peroxidases) and Horseradish Peroxidase	Covalent adsorption/ chitosan and APTS	Alizarin red/ 200	97.4 for Hematin 40 for Horseradish Peroxidase	Decolorisation is based on action of hematin as peroxidase active site, comparison with immobilised horseradish peroxidase is taking place, about 50% efficiency on 1st cycle, after 6 cycles efficiency drops to 34%, identification of possible reasons for decreased activity, comparison between 2 dyes (anthraquinone and azo)	474
Laccase	Adsorption/ magnetic carbon capsules	Reactive Blue 19/ 100-300 Acid Green 25/ up to 2000	18-54 for Reactive Blue 19, 18-360 for Acid Green 25	Decolorisation experiments for the 2 dyes were under different conditions, very high loading achieved (1g enzyme/g support), almost 80% decolorisation within 1st hour, 90% within 5 hours, excellent reusability (activity almost intact after 6 cycles), acknowledgment of dye adsorption on support, good storage stability (10% activity loss after 2 months)	270
Horseradish Peroxidase	ZnO nanowires-porous silica composite	Acid Violet 109, Reactive Blue 19/ 50	~50	Enzyme gets immobilised using epoxy based crosslinkers to prevent leaching, examination of various parameters affecting immobilisation, a max of 120mg/g loading was achieved, acknowledgement of dual action based on both enzyme and support, very positive results (100% dye removal, reuse for up to 12 cycles with 20% activity loss)	335

*values shown are for the optimised methods as presented by researchers and refer to removal of colour unless stated otherwise

**arbitrary value calculated to show the maximum removal capacity of any given method within an hour, based on the best results presented in each reference. In cases where the timescale of the decolorisation is within a few minutes, the assumption of decolorisation ability over continuous use for 1 h is made

Appendix II

Supporting information for Chapter 3

Section 1: Derivation of Michaelis – Menten equation

Reaction equation: [E] + [S] ←→ [ES] → [E] + [P] (Eqn. AIII. 1)

With rate of the reaction being: $\nu = k_2 \times [ES]$ (Eqn. AIII. 2)

where E: enzyme, S: substrate, ES: complex between enzyme and substrate, and P: product. The equivalent rate constants are k_1 for the [ES] production, k_{-1} for the [ES] dissociation back to [E] and [S] and k_2 for product formation.

a. **Steady state approach**: assumes that substrate is in a highly excessive concentration compared to the formed ES complex, allowing for the rate of ES formation to be assumed as zero. This is expressed as:

$\frac{d[ES]}{dt} = 0$ (Eqn. AIII.3)

Expressing all reagents present in Eqn. AIII.1 as rates, we get:

$\frac{d[E]}{dt} = k_{-1} \times [ES] + k_2 \times [ES] - k_1 \times [E][S]$ (Eqn. AIII.4)

$\frac{d[S]}{dt} = k_{-1} \times [ES] - k_1 \times [E][S]$ (Eqn. AIII.5)

$\frac{d[ES]}{dt} = k_1 \times [E][S] + k_1 \times [ES] - k_2 \times [ES]$ (Eqn. AIII.6)

$\frac{d[P]}{dt} = k_2 \times [ES]$ (Eqn. AIII.7)

$[E]_t = [E] + [ES]$ (Eqn. AIII.8).

From Eqn. AIII.2 and AIII.5, we get: $k_1 \times [E][S] = (k_{-1} + k_2) \times [ES]$, which solved to [ES] returns:

$[ES] = \frac{k_1 \times [E][S]}{k_{-1} + k_2}$ (Eqn. AIII.9)

Dividing Eqn. AIII. 2 with Eqn. AIII. 8 returns:

$\frac{\nu}{[E]_t} = \frac{k_2 \times [ES]}{[E]+[ES]}$ (Eqn. AIII. 10)

and substituting [ES] with the equivalent from Eqn. AIII. 9 gives:

$\nu = [E]_t \times \frac{k_2 \times \frac{k_1 \times [E][S]}{k_{-1} + k_2}}{[E] + \frac{k_1 \times [E][S]}{k_{-1} + k_2}}$ (Eqn. AIII. 11)

Neutralising [E] in Eqn. AIII. 11 and multiplying both numerator and denominator with $\frac{k_{-1} + k_2}{k_1}$ returns:

$\nu = [E]_t \times \frac{k_2 \times [S]}{\frac{k_{-1} + k_2}{k_1} + [S]}$ (Eqn. AIII. 12)

The constant values of $[E]_t$ and k_2 can be grouped together to form V_{max} and the constant values of the $\frac{k_{-1} + k_2}{k_1}$ expression represent the Michaelis constant, K_M. Hence, Eqn. AIII. 13 can be transformed to the following:

$\nu = \frac{V_{max} \times [S]}{K_M + [S]}$ (Eqn. AIII. 13)

Eqn. AIII. 14 is the well-known Michaelis – Menten expression.

b. **Rapid equilibrium approach**: assumes that product is formed in a much slower rate compared to the formation and dissociation of the ES complex, allowing for a rapid equilibrium relationship between enzyme [E], substrate [S] and complex [ES].

At the equilibrium point, the rate of complex formation is equal to the rate of complex dissociation. Using Eqn. AIII. 1 and expressing this equilibrium for [ES], we get: $k_1 \times [E][S] = k_{-1} \times [ES]$ (Eqn. AIII. 14)

Solving Eqn. AIII. 13 to [ES], we get: [ES] = $\frac{k_1 \times [E][S]}{k_{-1}}$ (Eqn. AIII. 15)

Using Eqn. AIII. 14 to substitute ES at Eqn. AIII. 10, returns:

$\nu = [E]_t \times \frac{k_2 \times k_1 \times \frac{[E][S]}{k_{-1}}}{[E] + \frac{k_1 \times [E][S]}{k_{-1}}}$ (Eqn. AIII. 16)

In Eqn. AIII. 16, [E] can be eliminated, and also, the constant combination $\frac{k_{-1}}{k_1}$ can be named dissociation constant (K_s), defined by the ratio of dissociation over formation of ES. These actions return:

$\nu = [E]_t \times \frac{k_2 \times \frac{[S]}{K_S}}{1 + \frac{[S]}{K_S}}$ (Eqn. AIII. 17)

By multiplying both the numerator and the denominator with K_s, we get:

$\nu = \frac{[E]_t \times k_2 \times [S]}{K_S + [S]}$ (Eqn. AIII. 18)

Similarly to the steady state assumption, $[E]_t \times k_2$ is the maximum initial rate of the enzymatic reaction (V_{max}). In this case, K_S is different to K_M, and is indicative of how strongly the substrate binds on the enzyme.

Comparing K and K_M as defined earlier, we can result to the following equation:

$K_M = K_S + \frac{k_2}{k_1}$, so K_M could be assumed equal to K_S if k_2 is much smaller than k_{-1} (indicating that formation and dissociation of ES complex is much smaller than the formation of product, showing the extend of successful collisions between enzyme and substrate to form product).

Section 2: BIS synthesis

Table 0-6: Mass balance and pH measurement for BIS produced with both additives (PEHA, PAH), without presence of enzyme. Solids were separated from supernatant at pH7, or were eluted with more acid to target pH of 5 or 2.

Additive: PEHA		**BIS pH7**		**BIS pH 5**		**BIS pH2**	
		Mean of 15 samples	Standard deviation	Mean of 9 samples	Standard deviation	Mean of 6 samples	Standard deviation
	Silicate (target: 318.2 mg)	318.17	0.37	317.98	0.21	318.24	0.22
	Amine (target: 58.1 mg)	58.21	0.34	58.13	0.22	58.17	0.19
	HCl used (ml)	3.46	0.05	3.49	0.01	3.50 (+1.0)	0.01 (0.15)
	pH value achieved (target: 7.00/5.00/2.00)	7.04	0.07	7.02/5.02	0.02/0.04	7.02/2.05	0.03/0.03
	Theoretical mass yield (mg)	148.30	0.041	148.20	0.27	90.14	0.00
	Actual product (mg)	73.52	5.98	55.09	5.10	23.39	7.63
	Yield (%)	49.55	3.96	61.16	5.65	45.10	6.27
Additive: PAH		Mean of 13 samples	Standard deviation	Mean of 10 samples	Standard deviation	Mean of 6 samples	Standard deviation
	Silicate (target: 318.2 mg)	318.08	0.21	318.23	0.22	318.30	0.26
	Amine (target: 50.00 mg)	49.89	0.34	50.29	0.36	50.06	0.32
	HCl used (ml)	2.43	0.06	2.44	0.03	2.42/0.94	0.04/0.12
	pH value achieved (target: 7.00/5.00/2.00)	6.96	0.09	6.98/5.05	0.07/0.06	6.91/2.00	0.17/0.06
	Theoretical mass yield (mg)	140.02	0.00	140.43	0.40	90.16	0.00
	Isolated product (mg)	109.16	4.56	104.52	3.88	68.74	9.02
	Yield (%)	77.96	3.26	73.65	2.40	55.46	10.42

Appendix III

Supporting information for Chapters 4, 5, 6, 7, 8

Section 1: Information on RB19

Calculation of decolorisation based on absorbance at maximum wavelength:

%decolorisation = $\frac{A_{initial}-A_{final}}{A_{initial}}$*100%

Calculation of decolorisation based on the area under the curve:

%decolorisation = ($\sum_{x=400}^{x=700}(A_{x+1}-A_x)/2$ of treated sample - $\sum_{x=400}^{x=700}(A_{x+1}-A_x)/2$ of blank)*100%

Section 2: Assay protocols

Protocol used for ABTS oxidation

1. Prepare 0.2M $Na_2HPO_4.H_2O$ (1). Check the hydration state whilst preparing the solution
2. Prepare 0.1M $C_6H_8O_7.H_2O$ (2). check the hydration state whilst preparing this solution
3. Prepare citric acid- Na_2HPO_4 buffer of pH4 (3). For 10mL add 6.145mL of (2) and 3.855 of (1)
4. Prepare 10mM ABTS in (3) (4). Prepare freshly, ABTS should be stored in the fridge
5. Prepare 0.3% (w/w) H_2O_2 solution (5). Prepare freshly, 30% (w/w) H_2O_2 solution is stored in the fridge
6. Prepare 0.005mg/ml HRP in phosphate buffer pH4 (or other buffer as appropriate) (6), from enzyme solution of 1mg/ml, immediately before the assay. Lyophilised enzyme is stored in the fridge. After use store the enzyme solution in the fridge for short periods or in the freezer for longer periods.
7. For the assay prepare the reaction mixture below in cuvettes, in the order of reagents as proposed:

Components	**Sample (µL)**	**Control (µL)**
Enzyme	25	0
H_2O_2	50	50
Buffer	0	25
ABTS	2925	2925
Total volume	3000	3000

8. Upon addition of the enzyme and peroxide in the cuvette, allow 5minutes for incubation (cuvette should be covered).
9. Insert the cuvettes in the spectrophotometer and set up the measurement for absorbance at 420nm.
10. Initiate the reaction with addition of the ABTS and monitor kinetics for 5minutes.

Protocol used for RB19 degradation

1. Prepare 0.125mM RB19 in water
2. Prepare 0.3% (w/w) H_2O_2 solution. Prepare freshly, 30% (w/w) H_2O_2 solution is stored in the fridge.
3. Prepare 1mg/ml HRP in phosphate buffer pH4 (or other buffer as appropriate). Lyophilised enzyme is stored in the fridge. After use store the enzyme solution in the fridge for short periods or in the freezer for longer periods.
4. For the assay prepare the reaction mixture below in cuvettes, in the order of reagents as proposed:

Components	**Sample (μL)**	**Control (μL)**
Enzyme	50	0
H_2O_2	15	15
Buffer	0	50
RB19	2935	2935
Total volume	3000	3000

5. Upon addition of the enzyme and peroxide in the cuvette, allow 5minutes for incubation (cuvette should be covered).
6. Insert the cuvettes in the spectrophotometer and set up the measurement for absorbance at 595nm.
7. Initiate the reaction with addition of the RB19 and monitor kinetics for 10minutes.

Section 3: USAXS data interpretation

Table 0-7and Table 0-8 show the parameters obtained through USAXS measurement for every examined sample (one replicate). Figure 0-1 shows the logarithmic plot of Intensity vs Q for each sample, including experimental data and fitting. Sample correspondence to graphs is done through the Graph ID code as shown in the Tables, matching the legend of each graphs. Graphs are presented in order of sample appearance.

Table 0-7: Parameters obtained from analysis of USAXS data using suitable fitting tools. Samples in this table are BIS samples synthesised with PAH or PEHA as additive, in absence of enzyme. Level 1 and 2 represent identification of 2 particle sizes. G is the Guinier prefactor, Rg is the radius of gyration, B is the power-law prefactor at intermediate. S/V is the surface to volume ratio for the primary particles, dp is the Sauter mean diameter related to V/S for these particles, PDI is an index of primary particle polydispersity (1 for monodisperse spheres and larger values with higher particle size dispersion).

	Sample / Graph ID	G (cm^{-1})	Rg (Å)	B	P	S/V (m^2/cm^3)	d_p (nm)	PDI
Level 1	**BIS-PAH (pH 7)** / graph shown in Figure 5-6	85.78	67.03	1.91E-05	4	566.72	10.59	2.777
	BIS-PEHA (pH 7) / graph shown in Figure 5-6	745.5	303.2	7.43E-07	4	176.07	34.08	5.199
	BIS-PAH (pH 5) / 0504	92.73	72.44	1.35E-05	4	487.05	12.32	2.471
	BIS-PEHA (pH 5) / 0505	415.8	276.7	6.10E-07	4	194.78	30.8	5.309
	BIS-PAH (pH 2) / 0519	31.59	52.87	3.30E-05	4	995.074	6.03	5.039
	BIS-PEHA (pH 2) /0520	412.6	218.4	9.36E-07	4	189.02	31.74	3.189
Level 2	**BIS-PAH (pH 7)** / graph shown in Figure 5-6	2195	202.1	1.17E-05	4	554.645	10.82	5.471
	BIS-PEHA (pH 7) / graph shown in Figure 5-6	1.23E+06	1731	4.61E-07	4	1.95E+01	307	2.07
	BIS-PAH (pH 5) / 0504	1089	167.2	1.46E-05	4	814.15	7.37	6.458
	BIS-PEHA (pH 5) / 0505	2.50E+04	886.8	2.29E-07	4	5.99E+01	100.1	3.50E+00
	BIS-PAH (pH 2) / 0519	5.89E+02	104.4	1.18E-05	4	3.12E+02	19.26	1.47E+00
	BIS-PEHA (pH 2) /0520	1.22E+04	505.7	3.06E-07	4	4.09E+01	146.7	1.02E+00

Table 0-8: Parameters obtained from analysis of USAXS data using suitable fitting tools. Samples in this table are BIS samples synthesised with PAH or PEHA as additive, in presence of enzyme. Parameter explanation is the same as in Table 0-7.

	Sample	G (cm^{-1})	Rg (Å)	B	P	S/V (m^2/cm^3)	d_p (nm)	PDI
Level 1	**BIS-PAH-HRP (HRP added @ pH 7, 0.25mg/mL) /** graph shown in Figure 5-6	424.1	112.2	1.65E-05	4	407.001	14.74	3.813
	BIS-PEHA-HRP (HRP added @ pH 7, 0.25mg/mL) / graph shown in Figure 5-6**)**	1354	340.8	6.24E-07	4	134.48	44.62	3.838
	BIS-PAH-HRP (HRP added @ pH 7, eluted @ pH 5, 0.25mg/mL) / 0509	768.2	105.4	3.60E-05	4	418.216	14.35	3.577
	BIS-PEHA-HRP (HRP added @ pH 7, eluted @ pH 5, 0.25mg/mL) / 0910	3.327	28.56	2.77E-05	4	1504.4	3.988	3.416
	BIS-PAH-HRP (HRP added @ pH 7, eluted pH 2, 0.25mg/mL) / 0517	28.38	45.22	3.82E-05	4	959.672	6.252	3.477
	BIS-PEHA-HRP (HRP added @ pH 7, eluted pH 2, 0.25mg/mL) / 0518	1157	220.1	2.62E-06	4	190.567	31.49	3.275
	BIS-PAH-HRP (HRP added @ additive, 0.25mg/mL) /0514	95.91	129.3	2.90E-06	4	413.793	14.5	5.229
	BIS-PAH-HRP (HRP added @ silicate, 0.25mg/mL) /0515	393.7	128.4	1.53E-05	4	459.346	13.06	6.538
	BIS-PAH-HRP (HRP added @ mix additive-silicate, 0.25mg/mL) /0522	300.8	399.6	1.07E-07	4	138.35	43.37	5.615
	BIS-PAH-HRP (HRP added @ pH 7, eluted @ pH 5, 0.4mg/mL) / 0507	152.5	82.84	1.50E-05	4	466.28	12.87	2.853
	BIS-PEHA-HRP (HRP added @ pH 7, eluted @ pH 5, 0.4mg/mL) / 0508	299.6	198.4	9.29E-07	4	199.338	30.1	2.966
Level 2	**BIS-PEHA-HRP (HRP added @ pH 7, 0.25mg/mL) /** graph shown in Figure 5-6**)**	2.11E+06	1963	3.42E-07	4	1.33E+01	452.7	1.48
	BIS-PAH-HRP (HRP added @ pH 7, eluted @ pH 5, 0.25mg/mL) / 0509	3.82E+04	539.1	1.44E-05	4	3.15E+02	20.5	1.97
	BIS-PEHA-HRP (HRP added @ pH 7, eluted @ pH 5, 0.25mg/mL) / 0910	205.5	101.6	1.00E-05	4	693.91	8.647	3.195

	BIS-PAH-HRP (HRP added @ pH 7, eluted pH 2, 0.25mg/mL) / 0517	9.58E+02	114.1	3.38E-05	4	7.11E+02	8.435	3.69
	BIS-PEHA-HRP (HRP added @ pH 7, eluted pH 2, 0.25mg/mL) / 0518	7.57E+04	6.21E+02	3.08E-06	4	9.65E+01	62.2	3.74
	BIS-PAH-HRP (HRP added @ additive, 0.25mg/mL) /0514	4.51E+04	722.6	1.04E-06	4	8.24E+01	72.83	3.89
	BIS-PAH-HRP (HRP added @ silicate, 0.25mg/mL) /0515	2.09E+05	753.7	7.91E-06	4	1.17E+02	51.24	7.54
	BIS-PAH-HRP (HRP added @ mix additive-silicate, 0.25mg/mL) /0522	3.72E+03	837.3	1.44E-08	4	3.00E+01	222.4	1.17
	BIS-PAH-HRP (HRP added @ pH 7, eluted @ pH 5, 0.4mg/mL) / 0507	1216	154.5	1.69E-05	4	682.04	8.797	4.897
	BIS-PEHA-HRP (HRP added @ pH 7, eluted @ pH 5, 0.4mg/mL) / 0508	2.55E+04	659.1	1.53E-06	4	1.34E+02	44.76	6.97
Level 3	**BIS-PEHA-HRP (HRP added @ pH 7, eluted @ pH 5, 0.25mg/mL)** / 0910	4.83E+06	1275	1.04E-05	4	3.81E+01	157.5	3.50
	BIS-PEHA-HRP (HRP added @ pH 7, eluted pH 2, 0.25mg/mL) / 0518	3.55E+06	1531	3.84E-06	4	4.52E+01	132.8	3.66
	BIS-PEHA-HRP (HRP added @ pH 7, eluted @ pH 5, 0.4mg/mL) / 0508	8.42E+05	1368	2.50E-06	4	8.54E+01	70.26	6.42
Level 4	**BIS-PEHA-HRP (HRP added @ pH 7, eluted @ pH 5, 0.25mg/mL)** / 0910	1.53E+07	3286	3.03E-07	4	7.29E+00	823.4	1.43

Figure 0-1: Logarithmic plot of Intensity vs Q for BIS and BIS-HRP samples examined through USAXS measurement.

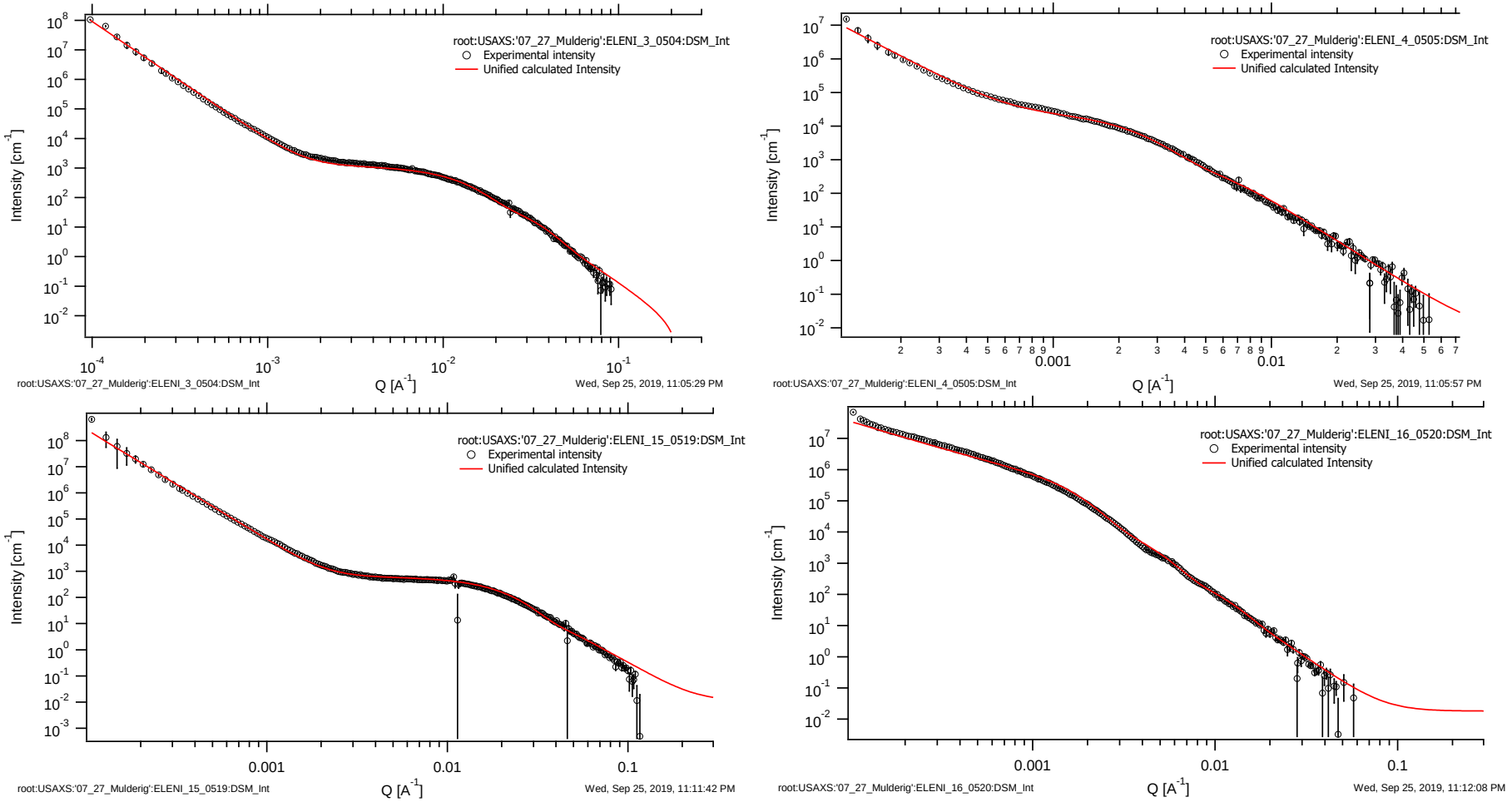

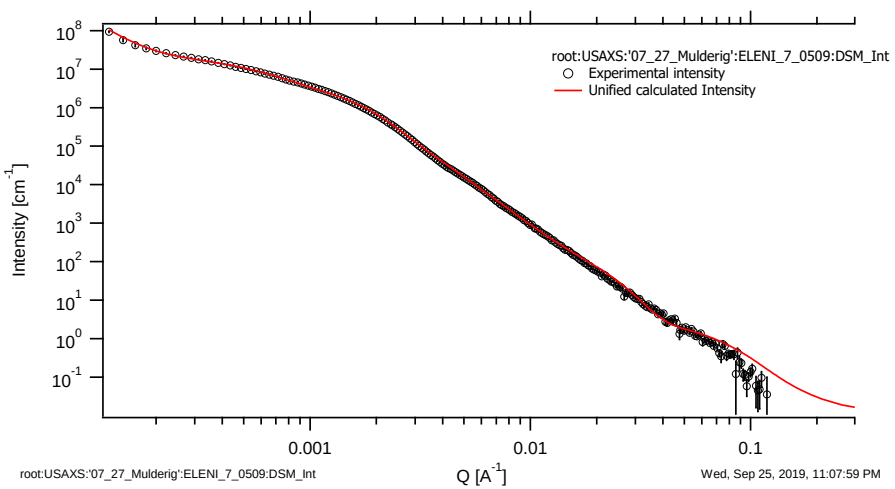
root:USAXS:'07_27_Mulderig':ELENI_7_0509:DSM_Int
Experimental intensity
Unified calculated Intensity
Intensity [cm^{-1}]
Q [A^{-1}]
root:USAXS:'07_27_Mulderig':ELENI_7_0509:DSM_Int
Wed, Sep 25, 2019, 11:07:59 PM

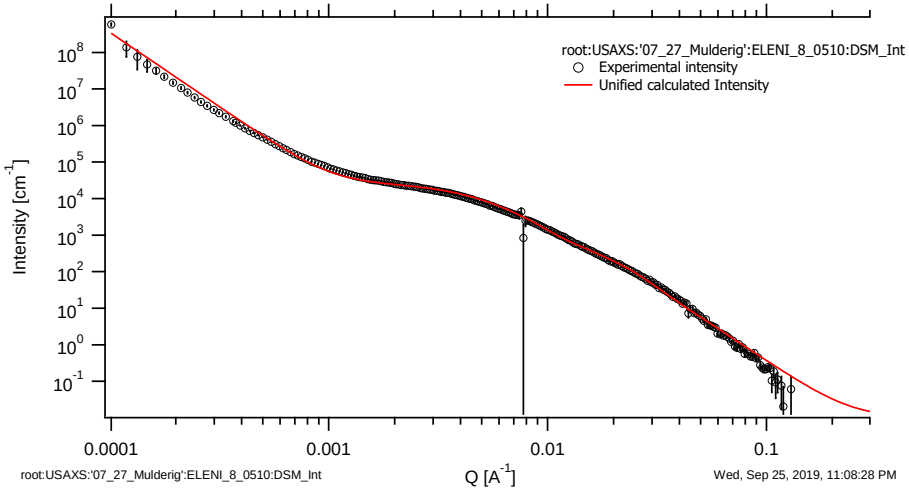
root:USAXS:'07_27_Mulderig':ELENI_8_0510:DSM_Int
Experimental intensity
Unified calculated Intensity
Intensity [cm^{-1}]
Q [A^{-1}]
root:USAXS:'07_27_Mulderig':ELENI_8_0510:DSM_Int
Wed, Sep 25, 2019, 11:08:28 PM

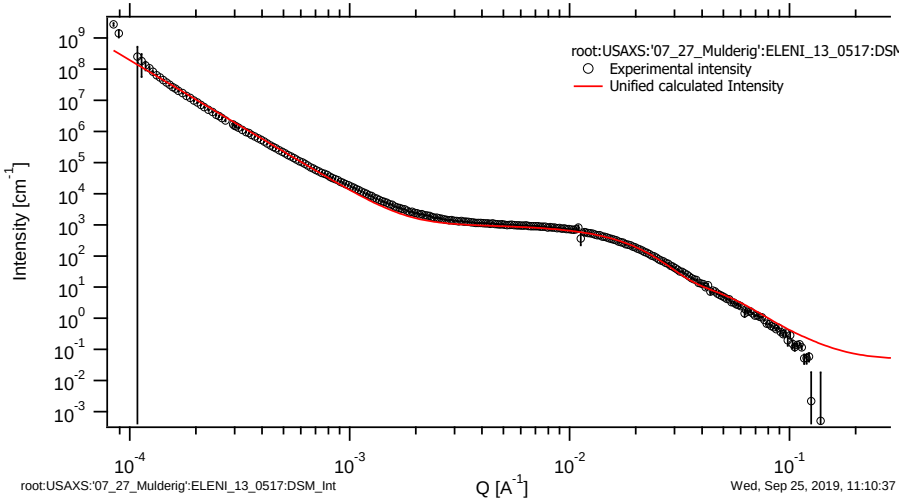
root:USAXS:'07_27_Mulderig':ELENI_13_0517:DSM_Int
Experimental intensity
Unified calculated Intensity
Intensity [cm^{-1}]
Q [A^{-1}]
root:USAXS:'07_27_Mulderig':ELENI_13_0517:DSM_Int
Wed, Sep 25, 2019, 11:10:37 PM

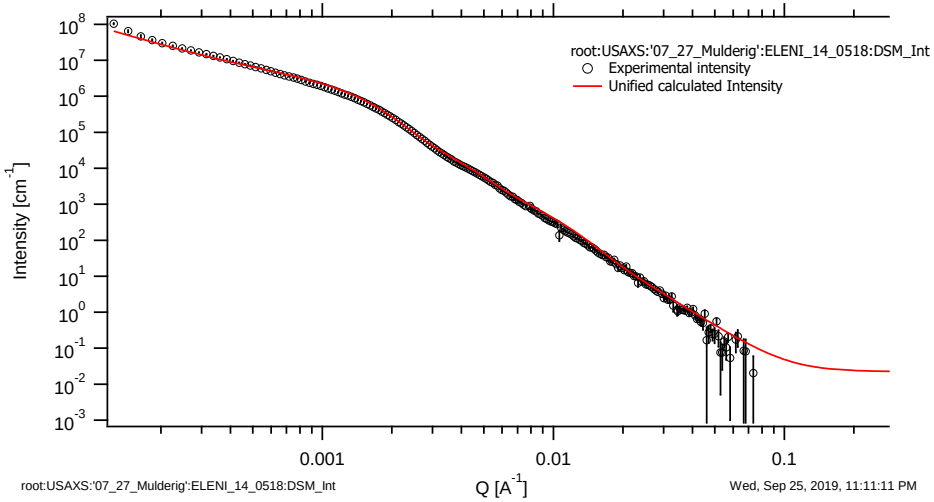
root:USAXS:'07_27_Mulderig':ELENI_14_0518:DSM_Int
Experimental intensity
Unified calculated Intensity
Intensity [cm^{-1}]
Q [A^{-1}]
root:USAXS:'07_27_Mulderig':ELENI_14_0518:DSM_Int
Wed, Sep 25, 2019, 11:11:11 PM

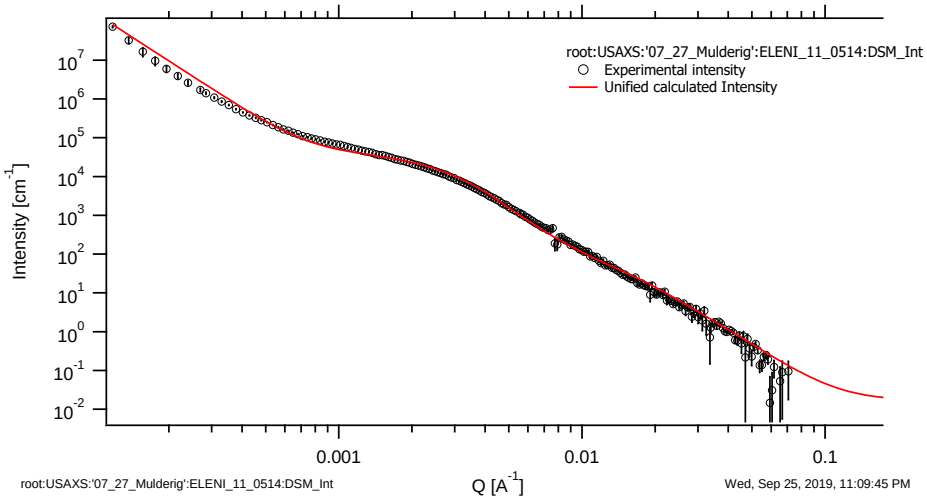
root:USAXS:'07_27_Mulderig':ELENI_11_0514:DSM_Int
Experimental intensity
Unified calculated Intensity
Intensity [cm^{-1}]
Q [A^{-1}]
root:USAXS:'07_27_Mulderig':ELENI_11_0514:DSM_Int
Wed, Sep 25, 2019, 11:09:45 PM

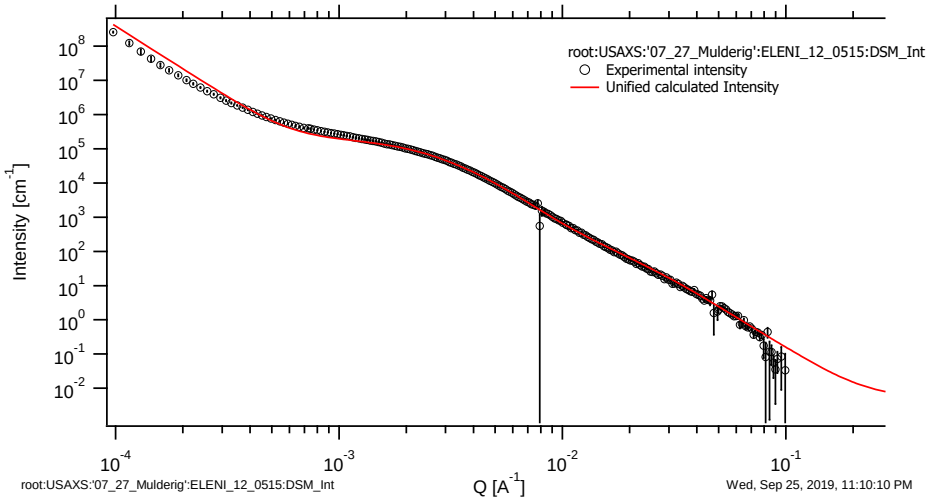
root:USAXS:'07_27_Mulderig':ELENI_12_0515:DSM_Int
Experimental intensity
Unified calculated Intensity
Intensity [cm^{-1}]
Q [A^{-1}]
root:USAXS:'07_27_Mulderig':ELENI_12_0515:DSM_Int
Wed, Sep 25, 2019, 11:10:10 PM

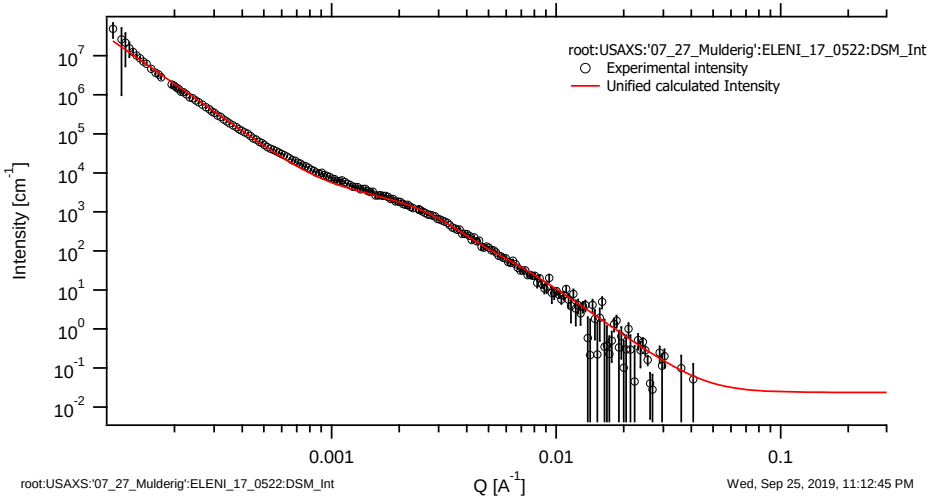
root:USAXS:'07_27_Mulderig':ELENI_17_0522:DSM_Int
Experimental intensity
Unified calculated Intensity
Intensity [cm^{-1}]
Q [A^{-1}]
root:USAXS:'07_27_Mulderig':ELENI_17_0522:DSM_Int
Wed, Sep 25, 2019, 11:12:45 PM

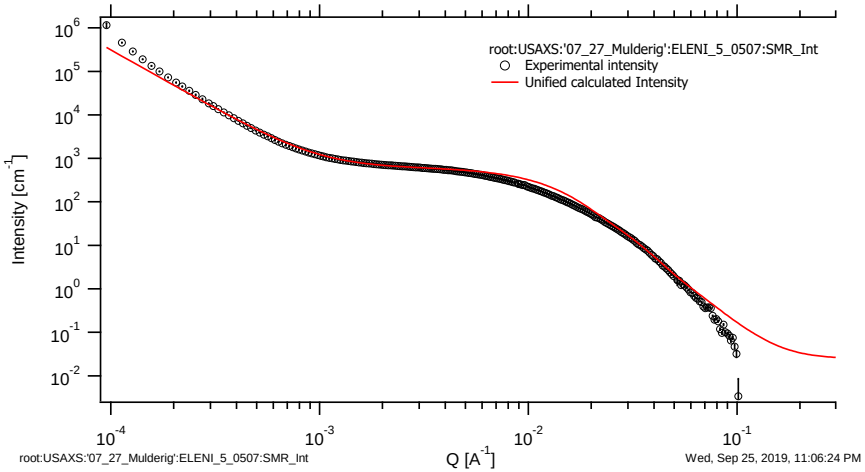
root:USAXS:'07_27_Mulderig':ELENI_5_0507:SMR_Int
Experimental intensity
Unified calculated Intensity
Intensity [cm^{-1}]
Q [A^{-1}]
root:USAXS:'07_27_Mulderig':ELENI_5_0507:SMR_Int
Wed, Sep 25, 2019, 11:06:24 PM

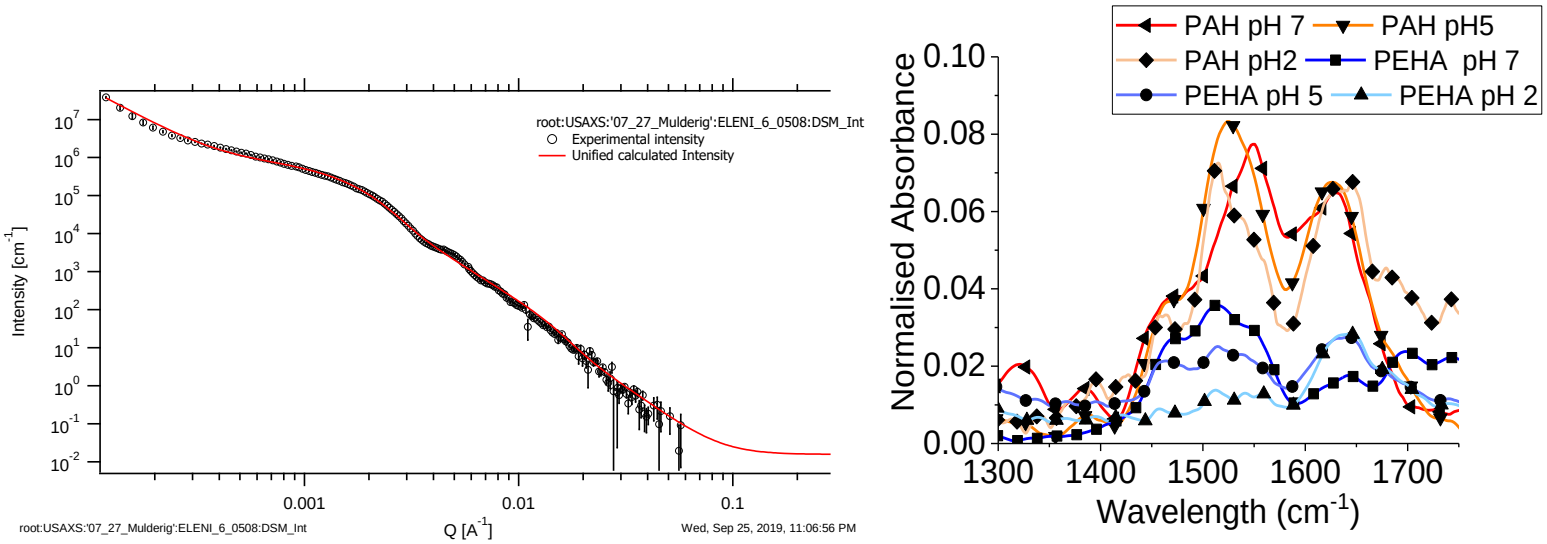

Figure 0-2: FTIR spectra of BIS synthesised with PAH or PEHA as additive, examining the effect of acid elution.

Section 4: Information on immobilised HRP from literature

Table 0-9: Examples of HRP used for decolorisation (Km, Vmax procured from Michaelis-Menten equation unless stated otherwise).

Enzyme form	Application/ substrate	Km (μM)/ Vmax (μM/s)	Comments	Ref.
Free	RB19 decolorisation	454.5/0.03	Inhibition by high dye C, pH opt was 5, broad T range, several factors examined	[20]
Free	RB5	58/0.238	Research on DyP but mentioning parameters for HRP	[176]
Free	Acid Blue 225, Acid Violet 109	221.3/0.016 (acid blue 225), 237.4/0.0273 (acid violet 109)	Different decolorisation time for each dye, same enzyme C for max % decolorisation, high C of H_2O_2 has inhibitory effect, high dye C is not	[133]

		Based on inhibition model	necessarily inhibitory, same pH opt for both dyes, same pattern of thermal deactivation	
Free	Remazol Blue, Crystal Violet	100/0.31 (Remazol blue), 18/0.005 (crystal violet)	Substrate inhibition in reaction pH over 6, dye degradation or precipitation in relation to dye structure, equimolar H_2O_2 consumption to dye concentration	[99]
Free/Immobilised	AV109	47/21.16 (free) 79/14.5 (immob.), based on inhibition model	Overall improved performance (decreased dye inhibition), not good reusability	[18]
Free/Immobilised	Various dyes, 1 anthraquinone (Acid Green 84)	-	Half the quantity of immobilised enzyme performs as double the amount of soluble, decent reuse potential (10 cycles), varying decolorisation % among dyes	[505]
Free/Immobilised	Acid Orange 7 and Acid Blue 25	-	Increased thermal stability, decent reusability (different for each dye), same pH optimum with free enzyme, same optimal amount of enzyme used for both dyes	[97]
Free/immobilised	Reactive Blue 221 and 198	46/1.57E-3 and 58/5.22E-3 for each dye (free HRP)	Immobilisation on alginate beads, exploration of mass transfer phenomena, poor reusability (10% efficiency by 3rd cycle), incomplete optimisation study	[433]

Table 0-10: Examples of immobilised HRP not used in decolorisation, (Km, Vmax procured from Michaelis-Menten equation unless stated otherwise).

Support/ method	**Application/substrate**	**Km (μM)/Vmax (μM/s)**	**Comments**	**Ref.**
Cinnamic carbohydrate esters/ adsorption	Immobilisation efficiency / ABTS	Varying between 92.8-126.6/0.06-0.34 across different immobilisation supports (based on inhibition model)	Too much time/steps involved, enhanced thermal stability, controversial stability at different pH, freezing and thawing examination, decreased storage stability, diffusional limitations/deactivation	[222]

BIS/encapsulation	Biosensor/ 4-AAP	-	In-situ encapsulation, customisable shape/size of nanoparticles, long-term stability	326
Activated acrylamide	pyrogallol	-	decrease of pH opt, increase of pH stability, same T opt, increased T stability, enhanced storage stability, good reuse potential, eventual denaturation of protein, increased stability in organic solvents	264
Silane modified ceramics/covalent attachment	Oily wastewater treatment/ 4-AAP	-	decent/high immob efficiency (1.16mg HRP/g support), good storage stability, enhanced pH stability, decent reusability	229
Activated alkylamine CPG Beads/covalent attachment	Decontamination /4-AAP	(calculation of similar coefficients based on in-house developed model)	Apparent kinetic parameters determination, comparison of kinetic model for free and immobilised enzyme	275
Graphene oxide/electrostatic interaction	Decontamination/ various phenols	-	high enzyme loading, increased stability in high pH, increased thermal stability, decent reusability, increased storage stability	381
Porous silica fibers/ In-situ encapsulation	4-AAP	650/8.3 (free)	inhibition by H2O2, enhanced thermal stability, enhanced pH stability, good reuse potential, flexibility of support	442
Aluminum pillar clay/adsorption	Decontamination/4-AAP, phenolic compounds	-	Activity enhancement by using PEG, increased phenol C is inhibitory, poor reusability, decent storage stability	203
Activated agarose beads/ covalent attachment (triple enzymatic system)	Decontamination w/ in-situ H_2O_2 production/ pyrogallol	-	very low activity of HRP due to glycoxyl groups present, not great immob efficiency but enhanced stability compared to soluble system	219
Nanoporous SBA-15	Immobilisation efficiency/ 4-AAP	270/2 (free), 310/0.146 (immob)	Enzyme confinement, increased thermal stability, decreased reaction rate but almost stable substrate affinity, increased stability to denaturising agents	506